

DEVELOPMENT OF VERSATILE STRATEGIES FOR ARYNE ANNULATION  
APPLICATIONS IN METHODOLOGY AND NATURAL PRODUCT  
TOTAL SYNTHESIS

VOLUME I

Thesis by  
Kevin McCormack Allan  
  
In Partial Fulfillment of the Requirements  
for the Degree of  
Doctor of Philosophy

CALIFORNIA INSTITUTE OF TECHNOLOGY  
Pasadena, California

2010  
(Defended March 25, 2010)

© 2010

Kevin McCormack Allan

All Rights Reserved

*To Dr. Ahamindra Jain*

*my friend and mentor*

## ACKNOWLEDGEMENTS

They say it takes a village to raise a child. I suppose one might then argue that it takes a department to raise a graduate student. And if so, then every single person in that department deserves thanks. So where to begin? I joined the Stoltz group in November of 2004, when the lab was already full to bursting. Yet Brian accepting me into his group without a moment's hesitation, and for that I am eternally grateful. Since joining, I have watched him spend his every effort on this lab, from early mornings in subgroup to late nights writing NIH grant proposals, and still have time to talk about chemistry at the drop of a hat. I have benefited through the years from his advice, support, and good humor. It goes without saying that none of what follows would have been possible without his continuous attention and involvement.

John Bercaw, the chairman of my thesis committee, has been a constant source of encouragement during these past five years. When discussing research, his inquiries are always complex and insightful. When discussing everything else, he conveys genuine interest and warmth of character. I thank him as well for his guidance as chairman of the instrumentation committee and the support he provided the NMR facility GLAs in a time of hectic transition.

I consider it a privilege to have been present for the advent of the Reisman group at Caltech. Since joining the faculty, Sarah has been an inspirational presence in class, at group meetings, and in everyday interactions. If I can continue to approach chemistry with half of the drive and determination she puts forth every day, I will consider myself fortunate.

I want to thank Peter Dervan for stepping in as the fourth member of my committee. His comments and suggestions concerning my proposals and the future of my career have been immensely helpful.

Scott Virgil joined the chemistry department in 2007, and from the very first day he became an active member of our group. I am certain that each and every one of us has been aided in some way by his encyclopedic knowledge of chemistry. He has managed the Herculean task of building, maintaining, and expanding a one-of-a-kind automated synthesis facility while simultaneously ensuring that the analytical machinery in both his lab and ours continues to run smoothly (and often better for having received his attention). And he does all of this without seeming to need (or get) a moment's rest. Caltech is lucky to have regained a mind like his.

I would also like to thank Dave MacMillan for his tenure as chairman of my candidacy committee. Though our interaction was brief, he provided a unique perspective on the finer points of synthetic research that I hope to carry with me.

I cannot possibly say enough to thank Ahamindra Jain for everything he has done for me. Simply put, he is the reason that I am a chemist. Before taking his course at Berkeley, my only contact with organic chemistry had come from brief lessons in nomenclature during high school and whispers of the “weeder” course overheard during my freshman year. He taught me that organic synthesis is an art form, and that doing it well requires both skill and imagination. As a member of his research group, I experienced firsthand the unending enthusiasm he had for this science, and I thank him for passing some of that on to me. It saddens me to say that our community is poorer for his passing.

I would also like to give my thanks to Dr. Jain's wife, Richa, for having the group over for tea so many times, and to his daughter, Divya, for beating us so graciously at Candy Land so many times.

I began my career in the Stoltz group sharing (or more accurately, overcrowding) a bay with Eric Ashley and Jenn Stockdill. I was tasked with continuing a total synthesis that Ash had begun a couple of years earlier, and I am sorry to say that this thesis does not contain that completed work. Still, the time I spent working with Ash showed me just what five years and a hell of a lot of work could accomplish. I am grateful for the time and effort he put into training me during those early days. The breakthroughs we were able to make in joining our aryne chemistry with the synthesis of the tetrahydroisoquinoline alkaloids are thanks in no small part to his pioneering work on leonomycin and cyanocycline A.

While Ash and Jenn were my first baymates at Caltech, John Enquist was my last. Since May 2005, we have shared bays in both 20 Gates and 4 Church. There is no one at Caltech with whom I have spent more time or shared more conversations. Working these past five years below ground, I am sure that I would have gone mad long ago without his constant camaraderie. The discussions we have had while running back-to-back columns have been wide-ranging and long-winded, wandering seamlessly from the philosophy of organic synthesis to the proper method for constructing a Rube Goldberg device. From Khan columns to clown chemistry (you'll have to look those up), he has helped to make each day in this lab interesting and enjoyable. And on top of it all, he is one of the most skilled, most meticulous synthetic chemists that I know. I wish him all the success in the world.

In addition to John, I have shared the trials and tribulations of candidacy, proposals, group meetings, and more with my two other classmates, Nat Sherden and Sandy Ma. It has been a thrill to grow as a chemist beside such talented people.

During my time in 20 Gates, I had the pleasure of sharing lab space with two postdoctoral fellows, Shyam Krishnan and Jun Chiba. Shyam was a fount of obscure chemical knowledge, and if I learned more from anyone else in that room, it would have been the endless string of books on tape that he played. While Jun was a quieter breed, I came to respect him just as much for his indomitable work ethic.

The evolution of aryne research in the Stoltz lab is thanks to the ongoing efforts of a number of people. Uttam Tambar is responsible for its commencement and its first application in total synthesis, and Dave Ebner played a large role in aiding the latter. Pam Tadross and Chris Gilmore were the next to join the team, and I have spent the last four years watching them take aryne chemistry to new heights. Chris and I collaborated on two of the projects presented in this thesis, and his work is much appreciated. While his research style is frantic to say the least, he demonstrates a real aptitude for bench chemistry and has accomplished a tremendous amount in his time here. Pam practices a more clearheaded approach to synthesis, and I have benefited a great deal from her involvement in my own research. While we have never collaborated directly, not a day goes by that one of us does not seek out the other for advice, assurance, or a fresh perspective. I know that my knowledge of benzyne and the ability to use it creatively have each grown in her presence, and I only hope to have had the same effect upon her. Most recently, our team has grown with the enlistment of Boram Hong. Boram and I collaborated on the aryne acyl-alkylation/condensation project, and his contributions to

that project were a boon. It is exciting to see the future of aryne research in such capable hands, and I look forward to witnessing the new directions that this research takes in the years to come.

Sometime between my third and fourth year, I began traveling to Ernie's Al Fresco for lunch across campus with several other members of the lab. In the two and a half years since, our lunchtime roster has grown to encompass more than half of the lab, including JT Mohr (and Sarah and Marie), Mike Krout, Dan Caspi, Dave White, Christian Defieber, Corinne Baumgartner, Nolan McDougal, Jan Streuff, Thomas Jensen, Alex Goldberg, Helene Kolding, Tomoko Ashizawa, Jen Alleva, and Kristy Tran. The hour spent each afternoon in the company of these people has been a welcome respite from the rigors of lab work, and I thank them for that. I would also like to acknowledge JT, Mike, and Corinne for their prowess on the racquetball court. I could not think of a better way to work off lunch at Ernie's than our weekly matches.

I suppose every graduate student finds a moment or two for a personal life, and I am happy that I was able to spend that time with friends like Kevin and Melissa Kuhn, Matt Winston, and Young In Oh. Kevin, Melissa, and I shared a love for coffee and movies that probably accounted for a hefty chunk of our monthly paychecks. I will always remember movie nights at House #1, barbequing in the back yard of House #2, and Thanksgiving dinner at House #3. More recently, I have had the good fortune to find close friends in Matt and Young In. Dinners at the tofu house and Saturday morning trips to the farmers' market have been peaceful interludes in what has all too often been a stressful year. I thank you both for listening patiently to my worries and woes these past few months. I am also extremely pleased to have found a matching caffeine addiction in

Matt, and I hope to have fulfilled my duties as a friend by fervently enabling that addiction. I look forward to our upcoming excursion and inevitably getting lost in the Japanese countryside.

The Caltech staff is truly without equal. Every bit of data that I have collected over the past five years was acquired with the help of the caring and capable people who manage our facilities. Dave VanderVelde and Scott Ross have built an NMR facility in which enormous amounts of information can be obtained with the push of a button. Mona Shahgholi and Naseem Torian have never failed to find a hi-res mass. Larry Henling was able to mount my amateur attempt at a crystal and collect usable data, and Mike Day refined that data to confirm our tentative structural assignments. Rick Gerhart has built (and rebuilt) almost every piece of glassware I own. Tom Dunn is the man who makes everything work, and his grasp of technology (from 100-year-old vacuum pumps to Mac OSX) is outmatched only by his kindness. I want to thank Paul Carroad for all of his help in setting up the Gates labs and in preparing for our move to the new Schlinger labs. Joe Drew and Ron Koen run a tight shop and have helped me on numerous occasions to track down chemical orders that have gone awry. The graduate office has kept me moving in the right direction for six years now. In particular, I would like to thank Dian Buchness, Laura Howe, and Agnes Tong for all of that they have done for me, as well as for the future of the department by organizing prospective student visitation weekends.

I would like to take this moment to express my gratitude to the people who took the time to edit this thesis: Pam Tadross, Chris Gilmore, Kristy Tran, Nolan McDougal, and Doug Behenna. I am long-winded on a good day, so you can imagine what they had to

slog through in my first drafts. Their careful attention and helpful suggestions aided in creating and refining the work you see before you, and I know that it has improved immensely with their input.

Finally, I want to express my gratitude for the love and support of my family. This thesis and the six years leading up to it never would have been possible without them. My parents have been there for me through it all. It was a tremendous comfort to know that when things got rough, all I had to do was jump in the car and drive down to Orange County to feel better. Having survived grad school, I can't describe how happy it makes me to see them embarking on their own adventure in the Pacific Northwest.

Thank you one and all.

## ABSTRACT

Since the elucidation of its structure in 1953, benzyne has been the focus of intense interest within the chemical community. Due to an unusually high degree of ring strain, benzyne displays reactivity uncharacteristic of common alkynes, including a tendency to react under mild metal-free conditions. This reactivity is exploited in the development of three novel methods for the synthesis of heterocyclic structures.

The first synthetic methodology includes two orthogonal annulation reactions taking place between functionalized enamines and arynes. The substitution at the nitrogen atom of the enamine determines the path of reactivity. Carbamates undergo a formal [3 + 2] cycloaddition with arynes to give rise to indolines, while amides undergo a formal [4 + 2] cycloaddition and dehydration to form isoquinolines. The latter reaction is applied to a three-step synthesis of the antispasmodic pavine alkaloid, papaverine.

This isoquinoline-forming alkyne annulation reaction is further employed in a concise asymmetric total synthesis of the tetrahydroisoquinoline antitumor antibiotic, (−)-quinocarcin. In addition to this key transformation, the synthetic route features an auxiliary-mediated diastereoselective dipolar cycloaddition to set the absolute stereochemistry and a novel two-step reduction to form the tetrahydroisoquinoline. In total, this strategy has enabled the shortest total synthesis of this important alkaloid reported to date.

The second methodology involves the synthesis of 3-hydroxyisoquinolines and 2-hydroxy-1,4-naphthoquinones from  $\beta$ -ketoesters using an alkyne acyl-alkylation reaction in combination with an in-situ condensation. This technology enables the preparation of highly functionalized polycyclic ring systems in two steps from readily available carboxylic acid starting materials. As a demonstration of its utility, this method is employed in a rapid synthesis of the *P,N*-ligand, QUINAP.

Finally, the development of a pair of three-component coupling reactions between arynes, isocyanides, and a third relay species is described. Phenyl esters and quinones lead to iminoisobenzofurans, while alkynes furnish iminoindenones. Procedures for the subsequent hydrolysis of these products are provided, thereby giving access to synthetically useful *ortho*-ketobenzamide and indenone compounds.

## TABLE OF CONTENTS

Dedication .....	iii
Acknowledgements.....	iv
Abstract .....	xi
Table of Contents.....	xii
List of Figures .....	xx
List of Schemes.....	xxxvi
List of Tables .....	xlii
List of Abbreviations .....	xlv

### **CHAPTER 1** 1

#### An Introduction to Benzyne

1.1	Introduction and Background .....	1
1.1.1	Early Observations of Aryne Reactivity.....	2
1.1.2	Mechanistic Investigations of a “Benzyne” Intermediate.....	6
1.1.3	Spectroscopic Evidence and Physical Properties of Benzyne.....	13
1.2	Arynes in Synthesis .....	18
1.2.1	Methods of Aryne Generation.....	18
1.2.2	Regioselectivity .....	21
1.3	Conclusion .....	24
1.4	Notes and References .....	26

### **CHAPTER 2** 36

#### Orthogonal Synthesis of Indolines and Isoquinolines via Aryne Annulation

2.1	Introduction .....	36
2.2	Previous Methods of Aryne Annulation .....	37
2.2.1	Aryne Annulation via Cycloaddition .....	37
2.2.1.1	[4 + 2] Cycloadditions .....	37
2.2.1.2	[3 + 2] Cycloaddition.....	39
2.2.2	Aryne Annulation via Stepwise Polar Mechanisms .....	41

2.2.2.1	Nucleophilic Addition and Cyclization .....	41
2.2.2.2	[2 + 2] Cycloadditions .....	44
2.2.2.3	Insertion into Activated $\sigma$ -Bonds .....	46
2.2.3	Transition Metal-Catalyzed Aryne Annulation .....	48
2.3	Orthogonal Synthesis of Indolines and Isoquinolines via Aryne Annulation .....	52
2.3.1	Rational Design of an Aryne Annulation Reaction for the Synthesis of Indolines .....	52
2.3.2	Synthesis of Isoquinolines via Aryne Annulation.....	57
2.3.3	Total Synthesis of Papaverine .....	65
2.3.4	An Alternative Approach to the Synthesis of Isoquinolines and Benzocyclobutenes via Aryne Annulation.....	66
2.3.5	Synthesis of Isoquinolones via Aryne Annulation.....	67
2.4	Conclusion.....	72
2.5	Experimental Section .....	74
2.5.1	Materials and Methods.....	74
2.5.2	Preparative Procedures and Spectroscopic Data .....	75
2.5.2.1	Representative Procedures for the Synthesis of Indolines and Isoquinolines via Aryne Annulation .....	75
2.5.2.2	Spectroscopic Data for Indolines .....	76
2.5.2.3	Spectroscopic Data for Isoquinolines .....	78
2.5.2.4	Synthesis of Additional Substrates.....	90
2.5.2.5	Total Synthesis of Papaverine .....	92
2.5.2.6	General Procedure for the Synthesis of Isoquinolones via Aryne Annulation .....	95
2.5.2.7	Spectroscopic Data for Isoquinolones .....	96
2.6	Notes and References .....	99

**APPENDIX 1****111**

Spectra Relevant to Chapter 2

**CHAPTER 3****182**

An Introduction to Quinocarcin

3.1	Introduction and Background .....	182
3.1.1	The Tetrahydroisoquinoline Antitumor Antibiotics .....	182

3.1.2	Isolation and Structural Characterization of Quinocarcin .....	185
3.1.3	Biosynthesis.....	186
3.1.4	Biological Activity.....	188
3.1.5	Mechanism of Action.....	192
3.2	Previous Total Syntheses of Quinocarcin .....	197
3.2.1	Fukuyama's Synthesis of ( $\pm$ )-Quinocarcin .....	197
3.2.2	Garner's Synthesis of (-)-Quinocarcin .....	200
3.2.3	Terashima's Synthesis of (-)-Quinocarcin.....	202
3.2.4	Myers' Synthesis of (-)-Quinocarcin .....	204
3.2.5	Zhu's Synthesis of (-)-Quinocarcin.....	207
3.3	Synthetic Studies Toward Quinocarcin .....	209
3.3.1	Danishefsky's Synthesis of ( $\pm$ )-Quinocarcinol Methyl Ester.....	210
3.3.2	Hirata's Approach to the ABCD Ring System .....	211
3.3.3	Weinreb's Approach to the Diazabicyclic.....	212
3.3.4	Joule's Approach to the Diazabicyclic.....	213
3.3.5	Williams' Synthesis of ( $\pm$ )-Quinocarcinamide .....	214
3.3.6	McMills' Approach to the ABCD Ring System .....	216
3.4	Conclusion .....	217
3.5	Notes and References .....	219

## CHAPTER 4 227

### A Concise Total Synthesis of (-)-Quinocarcin via Aryne Annulation

4.1	Introduction .....	227
4.1.1	Structure and Synthetic Challenges .....	227
4.1.2	Outline of Approach .....	228
4.2	First Generation Approach.....	230
4.2.1	Retrosynthetic Analysis .....	230
4.2.2	Dipolar Cycloaddition and Advancement to the <i>N</i> -Acyl Enamine.....	231
4.2.3	Attempts to Synthesize the Isoquinoline via Aryne Annulation.....	235
4.3	Second Generation Approach.....	237
4.3.1	Revision of Approach.....	237
4.3.2	Auxiliary-Mediated Diastereoselective Dipolar Cycloaddition and Aryne Annulation.....	238
4.3.3	Reduction of the Isoquinoline and Completion of Quinocarcin .....	243

4.4	Aryne Annulation Approaches to Additional Tetrahydroisoquinoline Antitumor Antibiotics.....	249
4.4.1	Jorumycin.....	250
4.4.2	Ecteinascidin 743.....	252
4.5	Conclusion.....	253
4.6	Experimental Section .....	255
4.6.1	Materials and Methods.....	255
4.6.2	Preparative Procedures and Spectroscopic Data .....	256
4.7	Notes and References .....	275

**APPENDIX 2** **282**  
**Synthetic Summary for (–)-Quinocarcin**

**APPENDIX 3** **284**  
**Spectra Relevant to Chapter 4**

**APPENDIX 4** **316**  
**Summary of Progress Toward the Total Synthesis of (+)-Cyanocycline A**

A4.1	Introduction and Background .....	316
A4.2	First Generation Synthetic Approach.....	318
A4.2.1	Outline of Approach and Retrosynthetic Analysis.....	318
A4.2.2	Styrene Synthesis and Oxidative Amination .....	320
A4.2.3	Oxazoline Route .....	322
A4.3	Second Generation Synthetic Approach.....	323
A4.3.1	Aryllithium Addition to an Aldehyde.....	323
A4.3.2	Petasis Three-Component Boronic Acid Mannich Reaction.....	325
A4.4	Future Directions .....	328
A4.5	Design of Novel Chiral Auxiliaries for a Diastereoselective Dipolar Cycloaddition: Application to the Enantioselective Total Synthesis of (+)-Cyanocycline A .....	330
A4.5.1	Introduction and Background .....	330

A4.5.2	Progress Toward an Auxiliary-Controlled Diastereoselective Dipolar Cycloaddition.....	334
A4.5.3	A Second Generation Auxiliary .....	337
A4.6	Conclusion.....	341
A4.7	Experimental Section .....	343
A4.7.1	Materials and Methods.....	343
A4.7.2	Preparative Procedures and Spectroscopic Data .....	344
A4.7.2.1	General Method for the Preparation of Amino Sulfonates.....	344
A4.7.2.2	General Method for the Preparation of Silyl Propargyl Amide Sulfonates.....	346
A4.7.2.3	General Method for the Preparation of Propargyl Amide Sulfonates .....	348
A4.7.2.4	General Method for the Preparation of Amide Sulfonate Cycloadducts.....	350
A4.7.2.5	General Method for the Preparation of Amino Silyl Ethers.....	352
A4.7.2.6	General Method for the Preparation of Propargyl Amide Silyl Ethers .....	354
A4.7.2.7	General Method for the Preparation of Silyl Ether Cycloadducts .....	356
A4.8	Notes and References .....	359

## **CHAPTER 5** 364

### Expedient Synthesis of 3-Hydroxyisoquinolines and 2-Hydroxy-1,4-Naphthoquinones via One-Pot Aryne Acyl-Alkylation / Condensation

5.1	Introduction and Background .....	364
5.1.1	The Direct Acyl-Alkylation of Arynes .....	364
5.1.2	Applications of Aryne Acyl-Alkylation in Natural Product Total Synthesis .....	371
5.1.2.1	Total Synthesis of (+)-Amurensinine .....	371
5.1.2.2	Total Synthesis of (–)-Curvularin .....	374
5.1.2.3	Progress Toward the Total Synthesis of Integrastatins A and B .....	375
5.2	Expedient Synthesis of 3-Hydroxyisoquinolines and 2-Hydroxy-1,4-naphthoquinones via One-Pot Aryne Acyl-Alkylation / Condensation.....	378
5.2.1	Previous Synthetic Methods.....	378
5.2.2	Proof of Principle .....	379
5.2.3	Development of a One-Pot Aryne Acyl-Alkylation / Ammonia Condensation Reaction Sequence for the Synthesis of 3-Hydroxyisoquinolines....	380
5.2.4	Development of a One-Pot Aryne Acyl-Alkylation / Intramolecular Condensation Reaction Sequence for the Synthesis of 2-Hydroxy-1,4-naphthoquinones.....	386
5.3	Conclusion.....	389

5.4	Experimental Section .....	390
5.4.1	Materials and Methods.....	390
5.4.2	Preparative Procedures and Spectroscopic Data .....	391
5.4.2.1	Representative Procedure for the Synthesis of $\beta$ -Ketoesters From Carboxylic Acids.....	391
5.4.2.2	Spectroscopic Data for $\beta$ -Ketoesters .....	392
5.4.2.3	Representative Procedure for the Synthesis of 3-Hydroxyisoquinolines From $\beta$ -Ketoesters .....	395
5.4.2.4	Spectroscopic Data for 3-Hydroxyisoquinolines .....	396
5.4.2.5	Synthesis of a 1,3-Diarylisoquinoline via Suzuki Coupling.....	408
5.4.2.6	Synthesis of QUINAP .....	410
5.4.2.7	Representative Procedure for the Synthesis of 2-Hydroxy-1,4-naphthoquinones From $\beta$ -Ketoesters .....	414
5.4.2.8	Spectroscopic Data for 2-Hydroxy-1,4-naphthoquinones.....	415
5.5	Notes and References .....	423

## **APPENDIX 5** **433**

### Spectra Relevant to Chapter 5

## **CHAPTER 6** **510**

### Multicomponent Aryne Reactions

6.1	Introduction and Background .....	510
6.1.1	Introduction to Multicomponent Reactions.....	510
6.1.2	Multicomponent Aryne Reactions .....	512
6.1.2.1	Three-Component Reactions .....	513
6.1.2.2	Four-Component Reactions .....	520
6.1.2.3	Multicomponent Aryne Reactions in Total Synthesis .....	522
6.2	Synthesis of Phenoxy Iminoisobenzofurans and Iminoindenones via Three-Component Coupling of Arynes, Isocyanides, and Esters or Alkynes.....	525
6.2.1	Outline of Approach and Initial Studies .....	525
6.2.2	Synthesis of Phenoxy Iminoisobenzofurans.....	527
6.2.3	Synthesis of Iminoindenones .....	536
6.2.4	Quinones as Relay Components.....	539

6.3	Conclusion .....	540
6.4	Experimental Section .....	542
6.4.1	Materials and Methods.....	542
6.4.2	Preparative Procedures and Spectroscopic Data .....	543
6.4.2.1	Representative Procedure for the Three-Component Synthesis of Phenoxy Iminoisobenzofurans from Arynes, Isocyanides, and Phenyl Esters .....	543
6.4.2.2	Spectroscopic Data for Phenoxy Iminoisobenzofurans .....	544
6.4.2.3	Representative Procedure for the One-Pot Synthesis of <i>ortho</i> -Ketobenzamides via Three-Component Synthesis and Hydrolysis of Phenoxy Iminoisobenzofurans.....	559
6.4.2.4	Spectroscopic Data for <i>ortho</i> -Ketobenzamides .....	560
6.4.2.5	Representative Procedure for the Copper-Catalyzed Intramolecular Coupling of 2-( <i>ortho</i> -Bromobenzoyl)benzamides .....	564
6.4.2.6	Spectroscopic Data for Dibenzoketocaprolactams.....	565
6.4.2.7	Representative Procedure for the Three-Component Synthesis of Iminoindenones from Arynes, Isocyanides, and Alkynes .....	567
6.4.2.8	Spectroscopic Data for Iminoindenones.....	568
6.4.2.9	Representative Procedure for the Three-Component Synthesis of Spirocycles from Arynes, Isocyanides, and Quinones .....	572
6.4.2.10	Spectroscopic Data for Spirocycles.....	573
6.5	Notes and References .....	576

**APPENDIX 6** **585**

Spectra Relevant to Chapter 6

**APPENDIX 7** **672**

X-ray Crystallography Reports Relevant to Appendix 6

**APPENDIX 8** **681**

Notebook Cross-Reference

Comprehensive Bibliography.....	687
Index .....	729
About the Author .....	735

## LIST OF FIGURES

### CHAPTER 1

Figure 1.1	Benzyne.....	2
Figure 1.2	<sup>1</sup> H and <sup>13</sup> C NMR spectra of benzyne.....	17

### APPENDIX 1

Figure A1.1.1	<sup>1</sup> H NMR (500 MHz, CDCl <sub>3</sub> ) of indoline <b>167</b> (Table 2.2, entry 1) .....	112
Figure A1.1.2	Infrared spectrum (thin film/NaCl) of indoline <b>167</b> (Table 2.2, entry 1).....	113
Figure A1.1.3	<sup>13</sup> C NMR (125 MHz, CDCl <sub>3</sub> ) of indoline <b>167</b> (Table 2.2, entry 1) .....	113
Figure A1.2.1	<sup>1</sup> H NMR (500 MHz, CDCl <sub>3</sub> ) of indoline <b>170a</b> and <b>170b</b> (Table 2.2, entry 2) .....	114
Figure A1.2.2	Infrared spectrum (thin film/NaCl) of indoline <b>170a</b> and <b>170b</b> (Table 2.2, entry 2) .....	115
Figure A1.2.3	<sup>13</sup> C NMR (125 MHz, CDCl <sub>3</sub> ) of indoline <b>170a</b> and <b>170b</b> (Table 2.2, entry 2) .....	115
Figure A1.3.1	<sup>1</sup> H NMR (500 MHz, CDCl <sub>3</sub> ) of indoline <b>170c</b> (Table 2.2, entry 3) .....	116
Figure A1.3.2	Infrared spectrum (thin film/NaCl) of indoline <b>170c</b> (Table 2.2, entry 3).....	117
Figure A1.3.3	<sup>13</sup> C NMR (125 MHz, CDCl <sub>3</sub> ) of indoline <b>170c</b> (Table 2.2, entry 3) .....	117
Figure A1.4.1	<sup>1</sup> H NMR (500 MHz, CDCl <sub>3</sub> ) of indoline <b>170d</b> (Table 2.2, entry 4) .....	118
Figure A1.4.2	Infrared spectrum (thin film/NaCl) of indoline <b>170d</b> (Table 2.2, entry 4) .....	119
Figure A1.4.3	<sup>13</sup> C NMR (125 MHz, CDCl <sub>3</sub> ) of indoline <b>170d</b> (Table 2.2, entry 4) .....	119
Figure A1.5.1	<sup>1</sup> H NMR (500 MHz, CDCl <sub>3</sub> ) of isoquinoline <b>176</b> (Table 2.4, entry 1).....	120
Figure A1.5.2	Infrared spectrum (thin film/NaCl) of isoquinoline <b>176</b> (Table 2.4, entry 1) .....	121
Figure A1.5.3	<sup>13</sup> C NMR (125 MHz, CDCl <sub>3</sub> ) of isoquinoline <b>176</b> (Table 2.4, entry 1).....	121
Figure A1.6.1	<sup>1</sup> H NMR (500 MHz, CDCl <sub>3</sub> ) of isoquinoline <b>181a</b> (Table 2.4, entry 2).....	122
Figure A1.6.2	Infrared spectrum (thin film/NaCl) of isoquinoline <b>181a</b> (Table 2.4, entry 2) .....	123
Figure A1.6.3	<sup>13</sup> C NMR (125 MHz, CDCl <sub>3</sub> ) of isoquinoline <b>181a</b> (Table 2.4, entry 2).....	123
Figure A1.7.1	<sup>1</sup> H NMR (500 MHz, CDCl <sub>3</sub> ) of isoquinoline <b>181b</b> (Table 2.4, entry 3) .....	124
Figure A1.7.2	Infrared spectrum (thin film/NaCl) of isoquinoline <b>181b</b> (Table 2.4, entry 3) .....	125
Figure A1.7.3	<sup>13</sup> C NMR (125 MHz, CDCl <sub>3</sub> ) of isoquinoline <b>181b</b> (Table 2.4, entry 3).....	125

Figure A1.8.1	$^1\text{H}$ NMR (500 MHz, $\text{CDCl}_3$ ) of isoquinoline <b>181c</b> (Table 2.4, entry 4).....	126
Figure A1.8.2	Infrared spectrum (thin film/NaCl) of isoquinoline <b>181c</b> (Table 2.4, entry 4) .....	127
Figure A1.8.3	$^{13}\text{C}$ NMR (125 MHz, $\text{CDCl}_3$ ) of isoquinoline <b>181c</b> (Table 2.4, entry 4).....	127
Figure A1.9.1	$^1\text{H}$ NMR (500 MHz, $\text{CDCl}_3$ ) of isoquinoline <b>181d</b> (Table 2.4, entry 5) .....	128
Figure A1.9.2	Infrared spectrum (thin film/NaCl) of isoquinoline <b>181d</b> (Table 2.4, entry 5) .....	129
Figure A1.9.3	$^{13}\text{C}$ NMR (125 MHz, $\text{CDCl}_3$ ) of isoquinoline <b>181d</b> (Table 2.4, entry 5).....	129
Figure A1.10.1	$^1\text{H}$ NMR (500 MHz, $\text{CDCl}_3$ ) of isoquinoline <b>181e</b> (Table 2.4, entry 6).....	130
Figure A1.10.2	Infrared spectrum (thin film/NaCl) of isoquinoline <b>181e</b> (Table 2.4, entry 6) .....	131
Figure A1.10.3	$^{13}\text{C}$ NMR (125 MHz, $\text{CDCl}_3$ ) of isoquinoline <b>181e</b> (Table 2.4, entry 6).....	131
Figure A1.11.1	$^1\text{H}$ NMR (500 MHz, $\text{CDCl}_3$ ) of isoquinoline <b>181f</b> (Table 2.4, entry 7) .....	132
Figure A1.11.2	Infrared spectrum (thin film/NaCl) of isoquinoline <b>181f</b> (Table 2.4, entry 7) .....	133
Figure A1.11.3	$^{13}\text{C}$ NMR (125 MHz, $\text{CDCl}_3$ ) of isoquinoline <b>181f</b> (Table 2.4, entry 7) .....	133
Figure A1.12.1	$^1\text{H}$ NMR (500 MHz, $\text{CDCl}_3$ ) of isoquinoline <b>181g</b> (Table 2.4, entry 8).....	134
Figure A1.12.2	Infrared spectrum (thin film/NaCl) of isoquinoline <b>181g</b> (Table 2.4, entry 8) .....	135
Figure A1.12.3	$^{13}\text{C}$ NMR (125 MHz, $\text{CDCl}_3$ ) of isoquinoline <b>181g</b> (Table 2.4, entry 8).....	135
Figure A1.13.1	$^1\text{H}$ NMR (500 MHz, $\text{CDCl}_3$ ) of isoquinoline <b>181h</b> (Table 2.4, entry 9) .....	136
Figure A1.13.2	Infrared spectrum (thin film/NaCl) of isoquinoline <b>181h</b> (Table 2.4, entry 9) .....	137
Figure A1.13.3	$^{13}\text{C}$ NMR (125 MHz, $\text{CDCl}_3$ ) of isoquinoline <b>181h</b> (Table 2.4, entry 9).....	137
Figure A1.14.1	$^1\text{H}$ NMR (500 MHz, $\text{CDCl}_3$ ) of isoquinoline <b>182a</b> (Table 2.5, entry 1).....	138
Figure A1.14.2	Infrared spectrum (thin film/NaCl) of isoquinoline <b>182a</b> (Table 2.5, entry 1) .....	139
Figure A1.14.3	$^{13}\text{C}$ NMR (125 MHz, $\text{CDCl}_3$ ) of isoquinoline <b>182a</b> (Table 2.5, entry 1).....	139
Figure A1.15.1	$^1\text{H}$ NMR (500 MHz, $\text{CDCl}_3$ ) of isoquinoline <b>182b</b> and <b>182c</b> (Table 2.5, entry 2) .....	140
Figure A1.15.2	Infrared spectrum (thin film/NaCl) of isoquinoline <b>182b</b> and <b>182c</b> (Table 2.5, entry 2) .....	141
Figure A1.15.3	$^{13}\text{C}$ NMR (125 MHz, $\text{CDCl}_3$ ) of isoquinoline <b>182b</b> and <b>182c</b> (Table 2.5, entry 2) .....	141
Figure A1.16.1	$^1\text{H}$ NMR (500 MHz, $\text{CDCl}_3$ ) of isoquinoline <b>182d</b> (Table 2.5, entry 3) .....	142
Figure A1.16.2	Infrared spectrum (thin film/NaCl) of isoquinoline <b>182d</b> (Table 2.5, entry 3) .....	143
Figure A1.16.3	$^{13}\text{C}$ NMR (125 MHz, $\text{CDCl}_3$ ) of isoquinoline <b>182d</b> (Table 2.5, entry 3).....	143
Figure A1.17.1	$^1\text{H}$ NMR (500 MHz, $\text{CDCl}_3$ ) of isoquinoline <b>182e</b> (Table 2.5, entry 4).....	144

Figure A1.17.2 Infrared spectrum (thin film/NaCl) of isoquinoline <b>182e</b> (Table 2.5, entry 4) .....	145
Figure A1.17.3 $^{13}\text{C}$ NMR (125 MHz, $\text{CDCl}_3$ ) of isoquinoline <b>182e</b> (Table 2.5, entry 4).....	145
Figure A1.18.1 $^1\text{H}$ NMR (500 MHz, $\text{CDCl}_3$ ) of isoquinoline <b>182f</b> (Table 2.5, entry 5) .....	146
Figure A1.18.2 Infrared spectrum (thin film/NaCl) of isoquinoline <b>182f</b> (Table 2.5, entry 5) .....	147
Figure A1.18.3 $^{13}\text{C}$ NMR (125 MHz, $\text{CDCl}_3$ ) of isoquinoline <b>182f</b> (Table 2.5, entry 5) .....	147
Figure A1.19.1 $^1\text{H}$ NMR (500 MHz, $\text{CDCl}_3$ ) of isoquinoline <b>187a</b> (Table 2.6, entry 1).....	148
Figure A1.19.2 Infrared spectrum (thin film/NaCl) of isoquinoline <b>187a</b> (Table 2.6, entry 1) .....	149
Figure A1.19.3 $^{13}\text{C}$ NMR (125 MHz, $\text{CDCl}_3$ ) of isoquinoline <b>187a</b> (Table 2.6, entry 1).....	149
Figure A1.20.1 $^1\text{H}$ NMR (500 MHz, $\text{CDCl}_3$ ) of isoquinoline <b>187b</b> (Table 2.6, entry 2) .....	150
Figure A1.20.2 Infrared spectrum (thin film/NaCl) of isoquinoline <b>187b</b> (Table 2.6, entry 2) .....	151
Figure A1.20.3 $^{13}\text{C}$ NMR (125 MHz, $\text{CDCl}_3$ ) of isoquinoline <b>187b</b> (Table 2.6, entry 2).....	151
Figure A1.21.1 $^1\text{H}$ NMR (500 MHz, $\text{CDCl}_3$ ) of isoquinoline <b>187c</b> (Table 2.6, entry 3).....	152
Figure A1.21.2 Infrared spectrum (thin film/NaCl) of isoquinoline <b>187c</b> (Table 2.6, entry 3) .....	153
Figure A1.21.3 $^{13}\text{C}$ NMR (125 MHz, $\text{CDCl}_3$ ) of isoquinoline <b>187c</b> (Table 2.6, entry 3).....	153
Figure A1.22.1 $^1\text{H}$ NMR (500 MHz, $\text{CDCl}_3$ ) of isoquinoline <b>A1-1</b> .....	154
Figure A1.22.2 Infrared spectrum (thin film/NaCl) of isoquinoline <b>A1-1</b> .....	155
Figure A1.22.3 $^{13}\text{C}$ NMR (125 MHz, $\text{CDCl}_3$ ) of isoquinoline <b>A1-1</b> .....	155
Figure A1.23.1 $^1\text{H}$ NMR (500 MHz, $\text{CDCl}_3$ ) of isoquinoline <b>187d</b> (Table 2.6, entry 4) .....	156
Figure A1.23.2 Infrared spectrum (thin film/NaCl) of isoquinoline <b>187d</b> (Table 2.6, entry 4) .....	157
Figure A1.23.3 $^{13}\text{C}$ NMR (125 MHz, $\text{CDCl}_3$ ) of isoquinoline <b>187d</b> (Table 2.6, entry 4).....	157
Figure A1.24.1 $^1\text{H}$ NMR (500 MHz, $\text{CDCl}_3$ ) of isoquinoline <b>A1-2</b> .....	158
Figure A1.24.2 Infrared spectrum (thin film/NaCl) of isoquinoline <b>A1-2</b> .....	159
Figure A1.24.3 $^{13}\text{C}$ NMR (125 MHz, $\text{CDCl}_3$ ) of isoquinoline <b>A1-2</b> .....	159
Figure A1.25.1 $^1\text{H}$ NMR (500 MHz, $\text{CDCl}_3$ ) of isoquinoline <b>187e</b> (Table 2.6, entry 5).....	160
Figure A1.25.2 Infrared spectrum (thin film/NaCl) of isoquinoline <b>187e</b> (Table 2.6, entry 5) .....	161
Figure A1.25.3 $^{13}\text{C}$ NMR (125 MHz, $\text{CDCl}_3$ ) of isoquinoline <b>187e</b> (Table 2.6, entry 5).....	162
Figure A1.26.1 $^1\text{H}$ NMR (500 MHz, $\text{CDCl}_3$ ) of isoquinoline <b>187f</b> (Table 2.6, entry 6) .....	162
Figure A1.26.2 Infrared spectrum (thin film/NaCl) of isoquinoline <b>187f</b> (Table 2.6, entry 6) .....	163
Figure A1.26.3 $^{13}\text{C}$ NMR (125 MHz, $\text{CDCl}_3$ ) of isoquinoline <b>187f</b> (Table 2.6, entry 6) .....	163
Figure A1.27.1 $^1\text{H}$ NMR (500 MHz, $\text{CDCl}_3$ ) of oxime <b>A1-4</b> .....	164

Figure A1.27.2	Infrared spectrum (thin film/NaCl) of oxime <b>A1-4</b> .....	165
Figure A1.27.3	$^{13}\text{C}$ NMR (125 MHz, $\text{CDCl}_3$ ) of oxime <b>A1-4</b> .....	165
Figure A1.28.1	$^1\text{H}$ NMR (500 MHz, $\text{CDCl}_3$ ) of enamine <b>A1-5</b> .....	166
Figure A1.28.2	Infrared spectrum (thin film/NaCl) of enamine <b>A1-5</b> .....	167
Figure A1.28.3	$^{13}\text{C}$ NMR (125 MHz, $\text{CDCl}_3$ ) of enamine <b>A1-5</b> .....	167
Figure A1.29.1	$^1\text{H}$ NMR (500 MHz, $\text{CDCl}_3$ ) of enamine <b>195</b> .....	168
Figure A1.29.2	Infrared spectrum (thin film/NaCl) of enamine <b>195</b> .....	169
Figure A1.29.3	$^{13}\text{C}$ NMR (125 MHz, $\text{CDCl}_3$ ) of enamine <b>195</b> .....	169
Figure A1.30.1	$^1\text{H}$ NMR (500 MHz, $\text{CDCl}_3$ ) of methyl papaverine-3-carboxylate ( <b>196</b> ).....	170
Figure A1.30.2	Infrared spectrum (thin film/NaCl) of methyl papaverine-3-carboxylate ( <b>196</b> ).....	171
Figure A1.30.3	$^{13}\text{C}$ NMR (125 MHz, $\text{CDCl}_3$ ) of methyl papaverine-3-carboxylate ( <b>196</b> ).....	171
Figure A1.31.1	$^1\text{H}$ NMR (500 MHz, $\text{CDCl}_3$ ) of papaverine ( <b>197</b> ) .....	172
Figure A1.31.2	Infrared spectrum (thin film/NaCl) of papaverine ( <b>197</b> ) .....	173
Figure A1.31.3	$^{13}\text{C}$ NMR (125 MHz, $\text{CDCl}_3$ ) of papaverine ( <b>197</b> ) .....	173
Figure A1.32.1	$^1\text{H}$ NMR (500 MHz, $\text{CDCl}_3$ ) of isoquinolone <b>202a</b> (Table 2.9, entry 1).....	174
Figure A1.32.2	Infrared spectrum (thin film/NaCl) of isoquinolone <b>202a</b> (Table 2.9, entry 1) .....	175
Figure A1.32.3	$^{13}\text{C}$ NMR (125 MHz, $\text{CDCl}_3$ ) of isoquinolone <b>202a</b> (Table 2.9, entry 1).....	175
Figure A1.33.1	$^1\text{H}$ NMR (500 MHz, $\text{CDCl}_3$ ) of isoquinolone <b>202b</b> (Table 2.9, entry 2) .....	176
Figure A1.33.2	Infrared spectrum (thin film/NaCl) of isoquinolone <b>202b</b> (Table 2.9, entry 2) .....	177
Figure A1.33.3	$^{13}\text{C}$ NMR (125 MHz, $\text{CDCl}_3$ ) of isoquinolone <b>202b</b> (Table 2.9, entry 2).....	177
Figure A1.34.1	$^1\text{H}$ NMR (500 MHz, $\text{CDCl}_3$ ) of isoquinolone <b>209</b> (Table 2.9, entry 3).....	178
Figure A1.34.2	Infrared spectrum (thin film/NaCl) of isoquinolone <b>209</b> (Table 2.9, entry 3) .....	179
Figure A1.34.3	$^{13}\text{C}$ NMR (125 MHz, $\text{CDCl}_3$ ) of isoquinolone <b>209</b> (Table 2.9, entry 3).....	179
Figure A1.35.1	$^1\text{H}$ NMR (500 MHz, $\text{CDCl}_3$ ) of isoquinolone <b>202c</b> (Table 2.9, entry 4).....	180
Figure A1.35.2	Infrared spectrum (thin film/NaCl) of isoquinolone <b>202c</b> (Table 2.9, entry 4) .....	181
Figure A1.35.3	$^{13}\text{C}$ NMR (125 MHz, $\text{CDCl}_3$ ) of isoquinolone <b>202c</b> (Table 2.9, entry 4).....	181

## CHAPTER 3

Figure 3.1	Representative structures of the tetrahydroisoquinoline antitumor antibiotics.....	184
------------	--	-----

Figure 3.2	Structures of quinocarcin and quinocarcinol .....	186
Figure 3.3	Elucidating the biosynthetic origins of saframycin A and naphthyridinomycin via isotopic labeling studies.....	187
Figure 3.4	a) Proposed mechanism of DNA alkylation by quinocarcin b) Calculated lowest energy conformation of quinocarcin covalently bound to DNA (stereo pair). c) Non-covalent hydrogen bonding interactions between quinocarcin and d(ATGCAT) <sub>2</sub> .....	194

## CHAPTER 4

Figure 4.1	Quinocarcin .....	228
Figure 4.2	Revised design of the <i>N</i> -acyl enamine .....	238
Figure 4.3	Additional tetrahydroisoquinoline natural product targets.....	250

## APPENDIX 3

Figure A3.1.1	<sup>1</sup> H NMR (500 MHz, CDCl <sub>3</sub> ) of ester <b>382</b> .....	285
Figure A3.1.2	Infrared spectrum (thin film/NaCl) of ester <b>382</b> .....	286
Figure A3.1.3	<sup>13</sup> C NMR (125 MHz, CDCl <sub>3</sub> ) of ester <b>382</b> .....	286
Figure A3.2.1	<sup>1</sup> H NMR (500 MHz, CDCl <sub>3</sub> ) of imide <b>381</b> .....	287
Figure A3.2.2	Infrared spectrum (thin film/NaCl) of imide <b>381</b> .....	288
Figure A3.2.3	<sup>13</sup> C NMR (125 MHz, CDCl <sub>3</sub> ) of imide <b>381</b> .....	288
Figure A3.3.1	<sup>1</sup> H NMR (500 MHz, CDCl <sub>3</sub> ) of <i>N</i> -acyl enamine <b>380</b> .....	289
Figure A3.3.2	Infrared spectrum (thin film/NaCl) of <i>N</i> -acyl enamine <b>380</b> .....	290
Figure A3.3.3	<sup>13</sup> C NMR (125 MHz, CDCl <sub>3</sub> ) of <i>N</i> -acyl enamine <b>380</b> .....	290
Figure A3.4.1	<sup>1</sup> H NMR (500 MHz, CDCl <sub>3</sub> ) of isoquinoline <b>392</b> .....	291
Figure A3.4.2	Infrared spectrum (thin film/NaCl) of isoquinoline <b>392</b> .....	292
Figure A3.4.3	<sup>13</sup> C NMR (125 MHz, CDCl <sub>3</sub> ) of isoquinoline <b>392</b> .....	292
Figure A3.5.1	<sup>1</sup> H NMR (500 MHz, CDCl <sub>3</sub> ) of diazabicycle <b>405a</b> .....	293
Figure A3.5.2	Infrared spectrum (thin film/NaCl) of diazabicycle <b>405a</b> .....	294
Figure A3.5.3	<sup>13</sup> C NMR (125 MHz, CDCl <sub>3</sub> ) of diazabicycle <b>405a</b> .....	294
Figure A3.6.1	<sup>1</sup> H NMR (500 MHz, CDCl <sub>3</sub> ) of methyl ester <b>402</b> .....	295
Figure A3.6.2	Infrared spectrum (thin film/NaCl) of methyl ester <b>402</b> .....	296
Figure A3.6.3	<sup>13</sup> C NMR (125 MHz, CDCl <sub>3</sub> ) of methyl ester <b>402</b> .....	296

Figure A3.6.4	Chiral SFC traces for racemic methyl ester <b>402</b> .....	297
Figure A3.6.5	Chiral SFC trace for enantioenriched methyl ester (–)- <b>402</b> (>99% ee) .....	298
Figure A3.7.1	<sup>1</sup> H NMR (500 MHz, CDCl <sub>3</sub> ) of imide <b>406</b> .....	299
Figure A3.7.2	Infrared spectrum (thin film/NaCl) of imide <b>406</b> .....	300
Figure A3.7.3	<sup>13</sup> C NMR (125 MHz, CDCl <sub>3</sub> ) of imide <b>406</b> .....	300
Figure A3.8.1	<sup>1</sup> H NMR (500 MHz, CDCl <sub>3</sub> ) of <i>N</i> -acyl enamine <b>407</b> .....	301
Figure A3.8.2	Infrared spectrum (thin film/NaCl) of <i>N</i> -acyl enamine <b>407</b> .....	302
Figure A3.8.3	<sup>13</sup> C NMR (125 MHz, CDCl <sub>3</sub> ) of <i>N</i> -acyl enamine <b>407</b> .....	302
Figure A3.9.1	<sup>1</sup> H NMR (500 MHz, CDCl <sub>3</sub> ) of isoquinoline <b>411</b> .....	303
Figure A3.9.2	Infrared spectrum (thin film/NaCl) of isoquinoline <b>411</b> .....	304
Figure A3.9.3	<sup>13</sup> C NMR (125 MHz, CDCl <sub>3</sub> ) of isoquinoline <b>411</b> .....	304
Figure A3.10.1	<sup>1</sup> H NMR (500 MHz, CDCl <sub>3</sub> ) of tetrahydroisoquinoline <b>415a</b> .....	305
Figure A3.10.2	Infrared spectrum (thin film/NaCl) of tetrahydroisoquinoline <b>415a</b> .....	306
Figure A3.10.3	<sup>13</sup> C NMR (125 MHz, CDCl <sub>3</sub> ) of tetrahydroisoquinoline <b>415a</b> .....	306
Figure A3.11.1	<sup>1</sup> H NMR (500 MHz, CDCl <sub>3</sub> ) of tetrahydroisoquinoline <b>415b</b> .....	307
Figure A3.11.2	Infrared spectrum (thin film/NaCl) of tetrahydroisoquinoline <b>415b</b> .....	308
Figure A3.11.3	<sup>13</sup> C NMR (125 MHz, CDCl <sub>3</sub> ) of tetrahydroisoquinoline <b>415b</b> .....	308
Figure A3.12.1	<sup>1</sup> H NMR (500 MHz, CDCl <sub>3</sub> ) of tetracycle <b>414</b> .....	309
Figure A3.12.2	Infrared spectrum (thin film/NaCl) of tetracycle <b>414</b> .....	310
Figure A3.12.3	<sup>13</sup> C NMR (125 MHz, CDCl <sub>3</sub> ) of tetracycle <b>414</b> .....	310
Figure A3.13.1	<sup>1</sup> H NMR (500 MHz, CDCl <sub>3</sub> ) of <i>N</i> -methyl amine <b>378</b> .....	311
Figure A3.13.2	Infrared spectrum (thin film/NaCl) of <i>N</i> -methyl amine <b>378</b> .....	312
Figure A3.13.3	<sup>13</sup> C NMR (125 MHz, CDCl <sub>3</sub> ) of <i>N</i> -methyl amine <b>378</b> .....	312
Figure A3.14.1	<sup>1</sup> H NMR (500 MHz, CD <sub>3</sub> OD) of (–)-quinocarcin ( <b>211</b> ) .....	313
Figure A3.14.2	<sup>1</sup> H NMR comparison of synthetic (above) and natural (below) (–)-quinocarcin ( <b>211</b> ) (500 MHz, CD <sub>3</sub> OD).....	314
Figure A3.14.3	Infrared spectrum (thin film/NaCl) of (–)-quinocarcin ( <b>211</b> ).....	315
Figure A3.14.4	<sup>13</sup> C NMR (125 MHz, CD <sub>3</sub> OD) of (–)-quinocarcin ( <b>211</b> ) .....	315

## APPENDIX 4

Figure A4.1	Translating a synthetic approach from leonomycin to cyanocycline A .....	319
-------------	--	-----

## CHAPTER 5

Figure 5.1	Natural products targeted for application of the aryne acyl-alkylation reaction .....	371
------------	---	-----

## APPENDIX 5

Figure A5.1.1	$^1\text{H}$ NMR (500 MHz, $\text{CDCl}_3$ ) of $\beta$ -ketoester <b>575h</b> (Table 5.5, entry 10).....	434
Figure A5.1.2	Infrared spectrum (thin film/NaCl) of $\beta$ -ketoester <b>575h</b> (Table 5.5, entry 10) .....	435
Figure A5.1.3	$^{13}\text{C}$ NMR (125 MHz, $\text{CDCl}_3$ ) of $\beta$ -ketoester <b>575h</b> (Table 5.5, entry 10).....	435
Figure A5.2.1	$^1\text{H}$ NMR (500 MHz, $\text{CDCl}_3$ ) of $\beta$ -ketoester <b>575i</b> (Table 5.5, entry 11).....	436
Figure A5.2.2	Infrared spectrum (thin film/NaCl) of $\beta$ -ketoester <b>575i</b> (Table 5.5, entry 11) .....	437
Figure A5.2.3	$^{13}\text{C}$ NMR (125 MHz, $\text{CDCl}_3$ ) of $\beta$ -ketoester <b>575i</b> (Table 5.5, entry 11).....	437
Figure A5.3.1	$^1\text{H}$ NMR (500 MHz, $\text{CDCl}_3$ ) of $\beta$ -ketoester <b>575j</b> (Table 5.5, entry 12).....	438
Figure A5.3.2	Infrared spectrum (thin film/NaCl) of $\beta$ -ketoester <b>575j</b> (Table 5.5, entry 12) .....	439
Figure A5.3.3	$^{13}\text{C}$ NMR (125 MHz, $\text{CDCl}_3$ ) of $\beta$ -ketoester <b>575j</b> (Table 5.5, entry 12).....	439
Figure A5.4.1	$^1\text{H}$ NMR (500 MHz, $\text{CDCl}_3$ ) of $\beta$ -ketoester <b>575k</b> (Table 5.5, entry 13).....	440
Figure A5.4.2	Infrared spectrum (thin film/NaCl) of $\beta$ -ketoester <b>575k</b> (Table 5.5, entry 13) .....	441
Figure A5.4.3	$^{13}\text{C}$ NMR (125 MHz, $\text{CDCl}_3$ ) of $\beta$ -ketoester <b>575k</b> (Table 5.5, entry 13).....	441
Figure A5.5.1	$^1\text{H}$ NMR (500 MHz, $\text{CDCl}_3$ ) of 3-hydroxyisoquinoline <b>569</b> .....	442
Figure A5.5.2	Infrared spectrum (thin film/NaCl) of 3-hydroxyisoquinoline <b>569</b> .....	443
Figure A5.5.3	$^{13}\text{C}$ NMR (125 MHz, $\text{CDCl}_3$ ) of 3-hydroxyisoquinoline <b>569</b> .....	443
Figure A5.6.1	$^1\text{H}$ NMR (500 MHz, $\text{CDCl}_3$ ) of 3-hydroxyisoquinoline <b>571a</b> (Table 5.4, entry 1) .....	444
Figure A5.6.2	Infrared spectrum (thin film/NaCl) of 3-hydroxyisoquinoline <b>571a</b> (Table 5.4, entry 1) .....	445
Figure A5.6.3	$^{13}\text{C}$ NMR (125 MHz, $\text{CDCl}_3$ ) of 3-hydroxyisoquinoline <b>571a</b> (Table 5.4, entry 1) .....	445
Figure A5.7.1	$^1\text{H}$ NMR (500 MHz, $\text{CDCl}_3$ ) of 3-hydroxyisoquinoline <b>571b</b> (Table 5.4, entry 2) .....	446
Figure A5.7.2	Infrared spectrum (thin film/NaCl) of 3-hydroxyisoquinoline <b>571b</b> (Table 5.4, entry 2) .....	447
Figure A5.7.3	$^{13}\text{C}$ NMR (125 MHz, $\text{CDCl}_3$ ) of 3-hydroxyisoquinoline <b>571b</b> (Table 5.4, entry 2) .....	447

Figure A5.8.1	$^1\text{H}$ NMR (500 MHz, $\text{CDCl}_3$ ) of 3-hydroxyisoquinoline <b>571c</b> (Table 5.4, entry 3) .....	448
Figure A5.8.2	Infrared spectrum (thin film/NaCl) of 3-hydroxyisoquinoline <b>571c</b> (Table 5.4, entry 3) .....	449
Figure A5.8.3	$^{13}\text{C}$ NMR (125 MHz, $\text{CDCl}_3$ ) of 3-hydroxyisoquinoline <b>571c</b> (Table 5.4, entry 3) .....	449
Figure A5.9.1	$^1\text{H}$ NMR (500 MHz, $\text{CDCl}_3$ ) of 3-hydroxyisoquinoline <b>571d</b> (Table 5.4, entry 4) .....	450
Figure A5.9.2	Infrared spectrum (thin film/NaCl) of 3-hydroxyisoquinoline <b>571d</b> (Table 5.4, entry 4) .....	451
Figure A5.9.3	$^{13}\text{C}$ NMR (125 MHz, $\text{CDCl}_3$ ) of 3-hydroxyisoquinoline <b>571d</b> (Table 5.4, entry 4) .....	451
Figure A5.10.1	$^1\text{H}$ NMR (500 MHz, $\text{CDCl}_3$ ) of 3-hydroxyisoquinoline <b>571e</b> (Table 5.4, entry 5) .....	452
Figure A5.10.2	Infrared spectrum (thin film/NaCl) of 3-hydroxyisoquinoline <b>571e</b> (Table 5.4, entry 5) .....	453
Figure A5.10.3	$^{13}\text{C}$ NMR (125 MHz, $\text{CDCl}_3$ ) of 3-hydroxyisoquinoline <b>571e</b> (Table 5.4, entry 5) .....	453
Figure A5.11.1	$^1\text{H}$ NMR (500 MHz, $\text{CDCl}_3$ ) of 3-hydroxy-5,6,7,8-tetrahydroisoquinoline <b>571f</b> (Table 5.4, entry 6) .....	454
Figure A5.11.2	Infrared spectrum (thin film/NaCl) of 3-hydroxy-5,6,7,8-tetrahydroisoquinoline <b>571f</b> (Table 5.4, entry 6) .....	455
Figure A5.11.3	$^{13}\text{C}$ NMR (125 MHz, $\text{CDCl}_3$ ) of 3-hydroxy-5,6,7,8-tetrahydroisoquinoline <b>571f</b> (Table 5.4, entry 6) .....	455
Figure A5.12.1	$^1\text{H}$ NMR (500 MHz, $\text{CDCl}_3$ ) of 3-hydroxyisoquinoline <b>576a</b> (Table 5.5, entry 1) .....	456
Figure A5.12.2	Infrared spectrum (thin film/NaCl) of 3-hydroxyisoquinoline <b>576a</b> (Table 5.5, entry 1) .....	457
Figure A5.12.3	$^{13}\text{C}$ NMR (125 MHz, $\text{CDCl}_3$ ) of 3-hydroxyisoquinoline <b>576a</b> (Table 5.5, entry 1) .....	457
Figure A5.13.1	$^1\text{H}$ NMR (500 MHz, $\text{CDCl}_3$ ) of 3-hydroxyisoquinoline <b>576b</b> (Table 5.5, entry 2) .....	458
Figure A5.13.2	Infrared spectrum (thin film/NaCl) of 3-hydroxyisoquinoline <b>576b</b> (Table 5.5, entry 2) .....	459
Figure A5.13.3	$^{13}\text{C}$ NMR (125 MHz, $\text{CDCl}_3$ ) of 3-hydroxyisoquinoline <b>576b</b> (Table 5.5, entry 2) .....	459
Figure A5.14.1	$^1\text{H}$ NMR (500 MHz, $\text{CDCl}_3$ ) of 3-hydroxyisoquinoline <b>576c</b> (Table 5.5, entry 3) .....	460
Figure A5.14.2	Infrared spectrum (thin film/NaCl) of 3-hydroxyisoquinoline <b>576c</b> (Table 5.5, entry 3) .....	461
Figure A5.14.3	$^{13}\text{C}$ NMR (125 MHz, $\text{CDCl}_3$ ) of 3-hydroxyisoquinoline <b>576c</b> (Table 5.5, entry 3) .....	461

Figure A5.15.1 $^1\text{H}$ NMR (500 MHz, $\text{CDCl}_3$ ) of 3-hydroxyisoquinoline <b>576d</b> (Table 5.5, entry 4) .....	462
Figure A5.15.2 Infrared spectrum (thin film/NaCl) of 3-hydroxyisoquinoline <b>576d</b> (Table 5.5, entry 4) .....	463
Figure A5.15.3 $^{13}\text{C}$ NMR (125 MHz, $\text{CDCl}_3$ ) of 3-hydroxyisoquinoline <b>576d</b> (Table 5.5, entry 4) .....	463
Figure A5.16.1 $^1\text{H}$ NMR (500 MHz, $\text{CDCl}_3$ ) of 3-hydroxyisoquinoline <b>576e</b> (Table 5.5, entry 5) .....	464
Figure A5.16.2 Infrared spectrum (thin film/NaCl) of 3-hydroxyisoquinoline <b>576e</b> (Table 5.5, entry 5) .....	465
Figure A5.16.3 $^{13}\text{C}$ NMR (125 MHz, $\text{CDCl}_3$ ) of 3-hydroxyisoquinoline <b>576e</b> (Table 5.5, entry 5) .....	465
Figure A5.17.1 $^1\text{H}$ NMR (500 MHz, $\text{CDCl}_3$ ) of 3-hydroxyisoquinoline <b>576f</b> (Table 5.5, entry 6) .....	466
Figure A5.17.2 Infrared spectrum (thin film/NaCl) of 3-hydroxyisoquinoline <b>576f</b> (Table 5.5, entry 6) .....	467
Figure A5.17.3 $^{13}\text{C}$ NMR (125 MHz, $\text{CDCl}_3$ ) of 3-hydroxyisoquinoline <b>576f</b> (Table 5.5, entry 6) .....	467
Figure A5.18.1 $^1\text{H}$ NMR (500 MHz, $\text{CDCl}_3$ ) of 3-hydroxyisoquinoline <b>576g</b> (Table 5.5, entry 7) .....	468
Figure A5.18.2 Infrared spectrum (thin film/NaCl) of 3-hydroxyisoquinoline <b>576g</b> (Table 5.5, entry 7) .....	469
Figure A5.18.3 $^{13}\text{C}$ NMR (125 MHz, $\text{CDCl}_3$ ) of 3-hydroxyisoquinoline <b>576g</b> (Table 5.5, entry 7) .....	469
Figure A5.19.1 $^1\text{H}$ NMR (500 MHz, $\text{CDCl}_3$ ) of 3-hydroxyisoquinoline <b>576h</b> (Table 5.5, entry 8) .....	470
Figure A5.19.2 Infrared spectrum (thin film/NaCl) of 3-hydroxyisoquinoline <b>576h</b> (Table 5.5, entry 8) .....	471
Figure A5.19.3 $^{13}\text{C}$ NMR (125 MHz, $\text{CDCl}_3$ ) of 3-hydroxyisoquinoline <b>576h</b> (Table 5.5, entry 8) .....	471
Figure A5.20.1 $^1\text{H}$ NMR (500 MHz, $\text{CDCl}_3$ ) of 3-hydroxyisoquinoline <b>576i</b> (Table 5.5, entry 9) .....	472
Figure A5.20.2 Infrared spectrum (thin film/NaCl) of 3-hydroxyisoquinoline <b>576i</b> (Table 5.5, entry 9) .....	473
Figure A5.20.3 $^{13}\text{C}$ NMR (125 MHz, $\text{CDCl}_3$ ) of 3-hydroxyisoquinoline <b>576i</b> (Table 5.5, entry 9) .....	473
Figure A5.21.1 $^1\text{H}$ NMR (500 MHz, $\text{CDCl}_3$ ) of 3-hydroxyisoquinoline <b>576j</b> (Table 5.5, entry 10) .....	474
Figure A5.21.2 Infrared spectrum (thin film/NaCl) of 3-hydroxyisoquinoline <b>576j</b> (Table 5.5, entry 10) .....	475
Figure A5.21.3 $^{13}\text{C}$ NMR (125 MHz, $\text{CDCl}_3$ ) of 3-hydroxyisoquinoline <b>576j</b> (Table 5.5, entry 10) .....	475

Figure A5.22.1 $^1\text{H}$ NMR (500 MHz, $\text{CDCl}_3$ ) of 3-hydroxyisoquinoline <b>576k</b> (Table 5.5, entry 11) .....	476
Figure A5.22.2 Infrared spectrum (thin film/NaCl) of 3-hydroxyisoquinoline <b>576k</b> (Table 5.5, entry 11) .....	477
Figure A5.22.3 $^{13}\text{C}$ NMR (125 MHz, $\text{CDCl}_3$ ) of 3-hydroxyisoquinoline <b>576k</b> (Table 5.5, entry 11) .....	477
Figure A5.23.1 $^1\text{H}$ NMR (500 MHz, $\text{CDCl}_3$ ) of 3-hydroxyisoquinoline <b>576l</b> (Table 5.5, entry 12) .....	478
Figure A5.23.2 Infrared spectrum (thin film/NaCl) of 3-hydroxyisoquinoline <b>576l</b> (Table 5.5, entry 12) .....	479
Figure A5.23.3 $^{13}\text{C}$ NMR (125 MHz, $\text{CDCl}_3$ ) of 3-hydroxyisoquinoline <b>576l</b> (Table 5.5, entry 12) .....	479
Figure A5.24.1 $^1\text{H}$ NMR (500 MHz, $\text{CDCl}_3$ ) of <i>bis</i> -(3-hydroxyisoquinoline) <b>576m</b> (Table 5.5, entry 13) .....	480
Figure A5.24.2 Infrared spectrum (thin film/NaCl) of <i>bis</i> -(3-hydroxyisoquinoline) <b>576m</b> (Table 5.5, entry 13) .....	481
Figure A5.24.3 $^{13}\text{C}$ NMR (125 MHz, $\text{CDCl}_3$ ) of <i>bis</i> -(3-hydroxyisoquinoline) <b>576m</b> (Table 5.5, entry 13) .....	481
Figure A5.25.1 $^1\text{H}$ NMR (500 MHz, $\text{CDCl}_3$ ) of isoquinoline triflate <b>A5-1</b> .....	482
Figure A5.25.2 Infrared spectrum (thin film/NaCl) of isoquinoline triflate <b>A5-1</b> .....	483
Figure A5.25.3 $^{13}\text{C}$ NMR (125 MHz, $\text{CDCl}_3$ ) of isoquinoline triflate <b>A5-1</b> .....	483
Figure A5.26.1 $^1\text{H}$ NMR (500 MHz, $\text{CDCl}_3$ ) of 1,3-diarylisoquinoline <b>578</b> .....	484
Figure A5.26.2 Infrared spectrum (thin film/NaCl) of 1,3-diarylisoquinoline <b>578</b> .....	485
Figure A5.26.3 $^{13}\text{C}$ NMR (125 MHz, $\text{CDCl}_3$ ) of 1,3-diarylisoquinoline <b>578</b> .....	485
Figure A5.27.1 $^1\text{H}$ NMR (500 MHz, $\text{CDCl}_3$ ) of isoquinoline triflate <b>579</b> .....	486
Figure A5.27.2 Infrared spectrum (thin film/NaCl) of isoquinoline triflate <b>579</b> .....	487
Figure A5.27.3 $^{13}\text{C}$ NMR (125 MHz, $\text{CDCl}_3$ ) of isoquinoline triflate <b>579</b> .....	487
Figure A5.28.1 $^1\text{H}$ NMR (500 MHz, $\text{CDCl}_3$ ) of 2-hydroxy-1,4-naphthoquinone <b>588a</b> (Table 5.6, entry 1) .....	488
Figure A5.28.2 Infrared spectrum (thin film/NaCl) of 2-hydroxy- 1,4-naphthoquinone <b>588a</b> (Table 5.6, entry 1) .....	489
Figure A5.28.3 $^{13}\text{C}$ NMR (125 MHz, $\text{CDCl}_3$ ) of 2-hydroxy-1,4-naphthoquinone <b>588a</b> (Table 5.6, entry 1) .....	489
Figure A5.29.1 $^1\text{H}$ NMR (500 MHz, $\text{CDCl}_3$ ) of 2-hydroxy-1,4-naphthoquinone <b>588b</b> (Table 5.6, entry 2) .....	490
Figure A5.29.2 Infrared spectrum (thin film/NaCl) of 2-hydroxy- 1,4-naphthoquinone <b>588b</b> (Table 5.6, entry 2) .....	491
Figure A5.29.3 $^{13}\text{C}$ NMR (125 MHz, $\text{CDCl}_3$ ) of 2-hydroxy-1,4-naphthoquinone <b>588b</b> (Table 5.6, entry 2) .....	491
Figure A5.30.1 $^1\text{H}$ NMR (500 MHz, $\text{CDCl}_3$ ) of 2-hydroxy-1,4-naphthoquinone <b>588c</b> (Table 5.6, entry 3) .....	492

Figure A5.30.2	Infrared spectrum (thin film/NaCl) of 2-hydroxy-1,4-naphthoquinone <b>588c</b> (Table 5.6, entry 3) .....	493
Figure A5.30.3	$^{13}\text{C}$ NMR (125 MHz, $\text{CDCl}_3$ ) of 2-hydroxy-1,4-naphthoquinone <b>588c</b> (Table 5.6, entry 3) .....	493
Figure A5.31.1	$^1\text{H}$ NMR (500 MHz, $\text{CDCl}_3$ ) of 2-hydroxy-1,4-naphthoquinone <b>588d</b> (Table 5.6, entry 4) .....	494
Figure A5.31.2	Infrared spectrum (thin film/NaCl) of 2-hydroxy-1,4-naphthoquinone <b>588d</b> (Table 5.6, entry 4) .....	495
Figure A5.31.3	$^{13}\text{C}$ NMR (125 MHz, $\text{CDCl}_3$ ) of 2-hydroxy-1,4-naphthoquinone <b>588d</b> (Table 5.6, entry 4) .....	495
Figure A5.32.1	$^1\text{H}$ NMR (500 MHz, $\text{CDCl}_3$ ) of 2-hydroxy-1,4-naphthoquinone <b>588e</b> (Table 5.6, entry 5) .....	496
Figure A5.32.2	Infrared spectrum (thin film/NaCl) of 2-hydroxy-1,4-naphthoquinone <b>588e</b> (Table 5.6, entry 5) .....	497
Figure A5.32.3	$^{13}\text{C}$ NMR (125 MHz, $\text{CDCl}_3$ ) of 2-hydroxy-1,4-naphthoquinone <b>588e</b> (Table 5.6, entry 5) .....	497
Figure A5.33.1	$^1\text{H}$ NMR (500 MHz, $\text{CDCl}_3$ ) of 2-hydroxy-1,4-naphthoquinone <b>588f</b> (Table 5.6, entry 6) .....	498
Figure A5.33.2	Infrared spectrum (thin film/NaCl) of 2-hydroxy-1,4-naphthoquinone <b>588f</b> (Table 5.6, entry 6) .....	499
Figure A5.33.3	$^{13}\text{C}$ NMR (125 MHz, $\text{CDCl}_3$ ) of 2-hydroxy-1,4-naphthoquinone <b>588f</b> (Table 5.6, entry 6) .....	499
Figure A5.34.1	$^1\text{H}$ NMR (500 MHz, $\text{CDCl}_3$ ) of 2-hydroxy-1,4-naphthoquinone <b>588g</b> (Table 5.6, entry 7) .....	500
Figure A5.34.2	Infrared spectrum (thin film/NaCl) of 2-hydroxy-1,4-naphthoquinone <b>588g</b> (Table 5.6, entry 7) .....	501
Figure A5.34.3	$^{13}\text{C}$ NMR (125 MHz, $\text{CDCl}_3$ ) of 2-hydroxy-1,4-naphthoquinone <b>588g</b> (Table 5.6, entry 7) .....	501
Figure A5.35.1	$^1\text{H}$ NMR (500 MHz, $\text{CDCl}_3$ ) of 2-hydroxy-1,4-naphthoquinone <b>588h</b> (Table 5.6, entry 8) .....	502
Figure A5.35.2	Infrared spectrum (thin film/NaCl) of 2-hydroxy-1,4-naphthoquinone <b>588h</b> (Table 5.6, entry 8) .....	503
Figure A5.35.3	$^{13}\text{C}$ NMR (125 MHz, $\text{CDCl}_3$ ) of 2-hydroxy-1,4-naphthoquinone <b>588h</b> (Table 5.6, entry 8) .....	503
Figure A5.36.1	$^1\text{H}$ NMR (500 MHz, $\text{CDCl}_3$ ) of 2-hydroxy-1,4-naphthoquinone <b>588i</b> (Table 5.6, entry 9) .....	504
Figure A5.36.2	Infrared spectrum (thin film/NaCl) of 2-hydroxy-1,4-naphthoquinone <b>588i</b> (Table 5.6, entry 9) .....	505
Figure A5.36.3	$^{13}\text{C}$ NMR (125 MHz, $\text{CDCl}_3$ ) of 2-hydroxy-1,4-naphthoquinone <b>588i</b> (Table 5.6, entry 9) .....	505
Figure A5.37.1	$^1\text{H}$ NMR (500 MHz, $\text{CDCl}_3$ ) of 2-hydroxy-1,4-naphthoquinone <b>588j</b> (Table 5.6, entry 10) .....	506

Figure A5.37.2	Infrared spectrum (thin film/NaCl) of 2-hydroxy-1,4-naphthoquinone <b>588j</b> (Table 5.6, entry 10).....	507
Figure A5.37.3	<sup>13</sup> C NMR (125 MHz, CDCl <sub>3</sub> ) of 2-hydroxy-1,4-naphthoquinone <b>588j</b> (Table 5.6, entry 10).....	507
Figure A5.38.1	<sup>1</sup> H NMR (500 MHz, CDCl <sub>3</sub> ) of 2-hydroxy-1,4-naphthoquinone <b>588k</b> (Table 5.6, entry 11).....	508
Figure A5.38.2	Infrared spectrum (thin film/NaCl) of 2-hydroxy-1,4-naphthoquinone <b>588k</b> (Table 5.6, entry 11).....	509
Figure A5.38.3	<sup>13</sup> C NMR (125 MHz, CDCl <sub>3</sub> ) of 2-hydroxy-1,4-naphthoquinone <b>588k</b> (Table 5.6, entry 11).....	509

## APPENDIX 6

Figure A6.1.1	<sup>1</sup> H NMR (500 MHz, CDCl <sub>3</sub> ) of phenoxy iminoisobenzofuran <b>680</b> .....	586
Figure A6.1.2	Infrared spectrum (thin film/NaCl) of phenoxy iminoisobenzofuran <b>680</b> .....	587
Figure A6.1.3	<sup>13</sup> C NMR (125 MHz, CDCl <sub>3</sub> ) of phenoxy iminoisobenzofuran <b>680</b> .....	587
Figure A6.2.1	<sup>1</sup> H NMR (500 MHz, CDCl <sub>3</sub> ) of phenoxy iminoisobenzofuran <b>683a</b> .....	588
Figure A6.2.2	Infrared spectrum (thin film/NaCl) of phenoxy iminoisobenzofuran <b>683a</b> .....	589
Figure A6.2.3	<sup>13</sup> C NMR (125 MHz, CDCl <sub>3</sub> ) of phenoxy iminoisobenzofuran <b>683a</b> .....	589
Figure A6.3.1	<sup>1</sup> H NMR (500 MHz, CDCl <sub>3</sub> ) of phenoxy iminoisobenzofuran <b>683b</b> .....	590
Figure A6.3.2	Infrared spectrum (thin film/NaCl) of phenoxy iminoisobenzofuran <b>683b</b> .....	591
Figure A6.3.3	<sup>13</sup> C NMR (125 MHz, CDCl <sub>3</sub> ) of phenoxy iminoisobenzofuran <b>683b</b> .....	591
Figure A6.4.1	<sup>1</sup> H NMR (500 MHz, CDCl <sub>3</sub> ) of phenoxy iminoisobenzofuran <b>683c</b> .....	592
Figure A6.4.2	Infrared spectrum (thin film/NaCl) of phenoxy iminoisobenzofuran <b>683c</b> .....	593
Figure A6.4.3	<sup>13</sup> C NMR (125 MHz, CDCl <sub>3</sub> ) of phenoxy iminoisobenzofuran <b>683c</b> .....	593
Figure A6.5.1	<sup>1</sup> H NMR (500 MHz, CDCl <sub>3</sub> ) of phenoxy iminoisobenzofuran <b>683d</b> .....	594
Figure A6.5.2	Infrared spectrum (thin film/NaCl) of phenoxy iminoisobenzofuran <b>683d</b> .....	595
Figure A6.5.3	<sup>13</sup> C NMR (125 MHz, CDCl <sub>3</sub> ) of phenoxy iminoisobenzofuran <b>683d</b> .....	595
Figure A6.6.1	<sup>1</sup> H NMR (500 MHz, CDCl <sub>3</sub> ) of phenoxy iminoisobenzofuran <b>683e</b> .....	596
Figure A6.6.2	Infrared spectrum (thin film/NaCl) of phenoxy iminoisobenzofuran <b>683e</b> .....	597
Figure A6.6.3	<sup>13</sup> C NMR (125 MHz, CDCl <sub>3</sub> ) of phenoxy iminoisobenzofuran <b>683e</b> .....	597
Figure A6.7.1	<sup>1</sup> H NMR (500 MHz, CDCl <sub>3</sub> ) of phenoxy iminoisobenzofuran <b>683f</b> .....	598
Figure A6.7.2	Infrared spectrum (thin film/NaCl) of phenoxy iminoisobenzofuran <b>683f</b> .....	599
Figure A6.7.3	<sup>13</sup> C NMR (125 MHz, CDCl <sub>3</sub> ) of phenoxy iminoisobenzofuran <b>683f</b> .....	599
Figure A6.8.1	<sup>1</sup> H NMR (500 MHz, CDCl <sub>3</sub> ) of phenoxy iminoisobenzofuran <b>683g</b> .....	600
Figure A6.8.2	Infrared spectrum (thin film/NaCl) of phenoxy iminoisobenzofuran <b>683g</b> .....	601

Figure A6.8.3	$^{13}\text{C}$ NMR (125 MHz, $\text{CDCl}_3$ ) of phenoxy iminoisobenzofuran <b>683g</b> .....	601
Figure A6.9.1	$^1\text{H}$ NMR (500 MHz, $\text{CDCl}_3$ ) of phenoxy iminoisobenzofuran <b>683h</b> .....	602
Figure A6.9.2	Infrared spectrum (thin film/NaCl) of phenoxy iminoisobenzofuran <b>683h</b> .....	603
Figure A6.9.3	$^{13}\text{C}$ NMR (125 MHz, $\text{CDCl}_3$ ) of phenoxy iminoisobenzofuran <b>683h</b> .....	603
Figure A6.10.1	$^1\text{H}$ NMR (500 MHz, $\text{CDCl}_3$ ) of phenoxy iminoisobenzofuran <b>683i</b> .....	604
Figure A6.10.2	Infrared spectrum (thin film/NaCl) of phenoxy iminoisobenzofuran <b>683i</b> .....	605
Figure A6.10.3	$^{13}\text{C}$ NMR (125 MHz, $\text{CDCl}_3$ ) of phenoxy iminoisobenzofuran <b>683i</b> .....	605
Figure A6.11.1	$^1\text{H}$ NMR (500 MHz, $\text{CDCl}_3$ ) of phenoxy iminoisobenzofuran <b>683j</b> .....	606
Figure A6.11.2	Infrared spectrum (thin film/NaCl) of phenoxy iminoisobenzofuran <b>683j</b> .....	607
Figure A6.11.3	$^{13}\text{C}$ NMR (125 MHz, $\text{CDCl}_3$ ) of phenoxy iminoisobenzofuran <b>683j</b> .....	607
Figure A6.12.1	$^1\text{H}$ NMR (500 MHz, $\text{CDCl}_3$ ) of phenoxy iminoisobenzofuran <b>683k</b> .....	608
Figure A6.12.2	Infrared spectrum (thin film/NaCl) of phenoxy iminoisobenzofuran <b>683k</b> .....	609
Figure A6.12.3	$^{13}\text{C}$ NMR (125 MHz, $\text{CDCl}_3$ ) of phenoxy iminoisobenzofuran <b>683k</b> .....	609
Figure A6.13.1	$^1\text{H}$ NMR (500 MHz, $\text{CDCl}_3$ ) of phenoxy iminoisobenzofuran <b>683l</b> .....	610
Figure A6.13.2	Infrared spectrum (thin film/NaCl) of phenoxy iminoisobenzofuran <b>683l</b> .....	611
Figure A6.13.3	$^{13}\text{C}$ NMR (125 MHz, $\text{CDCl}_3$ ) of phenoxy iminoisobenzofuran <b>683l</b> .....	611
Figure A6.14.1	$^1\text{H}$ NMR (500 MHz, $\text{CDCl}_3$ ) of phenoxy iminoisobenzofuran <b>683m</b> .....	612
Figure A6.14.2	Infrared spectrum (thin film/NaCl) of phenoxy iminoisobenzofuran <b>683m</b> .....	613
Figure A6.14.3	$^{13}\text{C}$ NMR (125 MHz, $\text{CDCl}_3$ ) of phenoxy iminoisobenzofuran <b>683m</b> .....	613
Figure A6.15.1	$^1\text{H}$ NMR (500 MHz, $\text{CDCl}_3$ ) of phenoxy iminoisobenzofuran <b>683n</b> .....	614
Figure A6.15.2	Infrared spectrum (thin film/NaCl) of phenoxy iminoisobenzofuran <b>683n</b> .....	615
Figure A6.15.3	$^{13}\text{C}$ NMR (125 MHz, $\text{CDCl}_3$ ) of phenoxy iminoisobenzofuran <b>683n</b> .....	615
Figure A6.16.1	$^1\text{H}$ NMR (500 MHz, $\text{CDCl}_3$ ) of phenoxy iminoisobenzofuran <b>683o</b> .....	616
Figure A6.16.2	Infrared spectrum (thin film/NaCl) of phenoxy iminoisobenzofuran <b>683o</b> .....	617
Figure A6.16.3	$^{13}\text{C}$ NMR (125 MHz, $\text{CDCl}_3$ ) of phenoxy iminoisobenzofuran <b>683o</b> .....	617
Figure A6.17.1	$^1\text{H}$ NMR (500 MHz, $\text{CDCl}_3$ ) of phenoxy iminoisobenzofuran <b>683p</b> .....	618
Figure A6.17.2	Infrared spectrum (thin film/NaCl) of phenoxy iminoisobenzofuran <b>683p</b> .....	619
Figure A6.17.3	$^{13}\text{C}$ NMR (125 MHz, $\text{CDCl}_3$ ) of phenoxy iminoisobenzofuran <b>683p</b> .....	619
Figure A6.18.1	$^1\text{H}$ NMR (500 MHz, $\text{CDCl}_3$ ) of phenoxy iminoisobenzofuran <b>683q</b> .....	620
Figure A6.18.2	Infrared spectrum (thin film/NaCl) of phenoxy iminoisobenzofuran <b>683q</b> .....	621
Figure A6.18.3	$^{13}\text{C}$ NMR (125 MHz, $\text{CDCl}_3$ ) of phenoxy iminoisobenzofuran <b>683q</b> .....	621
Figure A6.19.1	$^1\text{H}$ NMR (500 MHz, $\text{CDCl}_3$ ) of phenoxy iminoisobenzofuran <b>683r</b> .....	622
Figure A6.19.2	Infrared spectrum (thin film/NaCl) of phenoxy iminoisobenzofuran <b>683r</b> .....	623
Figure A6.19.3	$^{13}\text{C}$ NMR (125 MHz, $\text{CDCl}_3$ ) of phenoxy iminoisobenzofuran <b>683r</b> .....	623
Figure A6.20.1	$^1\text{H}$ NMR (500 MHz, $\text{CDCl}_3$ ) of phenoxy iminoisobenzofuran <b>683s</b> .....	624

Figure A6.20.2	Infrared spectrum (thin film/NaCl) of phenoxy iminoisobenzofuran <b>683s</b> .....	625
Figure A6.20.3	$^{13}\text{C}$ NMR (125 MHz, $\text{CDCl}_3$ ) of phenoxy iminoisobenzofuran <b>683s</b> .....	625
Figure A6.21.1	$^1\text{H}$ NMR (500 MHz, $\text{CDCl}_3$ ) of phenoxy iminoisobenzofuran <b>683t</b> .....	626
Figure A6.21.2	Infrared spectrum (thin film/NaCl) of phenoxy iminoisobenzofuran <b>683t</b> .....	627
Figure A6.21.3	$^{13}\text{C}$ NMR (125 MHz, $\text{CDCl}_3$ ) of phenoxy iminoisobenzofuran <b>683t</b> .....	627
Figure A6.22.1	$^1\text{H}$ NMR (500 MHz, $\text{CDCl}_3$ ) of phenoxy iminoisobenzofuran <b>683u</b> .....	628
Figure A6.22.2	Infrared spectrum (thin film/NaCl) of phenoxy iminoisobenzofuran <b>683u</b> .....	629
Figure A6.22.3	$^{13}\text{C}$ NMR (125 MHz, $\text{CDCl}_3$ ) of phenoxy iminoisobenzofuran <b>683u</b> .....	629
Figure A6.23.1	$^1\text{H}$ NMR (500 MHz, $\text{CDCl}_3$ ) of <i>ortho</i> -ketobenzamide <b>669a</b> .....	630
Figure A6.23.2	Infrared spectrum (thin film/NaCl) of <i>ortho</i> -ketobenzamide <b>669a</b> .....	631
Figure A6.23.3	$^{13}\text{C}$ NMR (125 MHz, $\text{CDCl}_3$ ) of <i>ortho</i> -ketobenzamide <b>669a</b> .....	631
Figure A6.24.1	$^1\text{H}$ NMR (500 MHz, $\text{CDCl}_3$ ) of <i>ortho</i> -ketobenzamide <b>669b</b> .....	632
Figure A6.24.2	Infrared spectrum (thin film/NaCl) of <i>ortho</i> -ketobenzamide <b>669b</b> .....	633
Figure A6.24.3	$^{13}\text{C}$ NMR (125 MHz, $\text{CDCl}_3$ ) of <i>ortho</i> -ketobenzamide <b>669b</b> .....	633
Figure A6.25.1	$^1\text{H}$ NMR (500 MHz, $\text{CDCl}_3$ ) of <i>ortho</i> -ketobenzamide <b>669c</b> .....	634
Figure A6.25.2	Infrared spectrum (thin film/NaCl) of <i>ortho</i> -ketobenzamide <b>669c</b> .....	635
Figure A6.25.3	$^{13}\text{C}$ NMR (125 MHz, $\text{CDCl}_3$ ) of <i>ortho</i> -ketobenzamide <b>669c</b> .....	635
Figure A6.26.1	$^1\text{H}$ NMR (500 MHz, $\text{CDCl}_3$ ) of <i>ortho</i> -ketobenzamide <b>669d</b> .....	636
Figure A6.26.2	Infrared spectrum (thin film/NaCl) of <i>ortho</i> -ketobenzamide <b>669d</b> .....	637
Figure A6.26.3	$^{13}\text{C}$ NMR (125 MHz, $\text{CDCl}_3$ ) of <i>ortho</i> -ketobenzamide <b>669d</b> .....	637
Figure A6.27.1	$^1\text{H}$ NMR (500 MHz, $\text{CDCl}_3$ ) of <i>ortho</i> -ketobenzamide <b>669e</b> .....	638
Figure A6.27.2	Infrared spectrum (thin film/NaCl) of <i>ortho</i> -ketobenzamide <b>669e</b> .....	639
Figure A6.27.3	$^{13}\text{C}$ NMR (125 MHz, $\text{CDCl}_3$ ) of <i>ortho</i> -ketobenzamide <b>669e</b> .....	639
Figure A6.28.1	$^1\text{H}$ NMR (500 MHz, $\text{CDCl}_3$ ) of <i>ortho</i> -ketobenzamide <b>669f</b> .....	640
Figure A6.28.2	Infrared spectrum (thin film/NaCl) of <i>ortho</i> -ketobenzamide <b>669f</b> .....	641
Figure A6.28.3	$^{13}\text{C}$ NMR (125 MHz, $\text{CDCl}_3$ ) of <i>ortho</i> -ketobenzamide <b>669f</b> .....	641
Figure A6.29.1	$^1\text{H}$ NMR (500 MHz, $\text{CDCl}_3$ ) of <i>ortho</i> -ketobenzamide <b>669g</b> .....	642
Figure A6.29.2	Infrared spectrum (thin film/NaCl) of <i>ortho</i> -ketobenzamide <b>669g</b> .....	643
Figure A6.29.3	$^{13}\text{C}$ NMR (125 MHz, $\text{CDCl}_3$ ) of <i>ortho</i> -ketobenzamide <b>669g</b> .....	643
Figure A6.30.1	$^1\text{H}$ NMR (500 MHz, $\text{CDCl}_3$ ) of dibenzoketocaprolactam <b>687a</b> .....	644
Figure A6.30.2	Infrared spectrum (thin film/NaCl) of dibenzoketocaprolactam <b>687a</b> .....	645
Figure A6.30.3	$^{13}\text{C}$ NMR (125 MHz, $\text{CDCl}_3$ ) of dibenzoketocaprolactam <b>687a</b> .....	645
Figure A6.31.1	$^1\text{H}$ NMR (500 MHz, $\text{CDCl}_3$ ) of dibenzoketocaprolactam <b>687b</b> .....	646
Figure A6.31.2	Infrared spectrum (thin film/NaCl) of dibenzoketocaprolactam <b>687b</b> .....	647
Figure A6.31.3	$^{13}\text{C}$ NMR (125 MHz, $\text{CDCl}_3$ ) of dibenzoketocaprolactam <b>687b</b> .....	647

Figure A6.32.1	$^1\text{H}$ NMR (500 MHz, $\text{CDCl}_3$ ) of dibenzoketocaprolactam <b>687c</b> .....	648
Figure A6.32.2	Infrared spectrum (thin film/NaCl) of dibenzoketocaprolactam <b>687c</b> .....	649
Figure A6.32.3	$^{13}\text{C}$ NMR (125 MHz, $\text{CDCl}_3$ ) of dibenzoketocaprolactam <b>687c</b> .....	649
Figure A6.33.1	$^1\text{H}$ NMR (500 MHz, $\text{CDCl}_3$ ) of iminoindenone <b>691</b> .....	650
Figure A6.33.2	Infrared spectrum (thin film/NaCl) of iminoindenone <b>691</b> .....	651
Figure A6.33.3	$^{13}\text{C}$ NMR (125 MHz, $\text{CDCl}_3$ ) of iminoindenone <b>691</b> .....	651
Figure A6.34.1	$^1\text{H}$ NMR (500 MHz, $\text{CDCl}_3$ ) of iminoindenone <b>675a</b> .....	652
Figure A6.34.2	Infrared spectrum (thin film/NaCl) of iminoindenone <b>698a</b> .....	653
Figure A6.34.3	$^{13}\text{C}$ NMR (125 MHz, $\text{CDCl}_3$ ) of iminoindenone <b>698a</b> .....	653
Figure A6.35.1	$^1\text{H}$ NMR (500 MHz, $\text{CDCl}_3$ ) of iminoindenone <b>698b</b> .....	654
Figure A6.35.2	Infrared spectrum (thin film/NaCl) of iminoindenone <b>698b</b> .....	655
Figure A6.35.3	$^{13}\text{C}$ NMR (125 MHz, $\text{CDCl}_3$ ) of iminoindenone <b>698b</b> .....	655
Figure A6.36.1	$^1\text{H}$ NMR (500 MHz, $\text{CDCl}_3$ ) of iminoindenone <b>698c</b> .....	656
Figure A6.36.2	Infrared spectrum (thin film/NaCl) of iminoindenone <b>698c</b> .....	657
Figure A6.36.3	$^{13}\text{C}$ NMR (125 MHz, $\text{CDCl}_3$ ) of iminoindenone <b>698c</b> .....	657
Figure A6.37.1	$^1\text{H}$ NMR (500 MHz, $\text{CDCl}_3$ ) of iminoindenone <b>698d</b> .....	658
Figure A6.37.2	Infrared spectrum (thin film/NaCl) of iminoindenone <b>698d</b> .....	659
Figure A6.37.3	$^{13}\text{C}$ NMR (125 MHz, $\text{CDCl}_3$ ) of iminoindenone <b>698d</b> .....	659
Figure A6.38.1	$^1\text{H}$ NMR (500 MHz, $\text{CDCl}_3$ ) of iminoindenone <b>698e</b> .....	660
Figure A6.38.2	Infrared spectrum (thin film/NaCl) of iminoindenone <b>698e</b> .....	661
Figure A6.38.3	$^{13}\text{C}$ NMR (125 MHz, $\text{CDCl}_3$ ) of iminoindenone <b>698e</b> .....	661
Figure A6.39.1	$^1\text{H}$ NMR (500 MHz, $\text{CDCl}_3$ ) of iminoindenone <b>698f</b> .....	662
Figure A6.39.2	Infrared spectrum (thin film/NaCl) of iminoindenone <b>698f</b> .....	663
Figure A6.39.3	$^{13}\text{C}$ NMR (125 MHz, $\text{CDCl}_3$ ) of iminoindenone <b>698f</b> .....	663
Figure A6.40.1	$^1\text{H}$ NMR (500 MHz, $\text{CDCl}_3$ ) of iminoindenone <b>698g</b> .....	664
Figure A6.40.2	Infrared spectrum (thin film/NaCl) of iminoindenone <b>698g</b> .....	665
Figure A6.40.3	$^{13}\text{C}$ NMR (125 MHz, $\text{CDCl}_3$ ) of iminoindenone <b>698g</b> .....	665
Figure A6.51.1	$^1\text{H}$ NMR (500 MHz, $\text{CDCl}_3$ ) of spirocycle <b>707</b> .....	666
Figure A6.51.2	Infrared spectrum (thin film/NaCl) of spirocycle <b>707</b> .....	667
Figure A6.51.3	$^{13}\text{C}$ NMR (125 MHz, $\text{CDCl}_3$ ) of spirocycle <b>707</b> .....	667
Figure A6.52.1	$^1\text{H}$ NMR (500 MHz, $\text{CDCl}_3$ ) of spirocycle <b>709</b> .....	668
Figure A6.52.2	Infrared spectrum (thin film/NaCl) of spirocycle <b>709</b> .....	669
Figure A6.52.3	$^{13}\text{C}$ NMR (125 MHz, $\text{CDCl}_3$ ) of spirocycle <b>709</b> .....	669
Figure A6.53.1	$^1\text{H}$ NMR (500 MHz, $\text{CDCl}_3$ ) of spirocycle <b>711</b> .....	670
Figure A6.53.2	Infrared spectrum (thin film/NaCl) of spirocycle <b>711</b> .....	671

Figure A6.53.3  $^{13}\text{C}$  NMR (125 MHz,  $\text{CDCl}_3$ ) of spirocycle **711** ..... 671

## APPENDIX 7

Figure A7.1 ORTEP drawing of phenoxy iminoisobenzofuran **683p** (shown with 50% probability ellipsoids) ..... 672

Figure A7.2 Phenoxy iminoisobenzofuran **683p** ..... 675

## LIST OF SCHEMES

### CHAPTER 1

Scheme 1.1	Stoermer & Kahlert – Unexpected rearrangement via “benzofuryne” .....	3
Scheme 1.2	Bachmann & Clarke – Proposal for a diradical intermediate .....	4
Scheme 1.3	Lüttringhaus & Säaf – Rearrangements of diphenyl ether.....	5
Scheme 1.4	Wittig – Proposal for a zwitterionic intermediate.....	6
Scheme 1.5	Unexpected rearrangements during nucleophilic aromatic substitution .....	7
Scheme 1.6	Benseker – Proposed rearrangement during nucleophilic aromatic Substitution.....	8
Scheme 1.7	Roberts – Nucleophilic aromatic substitution via a “benzyne” intermediate .....	9
Scheme 1.8	Roberts – proposed rearrangement during amination via aziridine <b>43</b> or diamine <b>44</b> .....	12
Scheme 1.9	Results in support of the aryne model .....	13
Scheme 1.10	Microdensitometer tracings showing absorbance by gaseous products of photolysis of phenyldiazonium-2-carboxylate.....	14
Scheme 1.11	Infrared spectrum of benzyne.....	16
Scheme 1.12	Methods for generating benzyne .....	19
Scheme 1.13	Inductive effects upon regioselectivity in nucleophilic aromatic substitution reactions.....	22
Scheme 1.14	a) Competing nucleophilic additions to 3- and 4-substituted arynes b) Substituent effects on regioselectivity c) Reactivity factor vs. $ \sigma' $ in dimethylamine where $\circ$ represents 3-substituted arynes and $\bullet$ represents 4-substituted arynes. ....	24

### CHAPTER 2

Scheme 2.1	Annulation of benzyne via Diels–Alder cycloaddition with furan .....	37
Scheme 2.2	Aryne annulation via [4 + 2] cycloaddition .....	39
Scheme 2.3	Aryne annulation via [3 + 2] cycloaddition .....	41
Scheme 2.4	Aryne annulation via nucleophilic addition and cyclization .....	43
Scheme 2.5	Aryne annulation via [2 + 2] cycloaddition .....	45
Scheme 2.6	Aryne annulation via insertion into activated $\sigma$ -bonds .....	47
Scheme 2.7	Transition metal-catalyzed aryne annulations.....	49

Scheme 2.8	Transition metal-catalyzed [2 + 2 + 2] cycloadditions .....	51
Scheme 2.9	a) Proposed indoline synthesis via aryne annulation	
	b) Bioactive indoline-containing natural products .....	53
Scheme 2.10	Orthogonal mechanisms for indoline formation via aryne annulation .....	57
Scheme 2.11	Unexpected formation of an isoquinoline through an alternative aryne annulation.....	58
Scheme 2.12	Arylation of <i>N</i> -vinyl acetamide .....	64
Scheme 2.13	Total synthesis of papaverine .....	65
Scheme 2.14	a) Synthesis of isoquinolones via aryne annulation	
	b) Bioactive isoquinolone- and 3,4-dihydroisoquinolone-containing natural products.....	68

## CHAPTER 3

Scheme 3.1	Proposed biosynthesis of quinocarcin .....	188
Scheme 3.2	Williams' proposed mechanism for superoxide formation via self-redox disproportionation of quinocarcin.....	197
Scheme 3.3	Fukuyama's synthesis of ( $\pm$ )-quinocarcin .....	199
Scheme 3.4	Garner's synthesis of (–)-quinocarcin .....	201
Scheme 3.5	Terashima's synthesis of (–)-quinocarcin.....	203
Scheme 3.6	Myers' synthesis of tetrahydroisoquinoline <b>313</b> .....	205
Scheme 3.7	Myers' synthesis of aminonitrile <b>318</b> .....	206
Scheme 3.8	Myers' completion of (–)-quinocarcin .....	207
Scheme 3.9	Zhu's synthesis of (–)-quinocarcin.....	209
Scheme 3.10	Danishefsky's synthesis of ( $\pm$ )-quinocarcinol methyl ester.....	211
Scheme 3.11	Hirata's approach toward quinocarcin.....	212
Scheme 3.12	Weinreb's approach toward quinocarcin.....	213
Scheme 3.13	Joule's approach toward quinocarcin .....	214
Scheme 3.14	Williams' synthesis of ( $\pm$ )-quinocarcinamide.....	216
Scheme 3.15	McMills' approach toward quinocarcin .....	217

## CHAPTER 4

Scheme 4.1	a) Pictet–Spengler condensation	
	b) Regioselective aryne annulation	
	c) Aryne annulation approach to an isoquinoline intermediate en route to quinocarcin.....	229
Scheme 4.2	Retrosynthetic analysis of quinocarcin.....	230
Scheme 4.3	a) Synthesis of <i>N</i> -methyl oxidopyrazinium iodide <b>387</b>	
	b) Dipolar cycloaddition .....	231
Scheme 4.4	Reductive opening of <i>N</i> -Boc lactam <b>389</b> en route to lemomomycin .....	232
Scheme 4.5	Proposed coordination conformations leading to lactam <b>382</b> and <i>N</i> -acyl enamine <b>380</b> .....	235
Scheme 4.6	Attempted aryne annulation using <i>N</i> -acyl enamine <b>380</b> .....	236
Scheme 4.7	Proposed mechanisms for the formation of isoquinoline <b>392</b> .....	237
Scheme 4.8	Synthesis of <i>N</i> -benzyl oxidopyrazinium bromide <b>401</b> and dipolar cycloaddition .....	239
Scheme 4.9	Auxiliary-mediated diastereoselective dipolar cycloaddition .....	240
Scheme 4.10	Advancement of diazabicycle <b>405a</b> to <i>N</i> -acyl enamine <b>407</b> .....	241
Scheme 4.11	Synthesis of 3-methoxy-2-(trimethylsilyl)phenyl triflate ( <b>108</b> ) .....	242
Scheme 4.12	Synthesis of isoquinoline <b>411</b> via aryne annulation.....	242
Scheme 4.13	a) One-step homogeneous reduction of isoquinoline <b>411</b>	
	b) Two-step reduction of isoquinoline <b>411</b> to tetrahydroisoquinolines <b>415a</b> and <b>415b</b> .....	246
Scheme 4.14	Models for diastereoselective reduction of isoquinoline <b>411</b> .....	247
Scheme 4.15	Completion of (–)-quinocarcin .....	249
Scheme 4.16	Retrosynthetic analysis of jorumycin.....	250
Scheme 4.17	Proposal for the synthesis of jorumycin via <i>bis</i> -isoquinoline <b>430</b> .....	252
Scheme 4.18	Retrosynthetic analysis of ecteinascidin 743.....	253

## APPENDIX 2

Scheme A2.1	Synthesis of the <i>N</i> -acyl enamine .....	283
Scheme A2.2	Synthesis of 3-methoxy-2-(trimethylsilyl)phenyl triflate .....	283
Scheme A2.3	Aryne annulation and completion of (–)-quinocarcin .....	283

## APPENDIX 4

Scheme A4.1	Cyanocycline A and naphthyridinomycin.....	317
Scheme A4.2	Retrosynthetic analysis of cyanocycline A .....	320
Scheme A4.3	Synthesis of silyl ether <b>438</b> .....	321
Scheme A4.4	Oxidative amination of styrene <b>438</b> .....	322
Scheme A4.5	Synthesis of oxazoline <b>437</b> .....	323
Scheme A4.6	Synthesis of benzylic ketone <b>457</b> via aldehyde <b>454</b> .....	324
Scheme A4.7	Reductive amination of a model benzylic ketone.....	325
Scheme A4.8	Proposed Petasis three-component coupling reaction .....	326
Scheme A4.9	Petasis three-component coupling via iminium boronate <b>466</b> .....	326
Scheme A4.10	a) Evaluating the Petasis reaction with aryl boronic acid <b>462</b> and amine <b>460</b>	
	b) Evaluating the Petasis reaction with amido aldehyde <b>474</b> .....	327
Scheme A4.11	Proposed advancement of benzylic amine <b>436</b> .....	329
Scheme A4.12	Proposed completion of cyanocycline A.....	330

## CHAPTER 5

Scheme 5.1	Discovery of the aryne acyl-alkylation reaction.....	365
Scheme 5.2	Total synthesis of (+)-amurensinine.....	372
Scheme 5.3	Total synthesis of (–)-curvularin.....	375
Scheme 5.4	a) Synthesis of $\beta$ -ketoester <b>547</b> b) Synthesis of <i>ortho</i> -silyl aryl triflate <b>550</b> .....	376
Scheme 5.5	a) Model acyl-alkylation using <i>ortho</i> -silyl aryl triflate <b>71</b> b) Aryne acyl-alkylation and strategy for the completion of integrastatins A and B .....	377
Scheme 5.6	a) Bentley’s synthesis of 3-hydroxyisoquinolines and 2-hydroxy-1,4-naphthoquinones from 2-acylhomoveratric esters b) Selected previous syntheses of functionalized isoquinoline and naphthoquinone motifs via transition metal-catalyzed cross coupling.....	379
Scheme 5.7	Aryne acyl-alkylation followed by condensation with ammonia or intramolecular condensation and aerobic oxidation .....	380
Scheme 5.8	a) Synthesis of 1,3-diarylisoquinoline <b>578</b> b) Synthesis of QUINAP .....	385

Scheme 5.9	Synthesis of 2-hydroxy-1,4-naphthoquinones via one-pot aryne acyl-alkylation, intramolecular condensation, and aerobic oxidation.....	386
------------	---	-----

## CHAPTER 6

Scheme 6.1	Laurent & Gerhardt – Synthesis of $\alpha$ -aminobenzonitrile.....	511
Scheme 6.2	a) Linear synthesis of a product containing four components b) One-step synthesis via four-component reaction c) Multicomponent reaction approach to library synthesis.....	512
Scheme 6.3	Benzyne as a relay species in multicomponent reactions.....	513
Scheme 6.4	Meyers – Synthesis of 2,3-disubstituted benzoic acid derivatives.....	514
Scheme 6.5	Three-component synthesis of phenanthridines ( <b>601</b> ) and xanthenes ( <b>605</b> ) using two aryne equivalents .....	515
Scheme 6.6	Three-component synthesis of nitrogen-containing products using three distinct components .....	517
Scheme 6.7	Transition metal-catalyzed three-component aryne reactions .....	520
Scheme 6.8	Four-component synthesis of anthracenamines ( <b>635</b> ) and isoquinolines ( <b>642</b> ) using multiple aryne equivalents .....	522
Scheme 6.9	a) Three-component synthesis of alcohols <b>648a</b> and <b>648b</b> en route to <i>ent</i> -clavilactone B b) Four-component synthesis of tricycle <b>634</b> en route to dehydroaltenuene B .....	524
Scheme 6.10	Passerini three-component synthesis of $\alpha$ -acyloxyamides .....	525
Scheme 6.11	Proposed benzyne analogue of the Passerini three-component coupling .....	526
Scheme 6.12	Attempted three-component coupling of benzyne, <i>tert</i> -butyl isocyanide, and carboxylate salts .....	527
Scheme 6.13	Revised approach to the synthesis of <i>ortho</i> -ketobenzamides via three-component coupling of arynes, isocyanides, and esters.....	528
Scheme 6.14	a) Attempted three-component coupling of benzyne, <i>tert</i> -butyl isocyanide, and ethyl acetate b) Three-component coupling of benzyne, <i>tert</i> -butyl isocyanide, and phenyl acetate .....	529
Scheme 6.15	a) Potential equilibration between iminoisobenzofuran and isoindolinone isomers b) X-ray crystal structure of phenoxy iminoisobenzofuran <b>683p</b> .....	533
Scheme 6.16	Two-step synthesis of dibenzoketocaprolactams .....	535
Scheme 6.17	a) Proposed three-component coupling of arynes, isocyanides, and a two-carbon relay species	

b) Three-component coupling of benzyne, <i>tert</i> -butyl isocyanide, and methyl propiolate .....	537
Scheme 6.18	
a) Hydrolysis of iminoindenone <b>698a</b>	
b) Indenone-derived natural products .....	539
Scheme 6.19	
Three-component coupling of benzyne, <i>tert</i> -butyl isocyanide, and quinones .....	540

## LIST OF TABLES

### CHAPTER 2

Table 2.1	Optimization of reaction conditions for indoline synthesis via aryne annulation.....	54
Table 2.2	Synthesis of indolines via aryne annulation .....	55
Table 2.3	Optimization of reaction conditions for isoquinoline synthesis via aryne annulation.....	59
Table 2.4	Synthesis of C(1)-substituted isoquinolines via aryne annulation .....	60
Table 2.5	Aryne substrate scope in isoquinoline synthesis .....	61
Table 2.6	<i>N</i> -Acyl enamine substrate scope .....	63
Table 2.7	Ramtahul – Isoquinoline and benzocyclobutene synthesis via aryne annulation.....	66
Table 2.8	Optimization of reaction conditions for isoquinolone synthesis via aryne annulation.....	70
Table 2.9	Synthesis of isoquinolones via aryne annulation .....	71

### CHAPTER 3

Table 3.1	Antibiotic activity of quinocarcin and quinocarcinol .....	189
Table 3.2	a) Time dependent $IC_{50}$ values of KW2152 against various cultured tumor cell lines	
	b) Response of human tumor xenografts to KW2152 and established anticancer agents.....	190
Table 3.3	Screening synthetic analogues of quinocarcin for tumor growth inhibition against HeLa S <sub>3</sub> epithelial carcinoma grown in vitro and P388 leukemia implanted in mice (in vivo) .....	191
Table 3.4	Effect of additives on the cleavage of supercoiled plasmid DNA by quinocarcin and analogues .....	195

### CHAPTER 4

Table 4.1	Lactam methanolysis .....	234
Table 4.2	Attempted heterogeneous reduction of isoquinoline <b>411</b> .....	244
Table 4.3	Comparison of <sup>1</sup> H NMR data for synthetic and natural quinocarcin .....	274

Table 4.4	Comparison of $^{13}\text{C}$ NMR data for synthetic and natural quinocarcin .....	274
-----------	--	-----

## CHAPTER 5

Table 5.1	Acyl-alkylation of benzyne with substituted $\beta$ -ketoesters .....	367
Table 5.2	Acyl-alkylation of substituted arynes.....	368
Table 5.3	Ring expansive aryne acyl-alkylation using cyclic $\beta$ -ketoesters.....	370
Table 5.4	Synthesis of 3-hydroxyisoquinolines via one-pot aryne acyl-alkylation and condensation with ammonia.....	381
Table 5.5	Two-step synthesis of 3-hydroxyisoquinolines from carboxylic acids .....	383
Table 5.6	Two-step synthesis of 2-hydroxy-1,4-naphthoquinones from carboxylic acids .....	388

## CHAPTER 6

Table 6.1	Optimization of reaction conditions for the three-component coupling of benzyne, <i>tert</i> -butyl isocyanide, and phenyl acetate.....	530
Table 6.2	Synthesis of phenoxy iminoisobenzofurans via three-component coupling of arynes, isocyanides, and phenyl esters .....	532
Table 6.3	Synthesis of <i>ortho</i> -ketobenzamides via one-pot three-component coupling and hydrolysis.....	534
Table 6.4	Three-component coupling of arynes, isocyanides, and alkynes.....	538

## APPENDIX 7

Table A7.1	Crystal data and structure refinement for phenoxy iminoisobenzofuran <b>683p</b> (CCDC 739396).....	673
Table A7.2	Atomic coordinates ( $\times 10^4$ ) and equivalent isotropic displacement parameters ( $\text{\AA}^2 \times 10^3$ ) for <b>683p</b> (CCDC 739396). $U(\text{eq})$ is defined as the trace of the orthogonalized $U^{ij}$ tensor.....	676
Table A7.3	Bond lengths [ $\text{\AA}$ ] and angles [ $^\circ$ ] for <b>683p</b> (CCDC 739396) .....	677
Table A7.4	Anisotropic displacement parameters ( $\text{\AA}^2 \times 10^4$ ) for <b>683p</b> (CCDC 739396). The anisotropic displacement factor exponent takes the form: $-2\pi^2 [ h^2 a^{*2} U^{11} + \dots + 2 h k a^* b^* U^{12} ]$ .....	679

Table A7.5	Hydrogen coordinates ( $\times 10^4$ ) and isotropic displacement parameters ( $\text{\AA}^2 \times 10^3$ ) for <b>683p</b> (CCDC 739396).....	680
------------	---	-----

## APPENDIX 8

Table A8.1	Compounds in Chapter 2 – Orthogonal Synthesis of Indolines and Isoquinolines via Aryne Annulation .....	682
Table A8.2	Compounds in Chapter 4 – A Concise Total Synthesis of (-)-Quinocarcin via Aryne Annulation.....	683
Table A8.3	Compounds in Chapter 5 – Expedient Synthesis of 3-Hydroxyisoquinolines and 2-Hydroxy-1,4-Naphthoquinones via One-Pot Aryne Acyl-Alkylation / Condensation.....	684
Table A8.4	Compounds in Chapter 6 – Multicomponent Aryne Reactions.....	685

## LIST OF ABBREVIATIONS

A	adenine
$[\alpha]_D$	angle of optical rotation of plane-polarized light
Å	angstrom(s)
<i>p</i> -ABSA	<i>para</i> -acetamidobenzenesulfonyl azide
Ac	acetyl
APCI	atmospheric pressure chemical ionization
app	apparent
aq	aqueous
Ar	aryl group
At	benztriazolyl
atm	atmosphere(s)
BHT	2,6-di- <i>tert</i> -butyl-4-methylphenol (“ <u>butylated hydroxytoluene</u> ”)
Bn	benzyl
Boc	<i>tert</i> -butoxycarbonyl
bp	boiling point
br	broad
Bu	butyl
<i>i</i> -Bu	<i>iso</i> -butyl
<i>n</i> -Bu	butyl or <i>norm</i> -butyl
<i>t</i> -Bu	<i>tert</i> -butyl
Bz	benzoyl
C	cytosine

<i>c</i>	concentration of sample for measurement of optical rotation
<sup>13</sup> C	carbon-13 isotope
<sup>14</sup> C	carbon-14 isotope
/C	supported on activated carbon charcoal
°C	degrees Celcius
calc'd	calculated
CAN	ceric ammonium nitrate
Cbz	benzyloxycarbonyl
CCDC	Cambridge Crystallographic Data Centre
CDI	1,1'-carbonyldiimidazole
cf.	consult or compare to (Latin: <i>confer</i> )
cm <sup>-1</sup>	wavenumber(s)
cod	1,5-cyclooctadiene
comp	complex
conc.	concentrated
Cy	cyclohexyl
CSA	camphor sulfonic acid
d	doublet
<i>d</i>	dextrorotatory
D	deuterium
dba	dibenzylideneacetone
DBU	1,8-diazabicyclo[5.4.0]undec-7-ene
DCE	1,2-dichloroethane

<i>de</i>	diastereomeric excess
DIAD	diisopropyl azodicarboxylate
DMAD	dimethyl acetylenedicarboxylate
DMAP	4-dimethylaminopyridine
DME	1,2-dimethoxyethane
DMF	<i>N,N</i> -dimethylformamide
DMSO	dimethylsulfoxide
DMTS	dimethylhexylsilyl
DNA	deoxyribonucleic acid
DPPA	diphenylphosphorylazide
dppp	1,3-bis(diphenylphosphino)propane
dr	diastereomeric ratio
DTT	dithiothreitol
<i>ee</i>	enantiomeric excess
E	methyl carboxylate ( $\text{CO}_2\text{CH}_3$ )
$\text{E}^+$	electrophile
<i>E</i>	trans (entgegen) olefin geometry
$\text{EC}_{50}$	median effective concentration (50%)
e.g.	for example (Latin: <i>exempli gratia</i> )
EI	electron impact
eq	equation
ESI	electrospray ionization
Et	ethyl

<i>et al.</i>	and others (Latin: <i>et alii</i> )
FAB	fast atom bombardment
Fmoc	fluorenlylmethyloxycarbonyl
g	gram(s)
G	guanine
h	hour(s)
<sup>1</sup> H	proton
<sup>2</sup> H	deuterium
<sup>3</sup> H	tritium
[H]	reduction
HATU	2-(7-aza-1 <i>H</i> -benzotriazol-1-yl)-1,1,3,3-tetramethyluronium hexafluorophosphate
HMDS	hexamethyldisilamide or hexamethyldisilazide
HMPT	hexamethylphosphoramide
<i>hν</i>	light
HPLC	high performance liquid chromatography
HRMS	high resolution mass spectrometry
Hz	hertz
IC <sub>50</sub>	half maximal inhibitory concentration (50%)
i.e.	that is (Latin: <i>id est</i> )
IR	infrared spectroscopy
<i>J</i>	coupling constant
<i>k</i>	rate constant
kcal	kilocalorie(s)

kg	kilogram(s)
L	liter or neutral ligand
<i>l</i>	levorotatory
LA	Lewis acid
LD <sub>50</sub>	median lethal dose (50%)
LDA	lithium diisopropylamide
LTMP	lithium 2,2,6,6-tetramethylpiperidide
m	multiplet or meter(s)
M	molar or molecular ion
<i>m</i>	meta
μ	micro
<i>m</i> -CPBA	<i>meta</i> -chloroperbenzoic acid
Me	methyl
mg	milligram(s)
MHz	megahertz
MIC	minimum inhibitory concentration
min	minute(s)
mL	milliliter(s)
MM	mixed method
mol	mole(s)
MOM	methoxymethyl
mp	melting point
Ms	methanesulfonyl (mesyl)

MS	molecular sieves
<i>m/z</i>	mass-to-charge ratio
N	normal or molar
NBS	<i>N</i> -bromosuccinimide
nm	nanometer(s)
NMR	nuclear magnetic resonance
NOE	nuclear Overhauser effect
NOESY	nuclear Overhauser enhancement spectroscopy
Nu <sup>-</sup>	nucleophile
<i>o</i>	ortho
[O]	oxidation
<i>t</i> -Oct	<i>tert</i> -octyl (1,1,3,3-tetramethylbutyl)
<i>p</i>	para
PCC	pyridinium chlorochromate
PDC	pyridinium dichromate
Ph	phenyl
pH	hydrogen ion concentration in aqueous solution
p <i>K<sub>a</sub></i>	acid dissociation constant
PMB	<i>para</i> -methoxybenzyl
ppm	parts per million
PPTS	pyridinium <i>para</i> -toluenesulfonate
Pr	propyl
<i>i</i> -Pr	isopropyl

<i>n</i> -Pr	propyl or <i>norm</i> -propyl
psi	pounds per square inch
py	pyridine
q	quartet
R	alkyl group
<i>R</i>	rectus
REDAL	sodium bis(2-methoxyethoxy)aluminum hydride
ref	reference
<i>R</i> <sub>f</sub>	retention factor
RNA	ribonucleic acid
s	singlet or seconds
<i>s</i>	selectivity factor = $k_{\text{rel(fast/slow)}} = \ln[(1 - C)(1 - ee)]/\ln[(1 - C)(1 + ee)]$ , where $C$ = conversion
<i>S</i>	sinister
sat.	saturated
SEM	2-(trimethylsilyl)ethoxymethyl
SOD	superoxide dismutase
Su	succinimide
t	triplet
T	thymine
TBAF	tetra- <i>n</i> -butylammonium fluoride
TBAT	tetra- <i>n</i> -butylammonium difluorotriphenylsilicate
TBDPS	<i>tert</i> -butyldiphenylsilyl
TBS	<i>tert</i> -butyldimethylsilyl

TCA	trichloroacetic acid
temp	temperature
TES	triethylsilyl
Tf	trifluoromethanesulfonyl
TFA	trifluoroacetic acid
TFE	2,2,2-trifluoroethanol
THF	tetrahydrofuran
THIQ	tetrahydroisoquinoline
TIPS	triisopropylsilyl
TLC	thin layer chromatography
TMEDA	<i>N,N,N',N'</i> -tetramethylethylenediamine
TMS	trimethylsilyl
TOF	time-of-flight
tol	tolyl
Troc	2,2,2-trichloroethoxycarbonyl
Ts	<i>para</i> -toluenesulfonyl (tosyl)
UV	ultraviolet
w/v	weight per volume
v/v	volume per volume
X	anionic ligand or halide
Z	cis (zusammen) olefin geometry

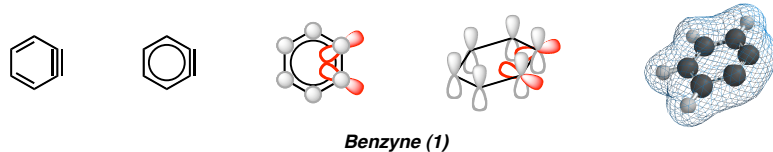
# CHAPTER 1

## *An Introduction to Benzyne*

### 1.1 INTRODUCTION AND BACKGROUND

Benzyne (**1**), the quintessential member of a larger class of arynes, is a six-membered aromatic ring containing a highly strained alkyne (Figure 1.1). Like all arynes, benzyne (or *ortho*-benzyne) is formally derived from the abstraction of two hydrogen atoms from the *ortho* positions of an aromatic ring, which has led to its alternative moniker, 1,2-dehydrobenzene. Due to the strain imparted on the alkyne by the small ring size, benzyne is a highly reactive species, most often playing the part of an electrophile in chemical transformations. Over the past 70 years, this reactivity has been harnessed in a number of inventive ways for the synthesis of a wide variety of arene-containing compounds. While it has evaded outright isolation thus far, several ingenious techniques have been devised for the purpose of observing and measuring benzyne *in situ*. Together, these studies have provided a better understanding of both the structure and electronic properties that lead to the unique reactivity displayed by this singular molecule.

Figure 1.1. Benzyne



The following chapter provides a general introduction to the history of benzyne as it relates to the discovery, characterization, and synthetic implementation of this intriguing reaction intermediate. There is, of course, a phenomenal body of literature already existent pertaining to each of these subjects in great detail.<sup>1,2</sup> As such, these pages are meant as more of a “crash course” to provide background and context for material presented in subsequent chapters. The topics discussed here will include historical examples of aryne reactivity, mechanistic investigations toward elucidation of the aryne bond structure, spectroscopic characterization of benzyne, and synthetic methods for generating benzyne *in situ*. Later chapters will focus on specific applications of aryne chemistry within synthetic methodology and natural product total synthesis.

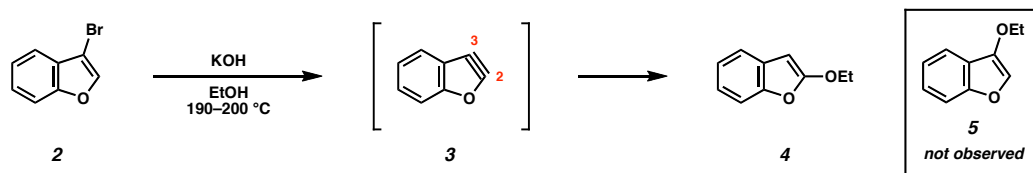
### 1.1.1 *Early Observations of Aryne Reactivity*

The first reported experimental results that can be attributed to the formation of aryne intermediates—albeit unintentional—date back to the early twentieth century. For the most part, these reports described the formation of isomeric product mixtures during attempts to carry out nucleophilic aromatic substitution of aryl halides using strong bases. Although the precise mechanism through which these reactions proceeded would not be fully understood until the early 1950s, the results of these experiments and the

mechanistic hypotheses they generated contributed greatly to the evolution of the fledgling field of aryne chemistry.

The first recorded observation of aryne reactivity was reported in 1902 by Stoermer and Kahlert.<sup>3</sup> In an attempt to prepare 3-ethoxybenzofuran (**5**), the authors treated 3-bromobenzofuran (**2**) with potassium hydroxide in absolute ethanol (Scheme 1.1). However, instead of **5**, the authors were surprised to find that 2-ethoxybenzofuran (**4**) was formed as the sole product. They suggested the possibility that an elimination of hydrogen bromide had produced an acetylenic intermediate, 2,3-dehydrobenzofuran (**3**). In analogy to previous experiments that noted the addition of ethanol to the less substituted terminus of phenyl acetylene,<sup>4</sup> the authors then proposed nucleophilic attack of potassium ethoxide at C(2) of **3** to form the isolated product (**4**). Attempts were made to isolate the theoretical intermediate, though not surprisingly, they were never met with success. Nonetheless, this report marks the first proposal for the formation of a transient aryne intermediate, and thus the birth of aryne chemistry.

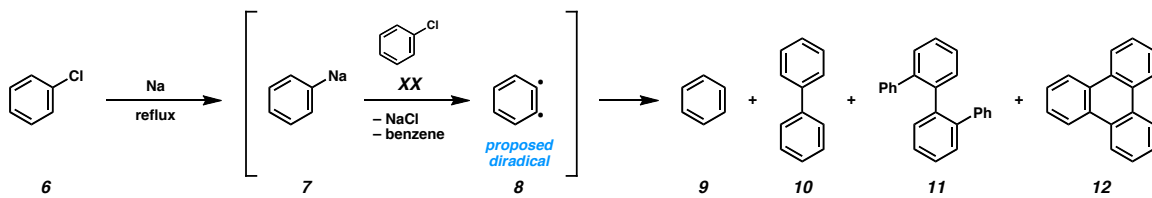
Scheme 1.1. Stoermer & Kahlert – Unexpected rearrangement via “benzofuryne”



Twenty five years later, Bachmann and Clarke communicated their efforts to prepare biphenyl (**10**) from chlorobenzene (**6**) using the Wurtz–Fittig process<sup>5</sup> (Scheme 1.2).<sup>6</sup> In the presence of sodium metal, chlorobenzene was expected to form phenyl sodium (**7**),

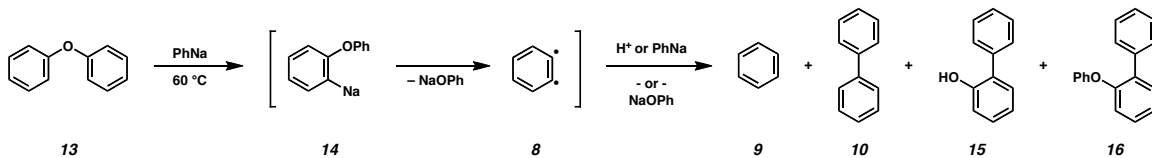
which would react with a second equivalent of chlorobenzene to produce biphenyl. However, in addition to the desired product, 1,1'-diphenylbiphenyl (**11**), triphenylene (**12**), and large quantities of benzene (**9**) were also isolated. Unable to rationalize the formation of triphenylene through a polar mechanism, the authors postulated the intermediacy of an *ortho*-phenylene diradical (**8**) capable of undergoing trimerization. Although no further experimental data was provided, this hypothetical compound represents the second invocation of an aryne intermediate and the first proposal for benzyne, albeit in a resonance form.

Scheme 1.2. Bachmann & Clarke – Proposal for a diradical intermediate



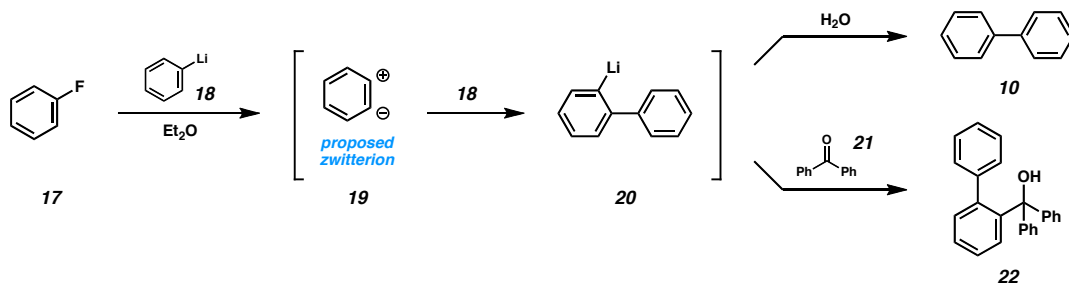
In 1939, Lüttringhaus and Säaf reported the rearrangement of diphenyl ether (**13**) to biphenyl (**10**) and related derivatives **15** and **16** upon treatment with phenylsodium (Scheme 1.3).<sup>7</sup> Among other explanations, the authors offered the possibility that metallation at the ortho position of **13** produced a sodium aryl species (**14**), which then decomposed through a radical process to sodium phenoxide and a phenylene diradical (**8**). Combination of **8** and **14** would then account for the formation of phenyl biphenyl ether (**16**). Although no connection was made to the previous work of Bachmann and Clarke, the notion of a symmetrical intermediate was clearly gaining ground as a means to rationalize these unexpected rearrangements.

Scheme 1.3. Lüttringhaus &amp; Sääf – Rearrangements of diphenyl ether



Between 1940 and 1942, Wittig *et al.* made a number of experimental observations that led to the emergence of the benzyne hypothesis.<sup>8</sup> The key discovery rested upon the finding that products of the reaction between fluorobenzene (**17**) and phenyllithium (**18**) depended upon the subsequent treatment of the reaction mixture (Scheme 1.4). When the reaction was quenched with water, biphenyl (**10**) was isolated. If instead, benzophenone (**21**) was added, 2-biphenyldiphenylcarbinol (**22**) resulted. Assuming nucleophilic addition to the variable electrophile is the final step, the products were traced back through lithiated biphenyl **20** to a unsymmetrical zwitterionic phenylene species (**19**). Interestingly, Wittig rejected the notion of a cyclic alkyne on the basis of presumably overwhelming ring strain. Instead, he proposed that reactions proceeding through **19** would occur in a regiospecific manner, wherein nucleophiles would always add to the cationic position previously occupied by the leaving group and electrophiles would always take the position originally occupied by the *ortho*-hydrogen. Although later studies would prove this to be incorrect, the experiments performed by Wittig and his predecessors represent an indispensable contribution to the body of knowledge that ultimately led to the discovery of benzyne.

Scheme 1.4. Wittig – Proposal of a zwitterionic intermediate

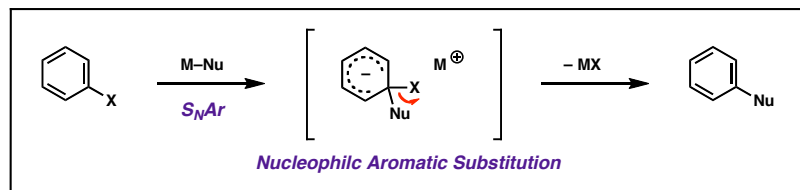


### 1.1.2 Mechanistic Investigation of a “Benzyne” Intermediate

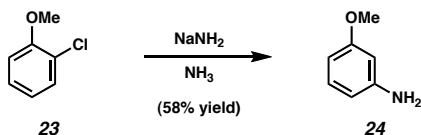
By the mid-1940s, the mechanism of amination operative in the conversion of aryl halides to anilines had become a point of heated discussion in the chemical community. The commonly accepted mechanism involved  $S_NAr$  displacement through nucleophilic attack at the ipso carbon followed by elimination of the halide (Scheme 1.5).<sup>9,10</sup> However, this mechanism could not account for the rearrangements that sometimes occurred when “non-activated” aryl halides were treated with alkali metal amides, or the fact that these rearrangements did not obey the same influences that governed other aromatic substitution reactions. For instance, it was well understood that a methoxy group would promote electrophilic aromatic nitration at the ortho and para positions, while a trifluoromethyl group would promote nitration at the meta position. However, when treated with alkali metal amides (e.g.,  $NaNH_2$ ,  $KNH_2$ ), *ortho*-methoxy<sup>11a,i</sup> (**23**) and *ortho*- and *meta*-trifluoromethyl aryl halides<sup>11h</sup> (**25** and **26**) both produced exclusively the corresponding *meta*-substituted anilines (**24** and **27**). Likewise, *para*-substituted aryl halides (**28**) produced mixtures of both *meta*- and *para*-substituted anilines (**29** and **30**).<sup>11g</sup> Similar results were also obtained during attempts to aminate *ortho*-chloro- and *ortho*-

bromothioanisoles, 4-iododibenzothiophene,<sup>11b</sup> *ortho*-bromophenyl methyl sulfone,<sup>11j</sup> and even *ortho*-bromo-*N,N*-dimethylaniline.<sup>11e</sup>

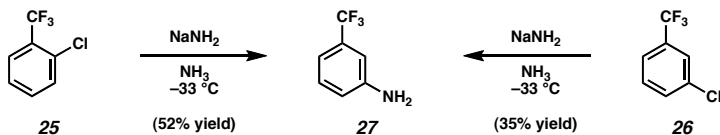
Scheme 1.5. Unexpected rearrangements during nucleophilic aromatic substitution



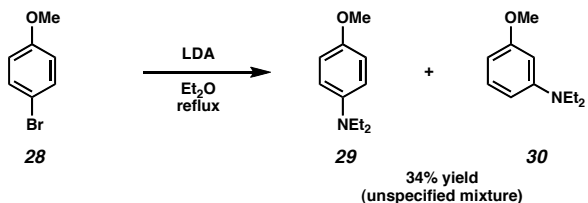
Gilman (1945)



Benkeser (1949)



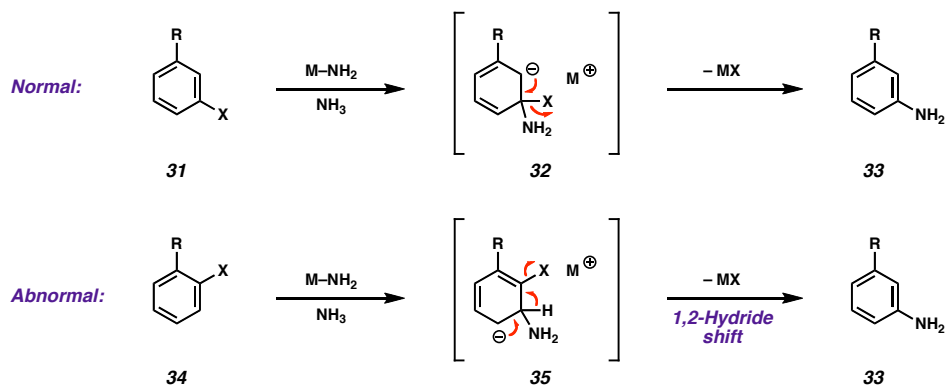
Gilman (1948)



In 1953, Benkeser and Schroll put forth an explanation for the observation that both *ortho*- (34) and *meta*-substituted aryl halides (31) converged to the *meta*-substituted anilines (33) (Scheme 1.6).<sup>12</sup> The authors suggested an  $S_NAr$ -like mechanism whereby *meta*-substituted aryl halides (32) proceeded through a “normal” mode of amination involving direct displacement, while the *ortho* isomers (34) reacted “abnormally” to generate rearranged products. In the abnormal mechanism, it was proposed that the

amide nucleophile would add to the carbon ortho to the halide (meta to the remaining substituent) to generate an intermediate anion (**35**) that would then undergo a 1,2-hydride shift to displace the halide. While this combination of mechanisms concurred with most previously observed rearrangements, the hydride shift and concomitant loss of the halide seems unlikely given the poor overlap between the C(sp<sup>3</sup>)–H and C(sp<sup>2</sup>)–X orbitals.

*Scheme 1.6. Benkeser – Proposed rearrangement during nucleophilic aromatic substitution*

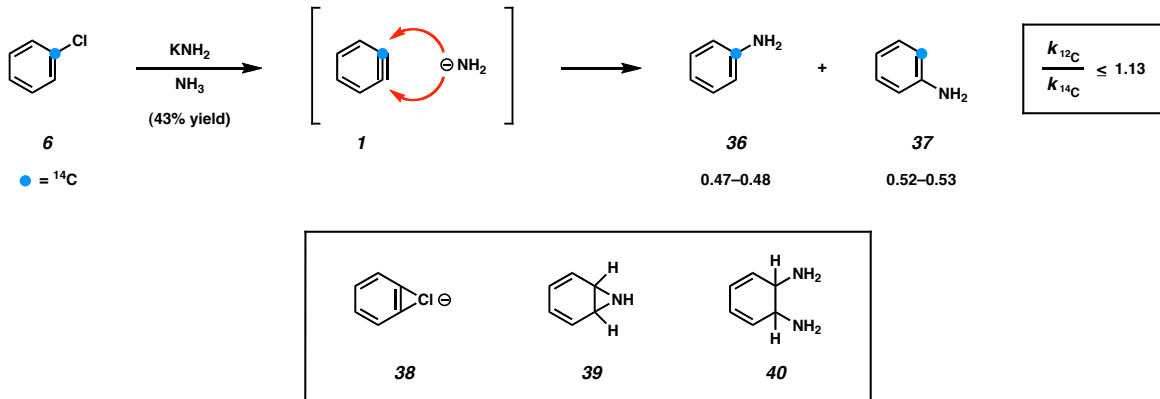


One month after Benkeser's proposal, Roberts and co-workers at the Massachusetts Institute of Technology published an alternative mechanism to explain this rearrangement.<sup>13</sup> The authors recognized that any suitable explanation must agree with several key observations: (1) the amination reactions are very rapid, even with chlorobenzene, in liquid ammonia at –33 °C; (2) the entering amino group is never found farther than one carbon away from the position of the leaving halide<sup>11</sup>; (3) the aryl halide substrates and the aniline products are not isomerized under the reaction conditions<sup>11i</sup>; (4) no reaction occurs when the substrate lacks a hydrogen ortho to the halide (e.g., bromomesitylene, bromodurene, and 2-bromo-3-methylanisole<sup>11i</sup>). With these facts in mind, Roberts *et al.* proposed an elimination/addition mechanism involving the transitory

existence of an electronically neutral species they termed “benzyne” (**1**) (Scheme 1.7).

In order to test their claim, the authors performed an amination reaction using an isotopically labeled unsubstituted aryl halide, chlorobenzene-1-<sup>14</sup>C (**6**). If a symmetrical intermediate such as **1** was indeed the electrophile that underwent amination, then the product should contain a mixture of aniline-1-<sup>14</sup>C (**36**) and aniline-2-<sup>14</sup>C (**37**) in a ratio reflecting the difference in the rates of addition to <sup>12</sup>C- and <sup>14</sup>C-labeled positions.<sup>14</sup> When the reaction was carried out, the desired mixture of <sup>14</sup>C-labeled anilines was isolated in 43% yield. More importantly, the measured yield of aniline-2-<sup>14</sup>C (**37**) reflected a 52–53% degree of rearrangement, consistent with the formation of a symmetrical intermediate and a kinetic isotope effect of  $\leq 1.13$ .<sup>15</sup> The authors noted, however, that at the time they could not rule out the potential formation of other symmetrical intermediates (e.g., **38–40**) in place of benzyne.

Scheme 1.7. Roberts – Nucleophilic aromatic substitution via a “benzyne” intermediate



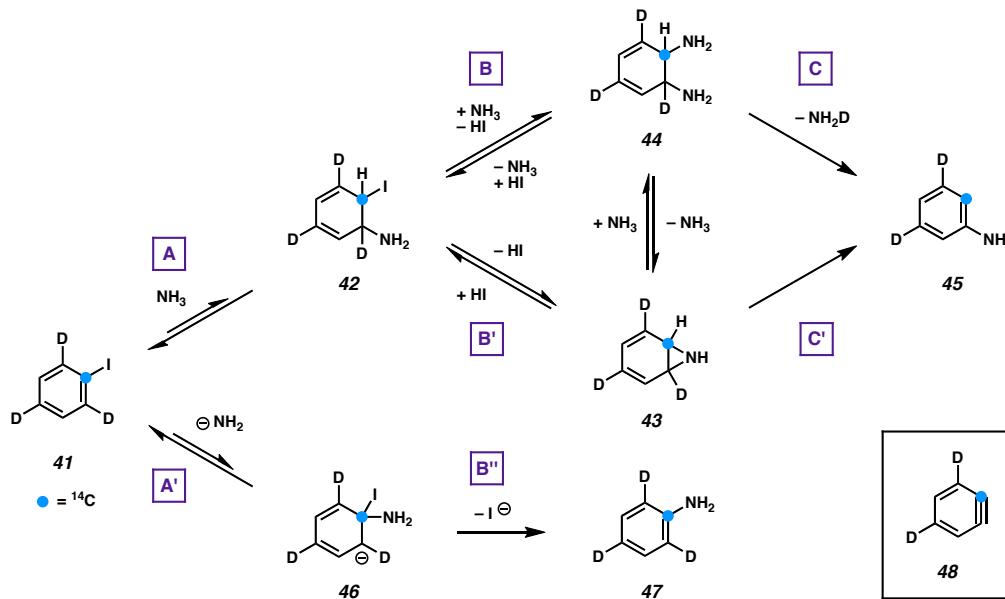
In order to address the notion that the formation of a nearly equivalent mixture of aniline-1-<sup>14</sup>C (**36**) and aniline-2-<sup>14</sup>C (**37**) resulted from a fortuitous combination of

Benkeser's "normal" and "abnormal" displacement mechanisms, Roberts *et al.* repeated the amination reaction with iodobenzene-1-<sup>14</sup>C.<sup>15</sup> The <sup>14</sup>C-labeled aniline isolated from this second reaction contained a mixture of isomers nearly identical to the first, leading the authors to posit that "it would be a remarkable coincidence if the two very different halogens had the same ratios of 'normal' to 'abnormal' reactions."

Having confirmed that aromatic aminations of haloarenes can proceed through a symmetrical intermediate, Roberts *et al.* redoubled their efforts to determine the exact structure of this elusive entity. In light of the fact that aryl halides lacking an *ortho*-hydrogen failed to react, the group sought to elucidate the role that this hydrogen played in the reaction mechanism. By performing a complex series of rate experiments using *ortho*-deuterated chloro- and bromobenzene, the authors were able to extract a kinetic isotope effect of 5.5–5.8, indicating that removal of the *ortho*-hydrogen occurred in the rate-determining step.<sup>15,16</sup> With this information in hand, they returned their attention to each of the candidates for the symmetrical intermediate. Anion **38** was dismissed upon the observation that aryl fluorides—like their chloride, bromide, and iodide analogues—reacted smoothly with lithium diethylamide to produce a corresponding mixture of rearranged and non-rearranged anilines. It was assumed that fluorine, as a second-row element, lacks the capacity to expand its valence shell to accommodate ten electrons. Furthermore, the fact that chlorobenzene and iodobenzene both produce the same ratio of isomeric anilines suggests that the halide is either absent during the product-forming step or at least relegated to such a distance from the reactive position as to have no appreciable effect on the outcome.

Eliminating aziridine **39** and diamine **40** as potential intermediates proved far more demanding since doing so required consideration of an altogether separate mechanism. An innovative experiment was designed to determine whether either of these species formed during the rearrangement of iodobenzene-1-<sup>14</sup>C-2,4,6-<sup>2</sup>H<sub>3</sub> (**41**) to aniline-2-<sup>14</sup>C-3,5-<sup>2</sup>H<sub>2</sub> (**45**) (Scheme 1.8).<sup>17</sup> Given that *ortho*-C–H bond scission occurs in the rate-determining step, the slow step of this alternative mechanism must be the final loss of NH<sub>2</sub>D (path C) or reestablishment of aromaticity (path C').<sup>18</sup> Replacing the *ortho*-hydrogens with deuterium was therefore expected to slow the rate of formation of the rearranged aniline (**45**) relative to the non-rearranged aniline (**47**), the latter of which was envisioned to form according to the normal S<sub>N</sub>Ar displacement (path A' → B''). Evidence for this rate difference—and thus the presence of either aziridine **43** or diamine **44** as the symmetrical intermediate—would be measurable as a decrease in the yield of aniline-2-<sup>14</sup>C-3,5-<sup>2</sup>H<sub>2</sub> (**45**) relative to aniline-1-<sup>14</sup>C-2,4,6-<sup>2</sup>H<sub>3</sub> (**47**), the formation of which does not require scission of a C–H(D) bond. When the amination was performed, however, anilines **45** and **47** were isolated in a ratio of 52.8 : 47.2, nearly identical to the ratio obtained upon amination of chlorobenzene-1-<sup>14</sup>C (cf., **36** : **37**). While these results remained consistent with the formation of a benzyne intermediate (e.g., **48**), they disproved the existence of aziridine **43** and diamine **44**. Moreover, they proved that rate determination and product determination occurred in separate steps, lending further credence to the notion of benzyne as the key intermediate.

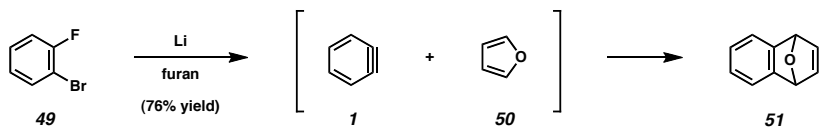
Scheme 1.8. Roberts – Proposed rearrangement during amination via aziridine 43 or diamine 44



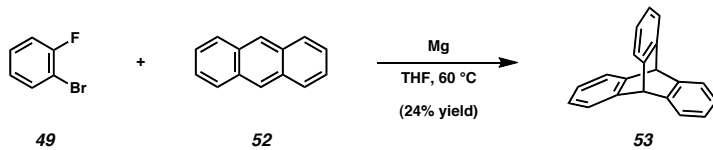
Over the next few years, several other labs published results in support of the aryne model (Scheme 1.9). In 1955, Wittig and Pohmer demonstrated that 2-bromofluorobenzene (**49**) reacts with lithium metal in furan solution to generate naphthalene-1,4-endoxide (**51**), presumably through a Diels–Alder cycloaddition between benzyne (**1**) and furan (**50**).<sup>19</sup> Similar results were obtained using anthracene (**52**) to generate triptycene (**53**), an intriguing  $D_{3h}$  symmetrical hydrocarbon resembling a paddlewheel.<sup>20</sup> Three years later, Huisgen and co-workers carried out the aromatic amination of six naphthyl halides (**54a–c** and **55a–c**)—both  $\alpha$ - and  $\beta$ -isomers of chloro-, bromo-, and iodonaphthalene.<sup>21</sup> In accordance with the formation of a “naphthalyne”<sup>22</sup> intermediate (**56**), all six substrates produced the same mixture of  $\alpha$ - and  $\beta$ -naphthylpiperidines (**57** and **58**). These findings further reinforced Roberts’ earlier observation that neither the position nor the identity of the halide affects the final partitioning of products.<sup>15</sup>

Scheme 1.9. Results in support of the aryne model

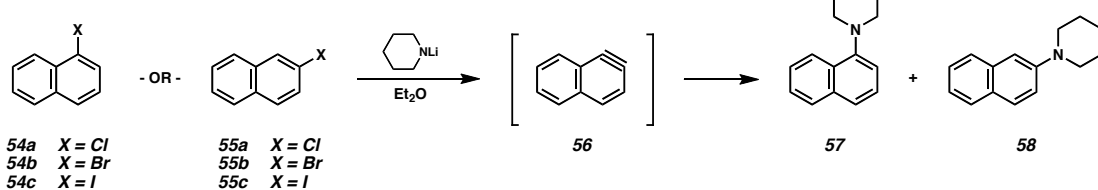
Wittig &amp; Pohmer (1955)



Wittig (1959)



Huisgen (1958)



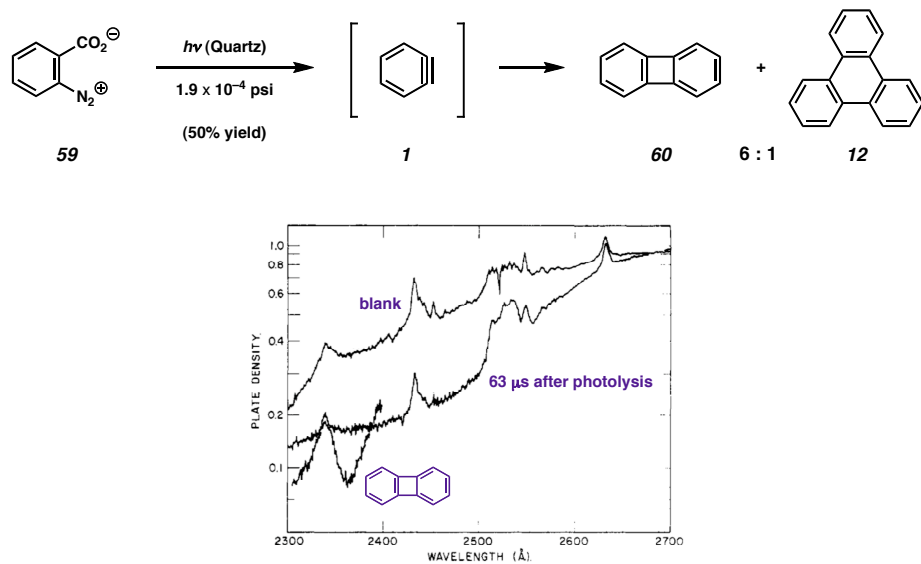
substrate	X	yield	57 : 58
54a	Cl	92%	31.5 : 68.5
54b	Br	93%	30.0 : 70.0
54c	I	83%	34.0 : 66.0
55a	Cl	92%	31.0 : 69.0
55b	Br	79%	31.0 : 69.0
55c	I	54%	31.5 : 68.5

### 1.1.3 Spectroscopic Evidence and Physical Properties of Benzyne

As the concept of benzyne gained general acceptance, chemists began to search for ways in which to observe and characterize this fleeting intermediate. Despite the elegant mechanistic work performed by Roberts, questions still remained as to whether arynes existed freely in solution or whether they were loosely associated with metal cations or halogen anions, and furthermore, whether they existed as strained alkynes or diradicals. In 1960, Stiles and Miller at the University of Michigan provided the first step along the path toward observing benzyne in the absence of external reagents by preparing phenyldiazonium-2-carboxylate (**59**), a precursor that generates benzyne (**1**) through the

loss of carbon dioxide and nitrogen when heated.<sup>23</sup> The compound was shown to produce biphenylene (**60**) and triphenylene (**12**) when subjected to flash photolysis in *vacuo* (Scheme 1.10).<sup>24</sup> When this reaction was monitored by UV spectroscopy, the authors noted strong absorbance in the region between 240 and 270 nm prior to the formation of biphenylene (10–200  $\mu$ s after irradiation). The peaks in this region were assigned to the  $n \rightarrow \pi^*$  and  $\pi \rightarrow \pi^*$  excitations of benzyne, marking the first acquisition of spectroscopic evidence of benzyne.

*Scheme 1.10. Microdensitometer tracings showing absorbance by gaseous products of flash photolysis of phenyldiazonium-2-carboxylate (**59**)*

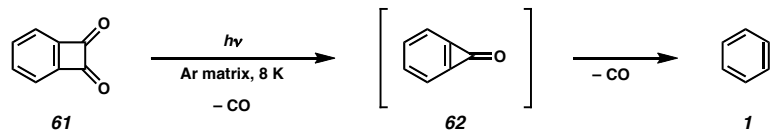


The next several years furnished additional data in support of benzyne, including detection of the parent ion by gas phase mass spectrometry<sup>25</sup> and measurement of its ionization potential (9.75 V).<sup>26</sup> In 1973, Chapman and co-workers recorded the first infrared spectrum of benzyne through low-temperature photolytic decomposition of

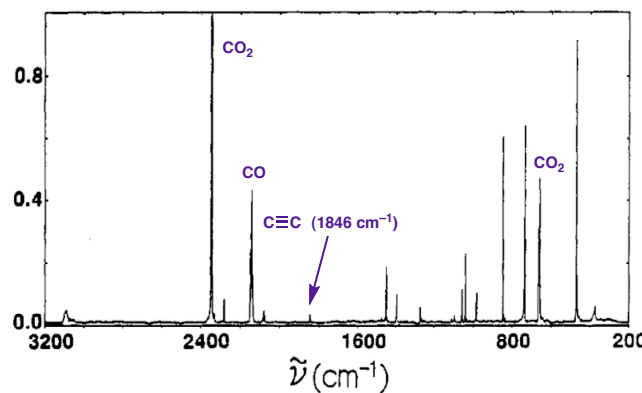
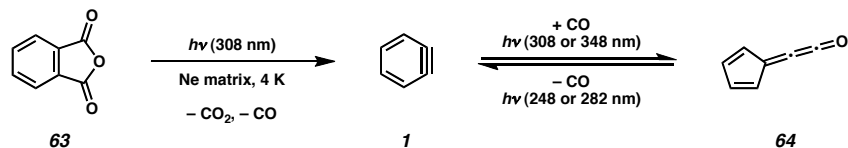
benzocyclobutenedione (**61**) (Scheme 1.11).<sup>27</sup> Among numerous peaks associated with byproducts such as carbon monoxide, biphenylene, triphenylene, and acetylene, two weak absorbances were noted at 1838 and 2085  $\text{cm}^{-1}$ . The authors attributed the former to the carbonyl stretch of benzocyclopropenone (**62**),<sup>28</sup> claiming that this band disappeared upon decarbonylation to produce benzyne (**1**). The latter was therefore attributed to the  $\text{C}\equiv\text{C}$  stretch of benzyne, given its proximity to the value known for acetylene (2165  $\text{cm}^{-1}$ ).<sup>29</sup> Although several other labs confirmed these results both computationally<sup>30</sup> and experimentally<sup>31</sup> over the next decade, doubts arose when Wentrup *et al.* identified a band at 2080  $\text{cm}^{-1}$  during flash vacuum pyrolysis of phthalic anhydride (**63**) and claimed that it consisted of two overlapping vibrations belonging both to benzyne and cyclopentadienylideneketene (**64**).<sup>32</sup> In 1992, Radziszewski and co-workers were able to eliminate the bands attributable to the by-products of photolytic decomposition (including **62** and **64**) by analyzing band shifts in the infrared spectra of deuterated and  $^{14}\text{C}$ -labeled isotopomers of phthalic anhydride (**63**).<sup>33</sup> When the extraneous bands were removed, a weak vibrational stretch at 1846  $\text{cm}^{-1}$  remained and was thereby assigned to the benzyne triple bond. Later studies employed ultraviolet photoelectron spectroscopy to measure the singlet-triplet splitting ( $37.5 \pm 0.3 \text{ kcal}\cdot\text{mol}^{-1}$ ),<sup>34</sup> CID mass spectrometry to determine the enthalpy of formation ( $106.6 \pm 3.0 \text{ kcal}\cdot\text{mol}^{-1}$ ),<sup>35</sup> and  $^{13}\text{C}$  dipolar NMR to calculate the  $\text{C}\equiv\text{C}$  bond length ( $1.24 \pm 0.02 \text{ \AA}$ ).<sup>36</sup> Together, these measurements provide conclusive evidence that benzyne does in fact exist as a highly strained alkyne—weaker, longer, and more reactive than a typical linear alkyne, but an alkyne nonetheless.

Scheme 1.11. Infrared spectrum of benzyne

Chapman (1973)



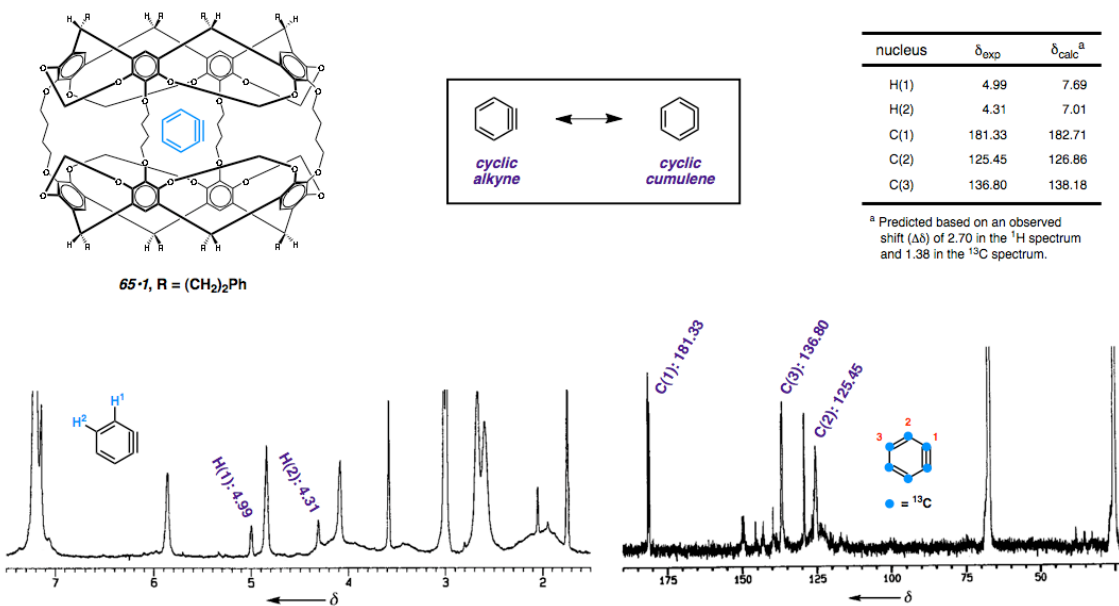
Wentrup (1988) and Radziszewski (1992)



In an impressive series of experiments carried out in 1997, Ralf Warmuth at the University of California, Los Angeles successfully obtained the  $^1\text{H}$  and  $^{13}\text{C}$  NMR spectra of benzyne (Figure 1.2).<sup>37</sup> By trapping phthalic anhydride within hemicarcerand **65**,<sup>38</sup> Warmuth was able to generate benzyne photolytically at 77 K within the protective inner cavity before measuring the spectra at 198 K. Because inclusion produces a shielding effect resulting in an upfield shift in each of the resonances, spectra were acquired for the analogous complex with benzene. By assuming that benzyne would experience the same degree of shielding as benzene, the chemical shifts of free benzyne in solution were predicted based on the observed resonance shift for benzene. Finally, by preparing a fully  $^{13}\text{C}$ -enriched isotopomer of phthalic anhydride, Warmuth was able to study the  $^{13}\text{C}$

coupling behavior. Noting that the coupling constant between C(2) and C(3) ( $J_{C2-C3}$ ) revealed a bond structure more closely related to two  $sp^2$ -hybridized carbon atoms connected through a single bond (as in 1,3-butadiene) than an aromatic system, the author was led to speculate as to whether benzyne would be better described as possessing significant cumulene character.

Figure 1.2.  $^1H$  and  $^{13}C$  NMR spectra of benzyne



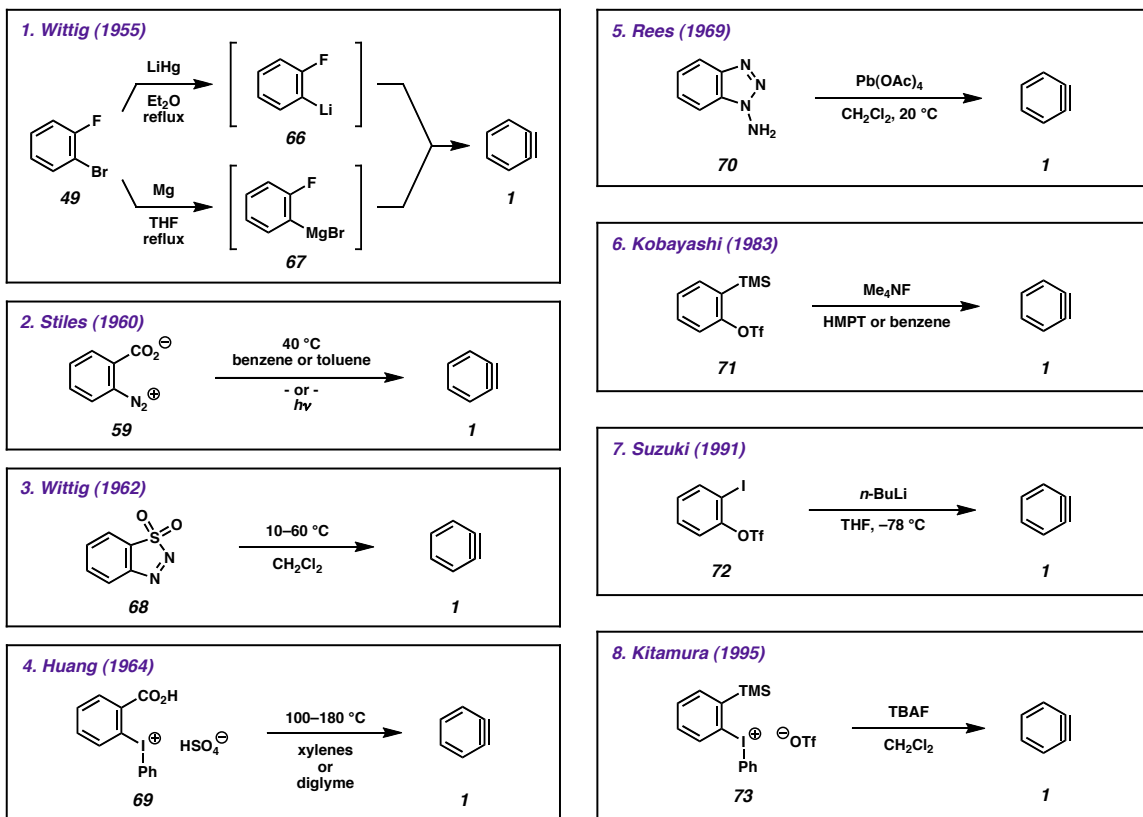
## 1.2 ARYNES IN SYNTHESIS

### 1.2.1 *Methods of Aryne Generation*

Today, benzyne is a commonly accepted reaction intermediate employed in a wide variety of synthetic transformations ranging from cycloadditions to organotransition metal chemistry. Several of these reaction classes—including ring-forming reactions and multicomponent processes—will be reviewed in depth in the following chapters. However, before focusing on reactions that involve benzyne as a reagent, it is first necessary to consider the reactions that produce benzyne. At the outset of aryne research in synthetic chemistry, the only available method consisted of the dehydrohalogenation of an aryl halide, a reaction typically accomplished under strongly basic conditions. In order to widen the scope of aryne technology, it therefore became necessary to develop milder conditions that would enable the use of more sensitive substrates.

The first method to circumvent the use of strong organometallic bases was provided by Wittig and Pohmer in 1955 (Scheme 1.12, eq 1).<sup>19a</sup> Instead of performing a direct deprotonation at the ortho position of a monohalogenated arene, the authors found that treating 2-bromofluorobenzene (**49**) with either lithium amalgam or magnesium metal effectively promoted metallation at the more labile C–Br bond to form an *ortho*-metallated aryl fluoride (**66** or **67**), which then underwent dehalometallation to produce benzyne (**1**). Over the next several years, this procedure featured prominently in a number of novel methodological studies, enabling the generation of benzyne in the presence of enamines,<sup>39</sup> dienes,<sup>40</sup> sulfides,<sup>41</sup> and various phosphorus compounds.<sup>42</sup>

Scheme 1.12. Methods for generating benzyne



Although Wittig and Pohmer discovered the first method to eliminate the need for a strong base, several labs—especially those interested in spectroscopically characterizing benzyne—desired a method for generating arynes under completely metal-free conditions. Between 1960 and 1964, the call was answered by three separate research groups. The first solution came in the form of phenyldiazonium-2-carboxylate (**59**), a derivative of anthranilic acid originally prepared by Hantzsch and Davidson in 1896,<sup>43</sup> but later applied to aryne chemistry by Stiles and Miller (eq 2).<sup>23</sup> Upon heating or photolysis,<sup>24</sup> this species releases two equivalents of gas to irreversibly generate benzyne as a lone intermediate. Similar approaches were subsequently adopted by Wittig and Huang using benzo-1,2,3-thiadiazole-1,1-dioxide<sup>44</sup> (**68**) (eq 3) and (2-

carboxyphenyl)phenyliodonium salts<sup>45</sup> (**69**) (eq 4), respectively. While the former decomposes to benzyne below room temperature, the latter requires extremely elevated temperatures and extended reactions times in order to fully react. Furthermore, each of these three compounds requires careful handling and low-temperature storage to avoid the danger of rapid gas evolution. Drawbacks aside, however, the ability to generate benzyne in the absence of additional activating agents popularized the use of these substrates in synthesis over the next several decades.<sup>46</sup>

Using a similar principle of irreversible gas release, Campbell and Rees described the use of 1-aminobenzotriazole (**70**)—a compound previously developed by Trave and Bianchetti<sup>47</sup>—for the generation of benzyne under mild conditions at room temperature (eq 5).<sup>48</sup> In the presence of lead(IV) tetraacetate, the amine hydrogen atoms are oxidatively removed to produce an intermediate nitrene, which decomposes to benzyne upon loss of two equivalents of nitrogen. Although the reaction proceeds immediately upon addition of the oxidant to generate benzyne in near-quantitative yield within minutes, the need for stoichiometric amounts of a toxic heavy metal has severely limited wide-scale application of this technique in synthesis.<sup>49</sup> In response to this drawback, Knight *et al.* developed an alternate set of conditions using *N*-iodosuccinimide as the oxidant.<sup>50</sup> However, these conditions can lead to the incorporation of an iodide within the final product.

In the thirty years following the discovery and elucidation of benzyne, aryne chemistry had become a mainstream field within organic synthesis, in part due to the advances in aryne generation described above. However, the available methods still required strong bases, metallic reagents, high temperatures, and/or extreme caution

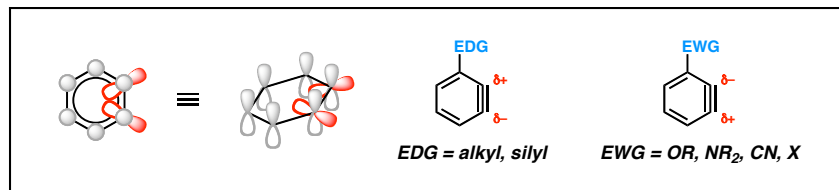
during preparation. Fortunately, this changed in 1983 when Kobayashi and co-workers reported a novel method for generating benzyne from 2-(trimethylsilyl)phenyl triflate (**71**) under exceedingly mild conditions (eq 6).<sup>51</sup> Upon adding a fluoride reagent at room temperature, the substrate undergoes a 1,2-elimination to generate benzyne in high yield within minutes. The authors went on to demonstrate that the reaction proceeded efficiently with a number of fluoride sources ( $\text{Me}_4\text{NF}$ ,  $n\text{-Bu}_4\text{NF}$ ,  $\text{CsF}$ , and  $\text{KF}/18\text{-crown-6}$ ) in several different solvents (HMPT, furan, benzene, acetonitrile). The most remarkable aspect of this technique, however, is the orthogonality that these conditions display toward most all other functionality. Aside from a few select groups susceptible to fluoride (e.g., silanes, sulfonates), these conditions can be applied to the formation of benzyne in the presence of amines,<sup>52</sup> epoxides,<sup>53</sup> allenes,<sup>54</sup> alkynes,<sup>55</sup> enamines,<sup>56</sup> phosphonates,<sup>57</sup> heteroarenes,<sup>58</sup> aldehydes,<sup>59</sup> aldimines,<sup>60</sup> ketones,<sup>61</sup> oximes,<sup>62</sup> esters,<sup>63</sup> amides,<sup>64</sup> isocyanides,<sup>65</sup> and diazo compounds,<sup>66</sup> among many other groups. Since the report by Kobayashi *et al.*, more recent examples of aryne generation have been developed by Suzuki<sup>67</sup> (eq 7) and Kitamura<sup>68</sup> (eq 8). However, no other aryne precursor has received more widespread application nor shown more compatibility with existing functionality than Kobayashi's *ortho*-silyl aryl triflate.

### 1.2.2 Regioselectivity

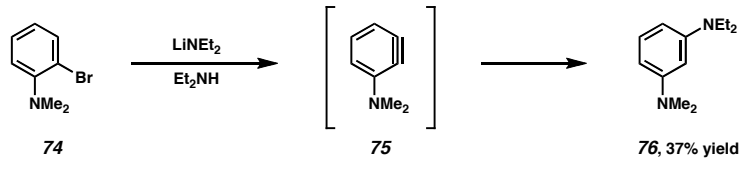
Aryne reactivity is highly susceptible to the influence of ring substitution (Scheme 1.13). Although highly strained, the triple bond is polarizable through electron donation or withdrawal from neighboring groups. In analogy to more traditional modes of aromatic substitution, the influence of a particular functional group is proportional to its

proximity. For instance, groups situated ortho to the triple bond exert a greater influence than those situated meta. It is extremely important to note, however, that the reactive  $\pi$ -orbitals of the aryne triple bond are located in the plane of the ring, as opposed to the  $\pi$ -orbitals of the aromatic system, which lie orthogonal to the plane. As such, the reactive orbitals do not interact with the delocalized  $\pi$ -system of the aromatic ring and are therefore largely immune to the resonance effects of ring substituents. Instead, polarization of the triple bond arises from inductive effects exerted through the  $\sigma$ -bond network. This leads to the rather unintuitive observation that ether<sup>11a,g,i</sup> and amine<sup>11e</sup> substituents (e.g., **75**)—normally viewed as electron-donating groups due to delocalization—function as electron-withdrawing groups due to the electronegativity of the heteroatom (cf., Scheme 1.5). In contrast, a carboxylate (**78a** and **b**) positioned ortho to the aryne triple bond has significantly less impact on regioselectivity.<sup>69</sup>

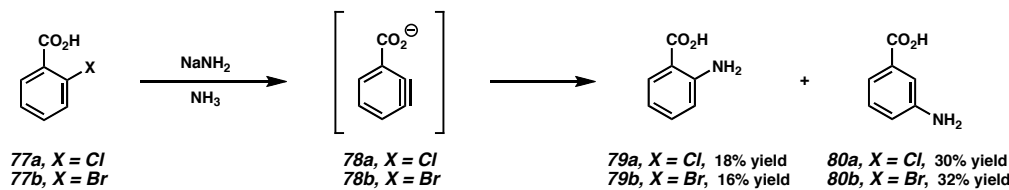
Scheme 1.13. Inductive effects upon regioselectivity in benzyne reactions



Gilman (1946)

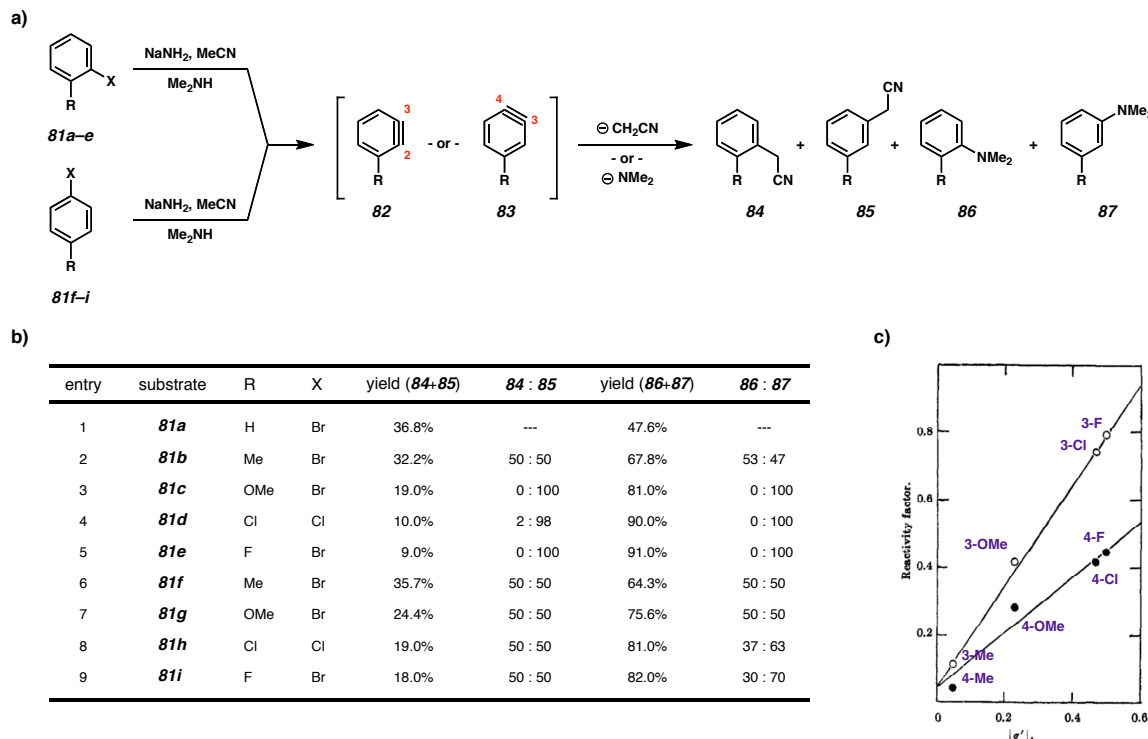


Biehl (1969)



In 1969, Biehl and co-workers performed an in-depth analysis of the effects that varying aryne substitution had upon the regioselectivity of nucleophilic addition (Scheme 1.14a).<sup>70</sup> The authors carried out a series of competition experiments using *ortho*- and *meta*-substituted arynes (**82** and **83**) in the presence of both a carbon ( $\text{NaCH}_2\text{CN}$ ) and nitrogen ( $\text{NaNMe}_2$ ) nucleophile. While the dimethylamide anion was unexpectedly found to outcompete the more reactive carbanion of acetonitrile to form the arylated product (**84+85** vs. **86+87**), this departure from the established trend was attributed merely to a greater abundance of the amine (Scheme 1.14b). More importantly, this study provided definitive evidence that reactivity and regioselectivity are each subject to the inductive effects of neighboring functionality. Interestingly, both inductive donation (entries 2 and 6) and withdrawal (entries 3–5 and 7–9) render the aryne more reactive than unsubstituted benzyne (entry 1). Withdrawing substituents in particular have a pronounced effect on regioselectivity, promoting nearly exclusive addition at C(3) when situated *ortho* to the triple bond (entries 3–5). However, this effect is drastically mitigated by moving the substituent to the *meta* position (entries 7–9). The weakly donating methyl group, on the other hand, fails to promote regioselective addition when located either *ortho* (entry 2) or *meta* (entry 6) to the aryne bond. Finally, using these product distributions, the authors were able to demonstrate a linear correlation between the absolute value of the Hammett substituent constant<sup>71,72</sup> ( $\sigma'$ ) and the reactivity factor,<sup>73</sup> thereby providing a general means to determine substituent effects upon aryne reactivity despite the formation of product mixtures (Scheme 1.14c).

Scheme 1.14. Biehl – a) Competing nucleophilic additions to 3- and 4-substituted arynes. b) Substituent effects on regioselectivity. c) Reactivity factor vs.  $|\sigma'|$  in dimethylamine where  $\circ$  represents 3-substituted arynes and  $\bullet$  represents 4-substituted arynes.



### 1.3 CONCLUSION

The twentieth century witnessed the birth of aryne chemistry. Beginning from a handful of unexpected rearrangements observed during attempts to carry out nucleophilic aromatic substitution of simple aryl halides, this field has grown to encompass an enormous variety of synthetic techniques focused on both the generation of arynes and their use in bond-forming reactions. The intricate studies performed by Roberts, Wittig, Huisgen, and others brought to light the unusual molecular structure of benzyne—an aromatic ring containing a highly strained alkyne. Over the next several decades, researchers confirmed this structural assignment using a host of spectroscopic techniques

including ultraviolet photoelectron spectroscopy, infrared and Raman spectroscopy, mass spectrometry, and nuclear magnetic resonance spectroscopy. Concurrent with these studies came advances in the chemical preparation of benzyne. Newer techniques abandoned the use of strong bases and metallic reagents in favor of mild, selective conditions amenable to the use of more highly functionalized reaction partners. This in turn enabled synthetic chemists to explore the different mechanistic pathways available to benzyne, using this reactive intermediate in a greater diversity of chemical transformations. Today, the once esoteric field of aryne chemistry enjoys mainstream recognition within the chemical community, regularly furnishing new synthetic techniques. Our research group in particular has been actively contributing to this growing body of knowledge for the past six years. The following chapters will describe in detail our work within this regime, focusing both on the design and development of novel synthetic methods for the synthesis of nitrogen-containing heterocycles and on the application of these methods toward the construction of complex bioactive natural products.

## 1.4 NOTES AND REFERENCES

- (1) For reviews on the history of arynes and their use in synthesis, see: (a) Bunnett, J. F. *J. Chem. Educ.* **1961**, *38*, 278–285. (b) Heaney, H. *Chem. Rev.* **1962**, *62*, 81–97. (c) Hoffmann, R. W. *Dehydrobenzene and Cycloalkynes*; Blomquist, A. T., Ed.; Academic Press: New York, 1967. (d) Kessar, S. V. *Acc. Chem. Res.* **1978**, *11*, 283–288. (e) Kessar, S. In *Comprehensive Organic Synthesis*; Trost, B. M.; Fleming, I., Eds.; Pergamon Press: New York, 1991; Vol. 4, pp 483–515. (f) Hart, H. In *The Chemistry of Triple-Bonded Functional Groups Supplement C2*; Patai, S., Ed.; Wiley: New York, 1994; pp 1017–1134. (g) Sander, W. *Acc. Chem. Res.* **1999**, *32*, 669–676. (h) Pellissier, H.; Santelli, M. *Tetrahedron* **2003**, *59*, 701–730. (i) Wenk, H. H.; Winkler, M.; Sander, W. *Angew. Chem., Int. Ed.* **2003**, *42*, 502–528.
- (2) For reviews focusing specifically on heteroarynes, see: (a) Kauffmann, T. *Angew. Chem., Int. Ed., Engl.* **1965**, *4*, 543–577. (b) Den Hertog, H. J.; Van Der Plas, H. C. *Adv. Heterocycl. Chem.* **1965**, *4*, 121–144. (c) Den Hertog, H. J.; Van Der Plas, H. In *Chemistry of Acetylenes*; Viehe, H. G., Ed.; Marcel Dekker: New York, 1969; Ch. 17. (d) Kauffmann, T.; Wirthwein, R. *Angew. Chem., Int. Ed., Engl.* **1971**, *10*, 20–33. (e) Reinecke, M. G. In *Reactive Intermediates*; Abramovitch, R. A., Ed.; Plenum Press: New York, 1982; Ch. 5. (f) Van Der Plas, H. C. In *The Chemistry of Triple Bonded Groups*, Supplement C of *The Chemistry of Functional Groups*; Patai, S.; Rappoport, Z., Eds.; Wiley: New York, 1982. (g) Reinecke, M. G. *Tetrahedron* **1982**, *38*, 427–498.
- (3) Stoermer, R.; Kahlert, B. *Ber. Dtsch. Chem. Ges.* **1902**, *35*, 1633–1640.
- (4) Nef, J. V. *Justus Liebigs Ann. Chem.* **1899**, *308*, 264–328.

(5) (a) Wurtz, A. *Ann. Chim. Phys.* **1855**, *44*, 275–312. (b) Wurtz, A. *Ann. Chem. Pharm.* **1855**, *96*, 364–375. (c) Fittig, R. *Justus Liebigs Ann. Chem.* **1864**, *132*, 201–215. (d) Fittig, R. *Ann. Chem. Pharm.* **1864**, *131*, 303–323. (e) Fittig, R. *Ann. Chem. Pharm.* **1867**, *144*, 277–294.

(6) Bachmann, W. E.; Clarke, H. T. *J. Am. Chem. Soc.* **1927**, *49*, 2089–2098.

(7) Lütteringhaus, A.; v. Säaf, G. *Justus Liebigs Ann. Chem.* **1939**, *542*, 241–258.

(8) (a) Wittig, G.; Pieper, G.; Fuhrmann, G. *Ber. Dtsch. Chem. Ges.* **1940**, *73*, 1193–1197. (b) Wittig, G.; Fuhrmann, G. *Ber. Dtsch. Chem. Ges.* **1940**, *73*, 1197–1218. (c) Wittig, G. *Naturwiss.* **1942**, *30*, 696–703.

(9) For a review of nucleophilic aromatic substitution reactions, see: Bunnett, J. F.; Zahler, R. E. *Chem. Rev.* **1951**, *49*, 273–412.

(10) (a) Bergstrom, F. W.; Wright, R. E.; Chandler, C.; Gilkey, W. A. *J. Org. Chem.* **1936**, *01*, 170–178. (b) Wright, R. E.; Bergstrom, F. W. *J. Org. Chem.* **1936**, *01*, 179–188. (c) Horning, C. H.; Bergstrom, F. W. *J. Am. Chem. Soc.* **1945**, *67*, 2110–2111.

(11) For results reported prior to 1953 highlighting rearrangements observed during the amination of substituted aryl halides, see: (a) Gilman, H.; Avakian, S. *J. Am. Chem. Soc.* **1945**, *67*, 349–351. (b) Gilman, H.; Nobis, J. F. *J. Am. Chem. Soc.* **1945**, *67*, 1479–1480. (c) Gilman, H.; Crounse, N. N.; Massie, S. P., Jr.; Benkeser, R. A.; Spatz, S. M. *J. Am. Chem. Soc.* **1945**, *67*, 2106–2108. (d) Urner, R. S.; Bergstrom, F. W. *J. Am. Chem. Soc.* **1945**, *67*, 2108–2109. (e) Gilman, H.; Kyle, R. H.; Benkeser, R. A. *J. Am. Chem. Soc.* **1946**, *68*, 143–144.

(f) Bergstrom, F. W.; Horning, C. H. *J. Org. Chem.* **1946**, *11*, 334–340. (g) Gilman, H.; Kyle, R. H. *J. Am. Chem. Soc.* **1948**, *70*, 3945–3946. (h) Benkeser, R. A.; Severson, R. G. *J. Am. Chem. Soc.* **1949**, *71*, 3838–3839. (i) Benkeser, R. A.; Buting, W. E. *J. Am. Chem. Soc.* **1952**, *74*, 3011–3014. (j) Gilman, H.; Martin, G. A. *J. Am. Chem. Soc.* **1952**, *74*, 5317–5319.

(12) Benkeser, R. A.; Schroll, G. *J. Am. Chem. Soc.* **1953**, *75*, 3196–3197.

(13) Roberts, J. D.; Simmons, H. E., Jr.; Carlsmith, L. A.; Vaughan, C. W. *J. Am. Chem. Soc.* **1953**, *75*, 3290–3291.

(14) Reaction rates for additions to  $^{14}\text{C}$ -labeled positions have been noted to be as much as 16% less than those to  $^{12}\text{C}$ -positions. For example, a difference in rates of 10% is calculated to produce a 47.8 : 52.4 ratio of 1- $^{14}\text{C}$  : 2- $^{14}\text{C}$ -labeled aniline (**36 : 37**). See: Ropp, G. A. *Nucleonics* **1952**, *10*, 22–27.

(15) Roberts, J. D.; Semenow, D. A.; Simmons, H. E., Jr.; Carlsmith, L. A. *J. Am. Chem. Soc.* **1956**, *78*, 601–611.

(16) Hall, G. E.; Piccolini, R.; Roberts, J. D. *J. Am. Chem. Soc.* **1955**, *77*, 4540–4543.

(17) Panar, M.; Roberts, J. D. *J. Am. Chem. Soc.* **1960**, *82*, 3629–3632.

(18) This, in turn, places a rather lofty requirement upon both the endothermic addition of ammonia (path A or A') and loss of the halogen (path B or B') to exist as rapid equilibria. Furthermore, this mechanism requires the (most likely) exothermic loss of ammonia (path C) or re-aromatization (path C') to exist as the slow step.

(19) (a) Wittig, G.; Pohmer, L. *Angew. Chem.* **1955**, *67*, 348. (b) Wittig, G.; Pohmer, L. *Chem. Ber.* **1956**, *89*, 1334–1351.

(20) Wittig, G. *Org. Synth.* **1959**, *39*, 75–77.

(21) Sauer, J.; Huisgen, R.; Hauser, A. *Chem. Ber.* **1958**, *91*, 1461–1473.

(22) (a) Bunnett, J. F.; Brotherton, T. K. *J. Am. Chem. Soc.* **1956**, *78*, 155–158. (b) Bunnett, J. F.; Brotherton, T. K. *J. Am. Chem. Soc.* **1956**, *78*, 6265–6269. (c) Bunnett, J. F.; Brotherton, T. K. *J. Org. Chem.* **1958**, *23*, 904–906.

(23) Stiles, M.; Miller, R. G. *J. Am. Chem. Soc.* **1960**, *82*, 3802.

(24) (a) Berry, R. S.; Spokes, G. N.; Stiles, R. M. *J. Am. Chem. Soc.* **1960**, *82*, 5240–5241. (b) Berry, R. S.; Spokes, G. N.; Stiles, R. M. *J. Am. Chem. Soc.* **1962**, *84*, 3570–3577.

(25) Berry, R. S.; Clardy, J.; Schafer, M. E. *J. Am. Chem. Soc.* **1964**, *86*, 2738–2739.

(26) Fisher, I. P.; Lossing, F. P. *J. Am. Chem. Soc.* **1963**, *85*, 1018–1019.

(27) (a) Chapman, O. L.; McIntosh, C. L.; Pacansky, J.; Calder, G. V.; Orr, G. *J. Am. Chem. Soc.* **1973**, *95*, 6134–6135. (b) Chapman, O. L.; Chang, C.-C.; Kolc, J.; Rosenquist, N. R.; Tomioka, H. *J. Am. Chem. Soc.* **1975**, *97*, 6586–6588.

(28) Benzocyclopropenone (**62**) was later fully characterized by low-temperature <sup>1</sup>H and <sup>13</sup>C NMR. See: Simon, J. G. G.; Schweig, A. *Chem. Phys. Lett.* **1993**, *201*, 377–382.

(29) Bell, E. E.; Neilsen, H. H. *J. Chem. Phys.* **1950**, *18*, 1382–1394.

(30) Dunkin, I. R.; MacDonald, J. G. *J. Chem. Soc., Chem. Commun.* **1979**, 772–773.

(31) (a) Laing, J. W.; Berry, R. S. *J. Am. Chem. Soc.* **1976**, *98*, 660–664. (b) Nam, N.-H.; Leroi, G. E. *Spectrochim. Acta* **1985**, *41*, 67–73. (c) Scheiner, A. C.; Schaefer, H. F., III; Liu, B. *J. Am. Chem. Soc.* **1989**, *111*, 3118–3124.

(32) (a) Wentrup, C.; Blanch, R.; Briehl, H.; Gross, G. *J. Am. Chem. Soc.* **1988**, *110*, 1874–1880. (b) Simon, J. G. G.; Münzel, N.; Schweig, A. *Chem. Phys. Lett.* **1990**, *170*, 187–192.

(33) Radziszewski, J. G.; Hess, B. A., Jr.; Zahradník, R. *J. Am. Chem. Soc.* **1992**, *114*, 52–57.

(34) The large singlet-triplet splitting ( $37.5 \pm 0.3 \text{ kcal}\cdot\text{mol}^{-1}$ ) suggests that benzyne preferentially occupies a singlet ground state. For measurements, see: (a) Wentholt, P. G.; Squires, R. R.; Lineberger, W. C. *J. Am. Chem. Soc.* **1998**, *120*, 5279–5290. (b) Leopold, D. G.; Miller, A. E. S.; Lineberger, W. C. *J. Am. Chem. Soc.* **1986**, *108*, 1379–1384.

(35) (a) Grützmacher, H.-F.; Lohmann, J. *Justus Liebigs Ann. Chem.* **1966**, 705, 81–90. (b) Pollack, S. K.; Hehre, W. J. *Tetrahedron Lett.* **1980**, *21*, 2483–2486. (c) Riveros, J. M.; Ingemann, S.; Nibbering, N. M. M. *J. Am. Chem. Soc.* **1991**, *113*, 1053. (d) Guo, Y.; Grabowski, J. J. *J. Am. Chem. Soc.* **1991**, *113*, 5923–5931. (e) Wentholt, P. G.; Paulino, J. A.; Squires, R. R. *J. Am. Chem. Soc.* **1991**, *113*, 7414–7415. (f) Wentholt, P. G.; Squires, R. R. *J. Am. Chem. Soc.* **1994**, *116*, 6401–6412.

(36) Orendt, A. M.; Facelli, J. C.; Radziszewski, J. G.; Horton, W. J.; Grant, D. M.; Michl, J. *J. Am. Chem. Soc.* **1996**, *118*, 846–852.

(37) Warmuth, R. *Angew. Chem., Int. Ed., Engl.* **1997**, *36*, 1347–1350.

(38) Robbins, T. A.; Knobler, C. B.; Bellew, D. R.; Cram, D. J. *J. Am. Chem. Soc.* **1994**, *116*, 111–122.

(39) Kuehne, M. E. *J. Am. Chem. Soc.* **1962**, *84*, 837–847.

(40) (a) Wittig, G.; Härle, H. *Justus Liebigs Ann. Chem.* **1959**, *623*, 17–34. (b) Huisgen, R.; Knorr, R. *Tetrahedron Lett.* **1963**, *4*, 1017–1021. (c) Wittig, G.; Ludwig, R. *Angew. Chem.* **1956**, *68*, 40. (d) Wittig, G.; Knauss, E. *Chem. Ber.* **1958**, *91*, 895–907. (e) Wittig, G.; Behnisch, W. *Chem. Ber.* **1958**, *91*, 2358–2365. (f) Wittig, G.; Knauss, E.; Niethamer, K. *Justus Liebigs Ann. Chem.* **1960**, *630*, 10–18. (g) Aitken, I. M.; Reid, D. H. *J. Chem. Soc.* **1960**, 663–665. (h) Simmons, H. E. *J. Am. Chem. Soc.* **1961**, *83*, 1657–1664. (i) Wittig, G.; Dürr, H. *Justus Liebigs Ann. Chem.* **1964**, *672*, 55–62. (j) Wolthuis, E.; De Boer, A. *J. Am. Chem. Soc.* **1965**, *30*, 3225–3227.

(41) Hellmann, H.; Eberle, D. *Justus Liebigs Ann. Chem.* **1963**, *662*, 188–201.

(42) (a) Seyferth, D.; Burlitch, J. M. *J. Org. Chem.* **1963**, *28*, 2463–2464. (b) Griffin, C.; Castellucci, N. *J. Org. Chem.* **1961**, *26*, 629–630.

(43) (a) Hantzsch, A.; Davidson, W. B. *Ber. Dtsch. Chem. Ges.* **1896**, *29*, 1522–1536. (b) Hantzsch, A.; Glogauer, R. *Ber. Dtsch. Chem. Ges.* **1897**, *30*, 2548–2559.

(44) (a) Wittig, G.; Hoffmann, R. W. *Chem. Ber.* **1962**, *95*, 2718–2728. (b) Wittig, G.; Hoffmann, R. W. *Org. Synth.* **1967**, *47*, 4–8.

(45) Beringer, F. M.; Huang, S. J. *J. Org. Chem.* **1964**, *29*, 445–448.

(46) For examples of aryne precursors **59**, **68**, and **69** employed in synthesis, see: (a) Huisgen, R.; Knorr, R.; Möbius, L.; Szeimies, G. *Chem. Ber.* **1965**, 4014–4021. (b) Nair, V.; Kim, K. H. *J. Org. Chem.* **1975**, *40*, 3784–3786. (c) Saá, C.; Gutián, E.; Castedo, L.; Suau, R.; Saá, J. M. *J. Org. Chem.* **1986**, *51*, 2781–2784. (d) Atanes, N.; Castedo, L.; Gutián, E.; Saá, C.; Saá, J. M.; Suau, R. *J. Org. Chem.* **1991**, *56*, 2984–2988. (e) Matsumoto, K.; Katsura, H.; Uchida, T.; Aoyama, K.; Machiguchi, T. *J. Chem. Soc., Perkin Trans. 1* **1996**, 2599–2602. (f) Yamabe, S.; Minato, T.; Ishiwata, A.; Irinimihira, O.; Machiguchi, T. *J. Org. Chem.* **2007**, *72*, 2832–2841.

(47) Trave, R.; Bianchetti, G. *Atti. Accad. Naz. Lincei, Rend. Classe Sci. Fis. Mat. Nat.* **1960**, *28*, 652.

(48) (a) Campbell, C. D.; Rees, C. W. *Proc. Chem. Soc.* **1962**, 296. (b) Campbell, C. D.; Rees, C. W. *J. Chem. Soc. C* **1969**, 742–747.

(49) For examples of 1-aminobenzotriazole (**70**) employed in synthesis, see: (a) Perera, R. C.; Smalley, R. K. *J. Chem. Soc. D: Chem. Commun.* **1970**, 1458–1459. (b) Rigby, J. H.; Holsworth, D. D.; James, K. *J. Org. Chem.* **1989**, *54*, 4019–4020. (c) Rigby, J. H.; Holsworth, D. D. *Tetrahedron Lett.* **1991**, *32*, 5757–5760. (d) Birkett, M. A.; Knight, D. W.; Little, P. B.; Mitchell, M. B. *Tetrahedron* **2000**, *56*, 1013–1023. (e) Vagin, S. I.; Frickenschmidt, A.; Kammerer, B.; Hanack, M. *Chem. Eur. J.* **2005**, *11*, 6568–6573.

(50) (a) Birkett, M. A.; Knight, D. W.; Mitchell, M. B. *Tetrahedron Lett.* **1993**, *34*, 6939–6940. (b) Birkett, M. A.; Knight, D. W.; Mitchell, M. B. *Synlett* **1994**, 253–254. (c) Knight, D. W.; Little, P. B. *Tetrahedron Lett.* **1998**, *39*, 5105–5108.

(51) Himeshima, Y.; Sonoda, T.; Kobayashi, H. *Chem. Lett.* **1983**, 1211–1214.

(52) (a) Yoshida, H.; Morishita, T.; Ohshita, J. *Org. Lett.* **2008**, *10*, 3845–3847. (b) Cant, A. A.; Bertrand, G. H. V.; Henderson, J. L.; Roberts, L.; Greaney, M. F. *Angew. Chem., Int. Ed.* **2009**, *48*, 5199–5202.

(53) Beltrán-Rodil, S.; Peña, D.; Gutián, E. *Synlett* **2007**, 1308–1310.

(54) Liu, Y.-L.; Liang, Y.; Pi, S.-F.; Huang, X.-C.; Li, J.-H. *J. Org. Chem.* **2009**, *74*, 3199–3202.

(55) (a) Hayes, M. E.; Shinokubo, H.; Danheiser, R. L. *Org. Lett.* **2005**, *7*, 3917–3920. (b) Jayanth, T. T.; Jeganmohan, M.; Cheng, M.-J.; Chu, S.-Y.; Cheng, C.-H. *J. Am. Chem. Soc.* **2006**, *128*, 2232–2233.

(56) (a) Ramtohul, Y.; Chartrand, A. *Org. Lett.* **2007**, *9*, 1029–1032. (b) Gilmore, C. D.; Allan, K. M.; Stoltz, B. M. *J. Am. Chem. Soc.* **2008**, *130*, 1558–1559. (c) Blackburn, T.; Ramtohul, Y. K. *Synlett* **2008**, 1159–1164. (d) Feltenberger, J. B.; Hayashi, R.; Tang, Y.; Babiash, E. S. C.; Hsung, R. P. *Org. Lett.* **2009**, *11*, 3666–3669.

(57) Liu, Y.-L.; Liang, Y.; Pi, S.-F.; Li, J.-H. *J. Org. Chem.* **2009**, *74*, 5691–5694.

(58) (a) Jeganmohan, M.; Cheng, C.-H. *Chem. Commun.* **2006**, 2454–2456. (b) Xie, C.; Zhang, Y. *Org. Lett.* **2007**, 9, 781–784. (c) Rogness, D. C.; Larock, R. C. *Tetrahedron Lett.* **2009**, 50, 4003–4008. (d) Giacometti, R. D.; Ramtohul, Y. K. *Synlett* **2009**, 2010–2016.

(59) (a) Yoshida, H.; Watanabe, M.; Fukushima, H.; Ohshita, J.; Kunai, A. *Org. Lett.* **2004**, 6, 4049–4051. (b) Yoshida, H.; Morishita, T.; Fukushima, H.; Ohshita, J.; Kunai, A. *Org. Lett.* **2007**, 9, 3367–3370. (c) Morishita, T.; Fukushima, H.; Yoshida, H.; Ohshita, J.; Kunai, A. *J. Org. Chem.* **2008**, 73, 5452–5457.

(60) Yoshida, H.; Fukushima, H.; Ohshita, J.; Kunai, A. *J. Am. Chem. Soc.* **2006**, 128, 11040–11041.

(61) Xie, C.; Zhang, Y.; Xu, P. *Synlett* **2008**, 3115–3120.

(62) Gerfaud, T.; Neuville, L.; Zhu, J. *Angew. Chem., Int. Ed.* **2009**, 48, 572–577.

(63) (a) Tambar, U. K.; Stoltz, B. M. *J. Am. Chem. Soc.* **2005**, 127, 5340–5341. (b) Yoshida, H.; Watanabe, M.; Ohshita, J.; Kunai, A. *Chem. Commun.* **2005**, 3292–3294.

(64) (a) Liu, Z.; Larock, R. C. *J. Am. Chem. Soc.* **2005**, 127, 13112–13113. (b) Dockendorff, C.; Sahli, S.; Olsen, M.; Milhau, L.; Lautens, M. *J. Am. Chem. Soc.* **2005**, 127, 15028–15029. (c) Webster, R.; Lautens, M. *Org. Lett.* **2009**, 11, 4688–4691.

(65) (a) Yoshida, H.; Fukushima, H.; Ohshita, J.; Kunai, A. *Angew. Chem., Int. Ed.* **2004**, 43, 3935–3938. (b) Yoshida, H.; Fukushima, H.; Ohshita, J.; Kunai, A. *Tetrahedron Lett.* **2004**, 45, 8659–8662.

(66) Jin, T.; Yamamoto, Y. *Angew. Chem., Int. Ed.* **2007**, *46*, 3323–3325.

(67) Matsumoto, T.; Hosoya, T.; Katsuki, M.; Suzuki, K. *Tetrahedron Lett.* **1991**, *32*, 6735–6736.

(68) Kitamura, T.; Yamane, M. *J. Chem. Soc., Chem. Commun.* **1995**, 983–984.

(69) Biehl, E. R.; Nieh, E.; Li, H.-M.; Hong, C.-I. *J. Org. Chem.* **1969**, *34*, 500–505.

(70) Biehl, E. R.; Nieh, E.; Hsu, K. C. *J. Org. Chem.* **1969**, *34*, 3595–3599.

(71) Hammett, L. P. *J. Am. Chem. Soc.* **1937**, *59*, 96–103.

(72) For a survey of Hammett substituent constants, see: Hansch, C.; Leo, A.; Taft, R. W. *Chem. Rev.* **1991**, *91*, 165–195.

(73) The reactivity factor (RF) is defined as follows:

$$RF = \log \left( \frac{\text{yield } \mathbf{86}+\mathbf{87}}{\text{yield } \mathbf{84}+\mathbf{85}} \right)_{\text{sub}} / \left( \frac{\text{yield } \mathbf{86a}+\mathbf{87a}}{\text{yield } \mathbf{84a}+\mathbf{85a}} \right)_{\text{unsub}}$$

where  $(\text{yield } \mathbf{86}+\mathbf{87})_{\text{sub}} / (\text{yield } \mathbf{84}+\mathbf{85})_{\text{sub}}$  is the product ratio for a substituted alkyne and  $(\text{yield } \mathbf{86a}+\mathbf{87a})_{\text{unsub}} / (\text{yield } \mathbf{84a}+\mathbf{85a})_{\text{unsub}}$  is the product ratio for benzyne (entry 1, R = H).

# CHAPTER 2

## *Orthogonal Synthesis of Indolines and Isoquinolines via Aryne Annulation*

### 2.1 INTRODUCTION

Aryne annulation is a powerful technique for the synthesis of fused arene-containing polycyclic systems.<sup>1</sup> In the present discussion, this term will be used to describe methods that construct a new fused ring at the two carbon atoms of the reactive triple bond of an aryne. Such methods may proceed through either a concerted pericyclic mechanism or a stepwise polar mechanism. The following sections describe the major synthetic approaches that have been developed within the field of aryne annulation and provide examples of each. While some of these techniques trace their origins back more than half a century, the focus of this chapter is given primarily to those applications reported most recently and often in the context of natural product total synthesis. Discussion is also limited to examples featuring at most two reaction partners (and occasionally two reactive sites within a single molecule), one of which is the aryne. A discussion of ring-forming reactions involving three or more reaction partners will be provided in Chapter 6.

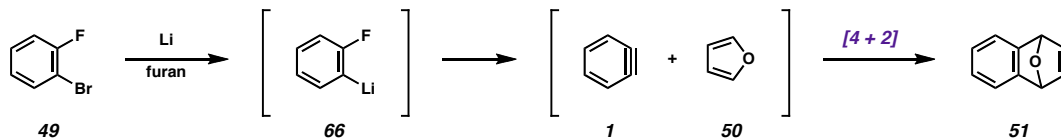
## 2.2 PREVIOUS METHODS OF ARYNE ANNULATION

### 2.2.1 Aryne Annulation via Cycloaddition

#### 2.2.1.1 [4 + 2] Cycloadditions

The earliest example of aryne annulation is a Diels–Alder cycloaddition between benzyne (**1**) and furan (**50**) carried out by Wittig and Pohmer in 1955 (Scheme 2.1).<sup>2</sup> In this report, the authors treated 2-bromofluorobenzene (**49**) with lithium metal to generate 2-fluorophenyllithium (**66**), an intermediate that undergoes elimination of an equivalent of lithium fluoride to form the reactive aryne in situ. When this reaction was performed in a solution of furan, a subsequent [4 + 2] cycloaddition occurred to produce benzannulated oxabicyclo[2.2.1]heptadiene **51** in 76% yield.

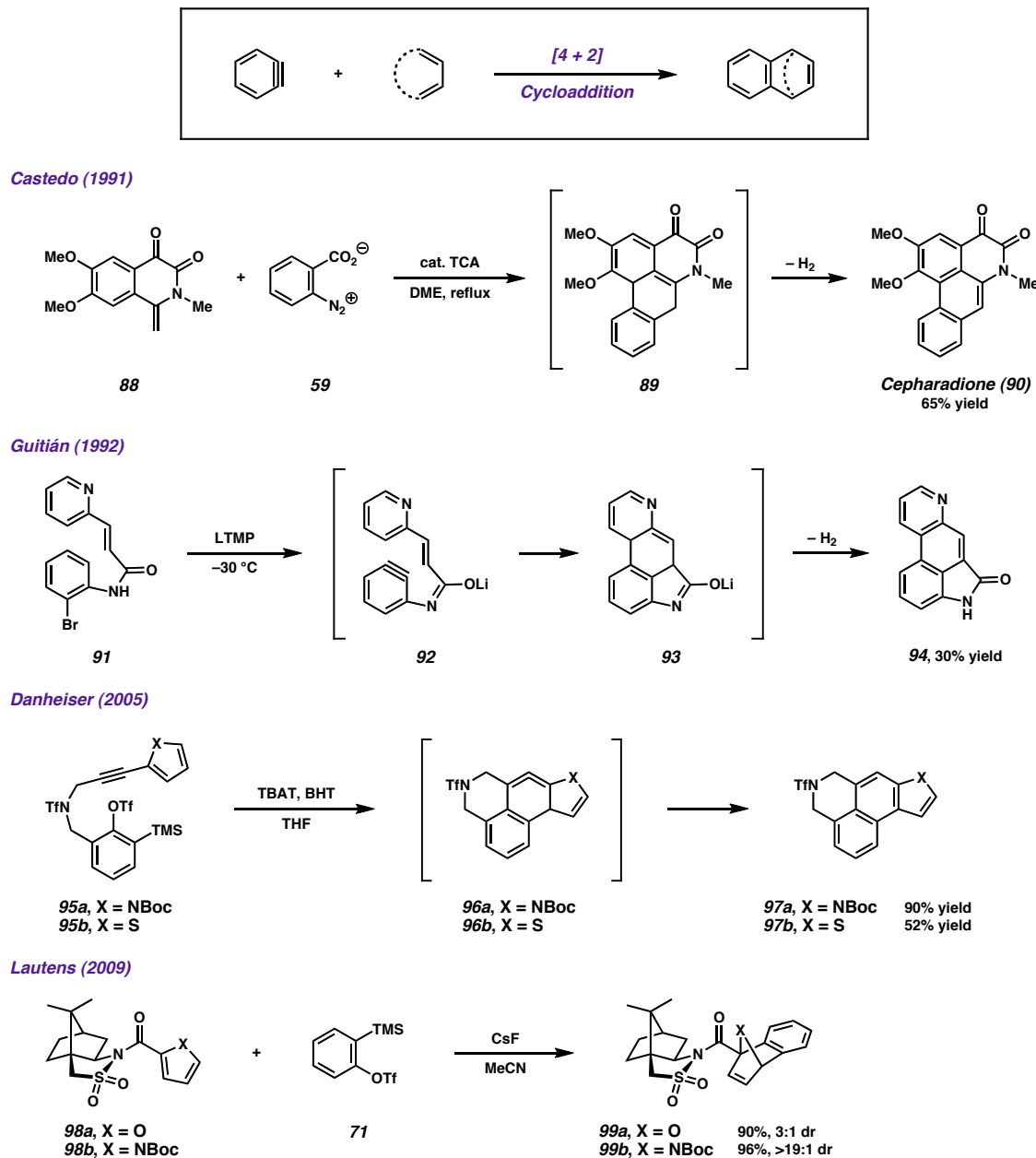
Scheme 2.1. Annulation of benzyne via Diels–Alder cycloaddition with furan



Since this initial discovery, numerous examples of [4 + 2] cycloadditions with arynes have been reported in the literature. The diene substrate scope is continually expanding, and now includes several nitrogen-, oxygen-, and sulfur-containing heterodienes,<sup>3</sup> transition metal complexes,<sup>4</sup> and even other aromatic structures.<sup>5</sup> Furthermore, aryne annulation via [4 + 2] cycloaddition has become a popular approach in natural product total synthesis.<sup>6</sup> In 1991, Castedo *et al.* developed an approach to the aporphinoids that employed a [4 + 2] cycloaddition between methylene isoquinolines such as **88** and arynes generated from aryl diazonium-2-carboxylates (**59**) (Scheme 2.2).<sup>7</sup> In the example shown,

the cycloaddition produces tetracycle **89**, which spontaneously undergoes dehydrogenation to furnish cephadione (**90**) in 65% yield. A year later, a collaborating laboratory reported a similar approach to the core of the ergot alkaloids (**94**) using an intramolecular aryne [4 + 2] cycloaddition with a vinyl pyridine (**91** → **92** → **93**).<sup>8</sup> More recently, the Danheiser research group showed that enynes (**95a** and **b**) are also capable of undergoing intramolecular [4 + 2] cycloaddition with tethered arynes to generate highly strained cyclic alenes (**96a** and **b**), which rearrange to more stable naphthalene products (**97a** and **b**).<sup>9</sup> Finally, the Lautens group has successfully employed benzyne in a number of auxiliary-mediated diastereoselective cycloadditions using pyrrole- and furan-2-carboxylates appended to Oppolzer's sultam (**98a** and **b**) as the chiral diene.<sup>10</sup> The heteroatom-bridged tricyclic products (**99a** and **b**) are isolated in excellent yield with high levels of diastereoselectivity. These results are particularly noteworthy given that only two other reports of stereoselective reactions involving arynes have been made thus far.<sup>11</sup>

*Scheme 2.2. Aryne annulation via [4 + 2] cycloaddition*

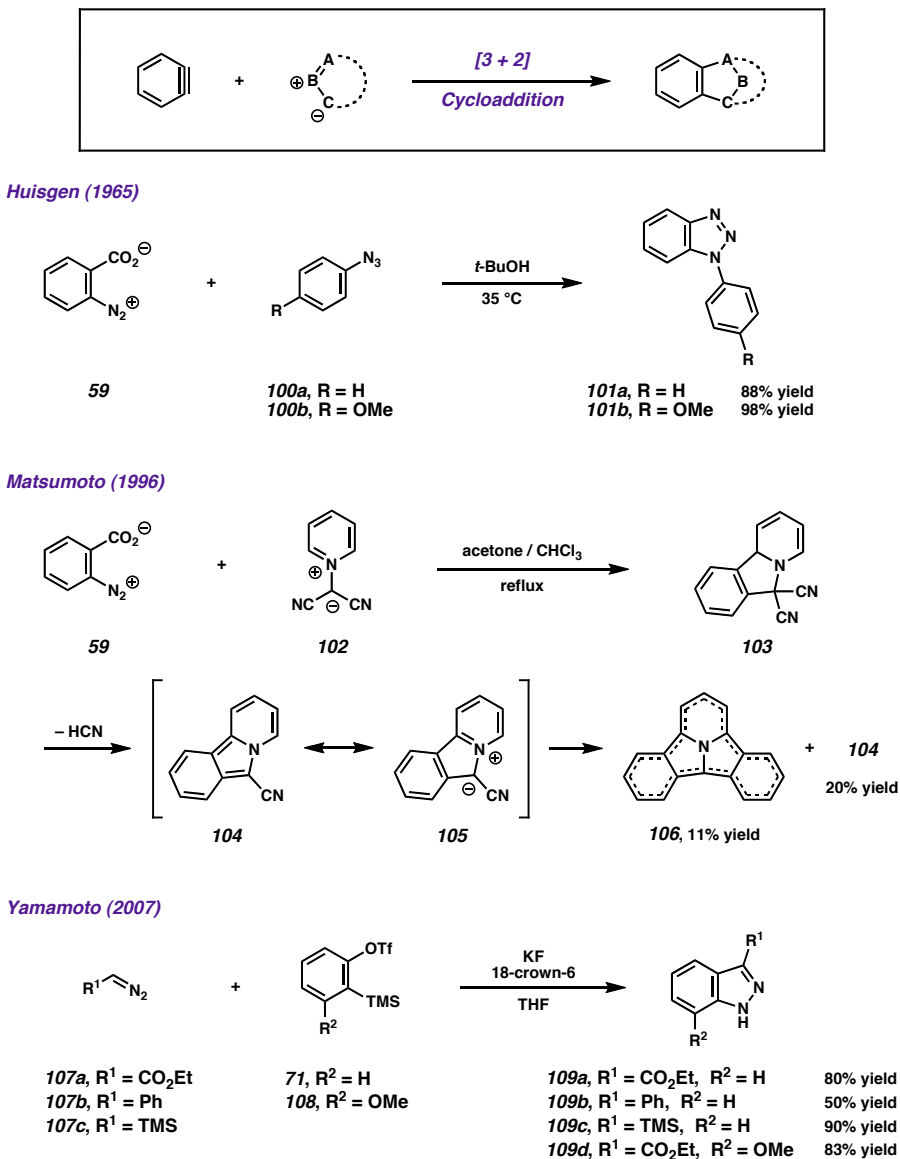


### 2.2.1.2 [3 + 2] Cycloadditions

In addition to cycloadditions with 1,3-dienes, benzyne has been shown to undergo [3 + 2] cycloadditions with a variety of stable 1,3-dipolar compounds. The earliest reports describe cycloadditions between arynes and organic azides (**100a** and **b**), including a

report by Huisgen and co-workers in which benzyne is generated from phenyldiazonium-2-carboxylate (**59**) (Scheme 2.3).<sup>12,13</sup> Unlike similar copper-catalyzed alkyne-azide cycloadditions,<sup>14</sup> the strained triple bond of benzyne is capable of reacting to form benzotriazoles such as **101a** and **b** in the absence of a transition metal catalyst.<sup>15</sup> Following these early discoveries, additional examples of aryne [3 + 2] cycloadditions have been demonstrated using nitrile oxides,<sup>16</sup> nitrones,<sup>17</sup> azomethine ylides,<sup>18</sup>  $\alpha$ -diazoketones,<sup>19</sup> and various nitrogen-containing heterocycle *N*-oxides.<sup>20</sup> In 1996, Matsumoto *et al.* reported the synthesis of an intriguing extended heteroaromatic polycycle (**106**) through two consecutive dipolar cycloadditions between benzyne and pyridinium cyanomethides **102** and **105**.<sup>21</sup> In a modern approach to a method originally developed by Huisgen,<sup>17a</sup> Yamamoto *et al.* accomplished the synthesis of a series of 1*H*-indazoles (**109a–d**) using a [3 + 2] cycloaddition between benzyne derived from *ortho*-silyl aryl triflates (**71** and **108**) and substituted derivatives of diazomethane (**107a–c**).<sup>22</sup> Yields and regioselectivities were generally good and, remarkably, the products did not undergo the 1,2-acyl shift characteristic of indazoles generated from  $\alpha$ -diazoketones.<sup>19,23</sup>

Scheme 2.3. Aryne annulation via [3 + 2] cycloaddition



## 2.2.2 Aryne Annulation via Stepwise Polar Mechanisms

### 2.2.2.1 Nucleophilic Addition and Cyclization

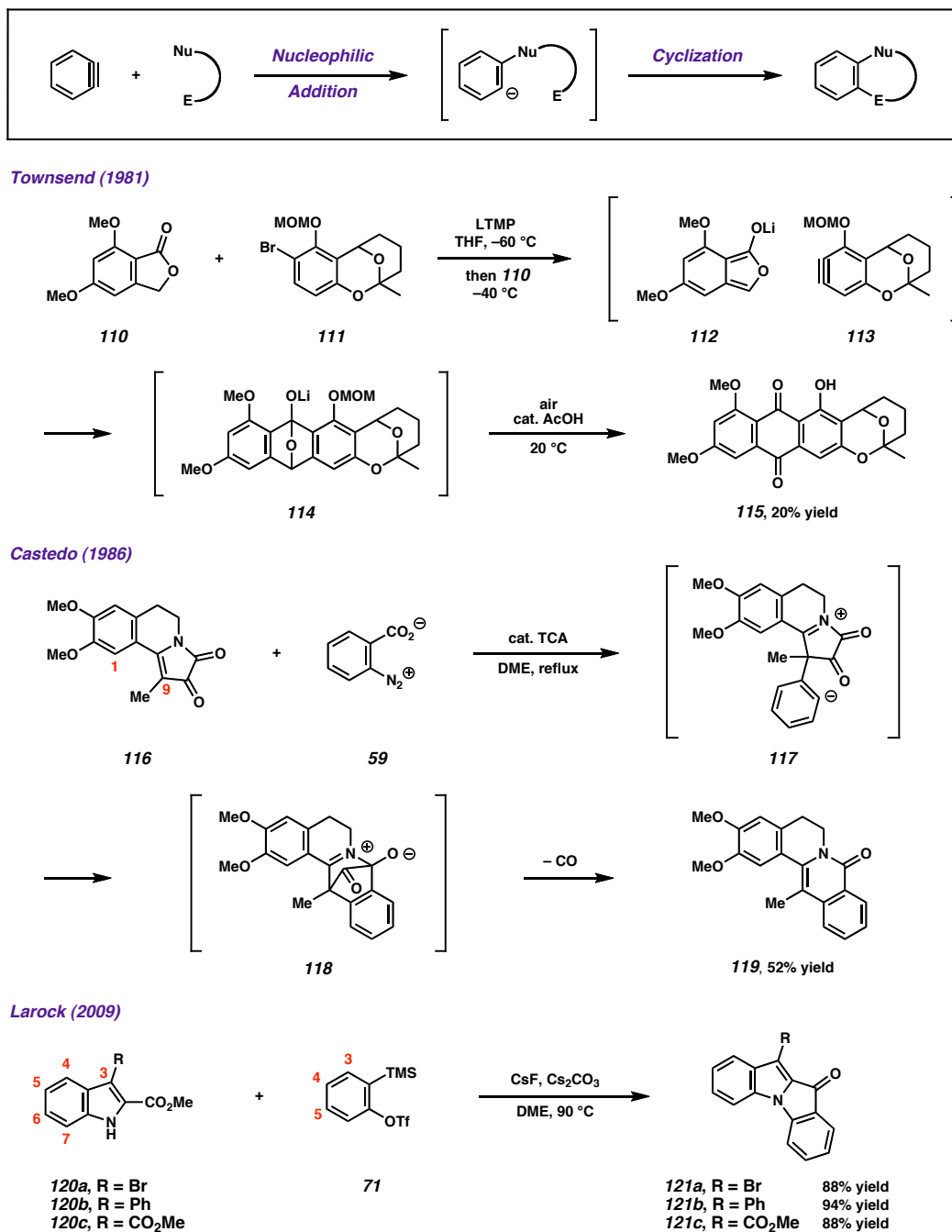
Examples of aryne annulation occurring through a stepwise addition pathway constitute the majority of reported approaches. While certain cases may be further classified as formal cycloadditions or bond insertions (*vide infra*), the general mechanism

common to each of these reactions includes an intermolecular attack by a nucleophile on the aryne triple bond followed by attack of the resulting aryl anion on an intramolecular electrophile in order to close a ring. Over the past several decades, aryne annulations have been carried out with a tremendous variety of nucleophiles, including amines,<sup>24</sup> epoxides,<sup>25</sup> indoles,<sup>26</sup> enolates,<sup>27</sup> and enamines.<sup>28</sup> In contrast, there is far less variation in the choice of terminating electrophile, and in most cases this group is a carbonyl.

In 1981, Townsend *et al.* developed a convergent approach to the polyketide, averufin, using an annulation between the lithium enolate of phthalide **110** and unsymmetrical aryne **113** to form the central ring of the anthraquinone (Scheme 2.4).<sup>29</sup> Following cyclization, the lithiated intermediate (**114**) was exposed to acetic acid and ambient air to generate averufin dimethyl ether (**115**) in 20% yield. Five years later, the Castedo research group at CSIC in Spain sought to use isoquinolinopyrrolidine diones such as **116** in an approach to aporphinoid alkaloids, forming bonds from C(1) and C(9) to an aryne using a [4 + 2] cycloaddition.<sup>30</sup> Instead, the authors isolated 8-oxoprotoberberine **119** in 52% yield, presumably arising through attack on the aryne by the *N*-acyl enamine to form zwitterion **117**. Addition of the aryl anion to the carbonyl of the *N*-acyl iminium ion followed by extrusion of an equivalent of carbon monoxide from **118** would then produce the observed tetracycle. In a final example, Larock *et al.* reported a facile method for the preparation of fused indole-indolone scaffolds (**121a–c**) through an addition/cyclization sequence between methyl indole-2-carboxylates (**120a–c**) and arynes.<sup>31</sup> Importantly, the reaction tolerated a wide range of substitution on the

indole framework at carbons 3–7 and on the aryne framework at carbons 3–5, providing access to over 20 novel heteroaromatic structures in rapid fashion.

Scheme 2.4. Aryne annulation via nucleophilic addition and cyclization



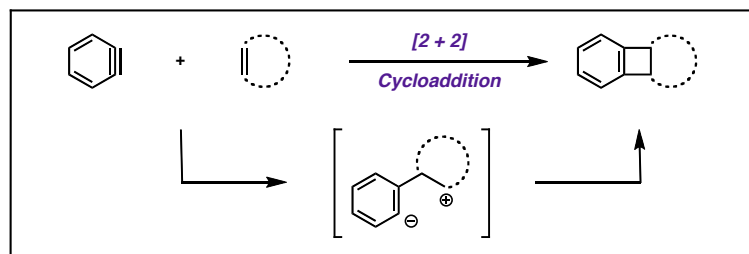
### 2.2.2.2 [2 + 2] Cycloadditions

Since its discovery, benzyne has been observed to undergo homodimerization to form biphenylene (**60**) in the absence of more reactive partners (Scheme 2.5).<sup>2,32</sup> Although this product appears to arise through a [2 + 2] cycloaddition, it is important to note that a concerted mechanism is disallowed under thermal conditions.<sup>33</sup> Therefore, the formation of benzocyclobutenes is envisioned to proceed through a polar mechanism beginning with a Prins-like addition of the olefin to the aryne triple bond followed by closure of the four-membered ring through addition of the aryl anion to the homobenzylic carbocation. This stepwise mechanism is supported by the high degree of regiochemical fidelity observed during the addition of a ketene acetal (**123**) to an unsymmetrical aryne derived from bromide **122**.<sup>34</sup> If the mechanism were concerted, the ketone (**125**) obtained upon hydrolysis of the benzocyclobutene acetal (**124**) would derive from a contra-steric cycloaddition. Instead, the observed selectivity more closely parallels the addition of simple nucleophiles to polarized arynes.

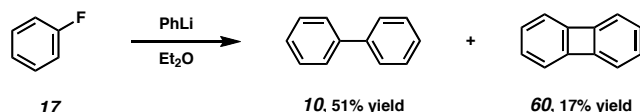
Arynes have been shown to participate in formal [2 + 2] cycloadditions with a wide variety of unsaturated species,<sup>35</sup> ranging from simple unsaturated hydrocarbons such as norbornadiene<sup>36</sup> (**126**) to heteroatom substituted olefins (**123**) and even azirines (**128**) en route to indoles (**130**).<sup>37</sup> In a remarkable demonstration of the versatility of aryne cycloaddition technology, Hsung *et al.* accomplished the synthesis of a series of arene-containing polycyclic amines (e.g., **134**) using a tandem sequence involving an aryne-enamine [2 + 2] cycloaddition followed by ring opening of the resulting benzocyclobutene (**132**) to form an intermediate *ortho*-quinone dimethide (**133**), which then undergoes a [4 + 2] cycloaddition with a tethered olefin to form the central six-

membered ring.<sup>38</sup> In total, this reaction creates four new C–C bonds and two new rings in the course of a procedurally simple one-pot process.

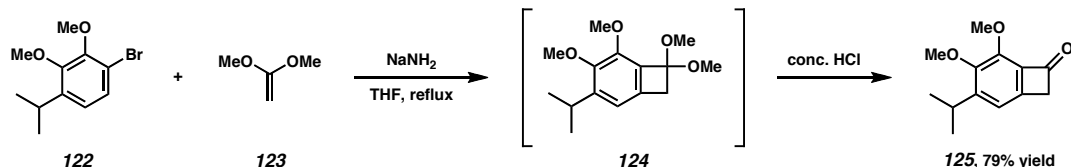
Scheme 2.5. Aryne annulation via [2 + 2] cycloaddition



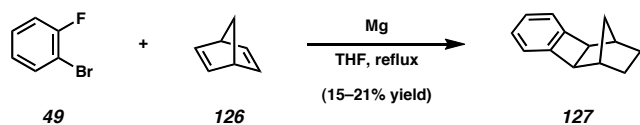
Wittig (1956)



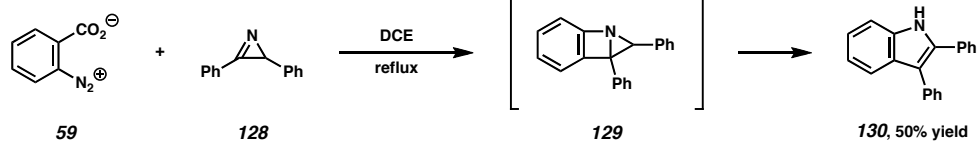
Stevens (1982)



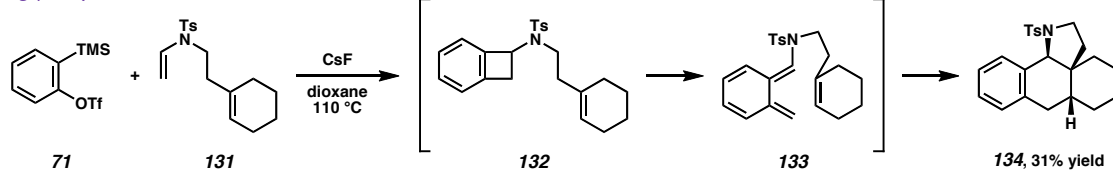
Simmons (1961)



Nair (1975)



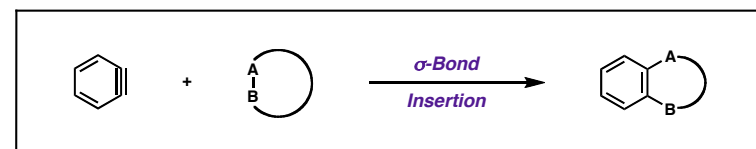
Hsung (2009)



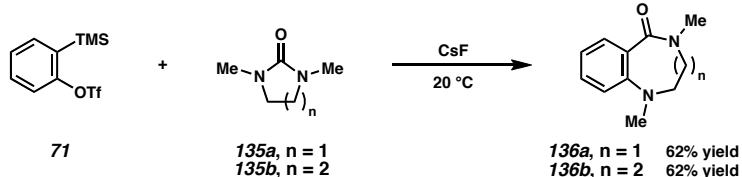
### 2.2.2.3 Insertion into Activated $\sigma$ -Bonds

The final class of aryne annulation reactions characterized by a stepwise polar mechanism consists of a small group of  $\sigma$ -bond insertions developed within the past seven years.<sup>39</sup> Like the formal [2 + 2] cycloadditions described above, reactions in this class can be adequately depicted as proceeding through a nucleophilic addition/cyclization mechanism.<sup>40</sup> However, since each of the five products shown below constitutes the two-carbon ring expansion of a cyclic substrate through the formal insertion of an aryne into a C–C or C–N bond, these reactions are given their own distinct subcategory.

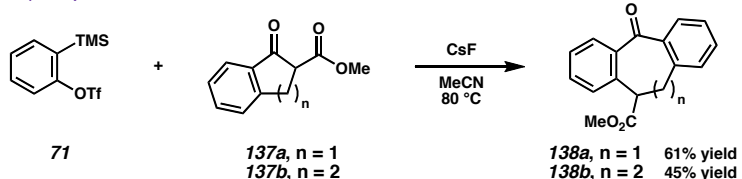
The first example of a formal  $\sigma$ -bond insertion was reported in 2002 by Shirakawa, Hiyama, and co-workers at Kyoto University.<sup>41</sup> The authors found that by adding *ortho*-silyl aryl triflates (**71**) to neat solutions of various cyclic ureas (**135a** and **b**) in the presence of caesium fluoride, they could achieve the synthesis of a wide range of benzannulated diazocines (**136a** and **b**) in good yield (Scheme 2.6). Three years later, our group communicated the formal insertion of an aryne into a C–C bond, accomplishing the synthesis of benzannulated and dibenzannulated carbocycles (**138a** and **b**) through the acyl-alkylation of arynes with cyclic  $\beta$ -ketoester substrates (**137a** and **b**).<sup>42,43</sup> In the next four years, three additional examples of C–C bond insertion have been reported by Kunai,<sup>44</sup> Li,<sup>45</sup> and Huang<sup>46</sup> using cyclic malonates (**139a** and **b**),  $\beta$ -ketophosphonates (**141**), and  $\beta$ -ketosulfones (**143a–d**), respectively, to form a variety of benzannulated medium rings.

Scheme 2.6. Aryne annulation via insertion into activated  $\sigma$ -bonds

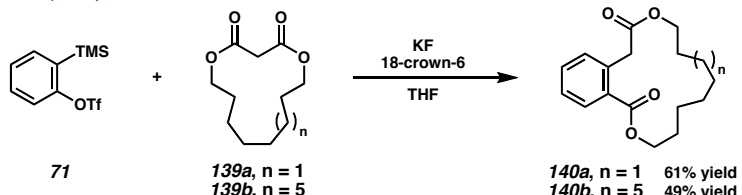
Yoshida (2002)



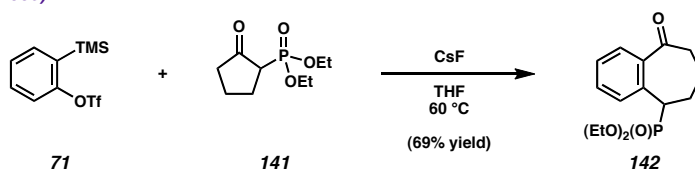
Stoltz (2005)



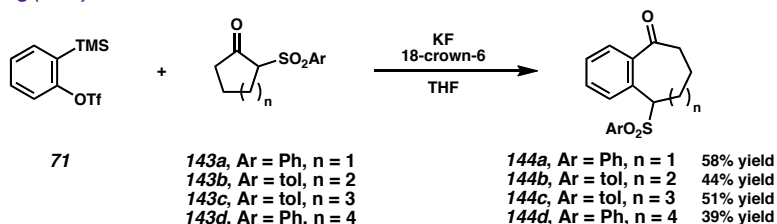
Yoshida (2005)



Li (2009)



Huang (2009)



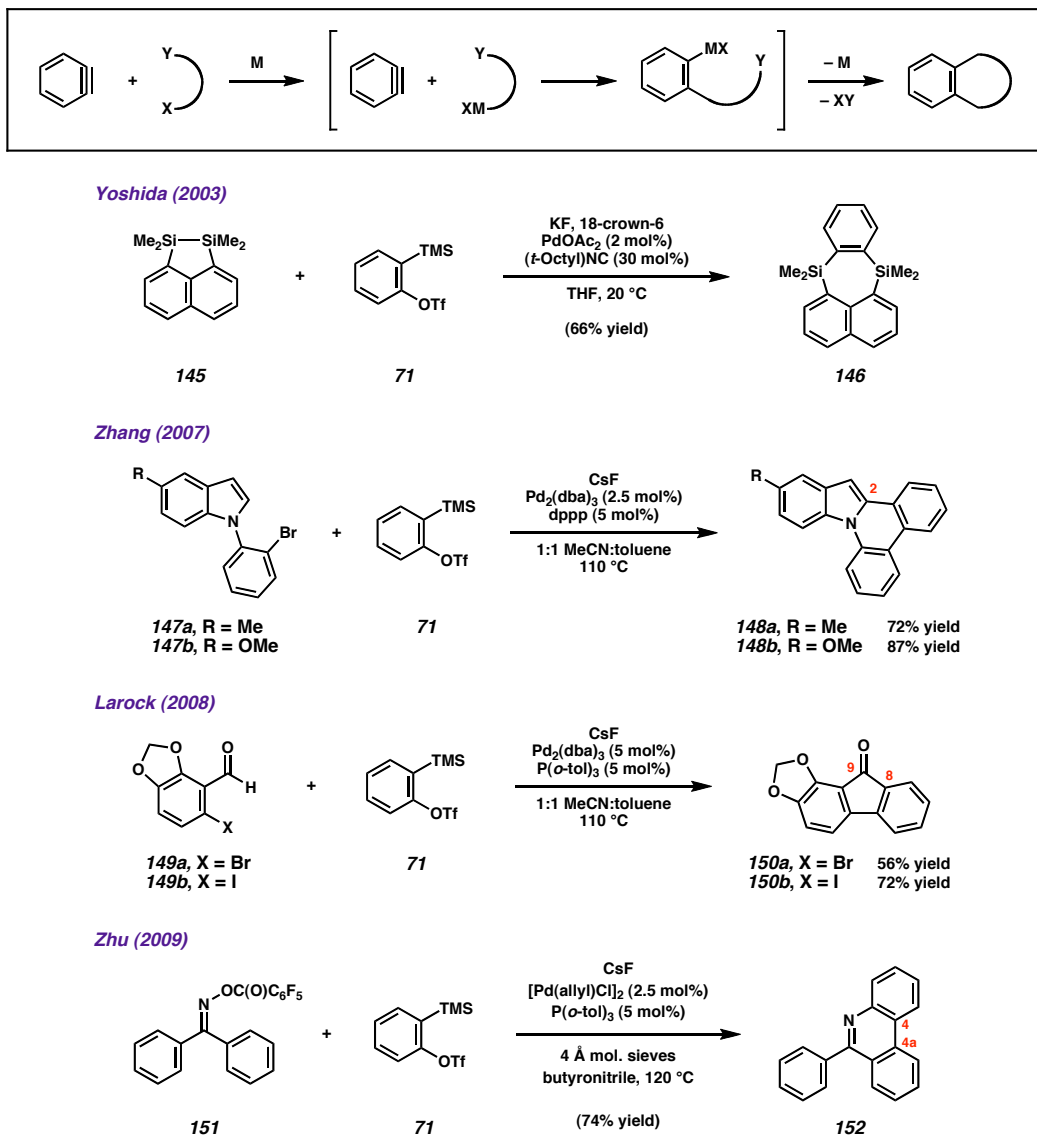
### 2.2.3 Transition Metal-Catalyzed Aryne Annulation

The examples of aryne annulation discussed prior to this point in the chapter proceed under metal-free conditions, typically requiring heat, fluoride, or a strong base as the only reagent in addition to the aryne precursor and its reaction partner. However, a number of transition metal-catalyzed reactions also incorporate arynes, often as a relay species in a Heck-type migratory insertion mechanism.<sup>47</sup> Due to the tremendous variation in the substrates employed in these reactions and the product structures they afford, it would be difficult to provide a comprehensive discussion of transition-metal catalyzed aryne annulation chemistry within this section. As such, a selection of representative reactions has been chosen to demonstrate a few of the products attainable using a catalyst-based approach.

In analogy to the  $\sigma$ -bond insertion approach discussed above, Kunai *et al.* developed a palladium-catalyzed synthesis of benzannulated disilacarbocycles (**146**) based on the formal insertion of an aryne into the Si–Si bond of five-membered cyclic disilanes such as **145** (Scheme 2.7).<sup>48</sup> The reaction employs a unique Pd(*tert*-octylisocyanide) complex, a catalyst developed by Ito *et al.* in 1991 for the bis-silylation of alkynes.<sup>49</sup> In 2007, Zhang and co-workers reported a palladium-catalyzed synthesis of indolo[1,2-*f*]phenanthridines (**148a** and **b**) from *N*-aryl indoles (**147a** and **b**) and arynes.<sup>50</sup> Given the expectation that oxidative insertion of palladium into the C–Br bond of **147** is followed by migratory insertion across benzyne, the authors propose C–H activation as the final step of the catalytic cycle to form the C–C bond between C(2) of the indole and the aryl ring. One year later, Larock *et al.* demonstrated a method for the preparation of fluoren-9-ones (**150a** and **b**) from *ortho*-halobenzaldehydes (**149a** and **b**) and arynes.<sup>51</sup> Similar to

the previous example, formation of the C(8)–C(9) bond requires an oxidative process, either palladium-catalyzed activation of the formyl C–H bond or migratory insertion of an intermediate Pd–C complex across the C=O bond followed by  $\beta$ -hydride elimination. Finally, Zhu and co-workers at CNRS developed a novel approach to the synthesis of substituted isoquinoline motifs (**152**) that proceeds through a palladium-catalyzed

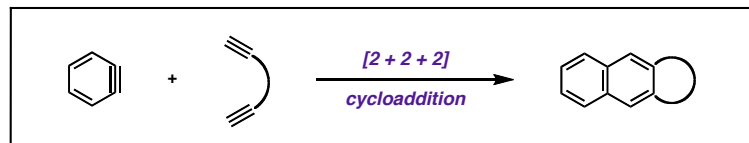
*Scheme 2.7. Transition metal-catalyzed aryne annulations*



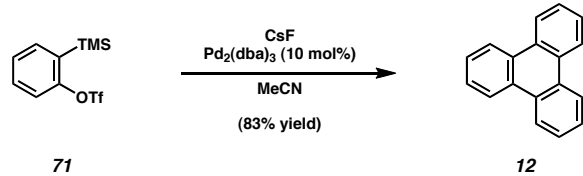
condensation between a benzophenone oxime (**151**) and an aryne.<sup>52</sup> Interestingly, the overall process is redox-neutral given that reductive scission of the oxime N–O bond is balanced by oxidative formation of the C(4)–C(4a) bond of the isoquinoline.

A subset of reactions within the class of transition metal-catalyzed aryne annulations includes cyclotrimerizations proceeding through a formal [2 + 2 + 2] cycloaddition between a diyne and an aryne (Scheme 2.8). While benzyne is known to produce small amounts of triphenylene (**12**) in the absence of an exogenous metal, recent efforts have been undertaken to promote this homocyclotrimerization by templating the reaction on a palladium catalyst.<sup>53</sup> However, far fewer examples of the analogous heterobimolecular process exist. One such case was reported by Pérez and co-workers in 2003 as part of an effort to develop an aryne-based approach to the kinamycin antibiotics.<sup>54</sup> Using a palladium-catalyzed [2 + 2 + 2] cycloaddition between diynes **153a–c** and benzyne, the authors achieved the synthesis of several differentially substituted benzo[*b*]fluorenones (**154a–c**) modest yield. A similar strategy was adopted by Mori and co-workers. a year later as a key step in their synthetic approach to the taiwanin lignans.<sup>55</sup> Carrying out a palladium-catalyzed cycloaddition between the aryne derived from *ortho*-silyl aryl triflate **155** and linear propiolate-propiolamide **156** generated tetracycle **157**, an intermediate en route to taiwanins C and E.

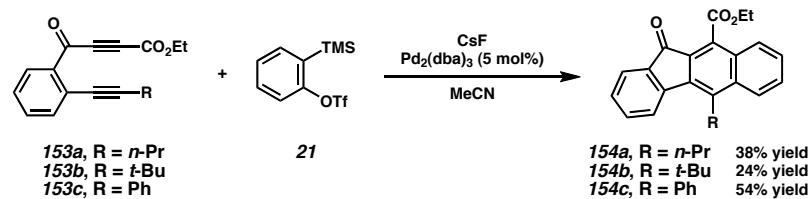
*Scheme 2.8. Transition metal-catalyzed [2 + 2 + 2] cycloadditions*



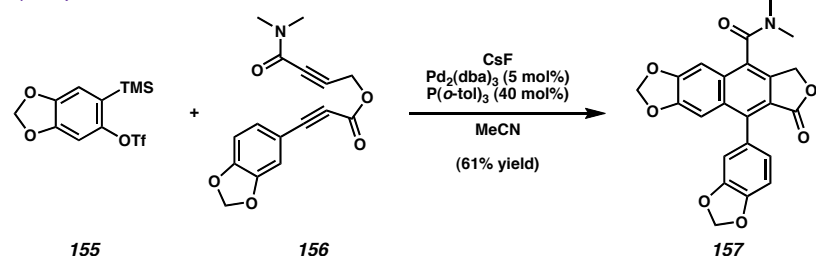
Pérez (1998)



Pérez (2003)



Mori (2004)



## 2.3 ORTHOGONAL SYNTHESIS OF INDOLINES AND ISOQUINOLINES

### VIA ARYNE ANNULATION<sup>†,56</sup>

#### 2.3.1 *Rational Design of an Aryne Annulation Reaction for the Synthesis of Indolines*

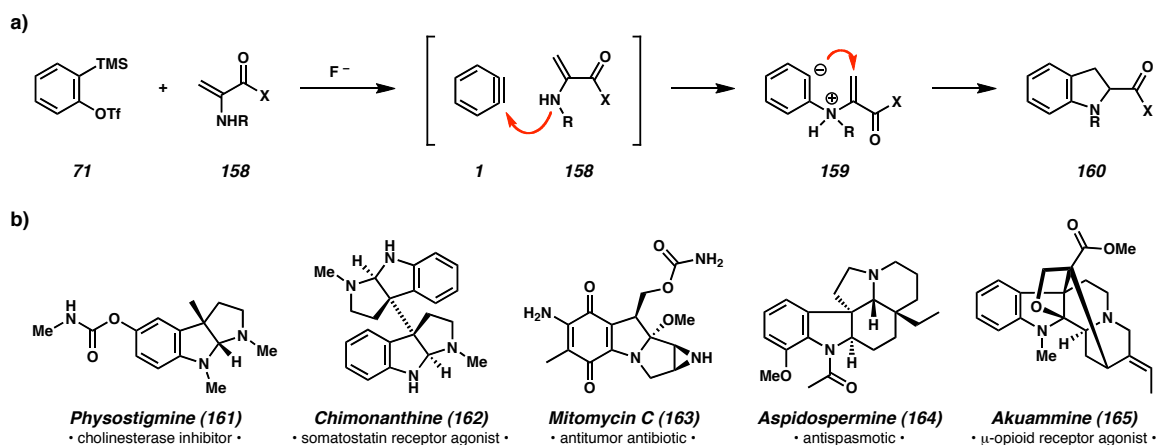
One year after the discovery of the aryne acyl-alkylation reaction,<sup>42</sup> our research group began investigating methods for the application of aryne chemistry to the synthesis of nitrogen-containing molecules. Given the rich history of aryne methodology, we were well aware that benzyne could act as a competent electrophile toward a wide range of nitrogen nucleophiles.<sup>24,26,28,37,57</sup> Furthermore, it was known that the intermediate aryl anion generated upon addition to benzyne could be utilized in subsequent additions to other electrophiles, either in an intramolecular (*vide supra*) or an intermolecular manner.<sup>58</sup> Taking these guidelines into consideration, we envisioned a novel method for the synthesis of indolines (**160**) from arynes (**1**) and  $\alpha,\beta$ -unsaturated carbonyl species bearing an amine at the  $\alpha$ -carbon (**158**) (Scheme 2.9a). Specifically, we expected the nitrogen atom of **158** to undergo nucleophilic addition to benzyne (**1**) to form an intermediate aryl anion (**159**), which would then add to the proximal  $\alpha,\beta$ -unsaturated carbonyl in a conjugate fashion to close the five-membered ring, yielding indoline **160**. While we were confident that the initial addition of the nitrogen nucleophile could be accomplished, there was no precedent at the time for conjugate addition as a means to quench the resultant anion.<sup>59</sup> We therefore undertook efforts to determine whether this could be a viable strategy for the synthesis of indolines. Given the prevalence of these

---

<sup>†</sup> This work was performed in collaboration with Christopher D. Gilmore, a fellow graduate student in the Stoltz research group. The initial discovery and optimization of both the indoline- and isoquinoline-forming aryne annulation reactions were accomplished by C. D. Gilmore.

heterocycles within a variety of bioactive natural products (e.g., **161–165**), the successful development of a direct method for their synthesis from easily preparable materials would open new avenues toward substances relevant to the advancement of medicine (Scheme 2.9b).<sup>60</sup>

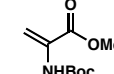
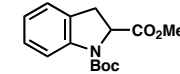
Scheme 2.9. a) Proposed indoline synthesis via aryne annulation. b) Bioactive indoline-containing natural products



Our initial investigations focused on substrates derived from amino acids, specifically *N*-Boc dehydroalanine methyl ester (**166**) (Table 2.1). Combining this reagent with Kobayashi's *ortho*-silyl aryl triflate (**71**),<sup>61,62</sup> we began by examining the conditions previously used to promote aryne acyl-alkylation (entry 1).<sup>42</sup> To our delight, this initial attempt produced the desired indoline methyl ester (**167**) in 35% yield, thereby confirming the feasibility of our aryne-based approach to nitrogen-containing heterocycles. We continued by examining alternative sources of fluoride for the in situ formation of benzyne. While both caesium fluoride (entries 1 and 2) and potassium fluoride (entries 3–6) promoted formation of the indoline, tetra-*n*-butylammonium

difluorotriphenylsilicate (TBAT) (entries 7–13) was identified as the optimal fluoride source. Unlike the alkali fluoride salts, this reagent is soluble in several common organic solvents, which facilitates purification by eliminating the need for filtration or aqueous extraction. Additionally, TBAT could be utilized at room temperature (25 °C) to generate yields comparable to those obtained with other fluoride sources at higher temperatures. By decreasing the concentration of the reaction to 0.02 M, the formation of minor undesired side products could be minimized, leading ultimately to the isolation of indoline **167** in 61% yield (entry 13).

Table 2.1. Optimization of reaction conditions for indoline synthesis via aryne annulation

 <b>71</b>		 <b>166</b>		 <b>167</b>			
entry	aryne equivalents	fluoride source	fluoride equivalents	solvent	conc. (M)	temp. (°C)	yield
1	1.5	CsF	2.0	MeCN	0.2	80	35%
2	1.5	CsF	2.0	MeCN	0.2	25	15%
3	1.5	KF / 18-Crown-6	2.0	THF	0.2	25	44%
4	1.5	KF / 18-Crown-6	2.0	THF	0.2	40	27%
5	1.0	KF / 18-Crown-6	1.5	THF	0.2	25	16%
6	2.0	KF / 18-Crown-6	2.0	THF	0.2	25	47%
7	2.0	TBAT	2.0	CH <sub>2</sub> Cl <sub>2</sub>	0.1	25	53%
8	2.0	TBAT	2.0	THF	0.2	25	45%
9	2.0	TBAT	2.0	THF	0.2	40	33%
10	2.0	TBAT	2.0	THF	0.1	25	45%
11	2.0	TBAT	2.0	THF	0.1	40	22%
12	2.0	TBAT	2.0	THF	0.02	40	47%
13	2.0	TBAT	2.0	THF	0.02	25	61%

Having identified the optimal reaction conditions, we set out to investigate the substrate tolerances by examining a series of substituted aryne precursors (**168**) in

combination with various enamines (**169**) (Table 2.2). Symmetrical aryne precursors were found to produce the expected indolines in good yield (entries 1 and 3). However, the unsymmetrically substituted aryne precursor, 3-methoxy-2-(trimethylsilyl)phenyl triflate (**108**), generated a 2.3:1 mixture of isomeric products, **170a** and **b** (entry 2). Interestingly, substituting the enamine derived from dehydroalanine (**171**) with a derivative of dehydrophenylalanine (**169b**) produced 2,3-disubstituted indoline **170d** in 40%, proving that substitution at C(3) does not have a significant impact on reactivity. Importantly, the syn relationship between the ester at C(2) and the phenyl ring at C(3) suggests that the reaction proceeds in a polar stepwise manner, as the product of a concerted reaction would reflect the anti relationship of the enamine substrate (**171**).

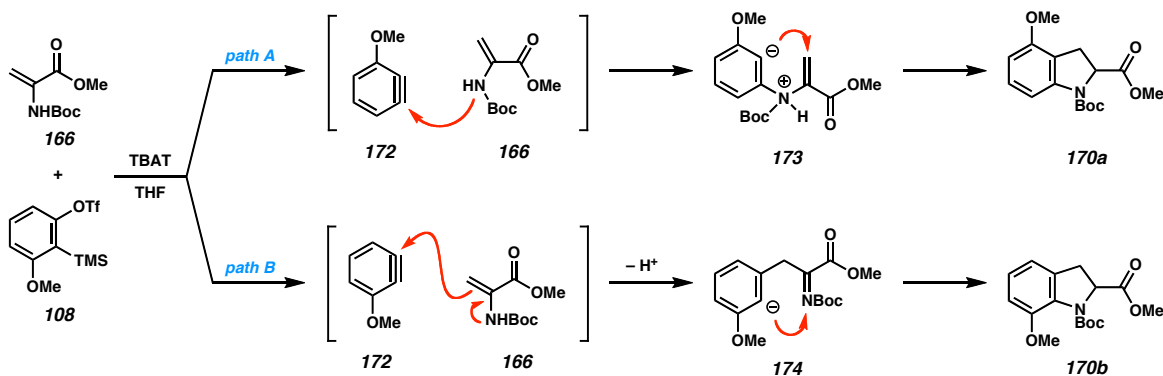
Table 2.2. Synthesis of indolines via aryne annulation<sup>a</sup>

		<b>168</b>	<b>169</b>	TBAT (2 equiv) THF (0.02 M) 23 °C, 6 h	<b>170</b>	
entry	silyl aryl triflate	ene carbamate		product	yield	
1					61%	
2					49%	
3					39%	
4					40%	

<sup>a</sup> Reaction performed with 2.0 equiv *ortho*-silyl aryl triflate **168** relative to enamine **169**.

We were intrigued by the observation that 3-methoxy-substituted aryne (derived from **108**) produced a mixture of isomeric indolines (**170a** and **b**) when this same compound had been shown previously to promote high levels of regioselectivity in several other reactions.<sup>63,64</sup> In an attempt to reconcile this result with our initially conceived mechanism, it appears that this poor regioselectivity can potentially be attributed to the occurrence of a competing reaction pathway (Scheme 2.10). If, in addition to the initially proposed nucleophilic attack of nitrogen meta to the methyl ether of aryne **171** (path A), the carbon terminus of enamine **166** was also capable of attacking the aryne (path B),<sup>65</sup> iminoester **174** would be generated as the intermediate anion instead of acrylate **173**. Then, in analogy to the putative intramolecular conjugate addition to produce indoline **170a**, the addition of the aryl anion to the imine nitrogen would close the five-membered ring to furnish the isomeric product, indoline **170b**. While nucleophilic addition directly to nitrogen is unusual, similar umpolung pathways have been reported with  $\alpha$ -iminoesters<sup>66</sup> and 2-iminomalonates<sup>67</sup> using Grignard and alkylaluminum reagents.<sup>68</sup> The observed product ratio would indicate, however, that an initial nucleophilic addition of the carbamate nitrogen is the more favorable mechanistic pathway (path A). Interestingly, this combination of mechanisms may in fact contribute to the formation of each of the indolines shown above (**167** and **170a–d**). However, this only becomes apparent in trials employing unsymmetrical arynes such as **172**.

Scheme 2.10. Orthogonal mechanisms for indoline formation via aryne annulation

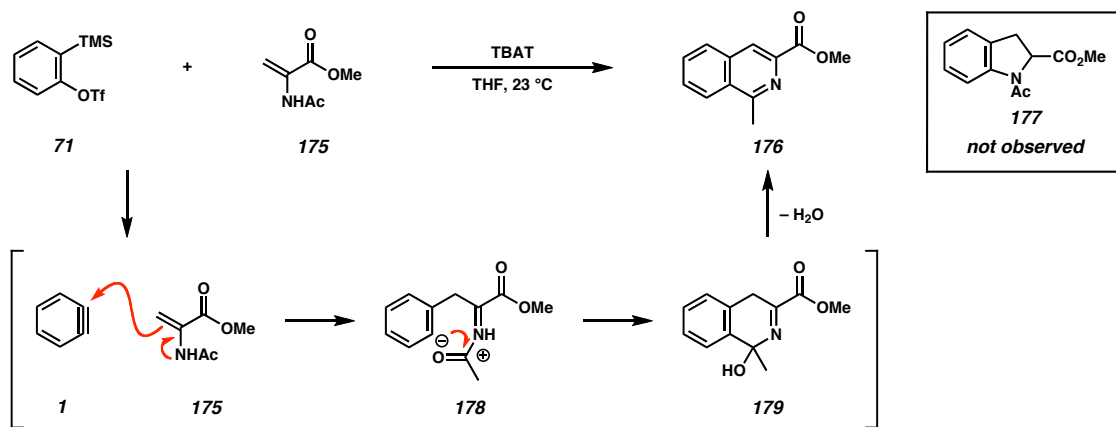


### 2.3.2 Synthesis of Isoquinolines via Aryne Annulation

In an effort to suppress the suspected mode of side reactivity and thus avoid further product mixtures, we set out to examine alternative nitrogen substituents that would decrease the nucleophilicity of the enamine  $\pi$ -system by sequestering the nitrogen lone pair. We considered an acetyl group due to its increased electron withdrawing potential relative to the *tert*-butyl carbamate. *N*-Boc dehydroalanine methyl ester (**166**) was therefore replaced with its *N*-acetyl congener (**175**) and the aryne annulation was attempted with 2-(trimethylsilyl)phenyl triflate (**71**) (Scheme 2.11). However, instead of isolating the expected *N*-acetyl indoline ester (**177**), we were surprised to find that methyl 1-methylisoquinoline-3-carboxylate (**176**) was the only product generated. This interesting structure most likely arises through nucleophilic addition of the enamine carbon to benzyne (**1**), followed by intramolecular addition of the aryl anion to the carbonyl of the intermediate *N*-acetyl imine (**178**). Subsequent aromatization through the loss of an equivalent of water from dihydroisoquinoline **179** would then produce the isoquinoline.<sup>69</sup> If this mechanism is indeed operative, it would indicate that exchanging the carbamate for the acetamide had little effect on the electronic properties of the

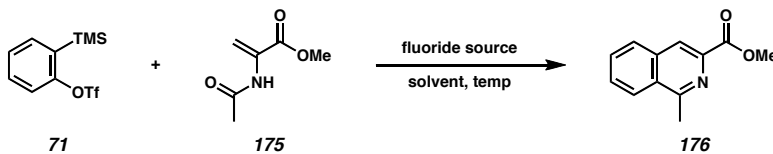
enamine, and instead only provided a carbonyl electrophile more reactive than the *N*-carbamoyl imine (**174**) to quench the intermediate aryl anion.

Scheme 2.11. Unexpected formation of an isoquinoline through an alternative aryne annulation



Having discovered this unexpected mode of orthogonal reactivity, we undertook a screen of reaction conditions to optimize the yield of isoquinoline **176** (Table 2.3). Caesium fluoride once again performed admirably as a fluoride source (entries 1–6), generating the desired isoquinoline in up to 65% yield at room temperature (entry 3). Potassium fluoride also proved effective, although less so than caesium fluoride (entries 7–9). As was the case in the previous indoline synthesis, however, TBAT was again identified as the optimal fluoride source (entries 11–14). Using this reagent, isoquinoline **176** could be isolated in up to 87% yield within 6 hours when the reaction was performed in THF at a slightly lower concentration (0.01 M) (entry 14).

Table 2.3. Optimization of reaction conditions for isoquinoline synthesis via aryne annulation



entry	aryne equivalents	fluoride source	fluoride equivalents	solvent	conc. (M)	temp. (°C)	yield
1	1.5	CsF	2.0	MeCN	0.2	25	57%
2	1.5	CsF	2.0	MeCN	0.1	25	61%
3	2.0	CsF	2.0	MeCN	0.2	25	65%
4	1.5	CsF	2.0	MeCN	0.1	25	30%
5	1.25	CsF	2.0	MeCN	0.2	25	50%
6	1.25	CsF	2.0	THF	0.2	25	0%
7	2.0	KF / 18-C-6	3.0	THF	0.2	25	36%
8	1.5	KF / 18-C-6	2.0	THF	0.2	25	34%
9	2.0	KF / 18-C-6	3.0	THF	0.2	40	40%
10	2.0	TBAF	2.0	CH <sub>2</sub> Cl <sub>2</sub>	0.2	25	13%
11	2.0	TBAT	2.0	CH <sub>2</sub> Cl <sub>2</sub>	0.2	25	71%
12 <sup>a</sup>	2.0	TBAT	2.0	CH <sub>2</sub> Cl <sub>2</sub>	0.2	120	56%
13	2.0	TBAT	2.0	THF	0.2	40	77%
14	2.0	TBAT	2.0	THF	0.01	25	87%

<sup>a</sup> Reaction performed in a microwave reactor.

From a synthetic standpoint, the isoquinoline carbon framework provides a number of sites for introduction of synthetic functionality, and furthermore, our aryne annulation technology enables a convergent approach to the assembly of these functionalized derivatives. In particular, isoquinolines bearing substitution at carbons 1, 3, and 4 can be prepared through manipulation of the dehydroamino ester, while substitution at carbons 5–8 originate from manipulation of the aryne. To systematically verify the capabilities of this approach, we began by preparing a series of *N*-acyl dehydroalanine methyl esters (**180**) for the synthesis of C(1)-substituted isoquinolines (**181**) (Table 2.4). To our delight, the reaction proved quite tolerant to the introduction of a wide variety of functionality at this position, ranging from linear and branched alkyl chains (entries 1–4)

to aryl groups (entries 5 and 6) and even heteroatom-functionalized sidechains (entries 7–9). Importantly, the carbon atom  $\alpha$  to the amide carbonyl can be introduced in several different oxidation states—from alkane (entries 1–5) to alcohol (entries 6 and 8) to carboxylic acid (entries 7 and 9)—without detriment to the product yield.

Table 2.4. Synthesis of C(1)-substituted isoquinolines via aryne annulation<sup>a</sup>

entry	<i>N</i> -acyl enamine ( <b>180</b> )	isoquinoline ( <b>181</b> )	yield
1	<b>180a</b> , R = Me	<b>176</b> , R = Me	87%
2	<b>180b</b> , R = <i>n</i> -Bu	<b>181a</b> , R = <i>n</i> -Bu	76%
3	<b>180c</b> , R = <i>i</i> -Pr	<b>181b</b> , R = <i>i</i> -Pr	66%
4	<b>180d</b> , R = <i>c</i> -Hex	<b>181c</b> , R = <i>c</i> -Hex	65%
5	<b>180e</b> , R = Bn	<b>181d</b> , R = Bn	72%
6	<b>180f</b> , R = Ph	<b>181e</b> , R = Ph	55%
7	<b>180g</b> , R = CF <sub>3</sub>	<b>181f</b> , R = CF <sub>3</sub>	57%
8	<b>180h</b> , R = CH <sub>2</sub> OMe	<b>181g</b> , R = CH <sub>2</sub> OMe	68%
9	<b>180i</b> , R = CO <sub>2</sub> Me	<b>181h</b> , R = CO <sub>2</sub> Me	51%

<sup>a</sup> Reaction performed with 2.0 equiv *ortho*-silyl aryl triflate **71** relative to enamine **180**.

Next, we turned our attention to the effect of aryne substitution on reactivity. Using methyl 2-acetamidoacrylate (**175**) as a model *N*-acyl enamine, we tested a pair of monosubstituted arynes displaying functionality *ortho* and *meta* to the reactive aryne triple bond (**108** and **183**) as well as three disubstituted arynes (**155**, **184**, and **185**) (Table 2.5). All five substrates performed well, providing the expected isoquinolines (**182a–f**) in good yield. Notably, both electron-rich (entries 1–4) and electron-deficient (entry 5) arynes successfully underwent aryne annulation. Not surprisingly, difluoroaryne **185**

proved to be the most productive substrate, most likely due to the increased reactivity provided by the inductively withdrawing halide substitution. We were also pleased to find that *ortho*-methoxy aryne **108** generated only one product isomer (**182a**) derived from the expected mode of nucleophilic attack meta to the ether. On the other hand, the *meta*- methyl aryne (**183**) provided a 1:1 mixture of isomeric isoquinolines (**182b** and **c**),

Table 2.5. Aryne substrate scope in isoquinoline synthesis

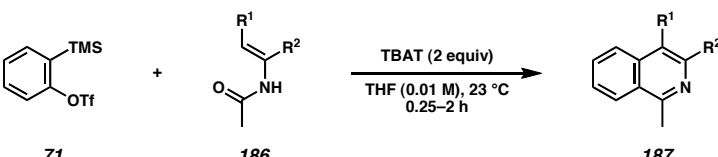
entry	substrate	product	yield
1			66%
2		+	59%
3			63%
4			60%
5			78%

<sup>a</sup> Reaction performed with 2.0 equiv *ortho*-silyl aryl triflate **168** relative to enamine **175**.

demonstrating the weak directing effect afforded by inductive donation from alkyl substituents.

Having confirmed that this orthogonal method of aryne annulation was capable of constructing several highly substituted isoquinoline esters, we began to reconsider the structural requirements for the enamine substrates in terms of our proposed mechanism. Dehydroamino esters were originally selected because they contained both a nitrogen nucleophile and a conjugate acceptor amenable to the preparation of indolines. We continued to employ these compounds after discovering that the *N*-acyl derivatives underwent a separate annulation to form isoquinolines. However, the mechanism we envision to lead to the formation of isoquinolines draws no benefit from the presence of the vestigial ester. We therefore set out to determine whether removing or replacing this group would have any effect upon reactivity.

The first substrates we tested were acetamides **186a** and **b**, derivatives of 3-pentanone and pinacolone, respectively.<sup>70</sup> Gratifyingly, both compounds produced the corresponding isoquinolines (**187a** and **b**) in very good yield and in far less time than required to form isoquinoline esters **181a–i** (entries 1 and 2).<sup>71</sup> This increase in rate lends credence to our hypothesis that the ester exerts a retarding effect upon the reactivity of the dehydroamino esters (**180a–i**) by removing electron density from the enamine carbon terminus. To further our investigation of *N*-acyl enamines, we prepared cyclic enamines **186c–f**, which furnished a series of tricyclic isoquinolines (**187c–f**) upon aryne annulation (entries 3–6). Importantly, it was possible to incorporate carbonyl functionality both within the ring (entry 5) and pendant to it (entry 6) without affecting reactivity.

Table 2.6. *N*-Acyl enamine substrate scope<sup>a</sup>


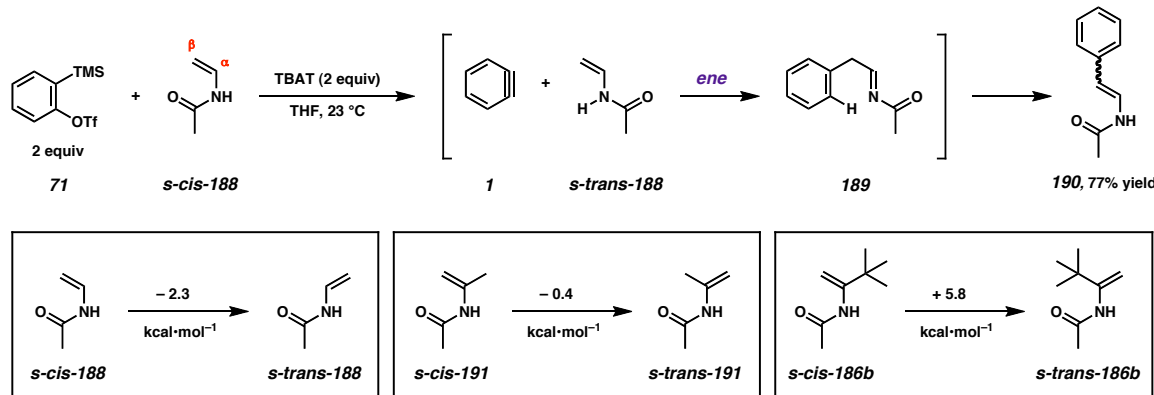
entry	substrate	product	yield
1	186a, R <sup>1</sup> = Et, R <sup>2</sup> = Me		72%
2	186b, R <sup>1</sup> = H, R <sup>2</sup> = t-Bu		83%
3	186c, n = 1, X = H <sub>2</sub>		66%
4	186d, n = 2, X = H <sub>2</sub>		67%
5	186e, n = 2, X = O		66%
6	186f		71%

<sup>a</sup> Reaction performed with 2.0 equiv *ortho*-silyl aryl triflate **71** relative to enamine **186**.

In order to test the lower limit of substitution on the *N*-acyl enamine substrate structure, we attempted an aryne annulation using *N*-vinyl acetamide (**188**), a compound lacking substitution at the carbon atom attached to nitrogen (Scheme 2.12). Unfortunately, instead of isolating the desired 1-methylisoquinoline, the substrate underwent exclusive arylation at the carbon terminus to produce styrene **190** as an inseparable mixture of olefin isomers in 77% yield.<sup>72</sup> One possible explanation for this phenomenon is a rotation about the C(α)–N bond of **188**, leading to an “*s-trans*-like” conformation.<sup>73</sup> This conformer would then be capable of undergoing an ene reaction with benzene (**1**) to generate intermediate *N*-acetyl imine **189**. Tautomerization to regenerate the enamine would then yield the observed styrene (**190**).<sup>74</sup>

The arylation of *N*-vinyl acetamide through an “*s-trans*-like” conformation would indicate a need for some form of substitution at C(α) in order to induce a preference for the “*s-cis*-like” conformation through steric interactions between the acetyl group and the C(α) substituent. To gain a better understanding of the relationship between enamine substitution and conformational preference, we calculated the ground state energies of each of the rotational conformers of *N*-vinyl acetamide (**188**), *N*-(2-propenyl)acetamide (**191**), and *N*-(3,3-dimethyl-2-butenyl)acetamide (**186b**).<sup>75</sup> In accordance with the postulated ene mechanism of *C*-arylation, the “*s-trans*-like” conformation of *N*-vinyl acetamide is preferred by 2.3 kcal·mol<sup>-1</sup>. The introduction of a methyl group at C(α) lowers the energy difference to 0.4 kcal·mol<sup>-1</sup>, only slightly in favor of the “*s-trans*-like” conformation. Conversely, the presence of a *tert*-butyl group at C(α) produces a strong preference for the “*s-cis*-like” conformation (5.8 kcal·mol<sup>-1</sup>), which helps to explain the observation that **186b** reacts faster than any other substrate we have tested to date.<sup>71</sup>

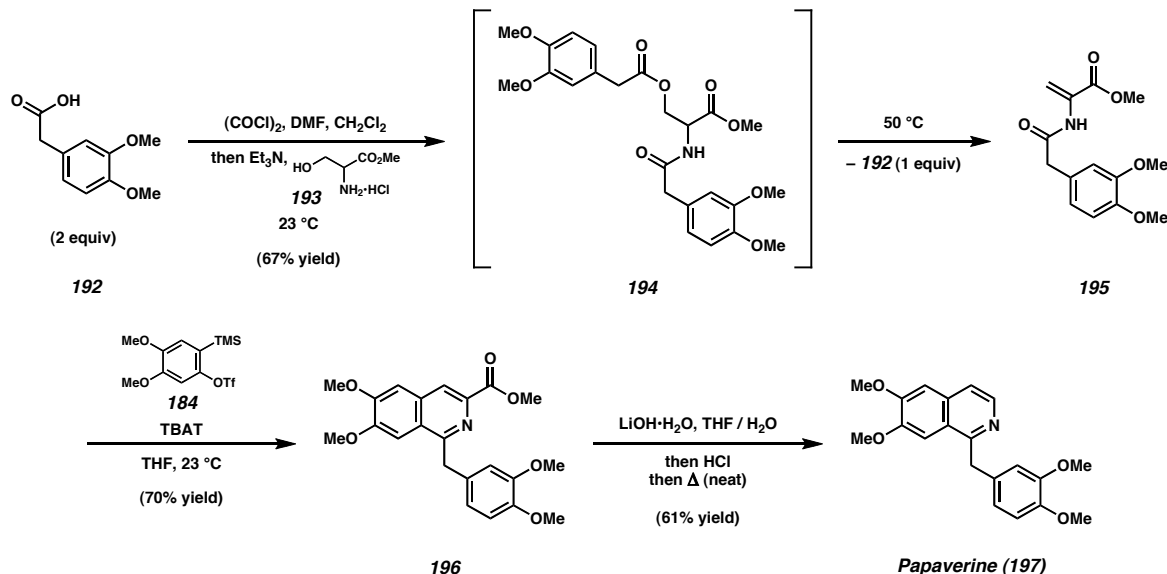
Scheme 2.12. Arylation of *N*-vinyl acetamide



### 2.3.3 Total Synthesis of Papaverine

Having developed this powerful condensation reaction for generating isoquinolines, we sought to demonstrate its utility in a rapid total synthesis of papaverine<sup>76</sup> (**197**), a clinically used non-narcotic antispasmodic agent that is a biosynthetic precursor to several of the pavine alkaloids and one of the four major constituents of opium (Scheme 2.13).<sup>77</sup> Our synthesis began with the condensation of homoveratric acid (**192**) and serine methyl ester•HCl (**193**), followed by elimination to provide *N*-acyl enamine **195**.<sup>78</sup> In the key annulation, enamide **195** underwent dehydrative addition to the aryne generated from *ortho*-silyl aryl triflate **184** to furnish isoquinoline ester **196** in 70% yield. Lastly, saponification and thermal decarboxylation<sup>79</sup> afforded papaverine (**197**) in 29% overall yield. Our synthesis totals three steps from commercially available materials, which marks the shortest synthesis of this important alkaloid reported to date.<sup>80,81</sup>

Scheme 2.13. Total synthesis of papaverine



### 2.3.4 An Alternative Approach to the Synthesis of Isoquinolines and Benzocyclobutenes via Aryne Annulation

Shortly after our communication detailing the development of two orthogonal aryne annulation methods, Blackburn and Ramtohul at Merck Frosst reported a similar approach to the synthesis of isoquinoline esters (**181**) (Table 2.7).<sup>82</sup> However, in addition to this heterocycle, the authors also noted the formation of a second annulation product—a benzocyclobutene amino ester (**198**). In contrast to the isoquinoline, which forms through a formal dehydrative [4 + 2] addition, the benzocyclobutene is the product

Table 2.7. Ramtohul – Isoquinoline and benzocyclobutene synthesis via aryne annulation

entry	R	yield (XX)	yield (XX)
1		64% <b>181a</b>	24% <b>198a</b>
2		59% <b>181b</b>	21% <b>198b</b>
3		64% <b>181c</b>	22% <b>198c</b>
4		62% <b>181d</b>	18% <b>198d</b>
5		51% <b>181e</b>	21% <b>198e</b>
6		66% <b>181f</b>	25% <b>198f</b>
7		69% <b>181g</b>	24% <b>198g</b>
8		56% <b>181h</b>	22% <b>198h</b>
9		42% <b>181i</b>	12% <b>198i</b>
10		66% <b>181j</b>	22% <b>198j</b>
11		42% <b>181k</b>	11% <b>198k</b>

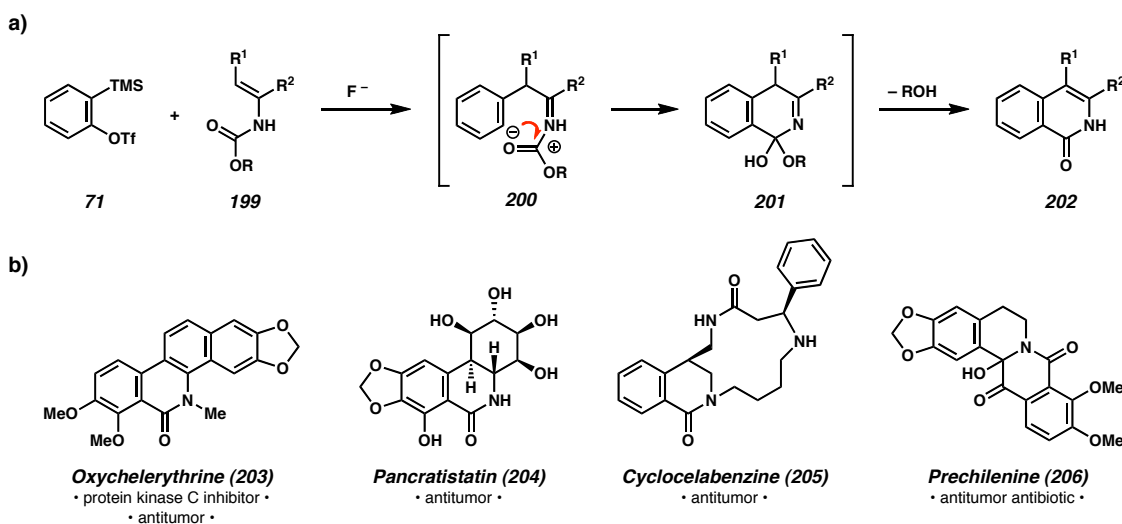
<sup>a</sup> Reaction performed with 1.25 equiv *ortho*-silyl aryl triflate **71** relative to enamine **180**.

of a [2 + 2] cycloaddition between enamine **180** and the aryne generated from *ortho*-silyl aryl triflate **71**. The authors demonstrated the substrate scope of this reaction, using caesium fluoride in acetonitrile to generate isoquinolines **181a–k** in good yield with modest yields of the accompanying benzocyclobutenes (**181a–k**).

### 2.3.5 Synthesis of Isoquinolones via Aryne Annulation

Recently, we began examining additional nitrogen-containing heteroaromatic structures that might be targeted using our aryne annulation approach. We postulated that by replacing the *tert*-butyl group of the *N*-Boc enamines previously used in the synthesis of indolines (e.g., **166**) with an electron-withdrawing group capable of activating the carbamate carbonyl toward intramolecular attack by the aryl anion (**200**), we could achieve a synthesis of isoquinolones (**202**) using the same general mechanism used to target isoquinolines (Scheme 2.14a).<sup>83</sup> If successful, this would open avenues to the convergent assembly of an even wider class of natural product targets, including several bioactive isoquinolone- and 3,4-dihydroisoquinolone-containing alkaloids (**203–206**) (Scheme 2.14b).

Scheme 2.14. a) Synthesis of isoquinolones via aryne annulation. b) Bioactive isoquinolone- and 3,4-dihydroisoquinolone containing natural products



We began our efforts by searching for an efficient method to prepare the carbamate substrates. Fortunately, a Curtius rearrangement carried out upon  $\alpha,\beta$ -unsaturated carboxylic acids (**207**) provided a concise route to the desired compounds, enabling the synthesis of a series of carbamates (**208**) with substitution at oxygen derived from the corresponding alcohols (Table 2.8).<sup>84,85</sup> Using *N*-cyclohexenyl carbamate **208** as a model substrate, we then turned our attention to a screen of both reaction conditions and optimal carbamate *O*-substitution in the synthesis of tricyclic isoquinolone **209**.

The screen commenced with the *O*-phenyl carbamate and caesium fluoride was evaluated as the fluoride source in both acetonitrile and DME (entries 1–4). While we were pleased to observe that this substrate successfully generated isoquinolone **209**, the yields were significantly lower than those obtained for the corresponding isoquinolines under similar conditions (cf., Table 2.3, entries 1–5). In order to obtain even modest yields of the product, it was necessary to elevate the temperature to the point of reflux.

We were further discouraged to find that exchanging caesium fluoride for TBAT—the optimal fluoride source in previous experiments—had little effect (entries 5–11). In light of the fact that performing the reaction in THF at 60 °C for 18 h resulted in the isolation of isoquinolone **209** in only 48% yield (accompanied by the reisolation of significant quantities of unreacted starting material), we resolved to explore microwave-assisted conditions in order to reach temperatures beyond the boiling point. While trials performed between 120 °C and 180 °C failed to achieve yields greater than 48%, the reactions did proceed to complete consumption of the carbamate in all cases (entries 12–15). Unfortunately, this occurred at the expense of product yield, as *N*-arylation of the isoquinolone (**209**) was observed as major side product. The quantity of *ortho*-silyl aryl triflate **71** was therefore decreased from 2.0 equivalents to 1.5, and the concentration was accordingly increased to 0.15 M (entries 16 and 17). Under these conditions, isoquinolone **209** can be prepared in up to 64% yield from the *N*-cyclohexenyl-*O*-phenyl carbamate when the reaction is run for 12 min in a microwave reactor (entry 17). We are currently applying these optimized conditions to an evaluation of additional carbamates featuring alternative electron-withdrawing substitution at oxygen (entries 18 and 19). At present, however, the *O*-phenyl carbamate remains the optimal substituent.

Table 2.8. Optimization of reaction conditions for isoquinolone synthesis via aryne annulation

entry	R	aryne equivalents	fluoride source	fluoride equivalents	solvent	conc. (M)	temp. (°C)	time	yield
1	Ph	2.0	CsF	2.0	MeCN	0.1	40	18 h	27%
2	Ph	2.0	CsF	2.0	MeCN	0.1	60	3 h	39%
3	Ph	2.0	CsF	2.0	MeCN	0.1	80	80 min	43%
4	Ph	2.0	CsF	2.0	DME	0.1	80	1 h	28%
5	Ph	2.0	TBAT	2.0	CH <sub>2</sub> Cl <sub>2</sub>	0.1	40	24 h	ND <sup>a</sup>
6	Ph	2.0	TBAT	2.0	DME	0.1	60	2 h	36%
7	Ph	2.0	TBAT	2.0	dioxane	0.1	60	10 h	41%
8	Ph	2.0	TBAT	2.0	dioxane	0.1	80	9 h	41%
9	Ph	2.0	TBAT	2.0	MeCN	0.1	60	24 h	40%
10	Ph	2.0	TBAT	2.0	THF	0.1	60	24 h	41%
11	Ph	3.0	TBAT	3.0	THF	0.1	60	18 h	48%
12 <sup>b</sup>	Ph	2.0	TBAT	2.0	THF	0.1	120	8 min	31% <sup>c</sup>
13 <sup>b</sup>	Ph	2.0	TBAT	2.0	THF	0.1	120	12 min	35% <sup>c</sup>
14 <sup>b</sup>	Ph	2.0	TBAT	2.0	THF	0.1	160	14 min	ND <sup>a,c</sup>
15 <sup>b</sup>	Ph	2.0	TBAT	2.0	THF	0.1	180	12 min	37% <sup>c</sup>
16 <sup>b</sup>	Ph	1.5	TBAT	1.5	THF	0.15	180	15 min	42%
17 <sup>b</sup>	Ph	1.5	TBAT	1.5	THF	0.15	180	12 min	64%
18 <sup>b</sup>	4-Br-C <sub>6</sub> H <sub>4</sub>	1.5	TBAT	1.5	THF	0.15	180	12 min	35%
19 <sup>b</sup>	CH <sub>2</sub> CCl <sub>3</sub>	1.5	TBAT	1.5	THF	0.15	180	12 min	22%

<sup>a</sup> ND = not determined.<sup>b</sup> Reaction performed in a microwave reactor.<sup>c</sup> N-arylation of isoquinolone **209** was observed as a major side product.

Concurrent with efforts to identify the optimal substituent at oxygen, we investigating the scope of substitution on the enamine fragment. Thus far, four products have been prepared using the aryne annulation method—isoquinolones **202a–c** and **209** (Table 2.9). These compounds display varying levels of alkyl substitution at C(3) and C(4), including five- and six-membered fused rings (entries 2–4). In the case of benzofuran-derived

carbamate **210d**, the product (**202c**) is a tetracycle featuring oxygen substitution at C(3) of the isoquinolone framework (entry 4). Ongoing efforts within this regime will center around a broadening of the substrate scope, focusing in particular on the incorporation of substituted aryne precursors and more highly functionalized *N*-vinyl carbamates. With a better grasp of the capabilities of this reaction, efforts will advance toward the application of this aryne annulation within the context of complex natural product total synthesis.

Table 2.9. Synthesis of isoquinolones via aryne annulation<sup>a</sup>

		TBAT (1.5 equiv)	202
entry	substrate	product	yield
1			46%
2			68%
3			64%
4 <sup>b</sup>			35%

<sup>a</sup> Reaction performed with 1.5 equiv *ortho*-silyl aryl triflate **71** relative to enamine **210**.

<sup>b</sup> Reaction performed at 120 °C for 10 min with 1.1 equiv carbamate **210d** relative to **71**.

## 2.4 CONCLUSION

As a general approach to the synthesis of fused arene-containing polycycles, the concept of aryne annulation has taken a number of different forms over the past several decades. While the earliest methods focused on cycloaddition reactions between arynes and various unsaturated substrates, modern approaches have incorporated stepwise addition/cyclization mechanisms,  $\sigma$ -bond insertions, and transition metal catalysis into the arsenal of ring-forming reactions. We originally entered this arena with the discovery that arynes underwent formal insertion into the  $\alpha,\beta$ -C–C bond of cyclic  $\beta$ -ketoesters to furnish a variety of benzannulated medium rings. With the development of this methodology, we turned our attention to the goal of employing aryne in a synthesis of nitrogen-containing heterocycles—specifically, indolines. Following a rational mechanistic approach, we envisioned a stepwise annulation using derivatives of dehydroamino acids, wherein addition of the nitrogen nucleophile to the aryne would precede ring closure via intramolecular conjugate addition. In practice, we found that a combination of dehydroamino esters protected as the corresponding carbamates and *ortho*-silyl aryl triflates produces indolines in good yield when TBAT is used as the fluoride source. However, upon finding that an unsymmetrical aryne produced a mixture of isomeric products, we were forced to consider the existence of a second competing mechanism involving initial nucleophilic attack by the enamine carbon. In an effort to limit the reaction to a single pathway, we therefore began examining *N*-acyl dehydroamino esters as alternative substrates. To our surprise, these compounds displayed a completely orthogonal mode of reactivity, producing isoquinolines in excellent yield. Expanding upon this serendipitous result, we demonstrated the synthesis

of a series of isoquinolines bearing varying levels of hydrocarbon and heteroatom substitution around the aromatic ring system. Furthermore, this methodology provided the key step in a short total synthesis of the antispasmodic isopavine alkaloid, papaverine. Efforts are now underway to translate this novel annulation strategy to the preparation of isoquinolones. Initial optimization studies have shown the effectiveness of microwave heating, and these findings have been applied to the synthesis of a small library of hydrocarbon-substituted isoquinolones. Further experimentation is expected to yield an expanded substrate scope and the results of these studies will be reported in due course. It is ultimately our goal to apply this technology to the synthesis of bioactive isoquinolone- and dihydroisoquinolone-containing natural products relevant to the advancement of human medicine.

## 2.5 EXPERIMENTAL SECTION

### 2.5.1 Materials and Methods

Unless stated otherwise, reactions were performed in flame-dried glassware under an argon or nitrogen atmosphere using dry, deoxygenated solvents. Commercially obtained reagents were used as received. Tetrabutylammonium difluorotriphenylsilicate (TBAT) was purchased from Sigma-Aldrich Chemical Company and azeotropically dried three times from acetonitrile prior to use. Brine solutions are saturated aqueous sodium chloride solutions. Known dehydroamino ester starting materials were prepared by the methods of Kobayashi<sup>86</sup> or Parsons<sup>78</sup> unless otherwise specified. 3-methoxy-2-(trimethylsilyl)phenyl triflate (**108**)<sup>87</sup> 4-methyl-2-(trimethylsilyl)phenyl triflate (**183**)<sup>88</sup> 4,5-dimethoxy-2-(trimethylsilyl)phenyl triflate (**184**)<sup>89</sup> 6-(trimethylsilyl)benzo[d][1,3]dioxol-5-yl triflate (**155**)<sup>42</sup> and 4,5-difluoro-2-(trimethylsilyl)phenyl triflate (**186**)<sup>62</sup> were prepared according to literature procedures. Reaction temperatures were controlled by an IKAmag temperature modulator. Microwave reactions were performed with a Biotage Initiator Eight 400 W apparatus at 2.45 GHz. Thin-layer chromatography (TLC) was performed using E. Merck silica gel 60 F254 precoated plates (0.25 mm) and visualized by UV fluorescence quenching, potassium permanganate, or CAM staining. SiliaFlash P60 Academic Silica gel (particle size 0.040–0.063 mm) was used for flash chromatography. <sup>1</sup>H and <sup>13</sup>C NMR spectra were recorded on a Varian Mercury 300 (at 300 MHz and 75 MHz, respectively) or a Varian Inova 500 (at 500 MHz and 125 MHz, respectively), with usage specified in each case, and are reported relative to Me<sub>4</sub>Si (δ 0.0). Data for <sup>1</sup>H NMR spectra are reported as follows: chemical shift (δ ppm) (multiplicity, coupling constant (Hz), integration). Data

for  $^{13}\text{C}$  NMR spectra are reported in terms of chemical shift relative to  $\text{Me}_4\text{Si}$  ( $\delta$  0.0).

IR spectra were recorded on a Perkin Elmer Paragon 1000 Spectrometer and are reported in frequency of absorption ( $\text{cm}^{-1}$ ). High resolution mass spectra were obtained from the Caltech Mass Spectral Facility.

## 2.5.2 *Preparative Procedures and Spectroscopic Data*

### 2.5.2.1 *Representative Procedures for the Synthesis of Indolines and Isoquinolines via Aryne Annulation*

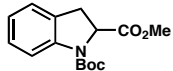
#### Method A

To a solution of TBAT (0.756 g, 1.40 mmol, 2.0 equiv) and enamine (0.70 mmol) in THF (35 mL) was added *ortho*-silyl aryl triflate **71** (0.340 mL, 1.40 mmol, 2.0 equiv) dropwise via syringe. The reaction was stirred under nitrogen at ambient temperature for 6 h, at which point the reaction was concentrated under reduced pressure and purified via flash chromatography.

#### Method B

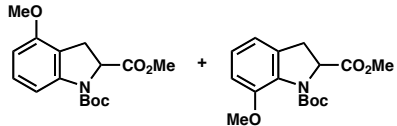
To a solution of TBAT (0.756 g, 1.40 mmol, 2.0 equiv) and enamine (0.70 mmol) in THF (70 mL) was added *ortho*-silyl aryl triflate **71** (0.340 mL, 1.40 mmol, 2.0 equiv) dropwise via syringe. The reaction was stirred under nitrogen at ambient temperature for 6 h, at which point the reaction was concentrated under reduced pressure and purified via flash chromatography.

### 2.5.2.2 Spectroscopic Data for Indolines



#### Indoline 167 (Table 2.2, Entry 1)

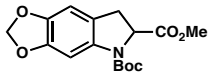
Reaction performed via Method A. Purified by flash chromatography (SiO<sub>2</sub>, 10:90 → 30:70 EtOAc/hexanes). 61% yield.  $R_f = 0.35$  (30:70 EtOAc/hexanes); <sup>1</sup>H NMR (300 MHz, CDCl<sub>3</sub>) δ 7.88 (d,  $J = 6.5$  Hz, 1H), 7.19 (d,  $J = 4.5$  Hz, 1H), 7.12 (d,  $J = 4.2$  Hz, 1H), 6.96 (t,  $J = 4.0$  Hz, 1H), 4.89 (br t,  $J = 2.0$  Hz, 1H), 3.77 (s, 3H), 3.65 (dd,  $J = 10.2$ , 8.0 Hz, 1H), 3.51 (dd,  $J = 9.0$ , 2.5 Hz, 1H), 1.49 (br s, 9H); <sup>13</sup>C NMR (125 MHz, CDCl<sub>3</sub>) δ 173.1, 152.2, 142.8, 134.0, 130.3, 128.2, 124.7, 122.5, 117.5, 81.7, 60.3, 52.2, 32.4, 28.6; IR (Neat Film, NaCl) 3066, 2928, 1754, 1603, 1485, 1289, 1319, 1277, 1203, 1169, 1046, 1022, 848, 751 cm<sup>-1</sup>; HRMS (EI+) *m/z* calc'd for C<sub>15</sub>H<sub>19</sub>NO<sub>4</sub> [M']<sup>+</sup>: 277.1314, found 277.1323.



#### Indolines 170a and b (Table 2.2, Entry 2)

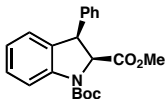
Reaction performed via Method A. Purified by flash chromatography (SiO<sub>2</sub>, 0:100 → 30:70 EtOAc/hexanes). 49% yield, isolated as a 2.3:1 mixture of inseparable 4- and 7-methoxyindolines.  $R_f = 0.21$  (30:70 EtOAc/hexanes); <sup>1</sup>H NMR (500 MHz, CDCl<sub>3</sub>) δ 7.0 (t,  $J = 7.3$  Hz, 1H), 6.80 (d,  $J = 3.6$  Hz, 2H), 6.78 (d,  $J = 2.9$  Hz, 1H), 5.08 (dd,  $J = 10.2$ , 2.2 Hz, 1H), 3.86 (s, 3H), 3.71 (s, 3H), 3.55 (dd,  $J = 16.8$ , 5.0 Hz, 1H), 3.07 (d,  $J = 16.8$ , 1.0 Hz, 1H), 1.45 (s, 9H); <sup>13</sup>C NMR (125 MHz, CDCl<sub>3</sub>) δ 172.8, 153.5, 149.8, 133.4,

130.8, 125.7, 117.1, 112.8, 81.3, 62.6, 55.7, 53.1, 33.9, 28.3; IR (Neat Film, NaCl) 2976, 2838, 1733, 1695, 1609, 1595, 1490, 1461, 1367, 1275, 1164, 1027, 947, 867, 766  $\text{cm}^{-1}$ ; HRMS (EI+)  $m/z$  calc'd for  $\text{C}_{16}\text{H}_{21}\text{NO}_5$   $[\text{M}^+]$ : 307.1420, found 307.1418.



### Indoline 170c (Table 2.2, Entry 3)

Reaction performed via Method A. Purified by flash chromatography ( $\text{SiO}_2$ , 10:90 → 30:70 EtOAc/hexanes). 39% yield.  $R_f = 0.33$  (30:70 EtOAc/hexanes);  $^1\text{H}$  NMR (500 MHz,  $\text{CDCl}_3$ )  $\delta$  7.58 (s, 1H), 6.58 (s, 1H), 5.89 (s, 2H), 4.84 (d,  $J = 11.0$  Hz, 1H) 2.78 (s, 1H), 3.55 (dd,  $J = 12.1, 5.7$  Hz, 1H), 3.07 (d,  $J = 15.9, 1.0$  Hz, 1H), 1.45 (s, 9H);  $^{13}\text{C}$  NMR (125 MHz,  $\text{CDCl}_3$ )  $\delta$  172.2, 151.9, 147.6, 143.3, 145.6, 128.2, 119.6, 105.0, 101.5, 98.3, 81.7, 61.7, 52.7, 33.0, 28.3; IR (Neat Film, NaCl) 2949, 1753, 1706, 1477, 1405, 1367, 1303, 1258, 1166, 1081, 1037, 938  $\text{cm}^{-1}$ ; HRMS (EI+)  $m/z$  calc'd for  $\text{C}_{16}\text{H}_{19}\text{NO}_6$   $[\text{M}^+]$ : 321.1212, found 321.1224.

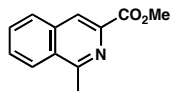


### Indoline 170d (Table 2.2, Entry 4)

Reaction performed via Method A. Purified by flash chromatography ( $\text{SiO}_2$ , 10:90 → 20:80 EtOAc/hexanes). 40% yield.  $R_f = 0.23$  (30:70 EtOAc/hexanes);  $^1\text{H}$  NMR (500 MHz,  $\text{CDCl}_3$ )  $\delta$  7.63 (d,  $J = 7.0$  Hz, 1H), 7.48 (dd,  $J = 7.6, 2.2$  Hz, 1H), 7.37 (comp m, 4H), 7.23 (d,  $J = 8.9$  Hz, 2H), 6.90 (t,  $J = 7.6$  Hz, 1H), 6.79 (d,  $J = 7.6$  Hz, 1H) 3.86 (t,  $J = 5.3$  Hz, 1H), 3.82 (s, 3H), 1.40 (s, 9H);  $^{13}\text{C}$  NMR (125 MHz,  $\text{CDCl}_3$ )  $\delta$  166.5, 158.9,

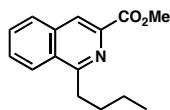
155.8, 135.2, 133.9, 133.0, 130.2, 129.9, 129.6, 129.0, 128.8, 128.0, 120.9, 115.1, 80.9, 67.5, 52.8, 47.8, 21.4; IR (Neat Film, NaCl) 2947, 1723, 1707, 1638, 1600, 1496, 1448, 1391, 1366, 1245, 1170, 1143, 755, 692  $\text{cm}^{-1}$ ; HRMS (EI+)  $m/z$  calc'd for  $\text{C}_{21}\text{H}_{23}\text{NO}_4$   $[\text{M}+\text{H}]^+$ : 352.1549, found 352.1564. Relative stereochemistry of substituents at C(2) and C(3) confirmed by 1D NOESY NMR studies.

### 2.5.2.3 Spectroscopic Data for Isoquinolines



#### Isoquinoline 176 (Table 2.4, entry 1)

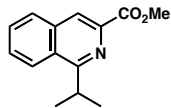
Reaction performed via Method B. Purified by flash chromatography ( $\text{SiO}_2$ , 10:90 → 30:70 EtOAc/hexanes). 87% yield.  $R_f = 0.33$  (30:70 EtOAc/hexanes);  $^1\text{H}$  NMR (300 MHz,  $\text{CDCl}_3$ )  $\delta$  8.47 (s, 1H), 8.20 (d,  $J = 9.2$ , 1H), 7.97 (d,  $J = 6.7$  Hz, 1H), 7.76 (app ddd,  $J = 5.2, 3.2, 1.9$  Hz, 2H), 4.04 (s, 3H), 3.05 (s, 3H);  $^{13}\text{C}$  NMR (125 MHz,  $\text{CDCl}_3$ )  $\delta$  165.4, 158.6, 141.4, 135.4, 131.0, 129.1, 128.6, 127.4, 125.4, 123.5, 51.5, 21.4; IR (Neat Film, NaCl) 2953, 1731, 1569, 1501, 1448, 1337, 1391, 1291, 1230, 1210, 795  $\text{cm}^{-1}$ ; HRMS (EI+)  $m/z$  calc'd for  $\text{C}_{12}\text{H}_{11}\text{NO}_2$   $[\text{M}^+]^+$ : 201.0790, found 201.0797.



#### Isoquinoline 181a (Table 2.4, entry 2)

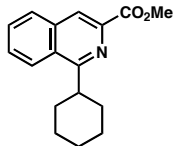
Reaction performed via Method B. Purified by flash chromatography ( $\text{SiO}_2$ , 10:90 → 30:70 EtOAc/hexanes). 76% yield.  $R_f = 0.40$  (30:70 EtOAc/hexanes);  $^1\text{H}$  NMR (500

MHz,  $\text{CDCl}_3$ )  $\delta$  8.45 (s, 1H), 8.18 (d,  $J$  = 9.6 Hz, 1H), 7.93 (d,  $J$  = 9.2 Hz, 1H), 7.70 (ddd,  $J$  = 5.0, 3.6, 2.3 Hz, 2H), 4.01 (s, 3H), 2.89 (d,  $J$  = 6.3 Hz, 2H), 1.63 (q,  $J$  = 5.2 Hz, 2H), 1.12 (app dt,  $J$  = 5.5, 3.3 Hz, 2H), 0.88 (t,  $J$  = 3.4 Hz, 3H);  $^{13}\text{C}$  NMR (125 MHz,  $\text{CDCl}_3$ )  $\delta$  168.5, 163.8, 141.4, 135.9, 131.0, 129.8, 129.1, 128.6, 126.0, 123.5, 53.5, 36.1, 33.2, 23.8, 14.3; IR (Neat Film, NaCl) 2855, 2870, 1721, 1449, 1293, 1246, 1213, 1175, 749  $\text{cm}^{-1}$ ; HRMS (EI+)  $m/z$  calc'd for  $\text{C}_{15}\text{H}_{17}\text{NO}_2$  [ $\text{M}^+$ ]: 243.1259, found 243.1256.



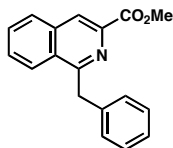
**Isoquinoline 181b (Table 2.4, entry 3)**

Reaction performed via Method B. Purified by flash chromatography ( $\text{SiO}_2$ , 10:90  $\rightarrow$  30:70 EtOAc/hexanes). 66% yield.  $R_f$  = 0.37 (30:70 EtOAc/hexanes);  $^1\text{H}$  NMR (300 MHz,  $\text{CDCl}_3$ ) 8.41 (s, 1H), 8.29 (d,  $J$  = 4.5 Hz, 1H), 7.96 (d,  $J$  = 3.5 Hz, 1H), 7.73 (app dt,  $J$  = 5.5, 3.3 Hz, 2H), 4.03 (s, 3H), 3.97 (m, 1H), 1.50 (d,  $J$  = 7.0 Hz, 6H);  $^{13}\text{C}$  NMR (125 MHz,  $\text{CDCl}_3$ )  $\delta$  166.9, 145.0, 140.8, 135.3, 130.4, 129.7, 129.3, 128.2, 125.2, 122.9, 53.0, 31.4, 22.7; IR (Neat Film, NaCl) 3965, 2929, 1718, 1565, 1501, 1449, 1323, 1267, 1221, 1207, 1150, 1117, 1077, 987, 781  $\text{cm}^{-1}$ ; HRMS (EI+)  $m/z$  calc'd for  $\text{C}_{14}\text{H}_{15}\text{NO}_2$  [ $\text{M}^+$ ]: 229.1103, found 229.1100.



**Isoquinoline 181c (Table 2.4, entry 4)**

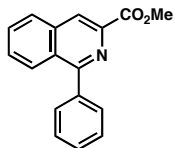
Reaction performed via Method B. Purified by flash chromatography (SiO<sub>2</sub>, 10:90 EtOAc/hexanes). 65% yield.  $R_f$  = 0.49 (30:70 EtOAc/hexanes); <sup>1</sup>H NMR (500 MHz, CDCl<sub>3</sub>) 8.44 (s, 1H), 8.28 (d,  $J$  = 4.3 Hz, 1H), 7.4 (d,  $J$  = 3.5 Hz, 1H), 7.73 (app dt,  $J$  = 5.2, 3.1 Hz, 2H), 4.02 (s, 3H), 3.59 (m, 1H), 1.98 (m, 8H), 1.57 (q,  $J$  = 5.1 Hz, 1H), 1.41 (q,  $J$  = 3.3 Hz, 1H); <sup>13</sup>C NMR (125 MHz, CDCl<sub>3</sub>)  $\delta$  167.0, 166.1, 140.7, 136.0, 129.9, 129.1, 127.8, 124.6, 122.2, 52.0, 42.1, 32.1, 27.1, 26.0; IR (Neat Film, NaCl) 2927, 2852, 1739, 1718, 1567, 1502, 1449, 1325, 1311, 1271, 1243, 1204, 1150, 1000, 780, 750 cm<sup>-1</sup>; HRMS (EI+) *m/z* calc'd for C<sub>14</sub>H<sub>15</sub>NO<sub>2</sub> [M<sup>+</sup>]: 269.1416, found 269.1424.



**Isoquinoline 181d (Table 2.4, entry 5)**

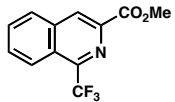
Reaction performed via Method B. Purified by flash chromatography (SiO<sub>2</sub>, 0:100 → 30:70 EtOAc/hexanes). 72% yield.  $R_f$  = 0.47 (30:70 EtOAc/hexanes); <sup>1</sup>H NMR (500 MHz, CDCl<sub>3</sub>)  $\delta$  8.53 (s, 1H), 8.20 (d,  $J$  = 6.7, 1H), 8.02 (d,  $J$  = 5.1 Hz, 1H), 7.74 (t,  $J$  = 7.1 Hz, 1H), 7.63 (t,  $J$  = 6.6 Hz, 1H), 7.22 (m, 4H), 7.18 (m, 1H), 4.80 (s, 2H) 4.14 (s, 3H); <sup>13</sup>C NMR (125 MHz, CDCl<sub>3</sub>)  $\delta$  167.3, 163.7, 141.4, 139.5, 135.4, 131.7, 129.8, 129.1, 128.3, 128.0, 126.3, 124.0, 53.5, 42.9; IR (Neat Film, NaCl) 2946, 2929, 1731,

1716, 1551, 1455, 1380, 1301, 1230, 1210, 995  $\text{cm}^{-1}$ ; HRMS (EI+)  $m/z$  calc'd for  $\text{C}_{18}\text{H}_{15}\text{NO}_2$   $[\text{M}+\text{H}]^+$ : 278.1103, found 278.1181.



### Isoquinoline 181e (Table 2.4, entry 6)

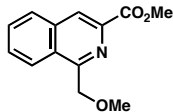
Reaction performed via Method B. Purified by flash chromatography ( $\text{SiO}_2$ , 0:100  $\rightarrow$  10:90 EtOAc/hexanes). 55% yield.  $R_f = 0.52$  (30:70 EtOAc/hexanes);  $^1\text{H}$  NMR (500 MHz,  $\text{CDCl}_3$ )  $\delta$  8.60 (s, 1H), 8.19 (d,  $J = 8.3$  Hz, 1H), 8.05 (d,  $J = 8.3$  Hz, 1H), 7.78 (t,  $J = 7.7$  Hz, 1H), 7.71, (dd,  $J = 7.7, 4.3$  Hz, 2H), 7.66 (d,  $J = 7.7$  Hz, 1H), 7.57 (t,  $J = 6.0$  Hz, 1H), 7.53 (d,  $J = 6.8$ , 1H), 7.49 (t,  $J = 4.3$  Hz, 1H), 4.03 (s, 3H);  $^{13}\text{C}$  NMR (125 MHz,  $\text{CDCl}_3$ )  $\delta$  166.0, 162.2, 141.2, 139.3, 137.7, 131.0, 130.4, 129.7, 128.6, 128.3, 128.2, 128.0, 127.8, 124.0; IR (Neat Film, NaCl) 2949, 1725, 1715, 1493, 1449, 1376, 1339, 1292, 1242, 1217, 1148, 1102, 997, 798, 766, 700  $\text{cm}^{-1}$ ; HRMS (EI+)  $m/z$  calc'd for  $\text{C}_{17}\text{H}_{13}\text{NO}_2$   $[\text{M}+\text{H}]^+$ : 264.1025, found 264.1020.



### Isoquinoline 181f (Table 2.4, entry 7)

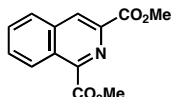
Reaction performed via Method B. Purified by flash chromatography ( $\text{SiO}_2$ , 20:80  $\rightarrow$  30:70 EtOAc/hexanes). 57% yield.  $R_f = 0.22$  (30:70 EtOAc/hexanes);  $^1\text{H}$  NMR (500 MHz,  $\text{CDCl}_3$ )  $\delta$  8.50 (s, 1H), 8.42 (d,  $J = 7.9$  Hz, 1H), 8.21 (d,  $J = 9.3$  Hz, 1H), 7.91 (t,  $J = 8.4$  Hz, 1H), 7.81 (t,  $J = 7.1$  Hz, 1H), 4.12 (s, 3H);  $^{13}\text{C}$  NMR (125 MHz,  $\text{CDCl}_3$ )  $\delta$

165.6, 148.3, 135.9, 135.1, 132.1, 131.4, 130.6, 124.6, 122.1, 118.2, 54.5; IR (Neat Film, NaCl) 2924, 2102, 1730, 1643, 1462, 1275, 1252, 1155, 1126, 897, 726  $\text{cm}^{-1}$ ; HRMS (EI+)  $m/z$  calc'd for  $\text{C}_{12}\text{H}_8\text{F}_3\text{NO}_2$  [ $\text{M}^+$ ]: 255.0507, found 255.0500.



**Isoquinoline 181g (Table 2.4, entry 8)**

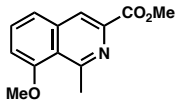
Reaction performed via Method B. Purified by flash chromatography ( $\text{SiO}_2$ , 25:75 → 50:50 EtOAc/hexanes). 68% yield.  $R_f = 0.50$  (50:50 EtOAc/hexanes);  $^1\text{H}$  NMR (500 MHz,  $\text{CDCl}_3$ )  $\delta$  8.57 (s, 1H), 8.43 (dd,  $J = 7.5, 1.0$  Hz, 1H), 7.99 (dd,  $J = 7.5, 2.0$  Hz, 1H), 7.78 (ddd,  $J = 8.0, 6.0, 1.0$  Hz, 1H), 7.77 (ddd,  $J = 9.0, 6.5, 1.5$  Hz, 1H), 5.13 (s, 2H), 4.06 (s, 3H), 3.49 (s, 3H);  $^{13}\text{C}$  NMR (125 MHz,  $\text{CDCl}_3$ )  $\delta$  166.6, 158.0, 140.4, 136.4, 131.2, 130.0, 128.9, 128.8, 126.4, 125.0, 75.5, 58.9, 53.2; IR (Neat Film, NaCl) 2950, 1736, 1718, 1450, 1295, 1248, 1210, 1100, 779  $\text{cm}^{-1}$ ; HRMS (ES+)  $m/z$  calc'd for  $\text{C}_{13}\text{H}_{14}\text{NO}_3$  [ $\text{M}+\text{H}$ ]: 232.0974, found 232.0968.



**Isoquinoline 181h (Table 2.4, entry 9)**

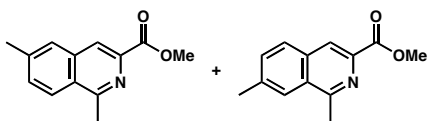
Reaction performed via Method B. Purified by flash chromatography ( $\text{SiO}_2$ , 20:80 → 30:70 EtOAc/hexanes). 51% yield.  $R_f = 0.21$  (30:70 EtOAc/hexanes);  $^1\text{H}$  NMR (500 MHz,  $\text{CDCl}_3$ )  $\delta$  8.85 (d,  $J = 8.2$  Hz, 1H), 8.78 (s, 1H), 8.05 (t,  $J = 3.5$  Hz, 1H), 7.81 (m, 2H), 4.13 (s, 3H), 4.09 (s, 3H);  $^{13}\text{C}$  NMR (125 MHz,  $\text{CDCl}_3$ )  $\delta$  165.9, 165.4, 149.1,

139.6, 136.3, 134.2, 131.0, 131.4, 128.4, 128.0, 127.2, 126.6, 53.6; IR (Neat Film, NaCl) 2959, 2924, 1725, 1713, 1449, 1300, 1251, 1232, 1205, 1146, 1055, 786, 760  $\text{cm}^{-1}$ ; HRMS (EI+)  $m/z$  calc'd for  $\text{C}_{13}\text{H}_{11}\text{NO}_4$  [ $\text{M}^+$ ]: 245.0688, found 245.0679.



### Isoquinoline 182a (Table 2.5, entry 1)

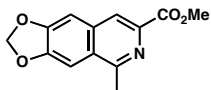
Reaction performed via Method B. Purified by flash chromatography ( $\text{SiO}_2$ , 20:80  $\rightarrow$  20:80 EtOAc/hexanes). 66% yield.  $R_f = 0.32$  (30:70 EtOAc/hexanes).  $^1\text{H}$  NMR (500 MHz,  $\text{CDCl}_3$ )  $\delta$  8.35 (s, 1H), 7.63 (t,  $J = 8.0$  Hz, 1H), 7.48 (d,  $J = 8.0$  Hz, 1H), 7.04 (d,  $J = 7.5$  Hz, 1H), 3.83 (s, 3H), 3.03 (s, 3H), 2.98 (s, 3H);  $^{13}\text{C}$  NMR (125 MHz,  $\text{CDCl}_3$ )  $\delta$  166.8, 159.8, 158.3, 140.6, 138.6, 131.4, 122.8, 121.8, 121.0, 109.0, 55.9, 53.0, 29.2; IR (Neat Film, NaCl) 2936, 2852, 1734, 1708, 1616, 1566, 1455, 1435, 1363, 1275, 1252, 1214, 1140, 1088, 1012, 787  $\text{cm}^{-1}$ ; HRMS (EI+)  $m/z$  calc'd for  $\text{C}_{13}\text{H}_{13}\text{NO}_3$  [ $\text{M}^+$ ]: 231.0895, found 231.0889.



### Isoquinolines 182b and c (Table 2.5, entry 2)

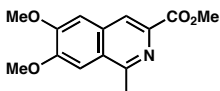
Reaction performed via Method B. Purified by flash chromatography ( $\text{SiO}_2$ , 10:90  $\rightarrow$  20:80 EtOAc/hexanes). 59% yield as a 1:1 mixture of isomers.  $R_f = 0.40$  (30:70 EtOAc/hexanes); Isolated as 1:1 mixture of isomers.  $^1\text{H}$  NMR (500 MHz,  $\text{CDCl}_3$ )  $\delta$  8.07 (s, 1H), 8.00 (s, 1H), 8.34 (s, 1H), 8.04 (s, 1H), 8.02 (s, 1H), 7.90, (s, 2H), 7.82 (s, 1H),

7.80, (s, 1H), 7.67 (s, 2H), 7.56 (d,  $J$  = 8.7 Hz, 1H), 7.52 (d,  $J$  = 8.7 Hz, 1H) 4.02 (s, 6H), 2.99 (d,  $J$  = 1.8 Hz, 6H), 2.57 (s, 3H), 2.54 (s, 3H);  $^{13}\text{C}$  NMR (125 MHz,  $\text{CDCl}_3$ )  $\delta$  167.1, 159.3, 158.9, 141.6, 140.1, 139.9, 133.8, 133.6, 132.0, 129.1, 128.5, 128.0, 127.8, 125.9, 125.0, 123.8, 122.6, 53.3, 23.1, 22.1, 21.9; IR (Neat Film, NaCl) 2951, 1718, 1438, 1392, 1287, 1245, 1212, 1116, 1009, 818  $\text{cm}^{-1}$ ; HRMS (EI+)  $m/z$  calc'd for  $\text{C}_{13}\text{H}_{13}\text{NO}_2$   $[\text{M}^+]$ : 215.0946, found 215.0898.



### Isoquinoline 182d (Table 2.5, entry 3)

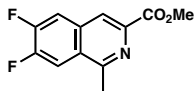
Reaction performed via Method B. Purified by flash chromatography ( $\text{SiO}_2$ , 10:90 → 40:60 EtOAc/hexanes). 63% yield.  $R_f$  = 0.25 (30:70 EtOAc/hexanes);  $^1\text{H}$  NMR (500 MHz,  $\text{CDCl}_3$ )  $\delta$  8.07 (s, 1H), 7.31 (s, 1H), 7.06 (s, 1H), 5.87 (s, 2H), 3.85 (s, 3H), 3.11 (s, 3H);  $^{13}\text{C}$  NMR (125 MHz,  $\text{CDCl}_3$ )  $\delta$  166.7, 157.1, 150.2, 149.3, 141.3, 133.6, 121.9, 104.2, 101.0, 100.7, 68.3, 51.7, 22.2; IR (Neat Film, NaCl) 2903, 2833, 1755, 1609, 1522, 1461, 1430, 1244, 1170, 1026, 931, 733  $\text{cm}^{-1}$ ; HRMS (EI+)  $m/z$  calc'd for  $\text{C}_{13}\text{H}_{11}\text{NO}_4$   $[\text{M}^+]$ : 245.0688, found 245.1003.



### Isoquinoline 182e (Table 2.5, entry 4)

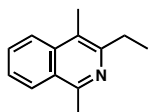
Reaction performed via Method B. Purified by flash chromatography ( $\text{SiO}_2$ , 10:90 → 40:60 EtOAc/hexanes). 60% yield.  $R_f$  = 0.34 (30:70 EtOAc/hexanes);  $^1\text{H}$  NMR (500 MHz,  $\text{CDCl}_3$ )  $\delta$  8.36 (s, 1H), 7.34 (s, 1H), 7.20 (s, 1H), 4.08 (s, 3H), 4.05 (s, 6H), 4.03 (s,

3H), 2.98 (s, 3H);  $^{13}\text{C}$  NMR (125 MHz,  $\text{CDCl}_3$ )  $\delta$  166.2, 156.6, 154.2, 152.1, 139.7, 132.1, 125.8, 123.9, 111.8, 105.2, 56.1, 51.5, 21.4; IR (Neat Film, NaCl) 2952, 2840, 1730, 1618, 1511, 1465, 1426, 1256, 1161, 1028, 733  $\text{cm}^{-1}$ ; HRMS (EI+)  $m/z$  calc'd for  $\text{C}_{14}\text{H}_{15}\text{NO}_4$   $[\text{M}^+]$ : 261.1001, found 261.1012.



### Isoquinoline 182f (Table 2.5, entry 5)

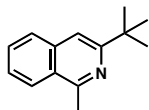
Reaction performed via Method B. Purified by flash chromatography ( $\text{SiO}_2$ , 30:70 EtOAc/hexanes). 66% yield.  $R_f = 0.29$  (1:1 EtOAc/hexanes);  $^1\text{H}$  NMR (500 MHz,  $\text{CDCl}_3$ )  $\delta$  8.40 (s, 1H), 7.93 (dd,  $J = 8.0, 1.9$  Hz, 1H), 7.70 (t,  $J = 8.7$  Hz, 1H), 4.05 (s, 3H), 3.01 (s, 3H);  $^{13}\text{C}$  NMR (125 MHz,  $\text{CDCl}_3$ )  $\delta$  166.4, 122.23, 115.1, 114.9, 113.9, 113.0, 60.7, 53.3, 31.3, 23.2, 21.4, 14.5; IR (Neat Film, NaCl) 2920, 1716, 1514, 1426, 1281, 1258, 1228, 1181, 1144, 1125, 928, 851, 792, 738, 611  $\text{cm}^{-1}$ ; HRMS (ES+)  $m/z$  calc'd for  $\text{C}_{19}\text{H}_{23}\text{NO}_2$   $[\text{M}^+]$ : 237.0601 found 237.0591.



### Isoquinoline 187a (Table 2.6, entry 1)

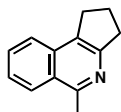
Reaction performed via Method B. Purified by flash chromatography ( $\text{SiO}_2$ , 0:100  $\rightarrow$  20:80 EtOAc/hexanes). 72% yield.  $R_f = 0.45$  (30:70 EtOAc/hexanes);  $^1\text{H}$  NMR (500 MHz,  $\text{CDCl}_3$ )  $\delta$  8.09 (d,  $J = 8.0$  Hz, 1H), 7.98 (d,  $J = 8.5$  Hz, 1H), 7.68 (ddd,  $J = 8.5, 7.0, 1.0$  Hz, 1H), 7.52 (ddd,  $J = 8.0, 7.0, 1.5$  Hz, 1H), 3.00 (q,  $J = 7.8$  Hz, 2H), 2.92 (s, 3H),

2.58 (s, 3H), 1.30 (t,  $J$  = 7.5 Hz, 3H);  $^{13}\text{C}$  NMR (125 MHz,  $\text{CDCl}_3$ )  $\delta$  151.9, 149.2, 129.5, 125.9, 125.3, 123.4, 29.3, 22.3, 14.3, 13.4; IR (Neat Film, NaCl) 2965, 1618, 1570, 1443, 1395, 1339, 1270, 755  $\text{cm}^{-1}$ ; HRMS (EI+)  $m/z$  calc'd for  $\text{C}_{13}\text{H}_{15}\text{N}$  [ $\text{M}^+$ ]: 185.1204, found 185.1266.



### Isoquinoline 187b (Table 2.6, entry 2)

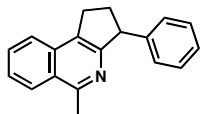
Reaction Performed via Method B. Purified by flash chromatography ( $\text{SiO}_2$ , 0:100  $\rightarrow$  4:96  $\text{Et}_2\text{O}$ /hexanes). 83% yield.  $R_f$  = 0.73 (15:85 EtOAc/hexanes);  $^1\text{H}$  NMR (500 MHz,  $\text{CDCl}_3$ )  $\delta$  8.07 (d,  $J$  = 9.0 Hz, 1H), 7.76 (d,  $J$  = 8.0 Hz, 1H), 7.61 (t,  $J$  = 7.0 Hz, 1H), 7.51 (t,  $J$  = 6.5 Hz, 1H), 7.45 (s, 1H), 2.95 (s, 3H), 1.45 (s, 9H);  $^{13}\text{C}$  NMR (125 MHz,  $\text{CDCl}_3$ )  $\delta$  161.8, 157.2, 136.6, 129.4, 127.2, 125.9, 125.6, 125.3, 112.5, 36.9, 30.1, 22.6; IR (Neat Film, NaCl) 3058, 2954, 1626, 1573, 1481, 1390, 1356, 878, 748  $\text{cm}^{-1}$ ; HRMS (EI+)  $m/z$  calc'd for  $\text{C}_{14}\text{H}_{17}\text{N}$  [ $\text{M}^+$ ]: 199.1361, found 199.1363.



### Isoquinoline 187c (Table 2.6, entry 3)

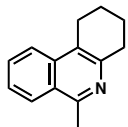
Reaction performed via Method B at 60 °C. Purified by flash chromatography ( $\text{SiO}_2$ , 0:100  $\rightarrow$  20:80 EtOAc/hexanes). 66% yield.  $R_f$  = 0.29 (30:70 EtOAc/hexanes);  $^1\text{H}$  NMR (500 MHz,  $\text{CDCl}_3$ )  $\delta$  8.12 (d,  $J$  = 8.5 Hz, 1H), 7.74 (d,  $J$  = 8.5 Hz, 1H), 7.67 (app t,  $J$  = 7.5 Hz, 1H), 7.52 (app t,  $J$  = 7.5 Hz, 1H), 3.20 (app dd,  $J$  = 9.0, 8.0 Hz, 4H), 2.95 (s, 3H),

2.26 (app quintet,  $J = 7.5$  Hz, 2H);  $^{13}\text{C}$  NMR (125 MHz,  $\text{CDCl}_3$ )  $\delta$  157.7, 156.4, 133.9, 130.1, 128.7, 126.6, 126.0, 125.7, 124.2, 35.1, 29.2, 22.7, 22.6; IR (Neat Film, NaCl) 2953, 1621, 1581, 1562, 1442, 1390, 1342, 1150, 755  $\text{cm}^{-1}$ ; HRMS (EI+)  $m/z$  calc'd for  $\text{C}_{13}\text{H}_{13}\text{N} [\text{M}^+]$ : 183.1048, found 183.1033.



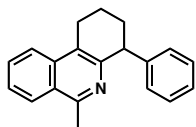
### A1-1

Reaction performed via Method B at 60 °C. Purified by flash chromatography ( $\text{SiO}_2$ , 0:100 → 20:80 EtOAc/hexanes). 21% yield, isolated as a side product of the reaction to form Table 2, Entry 12.  $R_f = 0.80$  (50:50 EtOAc/hexanes);  $^1\text{H}$  NMR (500 MHz,  $\text{CDCl}_3$ )  $\delta$  8.15 (d,  $J = 8.3$  Hz, 1H), 7.82 (d,  $J = 8.3$  Hz, 1H), 7.72 (ddd,  $J = 8.3, 6.8, 1.0$  Hz, 1H), 7.57 (ddd,  $J = 8.3, 6.8, 1.2$  Hz, 1H), 7.27 (app t,  $J = 7.1$  Hz, 2H), 7.19 (tt,  $J = 7.3, 1.2$  Hz, 1H), 7.14 (app d,  $J = 7.1$  Hz, 2H), 4.62 (dd,  $J = 8.8, 5.1$  Hz, 1H), 3.36 (ddd,  $J = 15.9, 7.8, 7.3$  Hz, 1H), 3.22 (ddd,  $J = 16.1, 9.0, 5.1$  Hz, 1H), 2.91 (s, 3H), 2.85-2.77 (m, 1H), 2.26-2.19 (m, 1H);  $^{13}\text{C}$  NMR (125 MHz,  $\text{CDCl}_3$ )  $\delta$  158.6, 157.5, 145.7, 135.5, 135.2, 130.3, 130.2, 128.7, 128.2, 128.1, 126.7, 126.4, 126.3, 126.2, 124.4, 52.6, 33.9, 27.8, 22.8; IR (Neat Film, NaCl) 3064, 2943, 1682, 1622, 1561, 1493, 1429, 1390, 1117, 1027, 758, 700  $\text{cm}^{-1}$ ; HRMS (ES+)  $m/z$  calc'd for  $\text{C}_{19}\text{H}_{18}\text{N} [\text{M}+\text{H}]^+$ : 260.1439, found 260.1438.



**Isoquinoline 187d (Table 2.6, entry 4)**

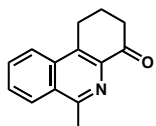
Reaction performed via Method B at 60 °C. Purified by flash chromatography (SiO<sub>2</sub>, 10:90 → 40:60 EtOAc/hexanes). 67% yield.  $R_f$  = 0.33 (30:70 EtOAc/hexanes); <sup>1</sup>H NMR (500 MHz, CDCl<sub>3</sub>) δ 8.09 (d,  $J$  = 8.0 Hz, 1H), 7.91 (d,  $J$  = 8.5 Hz, 1H), 7.68 (ddd,  $J$  = 8.5, 7.0, 1.0 Hz, 1H), 7.53 (ddd,  $J$  = 8.5, 7.0, 1.0 Hz, 1H), 3.04 (app dd,  $J$  = 5.0, 2.0 Hz, 4H), 2.92 (s, 3H), 1.95 (app quintet,  $J$  = 3.0 Hz, 4H); <sup>13</sup>C NMR (125 MHz, CDCl<sub>3</sub>) δ 156.0, 148.9, 135.7, 129.9, 126.3, 126.0, 125.8, 123.2, 122.7, 33.0, 24.9, 23.4, 23.0, 22.6; IR (Neat Film, NaCl) 2930, 1616, 1570, 1443, 1392, 1332, 1030, 754 cm<sup>-1</sup>; HRMS (EI+) *m/z* calc'd for C<sub>14</sub>H<sub>15</sub>N [M<sup>+</sup>]: 197.1204, found 197.1213.



**A1-2**

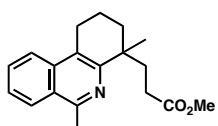
Reaction performed via Method B at 60 °C. Purified by flash chromatography (SiO<sub>2</sub>, 10:90 → 40:60 EtOAc/hexanes). 14% yield, isolated as a side product of the reaction to form Table 2, Entry 13.  $R_f$  = 0.84 (50:50 EtOAc/hexanes); <sup>1</sup>H NMR (500 MHz, CDCl<sub>3</sub>) δ 8.11 (d,  $J$  = 8.3 Hz, 1H), 8.00 (d,  $J$  = 8.5 Hz, 1H), 7.73 (ddd,  $J$  = 8.3, 6.8, 1.2 Hz, 1H), 7.58 (ddd,  $J$  = 8.3, 6.8, 1.2 Hz, 1H), 7.23 (app t,  $J$  = 7.1 Hz, 2H), 7.16 (tt,  $J$  = 7.3, 1.2 Hz, 1H), 7.00 (app d,  $J$  = 7.1 Hz, 2H), 4.48 (app t,  $J$  = 4.6 Hz, 1H), 3.23 (dt,  $J$  = 16.9, 4.9 Hz, 1H), 3.05 (dt,  $J$  = 16.9, 8.3 Hz, 1H), 2.84 (s, 3H), 2.29-2.21 (m, 1H), 2.08 (app dq,  $J$  = 13.4, 4.2 Hz, 1H), 1.88-1.83 (comp m, 2H); <sup>13</sup>C NMR (125 MHz, CDCl<sub>3</sub>) δ 156.6, 149.6,

146.6, 135.6, 135.2, 130.4, 130.0, 129.3, 128.2, 126.4, 126.3, 126.2, 125.9, 124.5, 123.0, 47.5, 32.4, 25.0, 22.7, 18.4; IR (Neat Film, NaCl) 3066, 2934, 1615, 1590, 1492, 1446, 1390, 1332, 1117, 1029, 756, 700  $\text{cm}^{-1}$ ; HRMS (ES+)  $m/z$  calc'd for  $\text{C}_{20}\text{H}_{20}\text{N}$   $[\text{M}+\text{H}]^+$ : 274.1596, found 274.1608.



**Isoquinoline 187e (Table 2.6, entry 5)**

Reaction performed via Method B. Purified by flash chromatography ( $\text{SiO}_2$ , 1:1 EtOAc/hexanes). 66% yield.  $R_f = 0.21$  (1:1 EtOAc/hexanes);  $^1\text{H}$  NMR (500 MHz,  $\text{CDCl}_3$ )  $\delta$  8.22 (d,  $J = 9.8$  Hz, 1H), 8.15 (d,  $J = 7.6$  Hz, 1H), 7.84 (t,  $J = 6.1$  Hz, 1H), 7.78 (t,  $J = 7.6$  Hz, 1H), 3.38 (t,  $J = 6.8$  Hz, 2H), 3.04 (s, 3H), 2.86 (d,  $J = 7.6$ , 2H), 2.33 (quintet,  $J = 4.5$ , 2H);  $^{13}\text{C}$  NMR (125 MHz,  $\text{CDCl}_3$ )  $\delta$  197.7, 158.6, 141.2, 136.0, 134.7, 130.9, 129.7, 128.9, 126.8, 124.7, 39.2, 25.2, 23.1, 22.5; IR (Neat Film, NaCl) 2944, 1682, 1628, 1407, 1385, 1164, 1129, 1031, 906, 759  $\text{cm}^{-1}$ ; HRMS (ES+)  $m/z$  calc'd for  $\text{C}_{19}\text{H}_{23}\text{NO}_2$   $[\text{M}+\text{H}]^+$ : 211.0997, found 211.0994.

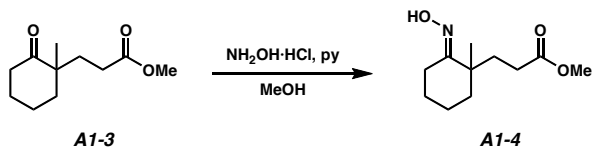


**Isoquinoline 187f (Table 2.6, entry 6)**

See below for synthesis of the enamide substrate SI-4. Purified by flash chromatography ( $\text{SiO}_2$ , 5:95 Et<sub>2</sub>O/hexanes). 71% yield.  $R_f = 0.48$  (15:85 EtOAc/hexanes);  $^1\text{H}$  NMR (500 MHz,  $\text{CDCl}_3$ )  $\delta$  8.06 (d,  $J = 8.0$  Hz, 1H), 7.90 (d,  $J = 8.5$  Hz, 1H), 7.65 (t,  $J = 7.0$  Hz,

1H), 7.52 (t,  $J$  = 7.0 Hz, 1H), 3.62 (s, 3H), 3.11 (dt,  $J$  = 16.5, 5.5 Hz, 1H), 2.99-2.93 (m, 1H), 2.90 (s, 3H), 2.33 (app d,  $J$  = 12.0 Hz, 2H), 2.08 (app d,  $J$  = 12.0 Hz, 2H), 2.02-1.90 (comp m, 2H), 1.85 (td,  $J$  = 13.0, 3.0 Hz, 1H), 1.74-1.69 (m, 1H), 1.41 (s, 3H);  $^{13}\text{C}$  NMR (125 MHz,  $\text{CDCl}_3$ )  $\delta$  175.0, 155.6, 153.9, 135.2, 129.3, 125.8, 125.5, 125.4, 122.9, 122.4, 51.4, 38.7, 36.5, 34.7, 29.9, 28.2, 25.5, 22.5, 18.9; IR (Neat Film, NaCl) 2934, 1737, 1570, 1439, 1205, 1171, 1118, 756, 710  $\text{cm}^{-1}$ ; HRMS (ES+)  $m/z$  calc'd for  $\text{C}_{19}\text{H}_{23}\text{NO}_2$  [M+H] $^+$ : 298.1807, found 298.1796.

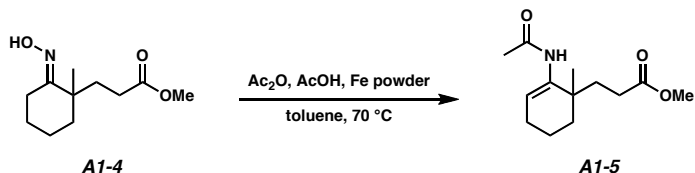
#### 2.5.2.4 Synthesis of Additional Substrates



#### Oxime A1-4

To a solution of ketoester **A1-3** (1.36 g, 6.86 mmol) in MeOH (27 mL) was added  $\text{NH}_2\text{OH}\cdot\text{HCl}$  (1.21 g, 17.4 mmol, 2.5 equiv) and pyridine (9.75 mL, 121 mmol, 17.6 equiv). The reaction was stirred at ambient temperature under nitrogen for 30 h, at which point it was concentrated under reduced pressure. The residue was dissolved in  $\text{CH}_2\text{Cl}_2$  (50 mL) and washed sequentially with water (50 mL) and brine (50 mL). The organic layer was dried over  $\text{MgSO}_4$ , filtered, and the filtrate was concentrated under reduced pressure to a pink oil. Purification by flash chromatography ( $\text{SiO}_2$ , 10:90 EtOAc:hexanes) provided oxime **A1-4** as a colorless oil (1.22 g, 83% yield).  $R_f$  = 0.33 (25:75 EtOAc/hexanes);  $^1\text{H}$  NMR (500 MHz,  $\text{CDCl}_3$ )  $\delta$  9.02 (br s, 1H), 3.66 (s, 3H), 3.01 (dt,  $J$  = 14.5, 4.5 Hz, 1H), 2.31 (dt,  $J$  = 10, 5 Hz, 1H), 2.19-2.11 (comp m, 2H), 2.04 (ddd,  $J$  = 14.5, 11.0, 5.0 Hz, 1H), 1.77-1.58 (comp m, 5H), 1.50-1.42 (comp m, 2H), 1.08 (s,

3H);  $^{13}\text{C}$  NMR (125 MHz,  $\text{CDCl}_3$ )  $\delta$  174.4, 163.9, 51.6, 40.0, 39.9, 32.5, 29.1, 25.8, 23.7, 21.1, 20.7; IR (Neat Film, NaCl) 3313, 2933, 2863, 1738, 1438, 1375, 1197, 1173, 936  $\text{cm}^{-1}$ ; HRMS (EI+)  $m/z$  calc'd for  $\text{C}_{11}\text{H}_{19}\text{NO}_3$   $[\text{M}^+]$ : 213.1365, found 213.1367.

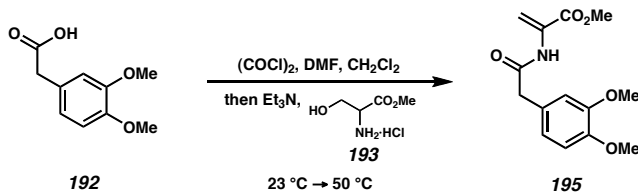


### **N**-Acetyl enamine **A1-5**

Reaction performed according to the method of Burk.<sup>70</sup> Acetic anhydride (7.0 mL, 74.1 mmol, 2.8 equiv) was added dropwise to a solution of oxime **A1-4** (5.61 g, 26.3 mmol) in toluene (45 mL) over a period of 5 min. After an additional 5 min, acetic acid (4.5 mL, 78.6 mmol, 3.0 equiv) was added dropwise over 2 min, followed by 325 mesh iron powder (2.94 g, 52.6 mmol, 2.0 equiv). A reflux condenser was attached and the mixture was heated to 70 °C under a nitrogen atmosphere for 4 h, during which time the color changed from dark grey to orange-brown. The reaction was cooled to ambient temperature and passed through a plug of Celite. The filtrate was diluted with EtOAc (100 mL) and washed with saturated aqueous sodium bicarbonate (2  $\times$  100 mL). The aqueous layer was extracted with EtOAc (2  $\times$  50 mL) and the combined organic layers were washed with brine (100 mL), dried over  $\text{MgSO}_4$ , filtered, and the filtrate was concentrated under reduced pressure to a yellow oil. Purification by flash chromatography ( $\text{SiO}_2$ , 25:75  $\rightarrow$  60:40 EtOAc:hexanes) provided acetamide **A1-5** (3.74 g, 60% yield) as a colorless oil.  $R_f$  = 0.21 (50:50 EtOAc/hexanes);  $^1\text{H}$  NMR (500 MHz,  $\text{CDCl}_3$ )  $\delta$  6.52 (br s, 1H), 6.16 (t,  $J$  = 4.0 Hz, 1H), 3.68 (s, 3H), 2.33 (dd,  $J$  = 9.5, 7.0 Hz,

1H), 2.26-2.09 (comp m, 3H), 2.05 (s, 3H), 1.88-1.82 (m, 1H), 1.64-1.56 (comp m, 4H), 1.44-1.39 (m, 1H), 1.08 (s, 3H);  $^{13}\text{C}$  NMR (125 MHz,  $\text{CDCl}_3$ )  $\delta$  175.0, 168.8, 135.7, 120.1, 51.8, 37.0, 34.7, 33.8, 29.0, 26.0, 24.8, 24.5, 18.6; IR (Neat Film, NaCl) 3301, 2934, 1738, 1672, 1658, 1531, 1436, 1371, 1272, 1198, 1173, 1001  $\text{cm}^{-1}$ ; HRMS (EI+)  $m/z$  calc'd for  $\text{C}_{13}\text{H}_{21}\text{NO}_3$  [M $^+$ ]: 239.1521, found 239.1527.

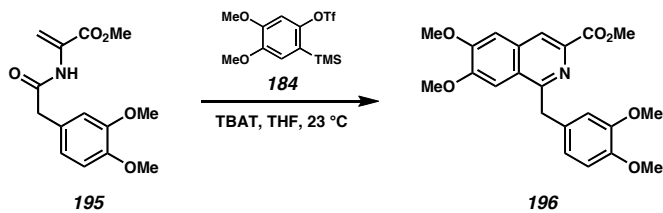
### 2.5.2.5 Total Synthesis of Papaverine



#### Methyl (3,4-dimethoxyphenyl)acetamidoacrylate (195)

Oxalyl chloride (2.6 mL, 29.8 mmol, 2.3 equiv) was slowly added to a solution of acid **192** (5.55 g, 28.3 mmol, 2.2 equiv) in  $\text{CH}_2\text{Cl}_2$  (40 mL), followed by DMF (0.10 mL, 1.29 mmol, 0.1 equiv). The solution was stirred at ambient temperature for 40 min, during which time it bubbled vigorously and the color changed from pale to bright yellow. In a separate flask, serine methyl ester-HCl (**193**) (2.02 g, 13.0 mmol) was suspended in  $\text{CH}_2\text{Cl}_2$  (120 mL), and  $\text{Et}_3\text{N}$  (5.91 mL, 42.0 mmol, 3.2 equiv) and DMAP (77.6 mg, 0.64 mmol, 0.05 equiv) were added. The mixture was stirred for 15 min until all solids had dissolved. The solution of acid chloride in the first flask was then transferred into the second flask via cannula under nitrogen over a period of 10 min, during which time the color of the serine methyl ester solution changed from colorless to orange. The reaction was maintained at ambient temperature under nitrogen for 2.5 h, at which time an additional portion of  $\text{Et}_3\text{N}$  (2.0 mL, 14.3 mmol, 1.1 equiv) was added. A reflux

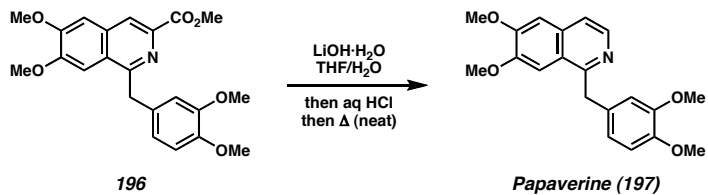
condenser was attached and the reaction was heated to 50 °C for 20 h. After cooling to ambient temperature, the solids were filtered off under vacuum and the filtrate was diluted in CH<sub>2</sub>Cl<sub>2</sub> (100 mL), washed with saturated aqueous sodium bicarbonate (150 mL), brine (150 mL), dried over MgSO<sub>4</sub>, filtered, and concentrated under reduced pressure to a yellow oil. In order to retrieve excess acid **192**, the aqueous layer was acidified with concentrated HCl (5 mL) and extracted with CH<sub>2</sub>Cl<sub>2</sub> (3 × 50 mL). The combined organic layers were dried over MgSO<sub>4</sub>, filtered, and concentrated under reduced pressure to a pale yellow solid (crude **195**). Purification of the original yellow oil by flash chromatography (SiO<sub>2</sub>, 25:75 → 45:55 EtOAc/hexanes) provided enamine **195** (2.43 g, 67% yield) as a colorless oil.  $R_f$  = 0.51 (50:50 EtOAc/hexanes); <sup>1</sup>H NMR (500 MHz, CDCl<sub>3</sub>) δ 7.82 (br s, 1H), 6.86 (s, 1H), 6.86 (d,  $J$  = 19.0 Hz, 1H), 6.82 (d,  $J$  = 19.5 Hz, 1H), 6.60 (s, 1H), 5.85 (d,  $J$  = 1.0 Hz, 1H), 3.88 (s, 3H), 3.87 (s, 3H), 3.78 (s, 3H), 3.61 (s, 2H); <sup>13</sup>C NMR (125 MHz, CDCl<sub>3</sub>) δ 169.9, 164.4, 149.4, 148.5, 130.8, 126.4, 121.6, 112.3, 111.6, 108.7, 55.9, 55.8, 52.9, 44.5; IR (Neat Film, NaCl) 3368, 2955, 1725, 1687, 1514, 1441, 1327, 1263, 1158, 1027 cm<sup>-1</sup>; HRMS (EI+) *m/z* calc'd for C<sub>14</sub>H<sub>17</sub>NO<sub>5</sub> [M<sup>+</sup>]: 279.1107, found 279.1118.



### Methyl 1-(3'4'-dimethoxybenzyl)-6,7-dimethoxyisoquinoline-3-carboxylate (196)

To a solution of methyl (3,4-dimethoxyphenyl)acetamidoacrylate **195** (156 mg, 0.56 mmol, 2.0 equiv) in THF (20 mL) was added TBAT (166 mg, 0.31 mmol, 1.1 equiv)

followed by *ortho*-silyl aryl triflate **184** (100 mg, 0.28 mmol) in THF (8 mL). The solution was stirred at ambient temperature under nitrogen for 72 h, at which point it was concentrated under reduced pressure to a yellow oil. Purification by flash chromatography (SiO<sub>2</sub>, 50:50 → 60:40 EtOAc/hexanes) provided isoquinoline **196** (77.6 mg, 70% yield) as tan solid.  $R_f$  = 0.15 (50:50 EtOAc/hexanes); <sup>1</sup>H NMR (500 MHz, CDCl<sub>3</sub>) δ 8.39 (s, 1H), 7.34 (s, 1H), 7.16 (s, 1H), 6.78 (app d,  $J$  = 6.5 Hz, 2H), 6.74 (d,  $J$  = 8.5 Hz, 1H), 4.63 (s, 2H), 4.05 (s, 3H), 4.01 (s, 3H), 3.86 (s, 3H), 3.81 (s, 3H), 3.74 (s, 3H); <sup>13</sup>C NMR (125 MHz, CDCl<sub>3</sub>) δ 166.9, 158.2, 152.8, 151.5, 149.0, 147.6, 139.6, 133.0, 132.0, 124.8, 122.4, 120.5, 111.9, 111.1, 106.5, 104.8, 56.1, 56.0, 55.8, 55.7, 52.8, 42.8; δ; IR (Neat Film, NaCl) 2951, 2835, 1730, 1618, 1511, 1465, 1426, 1256, 1161, 1028, 733 cm<sup>-1</sup>; HRMS (ES+) *m/z* calc'd for C<sub>22</sub>H<sub>23</sub>NO<sub>6</sub> [M+H]<sup>+</sup>: 398.1604, found 398.1584.



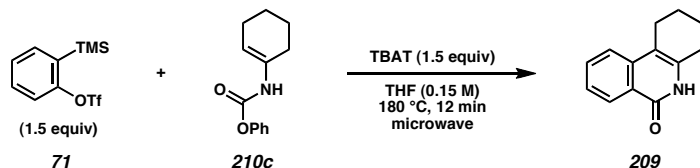
### Papaverine (197)

To a solution of isoquinoline ester **196** (20.0 mg, 50 μmol) in THF (1 mL) was added a solution of LiOH·H<sub>2</sub>O (10.6 mg, 253 μmol, 5.0 equiv) in H<sub>2</sub>O (0.5 mL). The biphasic mixture was vigorously stirred at ambient temperature under nitrogen for 3 h. The mixture was then concentrated under reduced pressure to remove the organic solvent and the aqueous layer was diluted with H<sub>2</sub>O (1 mL). The pH was adjusted to 4 with conc. HCl (20 μL), and the aqueous layer was extracted with CH<sub>2</sub>Cl<sub>2</sub> (3 × 10 mL). The

combined organic layers were dried over  $\text{MgSO}_4$ , filtered, and concentrated under reduced pressure to a solid tan foam. The vial containing the crude foam under nitrogen was then heated by passing intermittently through a Bunsen burner flame over 45 sec. The resulting brown oil was purified by flash chromatography ( $\text{SiO}_2$ , 40:60  $\rightarrow$  60:40  $\text{EtOAc/hexanes}$ ) to provide papaverine (**197**) (10.5 mg, 61% yield) as a yellow solid.  $R_f$  = 0.10 (50:50  $\text{EtOAc/hexanes}$ );  $^1\text{H}$  NMR (500 MHz,  $\text{CDCl}_3$ )  $\delta$  8.38 (d,  $J$  = 5.5 Hz, 1H), 7.43 (d,  $J$  = 5.5 Hz, 1H), 7.35 (s, 1H), 7.06 (s, 1H), 6.82 (app d,  $J$  = 7.0 Hz, 2H), 6.77 (d,  $J$  = 8.5 Hz, 1H), 4.54 (s, 2H), 4.01 (s, 3H), 3.91 (s, 3H), 3.83 (s, 3H), 3.77 (s, 3H);  $^{13}\text{C}$  NMR (125 MHz,  $\text{CDCl}_3$ )  $\delta$  155.9, 150.5, 147.8, 147.1, 145.6, 139.2, 131.5, 130.4, 121.0, 118.6, 116.8, 109.9, 109.2, 103.4, 102.3, 54.1, 54.0, 53.9, 53.8, 40.4; IR (Neat Film, NaCl) 2930, 2832, 1511, 1478, 1421, 1269, 1235, 1158, 1026, 855  $\text{cm}^{-1}$ ; HRMS (ES+)  $m/z$  calc'd for  $\text{C}_{20}\text{H}_{21}\text{NO}_4$  [M+H] $^+$ : 340.1549, found 340.1553.

### 2.5.2.6 General Procedure for the Synthesis of Isoquinolones via Aryne Annulation

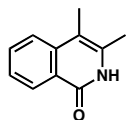
#### Annulation



A flame-dried 3 mL microwave vial equipped with a magnetic stir bar was charged with TBAT (0.186 g, 0.345 mmol, 1.5 equiv) and carbamate **210c** (0.050 g, 0.230 mmol). The vial was sealed with a teflon-silicone septum, then evacuated and back-filled with argon (x2). Tetrahydrofuran (1.5 mL) was added via syringe and the mixture was stirred until the solids fully dissolved. 2-(trimethylsilyl)phenyl triflate (**71**) (0.084 mL, 0.346

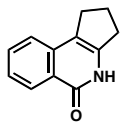
mmol, 1.5 equiv) was then added via syringe and the reaction was immediately irradiated in a Biotage Initiator microwave reactor at 240 W until the temperature reached 180 °C. The reaction was stirred at 180 °C for 12 min, at which point the vial was cooled to room temperature, the septum was removed, and the contents of the vial were passed through a plug of silica (2 cm circular diameter × 2 cm height) under EtOAc elution (30 mL). The solvent was removed under reduced pressure and the resulting residue was purified via flash chromatography over silica gel.

#### 2.5.2.7 Spectroscopic Data for Isoquinolones



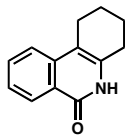
##### Isoquinolone 202a (Table 2.9, entry 1)

Purified by flash chromatography (SiO<sub>2</sub>, 25:75 → 40:60 EtOAc/hexanes) to yield a white solid (46% yield).  $R_f$  = 0.10 (25:75 EtOAc/hexanes); <sup>1</sup>H NMR (500 MHz, CDCl<sub>3</sub>) δ 9.93 (br s, 1H), 8.45 (dd,  $J$  = 7.8, 1.5 Hz, 1H), 7.71 (ddd,  $J$  = 7.8, 6.8, 1.5 Hz, 1H), 7.67 (d,  $J$  = 8.3 Hz, 1H), 7.47 (ddd,  $J$  = 7.8, 6.8, 1.5 Hz, 1H), 2.39 (s, 3H), 2.28 (s, 3H); <sup>13</sup>C NMR (125 MHz, CDCl<sub>3</sub>) δ 163.3, 139.0, 132.9, 132.6, 127.6, 125.5, 124.7, 122.8, 108.4, 17.7, 12.5; IR (Neat Film, NaCl) 2988, 2866, 1712, 1654, 1637, 1607, 1548, 1477, 1347, 1316 cm<sup>-1</sup>; HRMS (EI+) *m/z* calc'd for C<sub>11</sub>H<sub>11</sub>NO [M<sup>+</sup>]: 173.0841, found 173.0852.



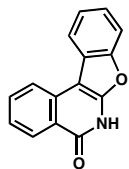
**Isoquinolone 202b (Table 2.9, entry 2)**

Purified by flash chromatography ( $\text{SiO}_2$ , 25:75  $\rightarrow$  40:60 EtOAc/hexanes) to yield a white solid (68% yield).  $R_f = 0.07$  (25:75 EtOAc/hexanes);  $^1\text{H}$  NMR (500 MHz,  $\text{CDCl}_3$ )  $\delta$  11.08 (br s, 1H), 8.44 (d,  $J = 8.3$  Hz, 1H), 7.68 (dd,  $J = 7.8, 7.3$  Hz, 1H), 7.48–7.42 (comp m, 2H), 3.00 (t,  $J = 7.3$  Hz, 2H), 2.94 (t,  $J = 6.8$  Hz, 2H), 2.24 (app quintet,  $J = 7.3$  Hz, 2H);  $^{13}\text{C}$  NMR (125 MHz,  $\text{CDCl}_3$ )  $\delta$  164.9, 140.6, 136.6, 132.6, 128.2, 125.3, 124.5, 123.0, 115.3, 31.6, 28.3, 22.0; IR (Neat Film, NaCl) 2899, 2849, 1657, 1643, 1606, 1545, 1476, 1386, 1339, 1324, 1154  $\text{cm}^{-1}$ ; HRMS (MM: ESI–APCI)  $m/z$  calc'd for  $\text{C}_{12}\text{H}_{11}\text{NO}$  [M+H] $^+$ : 186.0913, found 186.0916.



**Isoquinolone 209 (Table 2.9, entry 3)**

Purified by flash chromatography ( $\text{SiO}_2$ , 25:75  $\rightarrow$  50:50 EtOAc/hexanes) to yield a white solid (64% yield).  $R_f = 0.10$  (25:75 EtOAc/hexanes);  $^1\text{H}$  NMR (500 MHz,  $\text{CDCl}_3$ )  $\delta$  9.74 (br s, 1H), 8.43 (ddd,  $J = 8.1, 1.5, 0.5$  Hz, 1H), 7.69 (ddd,  $J = 8.3, 6.8, 1.5$  Hz, 1H), 7.61 (d,  $J = 7.8$  Hz, 1H), 7.46 (ddd,  $J = 7.8, 7.1, 1.2$  Hz, 1H), 2.74–2.69 (m, 2H), 2.68–2.63 (m, 2H), 1.94–1.86 (comp m, 4H);  $^{13}\text{C}$  NMR (125 MHz,  $\text{CDCl}_3$ )  $\delta$  163.1, 138.5, 134.9, 132.5, 127.7, 125.6, 124.9, 121.8, 109.8, 27.5, 23.1, 22.6, 22.0; IR (Neat Film, NaCl) 2931, 2859, 1652, 1640, 1608, 1549, 1476, 1380, 1355, 1331, 1260, 1170  $\text{cm}^{-1}$ ; HRMS (MM: ESI–APCI)  $m/z$  calc'd for  $\text{C}_{13}\text{H}_{13}\text{NO}$  [M+H] $^+$ : 200.1070, found 200.1073.

**Isoquinolone 202c (Table 2.9, entry 4)**

Purified by flash chromatography (SiO<sub>2</sub>, 2:98 → 5:95 EtOAc/hexanes) to yield a white solid (35% yield).  $R_f$  = 0.2 (25:75 EtOAc/hexanes); <sup>1</sup>H NMR (500 MHz, CDCl<sub>3</sub>) δ 10.51 (br s, 1H), 8.50 (dd,  $J$  = 7.8, 1.0 Hz, 1H), 8.11 (d,  $J$  = 7.8 Hz, 1H), 7.95 (d,  $J$  = 7.8 Hz, 1H), 7.78 (ddd,  $J$  = 8.3, 7.8, 1.0 Hz, 1H), 7.52 (d,  $J$  = 8.3 Hz, 1H), 7.45 (dd,  $J$  = 7.8, 7.3 Hz, 1H), 7.37 (dd,  $J$  = 8.3, 7.3 Hz, 1H), 7.27 (app t,  $J$  = 7.3 Hz, 1H); <sup>13</sup>C NMR (125 MHz, CDCl<sub>3</sub>) δ 162.9, 159.4, 140.0, 135.5, 133.6, 129.6, 129.4, 129.3, 128.2, 125.3, 124.3, 122.7, 119.6, 111.7, 111.6; IR (Neat Film, NaCl) 2919, 2851, 1667, 1630, 1524, 1454, 1290, 1246, 1208, 1137 cm<sup>-1</sup>; HRMS (ES+) *m/z* calc'd for C<sub>15</sub>H<sub>9</sub>NO<sub>2</sub> [M+H]<sup>+</sup>: 236.0706, found 236.0709.

## 2.6 NOTES AND REFERENCES

- (1) For reviews on the use of arynes in synthesis, including examples of aryne annulation, see: (a) Hoffmann, R. W. *Dehydrobenzene and Cycloalkynes*; Academic Press: New York, 1967. (b) Kessar, S. V. In *Comprehensive Organic Synthesis*; Trost, B. M.; Fleming, I., Eds.; Pergamon Press: New York, 1991; Vol. 4, pp 483–515. (c) Hart, H. In *The Chemistry of Triple-Bonded Functional Groups Supplement C2*; Patai, S., Ed.; Wiley: New York, 1994; pp 1017–1134. (d) Pellissier, H.; Santelli, M. *Tetrahedron* **2003**, *59*, 701–730. (e) Wenk, W. H.; Winkler, M.; Sander, W. *Angew. Chem., Int. Ed.* **2003**, *42*, 502–528.
- (2) (a) Wittig, G.; Pohmer, L. *Angew. Chem.* **1955**, *67*, 348. (b) Wittig, G.; Pohmer, L. *Chem. Ber.* **1956**, *89*, 1334–1351. (c) Wittig, G. *Angew. Chem.* **1957**, *69*, 245–251.
- (3) (a) Campbell, C. D.; Rees, C. W. *J. Chem. Soc.* **1969**, 748–751. (b) Whitney, S. E.; Rickborn, B. *J. Org. Chem.* **1988**, *53*, 5595–5596. (c) Rigby, J. H.; Holsworth, D. D.; James, K. *J. Org. Chem.* **1989**, *54*, 4019–4020.
- (4) (a) Wang, B.; Mu, B.; Chen, D.; Xu, S.; Zhou, X. *Organomet.* **2004**, *23*, 6225–6230.
- (5) (a) Wittig, G. *Org. Synth.* **1959**, *39*, 75–77. (b) Kornfield, E. C.; Barney, P.; Blankley, J.; Faul, W. *J. Med. Chem.* **1965**, *8*, 342–347.
- (6) For selected total syntheses featuring aryne annulation via [4 + 2] cycloaddition, see: (a) Best, W. M.; Wege, D. *Aust. J. Chem.* **1986**, *39*, 647–666. (b) Rigby, J. H.; Holsworth, D. D. *Tetrahedron Lett.* **1991**, *32*, 5757–5760. (c) Matsumoto, T.; Hosoya, T.; Suzuki, K. *J. Am. Chem. Soc.* **1992**, *114*, 3568–3570. (d) Pérez, D.; Gutián, E.; Castedo, L. *J. Org. Chem.* **1992**, *57*, 5911–5917. (e) Hosoya, T.;

Takashiro, E.; Matsumoto, T.; Suzuki, K. *J. Am. Chem. Soc.* **1994**, *116*, 1004–1015. (f) González, C.; Pérez, D.; Gutián, E.; Castedo, L. *J. Org. Chem.* **1995**, *60*, 6318–6326. (g) Venkatram, A.; Colley, T.; DeRuiter, J.; Smith, F. *J. Heterocycl. Chem.* **2005**, *42*, 297–301.

(7) Atanes, N.; Castedo, L.; Gutián, E.; Saá, C.; Saá, J. M.; Suau, R. *J. Org. Chem.* **1991**, *56*, 2984–2988.

(8) Gómez, B.; Gutián, E.; Castedo, L. *Synlett* **1992**, 903–904.

(9) Hayes, M. E.; Shinokubo, H.; Danheiser, R. L. *Org. Lett.* **2005**, *7*, 3917–3920.

(10) (a) Dockendorff, C.; Sahli, S.; Olsen, M.; Milhau, L.; Lautens, M. *J. Am. Chem. Soc.* **2005**, *127*, 15028–15029. (b) Webster, R.; Lautens, M. *Org. Lett.* **2009**, *11*, 4688–4691.

(11) (a) Caeiro, J.; Peña, D.; Cobas, A.; Pérez, D.; Gutián, E. *Adv. Synth. Catal.* **2006**, *348*, 2466–2474. (b) Peña, D.; Pérez, D.; Gutián, E. *Chem. Rec.* **2007**, *7*, 326–333.

(12) Huisgen, R.; Knorr, R.; Möbius, L.; Szeimies, G. *Chem. Ber.* **1965**, 4014–4021.

(13) While Huisgen contributed much to the advancement of knowledge pertaining to aryne [3 + 2] cycloadditions, a handful of reports preceded his work. These include the following: (a) Wittig, G.; Hoffmann, R. W. *Angew. Chem.* **1961**, *73*, 435–436. (b) Reynolds, G. A. *J. Org. Chem.* **1964**, *29*, 3733–3734.

(14) (a) Huisgen, R. *Angew. Chem., Int. Ed., Engl.* **1963**, *2*, 565–598. (b) Kolb, H. C.; Finn, M. G.; Sharpless, K. B. *Angew. Chem., Int. Ed.* **2001**, *40*, 2004–2021.

(15) For additional examples of aryne-azide [3 + 2] cycloadditions, see: (a) Mitchell, G.; Rees, C. W. *J. Chem. Soc., Perkin Trans. 1* **1987**, 403–412. (b) Zhang, F.; Moses, J. E. *Org. Lett.* **2009**, *11*, 1587–1590.

(16) (a) Minisci, F.; Quilico, A. *Chimica e Industria* **1964**, *46*, 428. (b) Kitamura, T.; Mansei, Y.; Fujiwara, Y. *J. Organomet. Chem.* **2002**, *646*, 196–199.

(17) (a) Huisgen, R.; Knorr, R. *Naturwiss.* **1961**, *48*, 716. (b) Matsumoto, T.; Sohma, T.; Hatazaki, S.; Suzuki, K. *Synlett* **1993**, 843–846.

(18) Matsumoto, K.; Uchida, T.; Sugi, T.; Yagi, Y. *Chem. Lett.* **1982**, 869–870.

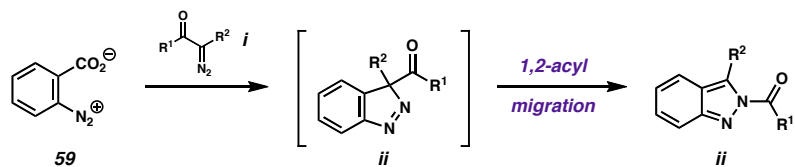
(19) (a) Yamazaki, T.; Shechter, H. *Tetrahedron Lett.* **1972**, *13*, 4533–4536. (b) Yamazaki, T.; Shechter, H. *Tetrahedron Lett.* **1973**, *14*, 1417–1420. (c) Yamazaki, T.; Baum, G.; Shechter, H. *Tetrahedron Lett.* **1974**, *15*, 4421–4424.

(20) (a) Kurita, J.; Kakusawa, N.; Yasuike, S.; Tsuchiya, T. *Heterocycles* **1990**, *31*, 1937–1940. (b) Kakusawa, N.; Imamura, M.; Kurita, J.; Tsuchiya, T. *Heterocycles* **1994**, *38*, 957–960. (c) Kakusawa, N.; Sakamoto, K.; Kurita, J.; Tsuchiya, T. *Heterocycles* **1996**, *43*, 2091–2094.

(21) Matsumoto, K.; Katsura, H.; Uchida, T.; Aoyama, K.; Machiguchi, T. *J. Chem. Soc., Perkin Trans. 1* **1996**, 2599–2602.

(22) Jin, T.; Yamamoto, Y. *Angew. Chem., Int. Ed.* **2007**, *46*, 3323–3325.

(23) 3-Acyl-3*H*-indazoles (**ii**) generated from  $\alpha$ -diazoketones (**i**) typically undergo spontaneous 1,2-acyl migration to furnish 2-acyl-2*H*-indazoles (**iii**). See refs. 19a–c.



(24) (a) Watanabe, M.; Kurosaki, A.; Furukawa, S. *Chem. Pharm. Bull.* **1984**, 32, 1264–1267. (b) Cant, A. A.; Bertrand, G. H. V.; Henderson, J. L.; Roberts, L.; Greaney, M. F. *Angew. Chem., Int. Ed.* **2009**, 48, 5199–5202.

(25) Beltrán-Rodil, S.; Peña, D.; Guitián, E. *Synlett* **2007**, 1308–1310.

(26) Giacometti, R. D.; Ramtohul, Y. K. *Synlett* **2009**, 2010–2016.

(27) (a) Bhawal, B. M.; Khanapure, S. P.; Zhang, H.; Biehl, E. R. *J. Org. Chem.* **1991**, 56, 2846–2849. (b) Zouaoui, M. A.; Mouaddib, A.; Jamart-Gregoire, B.; Ianelli, S.; Nardelli, M.; Caubere, P. *J. Org. Chem.* **1991**, 56, 4078–4081.

(28) Cobas, A.; Guitián, E.; Castedo, L. *J. Org. Chem.* **1992**, 57, 6765–6769.

(29) Townsend, C. A.; Davis, S. G.; Christensen, S. B.; Link, J. C.; Lewis, C. P. *J. Am. Chem. Soc.* **1981**, 103, 6885–6888.

(30) Saá, C.; Guitián, E.; Castedo, L.; Suau, R.; Saá, J. M. *J. Org. Chem.* **1986**, 51, 2781–2784.

(31) Rogness, D. C.; Larock, R. C. *Tetrahedron Lett.* **2009**, 50, 4003–4008.

(32) Wittig, G.; Hoffmann, R. W. *Chem. Ber.* **1962**, 95, 2718–2728.

(33) (a) Woodward, R. B.; Hoffmann, R. *J. Am. Chem. Soc.* **1965**, *87*, 395–397. (b) Hoffmann, R.; Woodward, R. B. *J. Am. Chem. Soc.* **1965**, *87*, 2046–2048. (c) Hoffmann, R.; Woodward, R. B. *Acc. Chem. Res.* **1968**, *1*, 17–22. (d) Woodward, R. B.; Hoffmann, R. *The Conservation of Orbital Symmetry*; Academic Press: New York, 1970. (e) Baldwin, J. E.; Andrist, A. H.; Pinschmidt, R. K., Jr. *Acc. Chem. Res.* **1972**, *5*, 402–406. (f) Shen, K.-W. *J. Chem. Ed.* **1973**, *50*, 238–242.

(34) (a) Stevens, R. V.; Bisacchi, G. S. *J. Org. Chem.* **1982**, *47*, 2393–2396. (b) Stevens, R. V.; Bisacchi, G. S. *J. Org. Chem.* **1982**, *47*, 2396–2399.

(35) For a review of methods for the synthesis of benzocyclobutenes, including [2 + 2] cycloadditions between arynes and olefins, see: Klundt, I. L. *Chem. Rev.* **1970**, *70*, 471–487.

(36) Simmons, H. E. *J. Am. Chem. Soc.* **1961**, *83*, 1657–1664.

(37) Nair, V.; Kim, K. H. *J. Org. Chem.* **1975**, *40*, 3784–3786.

(38) Feltenberger, J. B.; Hayashi, R.; Tang, Y.; Babiash, E. S. C.; Hsung, R. P. *Org. Lett.* **2009**, *11*, 3666–3669.

(39) For a short review highlighting recent developments in the field of aryne  $\sigma$ -bond insertion, see: Peña, D.; Pérez, D.; Guitián, E. *Angew. Chem., Int. Ed.* **2006**, *45*, 3579–3581.

(40) For a more in-depth discussion of the mechanism of aryne insertion into activated  $\sigma$ -bonds, see Chapter 5.

(41) Yoshida, H.; Shirakawa, E.; Honda, Y.; Hiyama, T. *Angew. Chem., Int. Ed.* **2002**, *41*, 3247–3249.

(42) Tambar, U. K.; Stoltz, B. M. *J. Am. Chem. Soc.* **2005**, *127*, 5340–5341.

(43) A more in-depth discussion of this methodology, including its application toward the total synthesis of four natural products, is provided in Chapter 5.

(44) Yoshida, H.; Watanabe, M.; Ohshita, J.; Kunai, A. *Chem. Commun.* **2005**, 3292–3294.

(45) Liu, Y.-L.; Liang, Y.; Pi, S.-F.; Li, J.-H. *J. Org. Chem.* **2009**, *74*, 5691–5694.

(46) Zhang, T.; Huang, X.; Xue, J.; Sun, S. *Tetrahedron Lett.* **2009**, *50*, 1290–1294.

(47) (a) Liu, Z.; Zhang, X.; Larock, R. C. *J. Am. Chem. Soc.* **2005**, *127*, 15716–15717. (b) Henderson, J. L.; Edwards, A. S.; Greaney, M. F. *J. Am. Chem. Soc.* **2006**, *128*, 7426–7427. (c) Worlikar, S. A.; Larock, R. C. *Org. Lett.* **2009**, *11*, 2413–2416. (d) Worlikar, S. A.; Larock, R. C. *J. Org. Chem.* **2009**, *74*, 9132–9139.

(48) Yoshida, H.; Ikadai, J.; Shudo, M.; Ohshita, J.; Kunai, A. *J. Am. Chem. Soc.* **2003**, *125*, 6638–6639.

(49) Ito, Y.; Suginome, M.; Murakami, M. *J. Org. Chem.* **1991**, *56*, 1948–1951.

(50) Xie, C.; Zhang, Y.; Huang, Z.; Xu, P. *J. Org. Chem.* **2007**, *72*, 5431–5434.

(51) Waldo, J. P.; Zhang, X.; Shi, F.; Larock, R. C. *J. Org. Chem.* **2008**, *73*, 6679–6685.

(52) Gerfaud, T.; Neuville, L.; Zhu, J. *Angew. Chem., Int. Ed.* **2009**, *48*, 572–577.

(53) (a) Peña, D.; Escudero, S.; Pérez, D.; Gutián, E.; Castedo, L. *Angew. Chem., Int. Ed.* **1998**, *37*, 2659–2661. (b) Peña, D.; Pérez, D.; Gutián, E.; Castedo, L. *Org. Lett.* **1999**, *1*, 1555–1557. (c) Peña, D.; Cobas, A.; Pérez, D.; Gutián, E.; Castedo, L. *Org. Lett.* **2000**, *2*, 1629–1632. (d) Peña, D.; Cobas, A.; Pérez, D.; Gutián, E.; Castedo, L. *Org. Lett.* **2003**, *5*, 1863–1866.

(54) Peña, D.; Pérez, D.; Gutián, E.; Castedo, L. *Eur. J. Org. Chem.* **2003**, 1238–1243.

(55) Sato, Y.; Tamura, T.; Mori. M. *Angew. Chem., Int. Ed.* **2004**, *43*, 2436–2440.

(56) Gilmore, C. D.; Allan, K. M.; Stoltz, B. M. *J. Am. Chem. Soc.* **2008**, *130*, 1558–1559.

(57) (a) Gilman, H.; Avakian, S. *J. Am. Chem. Soc.* **1945**, *67*, 349–351. (b) Bergstrom, F. W.; Horning, C. H. *J. Org. Chem.* **1946**, *11*, 334–340. (c) Roberts, J. D.; Simmons, H. E., Jr.; Carlsmith, L. A.; Vaughan, C. W. *J. Am. Chem. Soc.* **1953**, *75*, 3290–3291. (d) Ueda, N.; Tokuyama, T.; Sakan, T. *Bull. Chem. Soc. Jpn.* **1966**, *39*, 2012–2014. (e) Giumanini, A. G. *J. Am. Chem. Soc.* **1972**, *37*, 513–514. (f) Iida, H.; Aoyagi, S.; Kibayashi, C. *J. Chem. Soc., Perkin Trans. I* **1975**, 2502–2506. (g) Watanabe, M.; Kurosaki, A.; Furukawa, S. *Chem. Pharm. Bull.* **1984**, *32*, 1264–1267. (h) Cant, A. A.; Bertrand, G. H. V.; Henderson, J. L.; Roberts, L.; Greaney, M. F. *Angew. Chem., Int. Ed.* **2009**, *48*, 5199–5200.

(58) (a) Yoshida, H.; Morishita, T.; Fukushima, H.; Ohshita, J.; Kunai, A. *Org. Lett.* **2007**, *9*, 3367–3370. (b) Yoshida, H.; Morishita, T.; Ohshita, J. *Org. Lett.* **2008**, *10*, 3845–3847.

(59) An example of conjugate addition as the terminal step in a nucleophilic addition/cyclization sequence for aryne annulation has since been reported by Huang and Zhang for the synthesis of xanthenes and acridines. See: Huang, X.; Zhang, T. *J. Org. Chem.* **2010**, *75*, 506–509.

(60) For additional examples of direct indoline synthesis, see: (a) Yip, K.-T.; Yang, M.; Law, K.-L.; Zhu, N.-Y.; Yang, D. *J. Am. Chem. Soc.* **2006**, *128*, 3130–3131. (b) Ganton, M. D.; Kerr, M. A. *Org. Lett.* **2005**, *7*, 4777–4779. (c) Moutrille, C.; Zard, S. Z. *Tetrahedron Lett.* **2004**, *45*, 4631–4634.

(61) Himeshima, Y.; Sonoda, T.; Kobayashi, H. *Chem. Lett.* **1983**, 1211–1214.

(62) For a facile two-step preparation of *ortho*-silyl aryl triflates from the corresponding *ortho*-bromophenols, see: Peña, D.; Cobas, A.; Pérez, D.; Gutián, E. *Synthesis* **2002**, 1454–1458.

(63) For results highlighting regioselective additions to unsymmetrical arynes, see: (a) Huisgen, R.; Möbius, M. L. *Tetrahedron* **1960**, *9*, 29–39. (b) Huisgen, R.; Sauer, J. *Angew. Chem.* **1959**, *72*, 91–108. (c) Bunnett, J. F.; Happer, D. A. R.; Patsch, M.; Pyun, C.; Takayama, H. *J. Am. Chem. Soc.* **1966**, *88*, 5250–5254. (d) Biehl, E. R.; Nieh, E.; Hsu, K. C. *J. Org. Chem.* **1969**, *34*, 3595–3599. (e) Newman, M. S.; Kannan, R. *J. Org. Chem.* **1976**, *41*, 3356–3359. (f) Xin, H. Y.; Biehl, E. R. *J. Org. Chem.* **1983**, *48*, 4397–4399. (g) Han, X. Y.; Jovanovic, M. V.; Biehl, E. R. *J. Org. Chem.* **1985**, *50*, 1334–1337. (h) Biehl, E. R.; Razzuk, A.; Jovanovic, M. V.; Biehl, E. R. *J. Org. Chem.* **1986**, *51*, 1334–1337.

M. V.; Khanapure, S. P. *J. Org. Chem.* **1986**, *51*, 5157–5160. (i) Tielemans, M.; Areschka, V.; Colomer, J.; Promel, R.; Langenaeker, W.; Geerlings, P. *Tetrahedron* **1992**, *48*, 10575–10586.

(64) For computational studies of aryne electronic properties, see: (a) Hinchliffe, A.; Machado, H. J. S. *J. Mol. Struct.: THEOCHEM* **1994**, *313*, 265–273. (b) Langenaeker, W.; De Proft, F.; Geerlings, P. *J. Phys. Chem. A* **1998**, *102*, 5944–5950. (c) Johnson, W. T. G.; Cramer, C. J. *J. Am. Chem. Soc.* **2001**, *123*, 923–928. (d) Johnson, W. T. G.; Cramer, C. J. *J. Phys. Org. Chem.* **2001**, *14*, 597–603. (e) Cheong, P. H.-Y.; Paton, R. S.; Bronner, S. M.; Im, G.-Y. J.; Garg, N. K.; Houk, K. N. *J. Am. Chem. Soc.* **2010**, *132*, 1267–1269.

(65) Similar modes of enamine addition to intramolecular arynes generated from aryl halides under strongly basic conditions have been previously proposed. See: (a) Iida, H.; Yuasa, Y.; Kibayashi, C. *J. Org. Chem.* **1979**, *44*, 1074–1080. (b) Kessar, S. V.; Gupta, Y. P.; Balakrishnan, P.; Sawal, K. K.; Mohammad, T.; Dutt, M. *J. Org. Chem.* **1988**, *53*, 1708–1713.

(66) (a) Fiaud, J.-C.; Kagan, H. B. *Bull. Soc. Chim. Fr.* **1970**, 84–85. (b) Fiaud, J.-C.; Kagan, H. B. *Tetrahedron Lett.* **1971**, *12*, 1019–1022. (c) Yamamoto, Y.; Ito, W. *Tetrahedron* **1988**, *44*, 5415–5423. (d) Shimizu, M.; Niwa, Y. *Tetrahedron Lett.* **2001**, *42*, 2829–2832. (e) Shimizu, M. *Pure Appl. Chem.* **2006**, *78*, 1867–1876. (f) Dickstein, J. S.; Fennie, M. W.; Norman, A. L.; Paulose, B. J.; Kozlowski, M. C. *J. Am. Chem. Soc.* **2008**, *130*, 15794–15795.

(67) (a) Niwa, Y.; Takayama, K.; Shimizu, M. *Tetrahedron Lett.* **2001**, *42*, 5473–5476. (b) Niwa, Y.; Takayama, K.; Shimizu, M. *Bull. Chem. Soc. Jpn.* **2002**, *75*, 1819–1825.

(68) The nitrogen substituents reported in refs. 66 and 67 include aryl, sulfonyl, phosphoryl, and hydrazide groups. However, to our knowledge, the umpolung addition of a carbon nucleophile to the nitrogen atom of an *N*-carbamoyl imine has not been previously reported.

(69) For classical syntheses of isoquinolines, see: (a) Doebner, O. *Justus Liebigs Ann. Chem.* **1887**, *242*, 265–289. (b) Bischler, A.; Napieralski, B. *Ber. Dtsch. Chem. Ges.* **1893**, *26*, 1903–1912. (c) Pictet, A.; Gams, A. *Ber. Dtsch. Chem. Ges.* **1910**, *113*, 2384–2391. (d) Bevis, M. G.; Forbes, E. J.; Uff, D. C. *Tetrahedron* **1969**, *25*, 1585–1589.

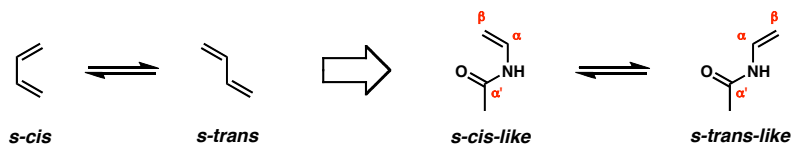
(70) *N*-acetyl enamines were synthesized from the corresponding ketones via an intermediate oxime according to the procedure of Burk *et al.* See: Burk, M. J.; Casy, G.; Johnson, N. B. *J. Org. Chem.* **1998**, *63*, 6084–6085.

(71) The reaction to form 1-methyl-3-*tert*-butylisoquinoline (**187b**) is complete within 15 min, as compared to the 6 h required to prepare isoquinolines **181a–i**.

(72) For similar examples of enamine *C*-arylation, see: Ramtohul, Y. K.; Chartrand, A. *Org. Lett.* **2007**, *9*, 1029–1032.

(73) The terms *s-cis* and *s-trans* are typically used to describe rotational conformations of 1,3-dienes. Here, the term “*s-cis*-like” is used to denote the rotational conformer in which the C(α')–N–C(α)–C(β) dihedral angle is 0°, while

the term “*s-trans-like*” is used to denote the rotational conformer in which the C( $\alpha'$ )–N–C( $\alpha$ )–C( $\beta$ ) dihedral angle is 180°.



- (74) As an alternative to the ene mechanism, nucleophilic attack as shown in Scheme 2.11 followed by protonation (either from an intramolecular or intermolecular proton source) would also generate styrene **190**.
- (75) Semiempirical calculations were performed at the AM1 level using Spartan '02 v1.0.8 (Wavefunction, Inc.).
- (76) For the isolation of papaverine, see: Merck, G. *Liebigs Ann. Chem.* **1848**, 66, 125–128.
- (77) (a) Bentley, K. W. In *The Isoquinoline Alkaloids*; Ravindranath, B., Ed.; Harwood Academic Publishers: Amsterdam, 1998; pp 107–122. (b) Bentley, K. W. *Nat. Prod. Rep.* **2005**, 22, 249–268.
- (78) Goodall, K.; Parsons, A. F. *Tetrahedron Lett.* **1995**, 36, 3259–3260.
- (79) Stanforth, S. P.; Tarbit, B.; Watson, M. D. *Tetrahedron* **2004**, 60, 8893–8897.
- (80) For previous total syntheses of papaverine, see: (a) Pictet, A.; Finkelstein, M. *Ber.* **1909**, 42, 1979–1989. (b) Rosenmund, K. W.; Nothnagel, M.; Riesenfeldt, H. *Ber.* **1927**, 60, 392–398. (c) Mannich, C.; Walther, O. *Arch. Pharm.* **1927**, 265, 1–11. (d) Galat, A. *J. Am. Chem. Soc.* **1951**, 73, 3654–3656. (e) Wahl, H. *Bull. Soc. Chim. Fr.* **1950**, 17, 680. (f) Popp, F. D.; McEwen, W. E. *J. Am.*

*Chem. Soc.* **1957**, *79*, 3773–3777. (g) Hirsenkorn, R. *Tetrahedron Lett.* **1991**, *32*, 1775–1778.

- (81) Decarboxylated products of this type (e.g., **197**) constitute those originally targeted in the attempt to accomplish aryne annulation using *N*-vinyl acetamide (**188**), thereby circumventing the undesired ene reactivity displayed by the latter.
- (82) Blackburn, T.; Ramtohul, Y. K. *Synlett* **2008**, 1159–1164.
- (83) A separate aryne-based synthesis of isoquinolones from *N*-vinyl isocyanates was reported by Rigby *et al.* See refs. 3c and 6b.
- (84) Shiori, T.; Ninomiya, K.; Yamada, S. *J. Am. Chem. Soc.* **1972**, *94*, 6203–6205.
- (85) The synthesis of *O*-substituted *N*-vinyl carbamates was accomplished using a modified version of the procedure employed by Rigby *et al.* See: Rigby, J. H.; Qabar, M. N. *J. Org. Chem.* **1993**, *58*, 4473–4475.
- (86) Yokoyama, Y.; Takahashi, M.; Tajashima, M.; Mitsuru, K.; Kohno, Y.; Kobayashi, H. *Chem. Pharm. Bull.* **1994**, *42*, 832–838.
- (87) Peña, D.; Pérez, D.; Gutián, E.; Castedo, L. *J. Am. Chem. Soc.* **1999**, *121*, 5827–5828.
- (88) Yoshikawa, E.; Radhakrishnan, K. V.; Yamamoto, Y. *J. Am. Chem. Soc.* **2000**, *122*, 7280–7286.
- (89) Liu, Z.; Zhang, X.; Larock, R. C. *J. Am. Chem. Soc.* **2005**, *127*, 15716–15717.

## APPENDIX 1

*Spectra Relevant to Chapter 2:  
Orthogonal Synthesis of Indolines and Isoquinolines  
via Aryne Annulation*

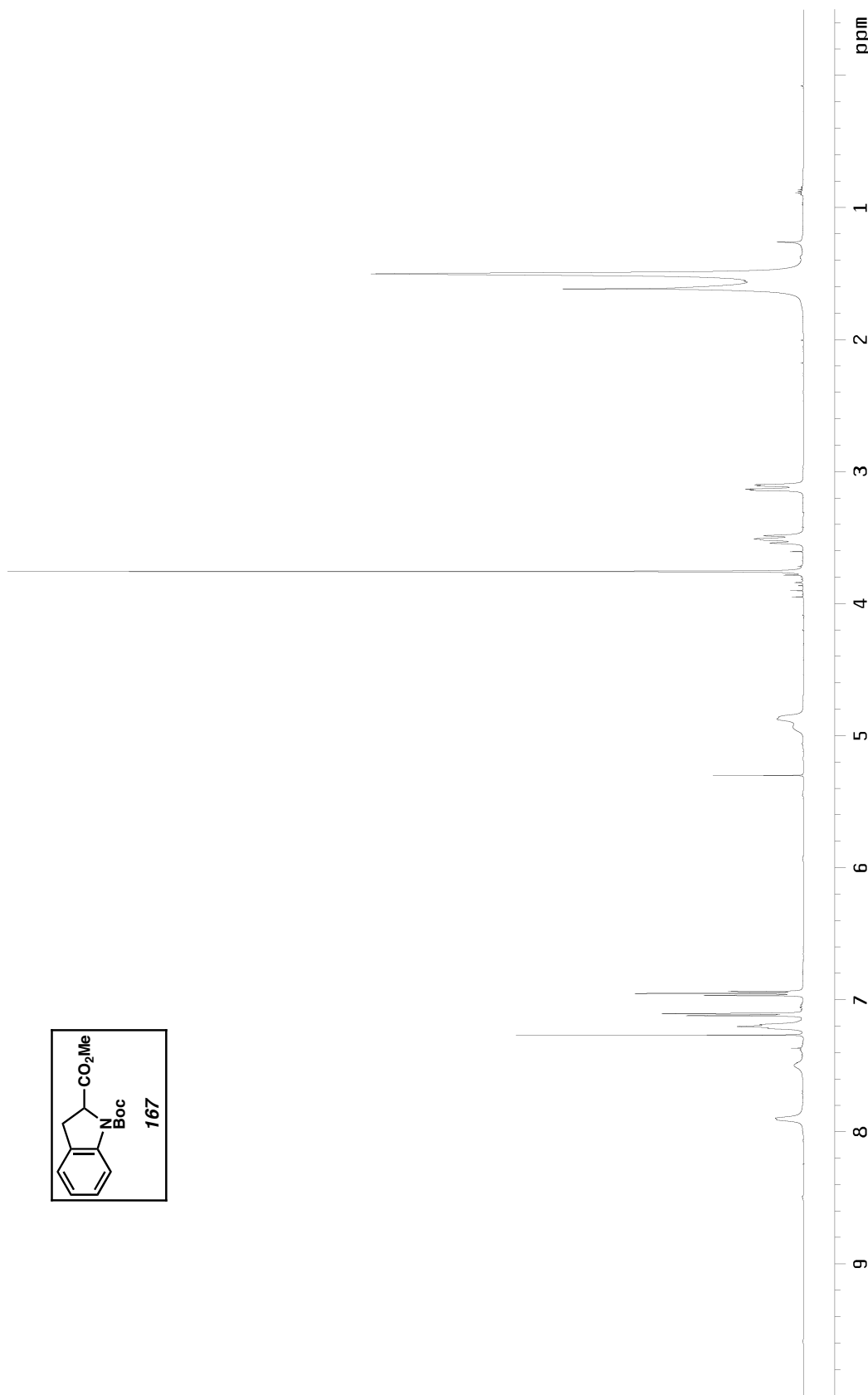


Figure A1.1.1  $^1\text{H}$  NMR (500 MHz,  $\text{CDCl}_3$ ) of indoline **167** (Table 2.2, entry 1).

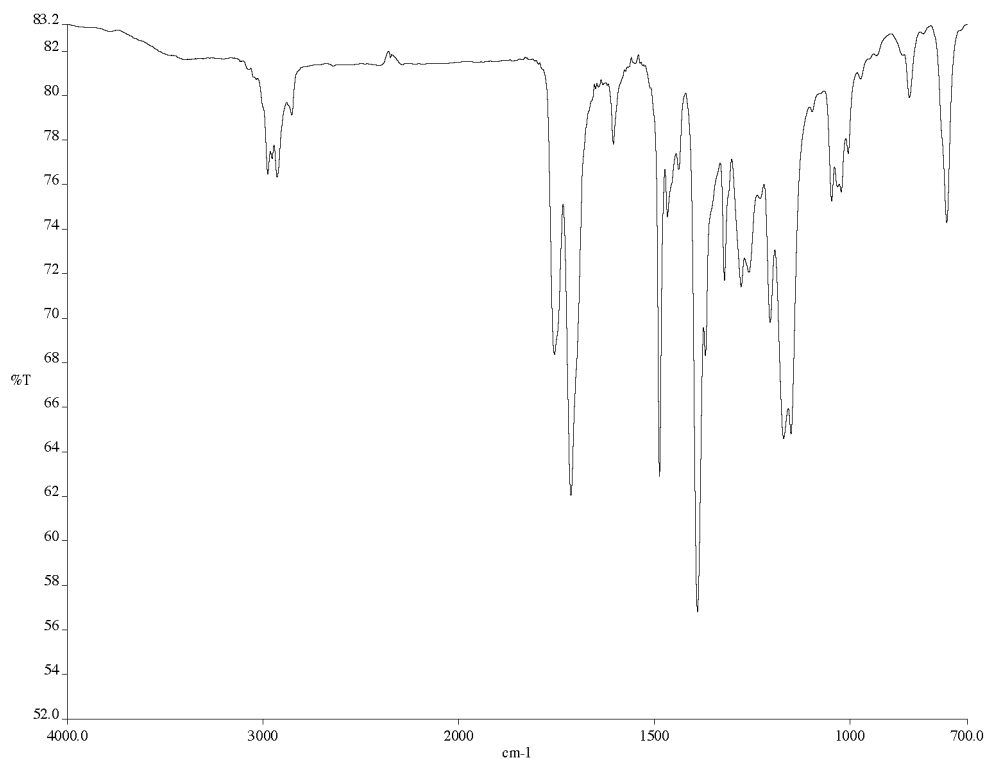


Figure A1.1.2 Infrared spectrum (thin film/NaCl) of indoline **167** (Table 2.2, entry 1).

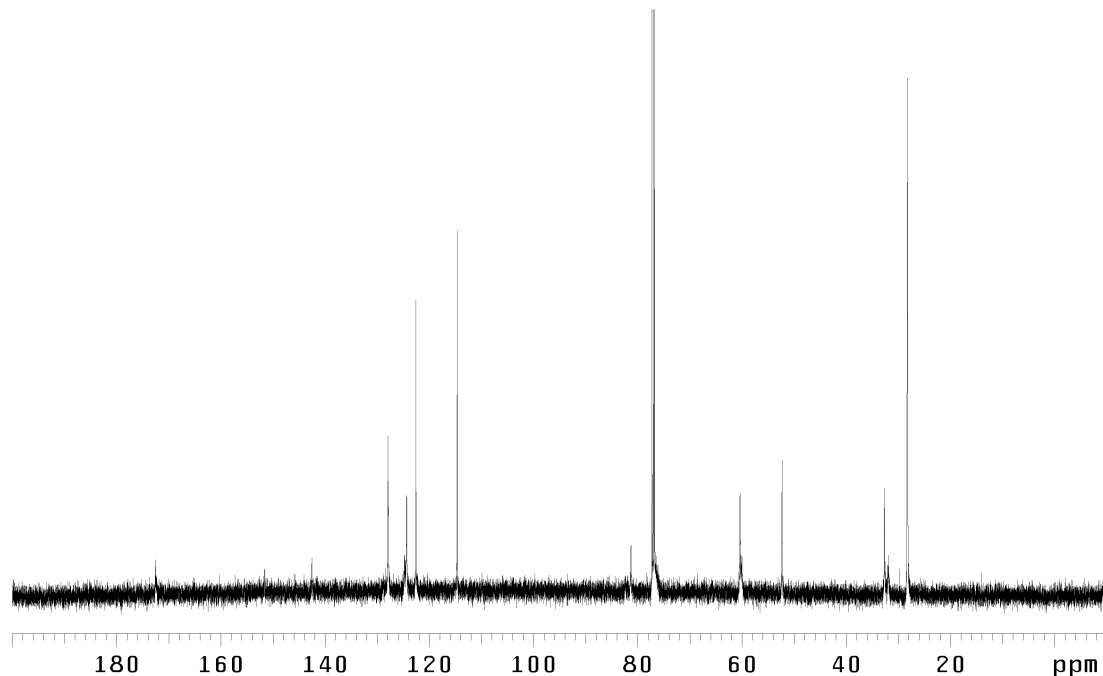


Figure A1.1.3 <sup>13</sup>C NMR (125 MHz, CDCl<sub>3</sub>) of indoline **167** (Table 2.2, entry 1).

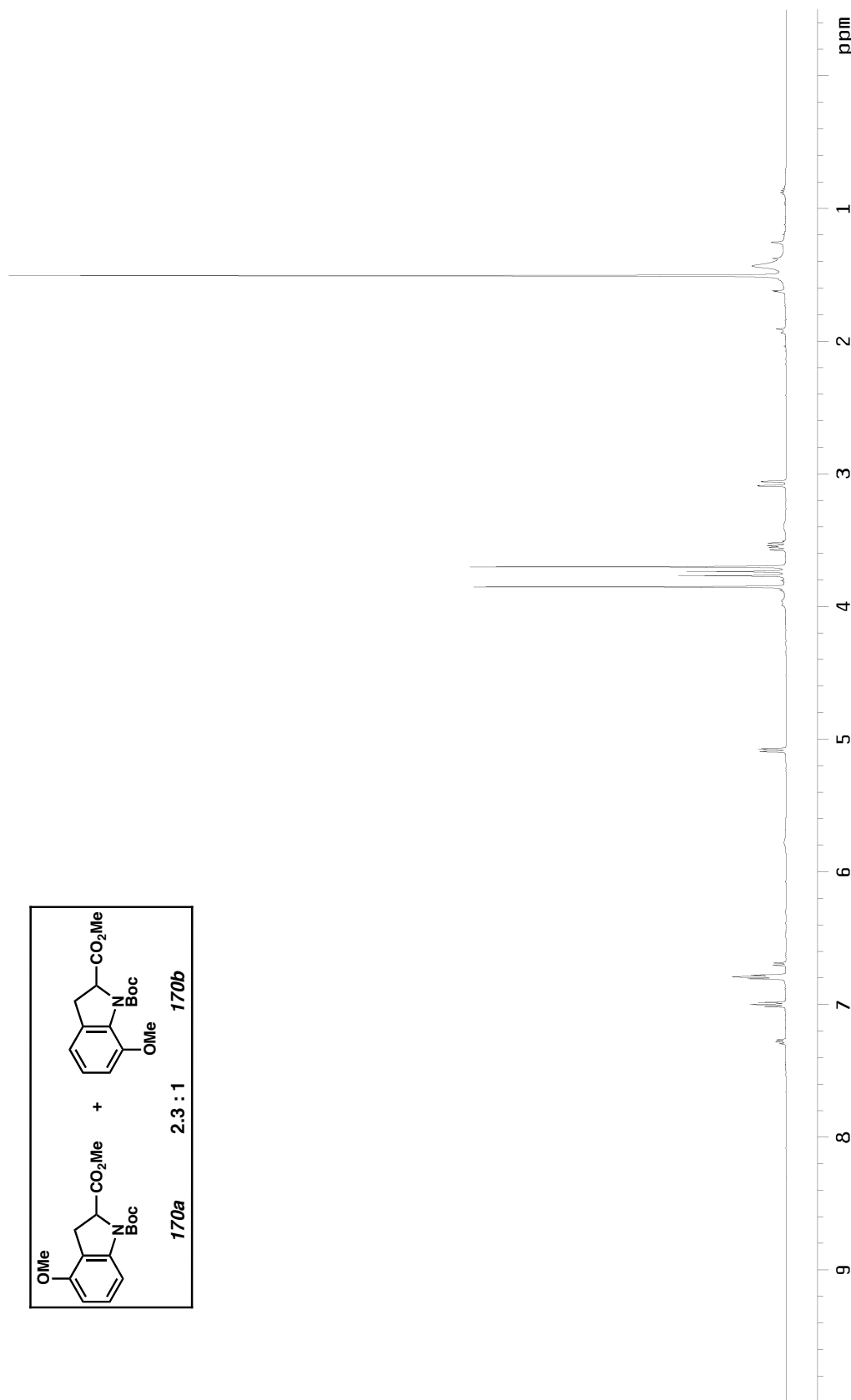


Figure A1.2.1  $^1\text{H}$  NMR (500 MHz,  $\text{CDCl}_3$ ) of indoline **170a** and **170b** (Table 2.2, entry 2).

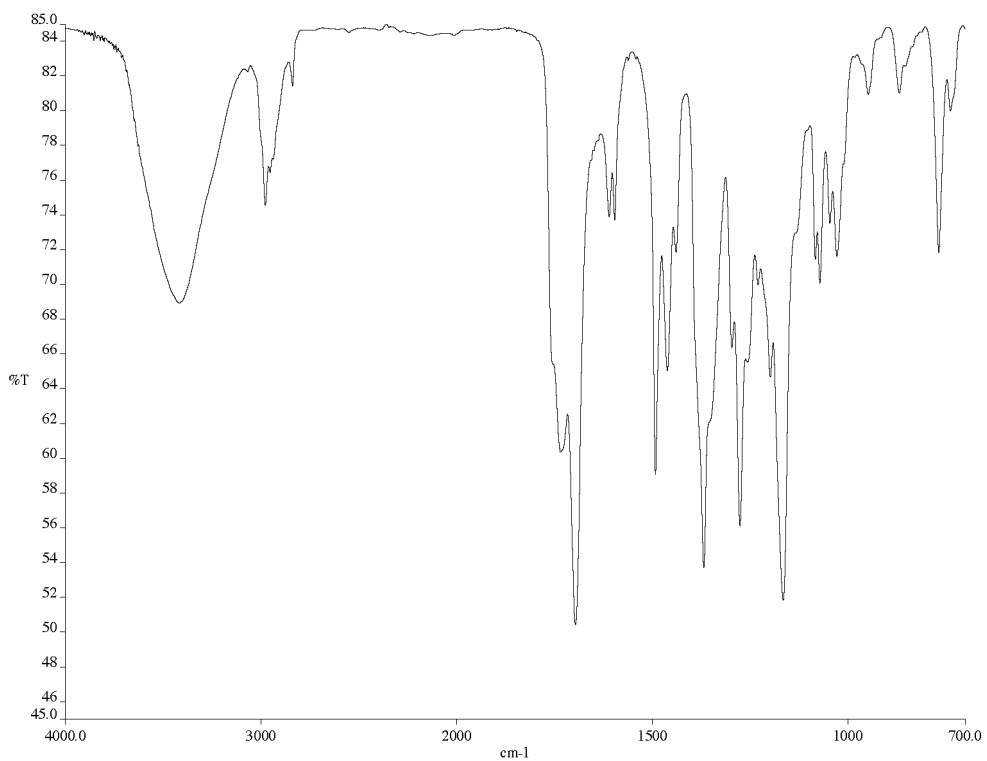


Figure A1.2.2 Infrared spectrum (thin film/NaCl) of indoline **170a** and **170b** (Table 2.2, entry 2).

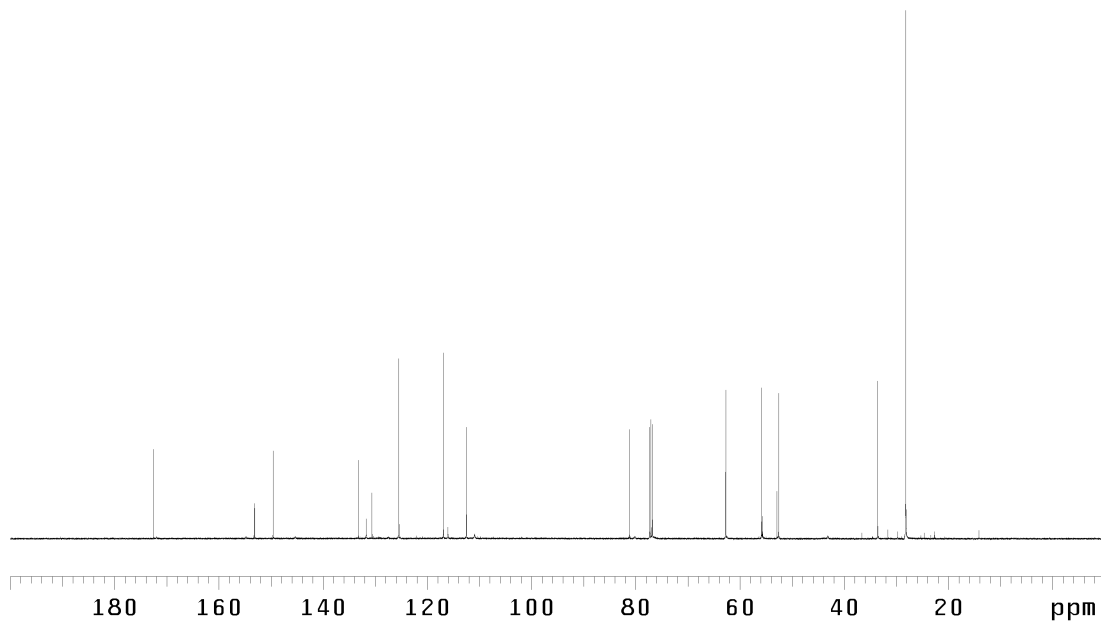


Figure A1.2.3  $^{13}\text{C}$  NMR (125 MHz,  $\text{CDCl}_3$ ) of indoline **170a** and **170b** (Table 2.2, entry 2).

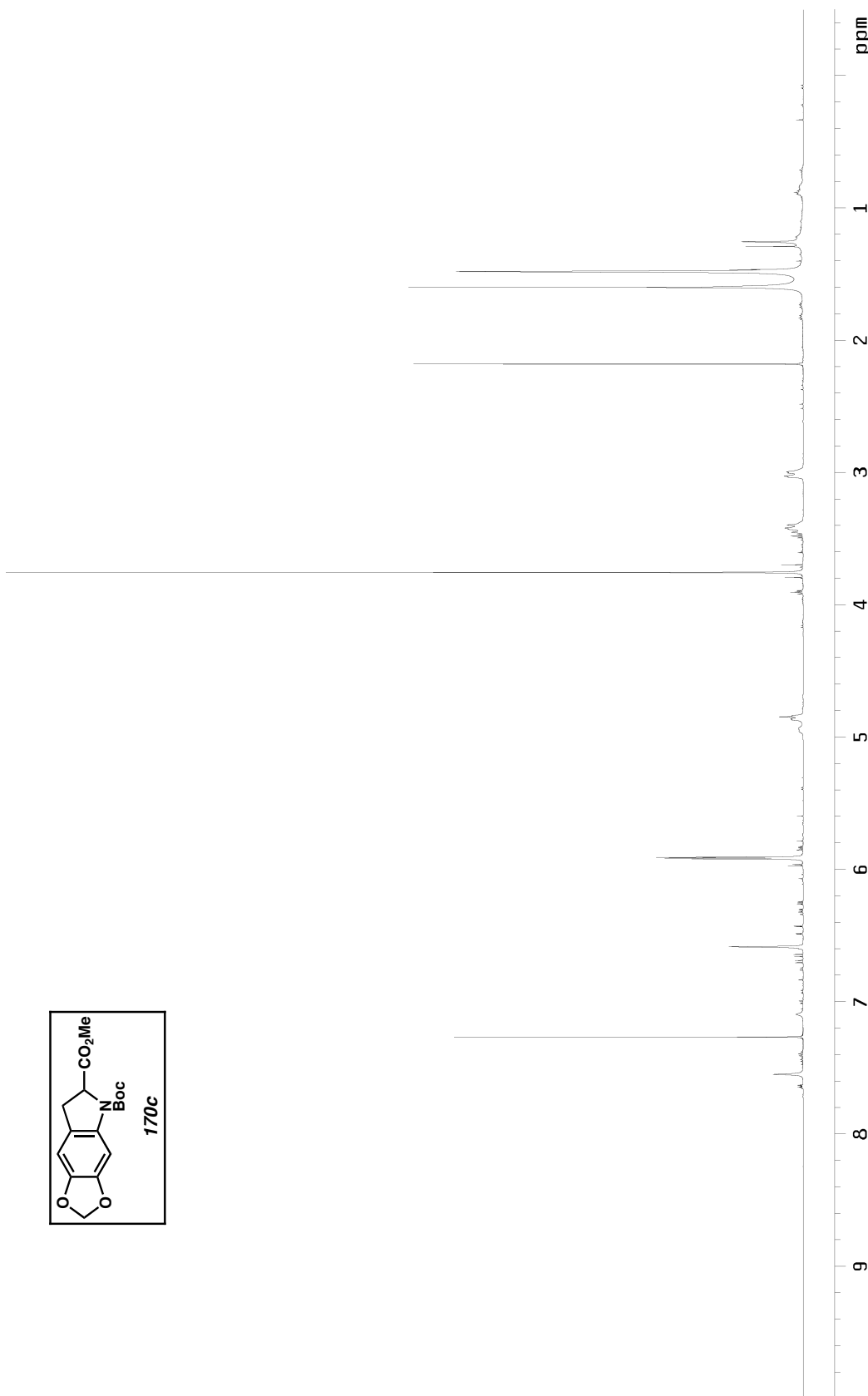
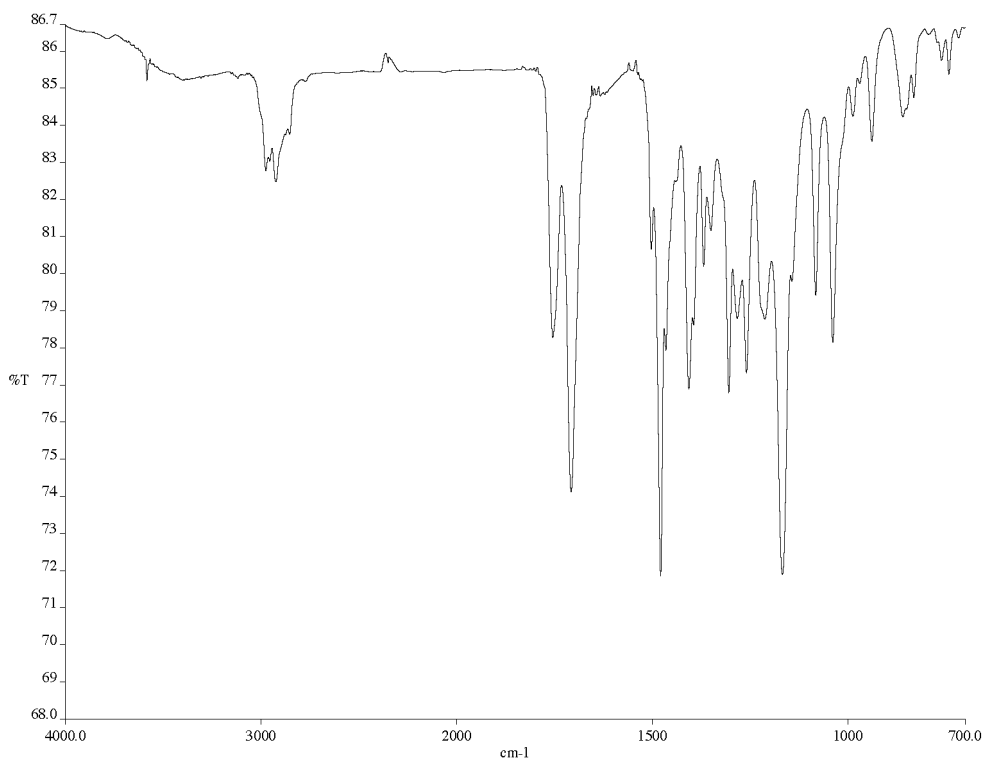
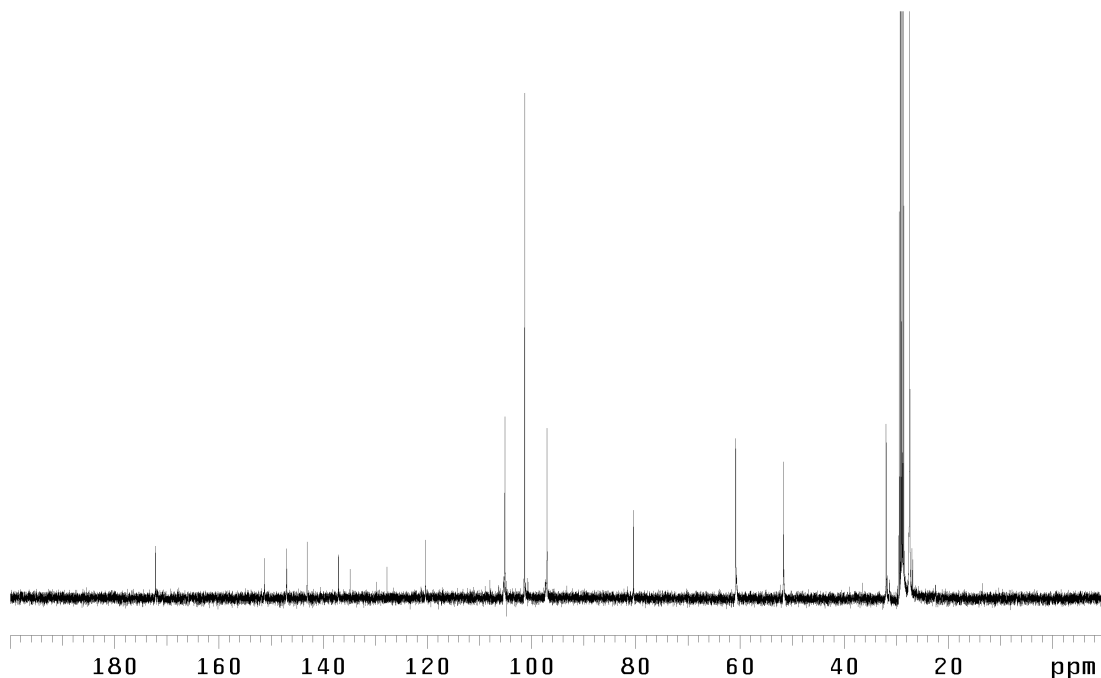


Figure A1.3.1  $^1\text{H}$  NMR (500 MHz,  $\text{CDCl}_3$ ) of indoline **170c** (Table 2.2, entry 3).



*Figure A1.3.2* Infrared spectrum (thin film/NaCl) of indoline **170c** (Table 2.2, entry 3).



*Figure A1.3.3* <sup>13</sup>C NMR (125 MHz, CDCl<sub>3</sub>) of indoline **170c** (Table 2.2, entry 3).

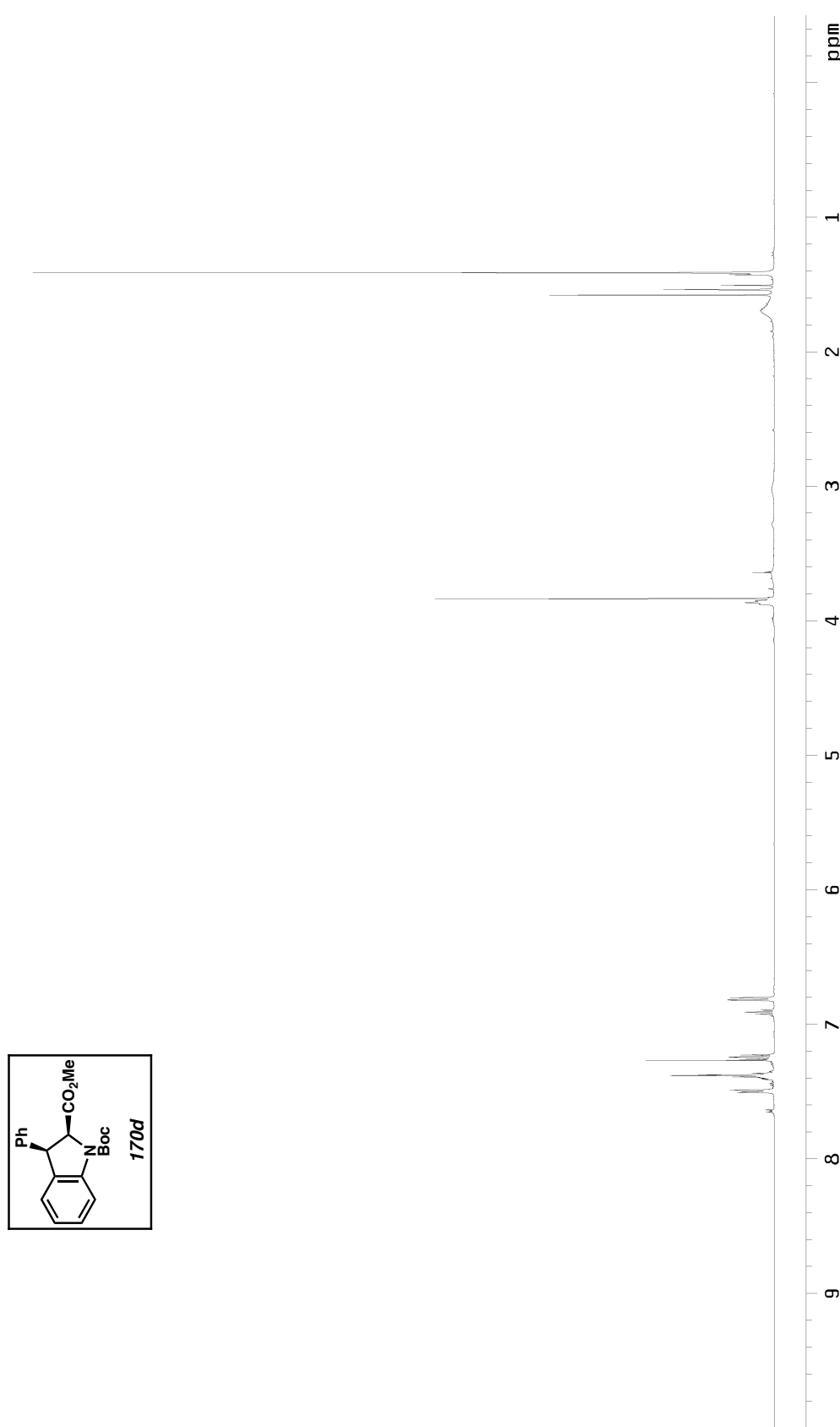
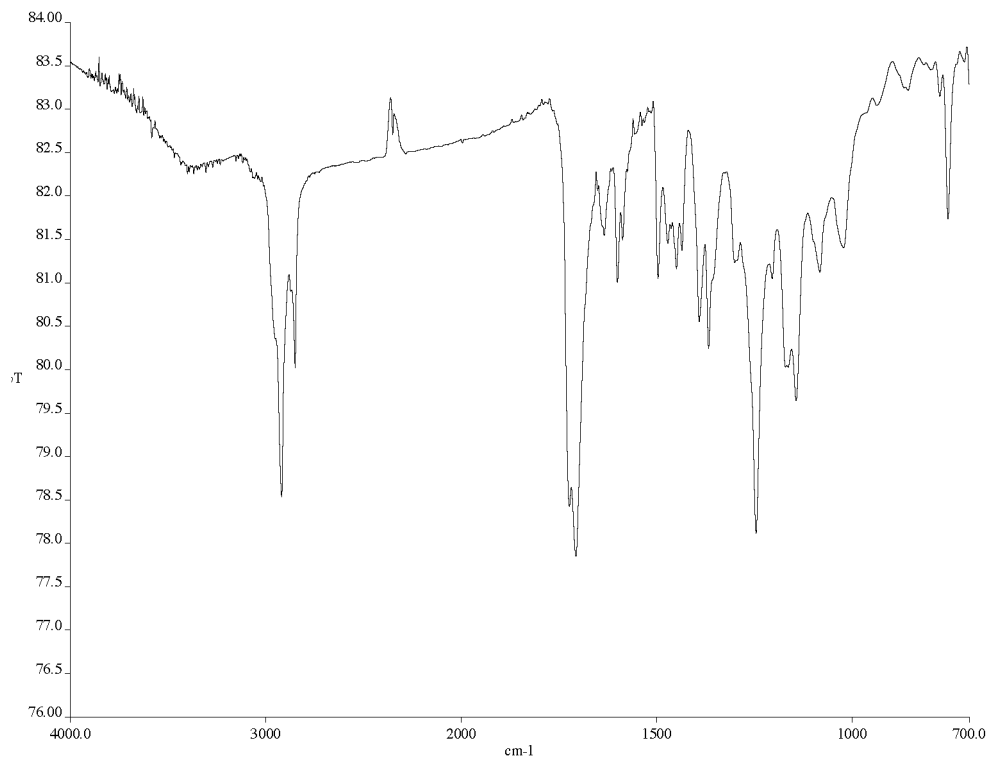
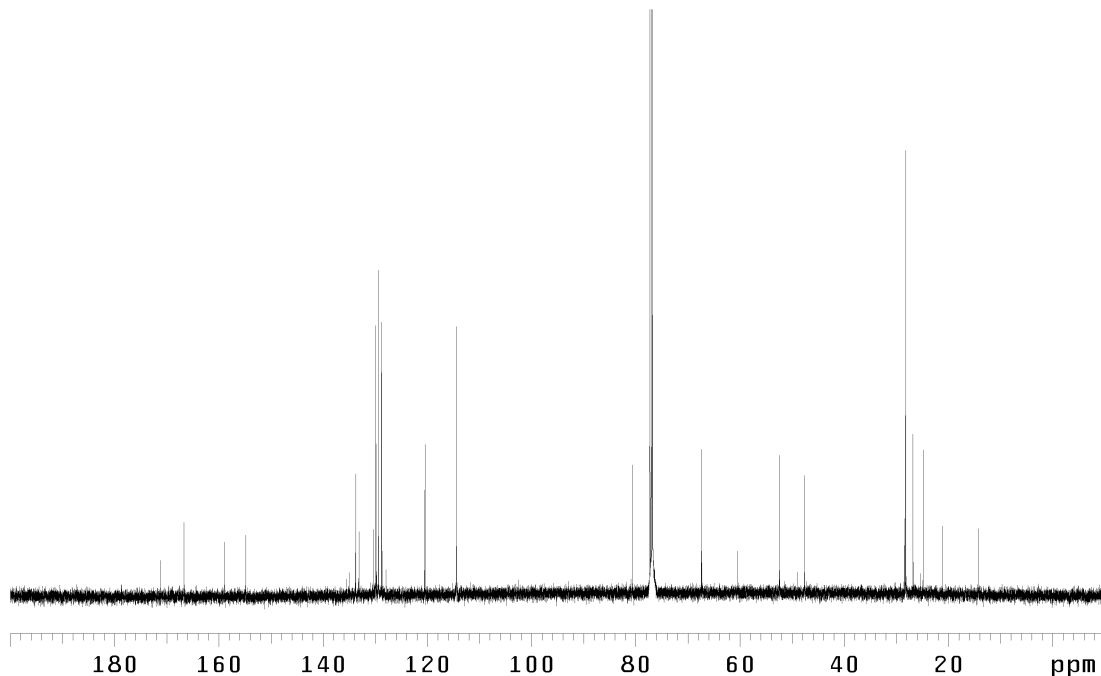


Figure A1.4.1  $^1\text{H}$  NMR (500 MHz,  $\text{CDCl}_3$ ) of indoline **170d** (Table 2.2, entry 4).



*Figure A1.4.2* Infrared spectrum (thin film/NaCl) of indoline **170d** (Table 2.2, entry 4).



*Figure A1.4.3* <sup>13</sup>C NMR (125 MHz, CDCl<sub>3</sub>) of indoline **170d** (Table 2.2, entry 4).

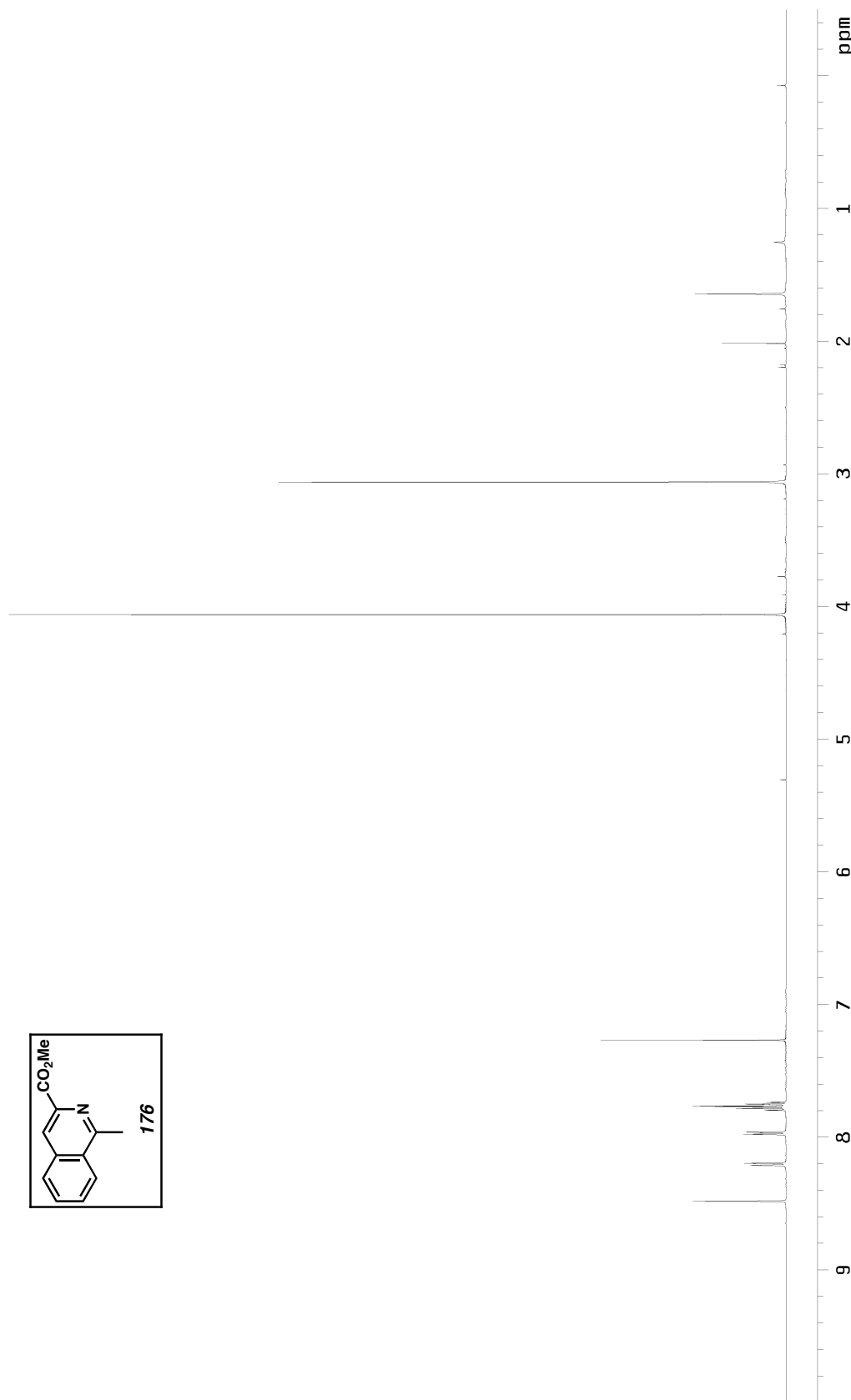


Figure A1.5.I  $^1\text{H}$  NMR (500 MHz,  $\text{CDCl}_3$ ) of isoquinoline **176** (Table 2.4, entry 1).

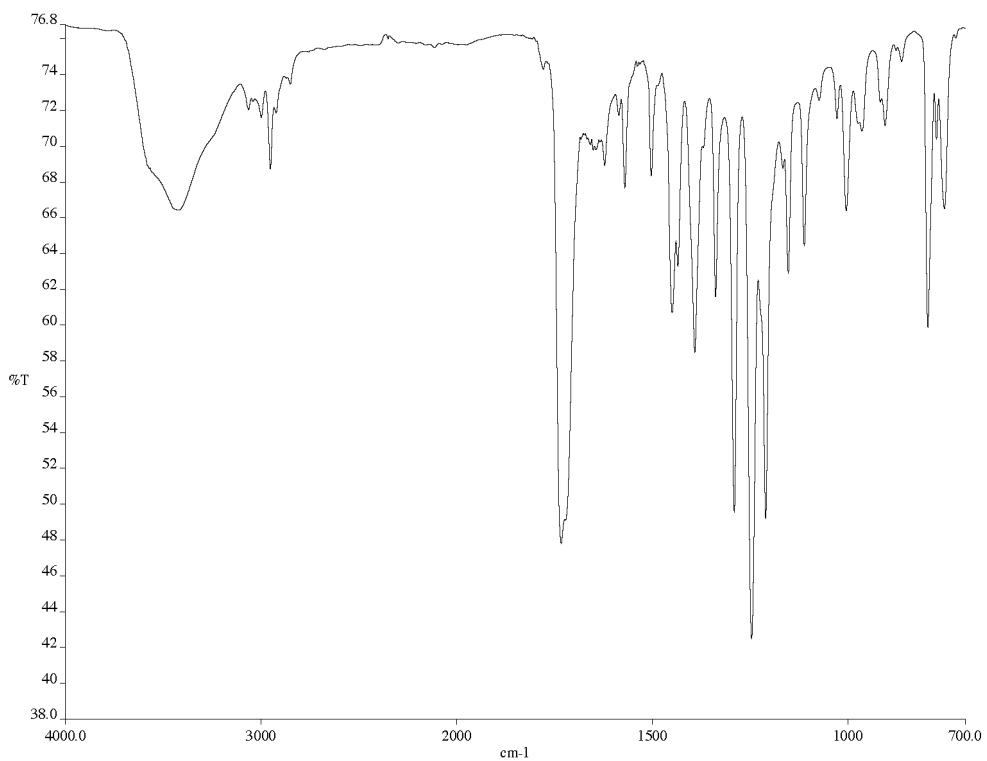


Figure A1.5.2 Infrared spectrum (thin film/NaCl) of isoquinoline **176** (Table 2.4, entry 1).

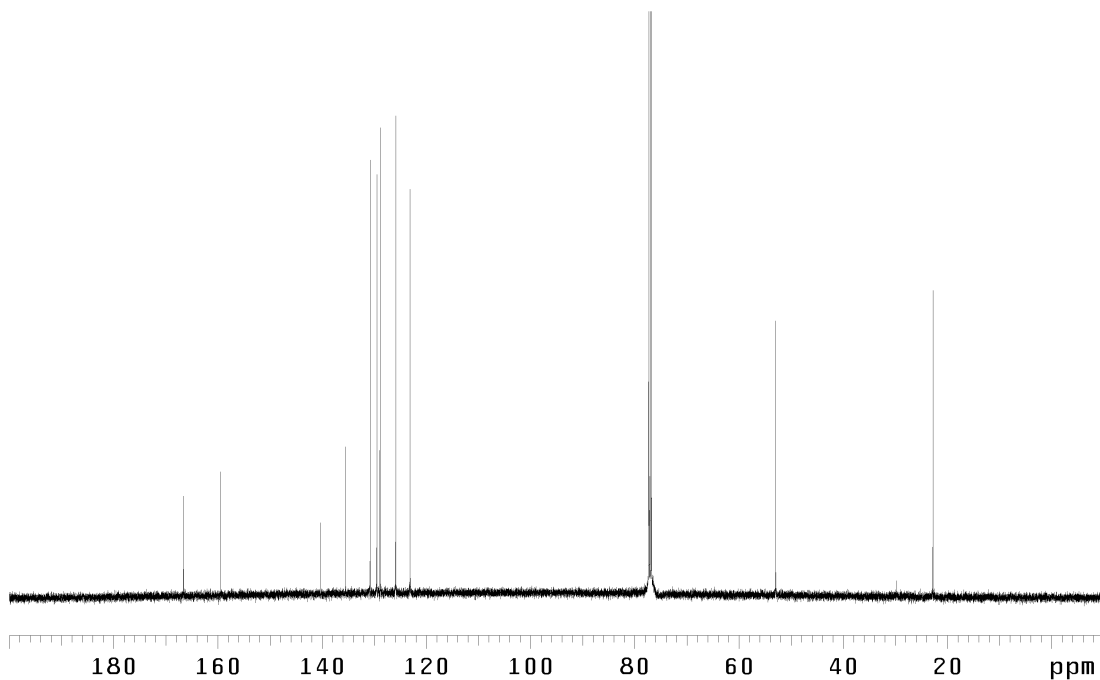


Figure A1.5.3 <sup>13</sup>C NMR (125 MHz, CDCl<sub>3</sub>) of isoquinoline **176** (Table 2.4, entry 1).

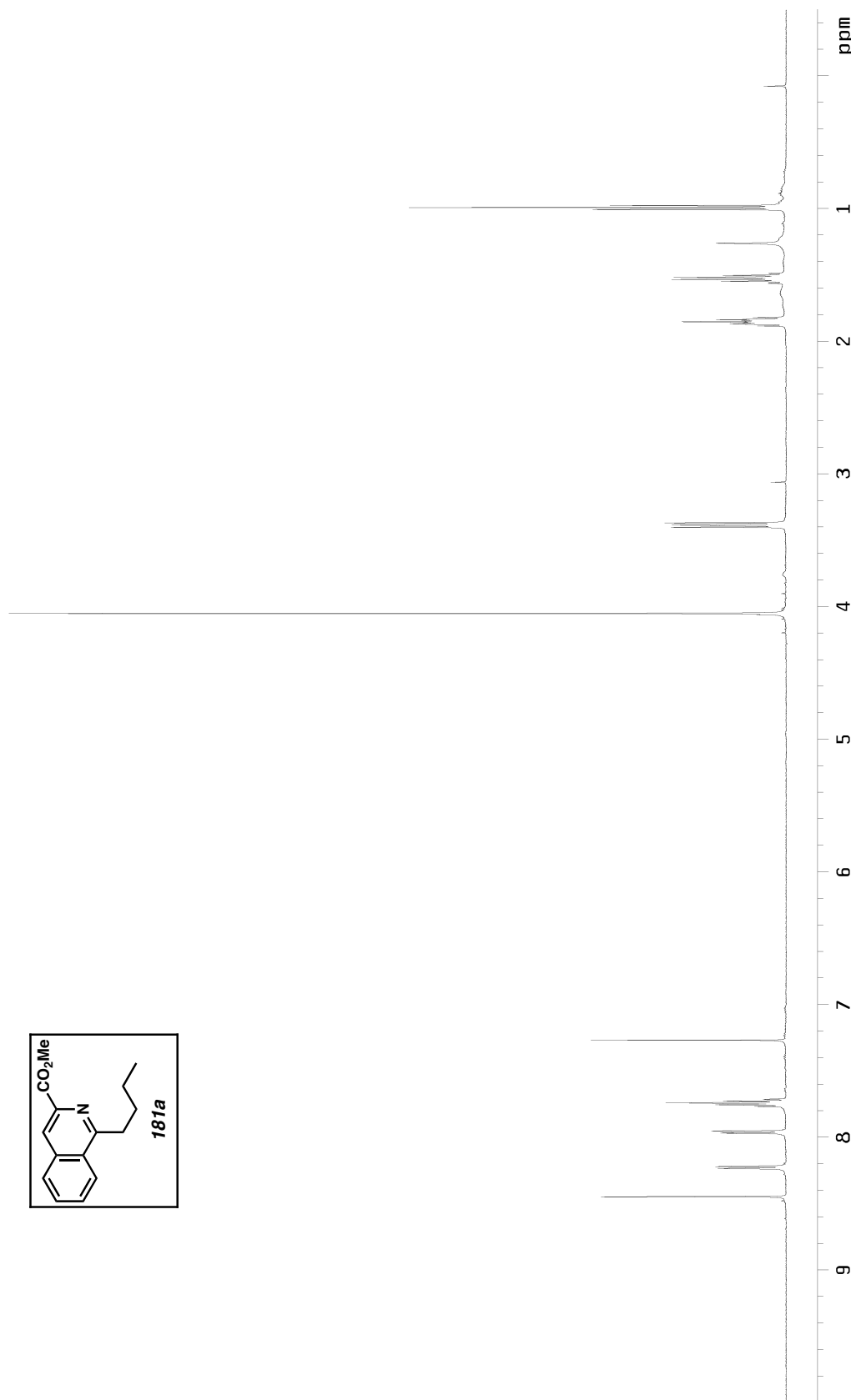


Figure AI.6.1  $^1\text{H}$  NMR (500 MHz,  $\text{CDCl}_3$ ) of isoquinoline **181a** (Table 2.4, entry 2).

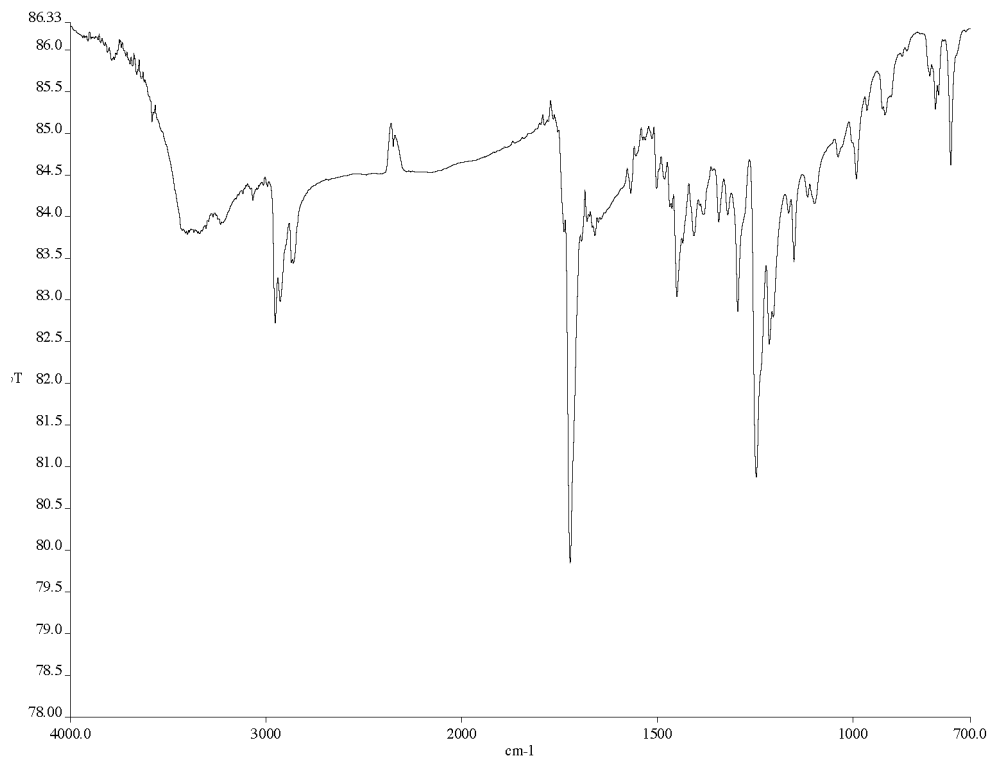


Figure A1.6.2 Infrared spectrum (thin film/NaCl) of isoquinoline **181a** (Table 2.4, entry 2).

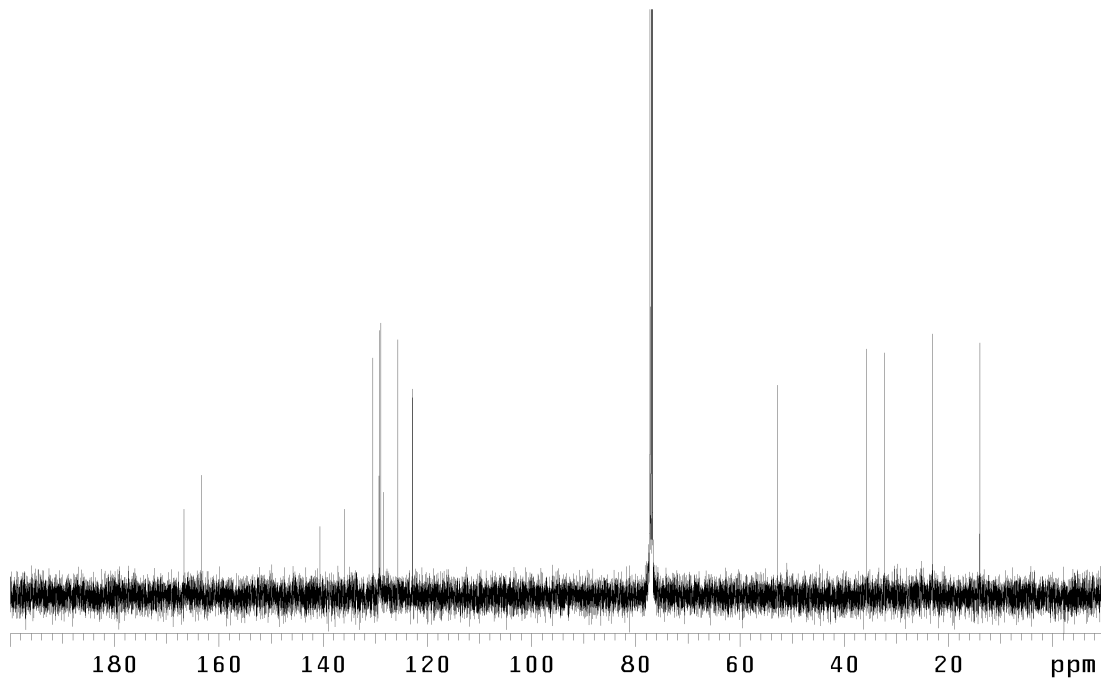


Figure A1.6.3  $^{13}\text{C}$  NMR (125 MHz,  $\text{CDCl}_3$ ) of isoquinoline **181a** (Table 2.4, entry 2).

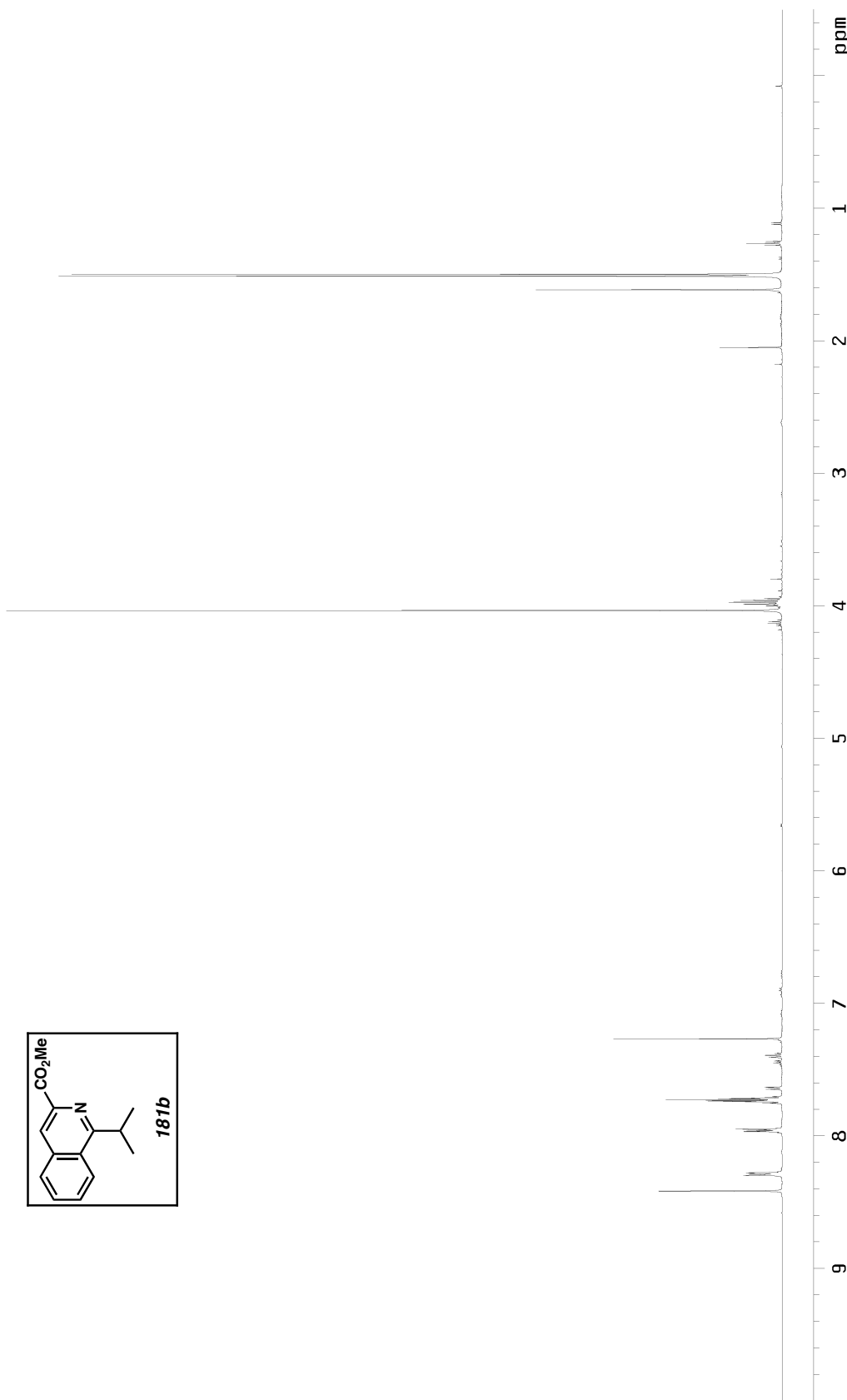


Figure A1.7.1  $^1\text{H}$  NMR (500 MHz,  $\text{CDCl}_3$ ) of isoquinoline **181b** (Table 2.4, entry 3).

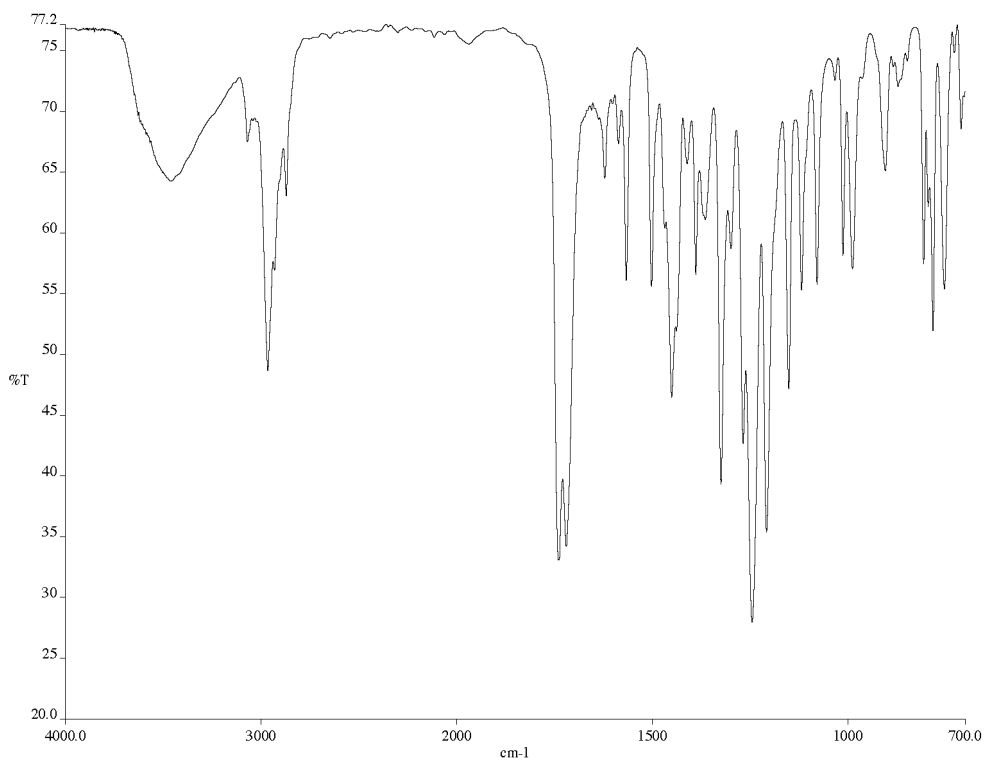


Figure A1.7.2 Infrared spectrum (thin film/NaCl) of isoquinoline **181b** (Table 2.4, entry 3).

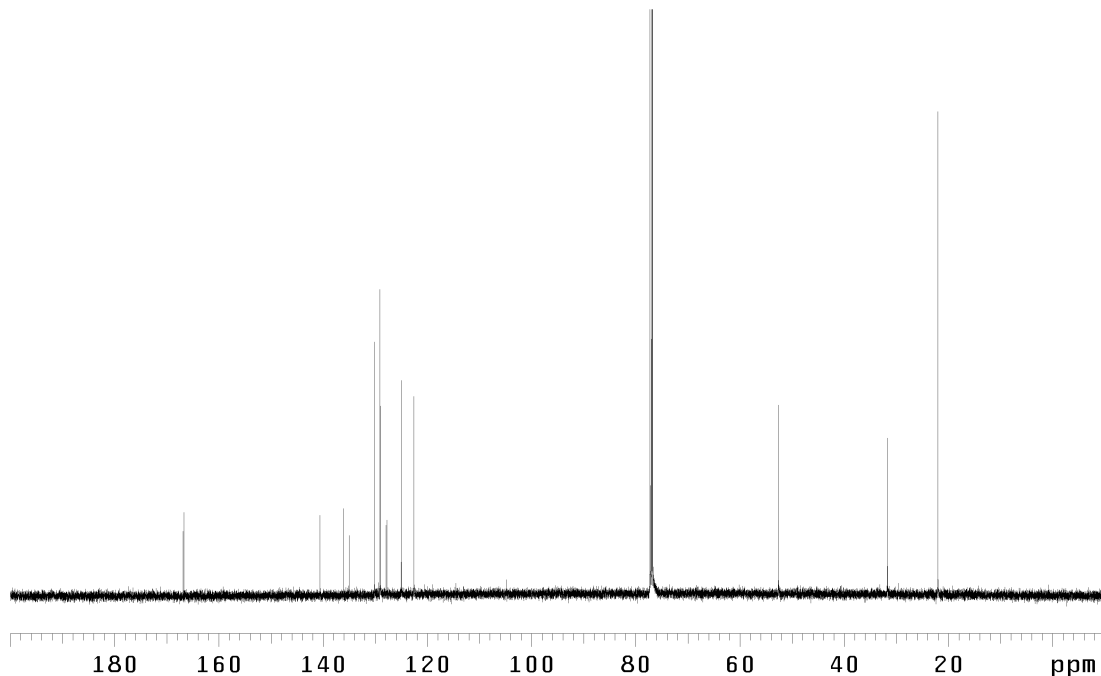


Figure A1.7.3  $^{13}\text{C}$  NMR (125 MHz,  $\text{CDCl}_3$ ) of isoquinoline **181b** (Table 2.4, entry 3).

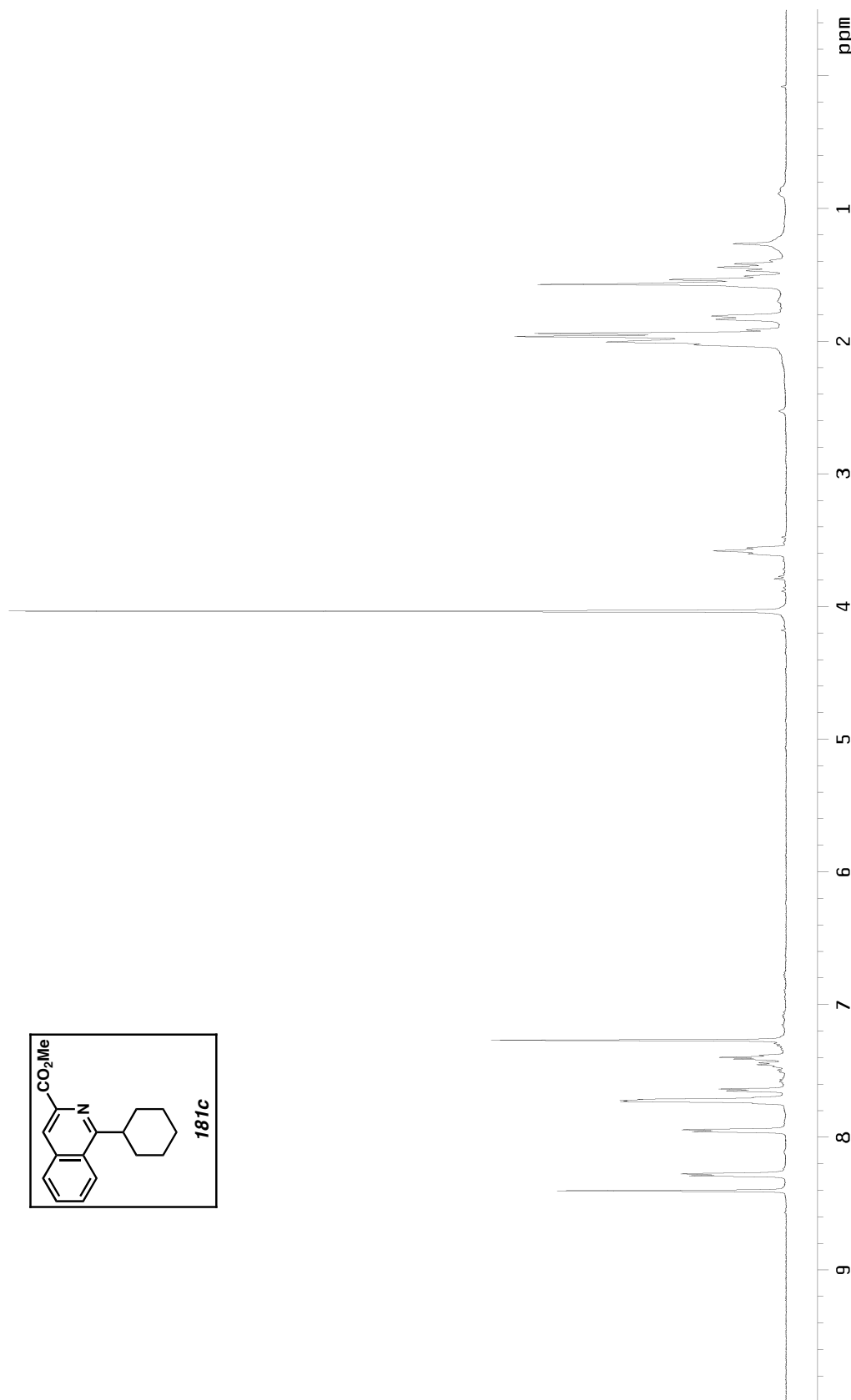


Figure A1.8.I  $^1\text{H}$  NMR (500 MHz,  $\text{CDCl}_3$ ) of isoquinoline **181c** (Table 2.4, entry 4).

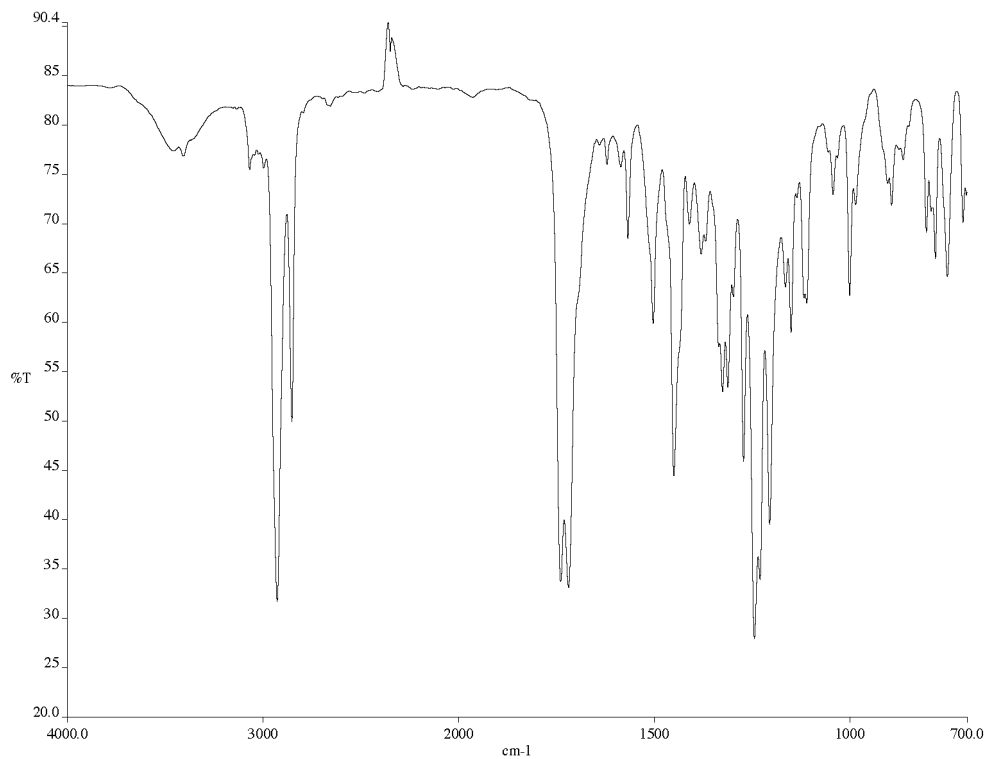


Figure A1.8.2 Infrared spectrum (thin film/NaCl) of isoquinoline **181c** (Table 2.4, entry 4).

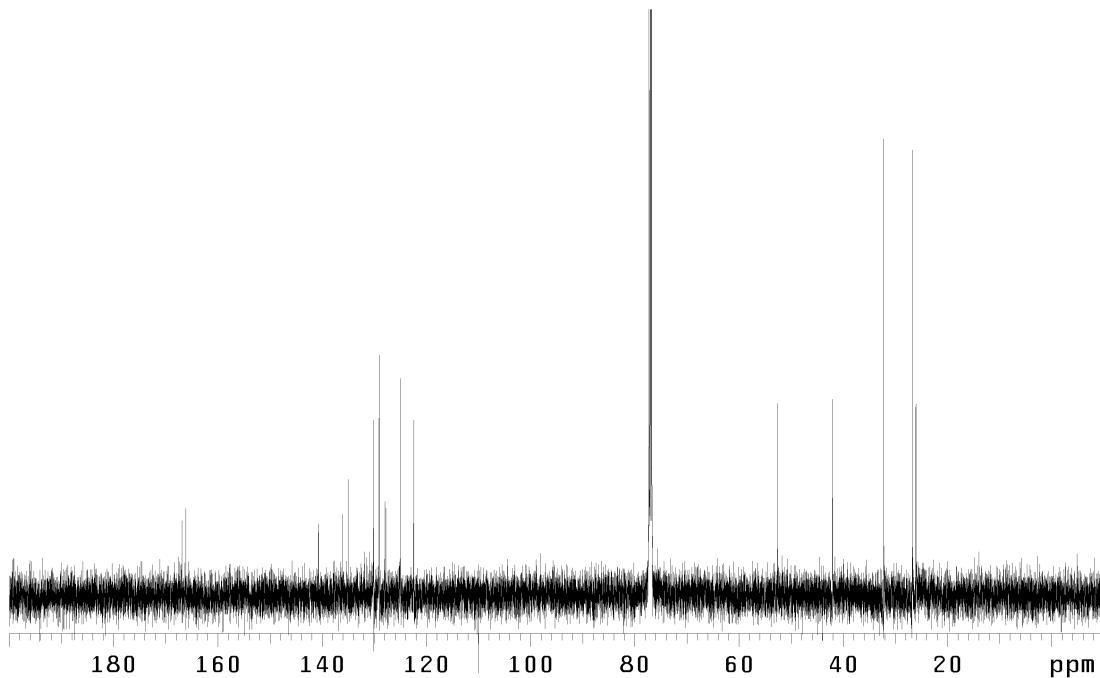


Figure A1.8.3 <sup>13</sup>C NMR (125 MHz, CDCl<sub>3</sub>) of isoquinoline **181c** (Table 2.4, entry 4).

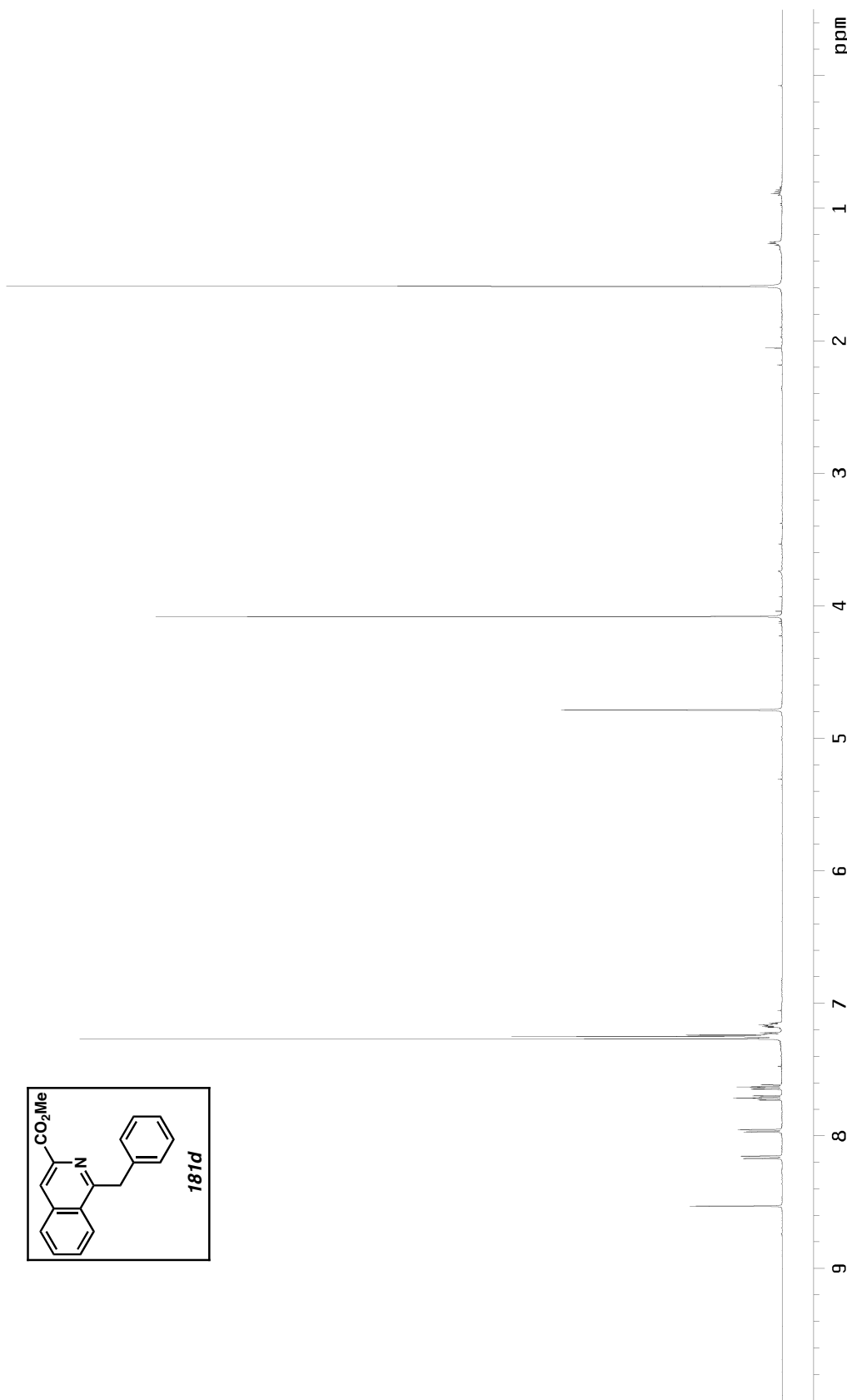
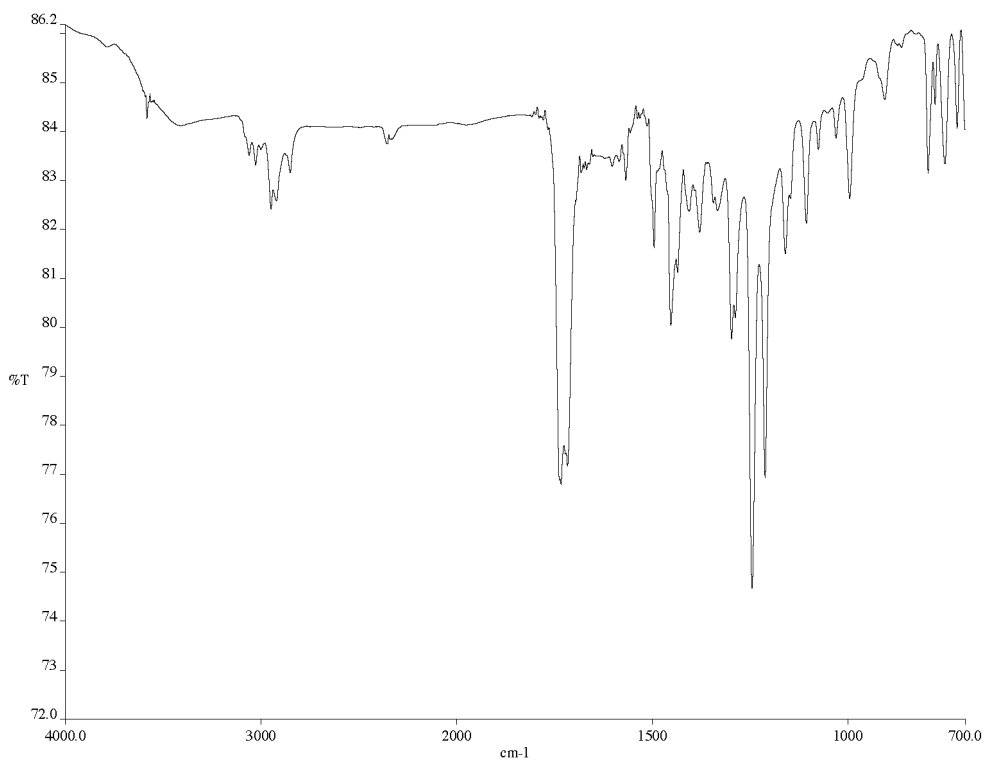
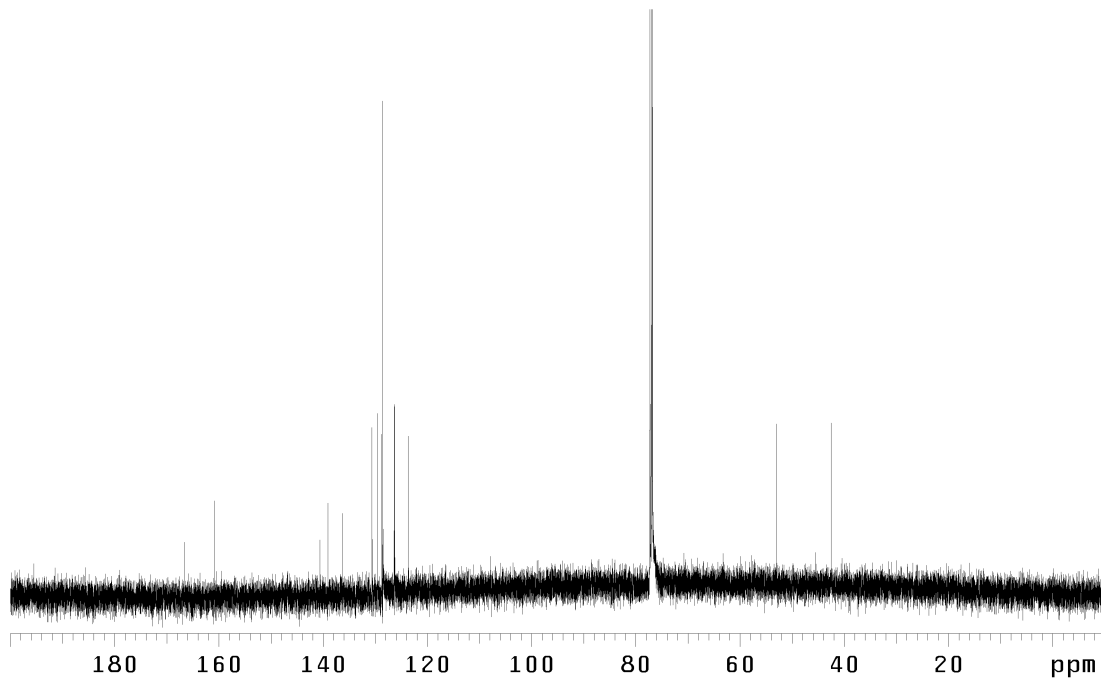


Figure A1.9.1  $^1\text{H}$  NMR (500 MHz,  $\text{CDCl}_3$ ) of isoquinoline **181d** (Table 2.4, entry 5).



*Figure A1.9.2* Infrared spectrum (thin film/NaCl) of isoquinoline **181d** (Table 2.4, entry 5).



*Figure A1.9.3* <sup>13</sup>C NMR (125 MHz, CDCl<sub>3</sub>) of isoquinoline **181d** (Table 2.4, entry 5).

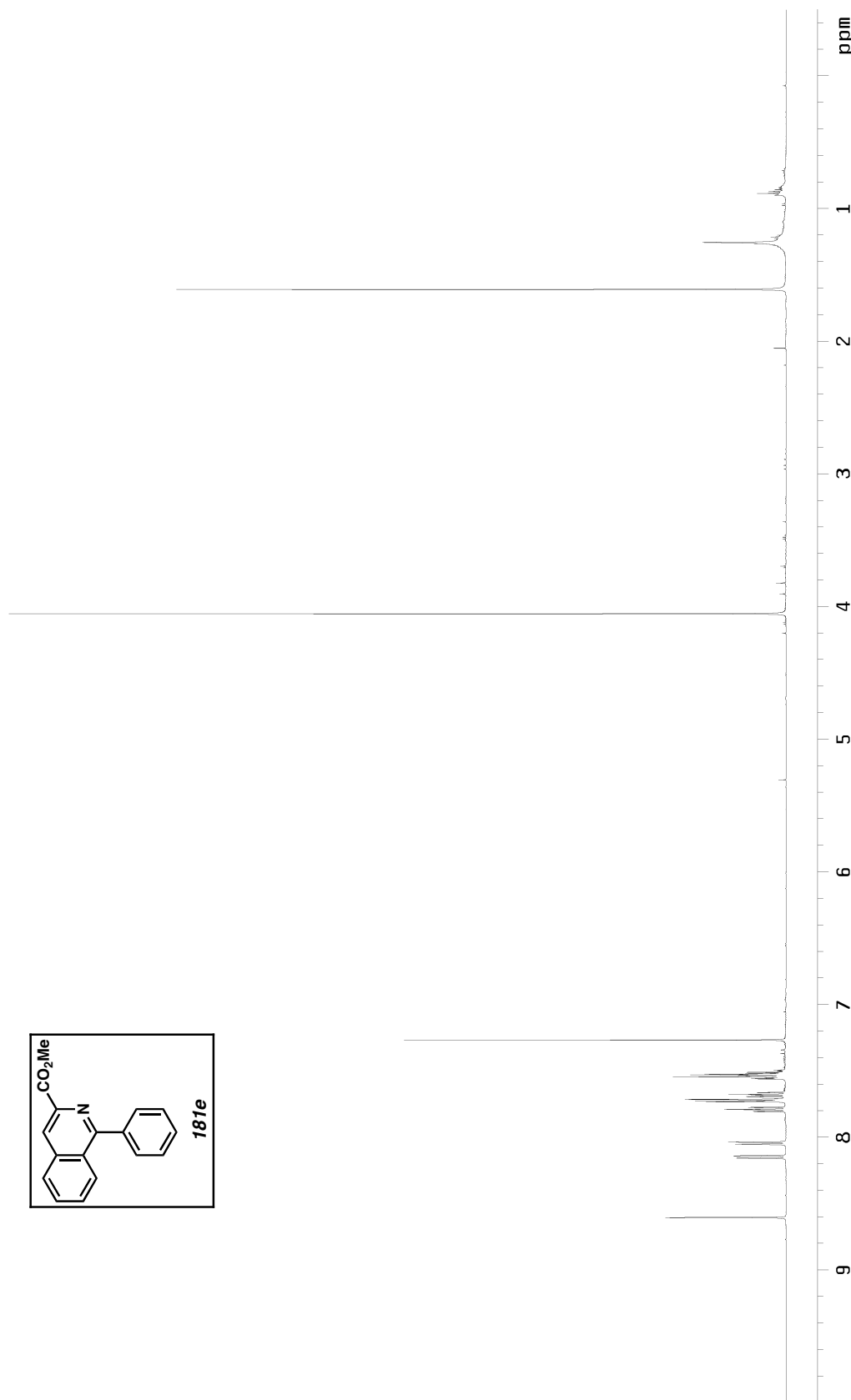


Figure A1.10.1  $^1\text{H}$  NMR (500 MHz,  $\text{CDCl}_3$ ) of isoquinoline **181e** (Table 2.4, entry 6).

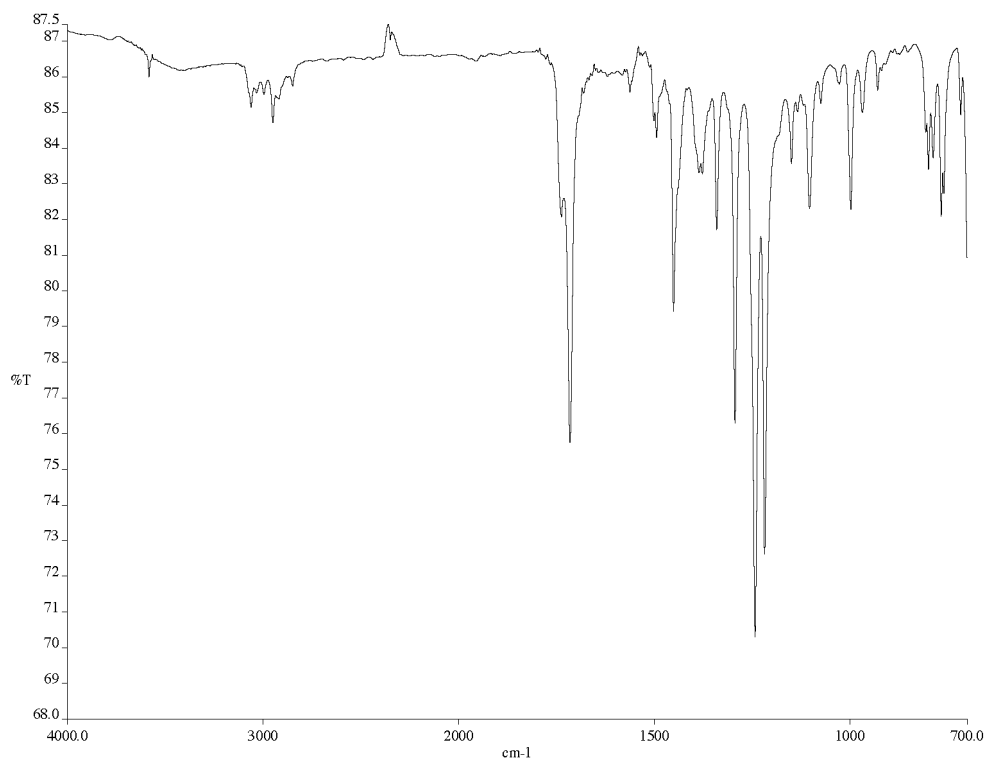


Figure A1.10.2 Infrared spectrum (thin film/NaCl) of isoquinoline **181e** (Table 2.4, entry 6).

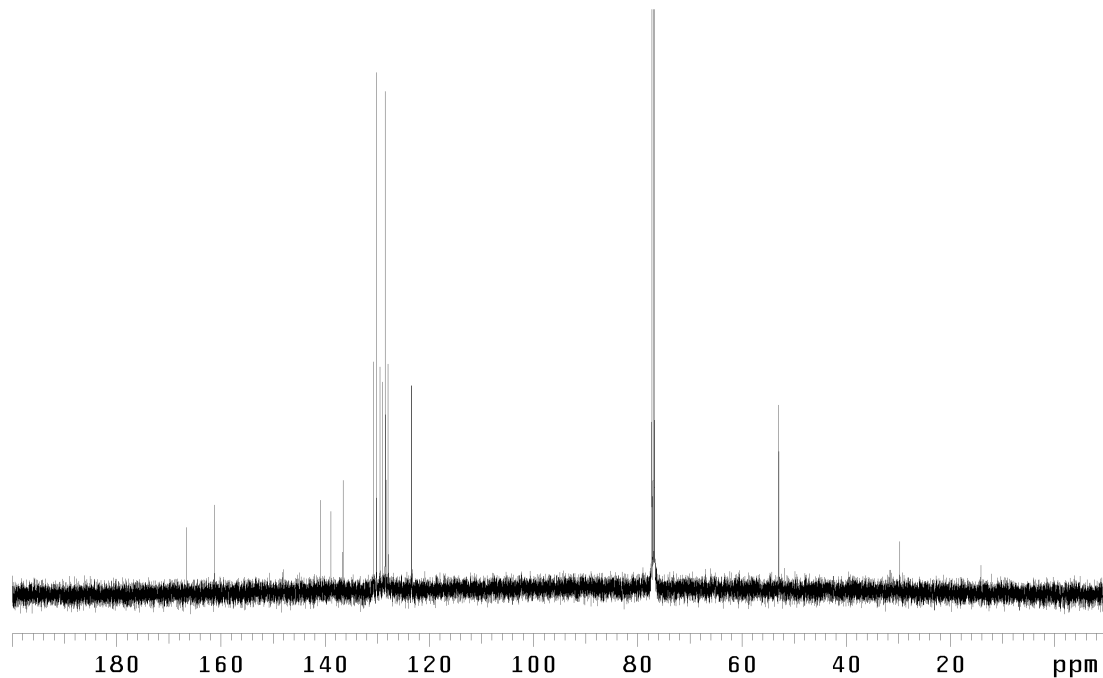


Figure A1.10.3  $^{13}\text{C}$  NMR (125 MHz,  $\text{CDCl}_3$ ) of isoquinoline **181e** (Table 2.4, entry 6).

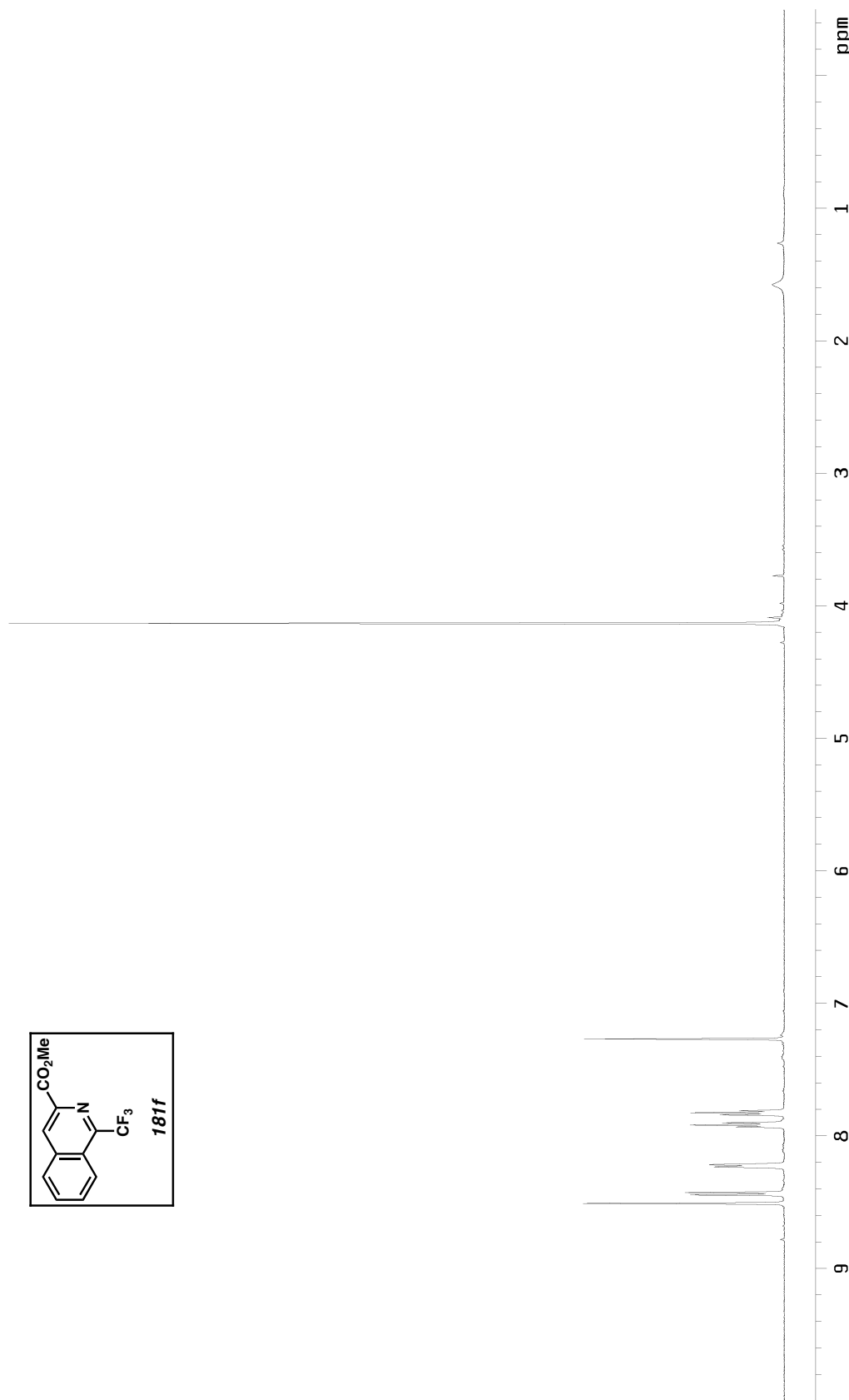


Figure A1.11.1  $^1\text{H}$  NMR (500 MHz,  $\text{CDCl}_3$ ) of isoquinoline **181f** (Table 2.4, entry 7).

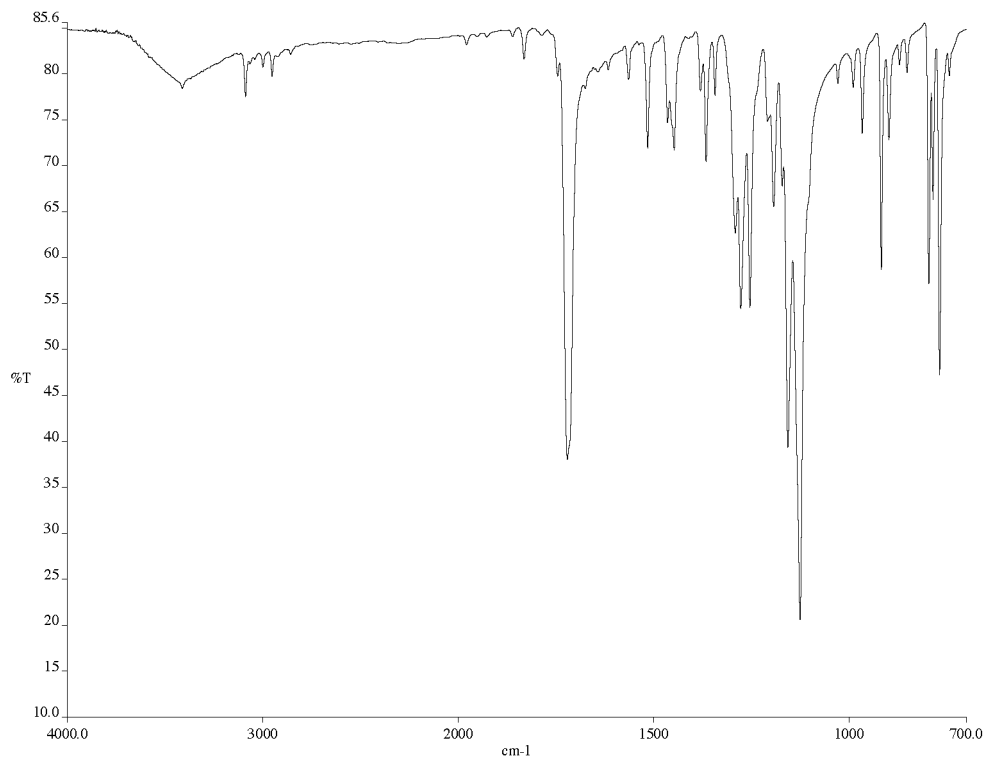


Figure A1.11.2 Infrared spectrum (thin film/NaCl) of isoquinoline **181f** (Table 2.4, entry 7).

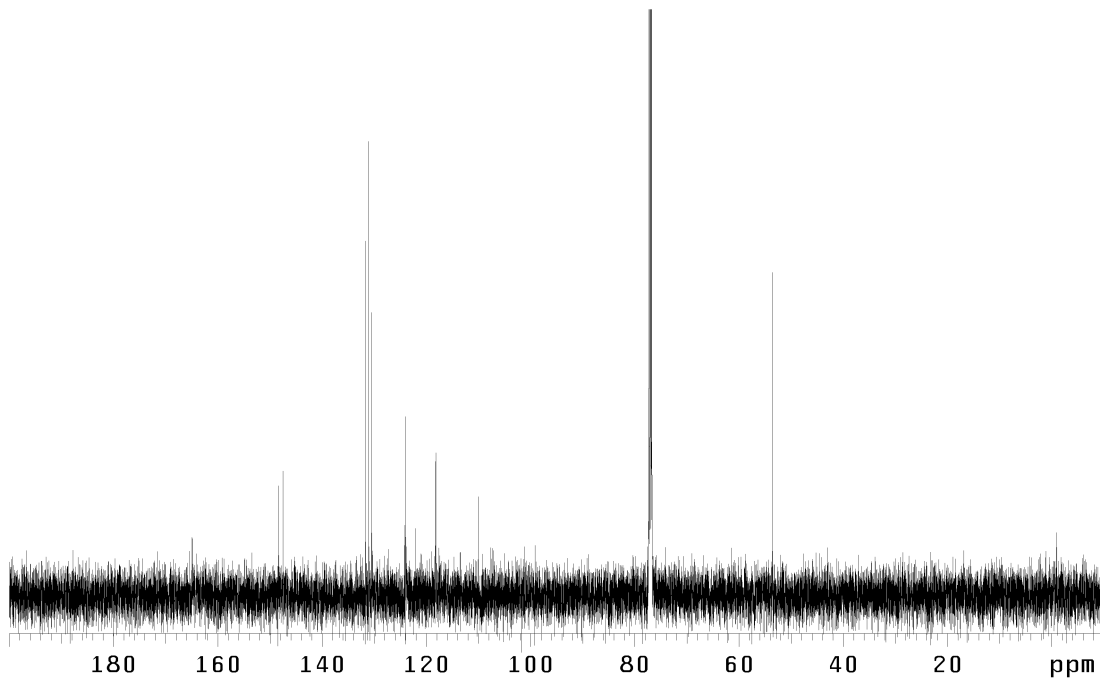


Figure A1.11.3  $^{13}\text{C}$  NMR (125 MHz,  $\text{CDCl}_3$ ) of isoquinoline **181f** (Table 2.4, entry 7).

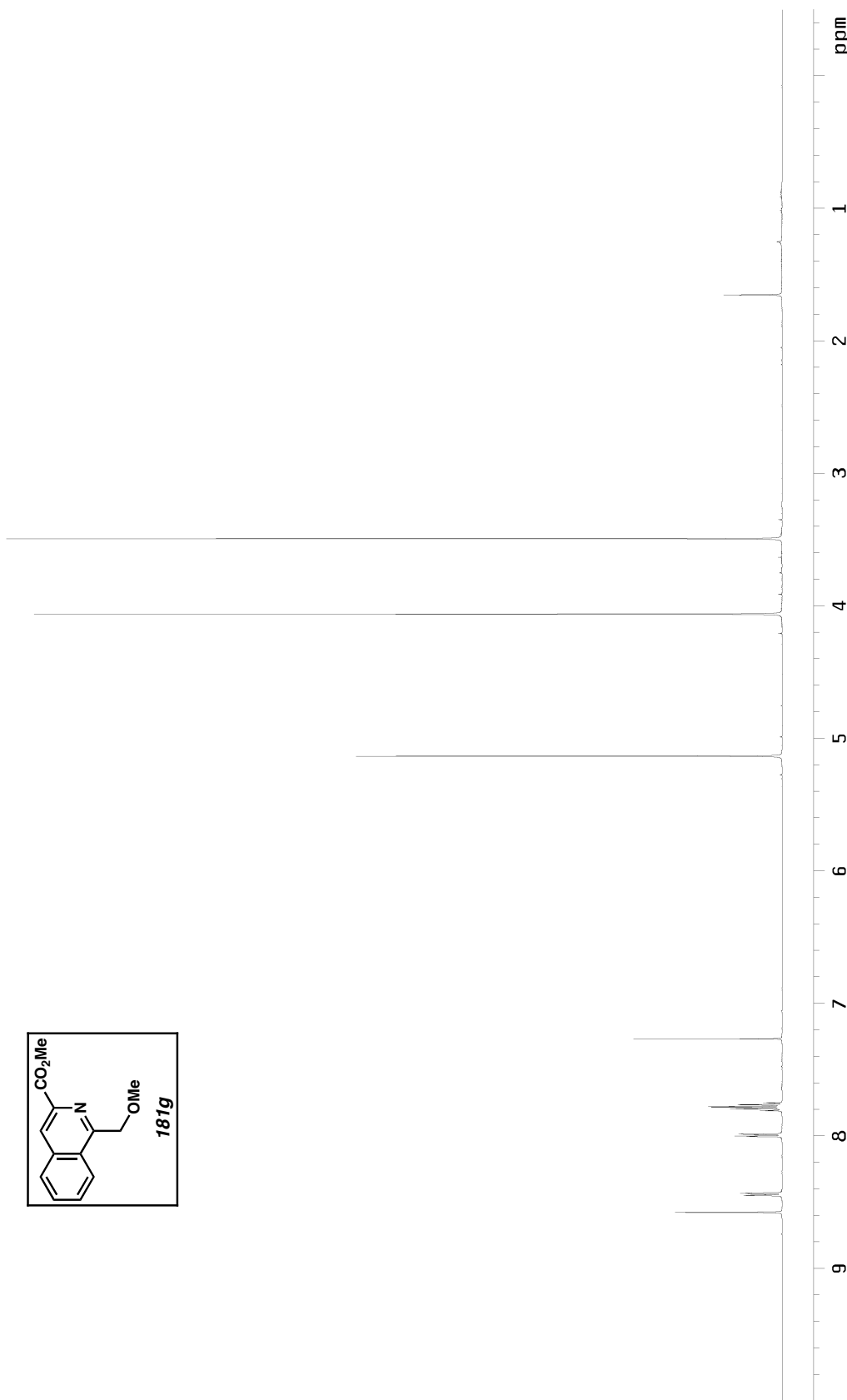


Figure A1.J2.I  $^1\text{H}$  NMR (500 MHz,  $\text{CDCl}_3$ ) of isoquinoline **181g** (Table 2.4, entry 8).

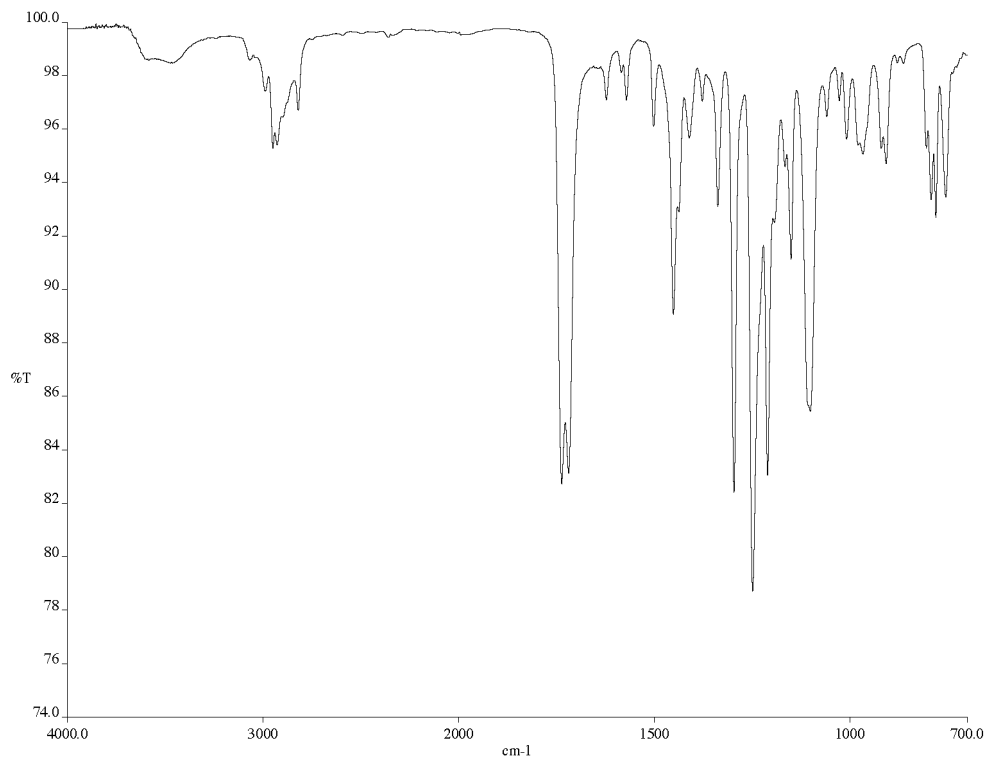


Figure A1.12.2 Infrared spectrum (thin film/NaCl) of isoquinoline **181g** (Table 2.4, entry 8).

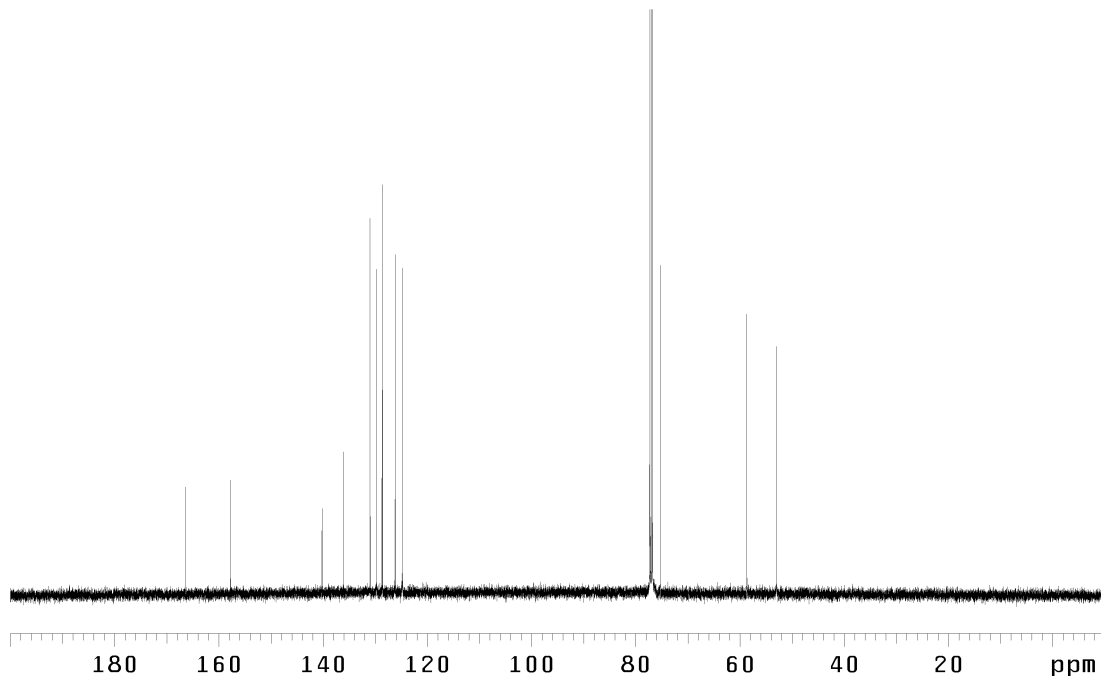


Figure A1.12.3 <sup>13</sup>C NMR (125 MHz, CDCl<sub>3</sub>) of isoquinoline **181g** (Table 2.4, entry 8).

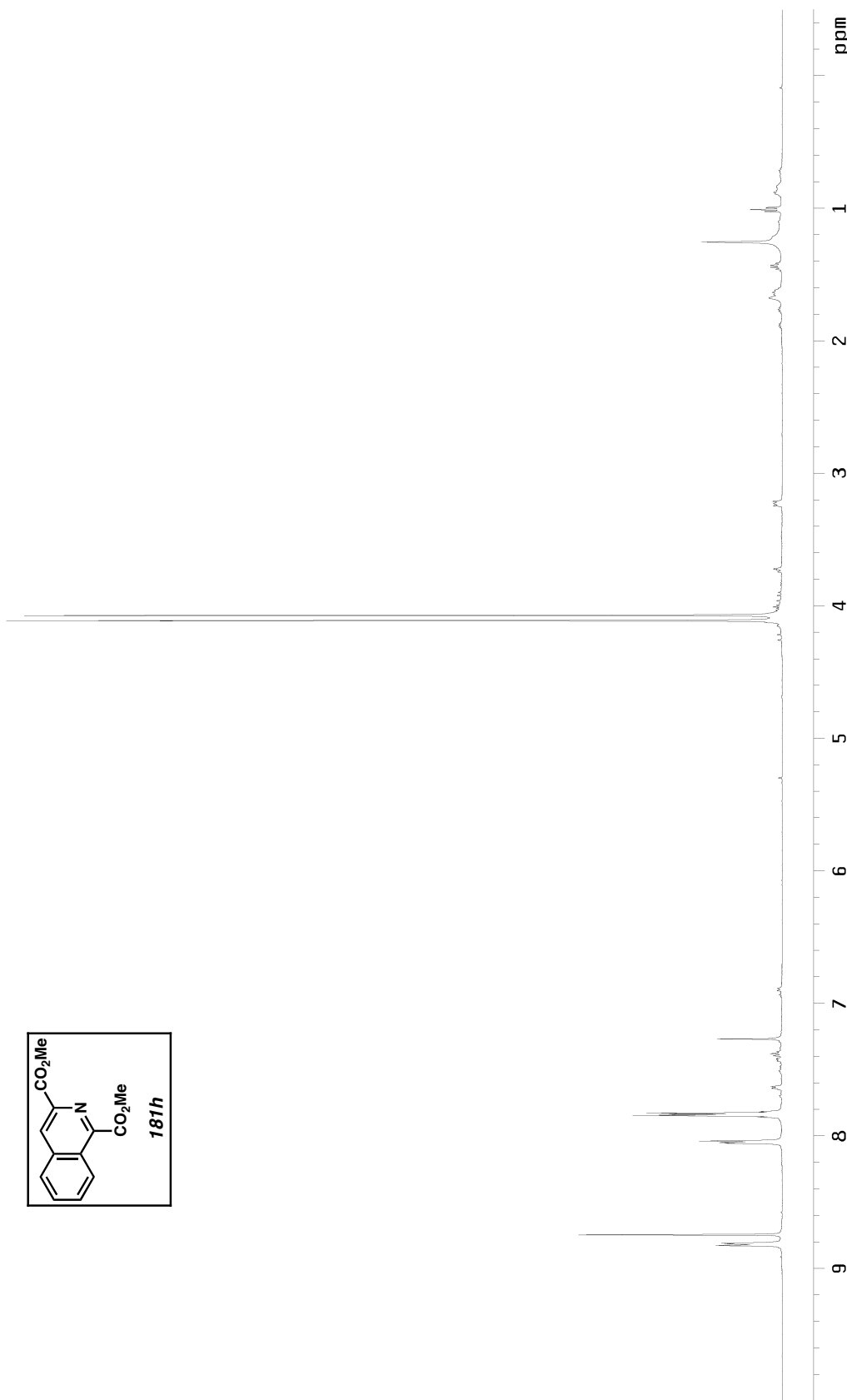


Figure A1.13.1  $^1\text{H}$  NMR (500 MHz,  $\text{CDCl}_3$ ) of isoquinoline **181h** (Table 2.4, entry 9).

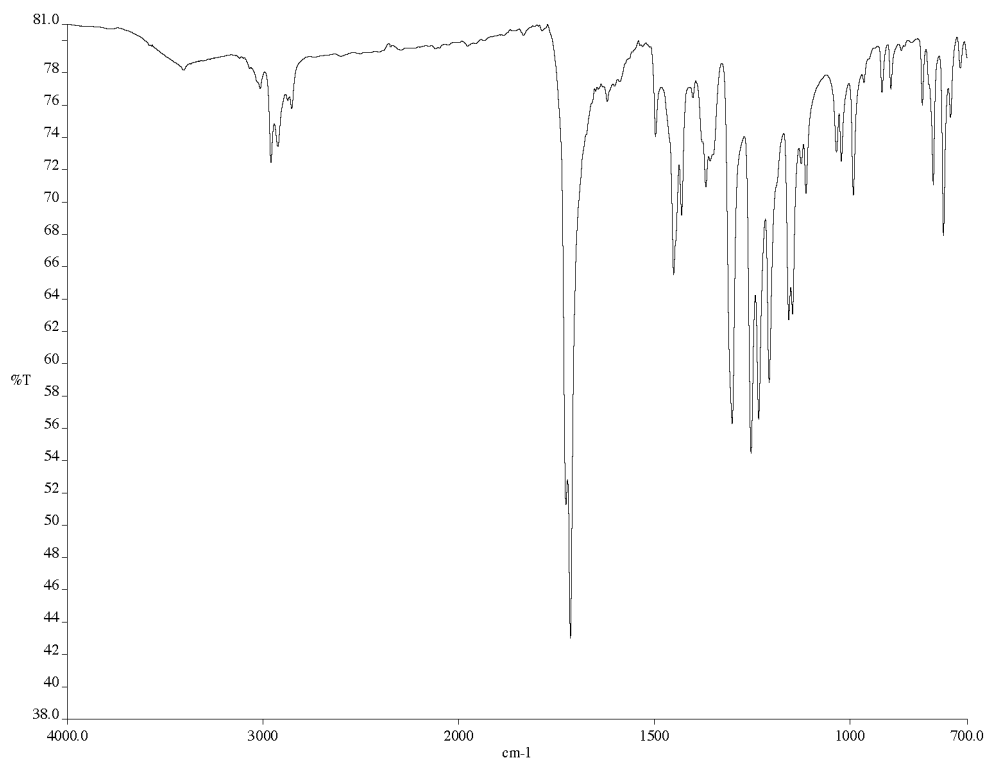


Figure A1.13.2 Infrared spectrum (thin film/NaCl) of isoquinoline **181h** (Table 2.4, entry 9).

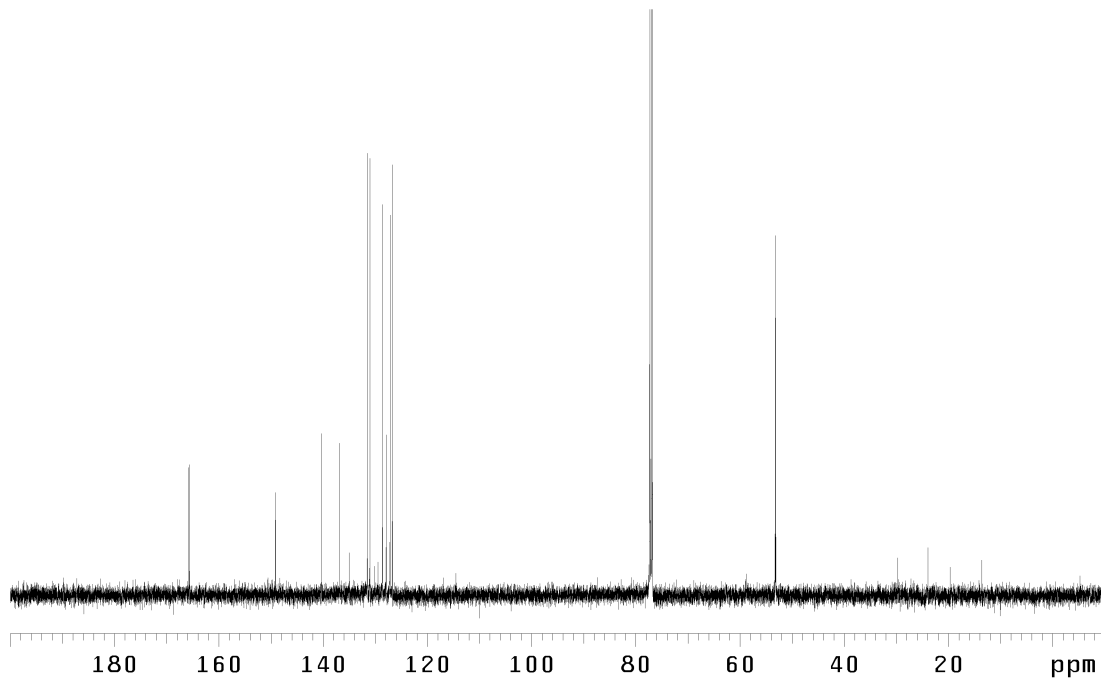


Figure A1.13.3 <sup>13</sup>C NMR (125 MHz,  $\text{CDCl}_3$ ) of isoquinoline **181h** (Table 2.4, entry 9).

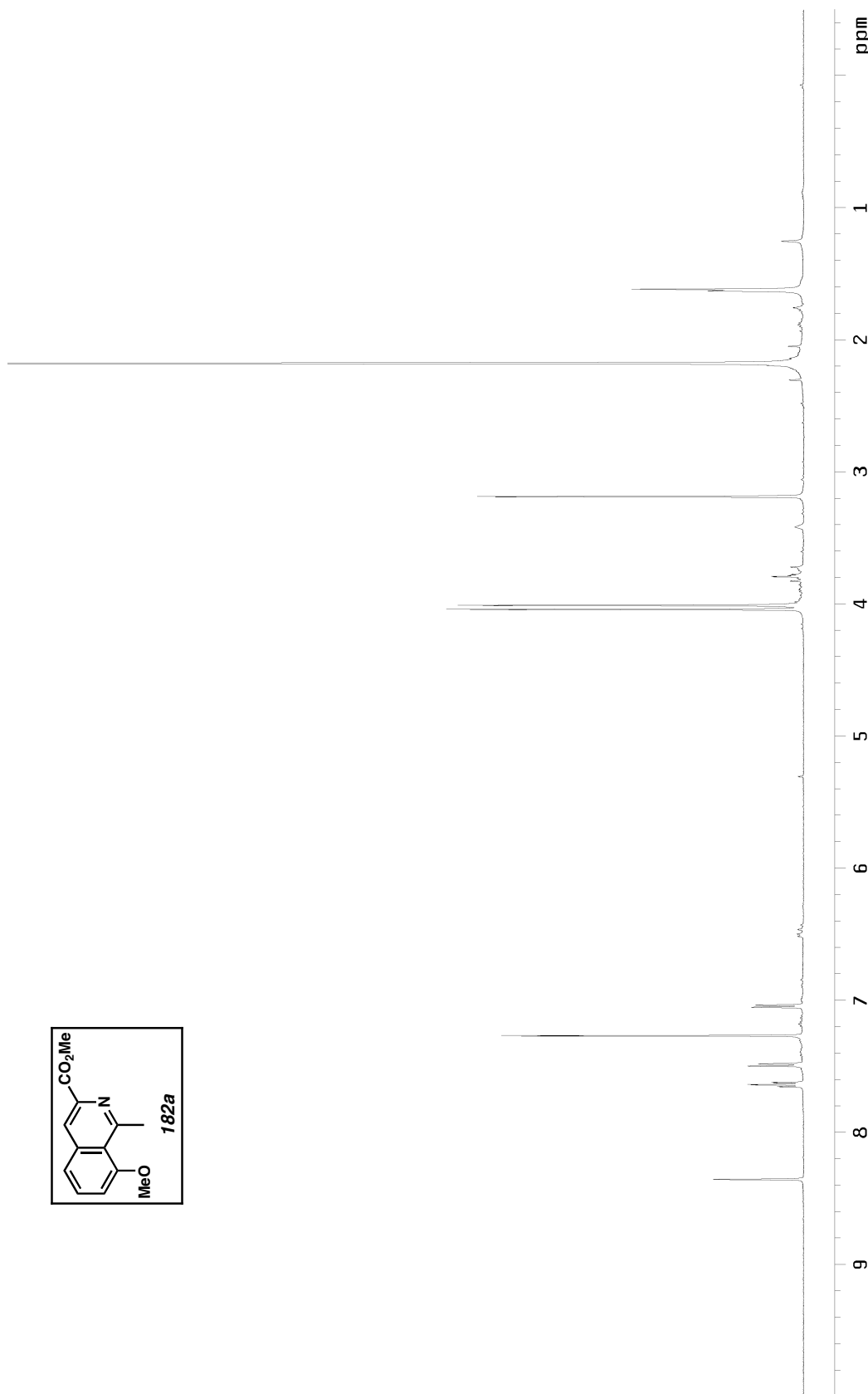


Figure A1.14.I  $^1\text{H}$  NMR (500 MHz,  $\text{CDCl}_3$ ) of isoquinoline **182a** (Table 2.5, entry 1).

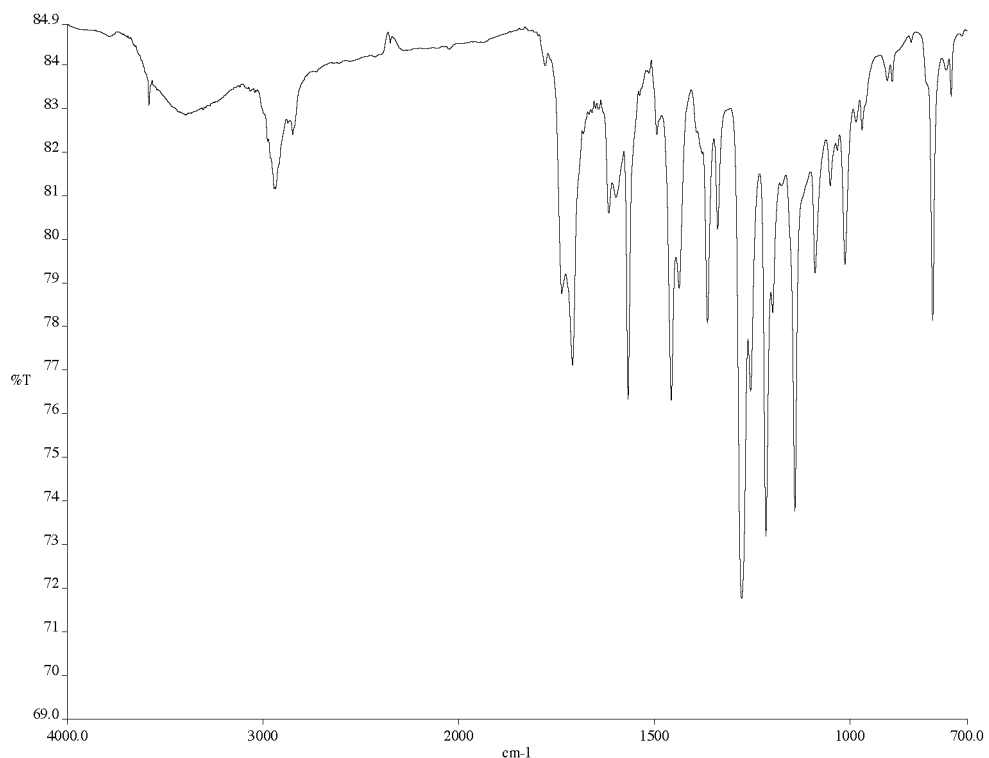


Figure A1.14.2 Infrared spectrum (thin film/NaCl) of isoquinoline **182a** (Table 2.5, entry 1).

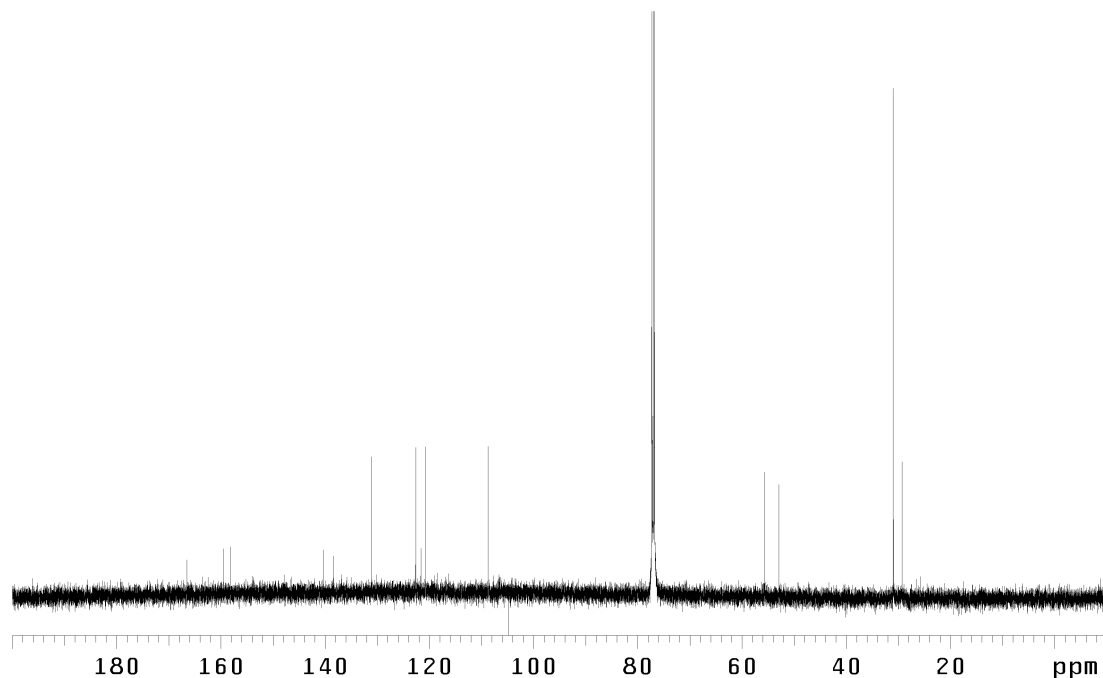


Figure A1.14.3  $^{13}\text{C}$  NMR (125 MHz,  $\text{CDCl}_3$ ) of isoquinoline **182a** (Table 2.5, entry 1).

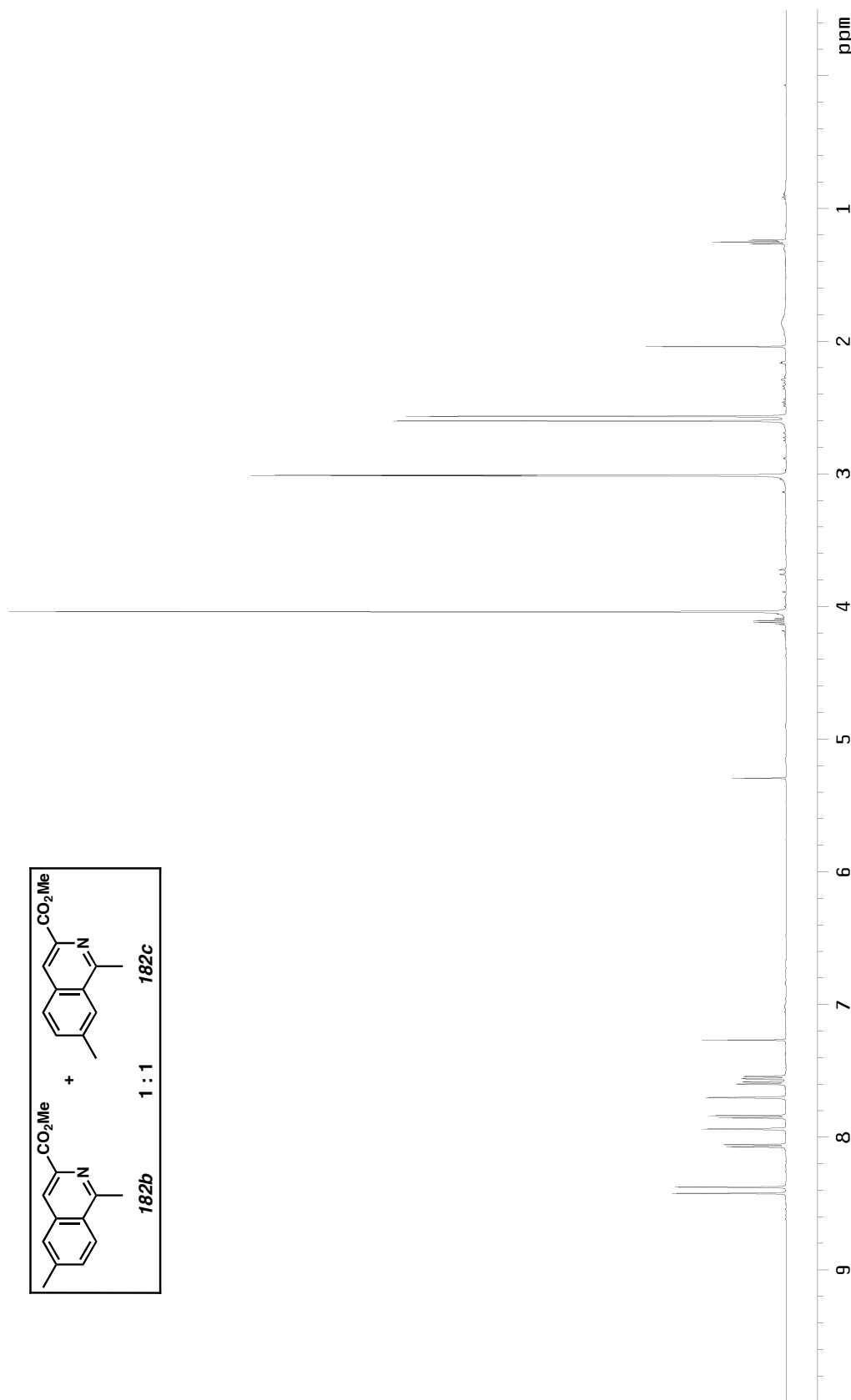


Figure AI.15.1  $^1\text{H}$  NMR (500 MHz,  $\text{CDCl}_3$ ) of isoquinoline **182b** and **182c** (Table 2.5, entry 2).

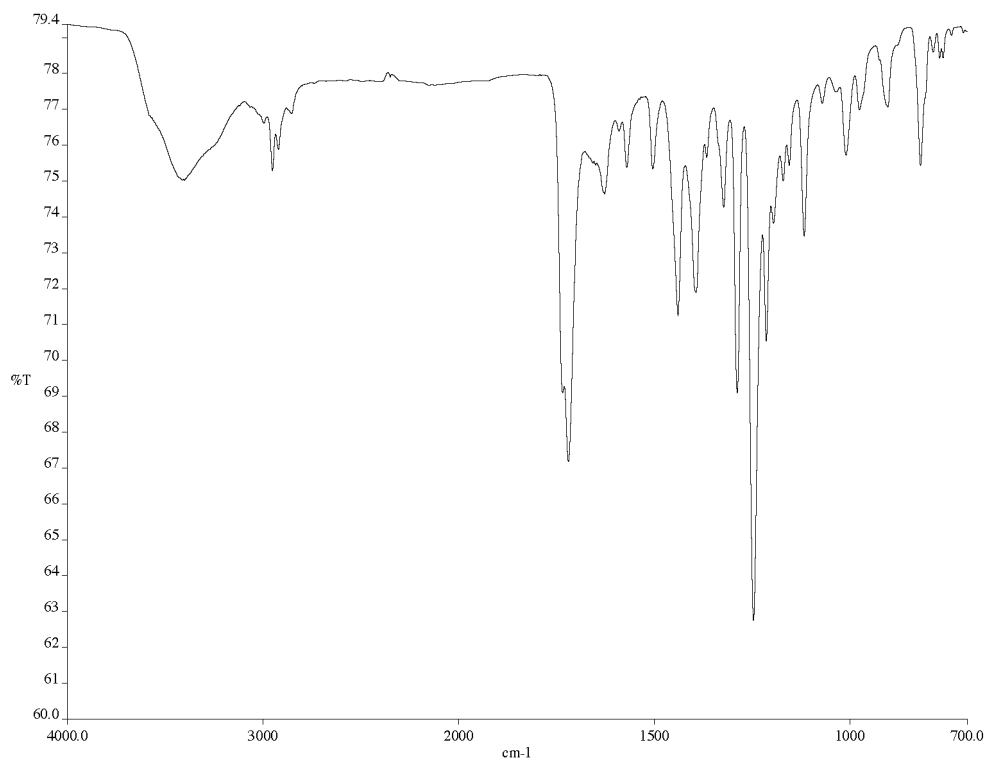


Figure A1.15.2 Infrared spectrum (thin film/NaCl) of isoquinoline **182b** and **182c** (Table 2.5, entry 2).

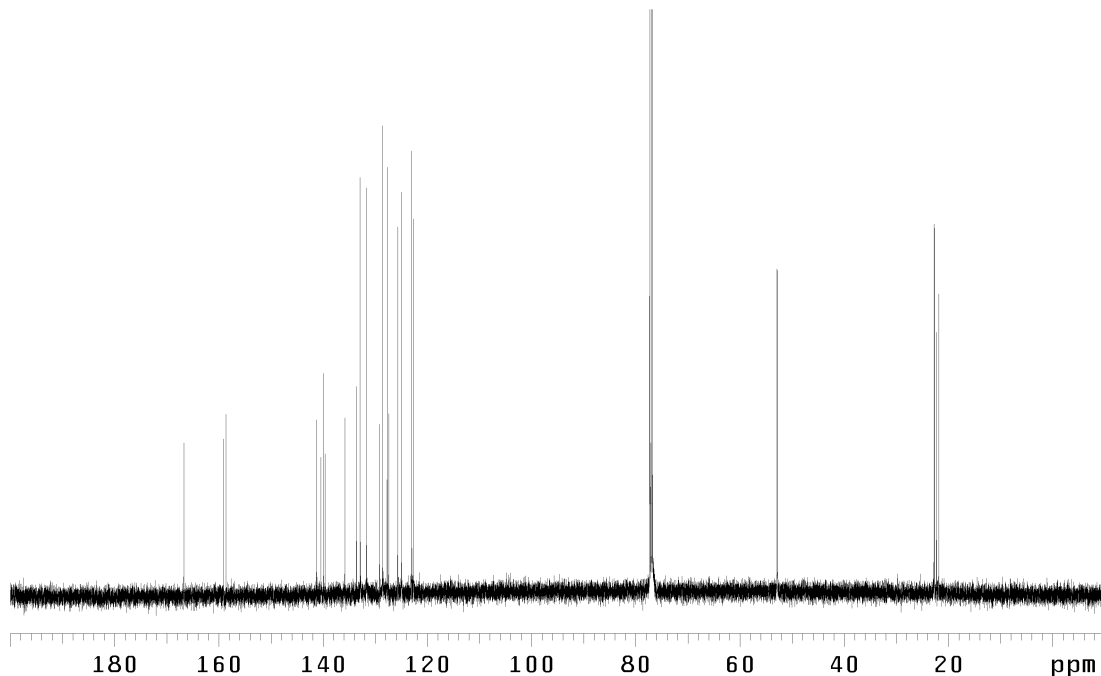


Figure A1.15.3 <sup>13</sup>C NMR (125 MHz, CDCl<sub>3</sub>) of isoquinoline **182b** and **182c** (Table 2.5, entry 2).

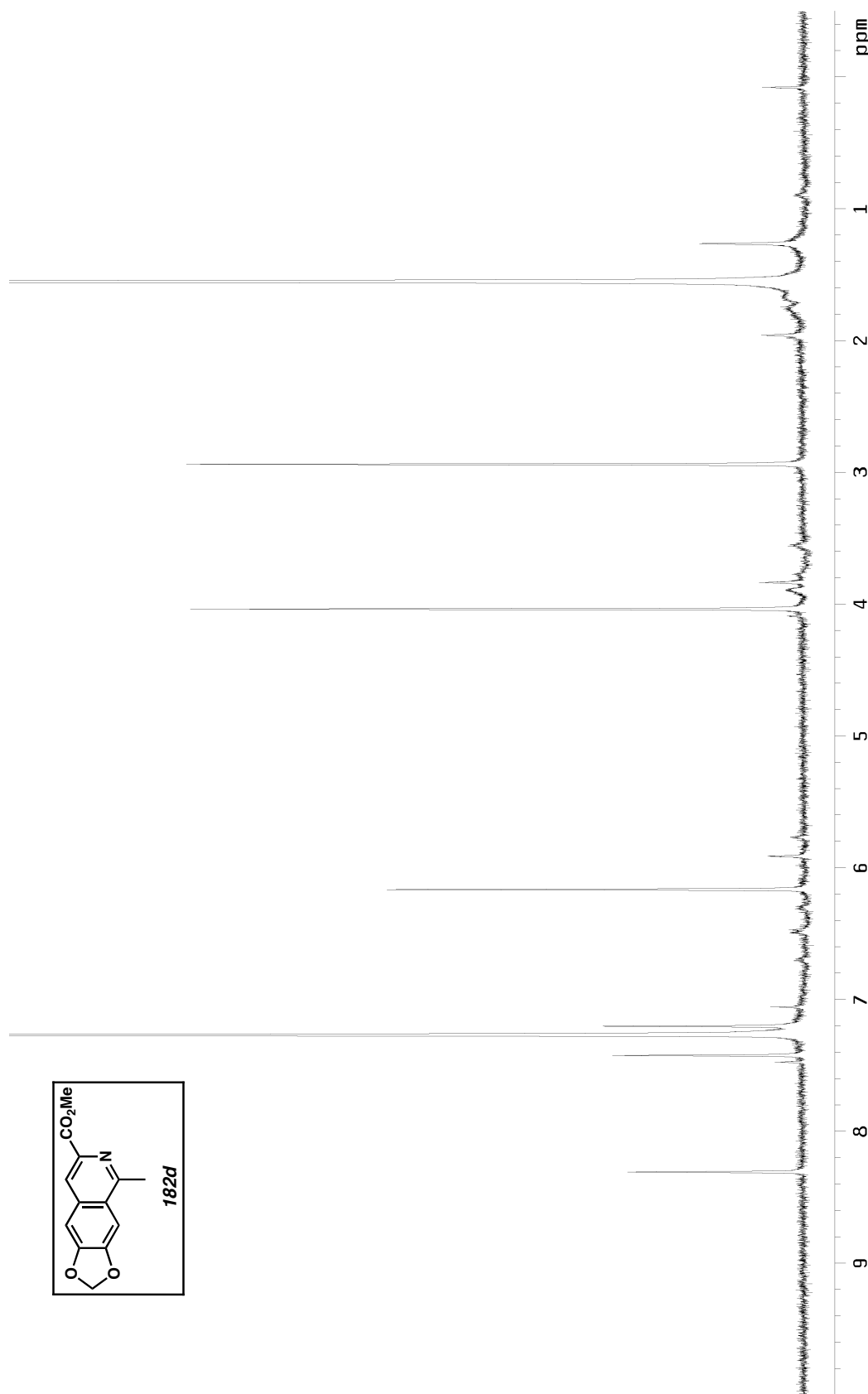


Figure A1.16.1  $^1\text{H}$  NMR (500 MHz,  $\text{CDCl}_3$ ) of isoquinoline **182d** (Table 2.5, entry 3).

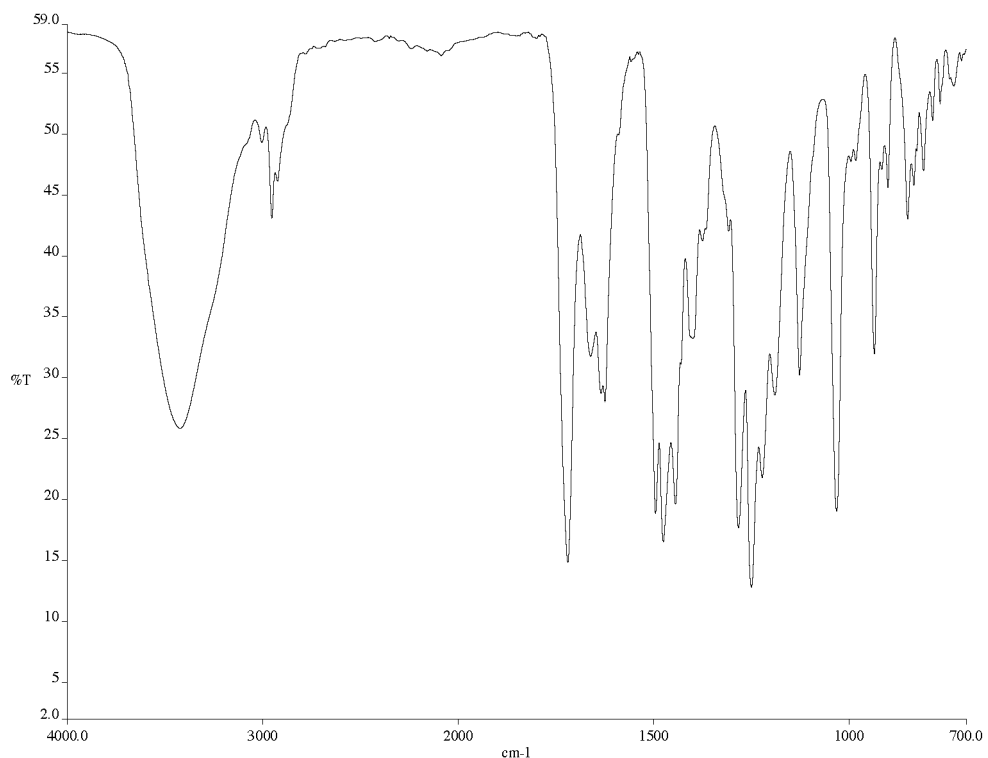


Figure A1.16.2 Infrared spectrum (thin film/NaCl) of isoquinoline **182d** (Table 2.5, entry 3).

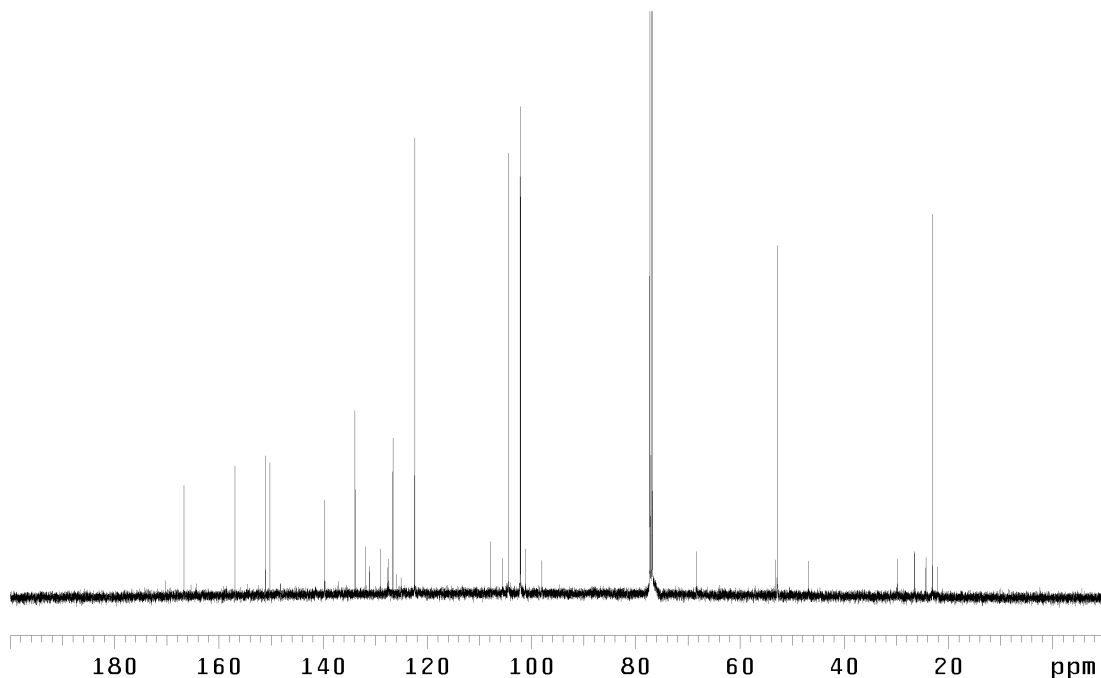


Figure A1.16.3 <sup>13</sup>C NMR (125 MHz, CDCl<sub>3</sub>) of isoquinoline **182d** (Table 2.5, entry 3).

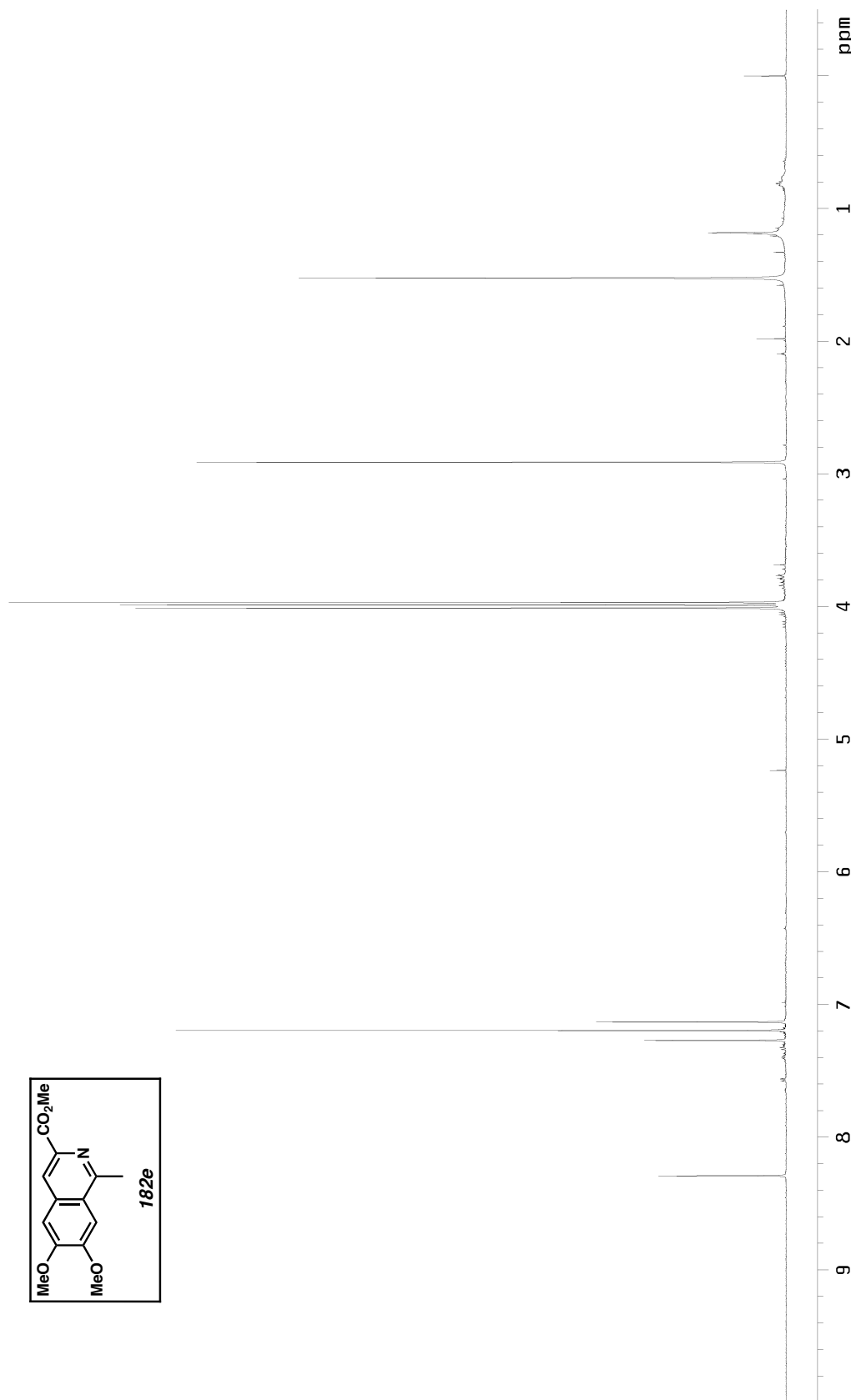


Figure A1.17.1  $^1\text{H}$  NMR (500 MHz,  $\text{CDCl}_3$ ) of isoquinoline **182e** (Table 2.5, entry 4).

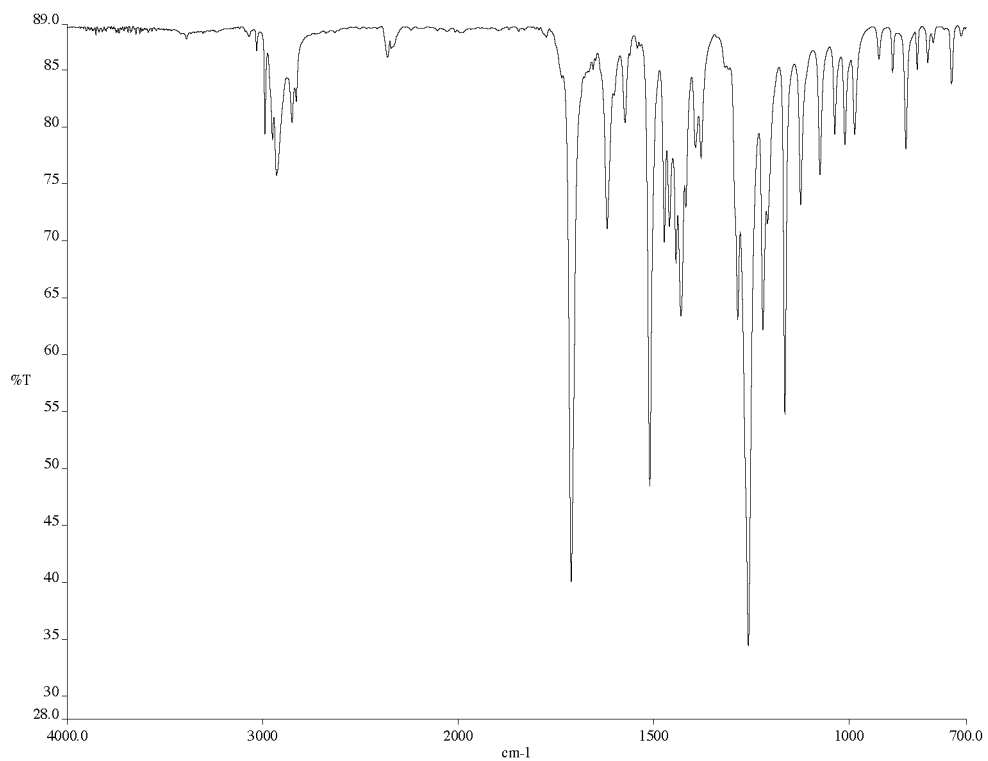


Figure A1.17.2 Infrared spectrum (thin film/NaCl) of isoquinoline **182e** (Table 2.5, entry 4).

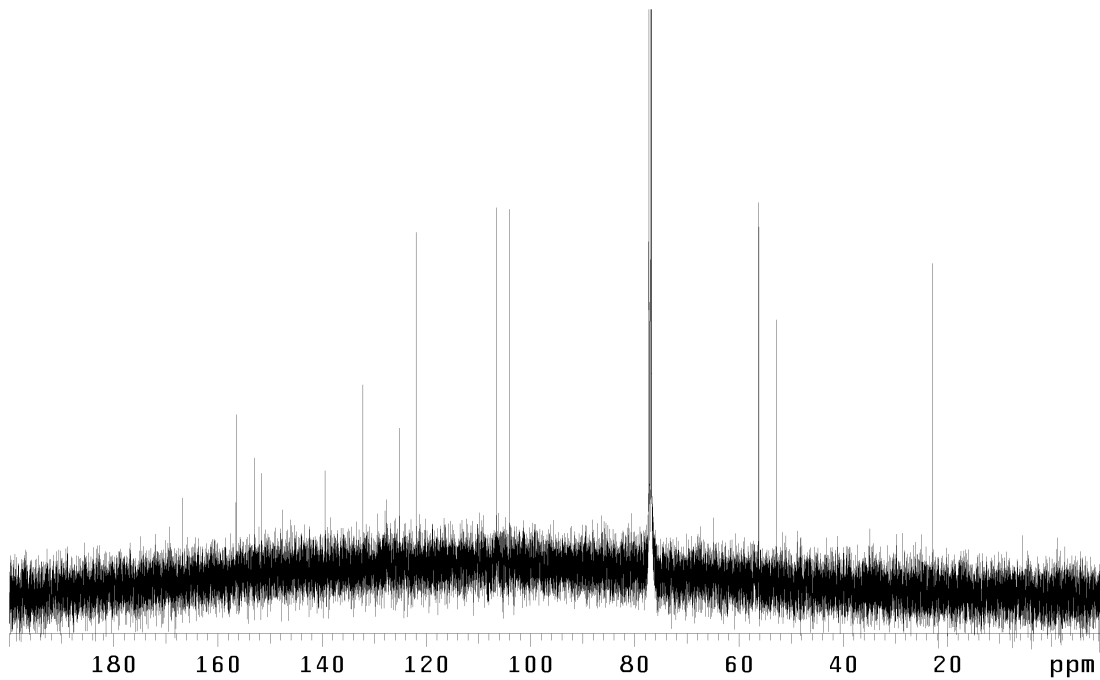


Figure A1.17.3 <sup>13</sup>C NMR (125 MHz, CDCl<sub>3</sub>) of isoquinoline **182e** (Table 2.5, entry 4).

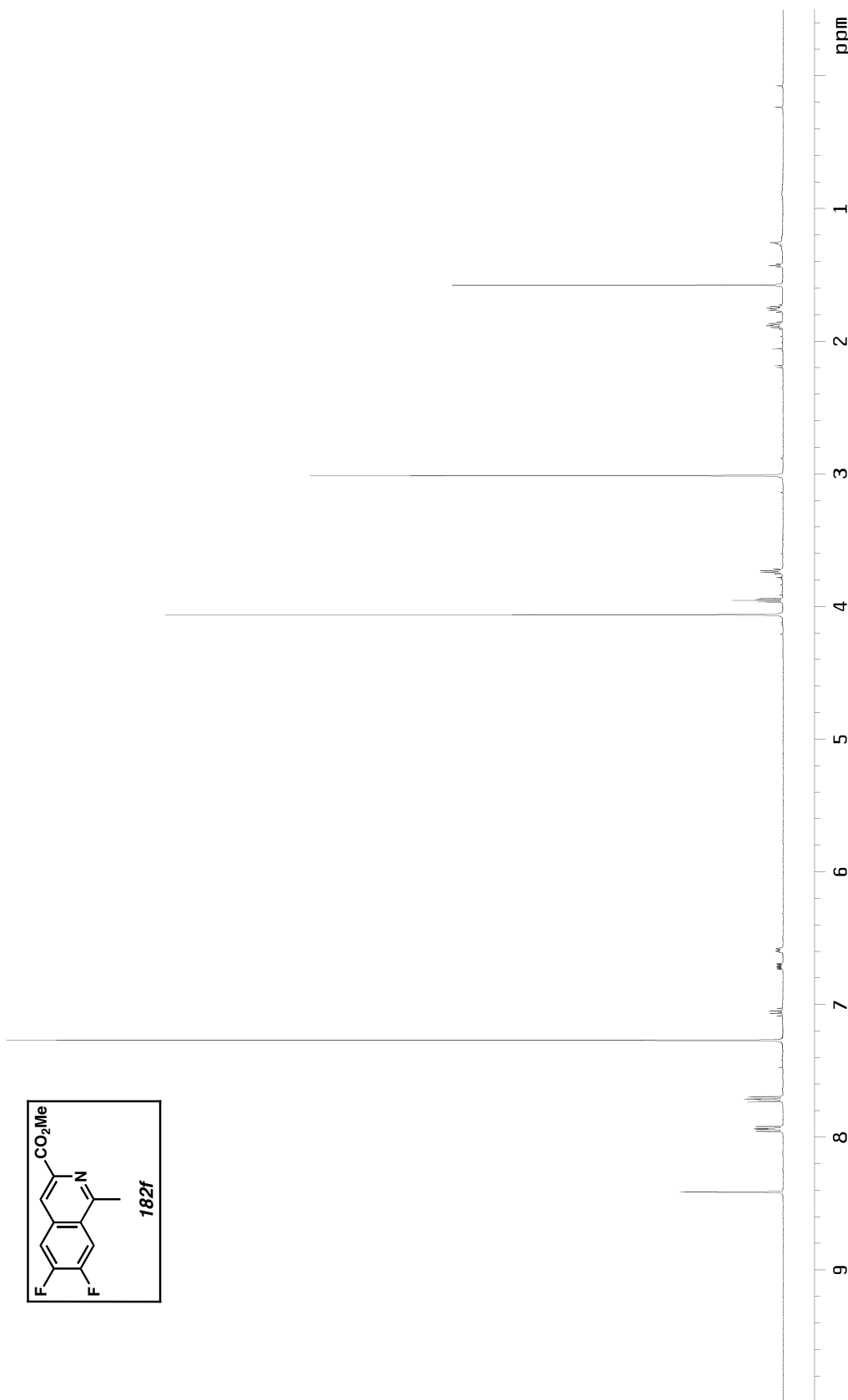


Figure A1.18.1  $^1\text{H}$  NMR (500 MHz,  $\text{CDCl}_3$ ) of isoquinoline **182f** (Table 2.5, entry 5).

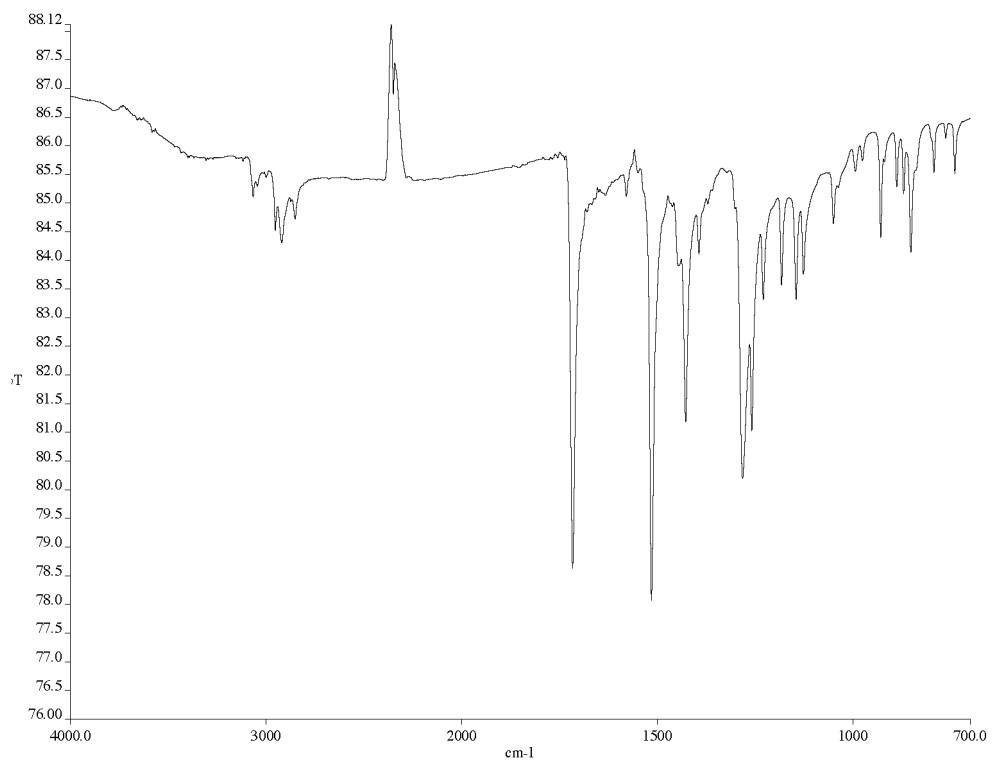


Figure A1.18.2 Infrared spectrum (thin film/NaCl) of isoquinoline **182f** (Table 2.5, entry 5).

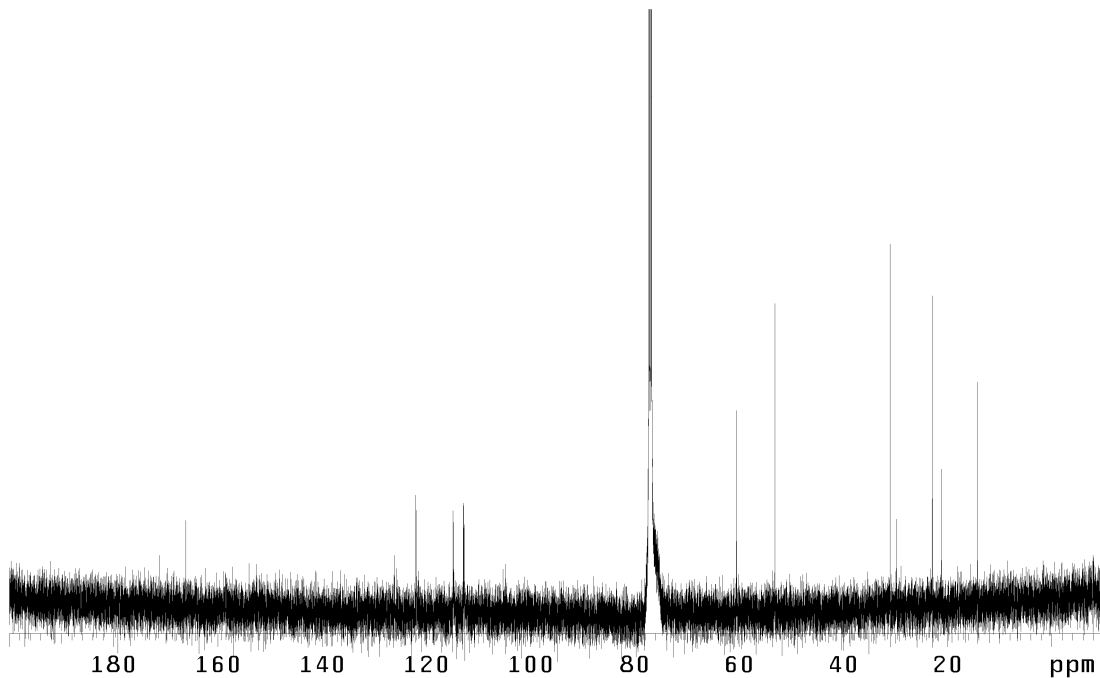


Figure A1.18.3  $^{13}\text{C}$  NMR (125 MHz,  $\text{CDCl}_3$ ) of isoquinoline **182f** (Table 2.5, entry 5).

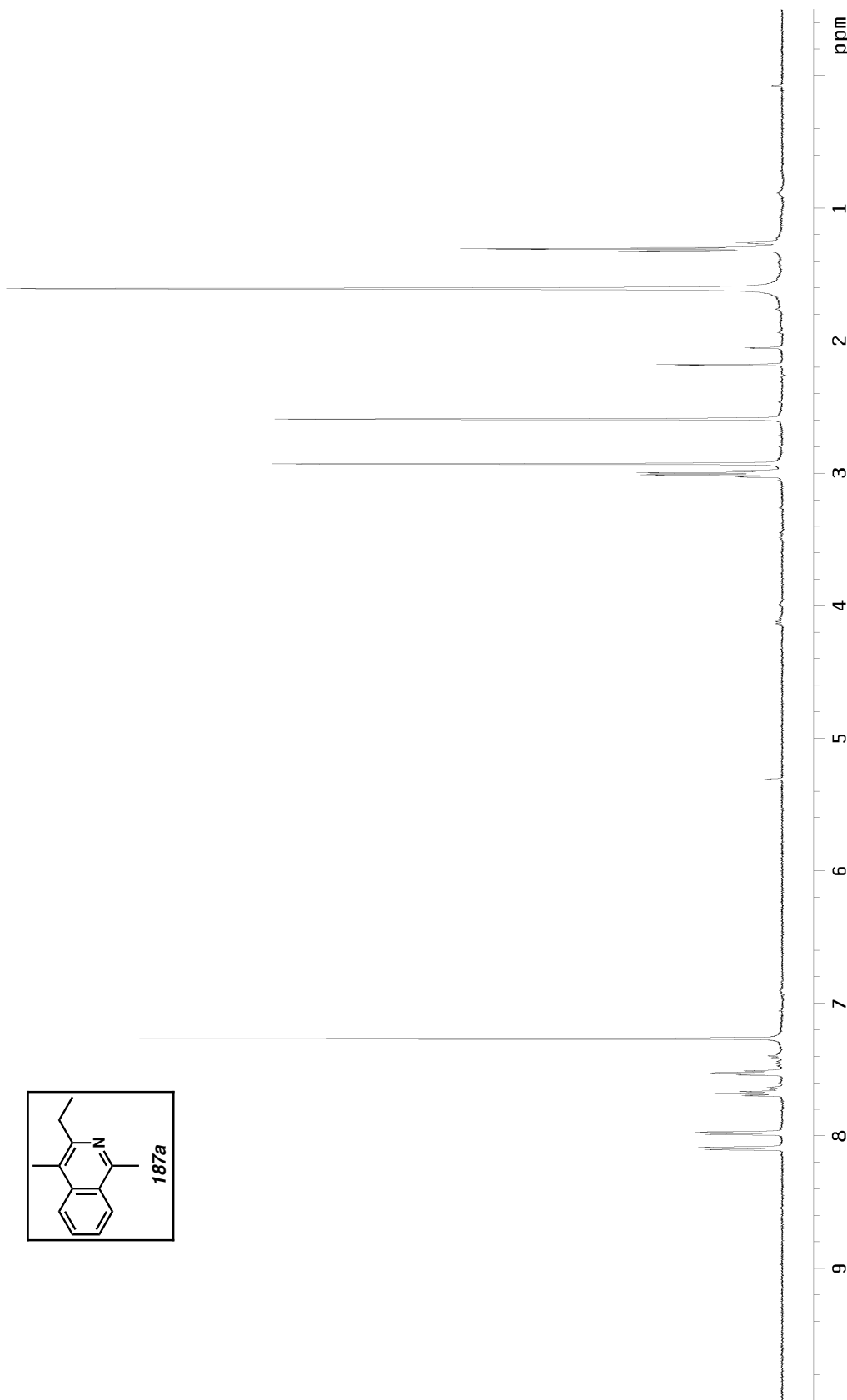


Figure A1.J9.1  $^1\text{H}$  NMR (500 MHz,  $\text{CDCl}_3$ ) of isoquinoline **187a** (Table 2.6, entry 1).

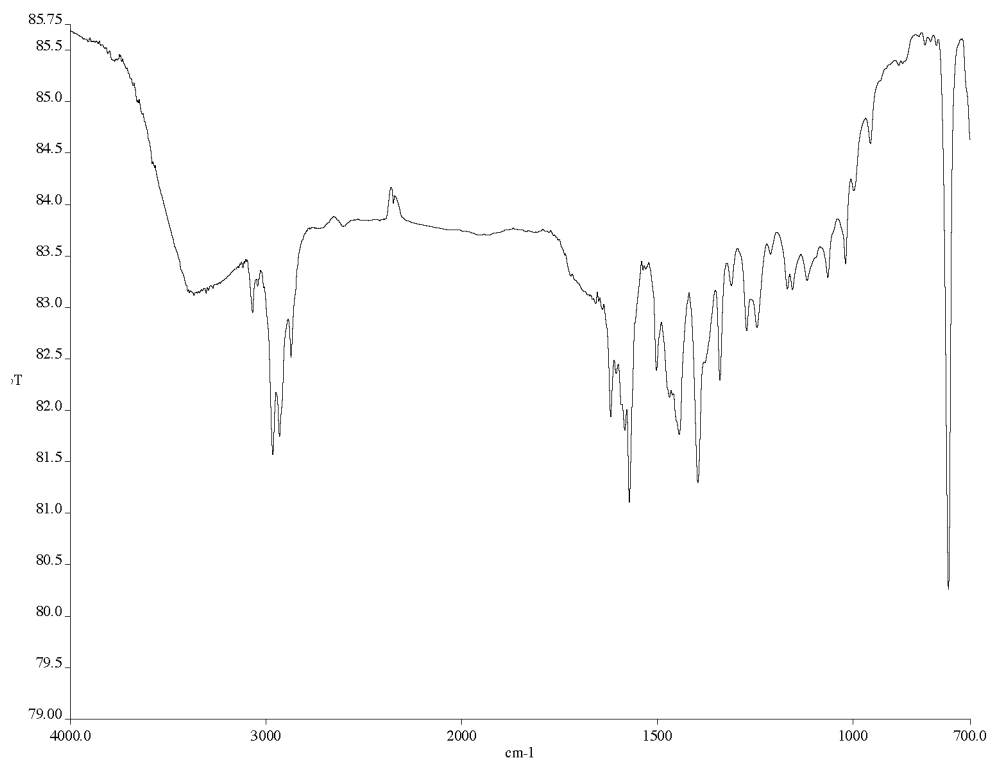


Figure A1.19.2 Infrared spectrum (thin film/NaCl) of isoquinoline **187a** (Table 2.6, entry 1).

Figure A1.19.3  $^{13}\text{C}$  NMR (125 MHz,  $\text{CDCl}_3$ ) of isoquinoline **187a** (Table 2.6, entry 1).

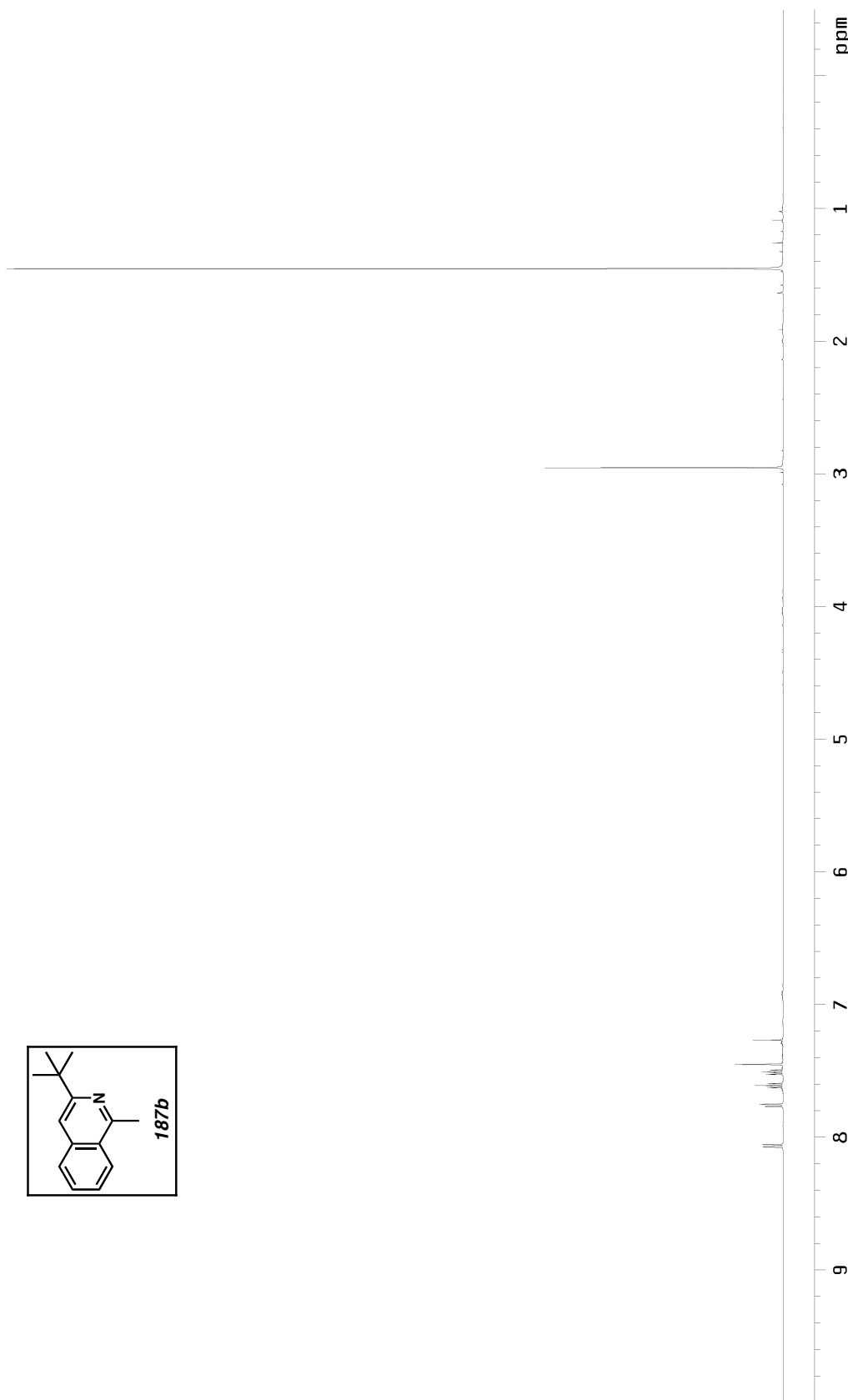


Figure A1.20.1  $^1\text{H}$  NMR (500 MHz,  $\text{CDCl}_3$ ) of isoquinoline **187b** (Table 2.6, entry 2).

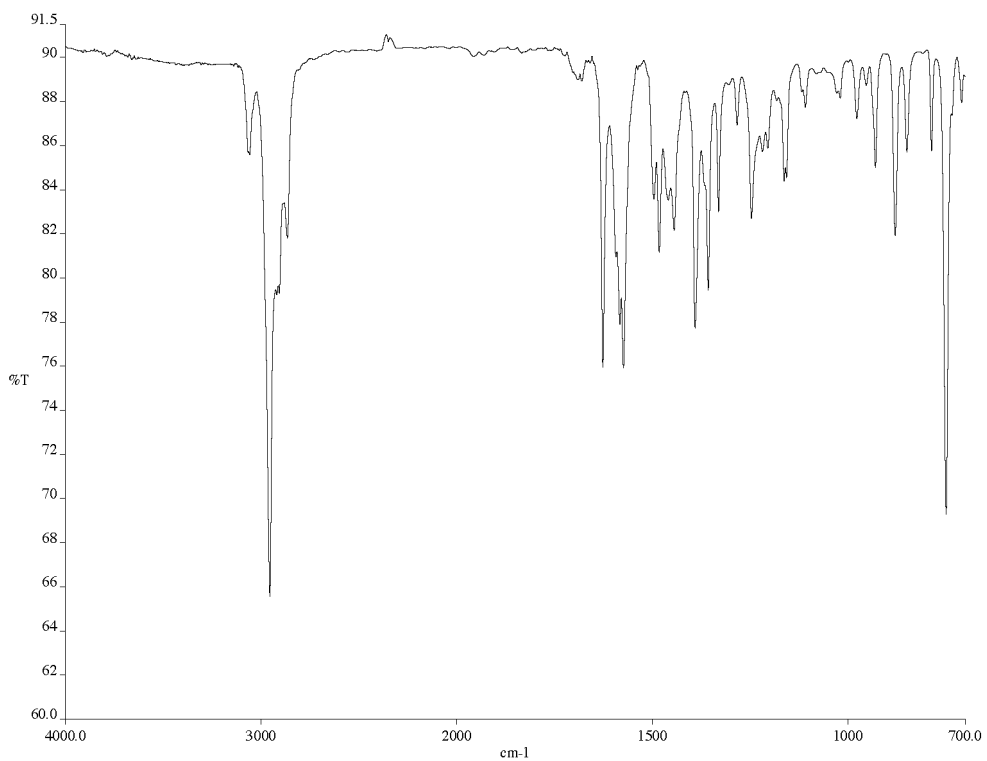


Figure A1.20.2 Infrared spectrum (thin film/NaCl) of isoquinoline **187b** (Table 2.6, entry 2).

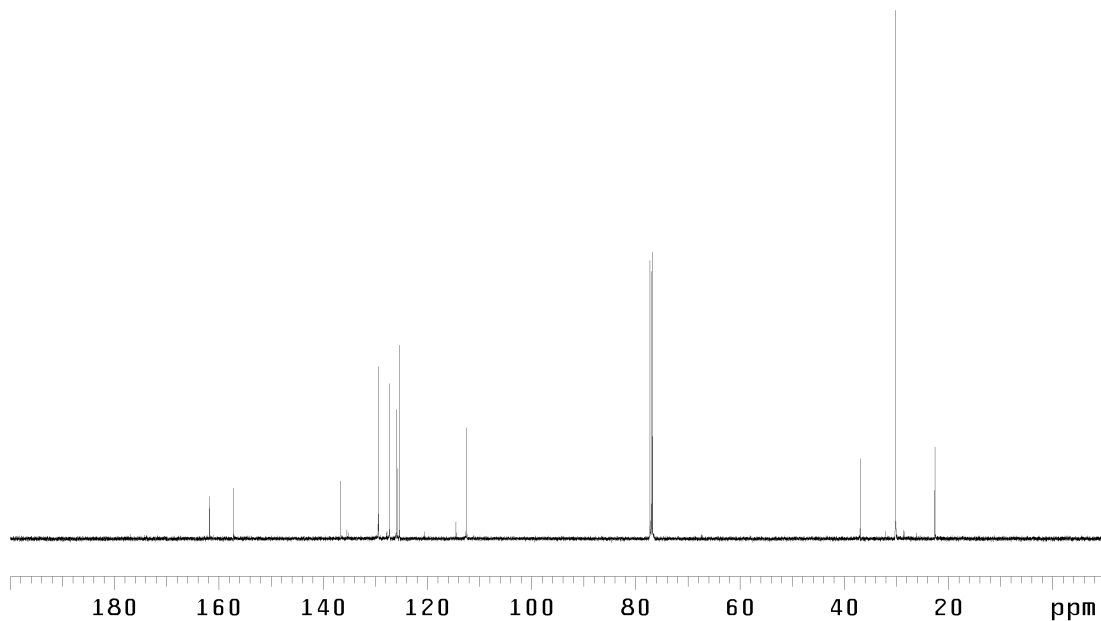


Figure A1.20.3  $^{13}\text{C}$  NMR (125 MHz,  $\text{CDCl}_3$ ) of isoquinoline **187b** (Table 2.6, entry 2).

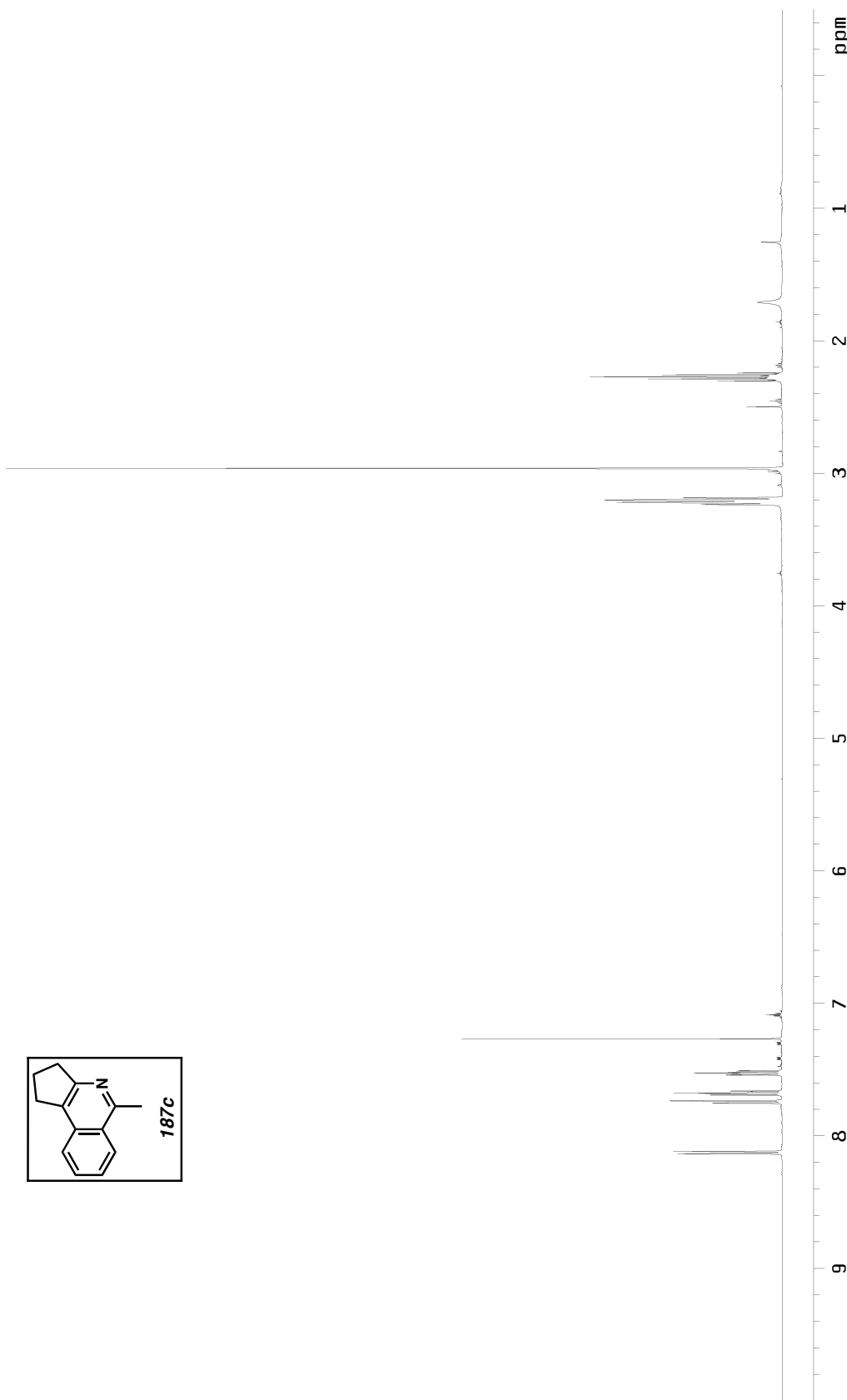


Figure A1.21.1  $^1\text{H}$  NMR (500 MHz,  $\text{CDCl}_3$ ) of isoquinoline **187c** (Table 2.6, entry 3).

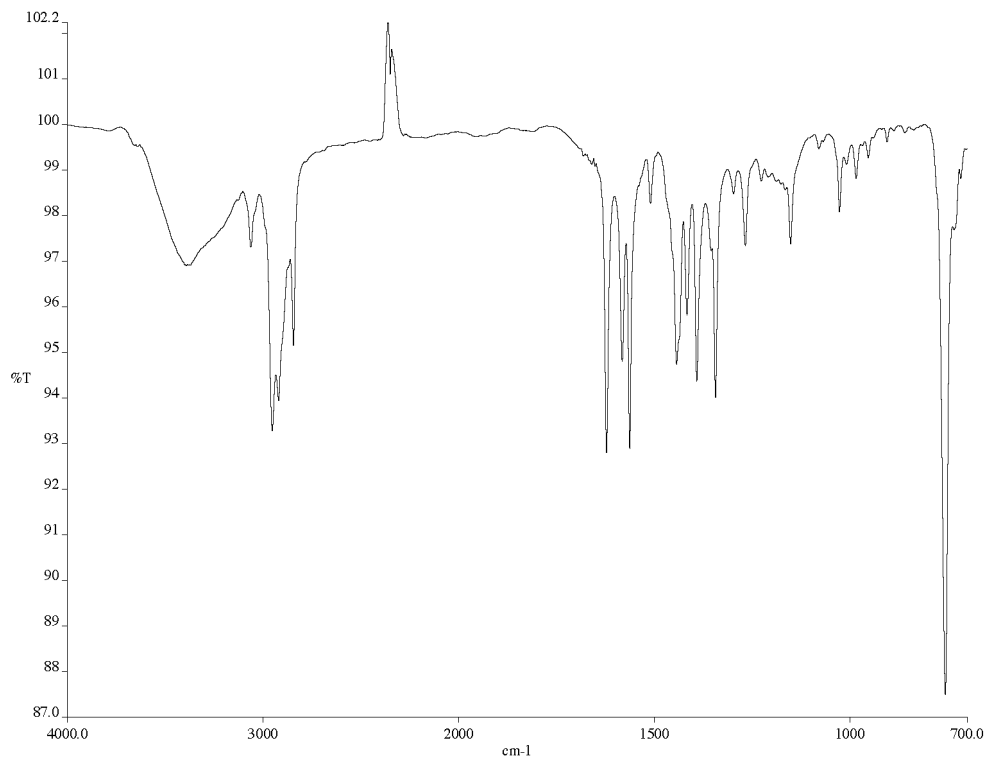


Figure A1.21.2 Infrared spectrum (thin film/NaCl) of isoquinoline **187c** (Table 2.6, entry 3).

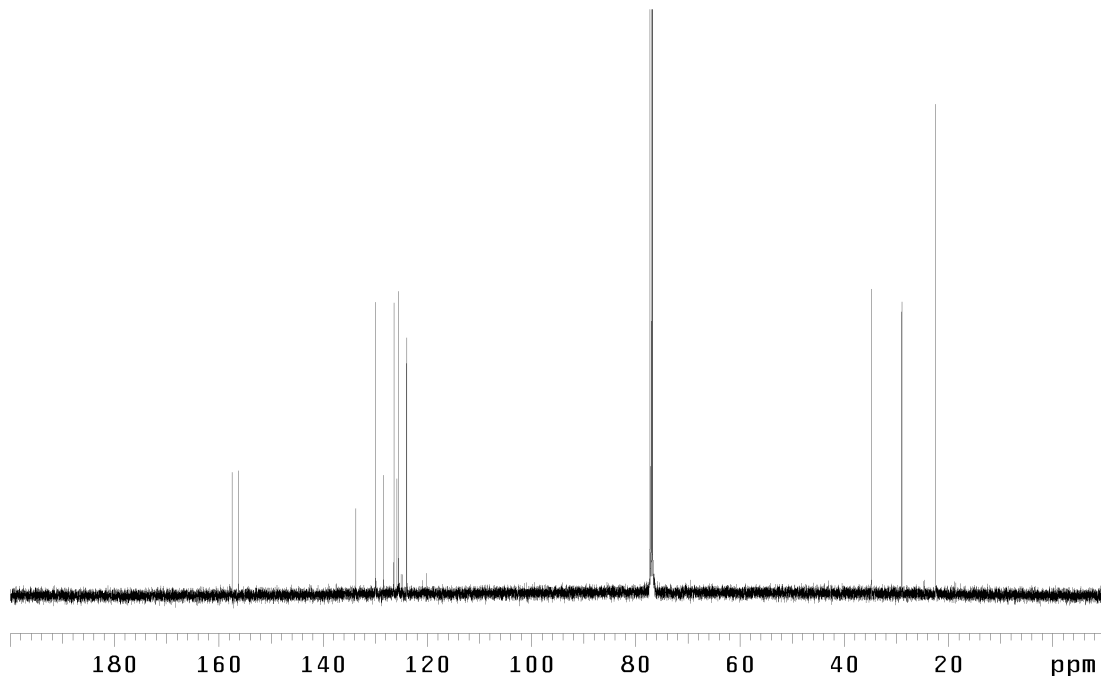


Figure A1.21.3  $^{13}\text{C}$  NMR (125 MHz,  $\text{CDCl}_3$ ) of isoquinoline **187c** (Table 2.6, entry 3).

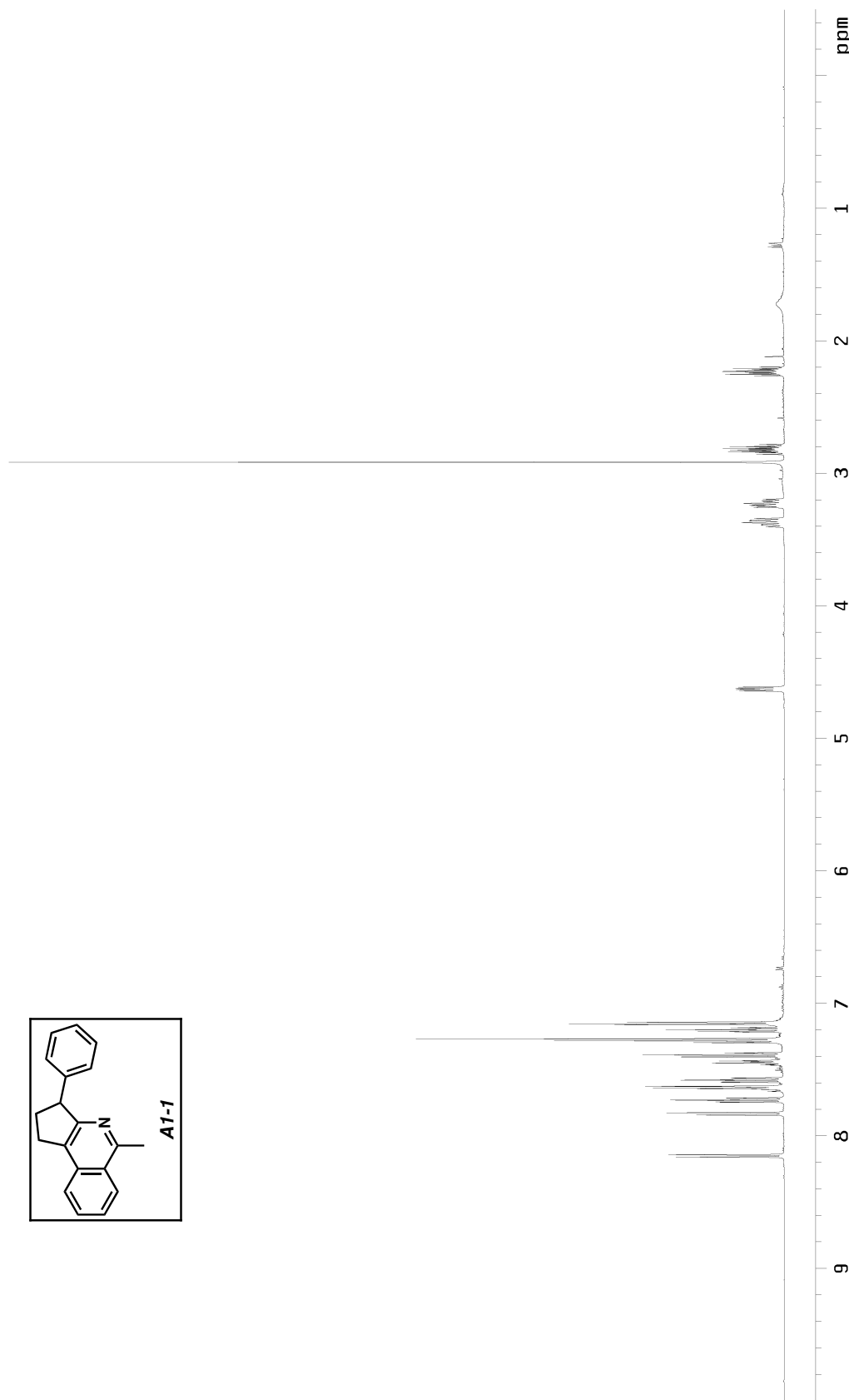


Figure A1.22.I  $^1\text{H}$  NMR (500 MHz,  $\text{CDCl}_3$ ) of isoquinoline A1-1.

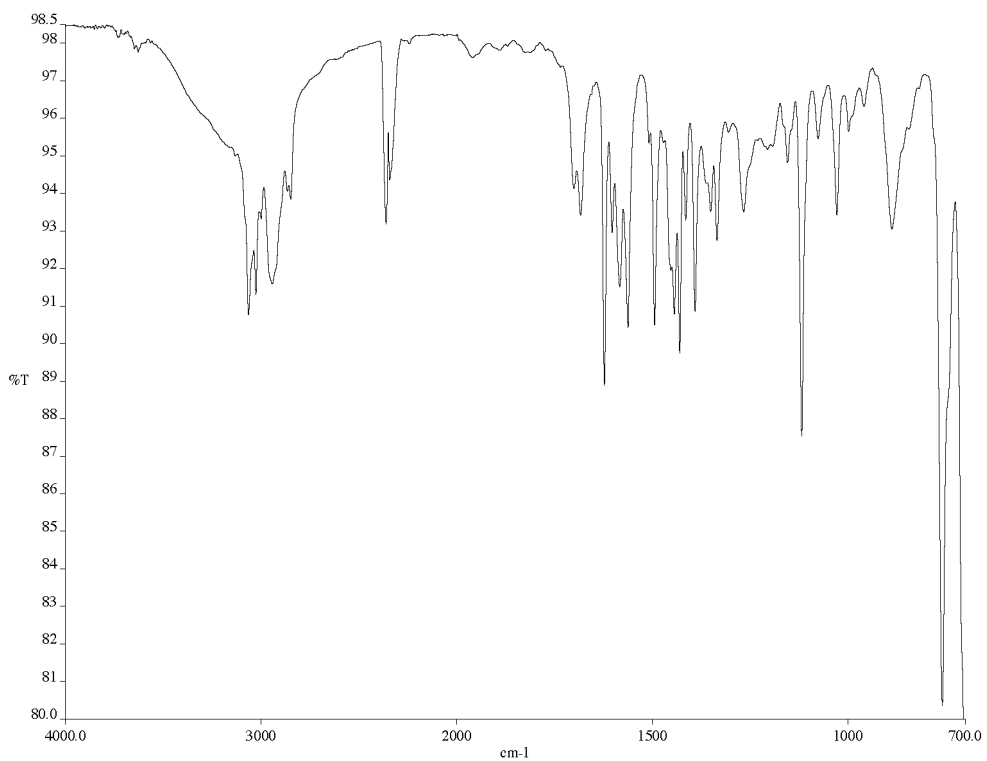


Figure A1.22.2 Infrared spectrum (thin film/NaCl) of isoquinoline **A1-1**.

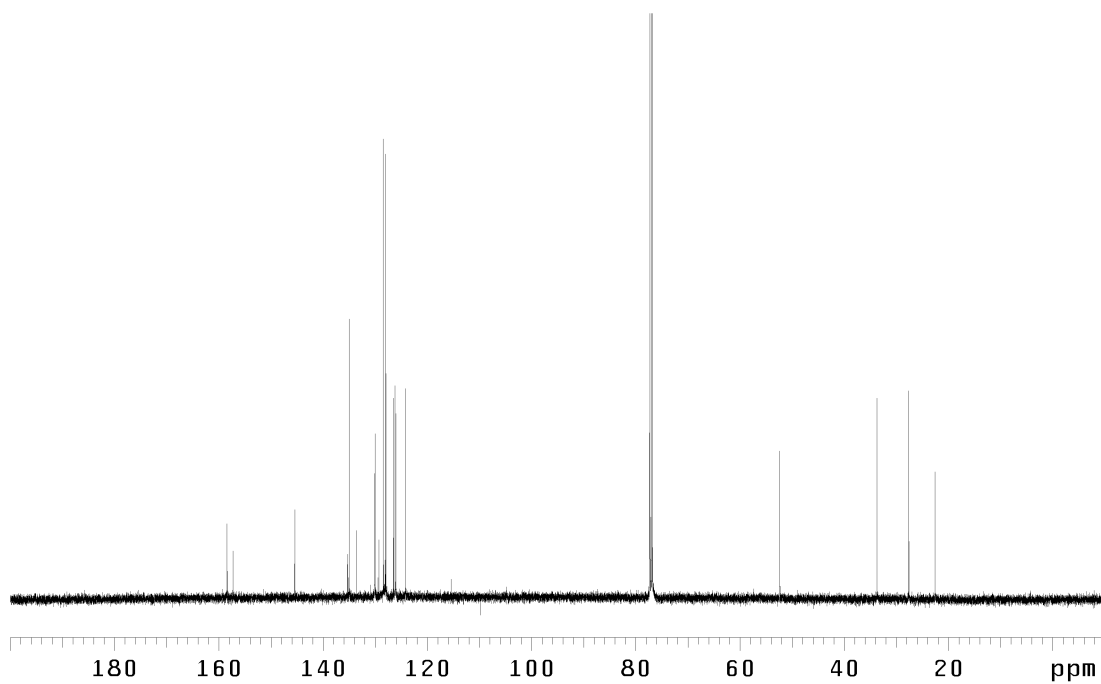


Figure A1.22.3  $^{13}\text{C}$  NMR (125 MHz,  $\text{CDCl}_3$ ) of isoquinoline **A1-1**.

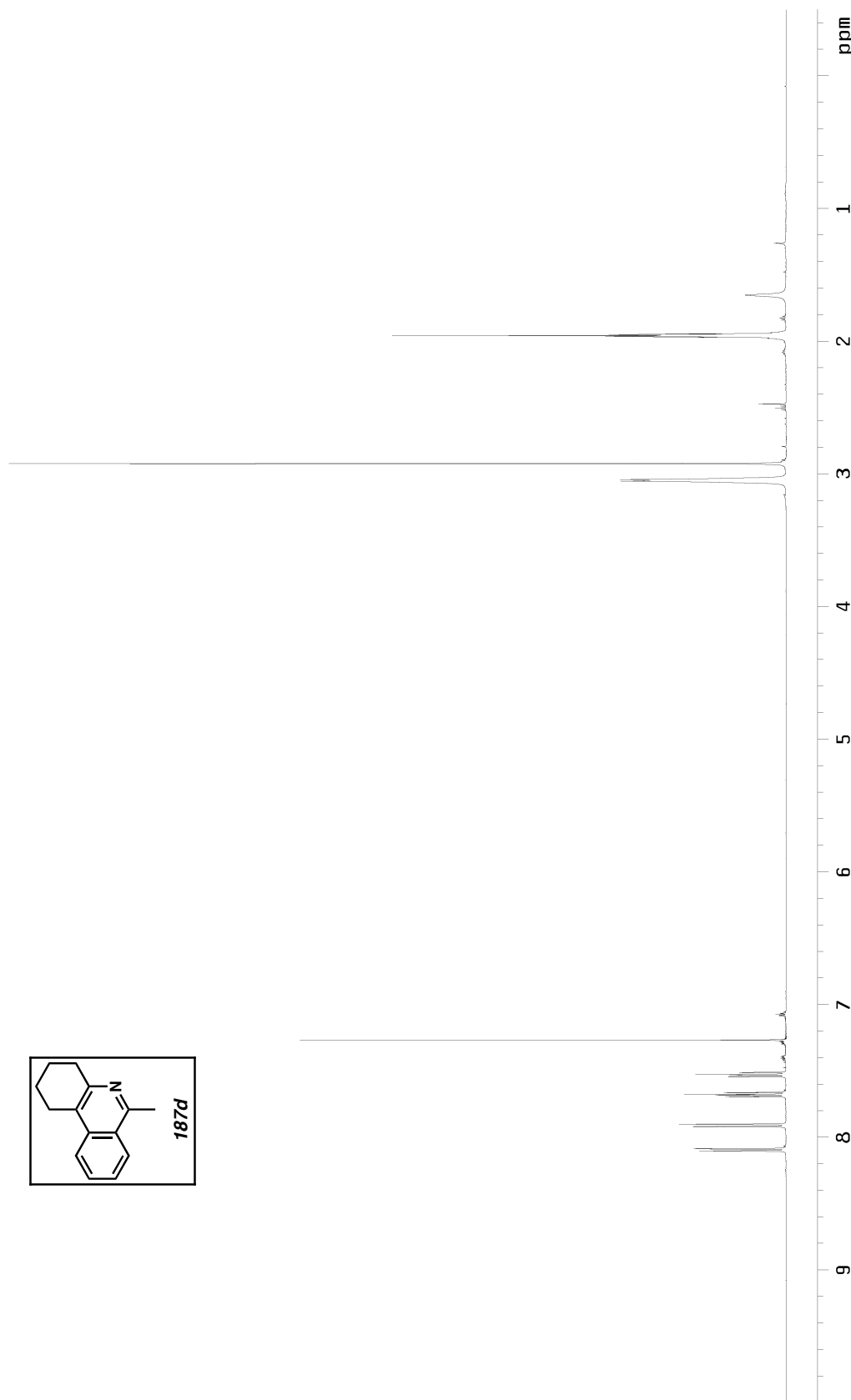


Figure A1.23.I  $^1\text{H}$  NMR (500 MHz,  $\text{CDCl}_3$ ) of isoquinoline **187d** (Table 2.6, entry 4).

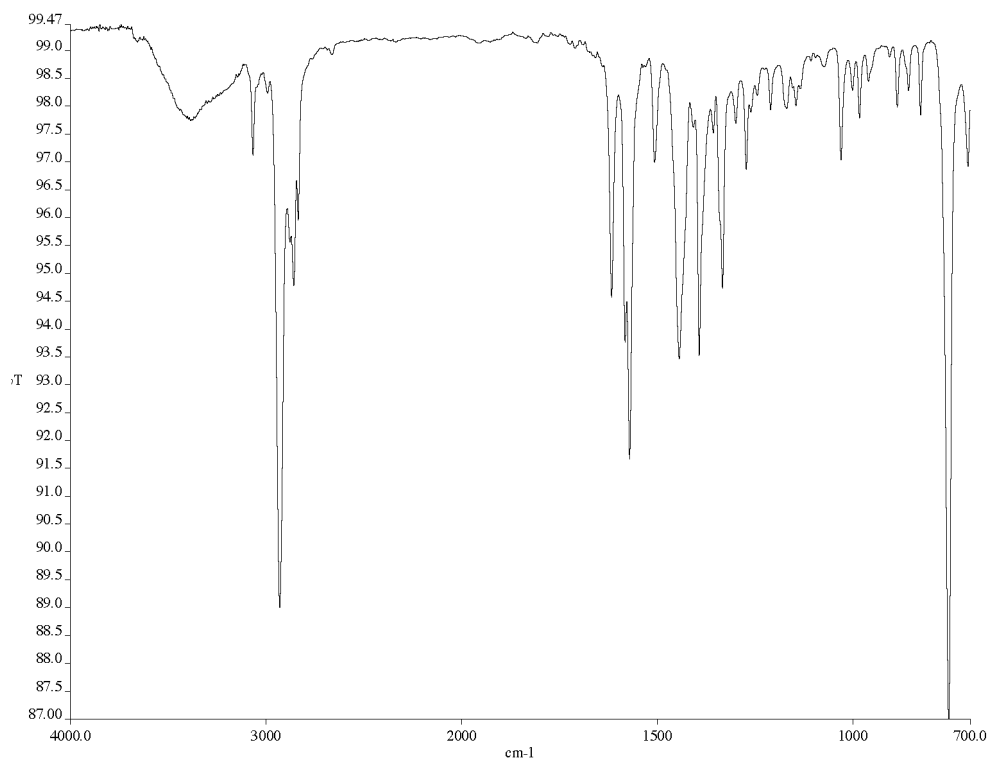


Figure A1.23.2 Infrared spectrum (thin film/NaCl) of isoquinoline **187d** (Table 2.6, entry 4).

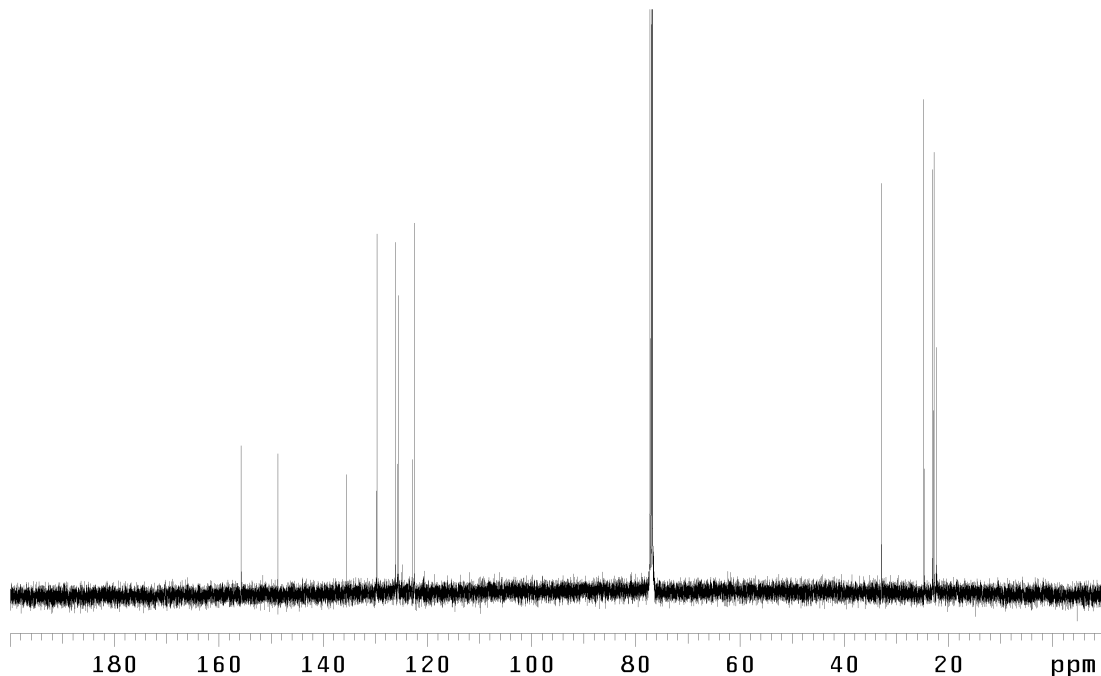


Figure A1.23.3  $^{13}\text{C}$  NMR (125 MHz,  $\text{CDCl}_3$ ) of isoquinoline **187d** (Table 2.6, entry 4).

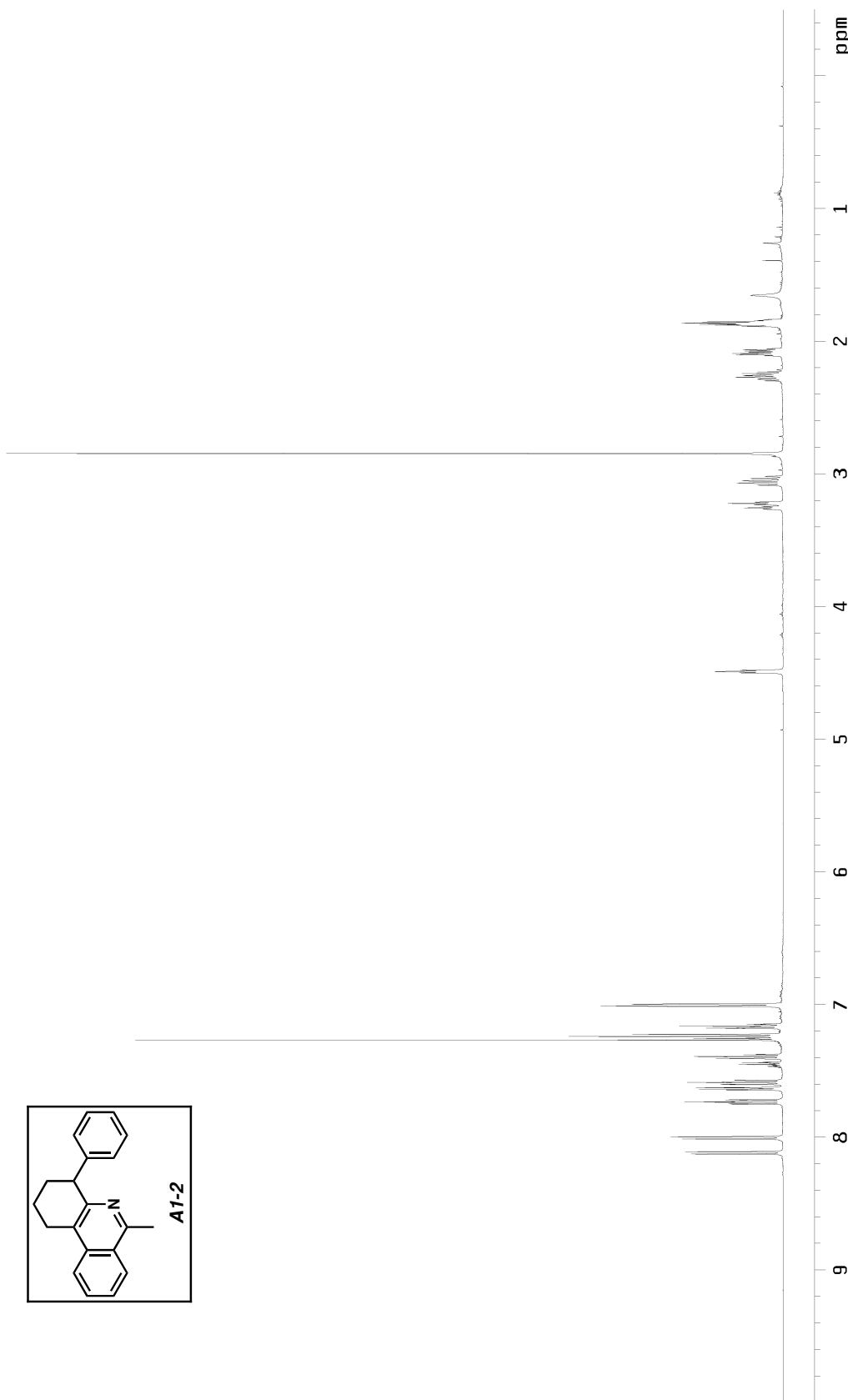


Figure A1.24.1  $^1\text{H}$  NMR (500 MHz,  $\text{CDCl}_3$ ) of isoquinoline A1-2.

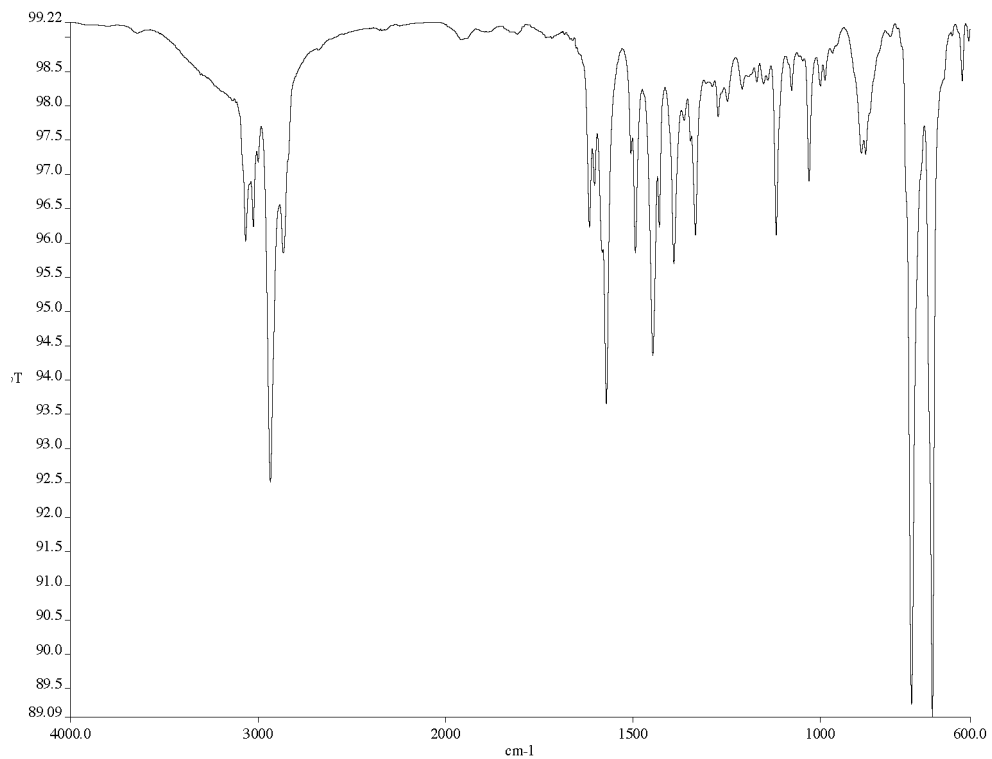


Figure A1.24.2 Infrared spectrum (thin film/NaCl) of isoquinoline **A1-2**.

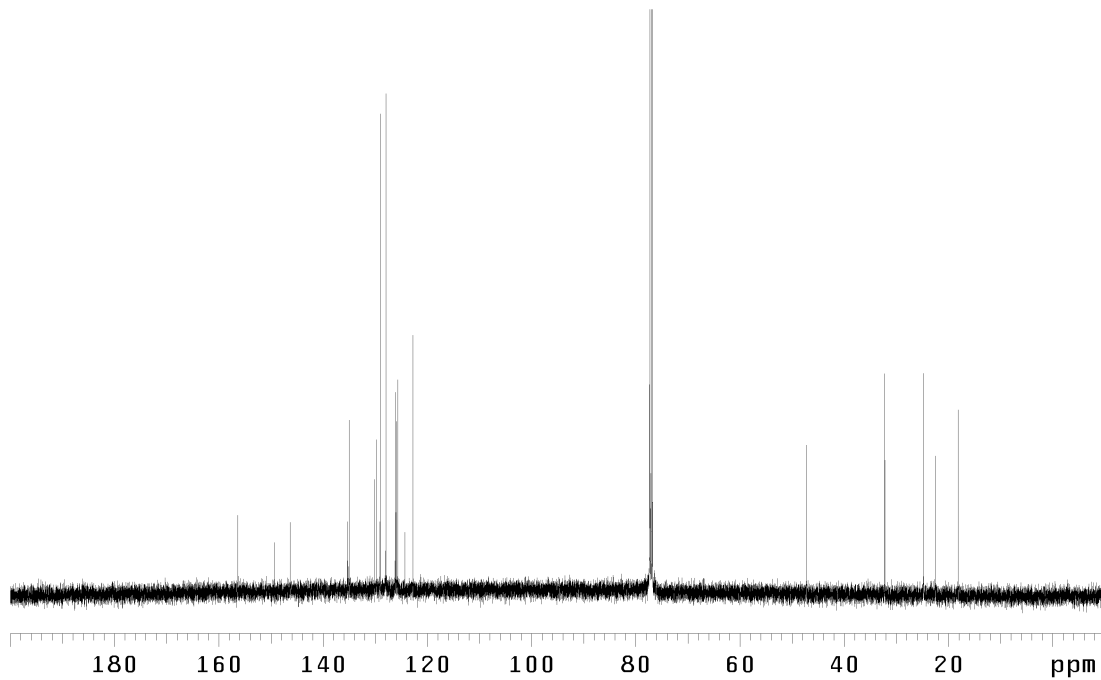


Figure A1.24.3  $^{13}\text{C}$  NMR (125 MHz,  $\text{CDCl}_3$ ) of isoquinoline **A1-2**.

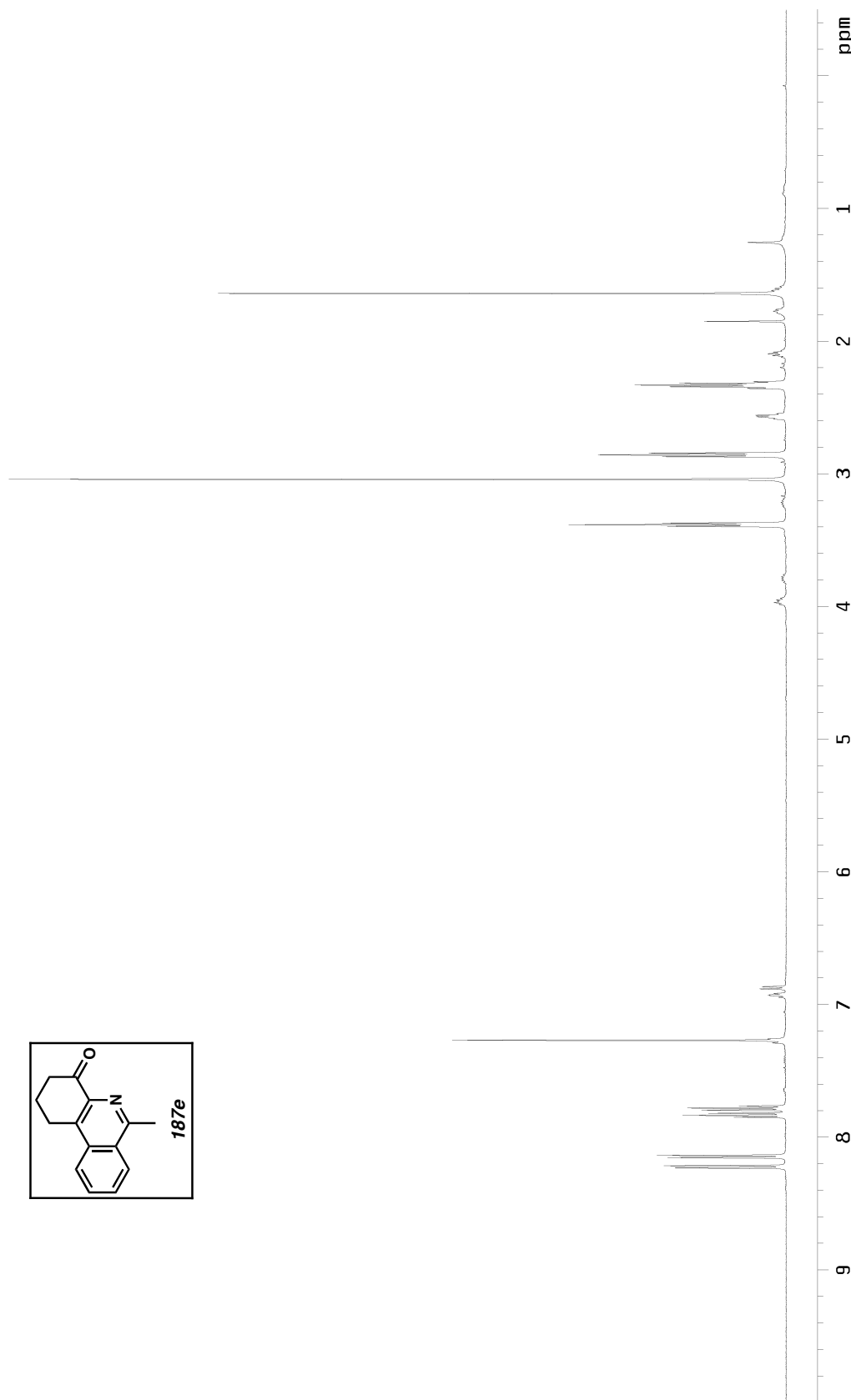


Figure A1.25.1  $^1\text{H}$  NMR (500 MHz,  $\text{CDCl}_3$ ) of isoquinoline **187e** (Table 2.6, entry 5).

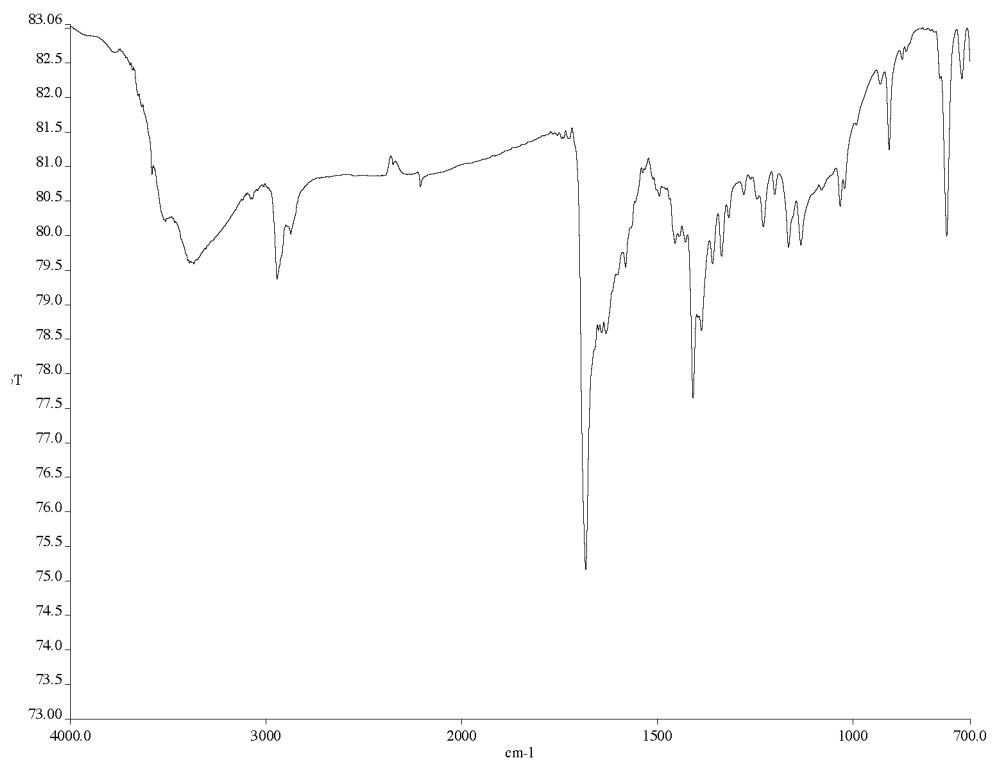


Figure A1.25.2 Infrared spectrum (thin film/NaCl) of isoquinoline **187e** (Table 2.6, entry 5).

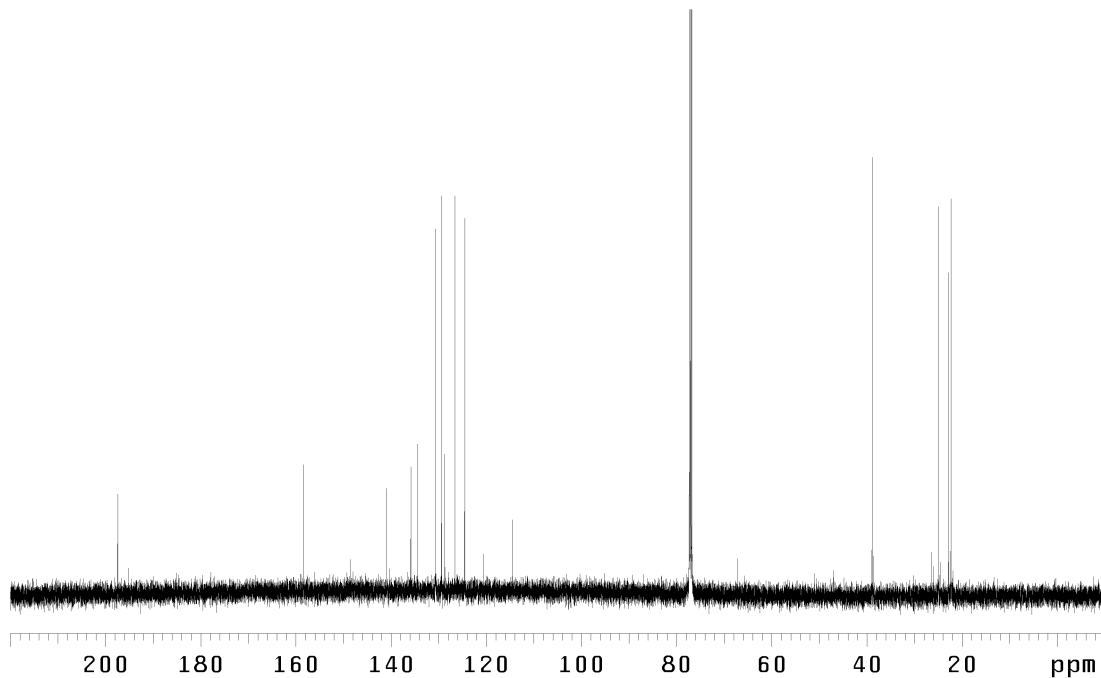


Figure A1.25.3  $^{13}\text{C}$  NMR (125 MHz,  $\text{CDCl}_3$ ) of isoquinoline **187e** (Table 2.6, entry 5).

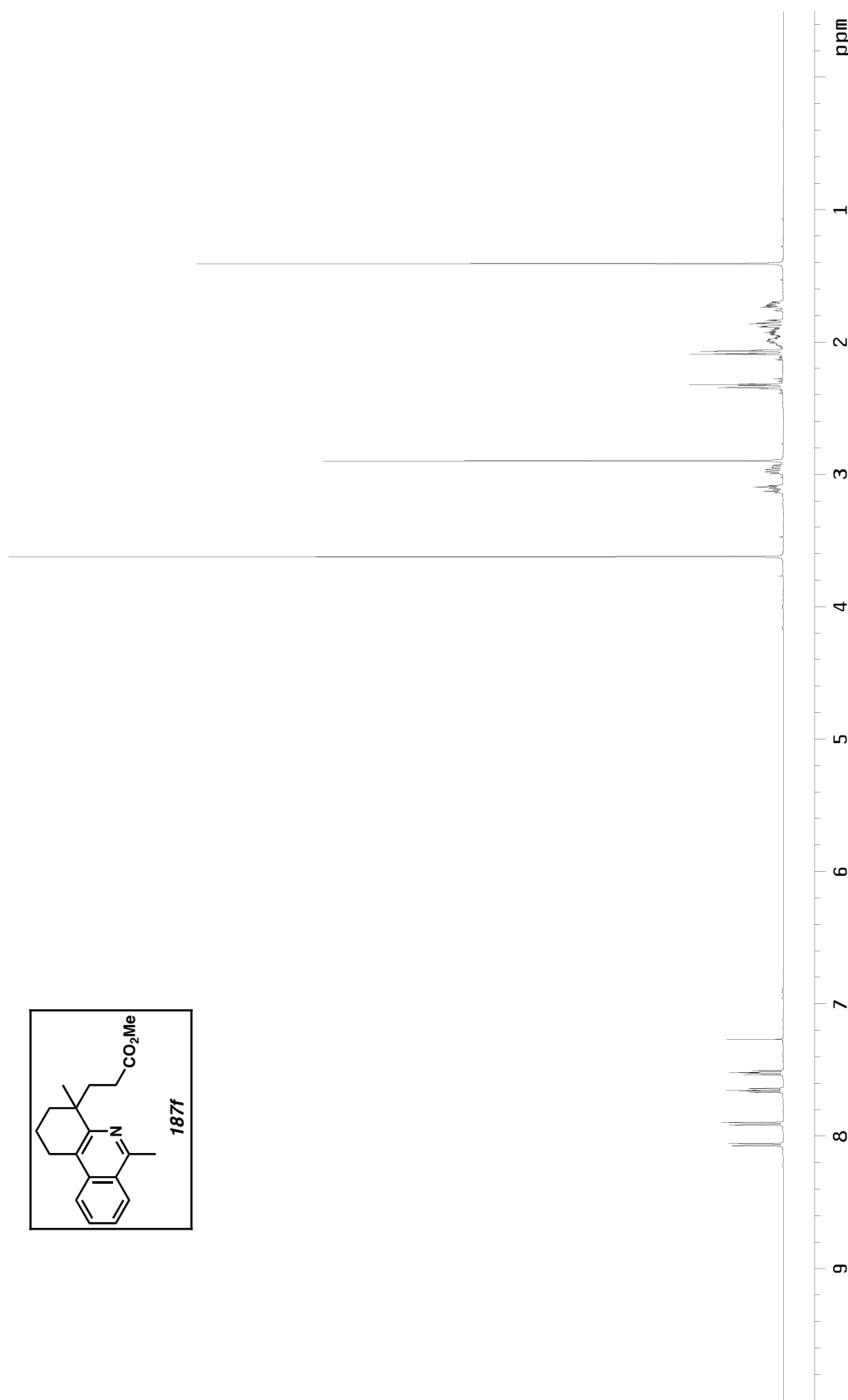


Figure A1.26.1  $^1\text{H}$  NMR (500 MHz,  $\text{CDCl}_3$ ) of isoquinoline **187f** (Table 2.6, entry 6).

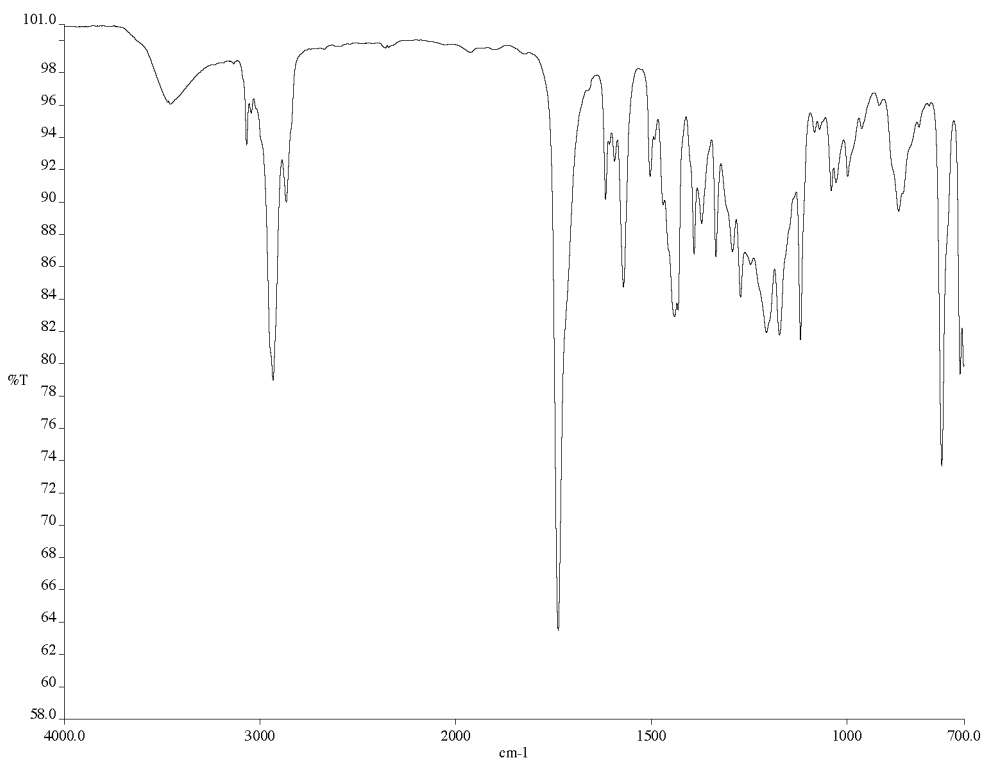


Figure A1.26.2 Infrared spectrum (thin film/NaCl) of isoquinoline **187f** (Table 2.6, entry 6).

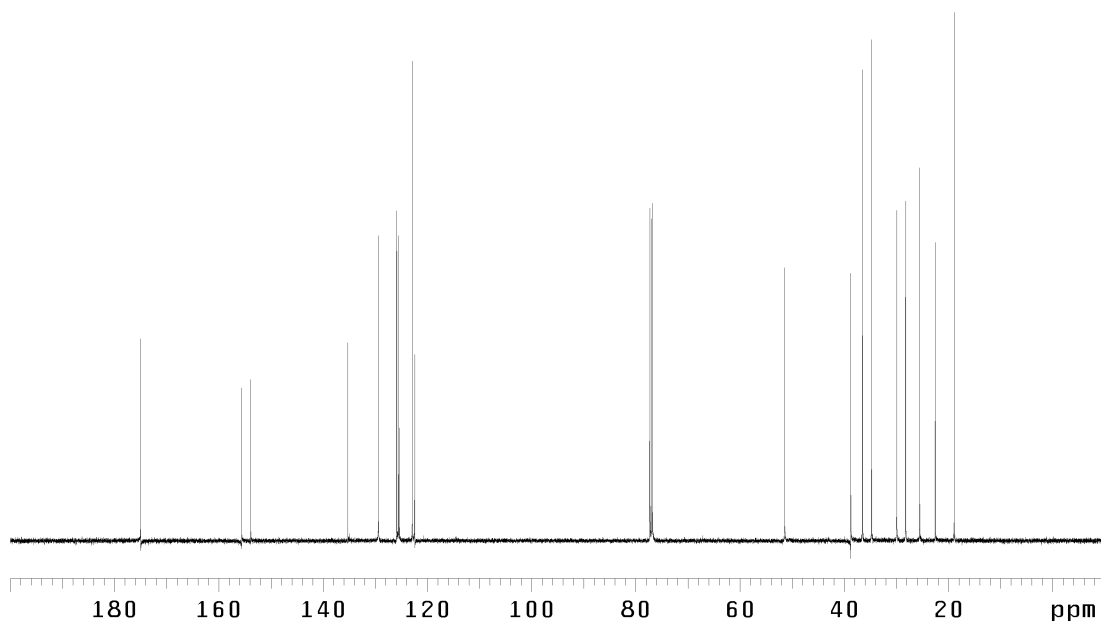


Figure A1.26.3  $^{13}\text{C}$  NMR (125 MHz,  $\text{CDCl}_3$ ) of isoquinoline **187f** (Table 2.6, entry 6).

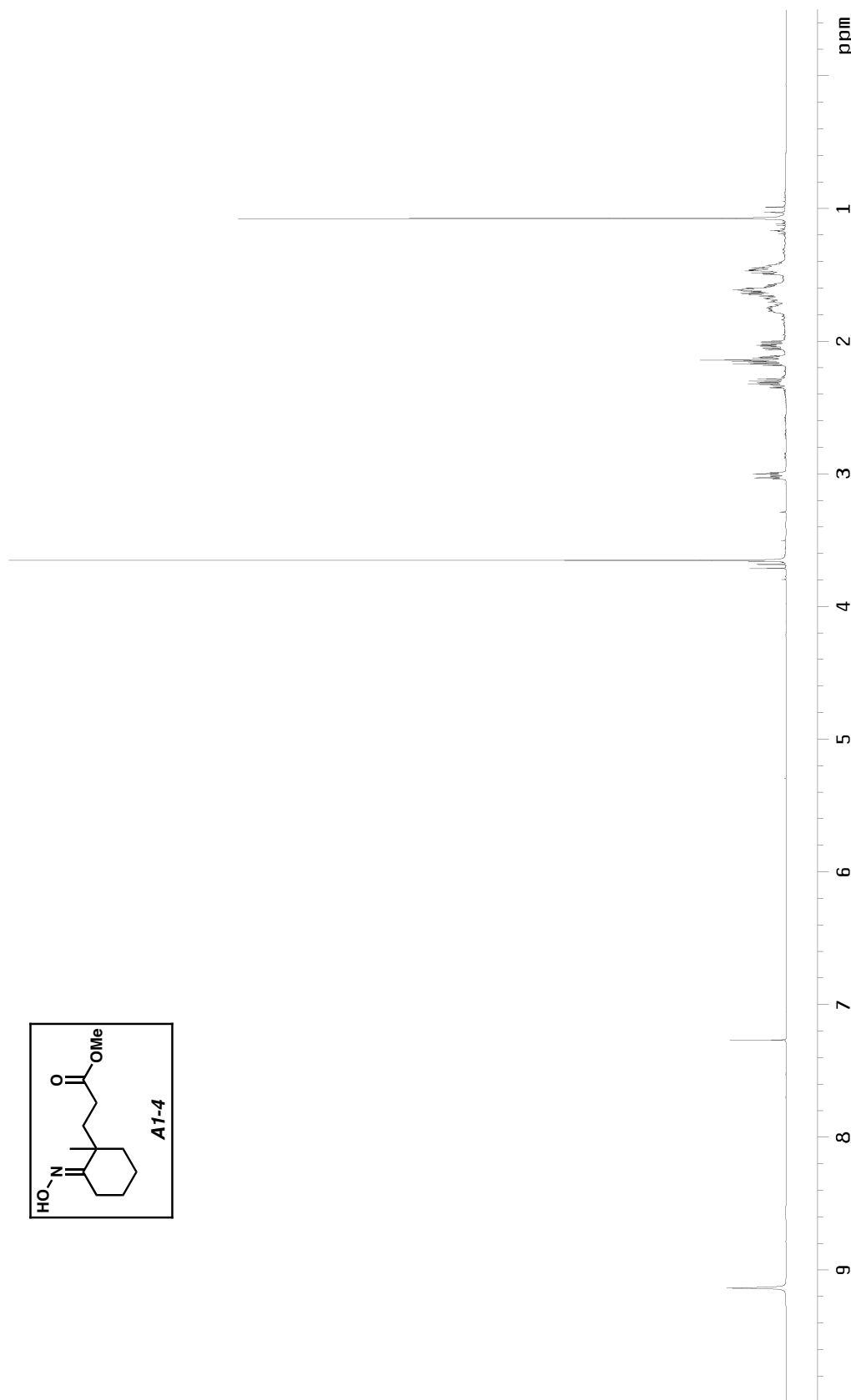


Figure A1.27.1  $^1\text{H}$  NMR (500 MHz, CDCl<sub>3</sub>) of oxime A1-4.

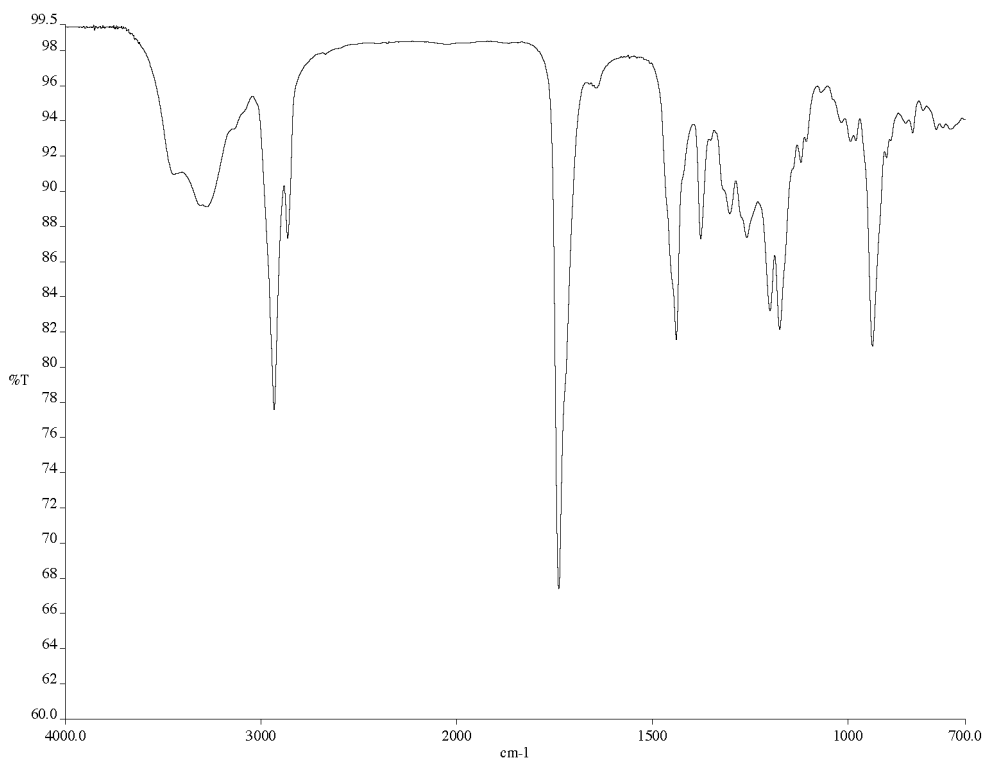


Figure A1.27.2 Infrared spectrum (thin film/NaCl) of oxime A1-4.

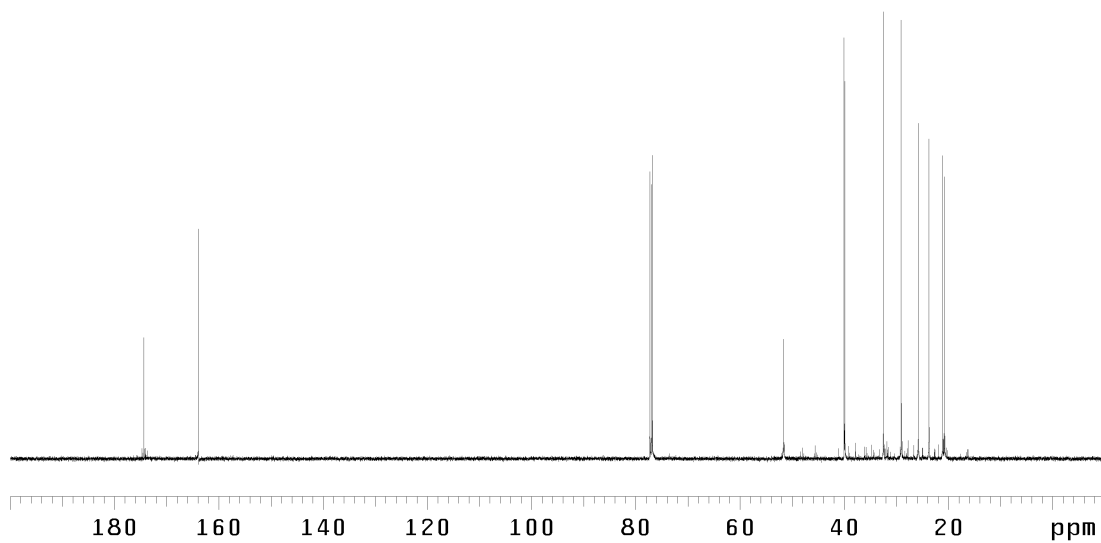


Figure A1.27.3  $^{13}\text{C}$  NMR (125 MHz,  $\text{CDCl}_3$ ) of oxime A1-4.

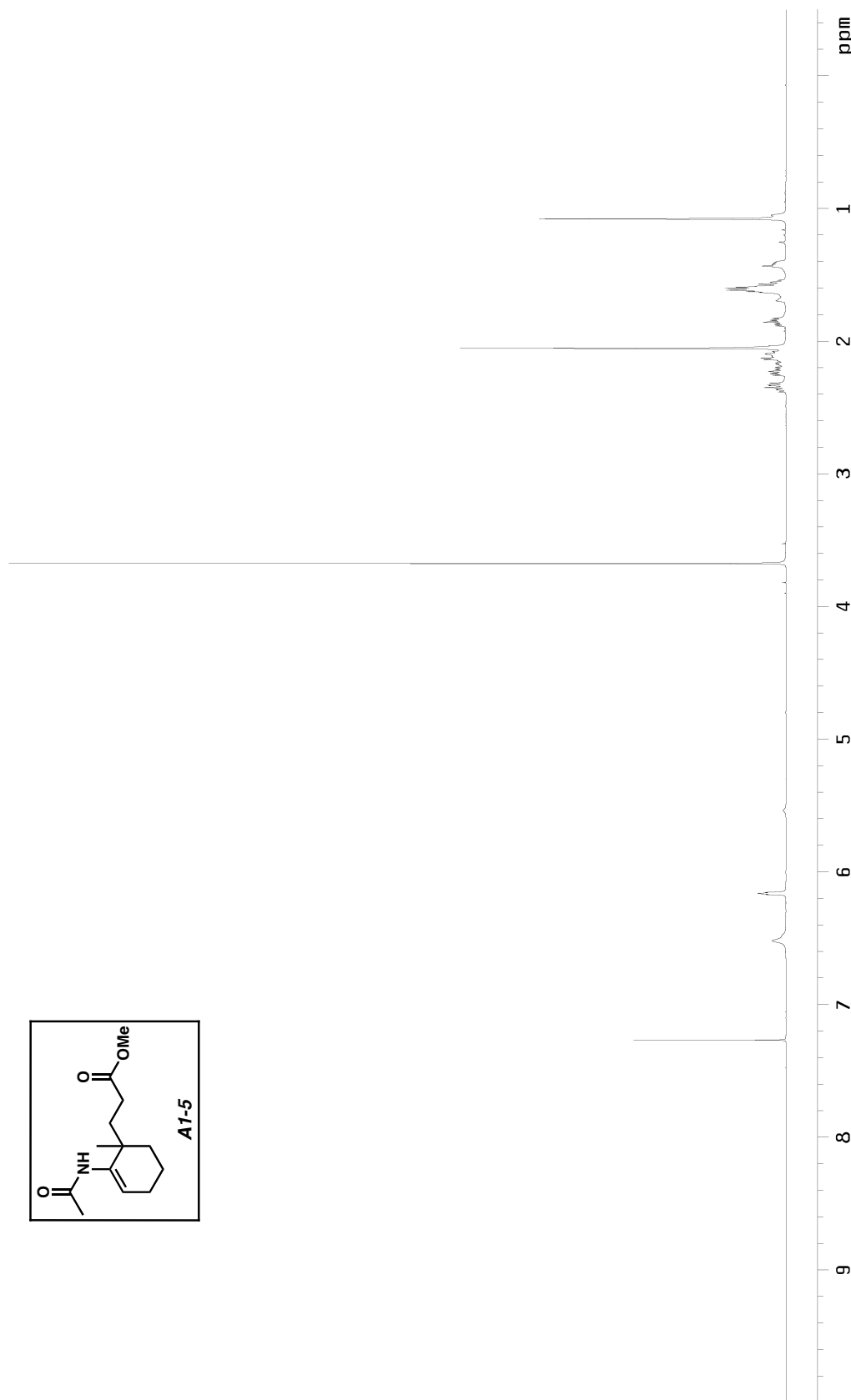


Figure A1.28.1  $^1\text{H}$  NMR (500 MHz,  $\text{CDCl}_3$ ) of *N*-acetyl enamine **A1-5**.

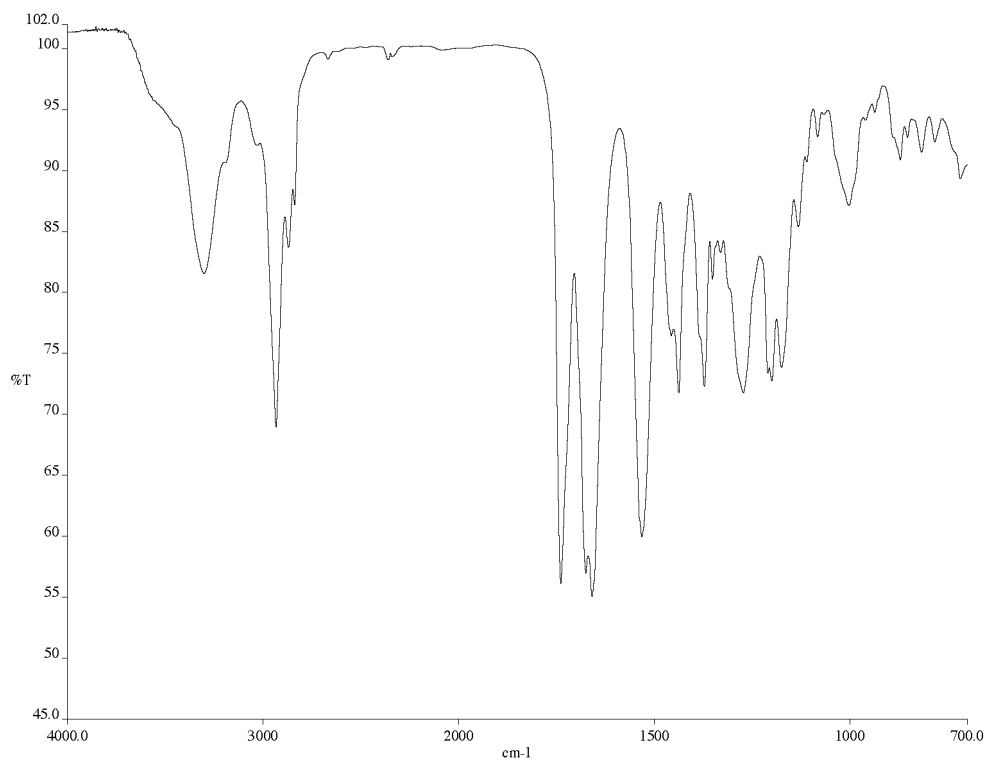


Figure A1.28.2 Infrared spectrum (thin film/NaCl) of *N*-acetyl enamine **A1-5**.

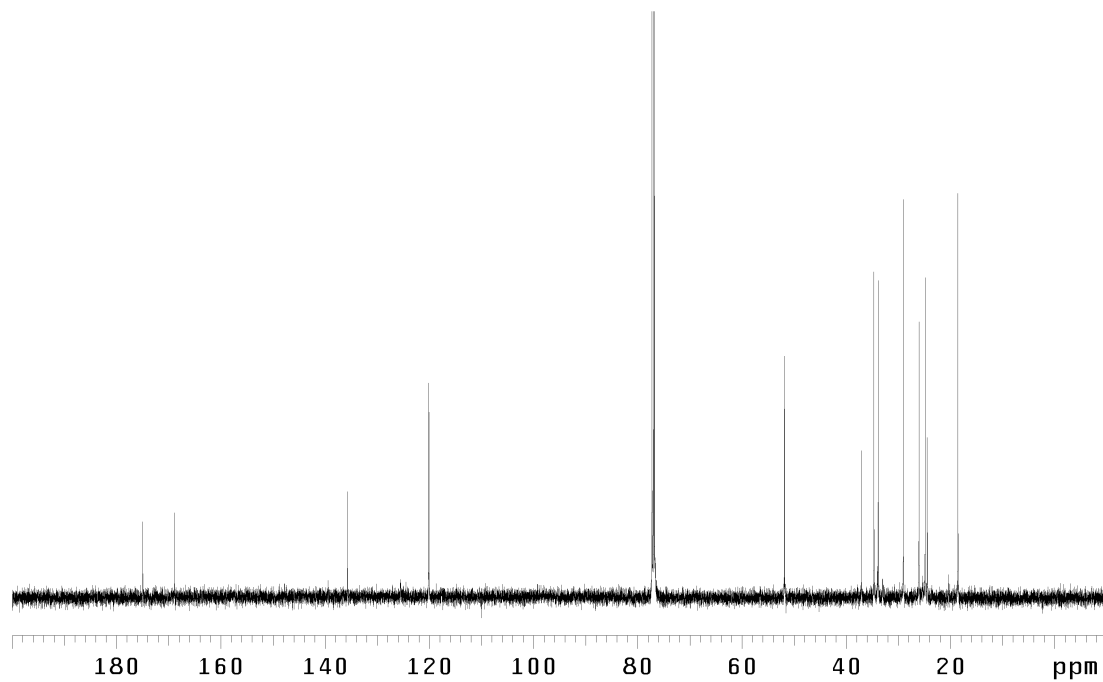


Figure A1.28.3  $^{13}\text{C}$  NMR (125 MHz,  $\text{CDCl}_3$ ) of *N*-acetyl enamine **A1-5**.

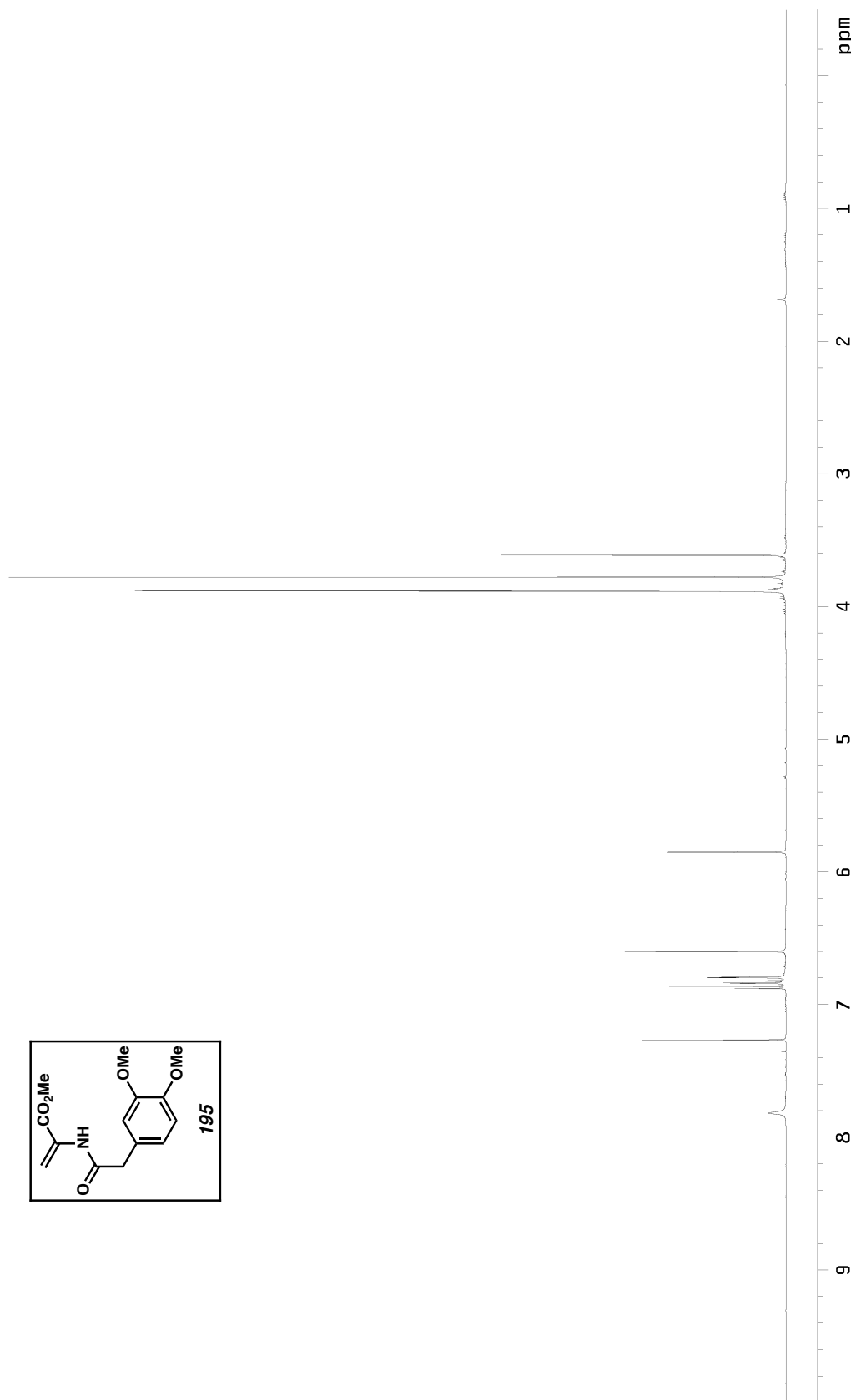


Figure A1.29.1  $^1\text{H}$  NMR (500 MHz,  $\text{CDCl}_3$ ) of *N*-acyl enamine 195.

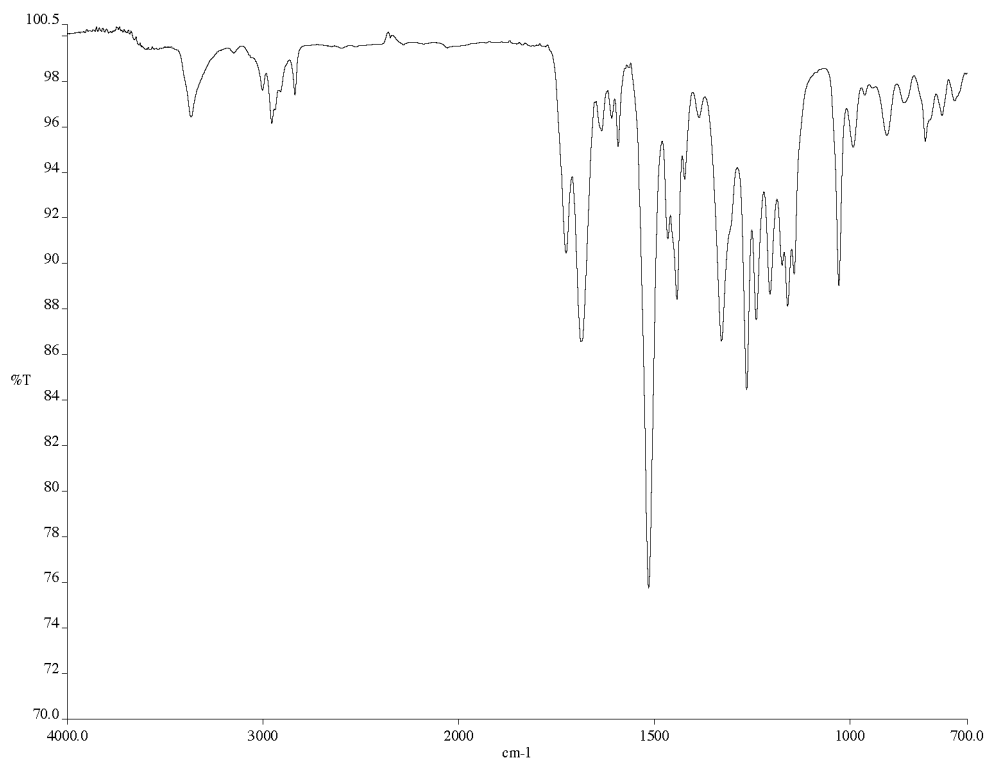


Figure A1.29.2 Infrared spectrum (thin film/NaCl) of *N*-acyl enamine **195**.

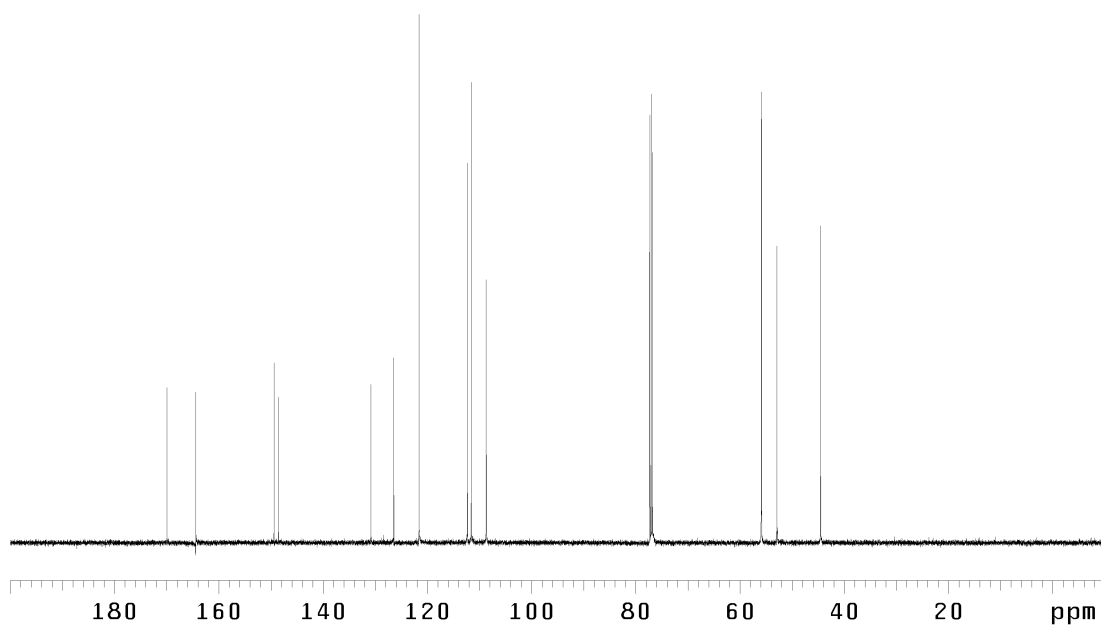


Figure A1.29.3  $^{13}\text{C}$  NMR (125 MHz,  $\text{CDCl}_3$ ) of *N*-acyl enamine **195**.

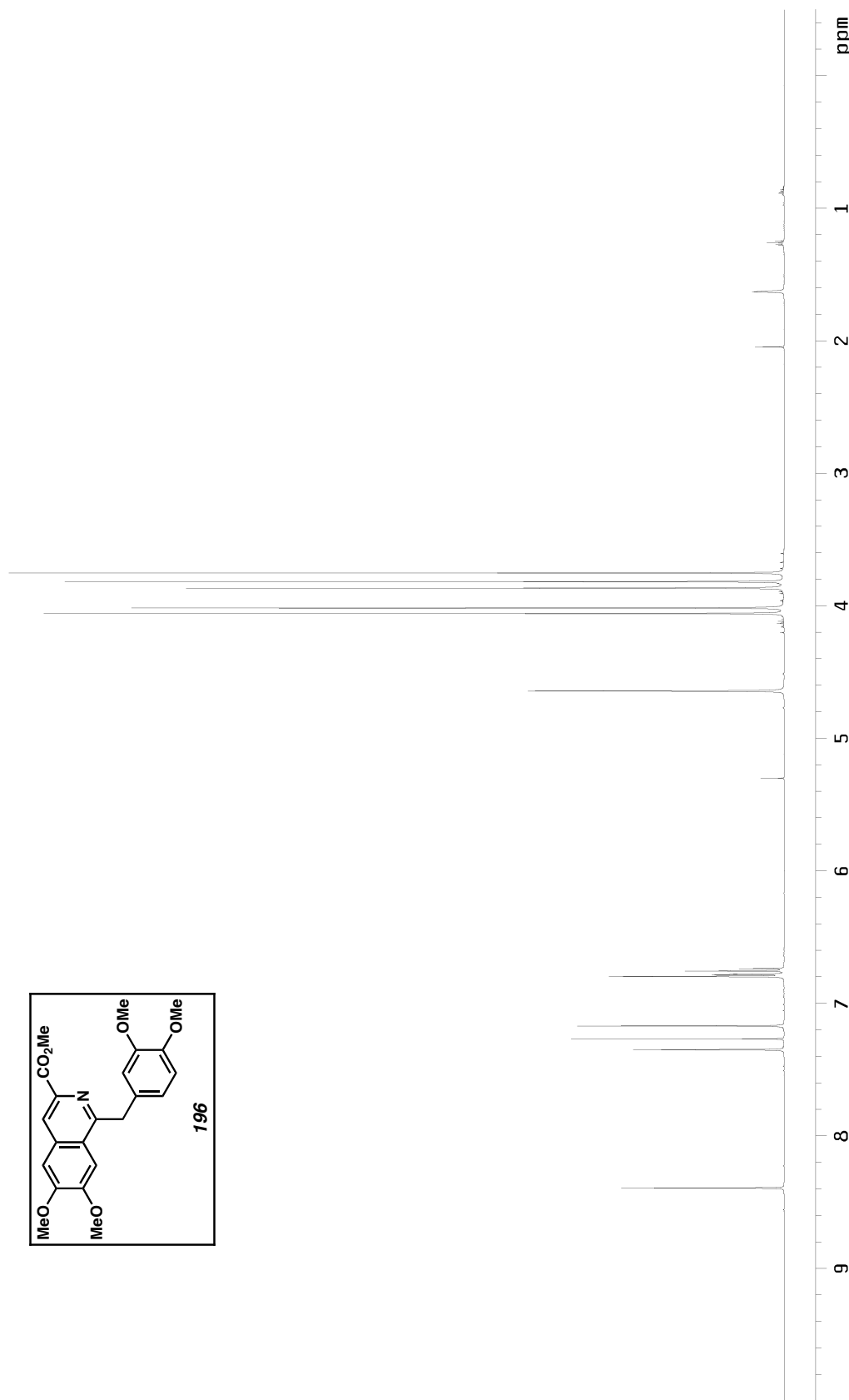


Figure AI.30.1  $^1\text{H}$  NMR (500 MHz,  $\text{CDCl}_3$ ) of methyl papaverine-3-carboxylate (196).

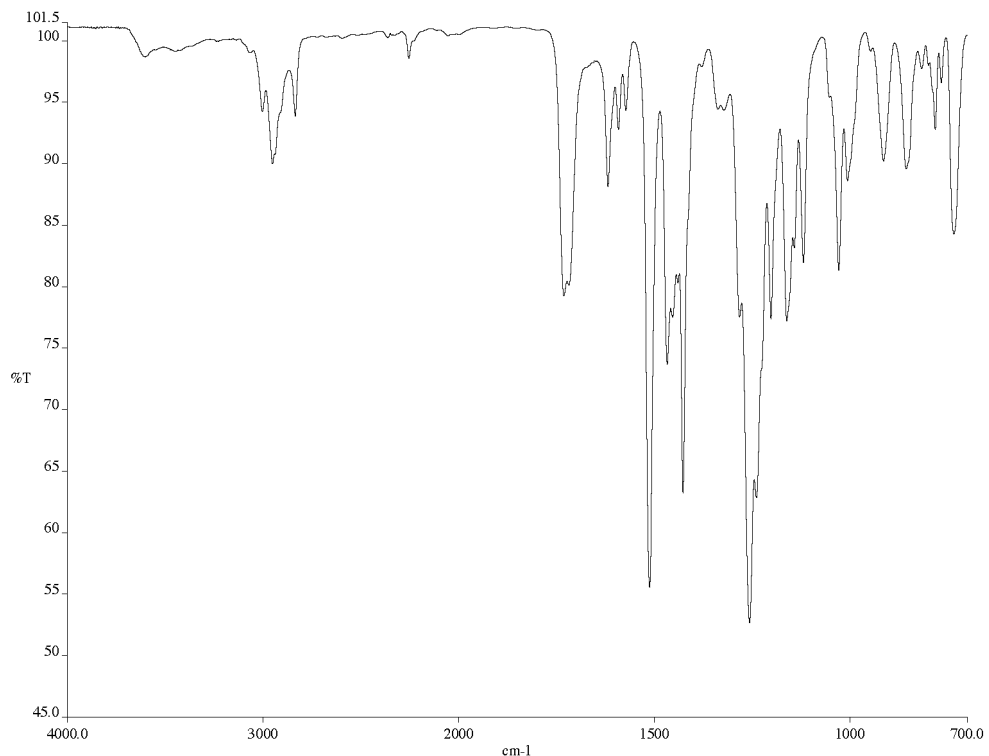


Figure A1.30.2 Infrared spectrum (thin film/NaCl) of methyl papaverine-3-carboxylate (**196**).

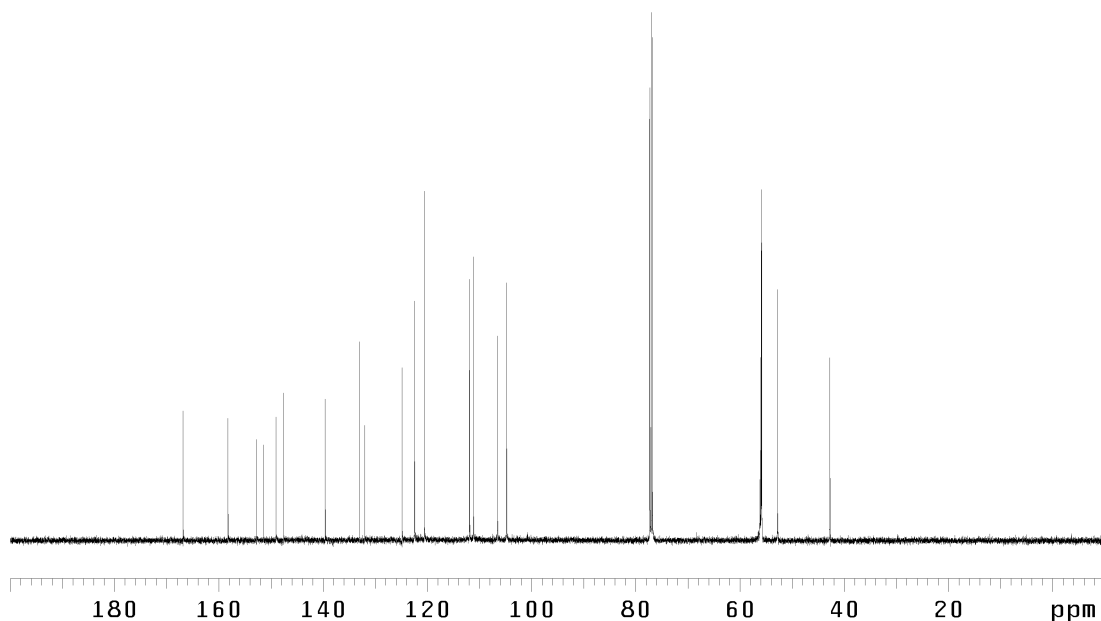


Figure A1.30.3 <sup>13</sup>C NMR (125 MHz, CDCl<sub>3</sub>) of methyl papaverine-3-carboxylate (**196**).



Figure A1.31.1  $^1\text{H}$  NMR (XXX MHz, XX) of papaverine (197).

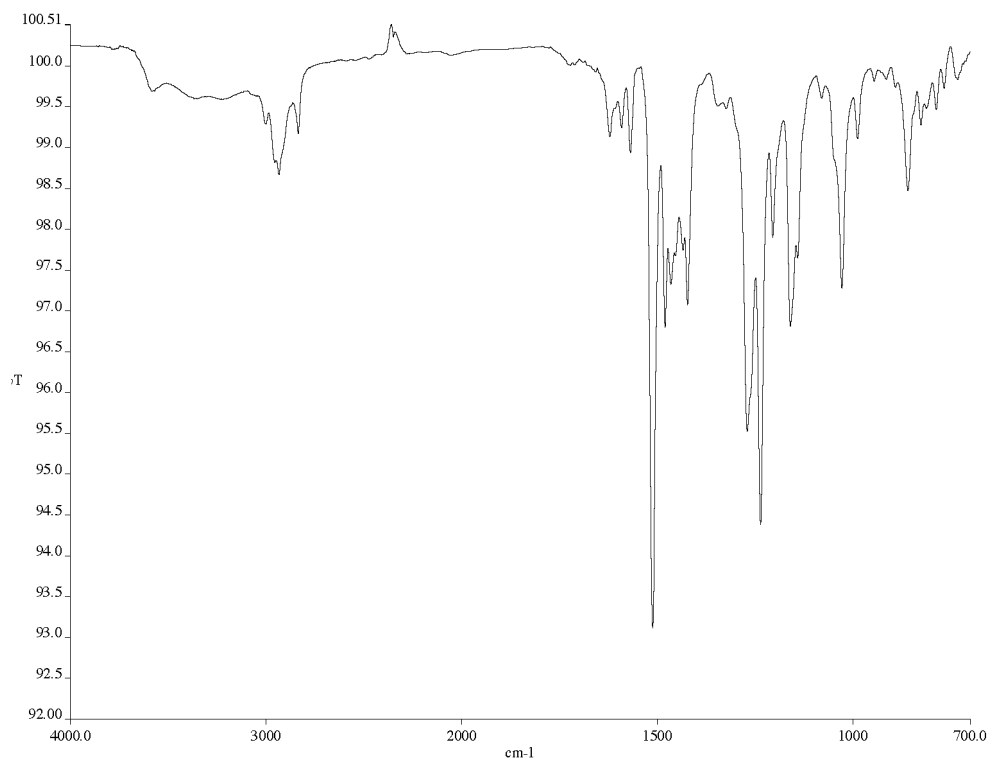


Figure A1.31.2 Infrared spectrum (thin film/NaCl) of papaverine (197).

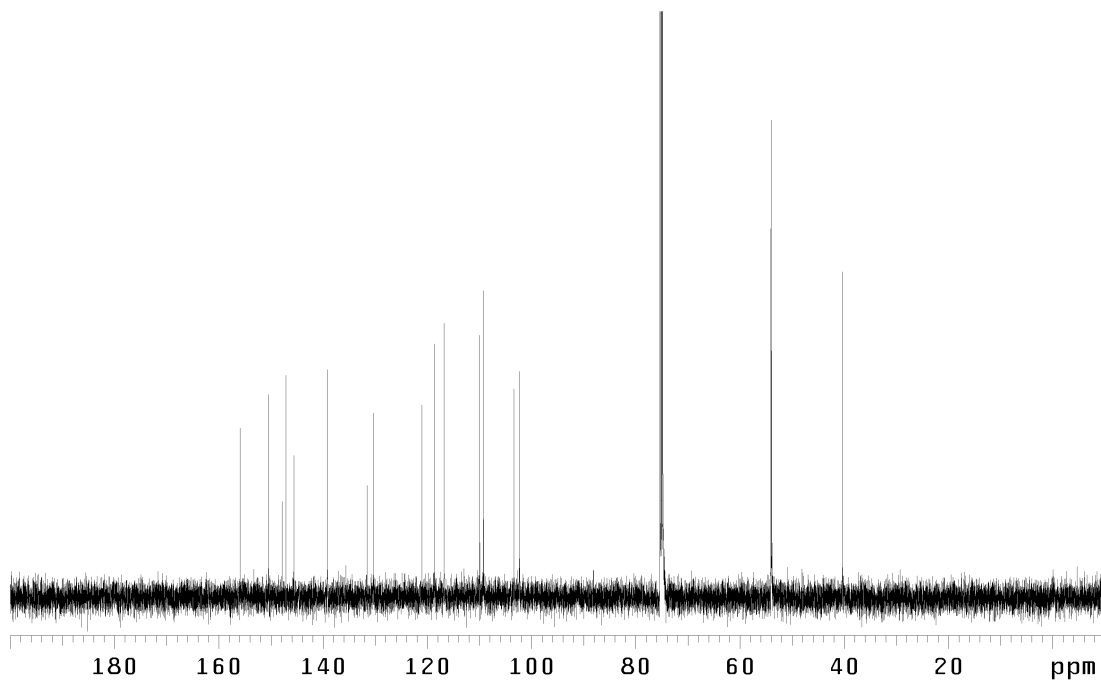


Figure A1.31.3 <sup>13</sup>C NMR (125 MHz, CDCl<sub>3</sub>) of papaverine (197).

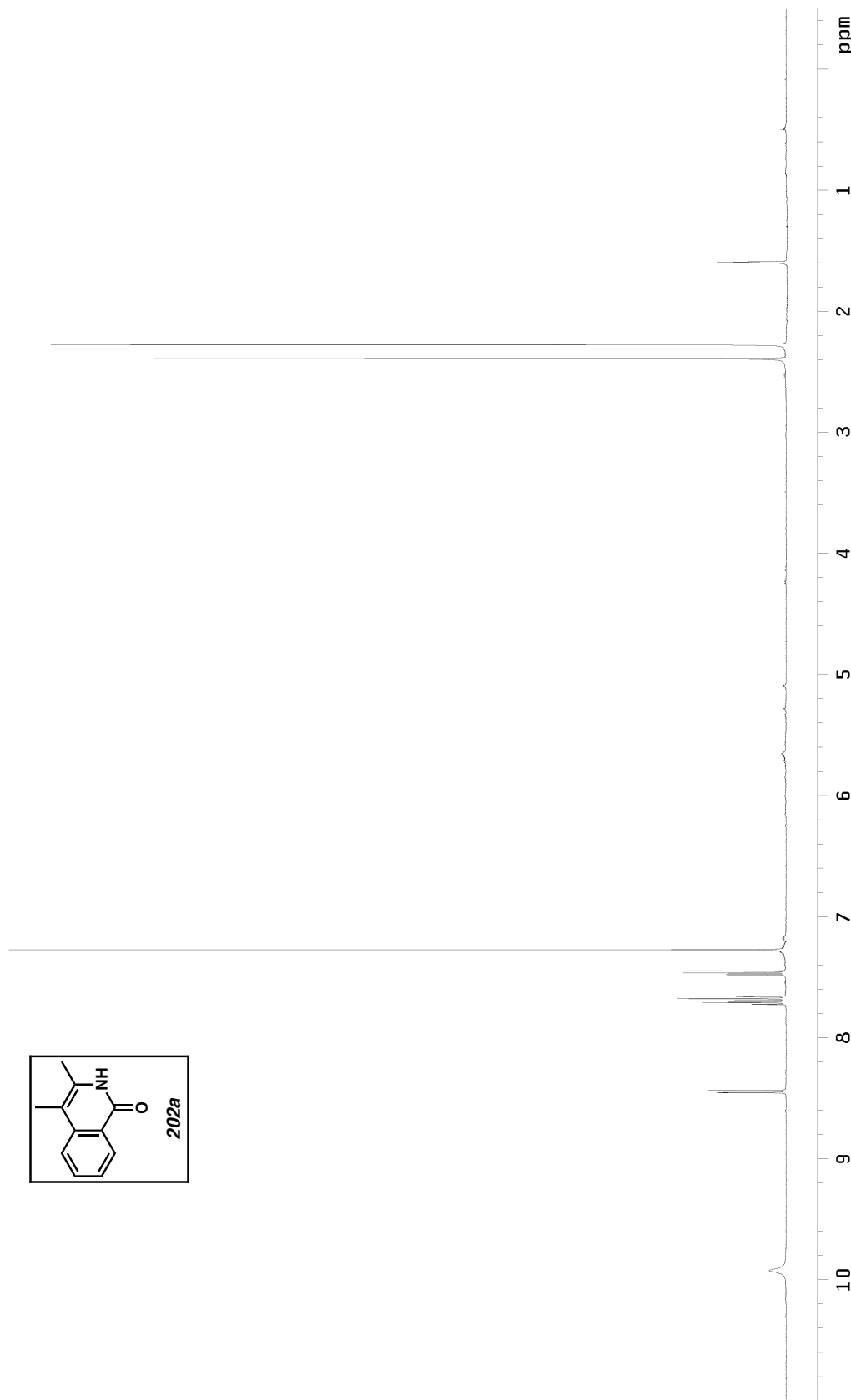


Figure A1.32.1  $^1\text{H}$  NMR (500 MHz,  $\text{CDCl}_3$ ) of isoquinolone **202a** (Table 2.9, entry 1).

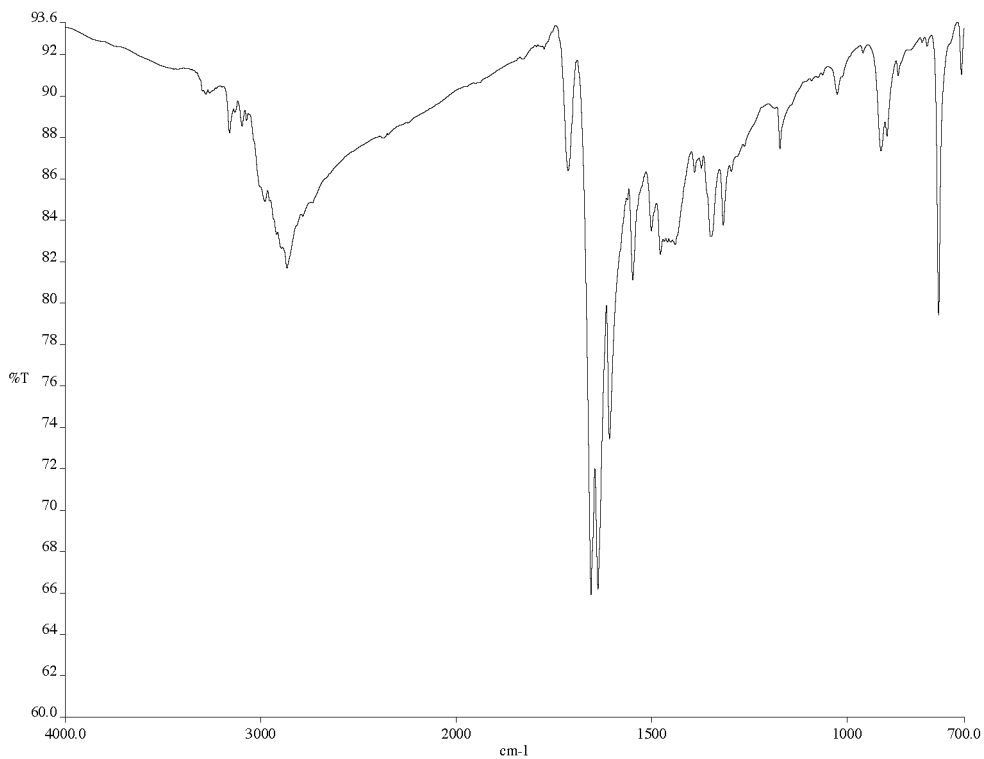


Figure A1.32.2 Infrared spectrum (thin film/NaCl) of isoquinolone **202a** (Table 2.9, entry 1).

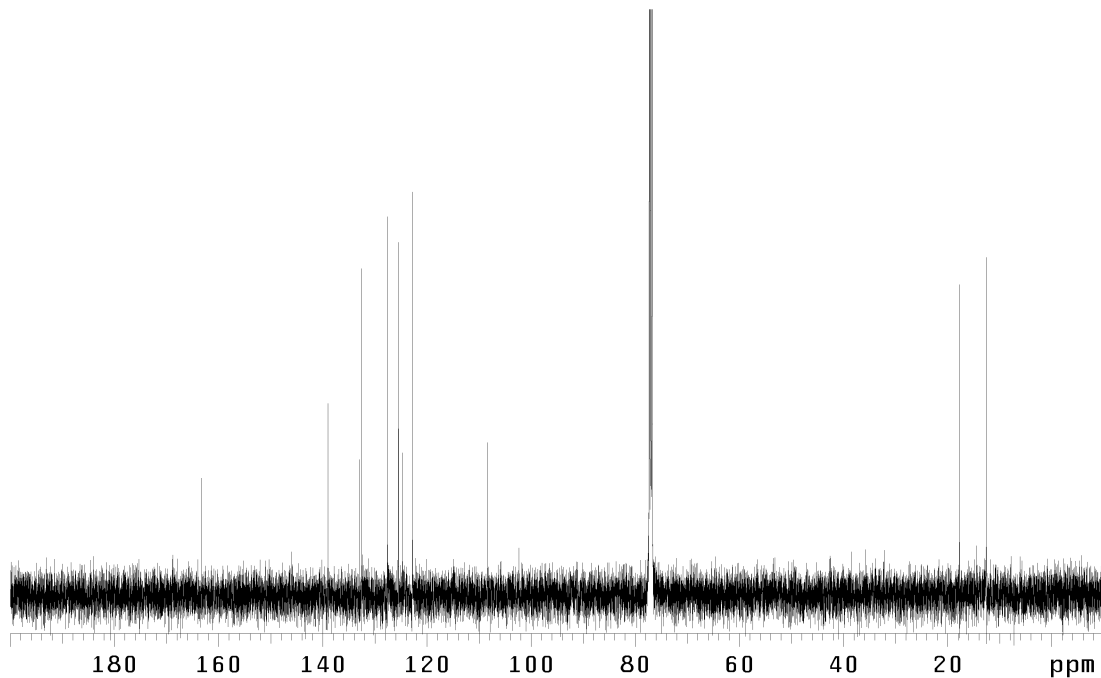


Figure A1.32.3  $^{13}\text{C}$  NMR (125 MHz,  $\text{CDCl}_3$ ) of isoquinolone **202a** (Table 2.9, entry 1).

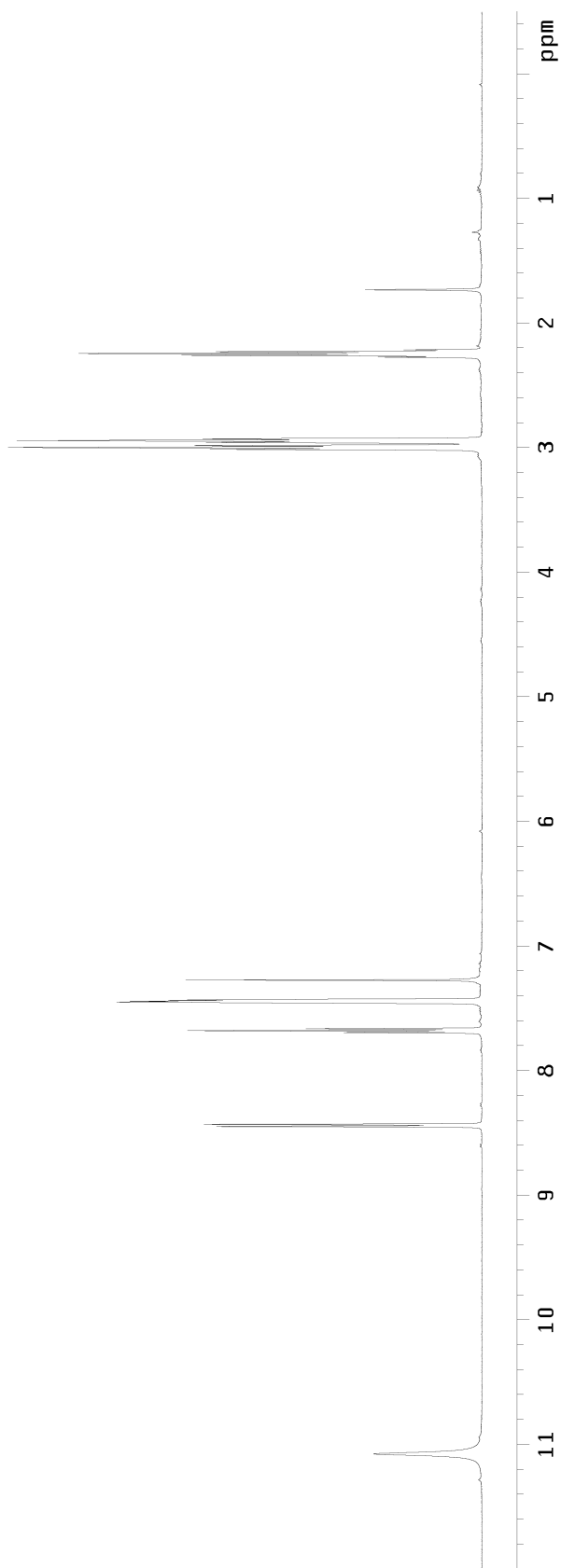
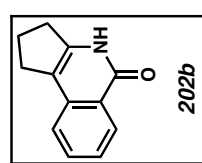


Figure A1.33.1  $^1\text{H}$  NMR (500 MHz,  $\text{CDCl}_3$ ) of isoquinolone **202b** (Table 2.9, entry 2).

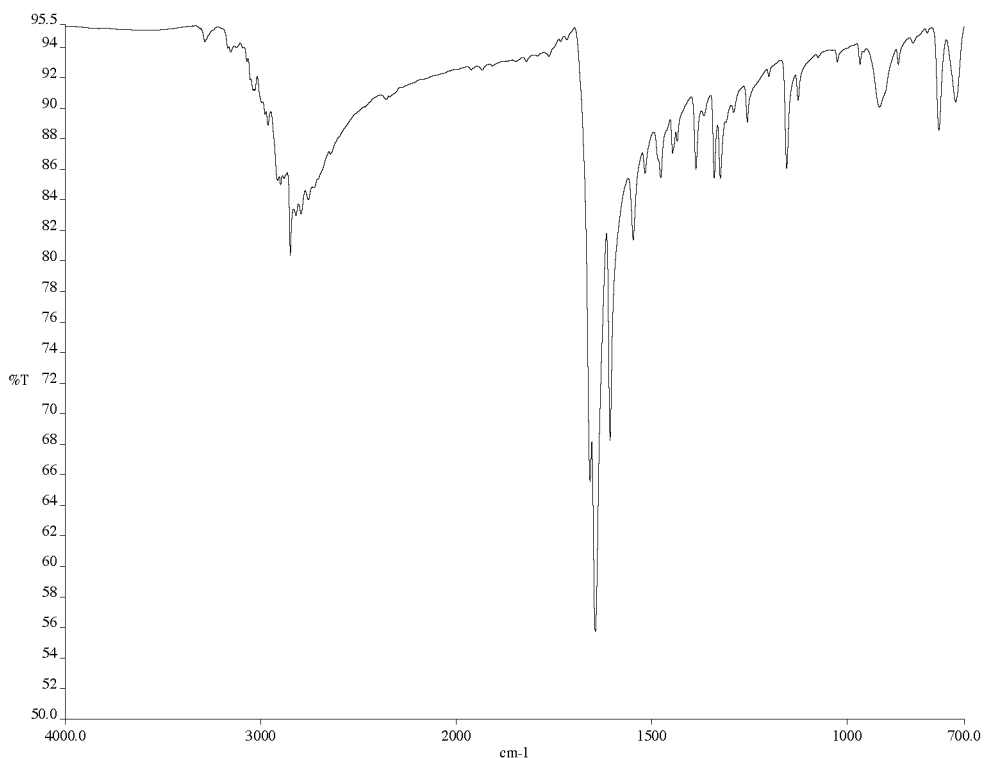


Figure A1.33.2 Infrared spectrum (thin film/NaCl) of isoquinolone **202b** (Table 2.9, entry 2).

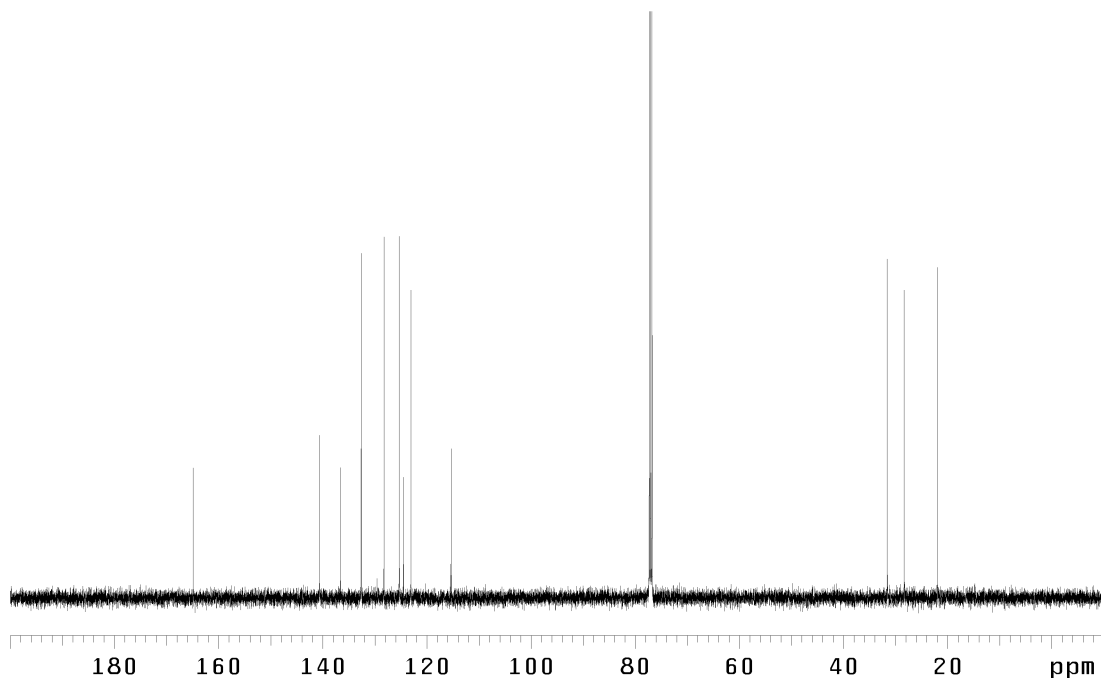


Figure A1.33.3 <sup>13</sup>C NMR (125 MHz, CDCl<sub>3</sub>) of isoquinolone **202b** (Table 2.9, entry 2).

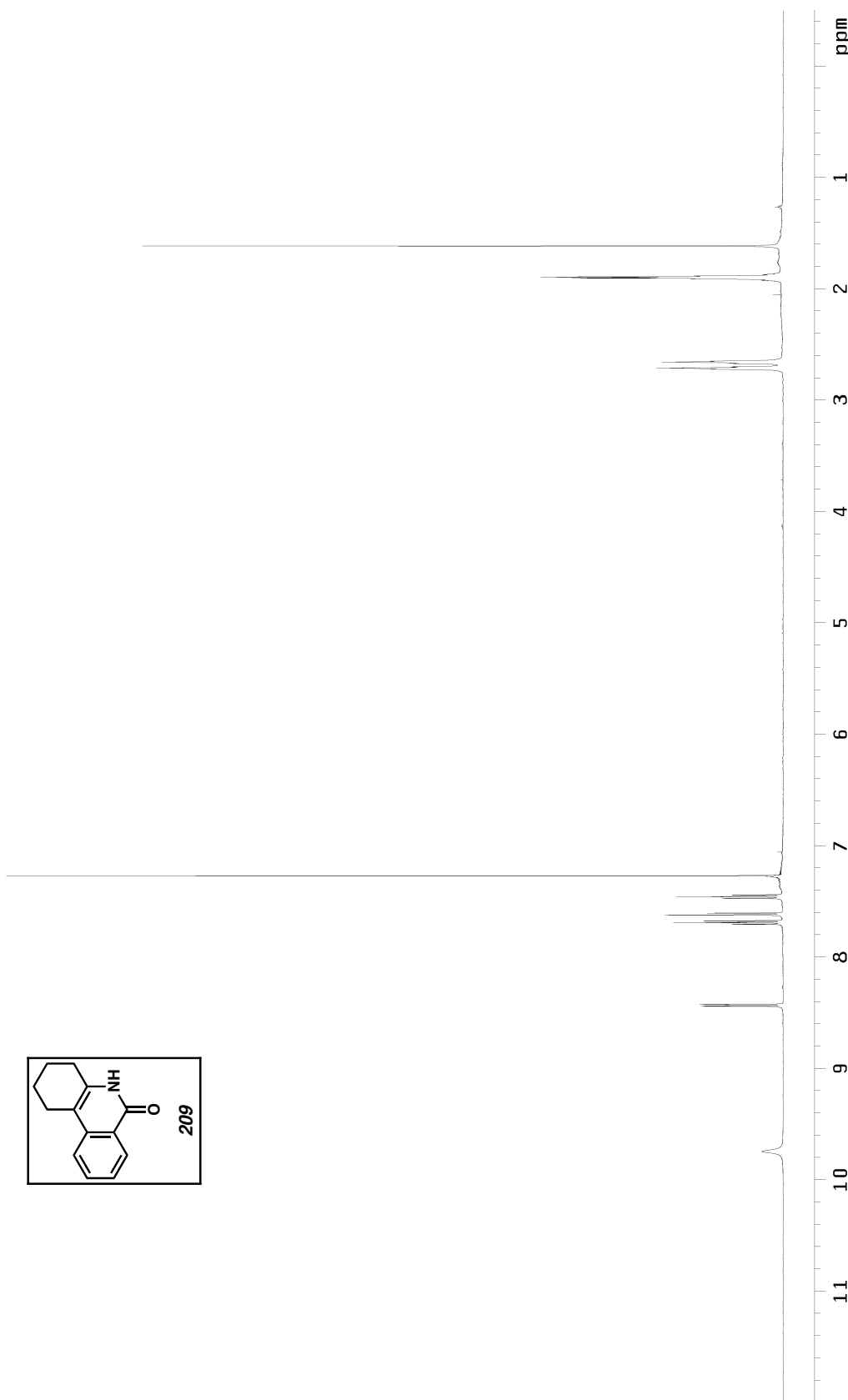
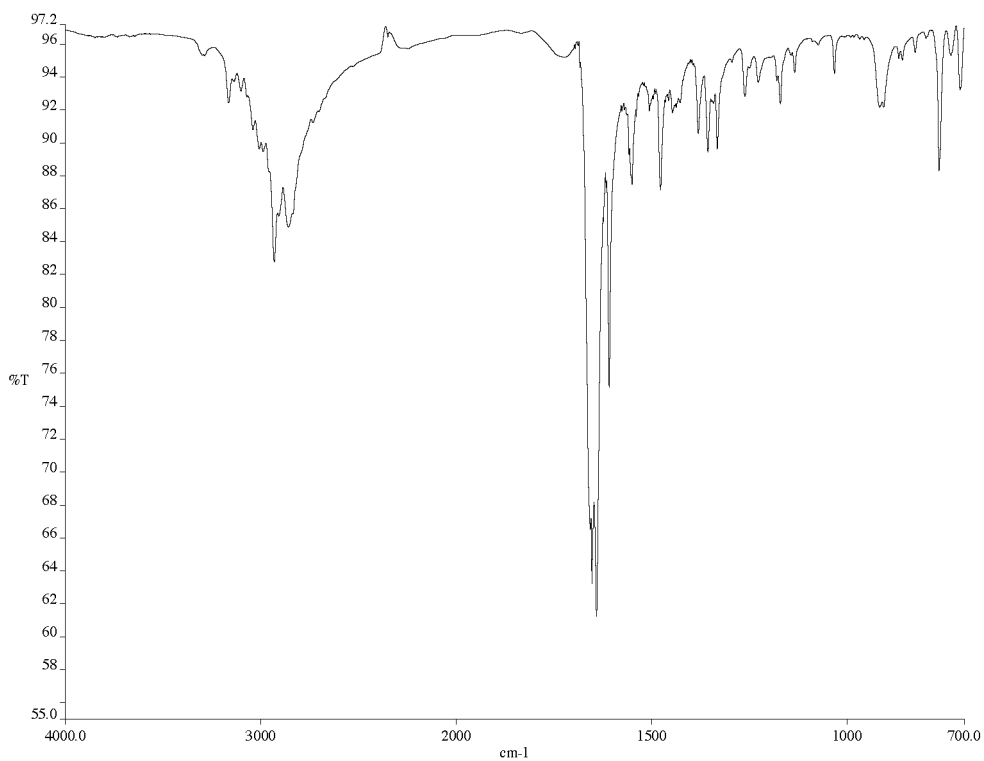
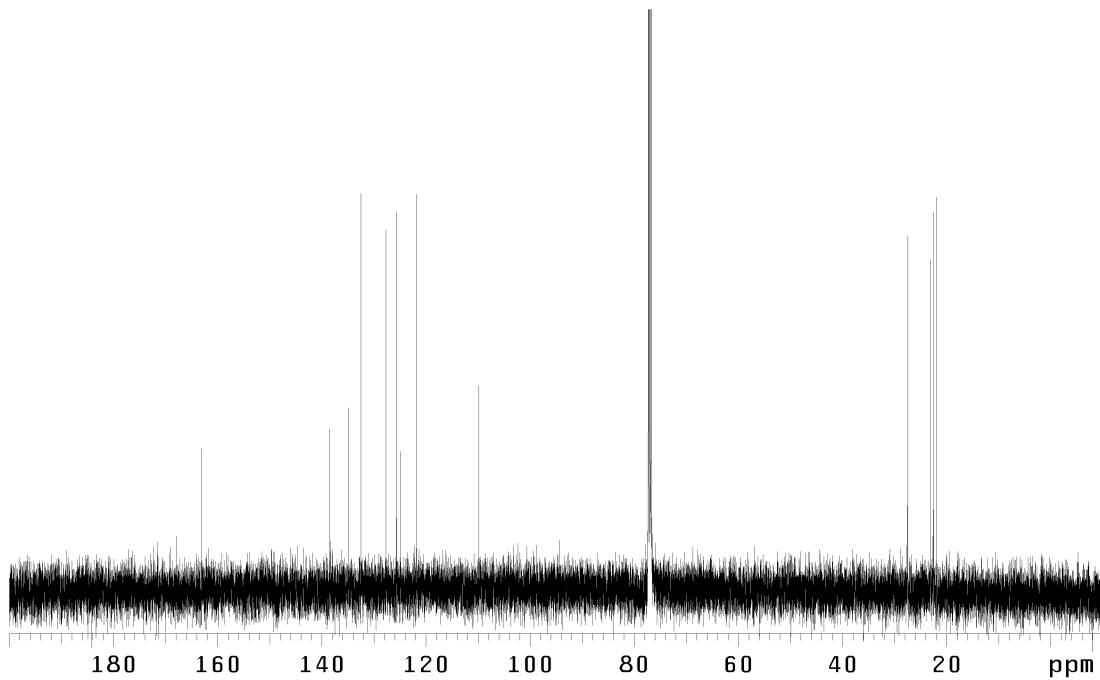


Figure A1.34.1  $^1\text{H}$  NMR (500 MHz,  $\text{CDCl}_3$ ) of isoquinolone **209** (Table 2.9, entry 3).



*Figure A1.34.2* Infrared spectrum (thin film/NaCl) of isoquinolone **209** (Table 2.9, entry 3).



*Figure A1.34.3*  $^{13}\text{C}$  NMR (125 MHz,  $\text{CDCl}_3$ ) of isoquinolone **209** (Table 2.9, entry 3).

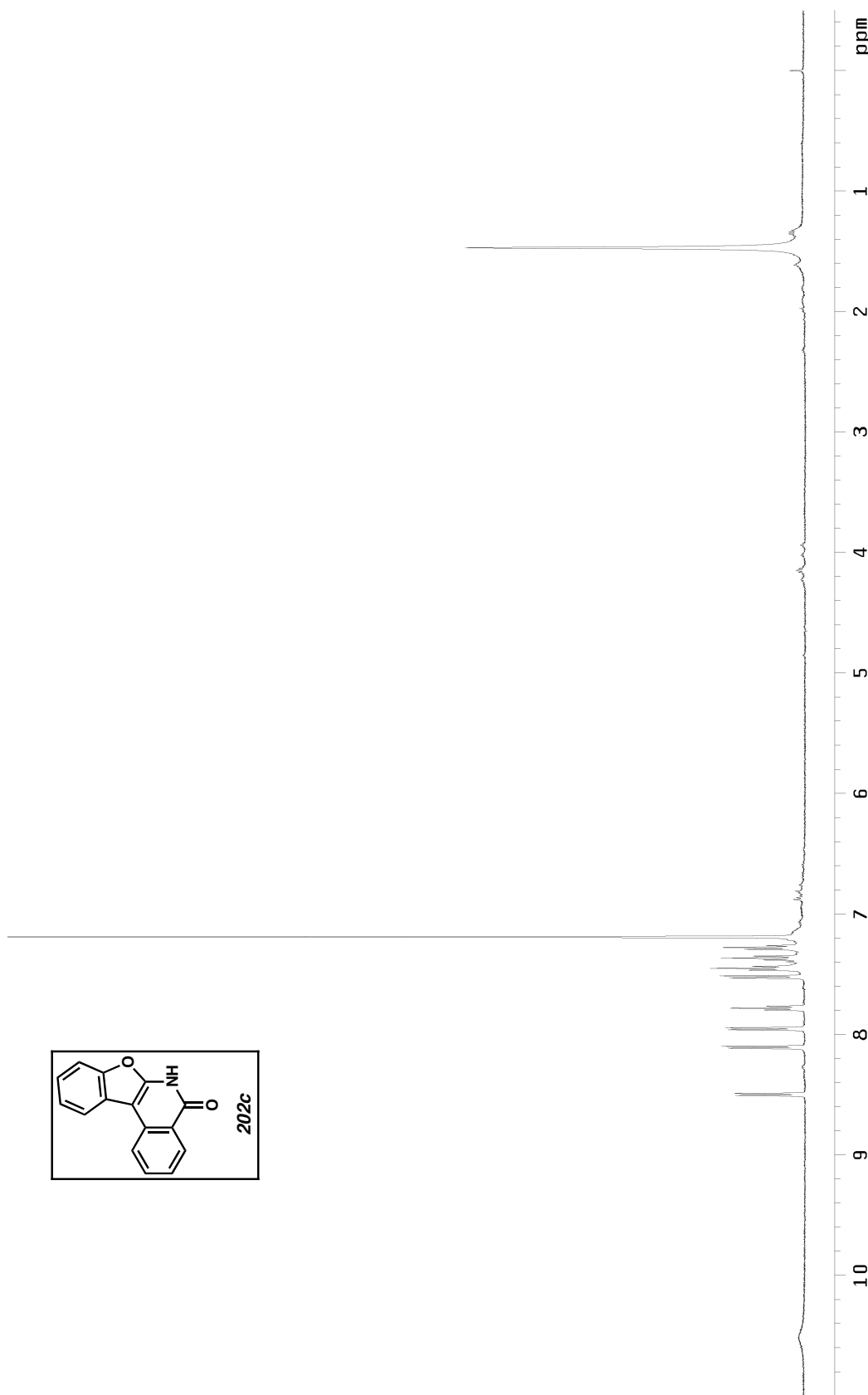


Figure A1.35.1  $^1\text{H}$  NMR (500 MHz,  $\text{CDCl}_3$ ) of isoquinolone **202c** (Table 2.9, entry 4).

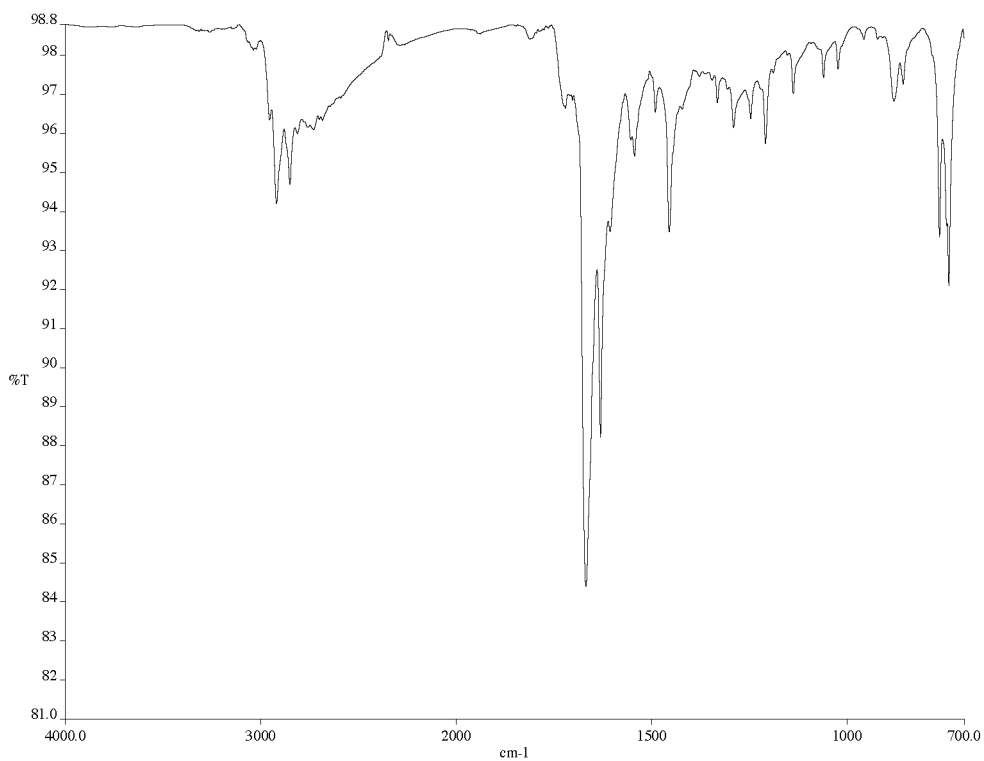


Figure A1.35.2 Infrared spectrum (thin film/NaCl) of isoquinolone **202c** (Table 2.9, entry 4).

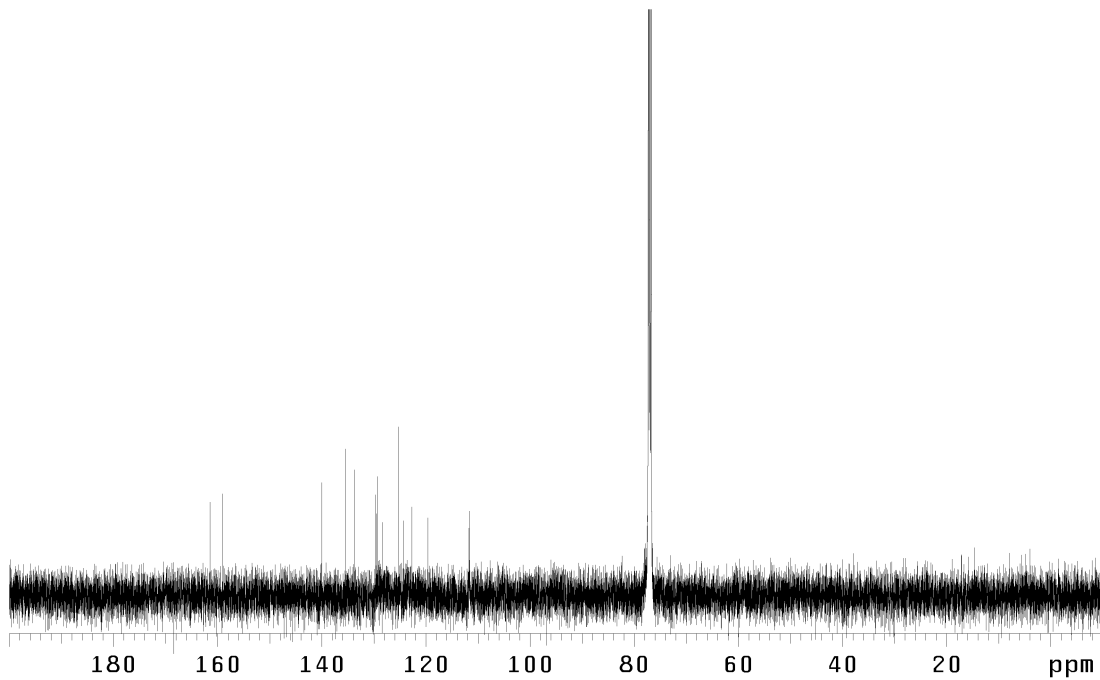


Figure A1.35.3  $^{13}\text{C}$  NMR (125 MHz,  $\text{CDCl}_3$ ) of isoquinolone **202c** (Table 2.9, entry 4).

# CHAPTER 3

## *An Introduction to Quinocarcin*

### 3.1 INTRODUCTION AND BACKGROUND

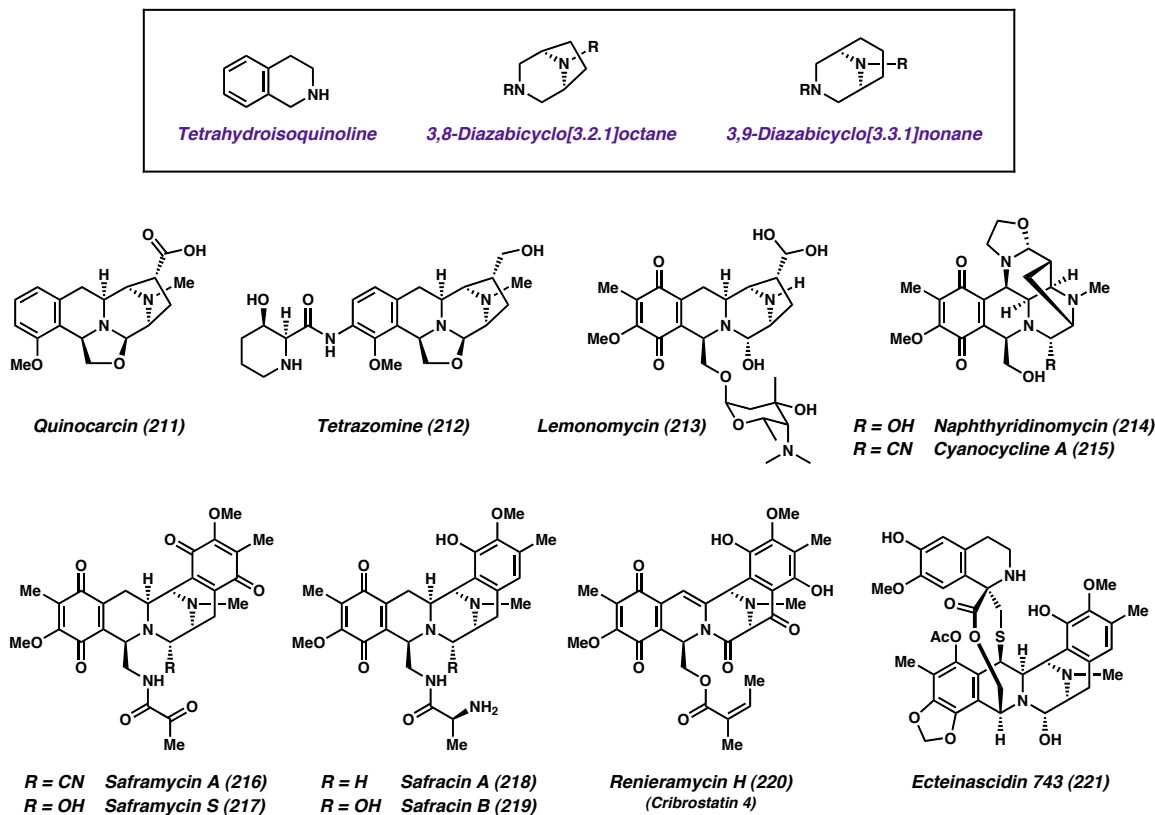
#### 3.1.1 *The Tetrahydroisoquinoline Antitumor Antibiotics*

Quinocarcin (**211**) belongs to a family of alkaloids known as the tetrahydroisoquinoline antitumor antibiotics (Figure 3.1).<sup>1</sup> To date, more than 60 members have been isolated from a wide variety of fauna, including soil actinomycetes of the genera *Streptomyces* and *Pseudomonas*, marine sponges, and tunicates. Representatives within this family are structurally characterized by the presence of one or more tetrahydroisoquinoline ring systems, often displayed in an oxidized quinone form, and assembled around either a 3,8-diazabicyclo[3.2.1]octane or a 3,9-diazabicyclo[3.3.1]nonane core. Those molecules bearing the former bridged ring system belong to one of two classes. The first class, typified by its prototypical member, quinocarcin, is distinguished by the presence of an oxygenated carbon substituent attached to the two-carbon bridge. Members include quinocarcin<sup>2</sup> (**211**), tetrazomine<sup>3</sup> (**212**), and lemomycin<sup>4</sup> (**213**). Alternatively, members of the naphthyridinomycin class

possess an oxazolidine ring linking the two-carbon bridge to the benzylic carbon of the tetrahydroisoquinoline, thereby resulting in a highly caged three-dimensional structure. This class includes naphthyridinomycin<sup>5</sup> (**214**) and cyanocycline A<sup>6,7</sup> (**215**), as well as the bioxalomycins,<sup>8</sup> dnacins,<sup>9</sup> and aclindomycins.<sup>10</sup> In general, members of these two classes contain only one tetrahydroisoquinoline ring system.

On the other hand, tetrahydroisoquinoline alkaloids exhibiting the 3,9-diazabicyclo[3.3.1]nonane core bear two tetrahydroisoquinoline units bordering the central piperazine ring and may possess as many as three in total. These molecules are divided among four classes—saframycins (e.g., **216** and **217**), safracins (e.g., **218** and **219**), renieramycins (e.g., **220**), and ecteinascidins (e.g., **221**). Members of the saframycin class represent the first tetrahydroisoquinoline alkaloids to be isolated and characterized.<sup>11</sup> These molecules possess a pentacyclic core bearing two quinones (or hydroquinones) and a pendant pyruvamide. Closely related to these structures are the safracins (**218** and **219**), differing only in the substitution of a phenol for one of the two quinones and the presence of an L-alanine residue in place of the pyruvamide.<sup>12</sup> Several of the renieramycins also closely resemble the structure of the saframycins and safracins, with the notable exception of an angelate ester in the lower quadrant.<sup>13</sup> However, renieramycin H (**220**) is unique in that it bears a single dihydroisoquinoline instead of the two namesake tetrahydroisoquinolines.<sup>14,15</sup> Finally, and arguably the most complex of the tetrahydroisoquinoline alkaloids are the members of the ecteinascidin group, a prominent example of which is ecteinascidin 743 (**221**).<sup>16</sup> The most notable structural feature of this class is the thioether-containing ten-membered ring, which is often spiro-fused to an additional tetrahydroisoquinoline or tetrahydropyridoindole ring system.

Figure 3.1. Representative structures of the tetrahydroisoquinoline antitumor antibiotics



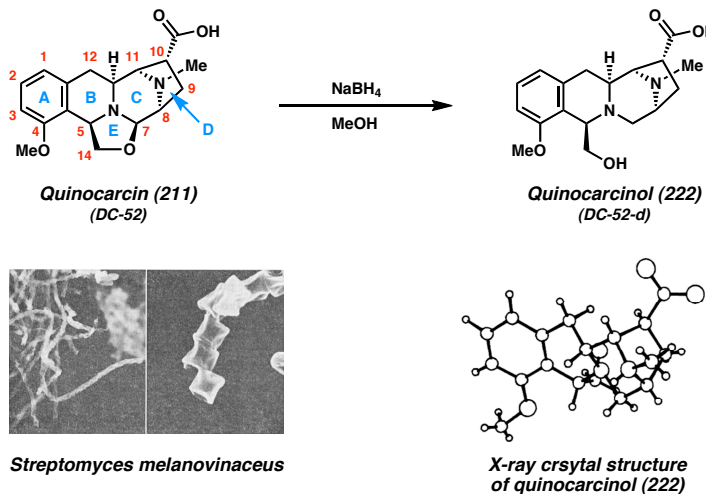
As their name implies, the tetrahydroisoquinoline antitumor antibiotics are potent broad-spectrum cytotoxins that display activity against both mammalian and bacterial cells.<sup>1</sup> Although tremendous variations in molecular structure exist within this family, two primary modes of action are shown to be conserved throughout each class. The most common biological mechanism is the alkylation of DNA base pairs within the minor groove, a pathway reliant upon the presence of a labile carbinolamine, aminonitrile, or oxazolidine functionality capable of forming an electrophilic iminium ion. The second is oxidative damage of DNA through the production of superoxide, a mechanism that has been invoked in cases where the molecule is capable of generating a semiquinone. However, an alternative pathway for the production of superoxide has been proposed for

quinocarcin and will be discussed Section 3.1.5. Two additional mechanisms have been proposed for ecteinascidin 743 (**221**): the induction of lethal DNA strand breaks by halting the transcription-coupled nucleotide excision repair machinery<sup>17</sup> and the interruption of microtubule formation.<sup>18</sup> However, thus far, these mechanisms are unique to ecteinascidin 743 and have yet to be observed in other tetrahydroisoquinoline antitumor antibiotics.

### 3.1.2 Isolation and Structural Characterization of Quinocarcin

In 1983, Tomita *et al.* at Kyowa Hakko Kogyo Co. isolated a novel antitumor antibiotic from a culture broth of *Streptomyces melanovinaceus* nov. sp. (labeled Actinomycete DO-52 at the time of isolation) collected in Machida-shi, Tokyo (Figure 3.2).<sup>2</sup> Quinocarcin (**211**), originally named DC-52, was isolated in a quantity of 90 mg as a colorless powder from 18 liters of broth. The structure was assigned based on <sup>1</sup>H and <sup>13</sup>C NMR data, as well as spectra collected for DC-52-d (quinocarcinol, **222**), a second isolate and the product obtained upon reduction of **211** with sodium borohydride in methanol.<sup>19</sup> Recrystallization of **222** from a water/ethanol/acetone solution provided a crystal suitable for X-ray diffraction, thereby confirming its structural assignment, as well as that of **211** by analogy.<sup>20</sup> However, the absolute stereochemistry remained unknown and the structure was arbitrarily assigned as *ent*-**211** by the isolation chemists. It was not until 1992 that the absolute configuration was determined, when Garner *et al.* prepared the natural enantiomer of quinocarcin through total synthesis.<sup>21</sup>

Figure 3.2. Structures of quinocarcin and quinocarcinol

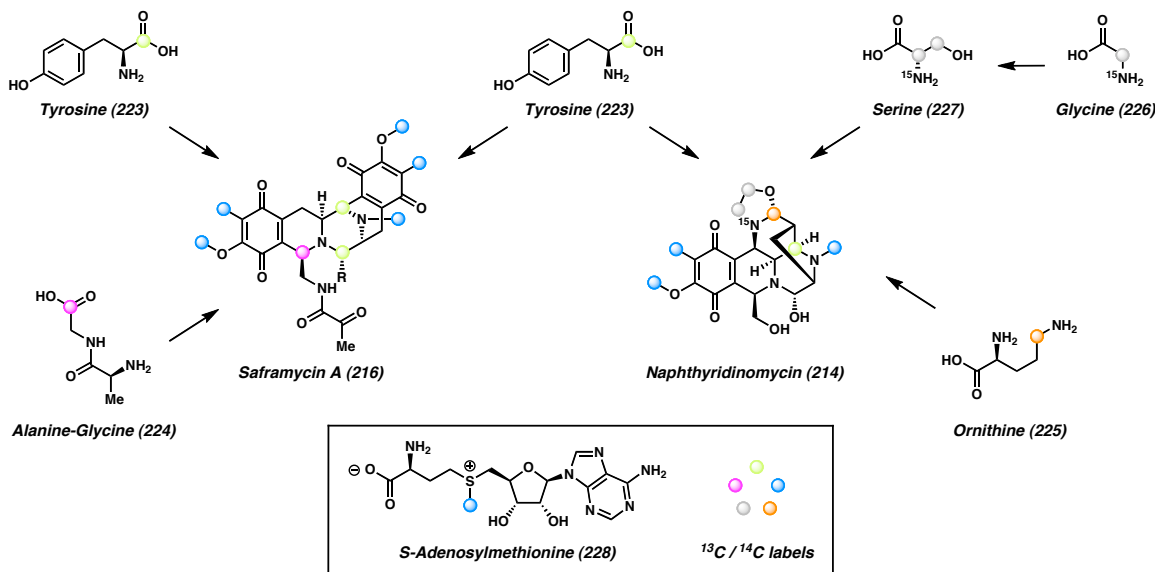


### 3.1.3 Biosynthesis

The tetrahydroisoquinoline antitumor antibiotics are biosynthetically derived from the condensation of amino acids. While the specific mechanisms involved in the biosynthesis of quinocarcin have not yet been studied in depth, certain implications can be drawn from more thoroughly investigated pathways such as those leading to saframycin A (**216**) and naphthyridinomycin (**214**) (Figure 3.3). Using <sup>13</sup>C-labeled amino acids, Mikami *et al.* showed that the majority of the pentacyclic core of saframycin A is biosynthesized through the condensation of two L-tyrosine residues (**223**),<sup>22</sup> while the southern quadrant of the left-hand tetrahydroisoquinoline and the pendant pyruvamide are derived from a preformed alanine-glycine dipeptide (**224**).<sup>23</sup> Similarly, Zmijewski *et al.* noted the incorporation of <sup>14</sup>C-labeled L-tyrosine (**223**) and L-ornithine (**225**) within the core structure of naphthyridinomycin,<sup>24</sup> while glycine (**226**), after being converted to serine (**227**), comprises the oxazolidine ring.<sup>25</sup> Finally, the methyl groups located on the

quinones and the tertiary amine of each product are installed by *S*-adenosylmethionine (**228**).

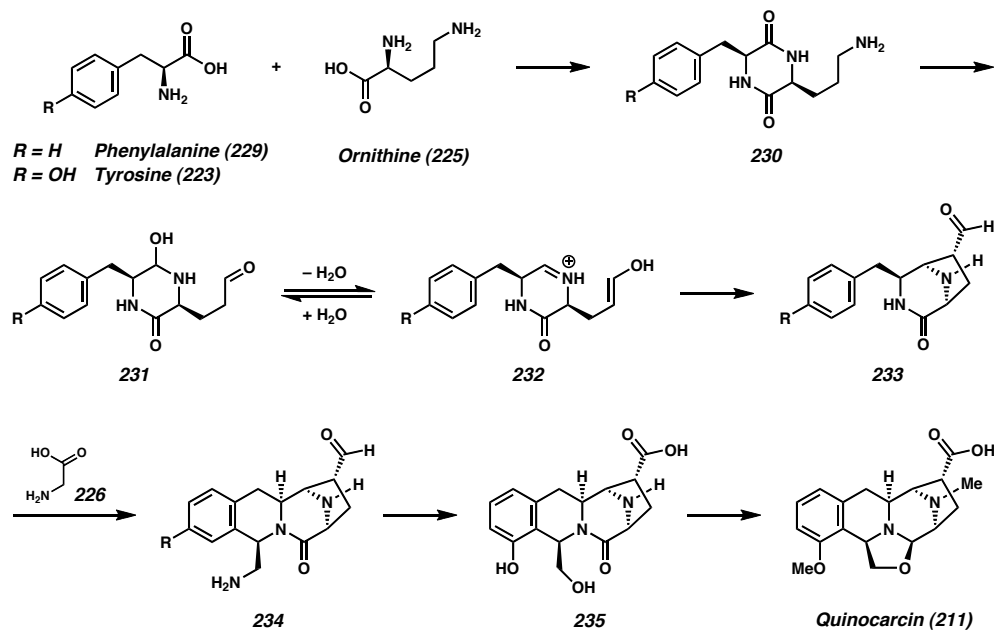
Figure 3.3. Elucidating the biosynthetic origins of saframycin A and naphthyridinomycin via isotopic labeling studies



Based on these previous studies, it is likely that quinocarcin arises through an initial condensation between L-ornithine (**226**) and either L-phenylalanine (**229**) or L-tyrosine (**223**) to form diketopiperazine **230** (Scheme 3.1). Oxidation of the primary amine and reduction of one of the lactam carbonyls leads to hemiaminal **231**, which then undergoes cyclization via intramolecular enol attack on an intermediate iminium ion (**232**) to form 3,8-diazabicyclo[3.2.1]octane **233**. The incorporation of an equivalent of glycine (**226**) closes the tetrahydroisoquinoline ring system to generate tetracycle **234**, after which functionalization of the arene ring, oxidation of the aldehyde, and conversion of the primary amine to an alcohol through oxidation, hydrolysis, and reduction leads to acid

**235.** Finally, installation of the methyl groups, lactam reduction, and closure of the oxazolidine ring furnish quinocarcin (**211**).

*Scheme 3.1. Proposed biosynthesis of quinocarcin*



### 3.1.4 Biological Activity

Shortly after its isolation, quinocarcin was tested for activity as both an antimicrobial and an antitumor agent.<sup>2</sup> The compound was found to possess moderate activity against Gram-positive bacteria such as *S. aureus* and *B. subtilis*, although it proved far less active against Gram-negative strains (Table 3.1). In each of the trials, quinocarcinol (**222**) was essentially inactive. When tested *in vivo* against murine lymphocytic leukemia P388, the administration of quinocarcin in a single dose of 12.5 mg/kg resulted in a 47% increase in life span ( $\text{LD}_{50} = 27$  mg/kg by intraperitoneal injection). Unfortunately, the instability of the natural product in aqueous media prevented more advanced biological testing.

Table 3.1. Antibiotic activity of quinocarcin and quinocarcinol

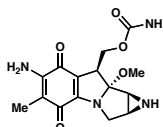
Bacterial strain	Gram + / -	Minimum inhibitory concentration ( $\mu\text{g/mL}$ )	
		quinocarcin (211)	quinocarcinol (222)
<i>Serratia marcescens</i>	(-)	>100	>100
<i>Pseudomonas cepacia</i>	(-)	>100	>100
<i>Escherichia coli</i>	(-)	>100	>100
<i>Proteus vulgaris</i>	(-)	25	>100
<i>Shigella sonnei</i>	(-)	>100	>100
<i>Salmonella typhosa</i>	(-)	>100	>100
<i>Klebsiella pneumoniae</i>	(-)	25	>100
<i>Staphylococcus aureus</i>	(+)	12.5	100
<i>Bacillus subtilis</i>	(+)	12.5	100

In 1987, Morimoto *et al.* at Kyowa Hakko Kogyo Co. reported an in-depth analysis of the anticancer properties of KW2152, the more stable monocitrate salt of quinocarcin.<sup>26</sup> In an initial assay against P388 leukemia, administration of KW2152 at doses of 2.1–6.1 mg/kg/day for 7 days resulted in an increase in life span of >80% in mice. The drug was most effective when administered daily and activity was observed to be schedule dependent. An IC<sub>50</sub> value of 5.3  $\mu\text{M}$  was observed after 1 hour, which decreased to 0.11  $\mu\text{M}$  after 72 hours. A broadened investigation revealed similar levels of activity in a number of additional tumor cell lines grown *in vitro* (Table 3.2a).<sup>27</sup> Most importantly, KW2152 performed comparably to established clinical anticancer treatments (Table 3.3b), even displaying activity against lung carcinoma cell lines resistant to mitomycin C and cisplatin.<sup>28</sup> These findings led researchers in Japan to advance KW2152 to clinical trials as an anticancer treatment.<sup>29</sup> However, the trials were discontinued in Phase I due to liver toxicity.

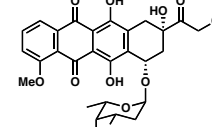
Table 3.2. a) Time-dependent  $IC_{50}$  values of KW2152 against various cultured tumor cell lines.  
 b) Response of human tumor xenografts to KW2152 and established anticancer agents

a)

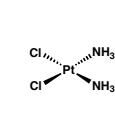
Cell line	$IC_{50}$ ( $\mu M$ )	
	1 h	72 h
P388 leukemia	5.3	0.11
L1210 leukemia	150	0.72
B16 melanoma	210	0.73
Sarcoma 180	1900	3.4
HeLa S <sub>3</sub> epithelial carcinoma	76	0.16
KB epidermal carcinoma	60	0.10
SK-MEL-28 melanoma	750	0.10



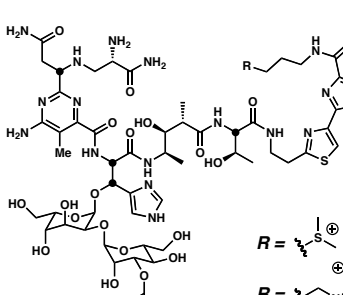
**Mitomycin C (236)**



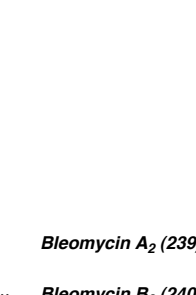
**Adriamycin (237)**



**Cisplatin (238)**



**Bleomycin A<sub>2</sub> (239)**



**Bleomycin B<sub>2</sub> (240)**

b)

Drug	T/C % <sup>a</sup> (dose, schedule)			
	MX-1 mammary tumor	Co-3 colon carcinoma	St-4 gastric carcinoma	St-15 gastric carcinoma
<b>KW2152</b>	0 (4.4 mg/kg, days 0–6)	18 (8.6 mg/kg, days 0–6)	27 (8.6 mg/kg, days 0–6)	29 (8.6 mg/kg, days 0–6)
<i>Mitomycin C</i>	0 (6.0 mg/kg, day 0)	38 (6.0 mg/kg, day 0)	32 (6.0 mg/kg, day 0)	7 (6.0 mg/kg, day 0)
<i>Adriamycin</i>	77 (10.0 mg/kg, day 0)	47 (15.0 mg/kg, day 0)	NT <sup>b</sup>	NT
<i>Cisplatin</i>	0 (7.1 mg/kg, days 0, 4, 8)	30 (7.1 mg/kg, days 0, 4, 8)	52 (7.1 mg/kg, days 0, 4, 8)	9 (7.1 mg/kg, days 0, 4, 8)
<i>Bleomycin</i>	NT	34 (80.1 mg/kg, days 0, 4, 8)	NT	NT

<sup>a</sup> T/C % = percentage of treated vs. control tumor volume

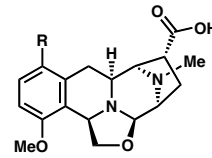
<sup>b</sup> NT = not tested

In the decade that followed the discovery of KW2152, researchers began assembling and screening hundreds of synthetic analogues of quinocarcin in an effort to uncover compounds that displayed comparable antitumor activity and fewer adverse side effects. Between 1990 and 1991, workers at Kyowa Hakko Kogyo Co. completed the synthesis and subsequent biological testing of a series of derivatives featuring additional arene ring substitution, oxidation to the hydroquinone or quinone, and ring opening of the oxazolidine to an aminonitrile (Table 3.3).<sup>30</sup> Based on assays for *in vitro* growth inhibition of a HeLa S<sub>3</sub> tumor cell line, the most promising lead compounds were those

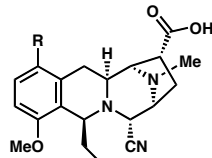
featuring halide substitution at C(1) (**241**, **242**, **244**, and **245**) or thioether substitution at C(2) and C(3) (**246**, **247**, **250**, and **251–259**), while quinones bearing no substitution (**248**) or amine and ether substitution (**249**) proved less effective. It is worthy of note, however, that an aminonitrile derivative featuring an unmodified arene ring (**243**, later given the name DX-52-1) performed comparably to the more highly substituted compounds. Further studies performed *in vivo* with each compound using P388-implanted mice showed moderate increases in life span of 17–69%.

Table 3.3. Screening synthetic analogues of quinocarcin for tumor growth inhibition against HeLa S<sub>3</sub> epithelial carcinoma grown *in vitro* and P388 leukemia implanted in mice (*in vivo*)

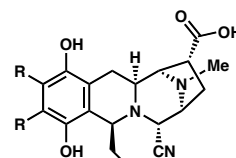
Analogue	HeLa S <sub>3</sub> IC <sub>50</sub> (μg/mL)	P388 dose (mg/kg)	ILS <sup>a</sup> (%)
<b>Quinocarcin</b>	0.05–0.11	10–20	27–56
<b>241</b>	0.04	12.5	40
<b>242</b>	0.04	25	24
<b>243</b>	0.05	20	26
<b>244</b>	0.042	12.5	23
<b>245</b>	0.11	50	31
<b>246</b>	0.09	6.25	47
<b>247</b>	<0.03	12.5	51
<b>248</b>	0.12	20	18
<b>249</b>	1.75	100	17
<b>250</b>	0.56	12.5	17
<b>251</b>	0.019	6.25	48
<b>252</b>	0.08	6.25	64
<b>253</b>	0.03	12.5	58
<b>254</b>	0.0019	6.25	69
<b>255</b>	0.13	12.5	53
<b>256</b>	0.11	12.5	50
<b>257</b>	0.05	25	56
<b>258</b>	0.012	25	65
<b>259</b>	0.004	25	48



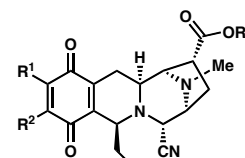
**241, R = Cl**  
**242, R = I**



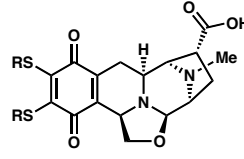
**DX-52-1 (243), R = H**  
**244, R = Cl**  
**245, R = I**



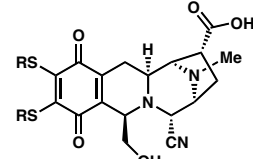
**246, R = MeS**  
**247, R = i-PrS**



**248, R<sup>1</sup> = H, R<sup>2</sup> = H, R<sup>3</sup> = Me**  
**249, R<sup>1</sup> = PhHN, R<sup>2</sup> = MeO, R<sup>3</sup> = H**  
**250, R<sup>1</sup> = MeO, R<sup>2</sup> = i-PrS, R<sup>3</sup> = H**



**251, R = Me**  
**252, R = Et**  
**253, R = n-Pr**  
**254, R = i-Pr**



**255, R = Me**  
**256, R = Et**  
**257, R = n-Pr**  
**258, R = i-Pr**  
**259, R = t-Bu**

<sup>a</sup> ILS = increase in life span

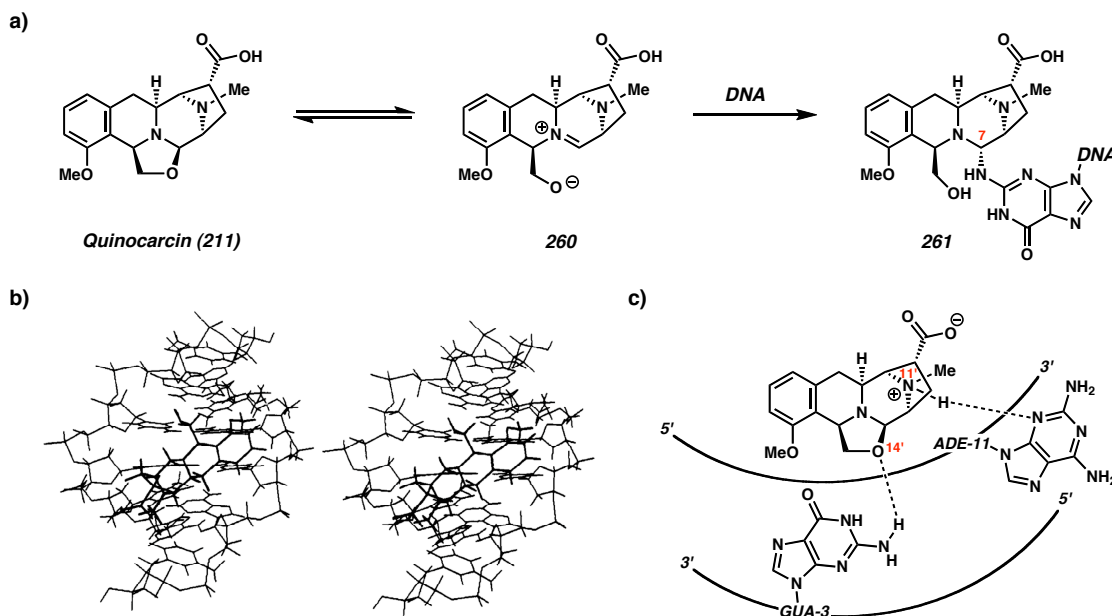
In 1985, the National Cancer Institute initiated a disease-oriented screening procedure for discovering new antitumor agents that employed 60 human tumor cell lines derived from seven cancer types (brain, color, leukemia, lung, melanoma, ovarian, and renal). The screen identified both KW2152 and DX-52-1 (**243**) as melanoma-specific inhibitors, which led researchers in the U.S. to submit the latter compound to Phase I clinical trials.<sup>31</sup> Unfortunately, the drug was poorly tolerated, causing dose-limiting gastrointestinal toxicity in an initial panel of 33 patients. Furthermore, the most efficacious treatment schedule indicated by prior *in vivo* antitumor studies was more than 60 times greater than the maximum tolerated dose (6 mg/m<sup>2</sup>/week) determined in the clinical trial. DX-52-1 was therefore not recommended for advancement to Phase II study.

### 3.1.5 Mechanism of Action

The biological mechanism of action of quinocarcin was originally investigated by Tomita *et al.* shortly after its isolation.<sup>32</sup> The effects of quinocarcin on the synthesis of DNA, RNA, and protein were examined by measuring the incorporation of [*methyl*-<sup>3</sup>H]thymidine, [2-<sup>14</sup>C]uracil, and [4,5-<sup>3</sup>H]-L-leucine, respectively, into acid-insoluble precipitates. At a high concentration (100 µg/mL), quinocarcin was found to inhibit DNA, RNA, and protein synthesis, while at a lower concentration (25 µg/mL), the inhibition of RNA and protein synthesis were minimal and could only be detected after 20 minutes. However, DNA synthesis was found to be completely blocked within 5 minutes at both concentrations, indicating that DNA was likely the primary target *in vivo*.

Previous DNA binding studies performed with the related tetrahydroisoquinoline alkaloids naphthyridinomycin<sup>33</sup> (**214**) and saframycin A<sup>34</sup> (**216**) suggested that members of this family of molecules might disrupt DNA transcription by alkylating in the minor groove. The carbinolamine and aminonitrile functionalities were envisioned to form electrophilic iminium species (**260**) that would react with nucleophilic groups on DNA, specifically the 2-amino group of a guanine residue, to form DNA adducts such as **261** (Figure 3.4a). In order to investigate the propensity for quinocarcin to participate in this mode of reactivity, Remers *et al.* performed a computer simulation of quinocarcin binding to the duplex DNA hexamer d(ATGCAT)<sub>2</sub>.<sup>35</sup> Since the absolute stereochemistry of the natural product was unknown at the time, the group simulated both covalent and non-covalent interactions between either enantiomer and a B-DNA helix. Conformations were investigated in which the arene ring of quinocarcin pointed either in the direction of the 3' or the 5' terminus, and alkylation at guanine produced either an *R* or *S* configuration at C(7). Of the eight possible scenarios, the lowest energy conformation was calculated to result from situating the arene ring in the 3' direction with an *R* configuration at C(7) (Figure 3.4b). This promoted hydrogen bonding between O(14') of quinocarcin and HN(2) of guanine-3, as well as between HN(11') of quinocarcin and N(3) of adenine-11 (Figure 3.4c). Interestingly, the group also came to the conclusion that the preferred absolute configuration of quinocarcin was likely the reverse of that arbitrarily chosen at the time of isolation. This was later confirmed by Garner *et al.* through total synthesis.<sup>21</sup>

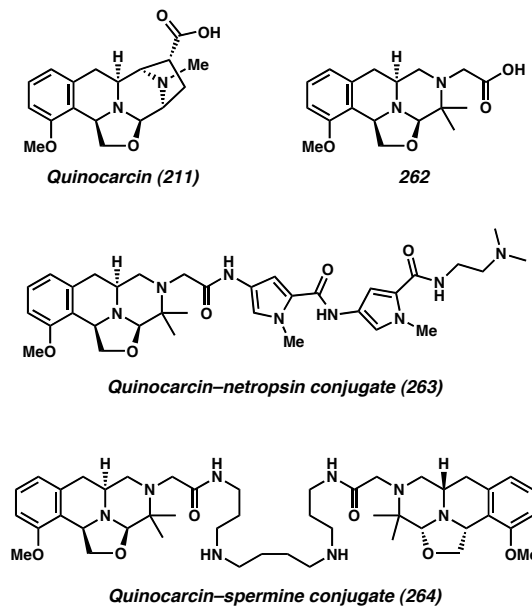
Figure 3.4. a) Proposed mechanism of DNA alkylation by quinocarcin. b) Calculated lowest energy conformation of quinocarcin covalently bound to DNA (stereo pair). c) Non-covalent hydrogen bonding interactions between quinocarcin and *d*(ATGCAT)<sub>2</sub>



Quinocarcin strongly inhibits the incorporation of [*methyl*-<sup>3</sup>H]thymidine into DNA in *Bacillus subtilis* *in vivo*.<sup>32</sup> This inhibition has been attributed both to the interruption of DNA polymerase activity and to the cleavage of double-stranded DNA. Williams *et al.* showed that the addition of superoxide dismutase (SOD), catalase, dithiothreitol (DTT), and various radical scavengers each inhibited strand cleavage of supercoiled plasmid DNA by quinocarcin, as well as analogues 262–264 (Table 3.4).<sup>36</sup> On the other hand, the addition of hydrogen peroxide produced a marked enhancement in activity.<sup>37</sup> Together, these results suggested that the mechanism of strand cleavage involved the generation of oxygen and/or hydroxyl radicals. In order to better understand this process, the authors measured the rate of superoxide formation over a pH range of 6.0–8.0 and found a positive correlation between pH and reaction rate with a maximum rate of  $6.8 \times 10^{-4}$

$M^{-1}s^{-1}$  at pH 8.0. Interestingly, this rate is  $10^4$ – $10^5$  times slower than the rate-limiting step of the Fenton<sup>38</sup>/Haber–Weiss<sup>39</sup> cycle (i.e., the Fenton reaction,  $k = 76 M^{-1} s^{-1}$ ), the process through which iron catalyzes the conversion of superoxide to hydroxyl radicals.<sup>40</sup> This helped to explain the unusual observation that the addition of Fe(III) does not affect the rate of DNA scission (entry 6), even though it has been demonstrated that superoxide alone is unable to cleave DNA and thus requires the presence of adventitious transition metals.<sup>41</sup> Finally, the authors noted that when monitoring DNA strand cleavage by gel electrophoresis, every cleavage band appeared as a doublet. This is characteristic of the generation of both 3'-phosphate and 3'-phosphoglycolate termini through Fenton-mediated cleavage by a non-selective diffusible oxidant such as a hydroxyl radical.

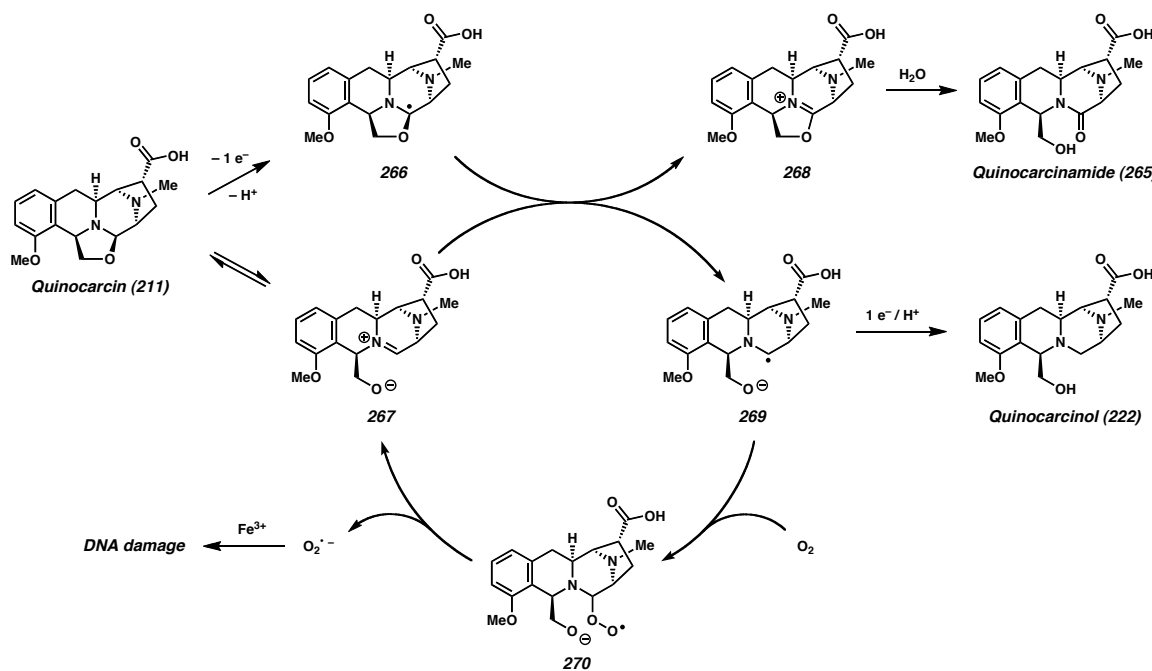
Table 3.4. Effect of additives on the cleavage of supercoiled plasmid DNA by quinocarcin and analogues



entry	substrate	additive	% inhibition	% enhancement
1	<b>211</b> (1 mM)	10 $\mu$ g/mL SOD	99	
2	<b>211</b> (1 mM)	100 $\mu$ g/mL catalase	83	
3	<b>211</b> (1 mM)	0.1 mM $H_2O_2$		143
4	<b>211</b> (1 mM)	10 mM picolinic acid	94	
5	<b>211</b> (1 mM)	5 mM DTT	98	
6	<b>211</b> (1 mM)	0.1 mM $NH_4Fe(SO_4)_2$	0	0
7	<b>262</b> (1 mM)	10 $\mu$ g/mL SOD	85	
8	<b>262</b> (1 mM)	100 $\mu$ g/mL catalase	65	
9	<b>262</b> (1 mM)	0.1 mM $H_2O_2$		19
10	<b>263</b> (1 mM)	10 $\mu$ g/mL SOD	0	0
11	<b>263</b> (1 mM)	100 $\mu$ g/mL catalase	3	
12	<b>263</b> (1 mM)	0.1 mM $H_2O_2$		95
13	<b>264</b> (1 mM)	10 $\mu$ g/mL SOD	83	
14	<b>264</b> (1 mM)	100 $\mu$ g/mL catalase	32	
15	<b>264</b> (1 mM)	0.1 mM $H_2O_2$		289

The observation that quinocarcin promotes DNA strand scission by forming superoxide is especially intriguing given that its molecular structure lacks functionality traditionally associated with radical formation (e.g., quinones, thiols). However, Williams *et al.* discovered that when quinocarcin is allowed to stand in deoxygenated deionized water at 25 °C under anaerobic conditions, two new products can be isolated—quinocarcinol (**222**), the product of reduction, and quinocarcinamide (**265**), the product of oxidation.<sup>37</sup> Based on these and previous observations,<sup>42</sup> the authors proposed a unifying mechanism for superoxide formation based primarily on a redox self-disproportion of quinocarcin similar to the Cannizarro reaction<sup>43</sup> (Scheme 3.2). However, unlike the Cannizarro disproportionation, which is believed to operate through a heterolytic two-electron mechanism, the authors invoke a single-electron process. Transfer of a single non-bonded electron from the oxazolidine nitrogen of quinocarcin (**211**) followed by deprotonation generates tertiary radical **266**. Oxidation of this radical by interaction with ring-opened iminium alkoxide **267** produces radical anion **269** and iminium **268**, the latter of which is then trapped by solvent water to furnish biologically inactive quinocarcinamide (**265**). Likewise, single electron transfer to radical anion **269** and subsequent protonation would yield the biologically inactive reduction product, quinocarcinol (**222**). However, under aerobic conditions, radical anion **269** would interact with molecular oxygen to produce peroxy radical **270**, which is capable of expelling superoxide to regenerate iminium alkoxide **267**. The superoxide thus produced would enter the Fenton/Haber–Weiss cycle, leading to the generation of reactive oxygen radicals and ultimately to the strand scission of DNA.

Scheme 3.2. Williams' proposed mechanism for superoxide formation via self-redox disproportionation of quinocarcin



### 3.2 PREVIOUS TOTAL SYNTHESSES OF QUINOCARCIN

The following sections detail the five completed total syntheses of quinocarcin—one racemic synthesis and four asymmetric syntheses of the natural enantiomer—reported prior to the communication of our own efforts. They are presented in chronological order.

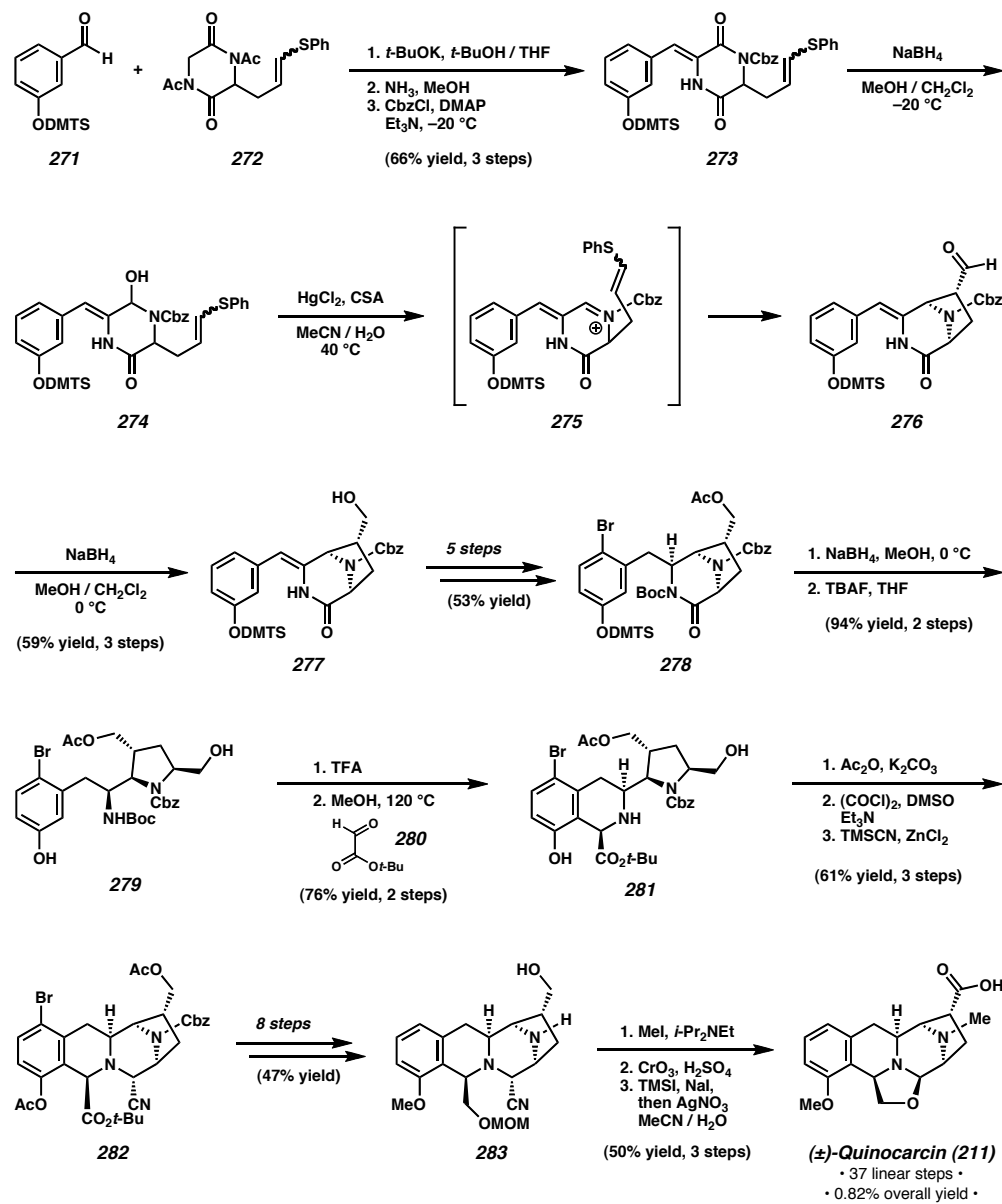
#### 3.2.1 Fukuyama's Synthesis of ( $\pm$ )-Quinocarcin

Five years after its isolation in 1983, the first total synthesis of quinocarcin was completed by Fukuyama and Nunes at Rice University.<sup>44</sup> With the discovery of DX-52-1 (243) one year prior,<sup>30</sup> the group sought to demonstrate the synthesis of quinocarcin (211)

via **243**, effectively devising routes toward both products in the process. Their synthesis began with the condensation of benzaldehyde **271** with diketopiperazine **272** (prepared from commercially available diethyl acetamidomalonate in seven steps and 39% overall yield), followed by ammonolysis of the acetyl groups and selective protection of the amide nitrogen to provide unsymmetrical diketopiperazine **273** (Scheme 3.3). Partial reduction of the activated amide generated carbinolamine **274** in preparation for a Lewis acid-catalyzed cyclization to construct diazabicycle **276** via acylium ion **275**. Reduction of the aldehyde then provided alcohol **277**, which was advanced through five additional steps to saturated intermediate **278**. Once again, reduction of the activated amide carbonyl was carried out to open the piperazinone ring, followed by desilylation to provide phenol **279**. Removal of the carbamate under acidic conditions revealed the primary amine necessary to perform a Pictet–Spengler cyclization upon addition of *tert*-butyl glyoxylate (**280**). Importantly, the aryl bromide blocks cyclization at the other ortho position, leading to the formation of a single tetrahydroisoquinoline isomer as an 8:1 mixture of diastereomers favoring the desired stereochemistry (**281**). Selective acetylation of the phenol was then followed by Swern oxidation of the remaining alcohol. Spontaneous cyclization of the resulting aldehyde effectively closed the piperazine ring to furnish an intermediate carbinolamine, which was converted to aminonitrile **282** via zinc-mediated Strecker addition. Over the next eight steps, reduction of the *tert*-butyl ester and removal of the aryl bromide, benzyl carbamate, and acetate protecting groups advanced this intermediate to amino alcohol **283**. Completion of the racemic natural product was then accomplished through methylation of the secondary amine, oxidation of the primary alcohol to a carboxylic acid, and removal of the methoxymethyl ether with

iodotrimethylsilane. This produced DX-52-1 (**243**) as an intermediate species, which underwent subsequent cyclization to form the oxazolidine ring when treated with silver nitrate. In full, the first total synthesis of  $(\pm)$ -quinocarcin (**211**) was accomplished in 37 linear steps and 0.82% overall yield.

Scheme 3.3. Fukuyama's synthesis of  $(\pm)$ -quinocarcin



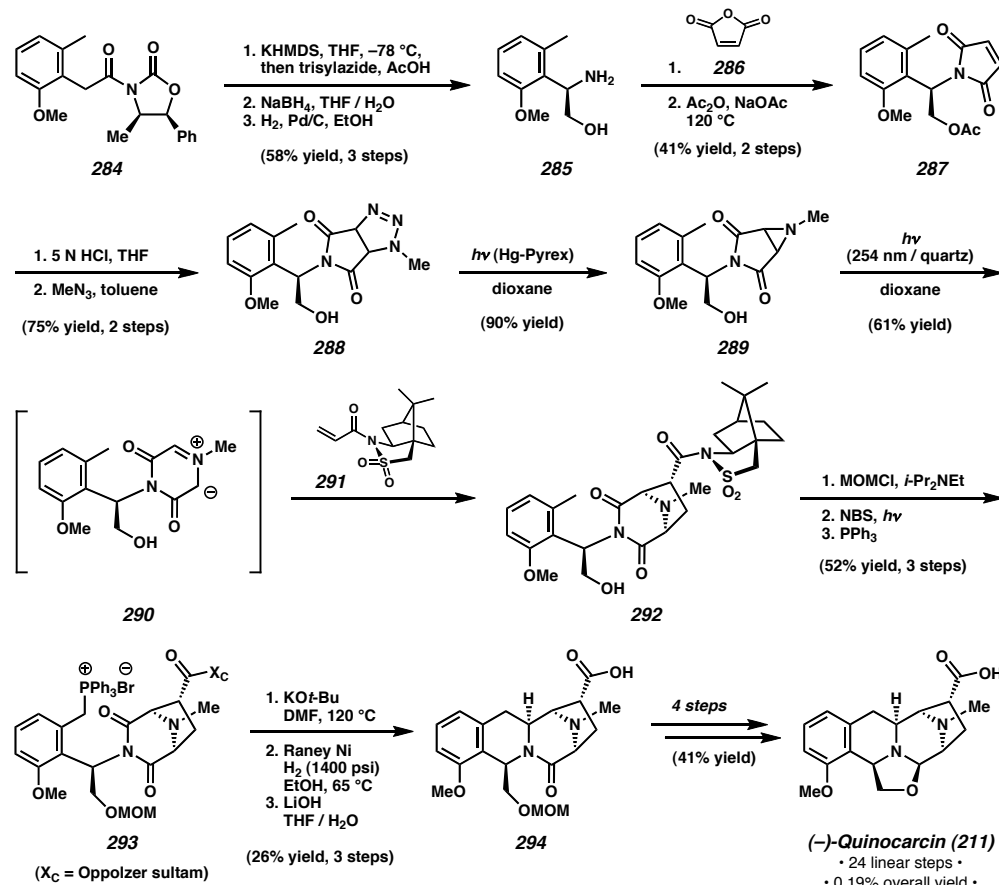
### 3.2.2 Garner's Synthesis of (–)-Quinocarcin

The first asymmetric total synthesis of quinocarcin was achieved in 1992 by Garner *et al.* at Case Western Reserve University.<sup>21</sup> Prior to their studies, the absolute configuration of quinocarcin had remained unknown, although computational models had suggested the enantiomer shown in Figure 3.4 would bind more favorably to DNA.<sup>35</sup> The group sought to construct the diazabicycle using an auxiliary-controlled dipolar cycloaddition with a photochemically generated azomethine ylide, a technique they had developed one year prior for this purpose.<sup>45</sup>

The synthesis began from chiral *N*-acyl oxazolidinone **284**, which was converted to amino alcohol **285** via asymmetric  $\alpha$ -azidation, reductive removal of the auxiliary, and reduction of the azide (Scheme 3.4). Condensation of the amine with maleic anhydride (**286**) produced an intermediate maleamic acid, which was heated in the presence of acetic anhydride to achieve both formation of the maleimide (**287**) and acetylation of the primary alcohol. Immediate removal of the acetyl group then preceded cycloaddition with methyl azide to generate triazoline **288**. When this compound was irradiated by a mercury lamp through a Pyrex filter, the triazoline decomposed through loss of nitrogen to form aziridine **289**. This intermediate was then further irradiated with UV light to generate azomethine ylide **290**, which underwent an auxiliary-controlled diastereoselective dipolar cycloaddition with the acrylamide of Oppolzer's sultam (**291**) to furnish diazabicycle **292** as a single diastereomer in 61% yield. Protection of the alcohol, radical benzylic bromination, and treatment with triphenyl phosphine then produced phosphonium bromide **293**. Heating this compound in the presence of a strong base resulted in a selective intramolecular olefination of one of the two imide carbonyls.

The authors ascribe the observed regioselectivity to a transition state that places the benzylic methine (rather than the  $\text{CH}_2\text{OMOM}$  group) in the plane of the imide such that the phosphine ylide approaches the *pro-R* imide carbonyl from the exo face. Hydrogenation of the newly formed olefin under forcing conditions was followed by saponification to remove the sultam auxiliary, yielding carboxylic acid **294**. This material was then advanced through four additional steps to (–)-quinocarcin (**211**). Comparing the optical rotation of this synthetic material to that of a natural sample confirmed the absolute stereochemistry of the natural product. In total, Garner’s asymmetric total synthesis was accomplished in 24 linear steps and 0.19% overall yield.

Scheme 3.4. Garner’s synthesis of (–)-quinocarcin



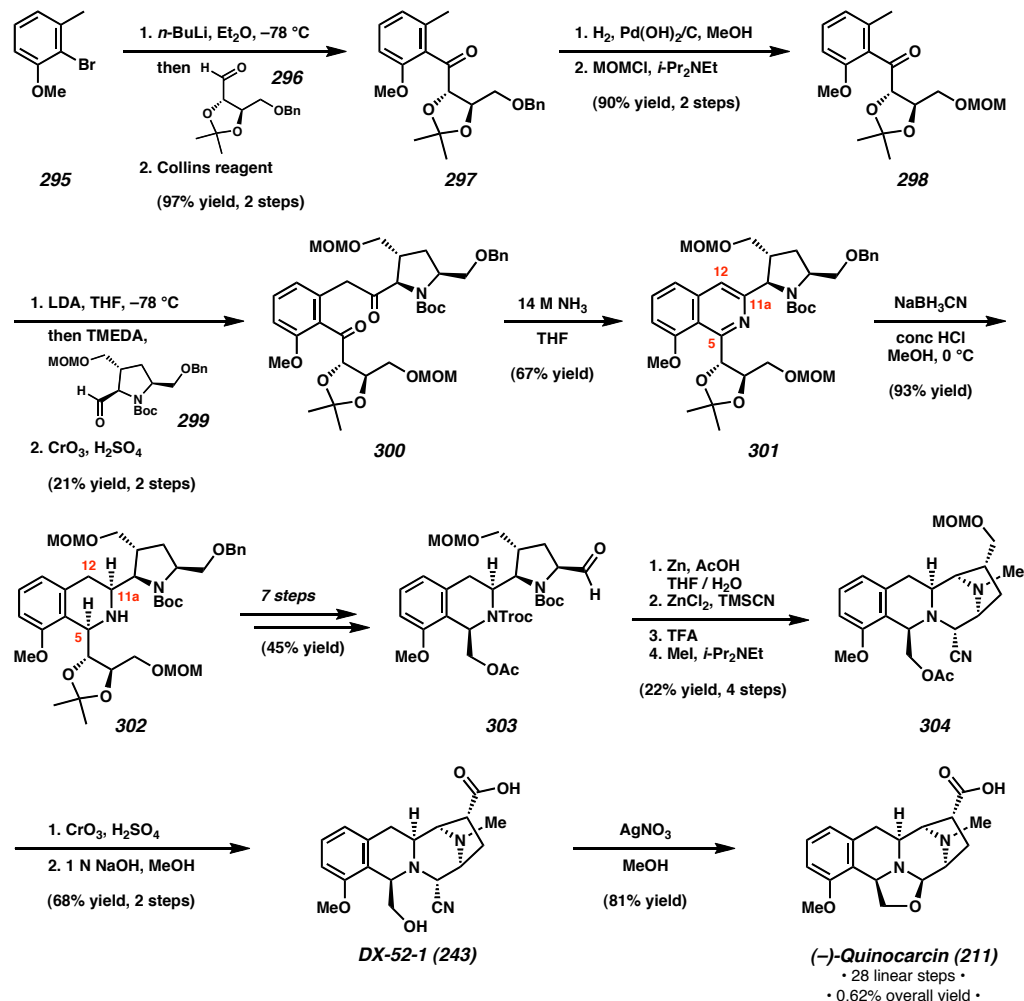
### 3.2.3 Terashima's Synthesis of (-)-Quinocarcin

In the 16 years following Garner's completion of (-)-quinocarcin, three additional asymmetric syntheses were achieved. The first of these was reported by Terashima *et al.* at the Sagami Chemical Research Center in Sagamihara, Japan, in 1994.<sup>46</sup> The total synthesis itself was part of a larger study aimed at the preparation of analogues designed to elucidate the structure-activity relationships displayed by quinocarcin *in vivo*.<sup>47</sup>

Beginning from 2-bromo-3-methylanisole (**295**), lithium-halogen exchange and addition to D-threose-derived aldehyde **296** delivered a benzylic alcohol, which was then oxidized to ketone **297** (Scheme 3.5). The benzyl ether was replaced by a methoxymethyl ether, after which the pyrrolidine fragment was introduced through the addition of aldehyde **299** to the extended enolate of **298**. Oxidation of the alcohol product then yielded diketone **300**, which was advanced to isoquinoline **301** through condensation with ammonia. Reduction of the isoquinoline was then accomplished using sodium cyanoborohydride. Due to the presence of the chiral dioxolane at C(5), initial reduction at this position was observed to be completely diastereoselective. Further reduction of the intermediate dihydroisoquinoline at the C(11a)–C(12) unsaturation proceeded from the same face to yield tetrahydroisoquinoline **302** in 93% yield as a single diastereomer. This material was advanced to aldehyde **303** through seven additional steps including removal of the acetonide and oxidative cleavage of the resulting diol, protection of the secondary amine, and two-step conversion of the benzyl ether to an aldehyde. Next, removal of the trichloroethyl carbamate revealed the secondary amine, which underwent addition to the proximal aldehyde to close the piperazine ring, producing an intermediate carbinolamine. Conversion to the aminonitrile

via Strecker addition, removal of the *tert*-butyl carbamate, and methylation then generated tetracycle **304**. Acidic hydrolysis of the methoxymethyl ether and oxidation of the resulting alcohol using Jones' reagent was followed by hydrolysis of the acetate protecting group to yield DX-52-1 (**243**). Finally, completion of the natural product was achieved through closure of the oxazolidine ring in the presence of silver nitrate, thus furnishing quinocarcin (**211**) in a total of 28 linear steps and 0.62% overall yield.

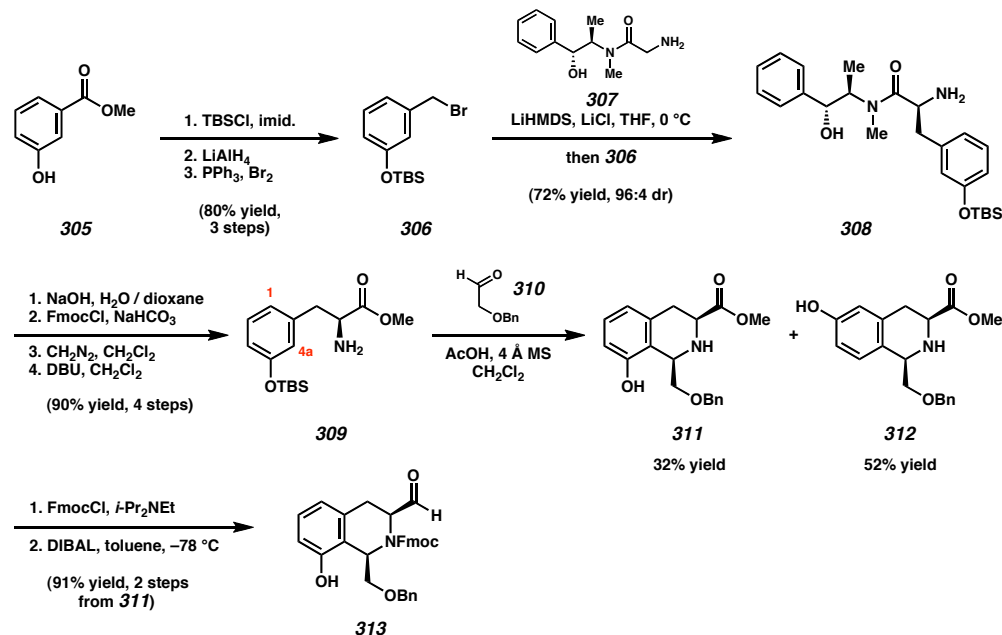
Scheme 3.5. Terashima's synthesis of (–)-quinocarcin



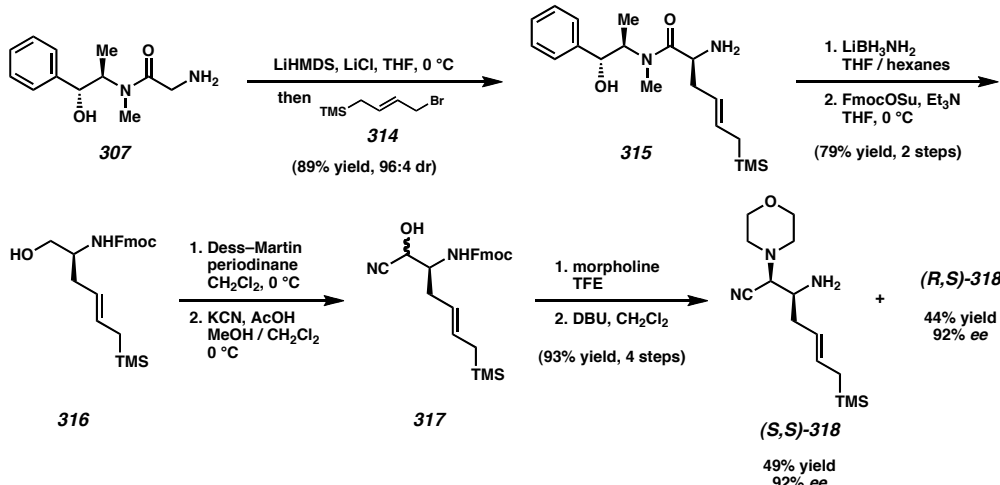
### 3.2.4 Myers' Synthesis of (–)-Quinocarcin

The next total synthesis of quinocarcin was reported 11 years after the completion of Terashima's work. This was accomplished by Myers *et al.* at Harvard University, as a demonstration of synthetic methodology they had previously applied toward the total synthesis of the related tetrahydroisoquinoline antitumor antibiotic, (–)-saframycin A<sup>48</sup> (**216**).<sup>49</sup> In particular, this approach featured the preparation of chiral  $\alpha$ -amino aldehyde equivalents using multiple auxiliary-mediated diastereoselective alkylations.

The synthesis of the tetrahydroisoquinoline ring system began from methyl 3-hydroxybenzoate (**305**), which was carried forward through silylation of the phenol, reduction of the ester, and conversion of the resulting alcohol to benzylic bromide **306** (Scheme 3.6). This electrophile was then used in an asymmetric alkylation of the enolate generated upon deprotonation of (*R,R*)-pseudoephedrine glycinate **307**, furnishing adduct **308** in 72% yield and 96:4 dr. The auxiliary was immediately removed by saponification, and the amine was temporarily protected as a fluorenyl carbamate in order to selectively methylate the carboxylate. Subsequent deprotection of the amine then provided amino ester **309**. A Pictet–Spengler condensation with benzyloxyacetaldehyde (**310**) was employed to construct the tetrahydroisoquinoline ring system. However, the presence of two nucleophilic ortho positions at C(1) and C(4a) of the arene resulted in the formation of two isomeric products—**311** and **312**—favoring attack from the less hindered ortho position at C(1) to form the undesired isomer (**312**) in greater yield. Despite this setback, the minor isomer was advanced through two additional steps to protected amino aldehyde **313**.

Scheme 3.6. Myers' synthesis of tetrahydroisoquinoline **313**

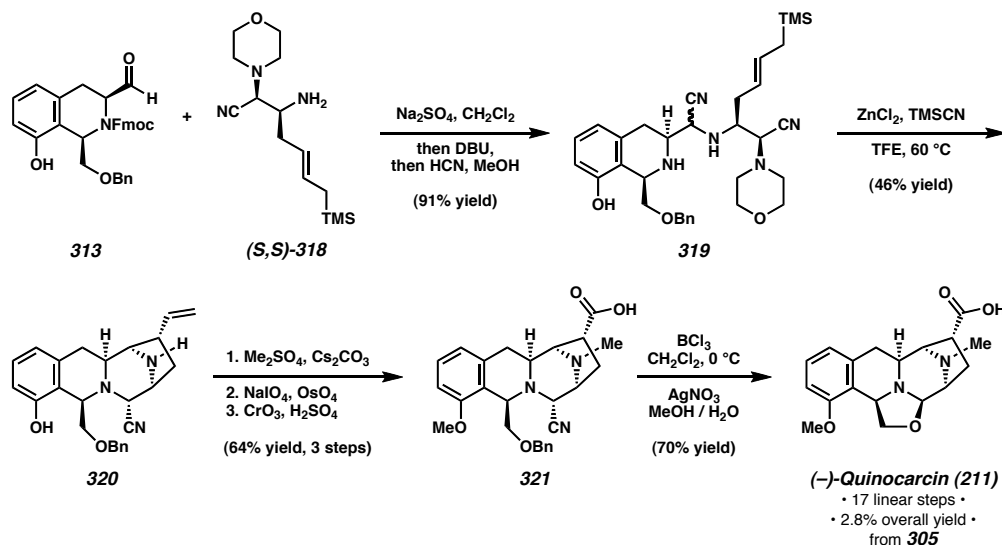
The synthesis of the left hand portion of quinocarcin began with the alkylation of a second equivalent of (*R,R*)-pseudoephedrine glycinamide **307** with allylic bromide **314** to provide allylic silane **315** in 89% yield and 96:4 dr (Scheme 3.7). Reduction of the amide and protection of the amine generated alcohol **316**, which underwent oxidation and conversion to a diastereomeric mixture of cyanohydrins (**317**). Finally, the hydroxyl group was exchanged for an equivalent of morpholine and the Fmoc protecting group was removed to furnish a mixture of diastereomeric aminonitriles—(*S,S*)-**318** and (*R,S*)-**318**—each in 92% *ee*.

Scheme 3.7. Myers' synthesis of aminonitrile **318**

With the precursors to the left and right halves of the molecule in hand, the fragments were condensed to form an intermediate imine, to which was added 1,8-diazabicyclo[5.4.0]undec-7-ene (DBU) to remove the Fmoc protecting group (Scheme 3.8). To this mixture was then added a methanolic solution of hydrogen cyanide, producing a mixture of diastereomeric bis-aminonitriles (**319**) via Strecker addition. In the key transformation, this mixture was exposed to  $\text{ZnCl}_2$  and  $\text{TMSCN}$  in trifluoroethanol, resulting in closure of the piperazine ring and cyclization of the allyl silane on to a transient iminium ion formed through loss of cyanide. The formation of two rings and four stereocenters thus furnished tetracycle **320** as a single diastereomer in 46% yield. Advancement of this intermediate through methylation of both the phenol and amine, oxidative cleavage of the terminal olefin, and further oxidation of the resulting aldehyde yielded carboxylic acid **321**. Treatment with boron trichloride effectively removed the benzyl ether to generate a small amount of quinocarcin in combination with the uncyclized aminonitrile, DX-52-1 (**243**). Exposure of this mixture

to silver nitrite then achieved full closure of the oxazolidine to yield quinocarcin (**211**) in an overall yield of 2.8% in 17 steps from methyl 3-hydroxybenzoate (**305**).

Scheme 3.8. Myers' completion of *(–)-quinocarcin*

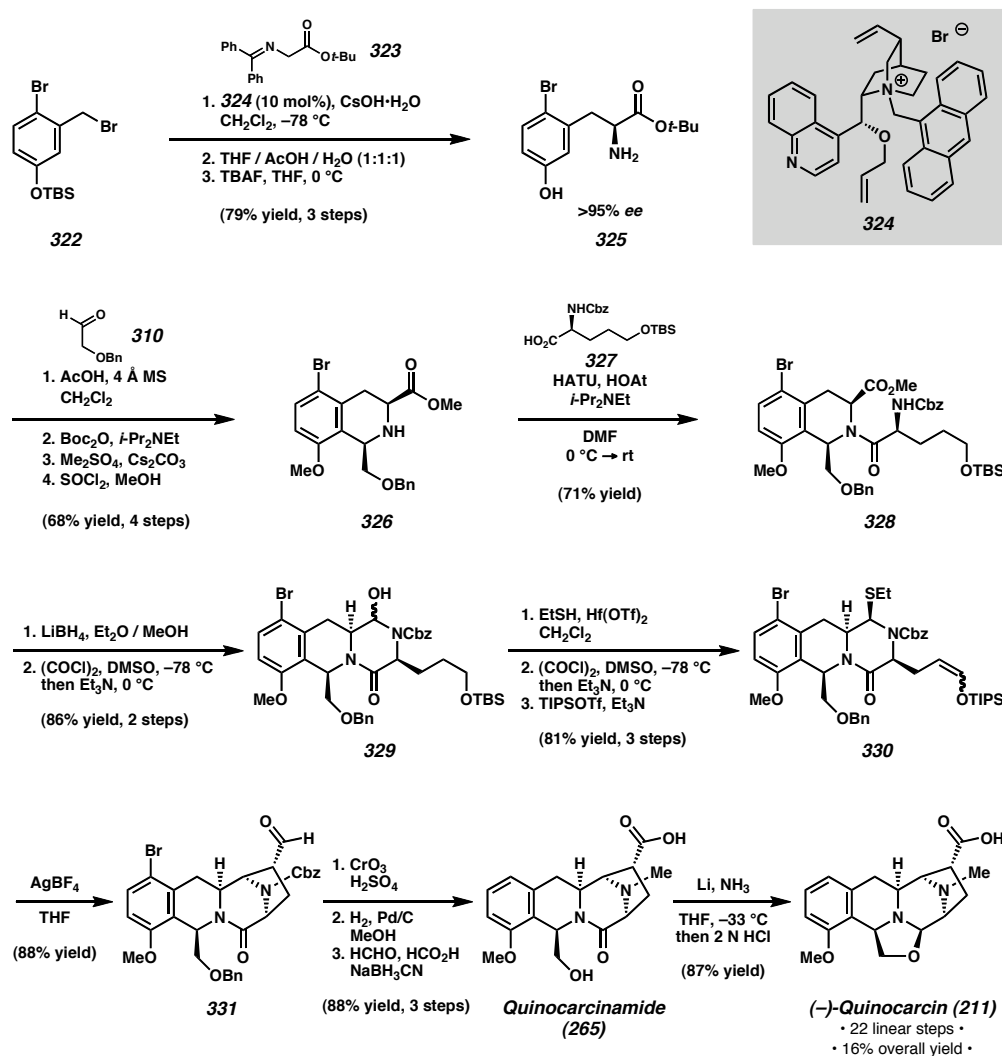


### 3.2.5 Zhu's Synthesis of *(–)-Quinocarcin*

The most recent asymmetric synthesis of *(–)-quinocarcin* was completed in early 2008 by Zhu *et al.* at the Centre National de la Recherche Scientifique (CNRS).<sup>50</sup> The synthetic route commenced with the asymmetric alkylation of a protected glycine derivative (**323**) using benzyl bromide **322** in the presence of the Corey–Lygo phase transfer catalyst (**324**) (Scheme 3.9).<sup>51,52</sup> Following hydrolysis of the imine, the *ee* and absolute configuration of the product were determined by analyzing the <sup>1</sup>H NMR chemical shifts of the corresponding *O*-methylmandelamide according to the method outlined by Trost.<sup>53</sup> The values obtained indicated the *de* of the mandelamide (and thus the *ee* of amine **325**) was higher than 95%.

Similar to previously developed synthetic routes,<sup>44,49</sup> a Pictet–Spengler condensation between amino ester **325** and benzyloxyacetaldehyde (**310**) was employed to assemble the tetrahydroisoquinoline. This was followed by temporary carbamoylation of the secondary amine, methylation of the phenol, and removal of the *tert*-butyl carbamate to provide tetrahydroisoquinoline **326**. The carbon framework of the eastern diazabicycle was introduced in the form of amino acid **327**, coupled with the amine to generate amide **328**. Ester reduction and oxidation of the resulting alcohol then provided an intermediate aldehyde, which underwent nucleophilic attack by the neighboring carbamate to form cyclic hemiaminal **329**. Treatment of this compound with thioethanol in the presence of  $\text{Hf}(\text{OTf})_2$  produced the more stable thioaminal while simultaneously removing the silyl ether. Swern oxidation, enolization, and trapping with  $\text{TiPSCl}$  then lead to silyl enol ether **330**. Using a strategy reminiscent of Fukuyama’s approach (cf., **274** → **276**, Scheme 3.3), construction of the bridged bicyclic was accomplished by treating the thioaminal with  $\text{AgBF}_4$ , producing a transient iminium ion that underwent cyclization with the silyl enol ether to furnish diazabicycle **331**. Oxidation of the newly formed aldehyde, hydrogenolysis, and reductive amination then provided quinocarcinamide (**265**). In the final step, partial reduction of the lactam under dissolving metal conditions generated an intermediate hemiaminal, which underwent dehydrative cyclization with the pendant alcohol upon the addition of 2 N  $\text{HCl}$  to form quinocarcin (**211**) in 87% yield. In total, Zhu’s synthetic route furnished the natural product in a total of 22 linear steps and an impressive 16% overall yield.

Scheme 3.9. Zhu's synthesis of (–)-quinocarcin

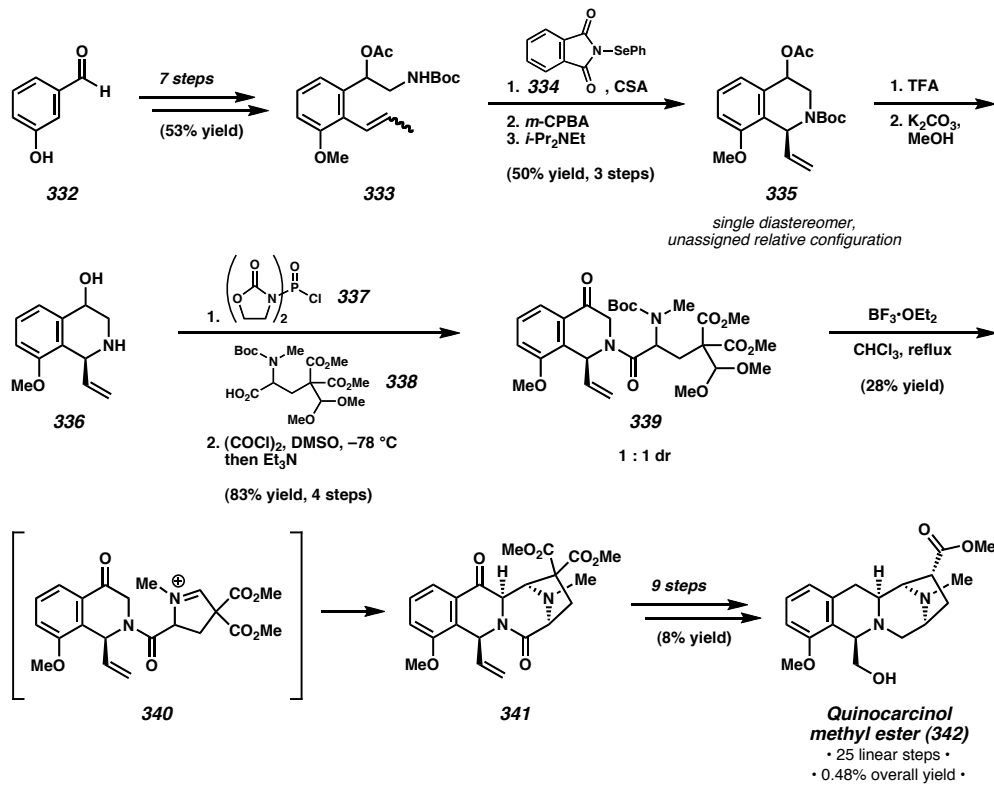


### 3.3 SYNTHETIC STUDIES TOWARD QUINOCARCIN

Although only five total syntheses of quinocarcin had been communicated prior to our own work, there have been several reports detailing approaches to various fragments of the natural product scaffold. The following section describes certain of these strategies in chronological order.

### 3.3.1 Danishefsky's Synthesis of ( $\pm$ )-Quinocarcinol Methyl Ester

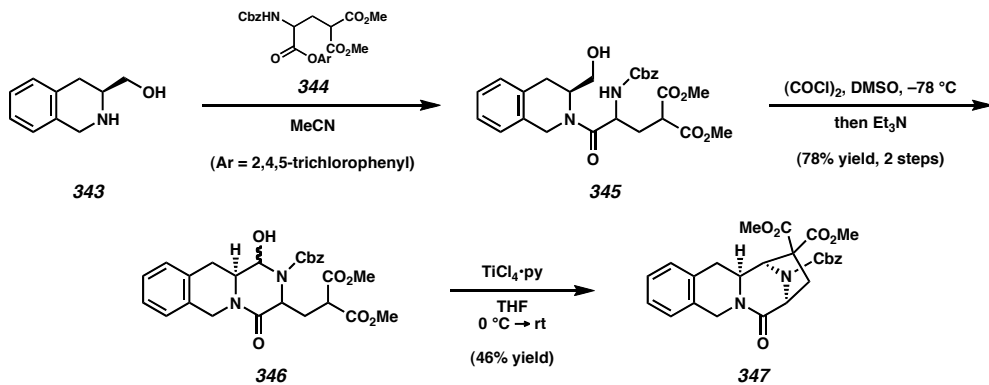
The earliest recorded approach to the core structure of quinocarcin was reported in 1985 by Danishefsky *et al.* at Yale University.<sup>54</sup> This group completed the racemic synthesis of quinocarcinol methyl ester (**342**), a biologically inactive analogue of quinocarcin that nonetheless bears all of the core atoms of the natural product (Scheme 3.10). The synthesis started from 3-hydroxybenzaldehyde (**332**), which was advanced through seven steps to amino styrene **333**. The tetrahydroisoquinoline ring system was closed through amino selenation of the olefin using *N*-phenylselenyl phthalimide (**334**) in the presence of camphor sulfonic acid. Oxidation of the selenide and elimination then provided vinyl tetrahydroisoquinoline **335**. Removal of the Boc and acetyl protecting groups readied this intermediate (**336**) for coupling with racemic amino acid **338**, after which Swern oxidation yielded ketone **339** as an equivalent mixture of diastereomers. In the key transformation, treatment with  $\text{BF}_3\text{-OEt}_2$  efficiently removed the Boc group and promoted cyclization of the secondary amine with the unmasked aldehyde to generate an iminium ion (**340**), which then underwent Mannich addition with the enolate of the proximal ketone to form tetracycle **341** in 28% yield. Although the yield is low, the authors note that this value represents a yield of 56% from the viable diastereomer. With the four rings in place, this material was advanced through nine additional steps to quinocarcinol methyl ester, resulting in an overall yield of 0.48% over 25 linear steps.

Scheme 3.10. Danishefsky's synthesis of ( $\pm$ )-quinocarcinol methyl ester

### 3.3.2 Hirata's Approach to the ABCD Ring System

Two years later, Saito and Hirata at Kyowa Hakko Kogyo Co. in Tokyo reported the construction of tetracycle **347**, a simplified version of the intermediate (**341**) employed in Danishefsky's approach (Scheme 3.11).<sup>55</sup> Beginning with amino alcohol **343** (prepared in enantioenriched form in three steps from L-phenylalanine<sup>56</sup>), condensation with 2,4,5-trichlorophenylester **344** produced amide **345**. Swern oxidation and cyclization with the neighboring carbamate generated a hemiaminal (**346**), which then underwent dehydrative cyclization with the pendant malonate in the presence of  $TiCl_4$ . In total, tetracycle **347** was assembled in 6 steps and 16% overall yield from L-phenylalanine.

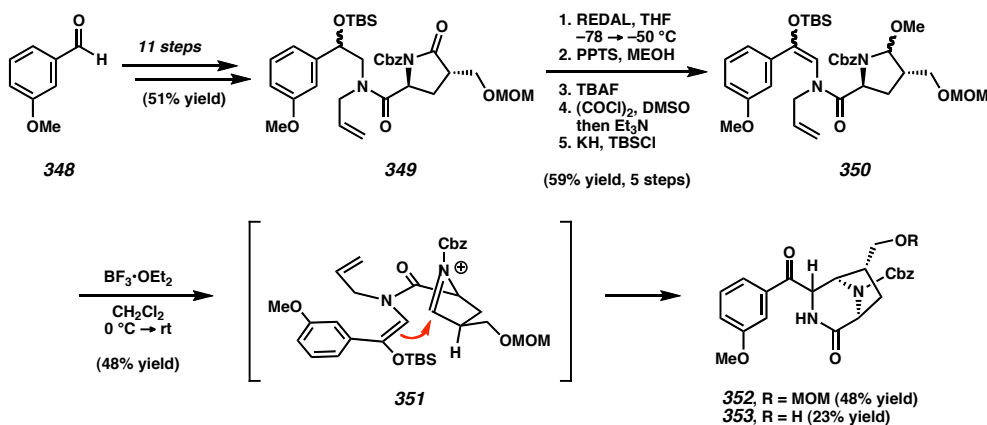
Scheme 3.11. Hirata's approach toward quinocarcin



### 3.3.3 Weinreb's Approach to the Diazabicyclic

In 1990, Weinreb *et al.* at Pennsylvania State University reported a strategy for the construction of the 3,8-diazabicyclo[3.2.1]octane utilizing a silyl enol ether-iminium addition similar to the Mannich addition employed previously by Danishefsky (cf., **339** → **341**, Scheme 3.10).<sup>57</sup> The starting material, 3-methoxybenzaldehyde (**348**), was advanced through 11 steps to pyrrolidone **349** (Scheme 3.12). Partial reduction of the lactam and subsequent trapping as the aminal was then followed by a three-step conversion of the benzylic silyl ether to a mixture of silyl enol ether isomers (**350**). Treatment with  $\text{BF}_3\text{-OEt}_2$  promoted loss of methanol to generate an intermediate iminium ion (**351**), which underwent nucleophilic addition of the silyl enol ether to furnish diazabicyclic **352** along with a small amount of the deprotected alcohol (**353**). Both compounds were isolated as 2:1 mixtures of unassigned epimers at the homobenzylic position.

Scheme 3.12. Weinreb's approach toward quinocarcin

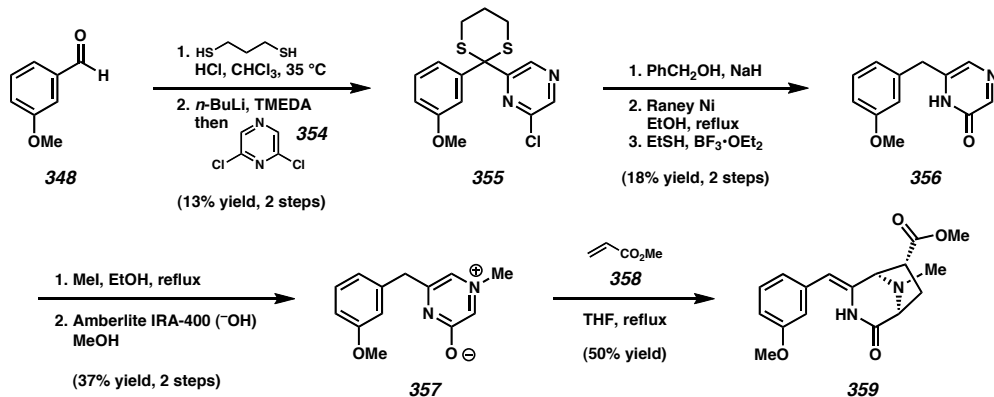


### 3.3.4 Joule's Approach to the Diazabicyclic

Between 1987 and 1990, Joule *et al.* at Manchester University developed a strategy for the construction of 3,8-diazabicyclo[3.2.1]octanes using a dipolar cycloaddition between oxidopyrazinium betaines and various electron-deficient dipolarophiles.<sup>58</sup> This approach was eventually applied toward the synthesis of diazabicyclic **359**, which constitutes three of the five rings of quinocarcin (Scheme 3.13).<sup>59</sup> 3-Methoxybenzaldehyde (**348**) was converted to a cyclic dithiane, which was deprotonated and used to displace one of the chloride atoms of 2,6-dichloropyrazine (**354**) to give rise to diaryl dithiane **355**. Displacement of the second chloride atom with benzyl alcohol followed by desulfurization and debenzylation then furnished pyrazinone **356**. Quaternization with methyl iodide provided an *N*-methyl pyrazinium salt, which formed the requisite betaine (**357**) upon deprotonation over anion exchange resin. A dipolar cycloaddition between this material and methyl acrylate (**358**) in refluxing THF efficiently constructed the eastern diazabicyclic, providing tricyclic **359**. The authors had shown previously that catalytic hydrogenation of similar species proceeds from the exo

face to provide the homobenzylic stereochemistry necessary for the synthesis of quinocarcin.<sup>58</sup>

Scheme 3.13. Joule's approach toward quinocarcin

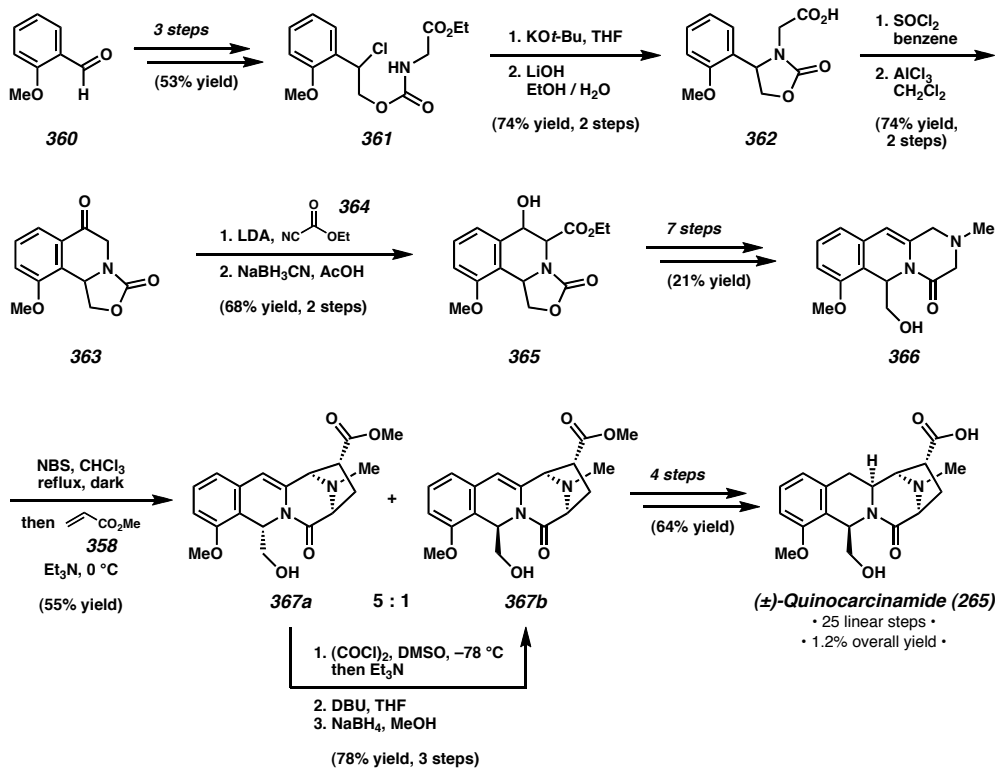


### 3.3.5 Williams' Synthesis of (±)-Quinocarcinamide

Beginning in the 1980s, the Williams group at Colorado State University became actively involved in studying the biological mechanism of action displayed by quinocarcin. In an effort to better understand this mechanism, they constructed simplified analogues to probe the effects of functionality and stereochemistry upon biological activity.<sup>42,60</sup> These studies eventually culminated in the synthesis of (±)-quinocarcinamide (**265**) in 1995,<sup>61</sup> constituting a formal racemic synthesis of quinocarcin due to Garner's earlier work.<sup>21</sup>

Williams' route toward quinocarcinamide commenced with *ortho*-anisaldehyde (**360**), which was advanced to chlorocarbamate **361** in three steps (Scheme 3.14). Displacement of the benzylic chloride and saponification provided oxazolidinone **362**, the pendant carboxylic acid of which was converted to an acid chloride. In the presence of AlCl<sub>3</sub>, this

intermediate underwent Friedel-Crafts acylation to form the tetrahydroisoquinoline ring system (**363**). Subsequent carboxylation with ethyl cyanoformate (**364**) and ketone reduction then yielded ester **365**, an intermediate key to the synthesis of several quinocarcin analogues examined by Williams *et al.*<sup>60</sup> For the purposes of quinocarcinamide, this compound was advanced to tricycle **366** through the introduction of a glycine subunit and subsequent cyclization to form the right-hand piperazinone. In order to assemble the diazabicycle, the authors developed a novel approach to the dipolar cycloaddition strategy previously employed by Joule<sup>58,59</sup> and Garner.<sup>21,45</sup> Treatment of tricycle **366** with *N*-bromosuccinimide resulted in bromination of the amine nitrogen followed by elimination of HBr and deprotonation to form an azomethine ylide, which participated in a dipolar cycloaddition with methyl acrylate (**358**) to form a mixture of diastereomeric diazabicycles (**367a** and **367b**) in 55% yield. Unfortunately, methyl acrylate favored approach from the less hindered face of the ylide opposite the benzylic CH<sub>2</sub>OH group, leading to a predominance of the undesired diastereomer (**367a**). In order to remedy this setback, alcohol **367a** was converted to **367b** in a three-step procedure consisting of Swern oxidation, epimerization, and reduction. With the polycyclic skeleton fully assembled, dihydroisoquinoline **367b** was carried forward in four steps to ( $\pm$ )-quinocarcinamide (**265**).

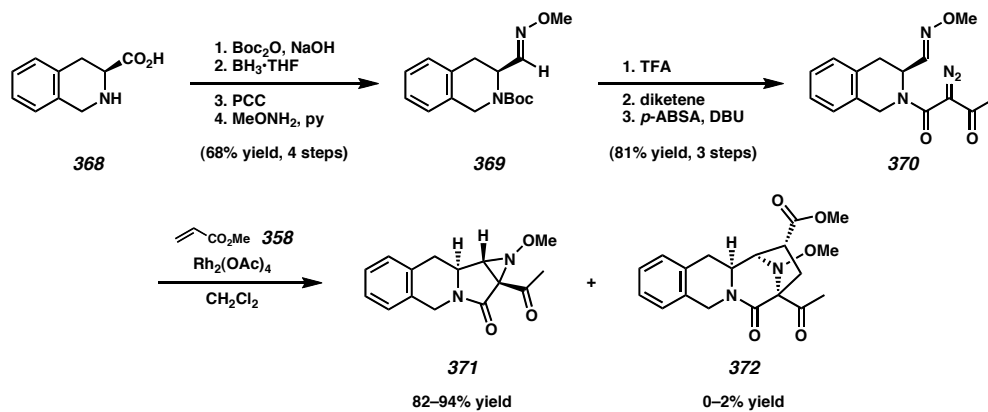
Scheme 3.14. Williams' synthesis of  $(\pm)$ -quinocarcinamide

### 3.3.6 McMills' Approach to the ABCD Ring System

By the mid-1990s, the use of a dipolar cycloaddition between an azomethine ylide and an acrylate derivative had become a popular method for the construction of the diazabicyclo[3.2.1]octane portion of quinocarcin. In 1996, McMills *et al.* at Ohio University developed a novel variation on this strategy in which the ylide species would be formed upon the addition of an oxime nitrogen to a rhodium carbenoid.<sup>62</sup> In order to test the feasibility of this approach,  $\alpha$ -diazo- $\beta$ -ketoamide **370** was assembled in six steps from commercially available tetrahydroisoquinoline **368** (Scheme 3.15). Amine protection, two-step conversion to the aldehyde, and treatment with methoxylamine provided oxime **369**, which further underwent Boc removal, addition to diketene, and

diazotization to generate the substrate. However, when  $\text{Rh}_2(\text{OAc})_4$  and methyl acrylate were added to this compound, the desired tetracycle (**372**) could only be isolated in trace quantities, while the bulk of the starting material was found to proceed to aziridine **371**. In fact, it was found that the aziridine was formed within 4–6 h simply upon standing at room temperature in the absence of catalyst. The authors report that investigations are underway to develop a photolytic opening of aziridine **371** in order to access synthetically useful azomethine ylide intermediates.

Scheme 3.15. McMills' approach toward quinocarcin



### 3.4 CONCLUSION

The tetrahydroisoquinoline antitumor antibiotics constitute a large family of structurally diverse alkaloids, many of which show promise as potential therapeutic agents for the clinical treatment of cancer. As an archetypal member of the 3,8-diazabicyclo[3.2.1]octane class within this family, quinocarcin has received a great deal of attention from scientific communities interested in both its fascinating chemical structure and its potent antitumor activity. Significant contributions made over the past

25 years have led to a better understanding of the biosynthetic origins and biological mechanisms of this important natural product. Furthermore, numerous synthetic approaches have been developed toward the construction of quinocarcin, and five of these have resulted in its total synthesis. At the commencement of our efforts, the shortest of these routes measured 17 linear steps from commercially available starting materials and the greatest overall yield achieved totaled 16%.

### 3.5 NOTES AND REFERENCES

- (1) For comprehensive review of the chemistry and biology of the tetrahydroisoquinoline antitumor antibiotics, see: Scott, J. D.; Williams, R. M. *Chem. Rev.* **2002**, *102*, 1669–1730.
- (2) Tomita, F.; Takahashi, K.; Shimizu, K. *J. Antibiot.* **1983**, *36*, 463–467.
- (3) Suzuki, K.; Sato, T.; Morioka, M.; Nagai, K.; Abe, K.; Yamaguchi, H.; Saito, T. *J. Antibiot.* **1991**, *44*, 479–485.
- (4) Whaley, H. A.; Patterson, E. L.; Dann, M.; Shay, A. J.; Porter, J. N. *Antimicrob. Agents Chemother.* **1964**, *8*, 83–86.
- (5) Kluepfel, D.; Baker, H. A.; Piattoni, S. N.; Sehgal, S. N.; Sidorowicz, A.; Singh, K.; Vézina, C. *J. Antibiot.* **1975**, *28*, 497–502.
- (6) For the first observation of cyanonaphthyridinomycin (cyanocycline A) through treatment of naphthyridinomycin with sodium cyanide, see: Zmijewski, M. J., Jr.; Goebel, M. *J. Antibiot.* **1982**, *35*, 524–526.
- (7) For the natural isolation of cyanocycline A, see: Hayashi, T.; Noto, T.; Nawata, Y.; Okazaki, H.; Sawada, M.; Ando, K. *J. Antibiot.* **1982**, *35*, 771–777.
- (8) (a) Bernan, V. S.; Montenegro, D. A.; Korshalla, J. D.; Maiese, W. M.; Steinberg, D. A.; Greenstein, M. *J. Antibiot.* **1994**, *47*, 1417–1424. (b) Zaccardi, J.; Alluri, M.; Ashcroft, J.; Bernan, V.; Korshalla, J. D.; Morton, G. O.; Siegel, M.; Tsao, R.; Williams, D. R.; Maiese, W.; Ellestad, G. A. *J. Org. Chem.* **1994**, *59*, 4045–4047.
- (9) (a) Tanida, S.; Hasegawa, T.; Muroi, M.; Higashide, E. *J. Antibiot.* **1980**, *33*, 1443–1448. (b) Muroi, M.; Tanida, S.; Asai, M.; Kishi, T. *J. Antibiot.* **1980**, *33*,

1499–1456. (c) Hida, T.; Muroi, M.; Tanida, S.; Harada, S. *J. Antibiot.* **1994**, *47*, 917–921.

(10) Gang, S.; Ohta, S.; Chiba, H.; Johdo, O.; Nomura, H.; Nagamatsu, Y.; Yoshimoto, A. *J. Antibiot.* **2001**, *54*, 304–307.

(11) (a) Arai, T.; Takahashi, K.; Kubo, A. *J. Antibiot.* **1977**, *30*, 1015–1018. (b) Arai, T.; Takahashi, K.; Ishiguro, K.; Yazawa, K. *J. Antibiot.* **1980**, *33*, 951–960. (c) Asaoka, T.; Yazawa, K.; Mikami, Y.; Arai, T.; Takahashi, K. *J. Antibiot.* **1982**, *35*, 1708–1710. (d) Yazawa, K.; Takahashi, K.; Mikami, Y.; Arai, T.; Saito, N.; Kubo, A. *J. Antibiot.* **1986**, *39*, 1639–1650. (e) Mikami, Y.; Takahashi, K.; Yazawa, K.; Hour-Young, C.; Arai, T.; Saito, N.; Kubo, A. *J. Antibiot.* **1988**, *41*, 734–740. (f) Trowitzsch-Kienast, W.; Irschik, H.; Reichenbach, H.; Wray, V.; Höfle, G. *Liebigs Ann. Chem.* **1988**, 475–481. (g) Irschik, H.; Trowitzsch-Kienast, W.; Gerth, K.; Höfle, G.; Reichenbach, H. *J. Antibiot.* **1988**, *41*, 993–998.

(12) (a) Ikeda, Y.; Idemoto, H.; Hirayama, F.; Yamamoto, K.; Iwao, K.; Asao, T.; Munakata, T. *J. Antibiot.* **1983**, *36*, 1279–1283. (b) Ikeda, Y.; Matsuki, H.; Ogawa, T.; Munakata, T. *J. Antibiot.* **1983**, *36*, 1284–1289.

(13) (a) Frincke, J. M.; Faulkner, D. J. *J. Am. Chem. Soc.* **1982**, *104*, 265–269. (b) He, H. Y.; Faulkner, D. J. *J. Org. Chem.* **1989**, *54*, 5822–5824. (c) Davidson, B. S. *Tetrahedron Lett.* **1992**, *33*, 3721–3724.

(14) Parameswaran, P. S.; Naik, C. G.; Kamat, S. Y.; Pramanik, B. N. *Ind. J. Chem.* **1998**, *37B*, 1258–1263.

(15) The originally assigned structure of renieramycin H was called into question when a similar alkaloid was isolated from *Cribrochalina* sp. The structure of renieramycin H was later revised to that of cibrostatin 4, see: (a) Pettit, G. R.; Knight, J. C.; Collins, J. C.; Herald, D. L.; Pettit, R. K.; Boyd, M. R.; Young, V. G. *J. Nat. Prod.* **2000**, *63*, 793–798. (b) Saito, N.; Sakai, H.; Suwanborirux, K.; Pummangura, S.; Kubo, A. *Heterocycles* **2001**, *55*, 21–28.

(16) (a) Rinehart, K. L.; Holt, T. G.; Fregeau, N. L.; Stroh, J. G.; Keifer, P. A.; Sun, F.; Li, L. H.; Martin, D. G. *J. Org. Chem.* **1990**, *55*, 4512–4515. (b) Rinehart, K. L.; Holt, T. G.; Fregeau, N. L.; Stroh, J. G.; Keifer, P. A.; Sun, F.; Li, L. H.; Martin, D. G. *J. Org. Chem.* **1991**, *56*, 1676. (c) Sakai, R.; Rinehart, K. L.; Guan, Y.; Wang, A. H. *Proc. Natl. Acad. Sci.* **1992**, *89*, 11456–11460. (d) Sakai, R.; Jares-Erijman, E. A.; Manzanares, I.; Elipe, M. V. S.; Rinehart, K. L. *J. Am. Chem. Soc.* **1996**, *118*, 9017–9023.

(17) Takebayashi, Y.; Pourquier, P.; Zimonjic, D. B.; Nakayama, K.; Emmert, S.; Ueda, T.; Urasaki, Y.; Kanzaki, A.; Akiyama, S.; Popescu, N.; Kraemer, K. H.; Pommier, Y. *Nat. Med.* **2001**, *7*, 961–966.

(18) Zewail-Foote, M.; Li, V.; Kohn, H.; Bearss, D.; Guzman, M.; Hurley, L. H. *Chem. Biol.* **2001**, *135*, 1–17.

(19) Takahashi, K.; Tomita, F. *J. Antibiot.* **1983**, *36*, 468–470.

(20) Hirayama, N.; Shirahata, K. *J. Chem. Soc., Perkin Trans. II* **1983**, 1705–1708.

(21) (a) Garner, P.; Ho, W. B.; Shin, H. *J. Am. Chem. Soc.* **1992**, *114*, 2767–2768. (b) Garner, P.; Ho, W. B.; Shin, H. *J. Am. Chem. Soc.* **1993**, *115*, 10742–10753.

(22) Mikami, Y.; Takahashi, K.; Yazawa, K.; Arai, T.; Namikoshi, M.; Iwasaki, S.; Okuda, S. *J. Biol. Chem.* **1985**, *260*, 344–348.

(23) Arai, T.; Yazawa, K.; Takahashi, K.; Maeda, A.; Mikami, Y. *Antimicrob. Agents Chemother.* **1985**, *28*, 5–11.

(24) Zmijewski, M. J., Jr.; Mikolajczak, M.; Viswanatha, V.; Hruby, V. J. *J. Am. Chem. Soc.* **1982**, *104*, 4969–4971.

(25) (a) Zmijewski, M. J., Jr. *J. Antibiot.* **1985**, *38*, 819–820. (b) Zmijewski, M. J., Jr.; Palaniswamy, V. P.; Gould, S. J. *J. Chem. Soc., Chem. Commun.* **1985**, 1261–1262.

(26) Fujimoto, K.; Oka, T.; Morimoto, M. *Cancer Res.* **1987**, *47*, 1516–1522.

(27) Inaba, S.; Shimoyama, M. *Cancer Res.* **1988**, *48*, 6029–6032.

(28) Chiang, C.; Kanzawa, F.; Matsushima, Y.; Nakano, H.; Nakagawa, K.; Tasahashi, H.; Terada, M.; Morinaga, S.; Tsuchiya, R.; Sasaki, Y.; Saijo, N. *J. Pharmacobiodyn.* **1987**, *10*, 431–435.

(29) Inoue, S.; Kubota, T.; Ohishi, T.; Kuzuoka, M.; Oka, S.; Shimoyama, Y.; Kikuyama, S.; Ishibiki, K.; Abe, O. *Keio J. Med.* **1988**, *37*, 355–364.

(30) (a) Saito, H.; Kobayashi, S.; Uosaki, Y.; Sato, A.; Fujimoto, K.; Miyoshi, K.; Ashizawa, T.; Morimoto, M.; Hirata, T. *Chem. Pharm. Bull.* **1990**, *38*, 1278–1285. (b) Saito, H.; Sato, A.; Ashizawa, T.; Morimoto, M.; Hirata, T. *Chem. Pharm. Bull.* **1990**, *38*, 3202–3210. (c) Saito, H.; Hirata, T.; Kasai, M.;

Fujimoto, K.; Ashizawa, T.; Morimoto, M.; Sato, A. *J. Med. Chem.* **1991**, *34*, 1959–1966.

(31) (a) Plowman, J.; Narayanan, V. L.; Abbott, B. J.; Inoue, K.; Hirata, T.; Grever, M. R. *Proc. Am. Assoc. Cancer Res.* **1993**, *34*, 368. (b) Plowman, J.; Dykes, D. J.; Narayanan, V. L.; Abbott, B. J.; Saito, H.; Hirata, T.; Grever, M. R. *Cancer Res.* **1995**, *55*, 862–867.

(32) Tomita, F.; Takahashi, K.; Tamaoki, T. *J. Antibiot.* **1984**, *37*, 1268–1272.

(33) Zmijewski, M. J., Jr.; Miller-Hatch, K.; Mikolajczak, M. *Chem.-Biol. Interact.* **1985**, *52*, 361–375.

(34) (a) Ishiguro, K.; Takahashi, K.; Yazawa, K.; Sakiyama, S.; Arai, T. *J. Biol. Chem.* **1981**, *256*, 2162–2167. (b) Lown, J. W.; Joshua, A. V.; Lee, J. S. *Biochemistry* **1982**, *21*, 419–428.

(35) Hill, G. C.; Wunz, T. P.; Remers, W. A. *J. Comput.-Aided Mol. Des.* **1988**, *2*, 91–106.

(36) Flanagan, M. E.; Rollins, S. E.; Williams, R. M. *Chem. Biol.* **1995**, *2*, 147–156.

(37) Williams, R. M.; Glinka, T.; Flanagan, M. E.; Gallegos, R.; Coffman, H.; Pei, D. *J. Am. Chem. Soc.* **1992**, *114*, 733–740.

(38) (a) Fenton, H. J. H. *J. Chem. Soc., Trans.* **1894**, *65*, 899–911. (b) Goldstein, S.; Meyerstein, D.; Czapski, G. *Free Rad. Biol. Med.* **1993**, *15*, 435–445.

(39) Haber, H.; Weiss, J. *Naturwiss.* **1932**, *51*, 948–950.

(40) Lesko, S. A.; Lorentzen, R. J.; Ts'o, P. O. P. *Biochemistry* **1980**, *19*, 3023–3028.

(41) Sutton, H. C.; Winterbourn, C. C. *Free Radical Biol. Med.* **1989**, *6*, 53–60.

(42) Williams, R. M.; Glinka, T.; Gallegos, R.; Ehrlich, P. P.; Flanagan, M. E.; Coffman, H.; Park, G. *Tetrahedron* **1991**, *47*, 2629–2642.

(43) Cannizarro, S. *Justus Liebigs Ann. Chem.* **1853**, *88*, 129–130.

(44) Fukuyama, T.; Nunes, J. J. *J. Am. Chem. Soc.* **1988**, *110*, 5196–5198.

(45) Garner, P.; Ho, W. B.; Grandhee, S. K.; Youngs, W. J.; Kennedy, V. O. *J. Org. Chem.* **1991**, *56*, 5893–5903.

(46) For the total synthesis of (–)-quinocarcin, see: Katoh, T.; Kirihsara, M.; Nagata, Y.; Kobayashi, Y.; Arai, K.; Minami, J.; Terashima, S. *Tetrahedron* **1994**, *50*, 6239–6258.

(47) For studies toward quinocarcin and the preparation of synthetic derivatives, see:  
(a) Saito, S.; Tamura, O.; Kobayashi, Y.; Matsuda, F.; Katoh, T.; Terashima, S. *Tetrahedron* **1994**, *50*, 6193–6208. (b) Saito, S.; Tanaka, K.; Nakatani, K.; Matsuda, F.; Katoh, T.; Terashima, S. *Tetrahedron* **1994**, *50*, 6209–6220. (c) Katoh, T.; Nagata, Y.; Kobayashi, Y.; Arai, K.; Minami, J.; Terashima, S. *Tetrahedron* **1994**, *50*, 6221–6238. (d) Katoh, T.; Kirihsara, M.; Yoshino, T.; Tamura, O.; Ikeuchi, F.; Nakatani, K.; Matsuda, F.; Yamada, K.; Gomi, K.; Ashizawa, T.; Terashima, S. *Tetrahedron* **1994**, *50*, 6259–6270.

(48) Myers, A. G.; Kung, D. W. *J. Am. Chem. Soc.* **1999**, *121*, 10828–10829.

(49) Kwon, S.; Myers, A. G. *J. Am. Chem. Soc.* **2005**, *127*, 16796–16797.

(50) Wu, Y.-C.; Liron, M.; Zhu, J. *J. Am. Chem. Soc.* **2008**, *130*, 7148–7152.

(51) Corey, E. J.; Xu, F.; Noe, M. C. *J. Am. Chem. Soc.* **1997**, *119*, 12414–12415.

(52) (a) Lygo, B.; Wainwright, P. G. *Tetrahedron Lett.* **1997**, *38*, 8595–8598. (b) Lygo, B.; Andrews, B. I. *Acc. Chem. Res.* **2004**, *37*, 518–525.

(53) Trost, B. M.; Bunt, R. C.; Pulley, S. R. *J. Org. Chem.* **1994**, *59*, 4202–4205.

(54) Danishefsky, S. J.; Harrison, P. J.; Webb, R. R., II; O'Neill, B. T. *J. Am. Chem. Soc.* **1985**, *107*, 1421–1423.

(55) Saito, H.; Hirata, T. *Tetrahedron Lett.* **1987**, *28*, 4065–4068.

(56) Yamada, S.; Kunieda, T. *Chem. Pharm. Bull.* **1967**, *15*, 490–498.

(57) Lessen, T. A.; Demko, D. M.; Weinreb, S. M. *Tetrahedron Lett.* **1990**, *31*, 2105–2108.

(58) Kiss, M.; Russell-Maynard, J.; Joule, J. A. *Tetrahedron Lett.* **1987**, *28*, 2187–2190.

(59) Allway, P. A.; Sutherland, J. K.; Joule, J. A. *Tetrahedron Lett.* **1990**, *31*, 4781–4782.

(60) Williams, R. M.; Ehrlich, P. P.; Zhai, W.; Hendrix, J. *J. Org. Chem.* **1987**, *52*, 2615–2617.

(61) Flanagan, M. F.; Williams, R. M. *J. Org. Chem.* **1995**, *60*, 6791–6797.

(62) McMills, M. C.; Wright, D. L.; Zubkowski, J. D.; Valente, E. J. *Tetrahedron Lett.* **1996**, 37, 7205–7208.

# CHAPTER 4

## *A Concise Total Synthesis of (–)-Quinocarcin via Aryne Annulation*

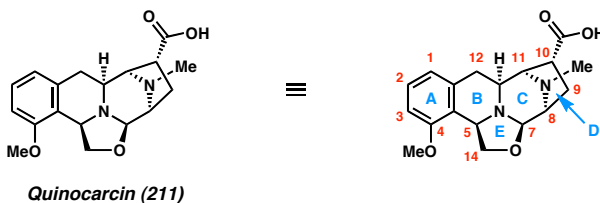
### 4.1 INTRODUCTION

#### 4.1.1 *Structure and Synthetic Challenges*

Quinocarcin (**211**) provides a formidable challenge to the chemist pursuing its total synthesis (Figure 4.1).<sup>1,2</sup> Possessing a total of six stereocenters set within a densely packed pentacyclic framework, this alkaloid represents the quintessential core structure of the 3,8-diazabicyclo[3.2.1]octane subclass. Fifteen carbon atoms make up the scaffold of quinocarcin, while two basic amines, a carboxylic acid, a trisubstituted arene, and an oxazolidine ring comprise the remaining functionality. This intriguing structure, coupled with an extensive list of anticancer properties,<sup>3</sup> has made quinocarcin a popular target within the chemical community. In the 27 years following its isolation, numerous synthetic approaches have been devised,<sup>4</sup> five of which have yielded the completed natural product.<sup>5,6</sup> In total, these routes have measured between 17 and 37 steps in length, providing quinocarcin in 0.2–16% overall yield. When we entered this forum, we had recently completed the total synthesis of (–)-lemonomycin,<sup>7,8</sup> a related member of the

tetrahydroisoquinoline family. Seeking to combine the strategies we had devised during that synthesis with our recently developed aryne technology, we undertook efforts toward (–)-quinocarcin. The following chapter details our work in this regime, which has produced the shortest total synthesis of this biologically important alkaloid yet reported.<sup>9</sup>

Figure 4.1. Quinocarcin

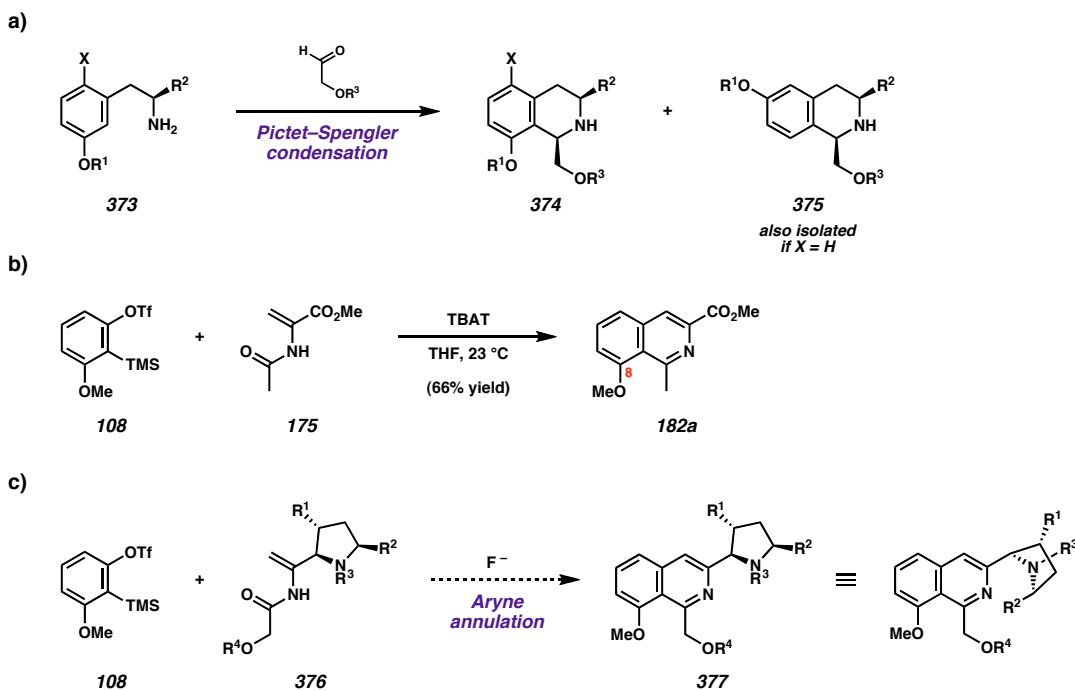


#### 4.1.2 Outline of Approach

Our primary goal in designing a synthetic route toward quinocarcin was to utilize our recently developed aryne annulation technology<sup>10</sup> for the preparation of an isoquinoline intermediate en route to the core of the natural product. We considered this a novel strategy given that three of the previous five syntheses had employed a Pictet–Spengler condensation to close the tetrahydroisoquinoline (Scheme 4.1a).<sup>5,6d,e</sup> While effective, this latter approach requires the installation of a blocking group (X) at one of the two ortho positions of the  $\beta$ -arylethylamine (**373**) in order to avoid the formation of isomeric products (**374** and **375**).<sup>6d</sup> In contrast, our aryne annulation reaction proceeds with a high degree of regioselectivity, generating 8-methoxyisoquinoline **182a** in good yield from readily available dehydroamino ester **175** and ether-substituted *ortho*-silyl aryl triflate **108** (Scheme 4.1b). Based on this result, we envisioned a synthetic approach to quinocarcin that would take advantage of this same aryne precursor in conjunction with a

functionalized *N*-acyl enamine (**376**) bearing the D-ring pyrrolidine of the natural product (Scheme 4.1c). If successful, this reaction would generate a tricyclic isoquinoline (**377**) comprising the entire carbon framework of quinocarcin. From this point, advancement to the natural product would be a matter of isoquinoline reduction and closure of the two remaining rings. In comparison to previous syntheses of quinocarcin, we anticipated that a convergent approach utilizing our aryne annulation methodology as the key bond-forming step would enable a much shorter overall synthetic route.

*Scheme 4.1. a) Pictet–Spengler condensation. b) Regioselective aryne annulation. c) Aryne annulation approach to an isoquinoline intermediate en route to quinocarcin.*

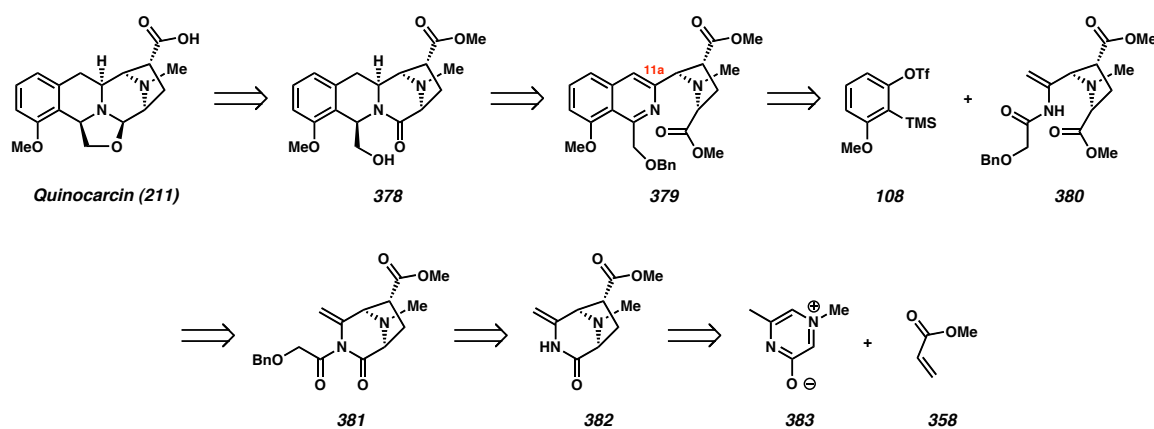


## 4.2 FIRST GENERATION APPROACH

### 4.2.1 Retrosynthetic Analysis

In our retrosynthetic analysis of quinocarcin (**211**), we recognized the need for late-stage installation of the sensitive carboxylic acid and oxazolidine functionality (Scheme 4.2). Thus, the natural product was envisioned to arise through redox manipulation and ring closure of a tetracyclic ester such as **378**. As it was ultimately our goal to employ our aryne methodology in the key bond-forming step, this intermediate was further simplified to an isoquinoline (**379**) bearing a trisubstituted pyrrolidine ring appended at C(11a). By invoking an aryne annulation disconnect, this compound was divided in two to reveal 3-methoxy-2-(trimethylsilyl)phenyl triflate (**108**) and *N*-acyl enamine **380**. While preparation of the former substrate is known, the latter was anticipated to derive from selective lactam methanolysis of imide **381**. Further simplification then led back to diazabicycle **382**, a compound we recognized from our previous studies as arising from a dipolar cycloaddition between oxidopyrazinium dipole **383** and methyl acrylate (**358**).

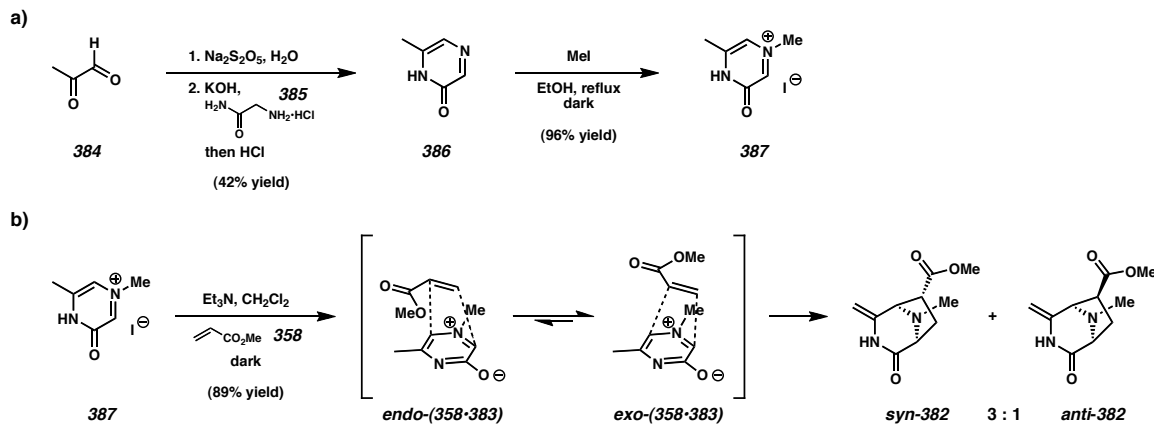
Scheme 4.2. Retrosynthetic analysis of quinocarcin



#### 4.2.2 Dipolar Cycloaddition and Advancement to the N-Acyl Enamine

We began our efforts toward the synthesis of quinocarcin by preparing *N*-methyl oxidopyrazinium iodide **387** (Scheme 4.3a). According to a procedure originally developed by Jones<sup>11</sup> and later modified by Meltzer *et al.*,<sup>12</sup> pyruvaldehyde (**384**) was condensed with glycinamide hydrochloride (**385**) under basic conditions to produce pyrazinone **386**. Although the yield is modest, the ready availability of the starting materials has enabled the preparation of up to 50 g of pyrazinone **386**. Following this, alkylation with methyl iodide furnished *N*-methyl oxidopyrazinium iodide **387**, the substrate for the upcoming dipolar cycloaddition.

Scheme 4.3. a) Synthesis of *N*-methyl oxidopyrazinium iodide **387**. b) Dipolar cycloaddition.

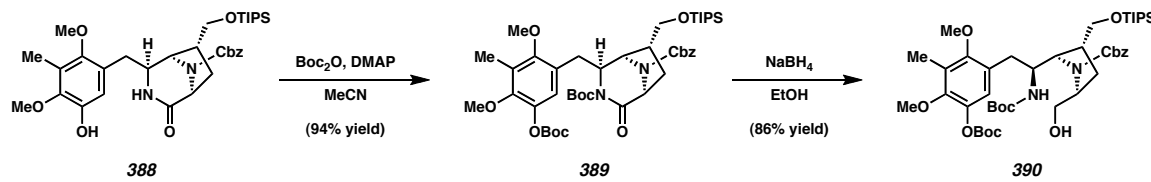


When treated with an amine base such as triethylamine, the oxidopyrazinium salt (**387**) undergoes deprotonation to form the active dipole (**383**) *in situ* (Scheme 4.3b). In the presence of a suitable dipolarophile such as methyl acrylate (**358**), this species will then participate in a [3 + 2] cycloaddition through one of two possible transition states—*endo*-(**358**•**383**) or *exo*-(**358**•**383**)—to generate a mixture of diazabicyclic

products (*syn*-382 and *anti*-382) in 89% yield.<sup>13–15</sup> Given the smaller degree of steric interaction between the methyl ester and the pyrazine ring in the exo transition state, *syn*-382 is formed as the major diastereomer in a ratio of 3:1.

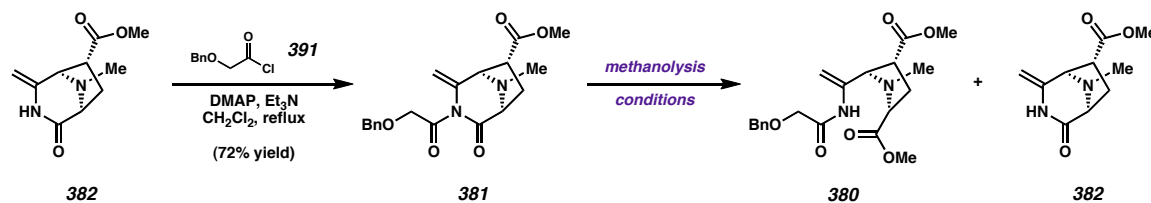
Our next task was to open the lactam in order to reveal the *N*-acyl enamine necessary for the key aryne annulation. In our previous total synthesis of leonomycin, a similar transformation was carried out by first protecting the lactam nitrogen as a *tert*-butyl carbamate (389) (Scheme 4.4).<sup>7,8</sup> This effectively increased the electrophilicity of the lactam carbonyl by partially sequestering the nitrogen lone pair. Upon treatment with sodium borohydride, the *N*-Boc lactam (389) underwent selective reduction at the endocyclic carbonyl to furnish primary alcohol 390. In designing a strategy toward quinocarcin, however, we sought to retain the methyl ester of cycloadduct 382 throughout the course of the synthesis, given that it constituted a masked form of the carboxylic acid present in the natural product. Thus, we advocated an approach in which the lactam ring would be opened under redox-neutral methanolysis conditions rather than by a reductive transformation, thereby giving rise to a diester such as 380. Specifically, imide 381 was pursued in favor of an *N*-carboxy lactam such as 389 in light of the fact that the methanolysis step would directly produce the *N*-acyl enamine necessary for the key aryne annulation.

Scheme 4.4. Reductive opening of *N*-Boc lactam 389 en route to leonomycin



The first step toward the eventual goal of opening the lactam was the acylation of cycloadduct **382** with benzyloxyacetyl chloride (**391**), which furnished imide **381** in 72% yield (Table 4.1). From this intermediate, methanolysis at the endocyclic carbonyl would open the lactam to produce *N*-acyl enamine **380**. However, an alternative methanolysis at the exocyclic carbonyl would cleave the newly installed benzyloxyacetyl sidearm to simply regenerate the secondary lactam (**382**). We therefore undertook a thorough screen of reaction conditions in order to determine whether regioselective methanolysis at the internal carbonyl was possible. Unfortunately, initial results were all but promising. In the presence of base (entry 1), protic acid (entry 2), or heat (entry 3), lactam **382** was generated as the sole product. Attempts to carry out the analogous alcoholysis with potassium *tert*-butoxide (entry 4) or heated *tert*-butanol (entry 5) gave similar results. Even an initial attempt using magnesium bromide as a Lewis acid in the presence of a limited quantity of methanol produced only lactam **382** (entry 6). However, further attempts were made using metal triflate salts as stoichiometric Lewis acids, and these reactions began to provide modest yields of *N*-acyl enamine **380**, albeit accompanied by minor quantities of lactam **382** (entries 7–10). Of the four metal triflates examined, yttrium(III) triflate provided the highest yield of **380** (entry 8).

Table 4.1. Lactam methanolysis



entry	conditions	product	yield <sup>a</sup>
1	$\text{K}_2\text{CO}_3$ , MeOH	382	ND
2	HCl, MeOH	382	ND
3	MeOH, reflux	382	ND
4	<i>t</i> -BuOK, <i>t</i> -BuOH	382	ND
5	<i>t</i> -BuOH, 80 °C	382	ND
6	$\text{MgBr}_2$ , MeOH / $\text{CH}_2\text{Cl}_2$ (1:10)	382	ND
7 <sup>b</sup>	$\text{Sc}(\text{OTf})_3$ , MeOH, $\text{CH}_2\text{Cl}_2$	380	19% <sup>c</sup>
8 <sup>b</sup>	$\text{Y}(\text{OTf})_3$ , MeOH, $\text{CH}_2\text{Cl}_2$	380	47% <sup>c</sup>
9 <sup>b</sup>	$\text{Zn}(\text{OTf})_2$ , MeOH, $\text{CH}_2\text{Cl}_2$	380	40% <sup>c</sup>
10 <sup>b</sup>	$\text{Sm}(\text{OTf})_3$ , MeOH, $\text{CH}_2\text{Cl}_2$	380	23% <sup>c</sup>

<sup>a</sup> ND = not determined

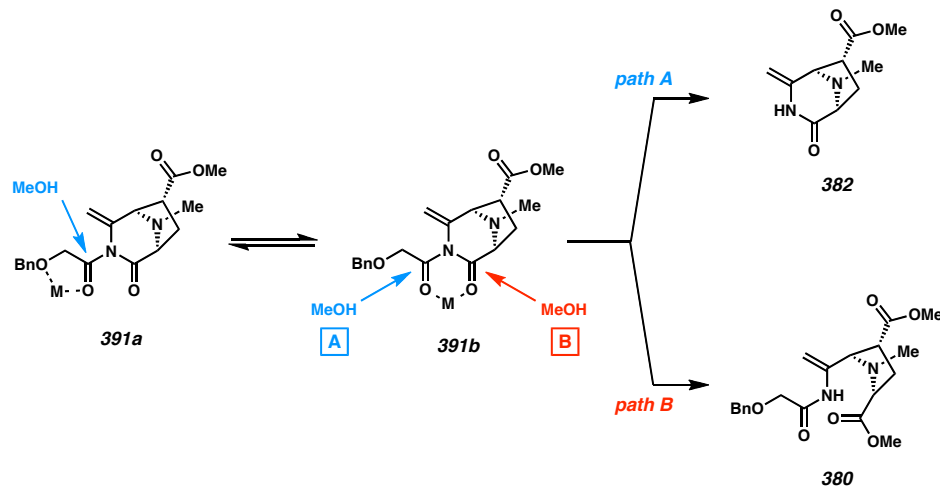
<sup>b</sup> Reaction performed with 10 equiv MeOH.

<sup>c</sup> Lactam 382 isolated as a minor side product.

During the course of these trials, we began to suspect that the benzyl ether might be interacting with the Lewis acid and interrupting its coordination to the imide by forming a five-membered chelate (**391a**) with the exocyclic carbonyl (Scheme 4.5). Given that only the left hand carbonyl is activated by this interaction, methanolysis of this coordination complex is anticipated to lead only to deacylated lactam **382**. On the other hand, the five-membered chelate is expected to be in equilibrium with a six-membered chelate (**391b**) involving coordination of the metal between the two carbonyls.<sup>16</sup> In this case, activation of either carbonyl is possible, and as such, methanolysis of this complex can be envisioned to lead to either lactam **382** or the desired *N*-acyl enamine (**380**). Although it is difficult to distinguish a clear trend in regioselectivity across the sample set of Lewis acids, it seems that metals with smaller cationic radii generally provide higher yields of

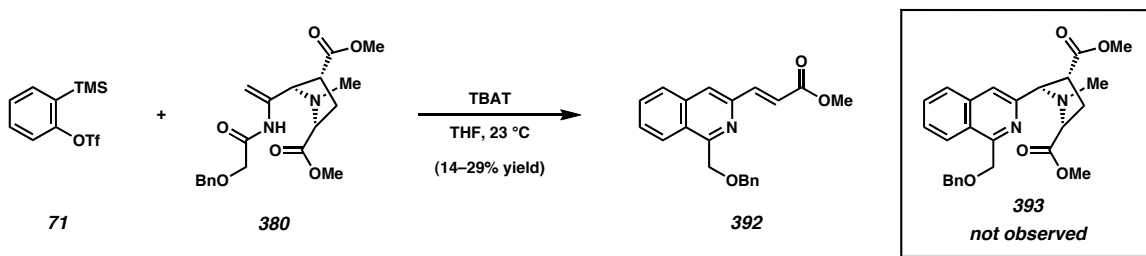
the *N*-acyl enamine (**380**), possibly by favoring formation of the six- (**391b**) rather than the five-membered chelate (**391a**). Further selectivity for methanolysis at the endocyclic carbonyl may be due to the release of ring strain that occurs during the formation of *N*-acyl enamine **380**.

Scheme 4.5. Proposed coordination conformations leading to lactam **382** and *N*-acyl enamine **380**



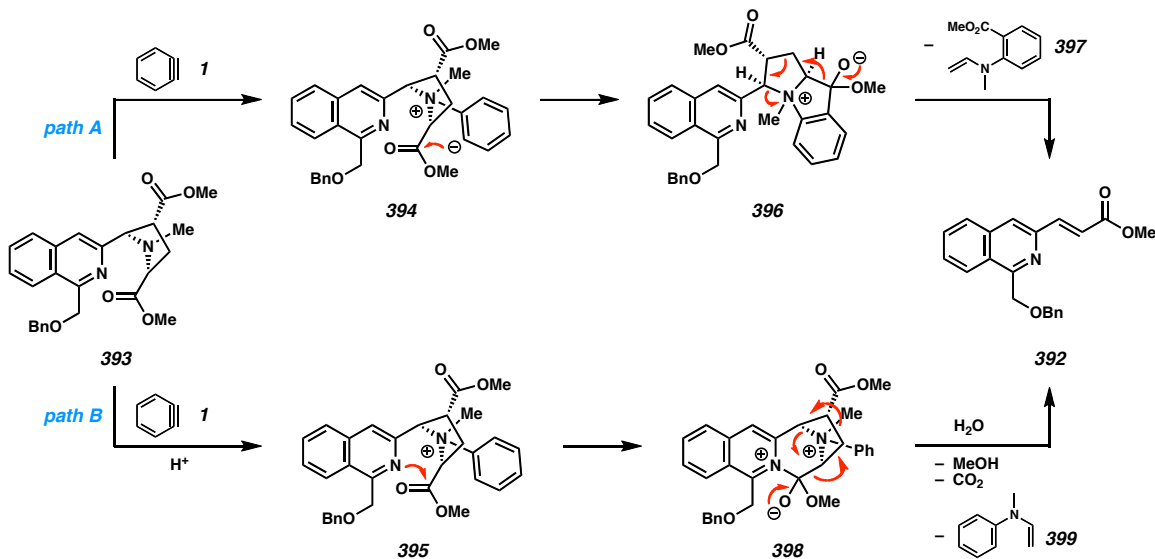
#### 4.2.3 Attempts to Synthesize the Isoquinoline via Aryne Annulation

With a route to *N*-acyl enamine **380** in hand, we turned our attention to the key aryne annulation. Before employing 3-methoxy-2-(trimethylsilyl)phenyl triflate (**108**), we decided to test the substrate in a model system using the unsubstituted benzyne precursor (**71**) (Scheme 4.6). When the reaction was performed under the standard conditions,<sup>10</sup> we were intrigued to find that an isoquinoline (**392**) had indeed formed, though it was not the expected product (**393**). The isoquinoline that was isolated lacked a majority of the *N*-methyl pyrrolidine ring originally appended to the enamine, and instead featured a simple  $\alpha,\beta$ -unsaturated ester.

Scheme 4.6. Attempted aryne annulation using *N*-acyl enamine **380**

Fascinated by this observation, we sought to understand the mechanism through which the product had formed (Scheme 4.7). Given the presence of the isoquinoline moiety, it was obvious that the aryne annulation had taken place. Assuming this reaction occurred prior to decomposition of the pyrrolidine, the desired product (**393**) would exist as a transient intermediate. In this case, the mechanism responsible for conversion of **393** to **392** would most likely involve activation of the tertiary amine through quaternization with a second equivalent of benzyne. Direct attack upon benzyne would yield zwitterion **394** (path A), while subsequent protonation would generate ammonium ion **395** (path B). Addition of the aryl anion of **394** to the neighboring ester would generate a tricyclic intermediate (**396**), which could proceed to  $\alpha,\beta$ -unsaturated ester **392** through elimination of methyl anthranilate **397**. Alternatively, the isoquinoline nitrogen (or an external nucleophile) may add to the proximal ester (**395**) in the absence of the aryl anion. Similar to path A, this intermediate (**398**) would decompose to the isolated product (**392**) through loss of aniline **399** and equivalents of methanol and carbon dioxide.

Scheme 4.7. Proposed mechanisms for the formation of isoquinoline 392

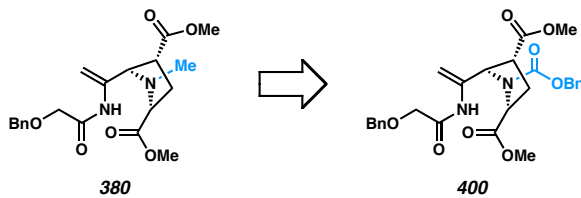


### 4.3 SECOND GENERATION APPROACH

#### 4.3.1 Revision of Approach

Thus far, our attempts to carry out an aryne annulation reaction using a pyrrolidine-appended *N*-acyl enamine had met with little success. While we had accomplished the formation of an isoquinoline, the subsequent fragmentation event had rendered the substrate for this reaction unusable in the synthesis of quinocarcin. As this undesired reactivity was most likely attributable to the nucleophilicity of the tertiary amine, we sought to design an alternative pyrrolidine substrate in which the nitrogen lone pair would be sequestered by an electron-withdrawing group. Fortunately, a benzyloxycarbonyl (Cbz) group had served this purpose quite effectively in our previous synthesis of lemomycin.<sup>7</sup> Thus, we decided to target a carbamate analogue (**400**) of our original *N*-benzyloxyacetyl enamine (**380**) in a revised approach to the total synthesis of quinocarcin (Figure 4.2).

Figure 4.2. Revised design of the N-acyl enamine

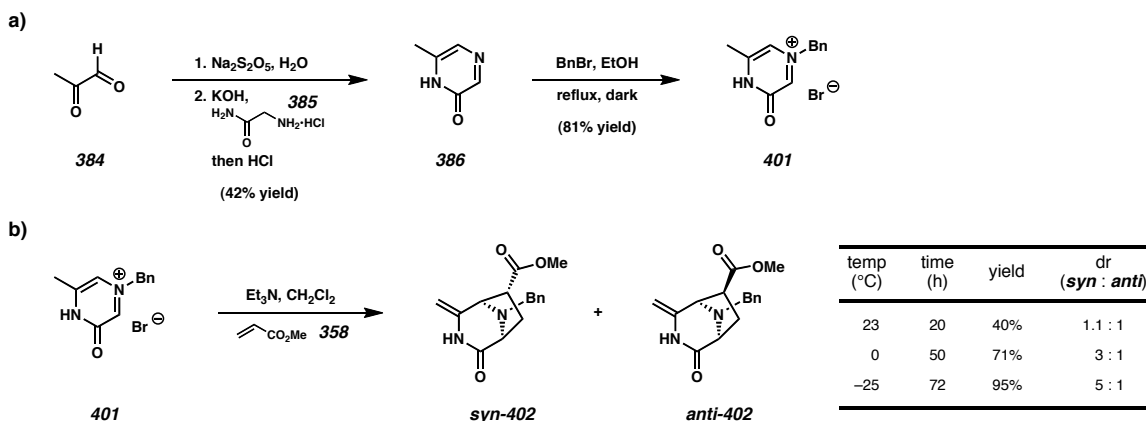


### 4.3.2 Auxiliary-Mediated Diastereoselective Dipolar Cycloaddition and Aryne Annulation

In order to construct carbamate **400**, it was necessary to return to the dipolar cycloaddition step and proceed forward using an alternate substrate. As we anticipated difficulty generating a stable *N*-benzyloxycarbonyl analogue of *N*-methyl oxidopyrazinium salt **387**, we decided to install a benzyl group that could later be exchanged for the carbamate. Alkylation of pyrazinone **386** was carried out with benzyl bromide to furnish *N*-benzyl oxidopyrazinium bromide **401** in 81% yield (Scheme 4.8a). However, when the subsequent dipolar cycloaddition was carried out at room temperature under the conditions previously used to generate *N*-methyl diazabicycle **382**, the resulting *N*-benzyl diazabicycles (*syn*-**402** and *anti*-**402**) were isolated in only a 1.1:1 ratio (Scheme 4.8b). This is envisioned to be due to the destabilizing effect that the larger benzyl substituent has upon the exo transition state, thereby decreasing the difference in energy between the endo and exo pathways. Fortunately, diastereoselectivity was found to be temperature sensitive and the ratio could be augmented in favor of the desired *syn* diastereomer by cooling the reaction. Not surprisingly, the reaction proceeds more slowly at lower temperatures, and  $-25\text{ }^{\circ}\text{C}$  was found to be the approximate lower limit to observe full conversion within a reasonable timeframe. At this temperature, the dipolar

cycloaddition between methyl acrylate (**358**) and the oxidopyrazinium betaine derived from **401** generates diazabicycle **402** in 95% yield and 5:1 dr over 72 h.

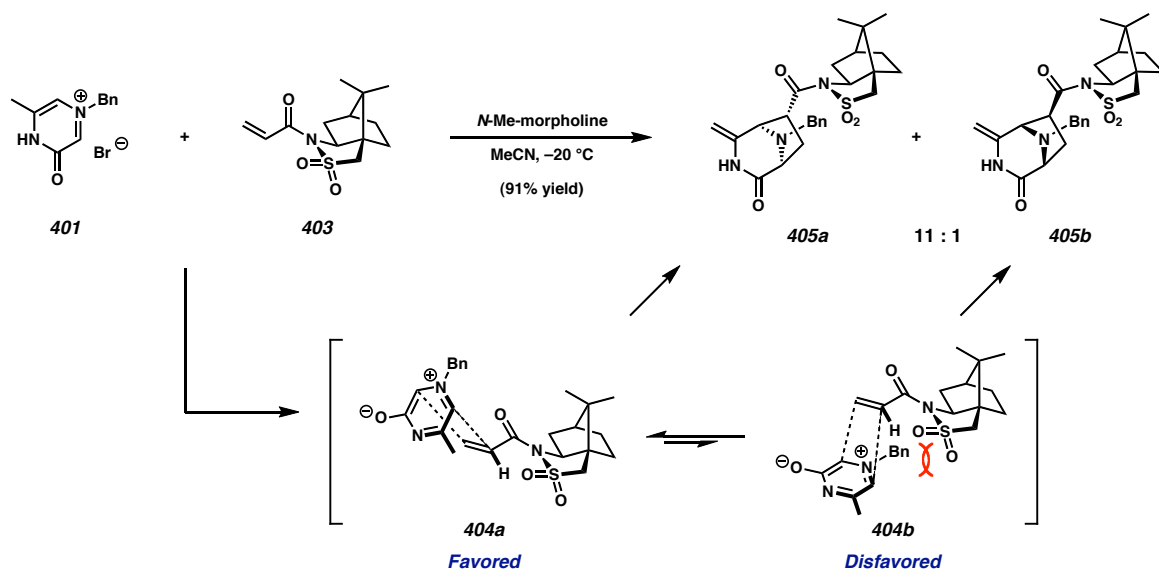
Scheme 4.8. Synthesis of *N*-benzyl oxidopyrazinium bromide **401** and dipolar cycloaddition



Up to this point, our efforts had focused upon the development of a racemic route to the *N*-acyl enamine substrate for the key aryne annulation. However, in light of our ultimate goal to prepare the natural enantiomer of quinocarcin, we resolved to introduce asymmetry during construction of the first three stereocenters. Drawing from our previous synthesis of leonomycin,<sup>7,8</sup> we chose to build the diazabicycle using an auxiliary-controlled diastereoselective variant of the dipolar cycloaddition employing the acrylamide of Oppolzer's sultam (**403**) in place of methyl acrylate (**358**) (Scheme 4.9).<sup>17</sup> According to proposed models,<sup>18</sup> the carbonyl is expected to occupy the plane of the N–S π-system and adopt an anti relationship with respect to the N–S bond in order to avoid dipole interactions with the sulfonamide. The olefin is then predicted to favor an *s*-*trans* geometry with respect to the carbonyl in order to avoid steric interactions with the flanking sulfonamide and methylene groups. In this orientation, the oxidopyrazinium

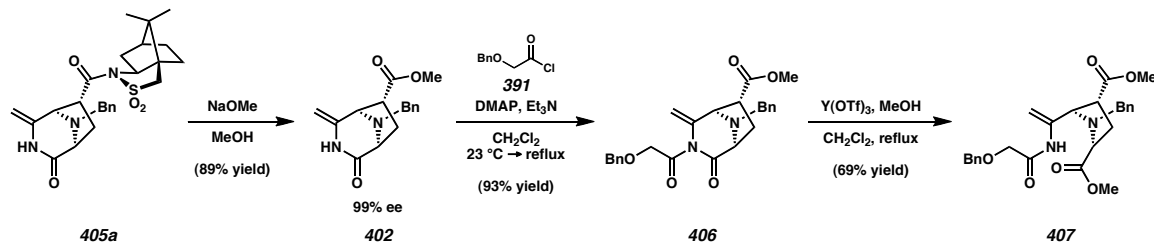
betaine can be envisioned to approach from either the top (**404a**) or bottom (**404b**) face of the olefin in either an endo or exo configuration relative to the acrylamide. Similar to the formation of diazabicycle **382**, the exo transition state leading to cycloadducts **405a** and **405b** is expected to predominate due to steric interactions between the *N*-alkyl substituent and the group appended to the acryloyl functionality (in this case, the camphor auxiliary). Given that additional interactions with the pseudoaxial oxygen of the sulfonamide disfavor transition state **404b**, selective approach from the top face is anticipated to lead to diazabicycle **405a** as the major product. In support of this hypothesis, cycloadducts **405a** and **405b** were isolated in 91% combined yield and an 11:1 ratio when the reaction was performed at –20 °C in acetonitrile using *N*-methyl morpholine as the base. Furthermore, recrystallization of diazabicycle **405a** from the crude mixture could be accomplished to provide the major diastereomer in 83% yield, suitable for advancement to the *N*-acyl enamine.

Scheme 4.9. Auxiliary-mediated diastereoselective dipolar cycloaddition



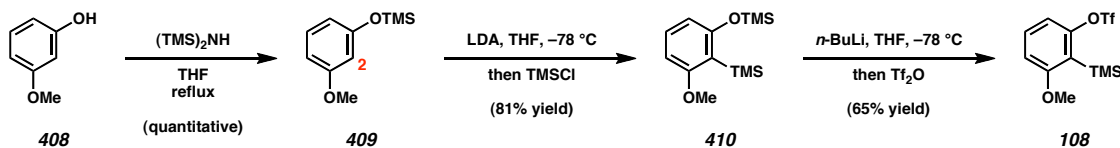
In order to intercept the route previously used to prepare *N*-acyl enamine **380**, the auxiliary was removed via methanolysis under basic conditions to provide ester **402** in 89% yield and 99% ee (Scheme 4.10). The lactam nitrogen was then acylated with benzyloxyacetyl chloride (**391**) to afford imide **406**. Using the optimal conditions identified for regioselective methanolysis of imide **381**, this material was advanced to *N*-acyl enamine **407** via lactam ring opening in the presence of yttrium(III) triflate.

Scheme 4.10. Advancement of diazabicycle **405a** to *N*-acyl enamine **407**

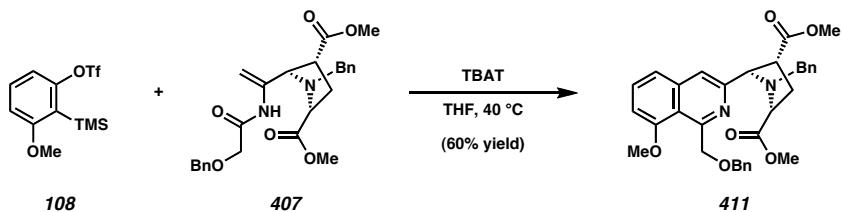


The synthesis of *ortho*-methoxy aryne precursor (**108**) was completed according to the procedure previously reported by Pérez *et al.*, which proceeds in three steps from commercially available 3-methoxyphenol (**408**) (Scheme 4.11).<sup>19</sup> Silylation of the phenol in refluxing hexamethyldisilamide generates silyl ether **409**, which then undergoes deprotonation and subsequent silylation at C(2) to furnish aryl silane **410**. Treatment with *n*-butyllithium then removes the silyl ether to form an intermediate lithium phenoxide, which is quenched by the addition of triflic anhydride to yield *ortho*-silyl aryl triflate **108**.

Scheme 4.11. Synthesis of 3-methoxy-2-(trimethylsilyl)phenyl triflate (108)



With both *N*-acyl enamine **407** and *ortho*-silyl aryl triflate **108** in hand, we were tempted to test the aryne annulation before exchanging the benzyl protecting group for a carbamate. To our delight, combining these two substrates in the presence of tetra-*n*-butylammonium difluorotriphenylsilicate (TBAT) and heating the reaction to 40 °C resulted in the formation of isoquinoline **411** in 60% yield as a single isomer (Scheme 4.12). While the reaction generates several minor side products—some likely forming through pathways analogous to those depicted in Scheme 4.7—this result represents the most highly functionalized isoquinoline we have yet been able to produce using our aryne annulation technology. Moreover, the structure of isoquinoline **411** contains the entire carbon skeleton of quinocarcin, assembled in only five steps from known materials.

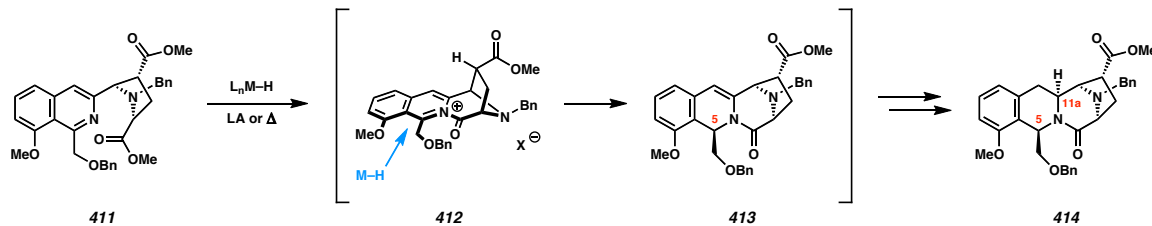
Scheme 4.12. Synthesis of isoquinoline **411** via aryne annulation

### 4.3.3 Reduction of the Isoquinoline and Completion of (–)-Quinocarcin

Proceeding forward from isoquinoline **411**, advancement to the natural product required stereoselective reduction of the isoquinoline to introduce the stereocenters at C(5) and C(11a). In developing a strategy to accomplish this task, we envisioned a sequence of events wherein reduction to the tetrahydroisoquinoline and closure of the D ring could be achieved in a single reaction using heterogeneous catalytic hydrogenation conditions. In the presence of either a Lewis acid or heat, the isoquinoline nitrogen was expected to add to the proximal ester to form a cationic isoquinolinium intermediate (**412**) (Table 4.2). The anticipated benefits of this formation were twofold: *N*-acylation of the isoquinoline would increase the electrophilicity of the heterocyclic ring toward reduction and rigidify the structure in order to position the two-carbon bridge and methyl ester on the  $\beta$ -face, thus obstructing hydrogenation from this side.<sup>20</sup> The dihydroisoquinoline (**413**) thus formed would then undergo further reduction from the  $\alpha$ -face to provide tetracyclic tetrahydroisoquinoline **414**. Unfortunately, attempts to carry out this hydrogenation sequence failed under a variety of heterogeneous conditions. Palladium on charcoal (entries 1–4) displayed little reactivity toward isoquinoline **411**, resulting either in slow conversion of the starting material or hydrogenolysis of the benzyl groups. Reactivity increased at higher temperatures and hydrogen pressures, though often resulting in the formation of complex product mixtures (entries 5–7). Reactions employing Pearlman’s catalyst<sup>21</sup> (entries 8–10) or Adam’s catalyst<sup>22</sup> (entries 11–15) yielded similar results, either proceeding too slowly or removing the benzyl groups without reducing the isoquinoline. Raney nickel<sup>23</sup> proved inactive at room temperature (entry 16), though the catalyst promoted rapid decomposition of the starting

material at 60 °C at both atmospheric (entry 17) and increased pressures (entry 18). The addition of Lewis acids (e.g.,  $\text{BF}_3 \bullet \text{OEt}_2$ ,  $\text{AlCl}_3$ ,  $\text{SnCl}_4$ ,  $\text{TiCl}_4$ ) had little effect upon the outcome, most often resulting only in decomposition of the starting material.

Table 4.2. Attempted heterogeneous reduction of isoquinoline 411



entry	catalyst	catalyst loading (mol %)	$\text{H}_2$ pressure (atm)	solvent	temp (°C)	time (h)	result
1	Pd/C	10	1.0	EtOH	23	18	benzyl hydrogenolysis
2	Pd/C	50	1.0	EtOH	23	18	benzyl hydrogenolysis
3	Pd/C	10	1.0	EtOAc	23	18	low conversion
4	Pd/C	10	1.0	AcOH	23	8	decomposition
5 <sup>a</sup>	Pd/C	10	1.0	EtOH	60	12	several products
6	Pd/C	10	68.0	EtOAc	60	8	several products
7	Pd/C	50	1.0	1,4-dioxane	80	12	several products
8	Pd(OH) <sub>2</sub> /C	10	1.0	EtOH	23	12	benzyl hydrogenolysis
9	Pd(OH) <sub>2</sub> /C	10	1.0	EtOAc	60	12	several products
10	Pd(OH) <sub>2</sub> /C	10	1.0	EtOH	23	12	benzyl hydrogenolysis
11	PtO <sub>2</sub>	25	1.0	EtOH	23	18	low conversion
12	PtO <sub>2</sub>	25	1.0	DME	23	18	low conversion
13	PtO <sub>2</sub>	25	1.0	DME	80	8	several products
14	PtO <sub>2</sub>	25	1.0	1,4-dioxane	80	18	low conversion
15	PtO <sub>2</sub>	25	1.0	AcOH	23	12	decomposition
16	Raney Ni	50	1.0	EtOH	23	18	low conversion
17	Raney Ni	50	1.0	EtOH	60	8	decomposition
18 <sup>a</sup>	Raney Ni	50	68.0	EtOH	60	4	decomposition

<sup>a</sup> Reaction performed in a stainless steel hydrogenation bomb.

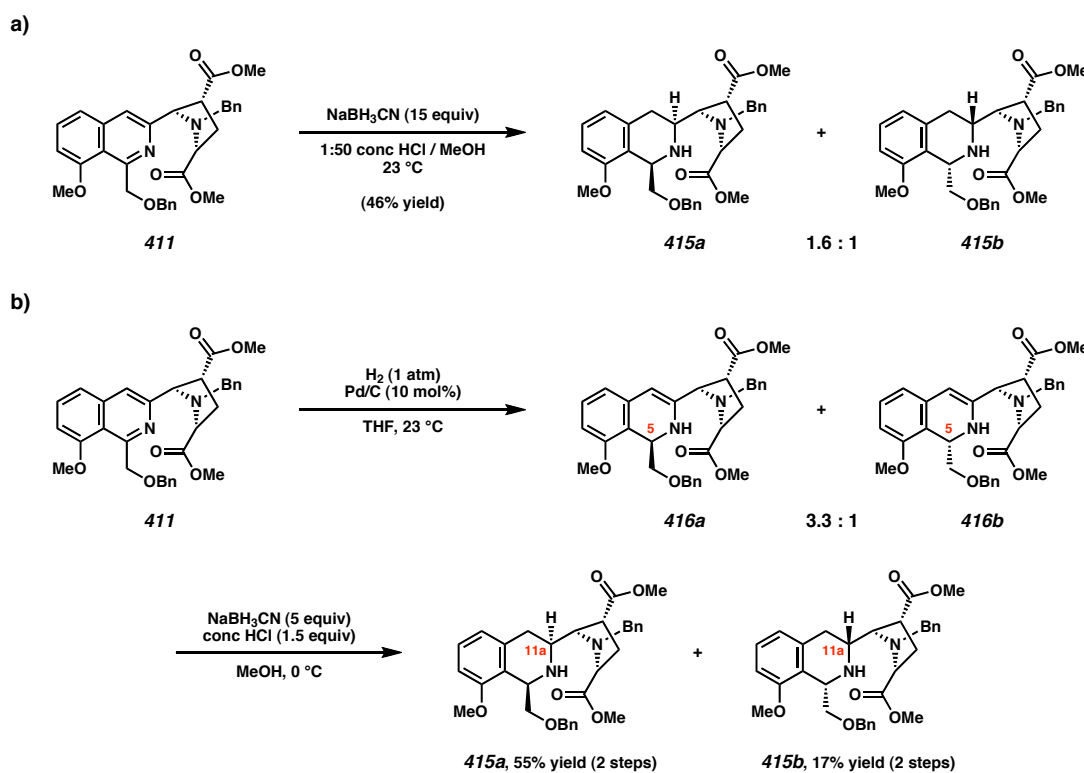
Concurrent with our efforts to find a suitable heterogeneous catalyst for hydrogenation of the isoquinoline ring, we examined homogeneous reductants known to display similar reactivity toward nitrogen-containing heterocycles. In their synthesis of (–)-quinocarcin, Terashima *et al.* carried out the reduction of an isoquinoline at 0 °C using sodium cyanoborohydride in the presence of concentrated hydrochloric acid.<sup>6c</sup>

Although the identical conditions failed to reduce isoquinoline **411**, warming the reaction to room temperature produced a mixture of diastereomeric tetrahydroisoquinolines **415a** and **415b** in a 1.6:1 ratio (Scheme 4.13). While this reduction proceeded in only 46% yield, we took encouragement from the fact that the major diastereomer (**415a**) possessed the same stereochemistry present in the natural product.

In an effort to promote greater diastereoselectivity in the isoquinoline reduction, we sought to fix the conformation of the pyrrolidine ring through the formation of internal hydrogen bonds between the unprotected alcohol and amine functionalities. It therefore became our goal to remove the benzyl protecting groups. When the hydrogenolysis was attempted using palladium on charcoal in tetrahydrofuran<sup>24</sup> under a balloon of hydrogen, we were surprised to find that instead of removing the two benzyl groups we had accomplished a 1,2-hydrogenation of the isoquinoline ring system to produce a 3.3:1 mixture of diastereomeric dihydroisoquinolines (**416a** and **416b**).<sup>25</sup> Given the difficulties we had encountered during our previous attempts to reduce isoquinoline **411**, we believe that this unexpected reactivity must be promoted only in THF. Similar to the reaction with sodium cyanoborohydride, reduction occurred primarily from the  $\alpha$ -face to generate the desired stereochemistry at C(5) as the major diastereomer (**416a**). At longer reaction times, removal of the benzyl groups was observed. As such, the hydrogenation was allowed to proceed for no more than 6 h in order to obtain an optimal yield of dihydroisoquinolines **416a** and **416b**. Additionally, these compounds proved unstable toward chromatography, and were therefore carried forward to the next step without separation. Treatment of the mixture with sodium cyanoborohydride according to

Terashima's procedure accomplished a second reduction to produce tetrahydroisoquinolines **415a** and **415b** in 72% combined yield over the two steps. Interestingly, this second reduction installs the stereocenter at C(11a) *syn* to the preexisting stereocenter at C(5) with complete selectivity to furnish **415a** and **415b** in a ratio of 3.3:1, equivalent to that of dihydroisoquinolines **416a** and **416b**.<sup>26</sup>

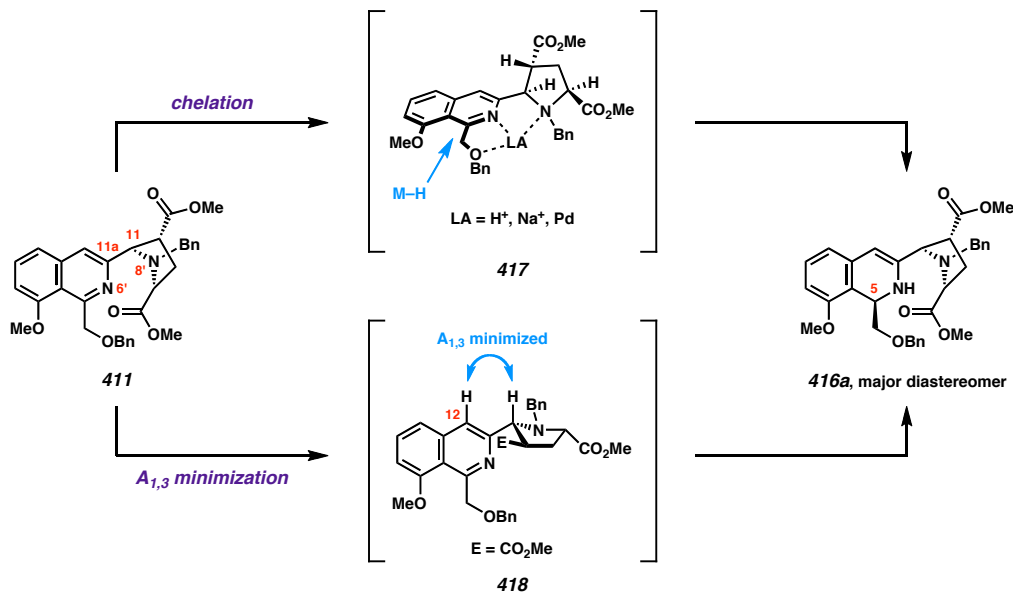
*Scheme 4.13. a) One-step homogeneous reduction of isoquinoline **411**. b) Two-step reduction of isoquinoline **411** to form tetrahydroisoquinolines **415a** and **415b**.*



Intrigued by the differences in diastereoselectivity observed when isoquinoline **411** was treated either under homogeneous or heterogeneous conditions, we were led to consider the factors affecting facial selectivity in this reduction (Scheme 4.14). Given the number of Lewis basic groups present in **411**, it is conceivable that chelation of a

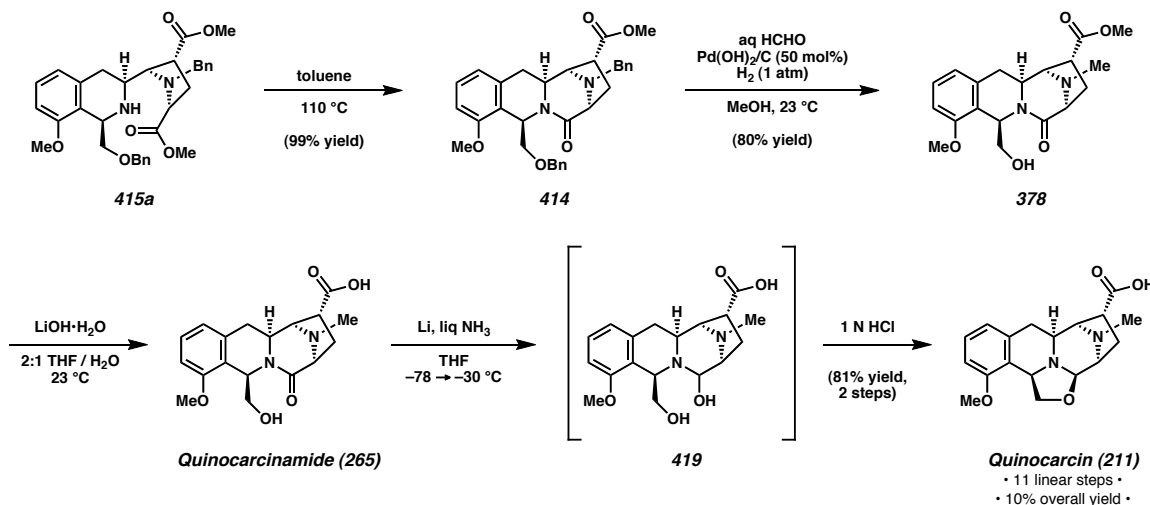
Brønsted or Lewis acid (e.g.,  $\text{H}^+$ ,  $\text{Na}^+$ , or  $\text{Pd}$ ) could serve to rigidify the structure **417** in a manner similar to that envisioned in our previous model for isoquinolinium ion **412**. In particular, planarizing the  $\text{N}(6')-\text{C}(11\text{a})-\text{C}(11)-\text{N}(8')$  bond system would position the bulk of the pyrrolidine ring over the  $\beta$ -face, blocking the approach of the reductant to this side of the isoquinoline. Delivery of hydrogen (or a hydride) to the  $\alpha$ -face would set the stereochemistry at  $\text{C}(5)$ , providing dihydroisoquinoline **416a**. Alternatively, diastereoselective reduction in the absence of a Lewis acidic group can be rationalized by minimizing allylic strain between the hydrogen atom at  $\text{C}(12)$  and the substituents at  $\text{C}(11)$  (**418**). Rotation of the pyrrolidine to place the  $\text{C}(11)-\text{H}$  bond in the plane of the isoquinoline ring would project the pseudoequatorial methyl ester over the  $\beta$ -face. In either case, however, the group responsible for blocking one particular face of the isoquinoline is situated far from the reaction center at  $\text{C}(5)$ , most likely accounting for the modest level of diastereoselectivity observed in this reaction.

Scheme 4.14. Models for diastereoselective reduction of isoquinoline **411**



Having finally identified a synthetic route to the preparation of tetrahydroisoquinoline **415a**, we set out to advance this intermediate to quinocarcin. Upon heating, we were pleased to observe the newly formed secondary amine selectively condense with only one of the two neighboring esters to form lactam **414** in 99% yield (Scheme 4.15). In light of the slow benzyl group hydrogenolysis implicit in the success of the previous heterogeneous reduction, we selected the more active Pearlman's catalyst to remove the two protecting groups. The addition of formaldehyde to this reaction mixture accomplished a subsequent methylation of the unmasked amine to provide tetracycle **378**. In the final two steps, saponification of the methyl ester generated quinocarcinamide (**265**), which was then subjected to dissolving metal conditions to effect a partial reduction of the lactam.<sup>6a,6b,6e,27</sup> Treatment of the resulting hemiaminal (**419**) with 1 N HCl resulted in closure of the oxazolidine ring to furnish (–)-quinocarcin (**211**) in 81% yield over two steps. In full, our synthetic route achieves the asymmetric total synthesis of (–)-quinocarcin in 10% overall yield via a longest linear sequence of 11 steps from known compounds (13 steps from commercially available materials), thus marking the shortest total synthesis of this important antitumor antibiotic reported to date.

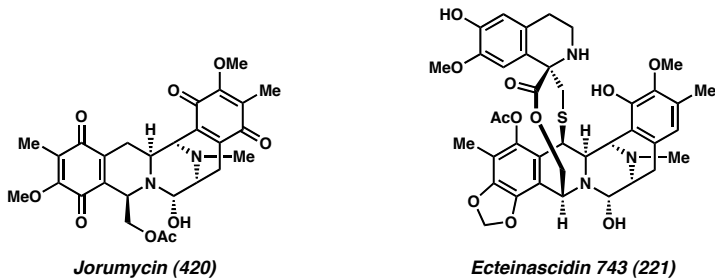
Scheme 4.15. Completion of (–)-quinocarcin



#### 4.4 ARYNE ANNULATION APPROACHES TO ADDITIONAL TETRAHYDROISOQUINOLINE ANTITUMOR ANTIBIOTICS

With the completion of (–)-quinocarcin, we began to consider other tetrahydroisoquinoline alkaloids that could be targeted using our unique aryne annulation approach. In particular, we were curious as to whether members of the 3,9-diazabicyclo[3.3.1]nonane class such as jorumycin (**420**) and ecteinascidin 743 (**221**) could be assembled through similar isoquinoline intermediates (Figure 4.3). Unlike quinocarcin, the core of each of these compounds contains two tetrahydroisoquinolines bound together through a central piperazine ring. As such, the key intermediate would necessarily consist of a *bis*-isoquinoline. Eager to test the capabilities of our aryne methodology, our group has undertaken efforts toward the total syntheses of (–)-jorumycin and (–)-ecteinascidin 743.

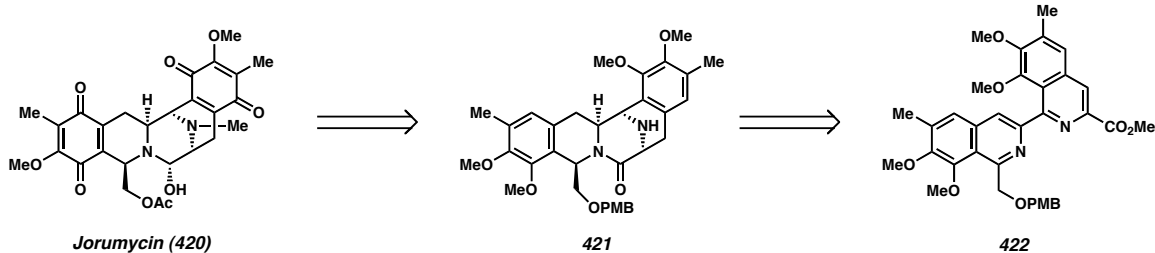
Figure 4.3. Additional tetrahydroisoquinoline natural product targets



#### 4.4.1 Jorumycin<sup>†</sup>

Jorumycin (**420**) was isolated in 2000 by Fontana *et al.* from the sea slug *Jorunna funebris* and displayed sub-nanomolar activity against A549 human lung carcinoma and HT29 human colon carcinoma cell lines ( $IC_{50} = 0.24$  nM).<sup>28</sup> Thus far, two independent total syntheses have been reported by the labs of Williams<sup>29</sup> and Zhu.<sup>30</sup> In each route, a Pictet–Spengler condensation was used to close at least one of the tetrahydroisoquinoline ring systems. We decided to take a different approach, envisioning jorumycin to arise from pentacycle **421**, which in turn could be obtained through reduction and cyclization of a *bis*-isoquinoline (**422**) (Scheme 4.16).

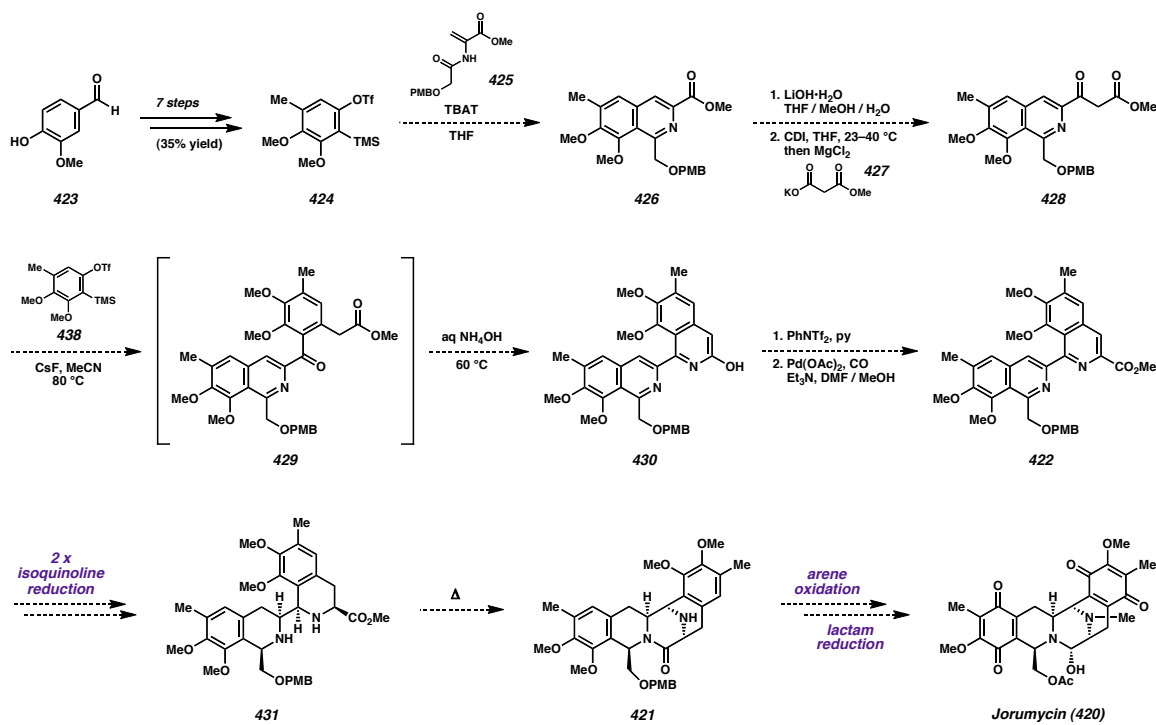
Scheme 4.16. Retrosynthetic analysis of jorumycin



<sup>†</sup> The asymmetric total synthesis of (–)-jorumycin is currently being pursued by Christopher D. Gilmore, a graduate student in the Stoltz research group.

In order to introduce the oxygenation pattern present in jorumycin prior to construction of the isoquinoline framework, trisubstituted *ortho*-silyl aryl triflate **424** was prepared in seven steps from commercially available vanillin (**423**) (Scheme 4.17).<sup>31</sup> This intermediate will be advanced to *bis*-isoquinoline **430** through a four-step sequence beginning with an aryne annulation reaction with dehydroalanine derivative **425** to form isoquinoline **426**. Following this, saponification of the ester followed by homologation with monomethyl malonate **427** according to the procedure of Masamune *et al.*<sup>32</sup> will provide  $\beta$ -ketoester **428**. Using an elaboration of our previously developed aryne acyl-alkylation methodology,<sup>33</sup> a second equivalent of the aryne will be inserted into the  $\alpha,\beta$ -C–C bond of  $\beta$ -ketoester **428** to generate intermediate **429**. This compound will then undergo condensation with ammonia to provide *bis*-isoquinoline **430**.<sup>34</sup> From this point, triflation of the alcohol and palladium-catalyzed carboxylation are expected to yield ester **422**. In the stereodetermining step, selective reduction of both isoquinoline rings from the  $\beta$ -face will provide *bis*-tetrahydroisoquinoline **431**. Cyclization of the secondary amine with the neighboring methyl ester will close the final ring to furnish pentacycle **421**. Completion of jorumycin (**420**) will then require methylation of the secondary amine, reduction of the lactam to a hemiaminal, oxidation of the two arenes to quinones, and acetylation of the primary alcohol.

Scheme 4.17. Proposal for the synthesis of jorumycin via bis-isoquinoline 430



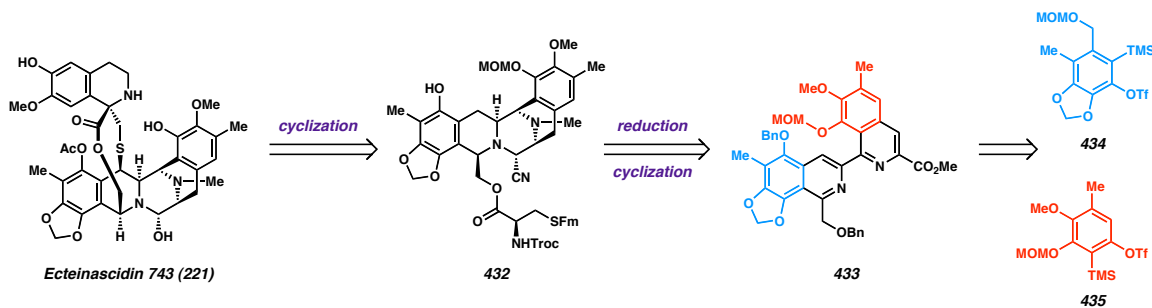
#### 4.4.2 Ecteinascidin 743<sup>‡</sup>

Concurrent with our efforts to synthesize jorumycin from *bis*-isoquinoline **430**, we are investigating the total synthesis of ecteinascidin 743 (**221**),<sup>35,36</sup> the most biologically active member of the tetrahydroisoquinoline antitumor antibiotics and a pharmaceutical agent marketed for the treatment of soft-tissue sarcomas under the trade name Yondelis.<sup>37</sup> Retrosynthetically, we plan to intercept hexacycle **432**, an intermediate employed by PharmaMar in the industrial semisynthesis of ecteinascidin 743 from cyanosafarin B (Scheme 4.18).<sup>36g,h</sup> We envision this compound to be available from *bis*-isoquinoline **433** using a reduction/cyclization sequence similar to that described above. However, unlike

<sup>‡</sup> The asymmetric total synthesis of (–)-ecteinascidin 743 is currently being pursued by Pamela M. Tadross, a graduate student in the Stoltz research group.

jorumycin, the right and left hand arene rings of ecteinascidin are not identical, and therefore require independent assembly of two separate *ortho*-silyl aryl triflates (**434** and **435**). At present, our attention is focused upon the preparation of these aryne precursors. Following their construction, our efforts will turn toward their application to the synthesis of *bis*-isoquinoline **433** and advancement of this intermediate to the natural product.

Scheme 4.18. Retrosynthetic analysis of ecteinascidin 743



## 4.5 CONCLUSION

We have successfully completed an extremely concise asymmetric total synthesis of (–)-quinocarcin in 10% overall yield via a longest linear sequence of 11 steps from known compounds (13 steps from commercially available materials). An auxiliary-mediated diastereoselective dipolar cycloaddition was employed as the stereodetermining event, and the resulting cycloadduct was advanced over three steps to an *N*-acyl enamine. By applying our aryne annulation methodology to the construction of the key isoquinoline intermediate, we are able to assemble the full carbon framework of the molecule after a total of only five steps. An exhaustive screen of reduction conditions uncovered a unique two-step procedure for the diastereoselective conversion of the isoquinoline to a tetrahydroisoquinoline. Following this, advancement of the material

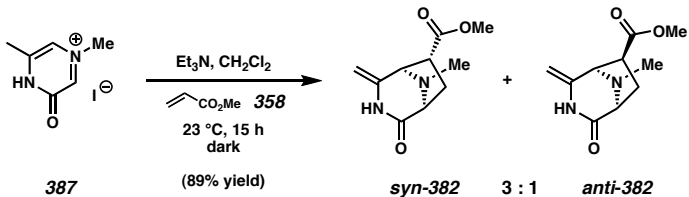
through four additional steps provided the natural product. In full, our aryne annulation strategy has enabled the shortest synthetic route to (–)-quinocarcin reported to date. Efforts are currently underway to apply this and other aryne technologies developed in our labs to the synthesis of additional members of the tetrahydroisoquinoline family of antitumor antibiotics.

## 4.6 EXPERIMENTAL SECTION

### 4.6.1 Materials and Methods

Unless stated otherwise, reactions were performed in flame-dried glassware under an argon or nitrogen atmosphere using dry, deoxygenated solvents (distilled or passed over a column of activated alumina). Commercially obtained reagents were used as received. Reaction temperatures were controlled by an IKAmag temperature modulator. Thin-layer chromatography (TLC) was performed using E. Merck silica gel 60 F254 precoated plates (0.25 mm) and visualized by UV fluorescence quenching, potassium permanganate, or ceric ammonium molybdate staining. SiliaFlash P60 Academic Silica gel (particle size 0.040–0.063 mm) was used for flash chromatography. Analytical chiral supercritical fluid chromatography was performed with a Berger Analytix SFC (Thar Technologies) using a Chiralcel OD-H column (250 mm × 4.6 mm, 5  $\mu$ m particle size, 2.0 mL/min flow rate). Preparatory reverse-phase HPLC was performed on a Waters HPLC with a Waters Delta-Pak column (100 mm × 2 mm, 15  $\mu$ m particle size, 1.5 mL/min flow rate) equipped with a guard, employing a variable gradient of methanol and water.  $^1\text{H}$  and  $^{13}\text{C}$  NMR spectra were recorded on a Varian Inova 500 (at 500 MHz and 125 MHz, respectively) and are reported relative to  $\text{Me}_4\text{Si}$  ( $\delta$  0.0). Data for  $^1\text{H}$  NMR spectra are reported as follows: chemical shift ( $\delta$  ppm) (multiplicity, coupling constant (Hz), integration). Data for  $^{13}\text{C}$  NMR spectra are reported in terms of chemical shift relative to  $\text{Me}_4\text{Si}$  ( $\delta$  0.0). IR spectra were recorded on a Perkin Elmer Paragon 1000 Spectrometer and are reported in frequency of absorption ( $\text{cm}^{-1}$ ). High resolution mass spectra were obtained from the Caltech Mass Spectral Facility. Optical rotations were measured on a Jasco P-1010 polarimeter using a 100 mm path-length cell.

#### 4.6.2 Preparative Procedures and Spectroscopic Data



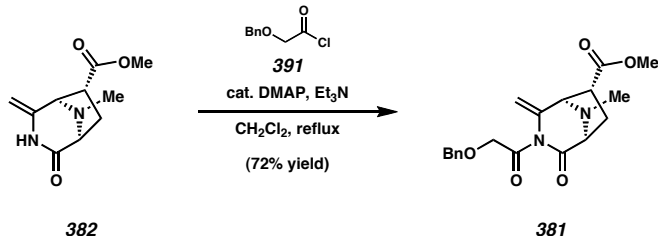
#### Esters *syn*-**382** and *anti*-**382**<sup>38</sup>

A flame-dried 5 mL round-bottomed flask wrapped in aluminum foil and equipped with a magnetic stir bar was charged with oxidopyrazinium iodide **387** (0.1012 g, 0.402 mmol). The flask was sealed with a rubber septum, evacuated, and back-filled with argon ( $\times 2$ ). Dichloromethane (2.0 mL) and  $\text{Et}_3\text{N}$  (0.064 mL, 0.459 mmol) were sequentially added via syringe and the reaction was stirred at  $23^\circ\text{C}$  for 20 min. Methyl acrylate (**358**) (0.108 mL, 1.20 mmol) was then added dropwise via syringe over 1 min and stirring was continued at  $23^\circ\text{C}$  for 15 h. The reaction solution was diluted with  $\text{CH}_2\text{Cl}_2$  (10 mL) and washed with saturated aqueous  $\text{NH}_4\text{Cl}$  (10 mL) and brine (10 mL). The organic layer was dried over  $\text{Na}_2\text{SO}_4$ , filtered, and concentrated to a pale yellow oil. This residue was purified via flash chromatography over silica gel (50:50  $\rightarrow$  80:20  $\text{EtOAc/hexanes}$ ) to yield ester *syn*-**382** (0.0564 g, 67% yield) and *anti*-**382** (0.0189 g, 22% yield) each as a white solid.

#### Ester *syn*-**382**

$R_f$  = 0.33 (75:25  $\text{EtOAc/hexanes}$ );  $^1\text{H}$  NMR (500 MHz,  $\text{CDCl}_3$ )  $\delta$  8.72 (br s, 1H), 4.31 (d,  $J$  = 1.2 Hz, 1H), 4.23 (s, 1H), 3.95 (s, 1H), 3.72 (s, 3H), 3.50 (d,  $J$  = 6.8 Hz, 1H), 2.98 (dd,  $J$  = 9.8, 5.6 Hz, 1H), 2.59 (ddd,  $J$  = 13.2, 7.1, 5.6 Hz, 1H), 2.42 (s, 3H), 2.29 (dd,  $J$  = 13.2, 9.8 Hz, 1H);  $^{13}\text{C}$  NMR (125 MHz,  $\text{CDCl}_3$ )  $\delta$  173.7, 171.7, 141.2, 91.7, 65.0, 64.8,

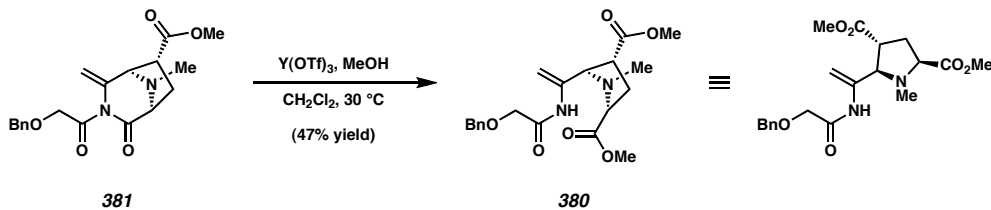
52.7, 48.6, 35.4, 33.8; IR (Neat Film, NaCl) 2955, 2925, 2854, 1733, 1686, 1459, 1377, 1316, 1273, 1204, 1173, 1125, 1071  $\text{cm}^{-1}$ ; HRMS (FAB+)  $m/z$  calc'd for  $\text{C}_{10}\text{H}_{14}\text{N}_2\text{O}_3$  [M+H] $^+$ : 211.1083, found 211.1130.



### Imide 381

A flame-dried 100 mL round-bottomed flask equipped with a magnetic stir bar and a reflux condenser was charged with benzyloxyacetic acid (**391**) (1.20 g, 7.22 mmol) and  $\text{CH}_2\text{Cl}_2$  (20 mL). To this solution was added oxalyl chloride (0.650 mL, 7.45 mmol) and *N,N*-dimethylformamide (0.028 mL, 0.362 mmol). **Warning:** vigorous gas evolution. The reaction was maintained at 23 °C until bubbling had ceased (45 min). A solution of ester **382** (0.508 g, 2.42 mmol), triethylamine (1.06 mL, 7.61 mmol), and 4-dimethylaminopyridine (0.044 g, 0.359 mmol) in  $\text{CH}_2\text{Cl}_2$  (4 mL) was then added dropwise via syringe over 5 min. The reaction was heated to 40 °C and maintained for 18 h. After cooling to room temperature, the reaction was quenched by the addition of saturated aqueous sodium bicarbonate (25 mL). The resulting biphasic mixture was stirred until bubbling ceased (15 min) and extracted with  $\text{CH}_2\text{Cl}_2$  ( $3 \times 100$  mL). The combined organics were washed with water (100 mL) and brine (100 mL), dried over  $\text{MgSO}_4$ , filtered, and concentrated to a brown oil. This residue was purified via flash chromatography over silica gel (40:60 → 45:55 EtOAc/hexanes) to yield imide **381**.

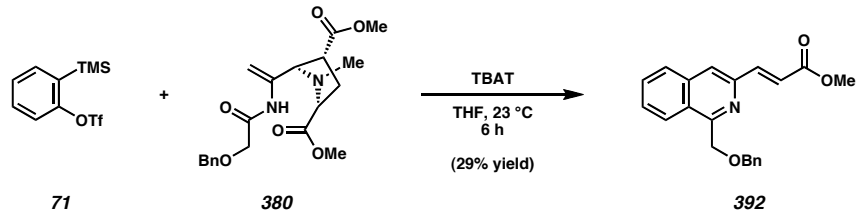
(0.6248 g, 72% yield) as a clear colorless oil.  $R_f = 0.50$  (50:50 EtOAc/hexanes);  $^1\text{H}$  NMR (500 MHz,  $\text{CDCl}_3$ )  $\delta$  7.38–7.33 (comp m, 4H), 7.33–7.28 (m, 1H), 5.22 (s, 1H), 4.68 (s, 1H), 4.60 (s, 2H), 4.52 (d,  $J = 17.1$  Hz, 1H), 4.43 (d,  $J = 17.1$  Hz, 1H), 4.00 (s, 1H), 3.74 (s, 3H), 3.61 (d,  $J = 6.8$  Hz, 1H), 3.03 (dd,  $J = 9.8, 5.9$  Hz, 1H), 2.58 (ddd,  $J = 13.2, 6.8, 5.9$  Hz, 1H), 2.44 (s, 3H), 2.23 (dd,  $J = 13.2, 9.8$  Hz, 1H);  $^{13}\text{C}$  NMR (125 MHz,  $\text{CDCl}_3$ )  $\delta$  175.5, 173.2, 171.8, 138.9, 137.0, 128.5, 128.1, 99.4, 73.7, 72.6, 67.2, 66.4, 52.5, 47.4, 35.4, 32.7; IR (Neat Film, NaCl) 2952, 2854, 2801, 1737, 1634, 1454, 1436, 1287, 1245, 1204, 1119, 1028  $\text{cm}^{-1}$ ; HRMS (FAB+)  $m/z$  calc'd for  $\text{C}_{19}\text{H}_{22}\text{N}_2\text{O}_5$  [M+H] $^+$ : 359.1601, found 359.1602.



### *N*-Acyl enamine 380

A flame-dried 25 mL round-bottomed flask equipped with a magnetic stir bar was charged with  $\text{Y(OTf)}_3$  (0.1677 g, 0.312 mmol) and  $\text{CH}_2\text{Cl}_2$  (10 mL). The flask was sealed with a rubber septum, evacuated, and back-filled with argon ( $\times 2$ ). A solution of imide **381** (0.110 g, 0.307 mmol) in  $\text{CH}_2\text{Cl}_2$  (12.5 mL) was added via syringe, and the suspension was heated to 30 °C. After stirring for 20 min, MeOH (0.087 mL, 2.15 mmol) was added dropwise via syringe over 1 min. The suspension cleared over the next 5 min and the solution was stirred for an additional 1.5 h. The reaction was cooled to room temperature and quenched by the addition of saturated aqueous sodium bicarbonate (12.5 mL). After stirring 10 min, the aqueous layer was diluted by the addition of water

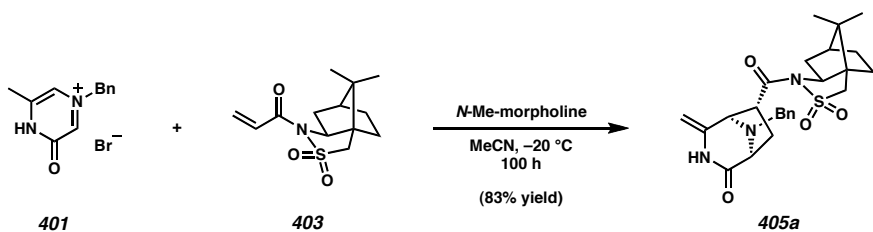
(20 mL) and then extracted with  $\text{CH}_2\text{Cl}_2$  ( $3 \times 20$  mL). The combined organics were washed with brine (40 mL), dried over  $\text{MgSO}_4$ , filtered, and concentrated to a yellow oil. This residue was purified via flash chromatography over silica gel (40:60 EtOAc/hexanes) to yield *N*-acyl enamine **380** (0.0567 g, 47% yield) as a clear colorless oil.  $R_f = 0.63$  (50:50 EtOAc/hexanes);  $^1\text{H}$  NMR (500 MHz,  $\text{CDCl}_3$ )  $\delta$  8.88 (br s, 1H), 7.37–7.32 (comp m, 4H), 7.32–7.29 (m, 1H), 5.94 (s, 1H), 4.71 (s, 1H), 4.63 (s, 2H), 4.05 (d,  $J = 15.1$  Hz, 1H), 4.01 (d,  $J = 15.1$  Hz, 1H), 3.69 (s, 3H), 3.63 (s, 3H), 3.37 (dd,  $J = 8.8, 6.3$  Hz, 1H), 3.30 (d,  $J = 8.3$  Hz, 1H), 2.95 (dd,  $J = 8.8, 8.3$  Hz, 1H), 2.37 (dd,  $J = 8.8, 6.8$  Hz, 1H), 2.37 (s, 3H), 2.21 (ddd,  $J = 6.8, 6.3, 2.9$  Hz, 1H);  $^{13}\text{C}$  NMR (125 MHz,  $\text{CDCl}_3$ )  $\delta$  173.4, 173.0, 169.2, 137.0, 136.9, 128.5, 128.0, 127.7, 101.1, 73.9, 73.3, 69.7, 66.1, 52.1, 52.0, 47.3, 38.9, 32.1; IR (Neat Film, NaCl) 3334, 2953, 2853, 1736, 1697, 1513, 1455, 1437, 1367, 1277, 1204, 1170, 1102  $\text{cm}^{-1}$ ; HRMS (FAB+)  $m/z$  calc'd for  $\text{C}_{20}\text{H}_{26}\text{N}_2\text{O}_6$  [ $\text{M}+\text{H}]^+$ : 391.1864, found 391.1867.



### Isoquinoline **392**

A flame-dried 1 dram vial equipped with a magnetic stir bar and a septum-bearing screw cap was charged with tetra-*n*-butylammonium difluorotriphenylsilicate (0.0214 g, 0.040 mmol) and *N*-acyl enamine **380** (0.010 g, 0.025 mmol). The vial was evacuated and back-filled with argon ( $\times 2$ ). Tetrahydrofuran (0.5 mL) was then added via syringe, followed by 2-(trimethylsilyl)phenyl triflate (**71**) (0.0075 mL, 0.031 mmol). The reaction

was stirred at 23 °C for 3 h, at which point an additional amount of 2-(trimethylsilyl)phenyl triflate (**71**) (0.003 mL, 0.012 mmol) was added. Stirring continued at 23 °C for 3 h, after which the reaction was diluted with EtOAc (10 mL) and washed with saturated aqueous sodium bicarbonate (10 mL), dried over Na<sub>2</sub>SO<sub>4</sub>, and concentrated to a yellow oil. The residue was purified via flash chromatography over silica gel (10:90 EtOAc/hexanes) to yield isoquinoline **392** (0.0024 g, 29% yield) as a white solid.  $R_f$  = 0.47 (30:70 EtOAc/hexanes); <sup>1</sup>H NMR (500 MHz, CDCl<sub>3</sub>) δ 8.38 (d,  $J$  = 8.3 Hz, 1H), 7.86 (d,  $J$  = 7.8 Hz, 1H), 7.83 (d,  $J$  = 15.4 Hz, 1H), 7.71 (ddd,  $J$  = 8.3, 6.8, 1.0 Hz, 1H), 7.70 (s, 1H), 7.64 (ddd,  $J$  = 8.3, 6.8, 1.0 Hz, 1H), 7.39–7.33 (comp m, 4H), 7.32–7.27 (m, 1H), 7.15 (d,  $J$  = 15.4 Hz, 1H), 5.15 (s, 2H), 4.65 (s, 2H), 3.85 (s, 3H); <sup>13</sup>C NMR (125 MHz, CDCl<sub>3</sub>) δ 168.2, 155.9, 145.2, 144.2, 137.8, 136.1, 134.3, 132.8, 130.6, 128.4, 128.1, 127.8, 126.2, 122.8, 117.2, 110.0, 73.1, 70.8, 54.1; IR (Neat Film, NaCl) 2949, 2920, 2850, 1716, 1640, 1580, 1435, 1295, 1262, 1164, 1090 cm<sup>-1</sup>; HRMS (FAB+) *m/z* calc'd for C<sub>21</sub>H<sub>19</sub>NO<sub>3</sub> [M+H]<sup>+</sup>: 334.1438, found 334.1454.



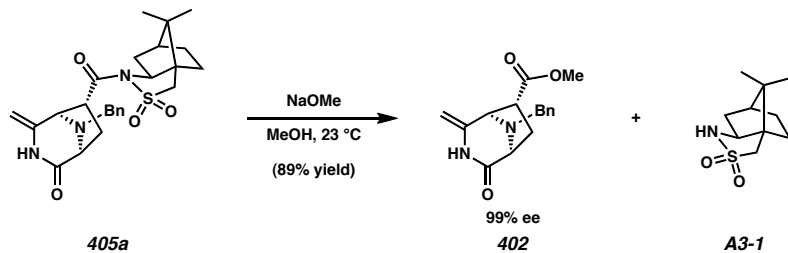
## Diazabicyclic 405a<sup>13,14</sup>

A flame-dried 1 L round-bottomed flask equipped with a stir bar was charged with 2-oxidopyrazinium bromide **401** (12.70 g, 45.2 mmol) and acetonitrile (250 mL). The suspension was cooled to  $-20^{\circ}\text{C}$  in a Thermo Scientific NESLAB CB-80 cold bath. *N*-methyl morpholine (14.9 mL, 136 mmol) was added via syringe and the mixture was

stirred until all solids had dissolved (10 min). A solution of acrylamide **403** (14.57 g, 54.1 mmol) in acetonitrile (350 mL) was then added and the reaction was maintained at –20 °C for 100 h. The reaction was then diluted cold in EtOAc (400 mL) and washed with water (2 × 300 mL). The combined aqueous layers were extracted with EtOAc (2 × 200 mL) and the combined organic layers were washed with brine (400 mL), dried over MgSO<sub>4</sub>, and concentrated under reduced pressure. The resulting crude orange-yellow solid was filtered through a plug of silica (CH<sub>2</sub>Cl<sub>2</sub> → 75:25 EtOAc/hexanes) to remove orange baseline material. Solvent was removed under reduced pressure to afford an off-white solid.<sup>39</sup> The crude solid was dissolved in a minimum amount of CH<sub>2</sub>Cl<sub>2</sub> (240 mL), and to this solution was added hexanes (300 mL) while swirling until the first crystals were visible. The solution was then allowed to stand at 23 °C for 8 h. Filtration under vacuum provided diazabicycle **405a** (14.85 g, 70% yield) as a white solid. The mother liquor was concentrated and the residue was resubmitted to recrystallization to provide additional diazabicycle **405a** (2.75 g, 13% yield – 83% combined yield) as a white solid.

*R*<sub>f</sub> = 0.38 (50:50 EtOAc/hexanes); <sup>1</sup>H NMR (500 MHz, CDCl<sub>3</sub>) δ 7.53 (br s, 1H), 7.31–7.21 (comp m, 5H), 4.38 (d, *J* = 1.2 Hz, 1H), 4.32 (d, *J* = 1.2 Hz, 1H), 3.94 (d, *J* = 12.8 Hz, 1H), 3.89 (dd, *J* = 7.8, 4.6 Hz, 1H), 3.74 (d, *J* = 7.8 Hz, 1H), 3.68 (s, 1H), 3.59 (dd, *J* = 9.0, 3.9 Hz, 1H), 3.57 (d, *J* = 12.8 Hz, 1H), 3.41 (s, 2H), 3.06 (ddd, *J* = 13.4, 7.8, 3.9 Hz, 1H), 2.15 (dd, *J* = 13.4, 9.0 Hz, 1H), 2.06 (dd, *J* = 13.9, 7.8 Hz, 1H), 1.91–1.84 (comp m, 3H), 1.82 (dd, *J* = 4.2, 3.7 Hz, 1H), 1.43–1.32 (comp m, 2H), 0.92 (s, 3H), 0.75 (s, 3H); <sup>13</sup>C NMR (125 MHz, CDCl<sub>3</sub>) δ 171.4, 171.3, 139.2, 138.2, 128.8, 128.5, 127.5, 94.0, 65.8, 63.4, 63.3, 53.3, 52.1, 49.2, 48.6, 47.9, 44.8, 38.5, 33.0, 31.3, 26.6, 20.8, 20.0; IR (Neat Film, NaCl) 3199, 2960, 1688, 1654, 1455, 1329, 1213, 1134, 853 cm<sup>–1</sup>; HRMS

(FAB+)  $m/z$  calc'd for  $C_{25}H_{32}N_3O_4S$   $[M+H]^+$ : 470.2108, found 470.2136;  $[\alpha]^{22}_D$  +100.72° ( $c$  1.0,  $CHCl_3$ ).

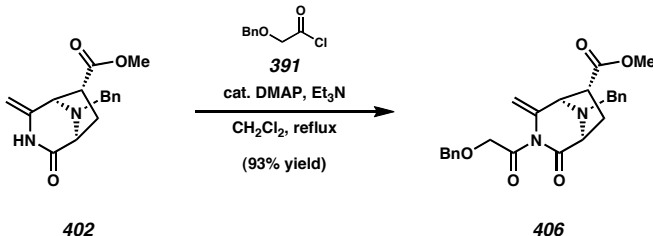


### Ester **402**

A flame-dried 500 mL round-bottomed flask equipped with a stir bar was charged with a 60% w/w suspension of  $NaH$  in mineral oil (1.32 g, 33.0 mmol). Methanol (200 mL) was slowly added with stirring at  $23\text{ }^\circ C$  under argon. **Warning:** vigorous gas evolution. The suspension was stirred until all solids had dissolved (15 min). A solution of diazabicycle **405a** (5.07 g, 10.8 mmol) in  $CH_2Cl_2$  (40 mL) was then added, and the reaction was maintained at  $23\text{ }^\circ C$  for 20 min. The reaction was quenched by the addition of saturated aqueous  $NH_4Cl$  (250 mL) and extracted into  $EtOAc$  ( $3 \times 200$  mL). The combined organic layers were washed with brine (300 mL), dried over  $MgSO_4$ , and concentrated under reduced pressure. The residue was purified via flash chromatography over silica gel (25:75 → 30:70  $EtOAc$ /hexanes) to afford methyl ester **402** (2.75 g, 89% yield) as a white solid and sultam **A3-1** (1.74 g, 75% yield) as a white crystalline solid.

$R_f$  = 0.45 (50:50  $EtOAc$ /hexanes);  $^1H$  NMR (500 MHz,  $CDCl_3$ )  $\delta$  8.35 (br s, 1H), 7.35–7.29 (comp m, 4H), 7.28–7.24 (m, 1H), 4.33 (d,  $J$  = 1.2 Hz, 1H), 4.19 (d,  $J$  = 1.2, 1H), 4.02 (s, 1H), 3.82 (d,  $J$  = 13.4 Hz, 1H), 3.74 (s, 3H), 3.73 (d,  $J$  = 13.4 Hz, 1H), 3.62 (d,  $J$  = 7.3 Hz, 1H), 3.02 (dd,  $J$  = 9.8, 5.6 Hz, 1H), 2.66 (ddd,  $J$  = 13.2, 7.3, 5.6 Hz, 1H),

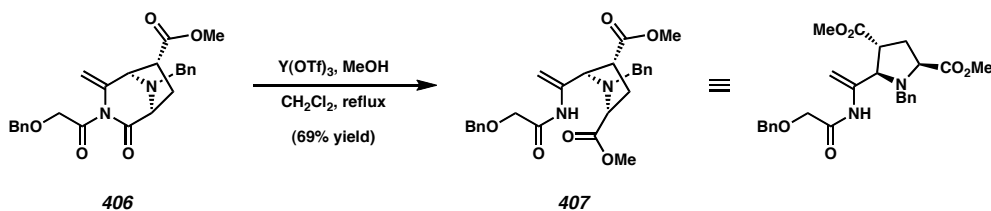
(dd,  $J = 13.2, 9.8$  Hz, 1H);  $^{13}\text{C}$  NMR (125 MHz,  $\text{CDCl}_3$ )  $\delta$  173.6, 171.6, 141.3, 137.9, 128.7, 128.6, 127.6, 91.7, 63.3, 62.5, 52.6, 52.5, 48.4, 33.5; IR (Neat Film, NaCl) 3202, 2953, 1737, 1684, 1656, 1454, 1318, 1200, 850  $\text{cm}^{-1}$ ; HRMS (FAB+)  $m/z$  calc'd for  $\text{C}_{16}\text{H}_{19}\text{N}_2\text{O}_3$  [ $\text{M}+\text{H}]^+$ : 287.1396, found 287.1390;  $[\alpha]^{26}_D -23.66^\circ$  ( $c$  1.0,  $\text{CHCl}_3$ ). Analytical chiral SFC assay: Chiralcel OD-H column, 10:90 2-propanol: $\text{CO}_2$ , 2.0 mL/min,  $\lambda = 254$  nm, 40 °C isothermal method over 20 min. Racemic **402**:  $t_{\text{fast}} = 11.31$  min ((–)-**402**, 49.9%),  $t_{\text{slow}} = 11.89$  min ((+)-**402**, 50.1%). Enantio-enriched **402**:  $t_{\text{fast}} = 11.39$  min ((–)-**402**, >99%) (the trace corresponding to (+)-**402** was below the threshold of detection).



### Imide **406**

A flame-dried 500 mL 3-neck round-bottomed flask equipped with a stir bar and a reflux condenser was charged with benzyloxyacetic acid (**391**) (8.76 g, 52.8 mmol) and  $\text{CH}_2\text{Cl}_2$  (140 mL). To this solution was added oxalyl chloride (4.53 mL, 51.9 mmol) and *N,N*-dimethylformamide (0.205 mL, 2.65 mmol). **Warning:** vigorous gas evolution. The reaction was maintained at 23 °C until bubbling had ceased (45 min). A solution of ester **402** (5.00 g, 17.5 mmol), triethylamine (7.9 mL, 56.7 mmol), and 4-dimethylaminopyridine (0.325 g, 2.66 mmol) in  $\text{CH}_2\text{Cl}_2$  (35 mL) was then added dropwise via syringe over 5 min. The reaction was heated to 40 °C and maintained for

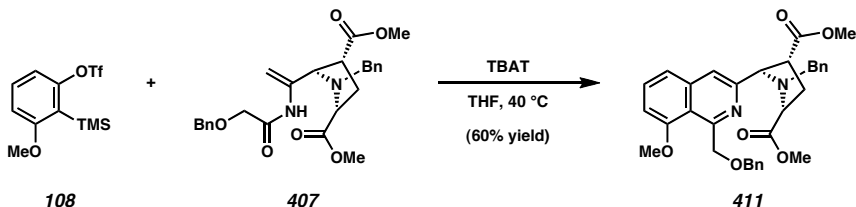
30 h. After cooling to room temperature, the solution was diluted in  $\text{CH}_2\text{Cl}_2$  (200 mL) and washed with saturated aqueous  $\text{NH}_4\text{Cl}$  (200 mL), water (200 mL), and brine (200 mL). The organic layer was dried over  $\text{MgSO}_4$  and concentrated under reduced pressure. The crude orange residue was purified via flash chromatography over silica gel (15:85 → 25:75 EtOAc/hexanes) to afford imide **406** (7.06 g, 93% yield) as a colorless oil.  $R_f = 0.47$  (30:70 EtOAc/hexanes);  $^1\text{H}$  NMR (500 MHz,  $\text{CDCl}_3$ )  $\delta$  7.41–7.34 (comp m, 4H), 7.34–7.29 (comp m, 4H), 7.29–7.24 (comp m, 2H), 5.25 (d,  $J = 1.2$  Hz, 1H), 4.65 (s, 2H), 4.59 (d,  $J = 1.2$  Hz, 1H), 4.56 (d,  $J = 16.8$  Hz, 1H), 4.49 (d,  $J = 16.8$  Hz, 1H), 4.04 (s, 1H), 3.77 (d,  $J = 4.9$  Hz, 2H), 3.74 (s, 3H), 3.68 (d,  $J = 7.1$  Hz, 1H), 3.04 (dd,  $J = 9.8, 6.0$  Hz, 1H), 2.62 (ddd,  $J = 13.4, 7.1, 6.0$  Hz, 1H), 2.26 (dd,  $J = 13.4, 9.8$  Hz, 1H);  $^{13}\text{C}$  NMR (125 MHz,  $\text{CDCl}_3$ )  $\delta$  175.9, 173.4, 172.1, 139.2, 137.4, 137.2, 128.8, 128.7, 128.6, 128.4, 128.3, 127.7, 99.8, 74.0, 72.9, 65.2, 64.7, 52.7, 52.7, 47.5, 32.7; IR (Neat Film, NaCl) 2952, 1736, 1634, 1454, 1200, 1117, 1028  $\text{cm}^{-1}$ ; HRMS (FAB+)  $m/z$  calc'd for  $\text{C}_{25}\text{H}_{27}\text{N}_2\text{O}_5$  [ $\text{M}+\text{H}]^+$ : 435.1920, found 435.1930;  $[\alpha]^{21}_{\text{D}} -51.53^\circ$  ( $c$  1.0,  $\text{CHCl}_3$ ).



### N-acyl enamine **407**

A flame-dried 500 mL 3-neck round-bottomed flask equipped with a stir bar and reflux condenser was charged with  $\text{Y}(\text{OTf})_3$  (2.59 g, 4.83 mmol) and  $\text{CH}_2\text{Cl}_2$  (120 mL). The suspension was heated to 40 °C and a solution of imide **406** (2.05 g, 4.72 mmol) in  $\text{CH}_2\text{Cl}_2$  (35 mL) was added. The mixture was maintained at 40 °C for 1 h, at which point

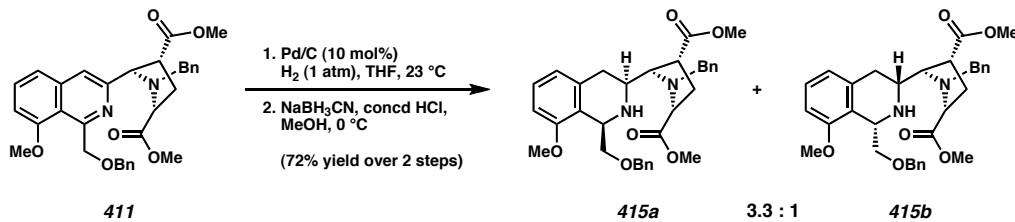
MeOH (1.35 mL, 33.3 mmol) was added via syringe. The suspension immediately cleared and stirring was continued at 40 °C for an additional 30 min. After cooling to room temperature, the reaction was concentrated to a cloudy yellow oil containing yttrium salts, which was suspended in a minimum amount of CH<sub>2</sub>Cl<sub>2</sub> (12 mL) and filtered through a plug of Celite. The filtrate was concentrated under reduced pressure and purified via flash chromatography over silica gel (25:75 → 40:60 EtOAc/hexanes) to yield *N*-acyl enamine **407** (1.52 g, 69% yield) as a pale yellow oil. *R*<sub>f</sub> = 0.70 (50:50 EtOAc/hexanes); <sup>1</sup>H NMR (500 MHz, CDCl<sub>3</sub>) δ 9.18 (br s, 1H), 7.43 (d, *J* = 6.6 Hz, 2H), 7.39 (dd, *J* = 7.2, 6.6 Hz, 2H), 7.34, (tt, *J* = 7.2, 1.5 Hz, 1H), 7.29–7.22 (comp m, 5H), 6.01 (s, 1H), 4.76 (d, *J* = 1.2 Hz, 1H), 4.75 (d, *J* = 12.4 Hz, 1H), 4.71 (d, *J* = 12.4 Hz, 1H), 4.06 (s, 2H), 3.97 (d, *J* = 13.7 Hz, 1H), 3.69 (s, 3H), 3.65 (d, *J* = 9.0 Hz, 1H), 3.60 (d, *J* = 13.7 Hz, 1H), 3.56 (dd, *J* = 9.5, 4.2 Hz, 1H), 3.40 (s, 3H), 3.09 (dd, *J* = 9.5, 8.8 Hz, 1H), 2.33 (dt, *J* = 12.9, 9.8 Hz, 1H), 2.13 (ddd, *J* = 12.7, 8.3, 4.2 Hz, 1H); <sup>13</sup>C NMR (125 MHz, CDCl<sub>3</sub>) δ 174.4, 173.2, 169.5, 137.4, 137.3, 136.8, 129.7, 128.8, 128.5, 128.3, 128.2, 127.8, 101.7, 73.7, 72.2, 70.0, 63.2, 56.4, 52.4, 52.0, 47.6, 33.1; IR (Neat Film, NaCl) 3316, 2951, 1737, 1696, 1512, 1454, 1436, 1201, 1174, 1028 cm<sup>−1</sup>; HRMS (ES+) *m/z* calc'd for C<sub>26</sub>H<sub>31</sub>N<sub>2</sub>O<sub>6</sub> [M+H]<sup>+</sup>: 467.2182, found 467.2188; [α]<sup>25</sup><sub>D</sub> −29.78° (c 1.0, CHCl<sub>3</sub>).



### Isoquinoline 411

A flame-dried 500 mL 3-neck round-bottomed flask equipped with a stir bar and reflux condenser was charged with tetra-*n*-butylammonium difluorotriphenylsilicate (5.45 g, 10.1 mmol) and THF (120 mL). A solution of *N*-acyl enamine **407** (2.35 g, 5.04 mmol) in THF (50 mL) was added at 23 °C, followed by silylaryl triflate **108**<sup>40</sup> (3.31 g, 10.1 mmol). The reaction was heated to 40 °C and maintained for 15 h, then cooled to room temperature and concentrated under reduced pressure. The yellow residue was purified via flash chromatography over silica gel (15:85 → 25:75 EtOAc/hexanes) to afford isoquinoline **411** (1.68 g, 60% yield) as a pale yellow oil.  $R_f$  = 0.65 (50:50 EtOAc/hexanes); <sup>1</sup>H NMR (500 MHz, CDCl<sub>3</sub>) δ 8.06 (s, 1H), 7.55 (dd, *J* = 8.1, 7.8 Hz, 1H), 7.44 (d, *J* = 7.6 Hz, 2H), 7.34 (dd, *J* = 7.8, 7.1 Hz, 2H), 7.32–7.25 (comp m, 4H), 7.22 (dd, *J* = 7.6, 7.1 Hz, 2H), 7.15 (t, *J* = 7.3 Hz, 1H), 6.90 (d, *J* = 7.8 Hz, 1H), 5.32 (d, *J* = 12.5 Hz, 1H), 5.29 (d, *J* = 12.5 Hz, 1H), 4.78 (d, *J* = 11.7 Hz, 1H), 4.68 (d, *J* = 11.7 Hz, 1H), 4.52 (d, *J* = 6.1 Hz, 1H), 4.04 (d, *J* = 13.4 Hz, 1H), 3.96 (s, 3H), 3.79 (d, *J* = 13.4 Hz, 1H), 3.77 (dd, *J* = 9.5, 7.6 Hz, 1H), 3.61 (s, 3H), 3.51 (s, 3H), 3.31 (dt, *J* = 8.3, 6.1 Hz, 1H), 2.44 (ddd, *J* = 12.7, 8.3, 6.1 Hz, 1H), 2.26 (ddd, *J* = 12.7, 8.1, 7.8 Hz, 1H); <sup>13</sup>C NMR (125 MHz, CDCl<sub>3</sub>) δ 174.8, 174.5, 157.7, 156.4, 154.2, 140.0, 139.2, 137.9, 130.4, 129.8, 128.5, 128.4, 128.2, 127.6, 127.4, 120.3, 118.0, 106.7, 75.2, 73.0, 72.7, 65.3, 58.1, 55.9, 52.2, 51.9, 50.6, 45.0, 32.9; IR (Neat Film, NaCl) 2950, 1736, 1733, 1619, 1566,

1454, 1361, 1201, 1171  $\text{cm}^{-1}$ ; HRMS (FAB+)  $m/z$  calc'd for  $\text{C}_{33}\text{H}_{35}\text{N}_2\text{O}_6$  [M+H] $^+$ : 555.2490, found 555.2497;  $[\alpha]^{24}_{\text{D}} -8.21^\circ$  ( $c$  1.0,  $\text{CHCl}_3$ ).



## Tetrahydroisoquinolines 415a and 415b

A flame-dried 10 mL round-bottomed flask equipped with a stir bar was charged with 10% w/w palladium on carbon (0.019 g, 0.018 mmol) followed by a solution of isoquinoline **411** (0.100 g, 0.180 mmol) in THF (3.6 mL). The flask was purged with hydrogen and a hydrogen balloon was attached. The reaction was maintained at 23 °C for 6 h, then filtered through a plug of silica with 30:70 EtOAc/hexanes. Removal of the solvents under vacuum provided a 3.3:1 mixture of dihydroisoquinolines **416a** and **416b**<sup>25</sup> (not shown) (0.082 g), which was carried on without further purification. A flame-dried 5 mL round-bottomed flask equipped with a stir bar was charged with dihydroisoquinolines **416a** and **416b** (0.082 g, 0.148 mmol) in methanol (2.9 mL), and the solution was cooled to 0 °C. Concentrated hydrochloric acid (0.018 mL, 0.216 mmol) was added via syringe followed by NaBH<sub>3</sub>CN (0.046 g, 0.732 mmol) added in portions, allowing for bubbling to subside. The reaction was maintained at 0 °C for 15 min, and then quenched with saturated aqueous NaHCO<sub>3</sub> (1.5 mL) followed by CH<sub>2</sub>Cl<sub>2</sub> (1.5 mL). The cloudy white mixture was vigorously stirred for 5 min, then 0.2 N NaOH was added dropwise until the mixture cleared (6 drops). The biphasic mixture was extracted with CH<sub>2</sub>Cl<sub>2</sub> (3 × 10 mL) and the combined organic phases were washed with

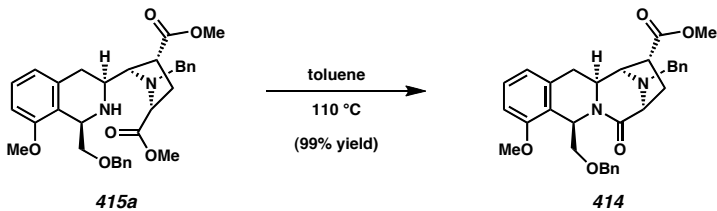
brine (15 mL), dried over  $\text{MgSO}_4$ , and concentrated under reduced pressure. The yellow residue was purified via flash chromatography over silica gel (15:85 EtOAc/hexanes) to yield tetrahydroisoquinoline **415a** (0.055 g, 55% yield over 2 steps) as a clear colorless oil and tetrahydroisoquinoline **415b** (0.017 g, 17% yield over 2 steps) as a clear colorless oil.

### Tetrahydroisoquinoline **415a**

$R_f$  = 0.38 (30:70 EtOAc/hexanes);  $^1\text{H}$  NMR (500 MHz,  $\text{CDCl}_3$ )  $\delta$  7.39 (d,  $J$  = 7.3 Hz, 2H), 7.36–7.29 (comp m, 4H), 7.29–7.23 (comp m, 3H), 7.21 (dd,  $J$  = 7.3, 7.1 Hz, 1H), 7.11 (t,  $J$  = 7.8 Hz, 1H), 6.72 (d,  $J$  = 7.6 Hz, 1H), 6.68 (d,  $J$  = 8.3 Hz, 1H), 4.66 (d,  $J$  = 12.2 Hz, 1H), 4.59 (d,  $J$  = 12.2 Hz, 1H), 4.47 (d,  $J$  = 7.1 Hz, 1H), 4.17 (dd,  $J$  = 8.8, 2.2 Hz, 1H), 3.99 (d,  $J$  = 13.9 Hz, 1H), 3.81 (d,  $J$  = 13.9 Hz, 1H), 3.76 (s, 3H), 3.71 (s, 3H), 3.63 (dd,  $J$  = 8.3, 7.8 Hz, 1H), 3.46–3.33 (comp m, 4H), 3.38 (s, 3H), 2.98 (ddd,  $J$  = 11.2, 2.9, 2.7 Hz, 1H), 2.65 (dd,  $J$  = 14.7, 11.2 Hz, 1H), 2.55 (dd,  $J$  = 14.7, 2.7 Hz, 1H), 2.35 (ddd,  $J$  = 12.5, 7.1, 3.8 Hz, 1H), 2.27 (ddd,  $J$  = 12.7, 9.0, 8.8 Hz, 1H);  $^{13}\text{C}$  NMR (125 MHz,  $\text{CDCl}_3$ )  $\delta$  176.1, 174.4, 157.1, 139.4, 139.1, 138.7, 129.3, 128.4, 128.3, 127.8, 127.5, 127.4, 127.1, 124.4, 121.8, 108.2, 75.2, 73.1, 72.0, 66.8, 59.1, 55.3, 53.6, 53.4, 52.3, 51.8, 45.0, 42.9, 34.5, 34.0; IR (Neat Film, NaCl) 2949, 1734, 1731, 1584, 1470, 1255, 1198, 1170, 1074  $\text{cm}^{-1}$ ; HRMS (FAB+)  $m/z$  calc'd for  $\text{C}_{33}\text{H}_{39}\text{N}_2\text{O}_6$  [M+H] $^+$ : 559.2803, found 559.2814;  $[\alpha]^{23}_{\text{D}} -52.71^\circ$  ( $c$  1.0,  $\text{CHCl}_3$ ).

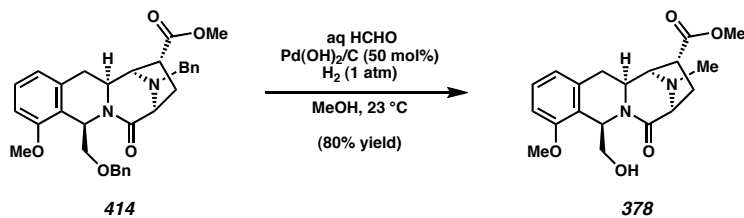
**Tetrahydroisoquinoline 415b**

$R_f$  = 0.18 (30:70 EtOAc/hexanes);  $^1\text{H}$  NMR (500 MHz,  $\text{CDCl}_3$ )  $\delta$  7.49 (d,  $J$  = 7.6 Hz, 2H), 7.38 (t,  $J$  = 7.6 Hz, 2H), 7.38–7.34 (comp m, 2H), 7.30 (t,  $J$  = 7.3 Hz, 1H), 7.19–7.14 (comp m, 3H), 7.12 (t,  $J$  = 7.8 Hz, 1H), 6.71 (d,  $J$  = 7.8 Hz, 1H), 6.65 (d,  $J$  = 8.1 Hz, 1H), 4.72 (d,  $J$  = 12.2 Hz, 1H), 4.68 (d,  $J$  = 12.2 Hz, 1H), 4.62 (dd,  $J$  = 9.5, 2.2 Hz, 1H), 4.03 (d,  $J$  = 13.4 Hz, 1H), 3.79 (d,  $J$  = 13.4 Hz, 1H), 3.76 (s, 3H), 3.70 (s, 3H), 3.67–3.56 (comp m, 3H), 3.60 (d,  $J$  = 9.3 Hz, 1H), 3.39–3.32 (comp m, 2H), 3.38 (s, 3H), 3.30 (app dt,  $J$  = 8.1, 7.1 Hz, 1H), 2.60 (d,  $J$  = 7.6 Hz, 2H), 2.35–2.21 (comp m, 2H);  $^{13}\text{C}$  NMR (125 MHz,  $\text{CDCl}_3$ )  $\delta$  176.2, 174.3, 156.6, 139.2, 138.2, 136.9, 129.8, 128.5, 128.3, 127.8, 127.6, 127.4, 123.8, 121.6, 107.7, 72.8, 71.5, 69.4, 66.8, 59.2, 55.4, 52.3, 51.8, 47.4, 42.7, 34.1, 32.4; IR (Neat Film, NaCl) 2949, 1733, 1588, 1454, 1257, 1198, 1171, 1074  $\text{cm}^{-1}$ ; HRMS (FAB+)  $m/z$  calc'd for  $\text{C}_{33}\text{H}_{39}\text{N}_2\text{O}_6$  [M+H] $^+$ : 559.2803, found 559.2825;  $[\alpha]^{21}_D$  –17.00° (c 0.5,  $\text{CHCl}_3$ ).

**Lactam 414**

A flame-dried 20 mL scintillation vial equipped with a stir bar was charged with tetrahydroisoquinoline **415a** (0.075 g, 0.135 mmol) in toluene (5.4 mL). The vial was sealed with a teflon cap and the reaction was heated to 110 °C for 24 h. The reaction was then cooled to room temperature and the solvent was removed under reduced pressure. Purification via flash chromatography over silica gel (25:75 EtOAc/hexanes) provided

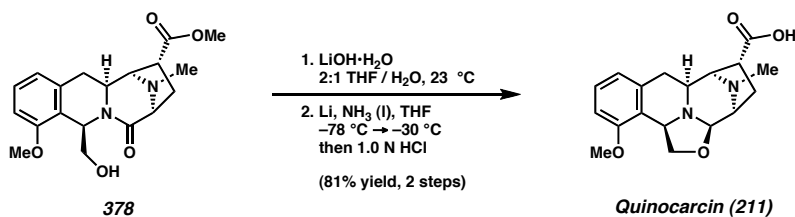
tetracyclic lactam **414** (0.071 g, 99% yield) as a pale yellow oil.  $R_f$  = 0.61 (50:50 EtOAc/hexanes);  $^1\text{H}$  NMR (500 MHz,  $\text{CDCl}_3$ )  $\delta$  7.34–7.22 (comp m, 9H), 7.21 (t,  $J$  = 8.0 Hz, 1H), 7.07 (dd,  $J$  = 7.6, 2.4 Hz, 1H), 6.79 (d,  $J$  = 8.3 Hz, 1H), 6.74 (d,  $J$  = 7.3 Hz, 1H), 5.64 (t,  $J$  = 2.2 Hz, 1H), 4.32 (d,  $J$  = 12.0 Hz, 1H), 4.29 (d,  $J$  = 12.0 Hz, 1H), 4.25 (dd,  $J$  = 9.5, 3.2 Hz, 1H), 3.79 (s, 3H), 3.76 (dd,  $J$  = 12.4, 2.2 Hz, 1H), 3.73 (s, 3H), 3.72 (br s, 1H), 3.68 (d,  $J$  = 6.4 Hz, 1H), 3.60 (br s, 1H), 3.48 (dd,  $J$  = 9.5, 2.0 Hz, 1H), 3.25 (app t,  $J$  = 8.1 Hz, 1H), 3.12 (app t,  $J$  = 13.4 Hz, 1H), 2.66 (app dt,  $J$  = 6.6, 6.6 Hz, 1H), 2.44 (dd,  $J$  = 14.2, 2.2 Hz, 1H), 2.21 (dd,  $J$  = 13.2, 9.5 Hz, 1H);  $^{13}\text{C}$  NMR (125 MHz,  $\text{CDCl}_3$ )  $\delta$  175.5, 170.8, 155.9, 138.7, 138.6, 138.3, 128.9, 128.6, 128.5, 128.1, 127.8, 127.6, 127.5, 123.2, 119.9, 108.9, 73.5, 70.9, 66.6, 65.2, 57.1, 55.5, 54.6, 52.4, 49.7, 41.2, 34.5, 32.4; IR (Neat Film, NaCl) 2950, 1735, 1654, 1474, 1437, 1265, 1208, 1099, 1069  $\text{cm}^{-1}$ ; HRMS (FAB+)  $m/z$  calc'd for  $\text{C}_{32}\text{H}_{35}\text{N}_2\text{O}_5$  [ $\text{M}+\text{H}]^+$ : 527.2540, found 527.2543;  $[\alpha]^{24}_{\text{D}}$  –85.60° ( $c$  1.0,  $\text{CHCl}_3$ ).



### N-Methyl amine 378

A flame-dried 1 dram vial equipped with a stir bar and a septum-bearing screw cap was charged with moist 20% w/w  $\text{Pd}(\text{OH})_2$  on carbon ( $\leq$ 50% water) (0.062 g, 0.044 mmol) followed by a solution of lactam **414** (0.0435 g, 0.083 mmol) in  $\text{MeOH}$  (0.85 mL). The vial was purged with hydrogen and a hydrogen balloon was attached. The reaction was maintained at 23 °C for 20 h, at which point a 37% w/w aqueous solution of

formaldehyde (0.310 mL, 4.14 mmol) was added via syringe. The reaction was maintained at 23 °C under hydrogen for an additional 20 h, and then filtered through a plug of Celite eluting with 10:90 MeOH/CH<sub>2</sub>Cl<sub>2</sub>. The solvent was removed under reduced pressure and the residue was purified via flash chromatography over silica (CH<sub>2</sub>Cl<sub>2</sub> → 2:98 MeOH/CH<sub>2</sub>Cl<sub>2</sub>) to afford *N*-methyl amine **378** (0.024 g, 80% yield) as a solid white foam. *R*<sub>f</sub> = 0.28 (10:90 MeOH/CH<sub>2</sub>Cl<sub>2</sub>); <sup>1</sup>H NMR (500 MHz, CDCl<sub>3</sub>) δ 7.21 (t, *J* = 7.8 Hz, 1H), 6.81 (d, *J* = 8.3 Hz, 1H), 6.78 (d, *J* = 7.6 Hz, 1H), 5.72 (dd, *J* = 5.6, 3.2 Hz, 1H), 3.91 (ddd, *J* = 11.3, 6.2, 2.9 Hz, 1H), 3.84 (s, 3H), 3.83 (app dt, *J* = 12.4, 2.4 Hz, 1H), 3.76 (s, 3H), 3.66 (dd, *J* = 1.5, 1.2 Hz, 1H), 3.60 (d, *J* = 6.4 Hz, 1H), 3.55 (ddd, *J* = 11.0, 5.6, 3.4 Hz, 1H), 3.31 (dd, *J* = 9.5, 6.6 Hz, 1H), 3.03 (dd, *J* = 5.6, 4.6 Hz, 1H), 2.96 (dd, *J* = 14.6, 12.7 Hz, 1H), 2.66 (app dt, *J* = 13.2, 6.6 Hz, 1H), 2.62 (dd, *J* = 14.6, 2.2 Hz, 1H), 2.48 (s, 3H), 2.39 (dd, *J* = 13.2, 9.5 Hz, 1H); <sup>13</sup>C NMR (125 MHz, CDCl<sub>3</sub>) δ 174.9, 173.5, 156.1, 137.5, 128.8, 121.8, 120.1, 109.3, 67.4, 67.3, 66.4, 55.7, 55.4, 52.7, 52.0, 41.6, 37.3, 34.8, 32.2; IR (Neat Film, NaCl) 3404, 2951, 1733, 1638, 1474, 1436, 1264, 1204, 1064, 915 cm<sup>–1</sup>; HRMS (EI+) *m/z* calc'd for C<sub>19</sub>H<sub>24</sub>N<sub>2</sub>O<sub>5</sub> [M]<sup>+</sup>: 360.1685, found 360.1701; [α]<sub>D</sub><sup>22</sup> –104.64° (c 1.0, CHCl<sub>3</sub>).



### Quinocarcin (211)<sup>41</sup>

A flame-dried 15 mL round-bottomed flask equipped with a stir bar was charged with *N*-methyl amine **378** (36.4 mg, 0.101 mmol) in THF (2.7 mL). A solution of LiOH·H<sub>2</sub>O

(0.0423 g, 1.01 mmol) in H<sub>2</sub>O (1.35 mL) was added via syringe and the mixture was vigorously stirred at 23 °C for 3 h. Ethyl acetate (4 mL) was added and the solution was neutralized to pH 7 with 2.0 N HCl (4 drops). The biphasic mixture was transferred to a 50 mL round-bottomed flask and the solvents were removed under reduced pressure. The resulting cloudy white residue was dried under high vacuum for 6 h, and then suspended in THF (7 mL) and cooled to –78 °C. Ammonia (14 mL) was condensed into the flask using a cold finger at –78 °C and lithium metal (0.0401 g, 5.78 mmol) was added. The mixture turned dark blue and was vigorously stirred for 2 min. The –78 °C cold bath was replaced with a –30 °C cold bath (MeCN/CO<sub>2</sub>) and stirring was continued for 15 min. The reaction was quenched by the addition of methanol (5 mL) down the side of the cold finger and stirred for an additional 5 min. Solid NH<sub>4</sub>Cl (0.960 g, 17.9 mmol) was added in portions, the cold bath was removed, and the ammonia was evaporated under a stream of argon at room temperature. Water (10 mL) was added and the mixture was neutralized to pH 7 with 1.0 N HCl (10 mL). The solvents were removed under reduced pressure, and the resulting solids were dissolved in a minimum amount of water (1 mL) and filtered through a 5 g Sep-Pak C<sub>18</sub> plug (H<sub>2</sub>O → 50:50 MeOH/H<sub>2</sub>O) to remove salts. The crude residue was purified via semi-preparative reverse-phase HPLC (20:80 → 70:30 MeOH/H<sub>2</sub>O, *t*<sub>R</sub> = 33 min) to afford quinocarcin (**211**) (0.0269 g, 81% yield over 2 steps) as a white solid. <sup>1</sup>H NMR (500 MHz, CD<sub>3</sub>OD) δ 7.17 (t, *J* = 7.8 Hz, 1H), 6.85 (d, *J* = 8.3 Hz, 1H), 6.76 (d, *J* = 7.6 Hz, 1H), 4.57 (d, *J* = 2.9 Hz, 1H), 4.55 (dd, *J* = 7.3, 2.9 Hz, 1H), 4.07 (br s, 2H), 3.82 (s, 3H), 3.68 (dd, *J* = 10.7, 2.9 Hz, 1H), 3.43–3.33 (comp m, 2H), 3.39 (dd, *J* = 10.7, 7.3 Hz, 1H), 2.79–2.74 (m, 1H), 2.77 (s, 3H), 2.64 (dd, *J* = 14.6, 2.4 Hz, 1H), 2.64–2.60 (m, 1H), 2.46 (dd, *J* = 13.9, 10.5 Hz, 1H); <sup>13</sup>C NMR (125 MHz,

CD<sub>3</sub>OD) δ 179.5, 157.2, 137.6, 129.1, 124.0, 121.3, 110.0, 92.6, 73.2, 68.2, 66.9, 56.3, 55.9, 55.7, 42.8, 40.7, 32.9, 28.3; IR (Neat Film, NaCl) 3370, 2941, 1590, 1474, 1383, 1264, 1054 cm<sup>–1</sup>; HRMS (FAB+) *m/z* calc'd for C<sub>18</sub>H<sub>23</sub>N<sub>2</sub>O<sub>4</sub> [M+H]<sup>+</sup>: 331.1652, found 331.1669; [α]<sub>22</sub><sup>D</sup> –31.57° (c 0.28, H<sub>2</sub>O). The analytical data for the synthetic sample matched those for the natural sample in all respects.<sup>6d</sup>

Table 4.3. Comparison of  $^1\text{H}$  NMR data for synthetic and natural quinocarcin

Synthetic (ppm)	Multiplicity	Natural <sup>6d</sup> (ppm)	Multiplicity
7.17	t	7.16	t
6.85	d	6.84	d
6.76	d	6.76	d
4.57	d	4.57	d
4.55	dd	4.54	dd
4.07	br s (2H)	4.08	br s (2H)
3.82	s (3H)	3.82	s (3H)
3.68	dd	3.67	dd
3.43–3.33	comp m (2H)	3.41–3.35	m (3H)
3.39	dd		
2.79–2.74	m	2.79–2.74	m
2.77	s (3H)	2.77	s (3H)
2.64	dd	2.64	dd
2.64–2.60	m	2.63–2.59	m
2.46	dd	2.47	dd

Table 4.4. Comparison of  $^{13}\text{C}$  NMR data for synthetic and natural quinocarcin<sup>42</sup>

Synthetic (ppm) <sup>a</sup>	Natural <sup>6d</sup> (ppm) <sup>b</sup>
179.5	174.9
157.2	157.2
137.6	137.0
129.1	129.1
124.0	123.8
121.3	121.3
110.0	110.0
92.6	92.1
73.2	72.3
68.2	67.9
66.9	66.8
56.3	56.3
55.9	55.9
55.7	53.4
42.8	40.6
40.7	40.3
32.9	32.5
28.3	27.3

<sup>a</sup>  $^{13}\text{C}$  NMR spectrum measured at 125 MHz in  $\text{CD}_3\text{OD}$ .<sup>b</sup>  $^{13}\text{C}$  NMR spectrum measured at 125 MHz in  $\text{CD}_3\text{OD}$ .

#### 4.7 NOTES AND REFERENCES

- (1) For the isolation and structural characterization of quinocarcin, see: (a) Tomita, F.; Takahashi, K.; Shimizu, K. *J. Antibiot.* **1983**, *36*, 463–467. (b) Takahashi, K.; Tomita, F. *J. Antibiot.* **1983**, *36*, 468–470. (c) Hirayama, N.; Shirahata, K. *J. Chem. Soc., Perkin Trans. II* **1983**, 1705–1708.
- (2) For a comprehensive review of the chemistry and biology of the tetrahydroisoquinoline antitumor antibiotics, see: Scott, J. D.; Williams, R. M. *Chem. Rev.* **2002**, *102*, 1669–1730.
- (3) For accounts detailing the cytotoxic activities of quinocarcin and various synthetic derivatives, see: (a) Tomita, F.; Takahashi, K.; Tamaoki, T. *J. Antibiot.* **1984**, *37*, 1268–1272. (b) Fujimoto, K.; Oka, T.; Morimoto, M. *Cancer Res.* **1987**, *47*, 1516–1522. (c) Inaba, S.; Shimoyama, M. *Cancer Res.* **1988**, *48*, 6029–6032. (d) Chiang, C.; Kanzawa, F.; Matsushima, Y.; Nakano, H.; Nakagawa, K.; Tasahashi, H.; Terada, M.; Morinaga, S.; Tsuchiya, R.; Sasaki, Y.; Saijo, N. *J. Pharmacobiodyn.* **1987**, *10*, 431–435. (e) Inoue, S.; Kubota, T.; Ohishi, T.; Kuzuoka, M.; Oka, S.; Shimoyama, Y.; Kikuyama, S.; Ishibiki, K.; Abe, O. *Keio J. Med.* **1988**, *37*, 355–364. (f) Saito, H.; Kobayashi, S.; Uosaki, Y.; Sato, A.; Fujimoto, K.; Miyoshi, K.; Ashizawa, T.; Morimoto, M.; Hirata, T. *Chem. Pharm. Bull.* **1990**, *38*, 1278–1285. (g) Saito, H.; Sato, A.; Ashizawa, T.; Morimoto, M.; Hirata, T. *Chem. Pharm. Bull.* **1990**, *38*, 3202–3210. (h) Saito, H.; Hirata, T.; Kasai, M.; Fujimoto, K.; Ashizawa, T.; Morimoto, M.; Sato, A. *J. Med. Chem.* **1991**, *34*, 1959–1966. (i) Plowman, J.; Narayanan, V. L.; Abbott, B. J.; Inoue, K.; Hirata, T.; Grever, M. R. *Proc. Am. Assoc. Cancer Res.* **1993**, *34*, 368. (j) Plowman, J.; Dykes, D. J.; Narayanan, V. L.; Abbott, B. J.; Saito, H.; Hirata, T.; Grever, M. R. *Cancer Res.* **1995**, *55*, 862–867.

(4) For synthetic work toward quinocarcin, see: (a) Danishefsky, S. J.; Harrison, P. J.; Webb, R. R., II; O'Neill, B. T. *J. Am. Chem. Soc.* **1985**, *107*, 1421–1423. (b) Saito, H.; Hirata, T. *Tetrahedron Lett.* **1987**, *28*, 4065–4068. (c) Lessen, T. A.; Demko, D. M.; Weinreb, S. M. *Tetrahedron Lett.* **1990**, *31*, 2105–2108. (d) Allway, P. A.; Sutherland, J. K.; Joule, J. A. *Tetrahedron Lett.* **1990**, *31*, 4781–4782. (e) Flanagan, M. F.; Williams, R. M. *J. Org. Chem.* **1995**, *60*, 6791–6797. (f) McMills, M. C.; Wright, D. L.; Zubkowski, J. D.; Valente, E. J. *Tetrahedron Lett.* **1996**, *37*, 7205–7208.

(5) For the total synthesis of (±)-quinocarcin, see: Fukuyama, T.; Nunes, J. J. *J. Am. Chem. Soc.* **1988**, *110*, 5196–5198.

(6) For asymmetric total syntheses of (–)-quinocarcin, see: (a) Garner, P.; Ho, W. B.; Shin, H. *J. Am. Chem. Soc.* **1992**, *114*, 2767–2768. (b) Garner, P.; Ho, W. B.; Shin, H. *J. Am. Chem. Soc.* **1993**, *115*, 10742–10753. (c) Katoh, T.; Kirihara, M.; Nagata, Y.; Kobayashi, Y.; Arai, K.; Minami, J.; Terashima, S. *Tetrahedron* **1994**, *50*, 6239–6258. (d) Kwon, S.; Myers, A. G. *J. Am. Chem. Soc.* **2005**, *127*, 16796–16797. (e) Wu, Y.-C.; Liron, M.; Zhu, J. *J. Am. Chem. Soc.* **2008**, *130*, 7148–7152.

(7) Ashley, E. R.; Cruz, E. G.; Stoltz, B. M. *J. Am. Chem. Soc.* **2003**, *125*, 15000–15001.

(8) Ashley, E. R. Ph.D. Thesis, California Institute of Technology, Pasadena, CA, 2005.

(9) Allan, K. M.; Stoltz, B. M. *J. Am. Chem. Soc.* **2008**, *130*, 17270–17271.

- (10) Gilmore, C. D.; Allan, K. M.; Stoltz, B. M. *J. Am. Chem. Soc.* **2008**, *130*, 1558–1559.
- (11) (a) Jones, R. G. U.S. Patent 2,520,088 (1950). (b) Jones, R. G. *Chem. Abstr.* **1950**, *44*, 10740.
- (12) Lutz, W. B.; Lazarus, S.; Klutchko, S.; Meltzer, R. I. *J. Org. Chem.* **1964**, *29*, 415–418.
- (13) The fundamental reaction protocol for this dipolar cycloaddition is based on the pioneering work of Joule. See: (a) Kiss, M.; Russell-Maynard, J.; Joule, J. A. *Tetrahedron Lett.* **1987**, *28*, 2187–2190. (b) Allway, P. A.; Sutherland, J. K.; Joule, J. A. *Tetrahedron Lett.* **1990**, *31*, 4781–4782. (c) Yates, N. D.; Peters, D. A.; Allway, P. A.; Beddoe, R. L.; Scopes, D. I. C.; Joule, J. A. *Heterocycles* **1995**, *40*, 331–347.
- (14) The specific experimental procedure for this dipolar cycloaddition is based on the previous synthesis of (–)-lemonomycin completed in our labs. See refs. 7 and 8.
- (15) The prefixes *syn* and *anti* are used to denote the stereochemical relationship between the methyl ester and the bridging amine.
- (16) An additional monodentate complex involving coordination to the right hand lone pair of the lactam carbonyl can also be envisioned, though it is expected that this complex would be thermodynamically less favorable than either of the chelates.
- (17) Garner *et al.* employed acrylamide **403** in a related dipolar cycloaddition using a photochemically generated azomethine ylide in their total synthesis of (–)-quinocarcin. See refs. 6a and b.

- (18) For a review of asymmetric thermal reactions using Oppolzer's camphor-derived sultam, see: Kim, B. H.; Curran, D. P. *Tetrahedron* **1993**, *49*, 293–318.
- (19) Peña, D.; Pérez, D.; Gutián, E.; Castedo, L. *J. Am. Chem. Soc.* **1999**, *121*, 5827–5828.
- (20) Similar heterogeneous hydrogenations of *N*-acyl quinolinium species have been carried out using copper(II) chromate or Raney nickel. See: (a) Clemo, G. R.; Nath, B. *J. Chem. Soc.* **1952**, 2196–2198. (b) Boekelheide, V.; Marinetti, G. *J. Am. Chem. Soc.* **1951**, *73*, 4015–4016.
- (21) Pearlman, W. M. *Tetrahedron Lett.* **1967**, *8*, 1663–1664.
- (22) Voorhees, V.; Adams, R. *J. Am. Chem. Soc.* **1922**, *44*, 1397–1405.
- (23) Raney, M. U.S. Patent 1,628,190 (1927).
- (24) Tetrahydrofuran has been shown to accelerate the rate of benzyl ether hydrogenolysis. See: (a) Tweedie, V. L.; Cuscurida, M. *J. Am. Chem. Soc.* **1957**, *79*, 5463–5466. (b) Tweedie, V. L.; Barron, B. G. *J. Org. Chem.* **1960**, *25*, 2023–2026. (c) Hawker, S.; Bhatti, M. A.; Griffin, K. G. *Chim. Oggi*, **1992**, *10*, 49–51.
- (25) In light of difficulties associated with stability encountered during chromatographic separation of dihydroisoquinolines **416a** and **416b**, the diastereomeric ratio was determined by <sup>1</sup>H NMR.

(26) For a similar example of asymmetric induction to form a *syn*-disubstituted tetrahydroisoquinoline, see: Ishida, A.; Fujii, H.; Nakamura, T.; Ohishi, T.; Aoe, K.; Nishibata, Y.; Kinumaki, A. *Chem. Pharm. Bull.* **1986**, *34*, 1994–2006.

(27) Evans, D. A.; Illig, C. R.; Saddler, J. C. *J. Am. Chem. Soc.* **1986**, *108*, 2478–2479.

(28) For the isolation of jorumycin, see: Fontana, A.; Cavaliere, P.; Wahidulla, S.; Naik, C. G.; Cimino, G. *Tetrahedron* **2000**, *56*, 7305–7308.

(29) Lane, J. W.; Chen, Y.; Williams, R. M. *J. Am. Chem. Soc.* **2005**, *127*, 12684–12690.

(30) Wu, Y.-C.; Zhu, J. *Org. Lett.* **2009**, *11*, 5558–5561.

(31) Tadross, P. M.; Gilmore, C. D.; Bugga, P.; Virgil, S. C.; Stoltz, B. M. *Org. Lett.* **2010**, *12*, 1224–1227.

(32) Brooks, D. E.; Lu, L. D.-L.; Masamune, S. *Angew. Chem., Int. Ed., Engl.* **1979**, *18*, 72–74.

(33) (a) Tambar, U. K.; Stoltz, B. M. *J. Am. Chem. Soc.* **2005**, *127*, 5340–5341. (b) Ebner, D. C.; Tambar, U. K.; Stoltz, B. M. *Org. Synth.* **2009**, *86*, 161–171.

(34) Allan, K. M.; Hong, B. D.; Stoltz, B. M. *Org. Biomol. Chem.* **2009**, *7*, 4960–4964.

(35) For the isolation and structure determination of ecteinascidin 743, see: (a) Rinehart, K. L.; Holt, T. G.; Fregeau, N. L.; Stroh, J. G.; Keifer, P. A.; Sun, F.; Li, L. H.; Martin, D. G. *J. Org. Chem.* **1990**, *55*, 4512–4515. (b) Rinehart, K. L.;

Holt, T. G.; Fregeau, N. L.; Stroh, J. G.; Keifer, P. A.; Sun, F.; Li, L. H.; Martin, D. G. *J. Org. Chem.* **1991**, *56*, 1676. (c) Wright, A. E.; Forleo, D. A.; Gunawardana, P. G.; Gunasekera, S. P.; Koehn, F. E.; McConnell, O. J. *J. Org. Chem.* **1990**, *55*, 4508–4512. (d) Sakai, R.; Rinehart, K. L.; Guan, Y.; Wang, A. H.-J. *Proc. Natl. Acad. Sci. U.S.A.* **1992**, *89*, 11456–11460. (e) Guan, Y.; Sakai, R.; Rinehart, K. L.; Wang, A. H.-J. *J. Biomol. Struct. Dyn.* **1993**, *10*, 793–818.

(36) For completed total syntheses and formal total syntheses of ecteinascidin 743, see:  
(a) Corey, E. J.; Gin, D. Y.; Kania, R. S. *J. Am. Chem. Soc.* **1996**, *118*, 9202–9203. (b) Martinez, E. J.; Corey, E. J. *Org. Lett.* **2000**, *2*, 993–996. (c) Endo, A.; Yanagisawa, A.; Abe, M.; Tohma, S.; Kan, T.; Fukuyama, T. *J. Am. Chem. Soc.* **2002**, *124*, 6552–6554. (d) Chen, J.; Chen, X.; Bois-Choussy, M.; Zhu, J. *J. Am. Chem. Soc.* **2006**, *128*, 87–89. (e) Zheng, S.; Chan, C.; Furuuchi, T.; Wright, B. J. D.; Zhou, B.; Guo, J.; Danishefsky, S. J. *Angew. Chem. Int. Ed.* **2006**, *45*, 1754–1759. (f) Fishlock, D.; Williams, R. M. *J. Org. Chem.* **2008**, *73*, 9594–9600. (g) Cuevas, C.; Pérez, M.; Martín, M. J.; Chicharro, J. L.; Fernández-Rivas, C.; Flores, M.; Francesch, A.; Gallego, P.; Zarzuelo, M.; de la Calle, F.; García, J.; Polanco, C.; Rodríguez, I.; Manzanares, I. *Org. Lett.* **2000**, *2*, 2545–2548. (h) Cuevas, C.; Francesch, A. *Nat. Prod. Rep.* **2009**, *26*, 322–337.

(37) (a) Verschraegen, C. F.; Glover, K. *Curr. Opin. Investig. Drugs* **2001**, *2*, 1631–1638. (b) Ryan, D. P.; Supko, J. G.; Eder, J. P.; Seiden, M. V.; Demetri, G.; Lynch, T. J.; Fischman, A. J.; Davis, J.; Jimeno, J.; Clark, J. W. *Clin. Cancer Res.* **2001**, *7*, 231–242.

(38) For spectroscopic data and experimental spectra for ester **anti-382**, see ref. 8.

(39)  $^1\text{H}$  NMR analysis shows this crude material to be an 11:1 mixture of diastereomeric cycloadducts. The major diastereomer (**405a**) is purified via subsequent recrystallization.

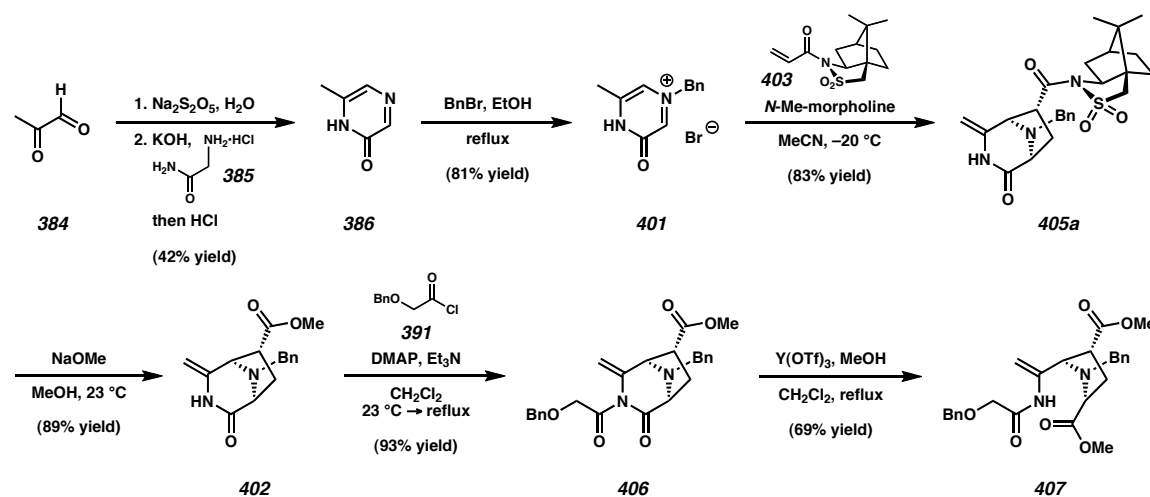
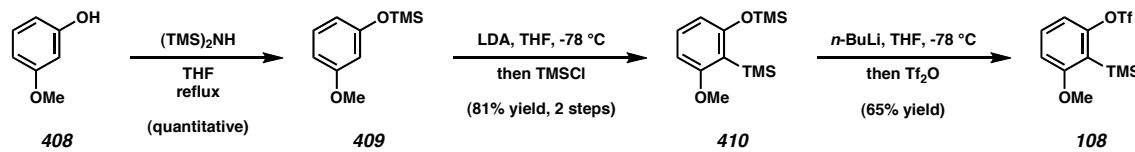
(40) 3-Methoxy-2-(trimethylsilyl)phenyl triflate (**108**) is prepared in three steps from 3-methoxyphenol. See ref. 20.

(41) The experimental procedure for the dissolving metal reduction is based on similar procedures carried out individually by Evans, Garner, and Zhu. See refs. 6a, 6b, 6e, and 28.

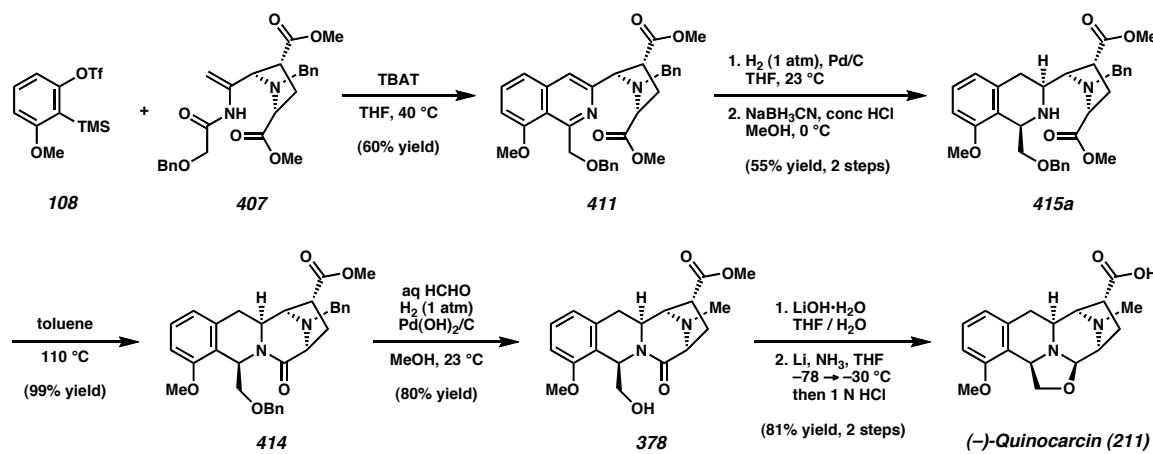
(42) Fukuyama noted that the pH of the analytical solution had a dramatic effect on the chemical shifts in both the  $^1\text{H}$  and  $^{13}\text{C}$  NMR spectra of quinocarcin, accounting for observed differences between natural and synthetic spectra. See ref. 5.

## APPENDIX 2

*Synthetic Summary for (–)-Quinocarcin*

Scheme A2.1. Synthesis of *N*-acyl enamine **407**Scheme A2.2. Synthesis of 3-methoxy-2-(trimethylsilyl)phenyl triflate **108**

Scheme A2.3. Aryne annulation and completion of (–)-quinocarcin



## APPENDIX 3

*Spectra Relevant to Chapter 4:*

*A Concise Total Synthesis of (–)-Quinocarcin via Aryne Annulation*

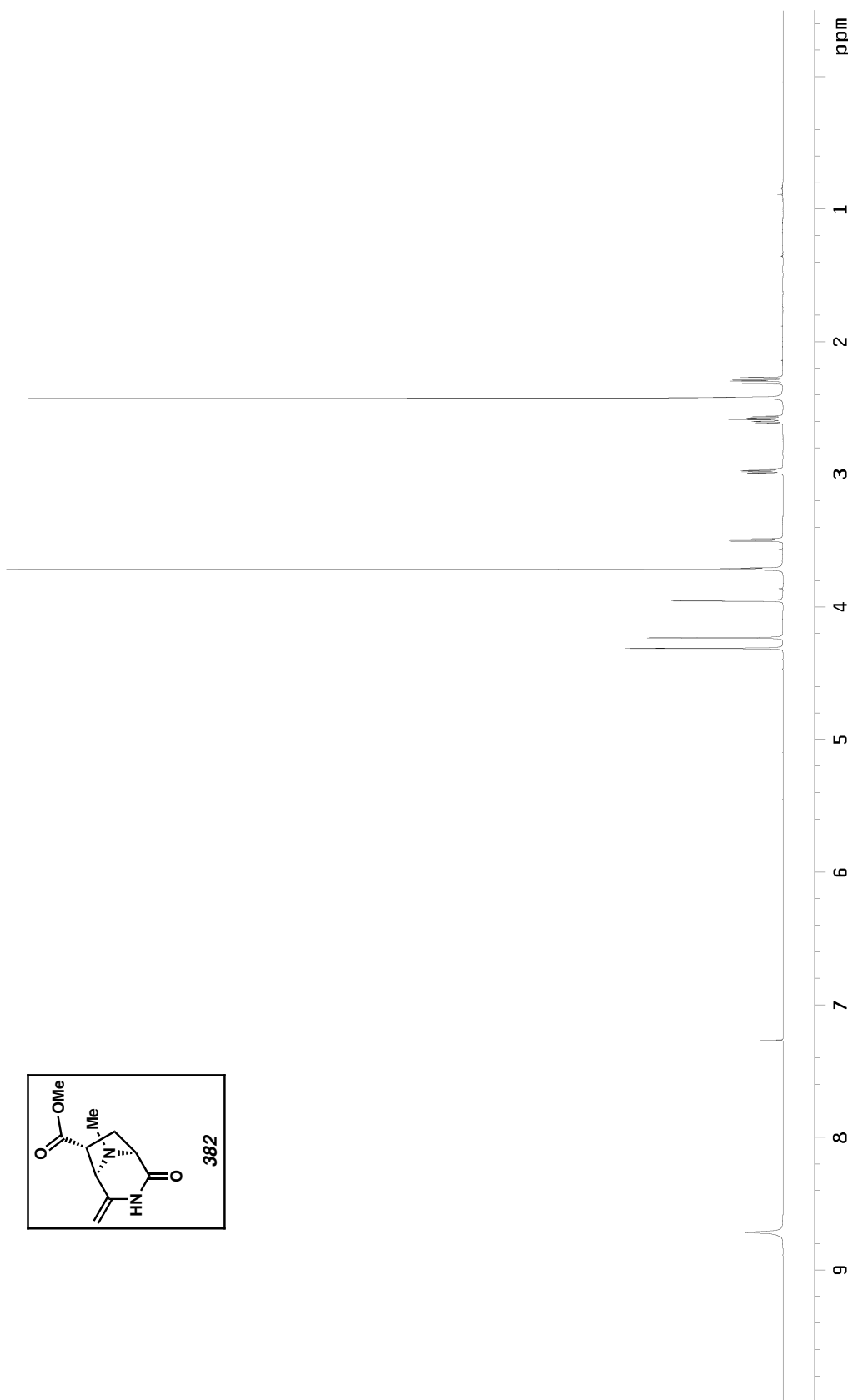


Figure A3.1.1  $^1\text{H}$  NMR (500 MHz,  $\text{CDCl}_3$ ) of ester 382.

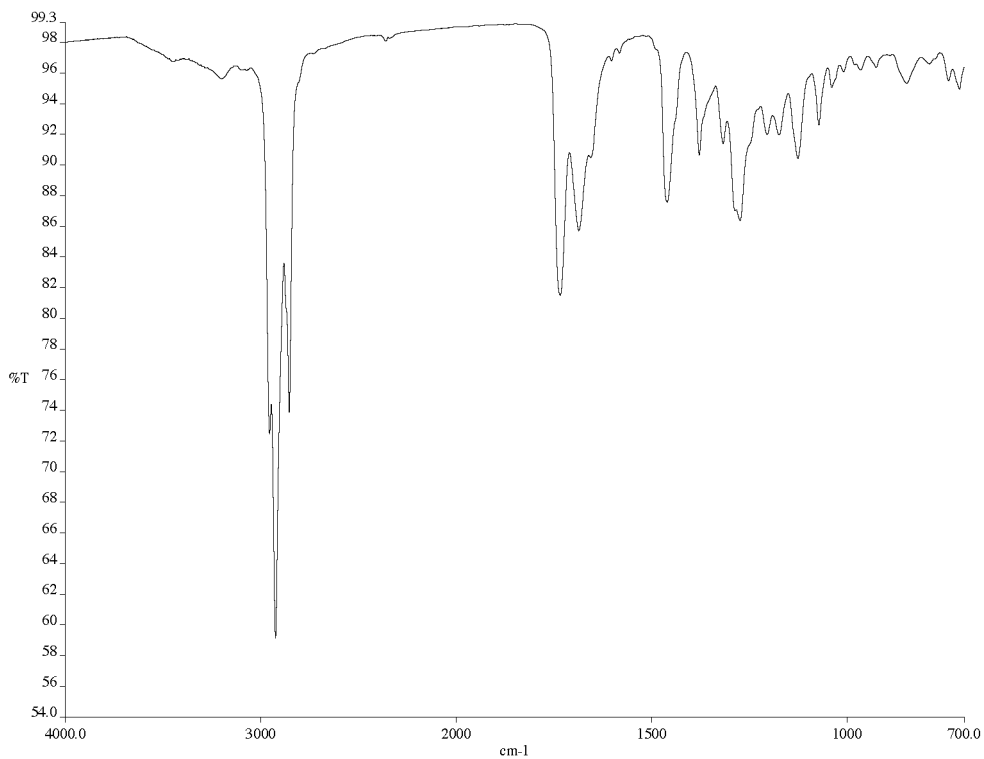


Figure A3.1.2 Infrared spectrum (thin film/NaCl) of ester **382**.

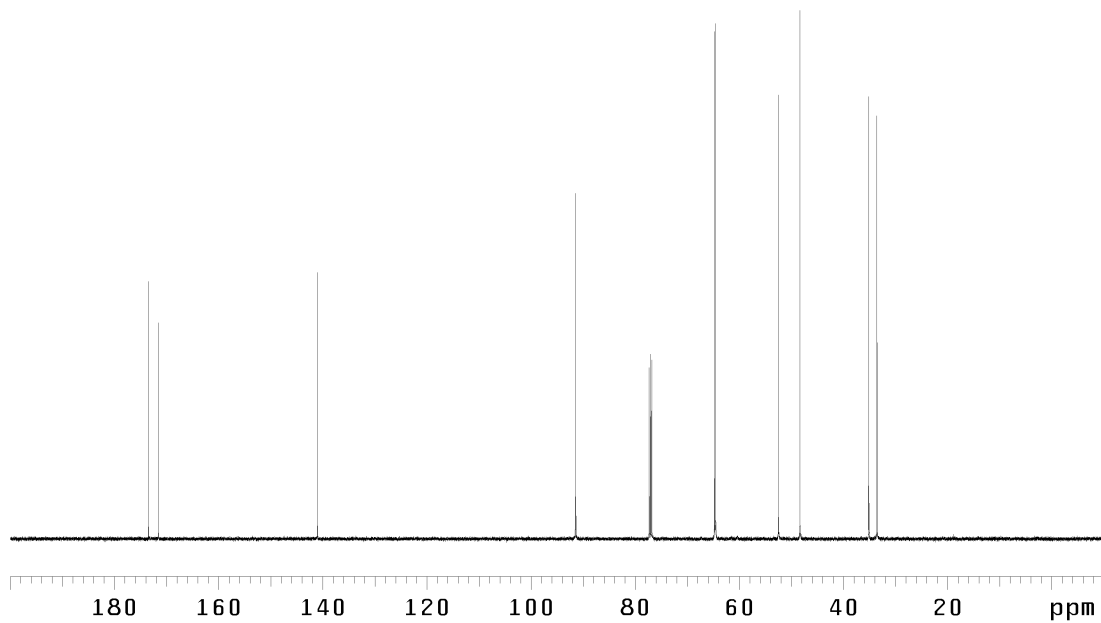


Figure A3.1.3  $^{13}\text{C}$  NMR (125 MHz,  $\text{CDCl}_3$ ) of ester **382**.

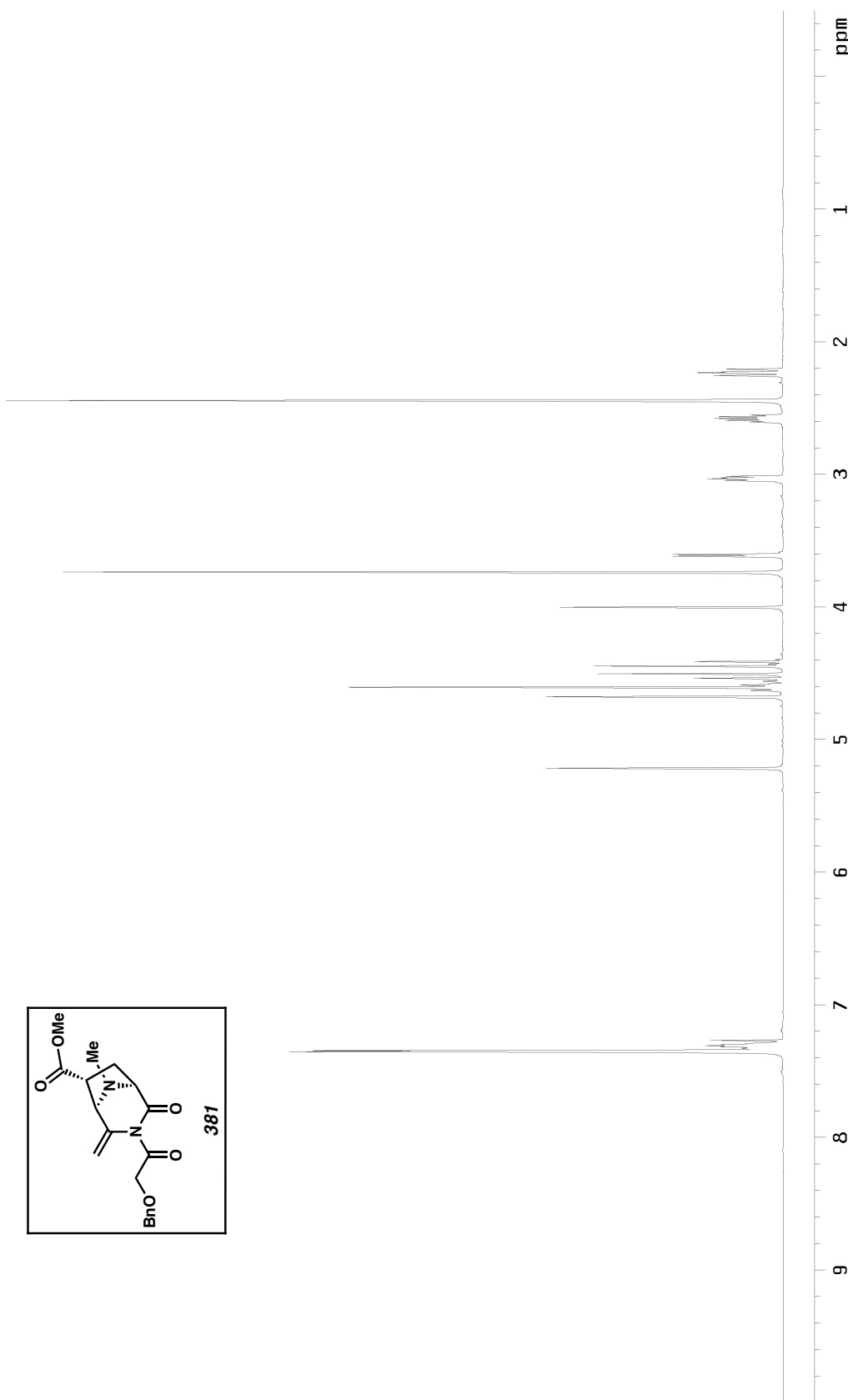


Figure A3.2.I  $^1\text{H}$  NMR (500 MHz,  $\text{CDCl}_3$ ) of imide 381.

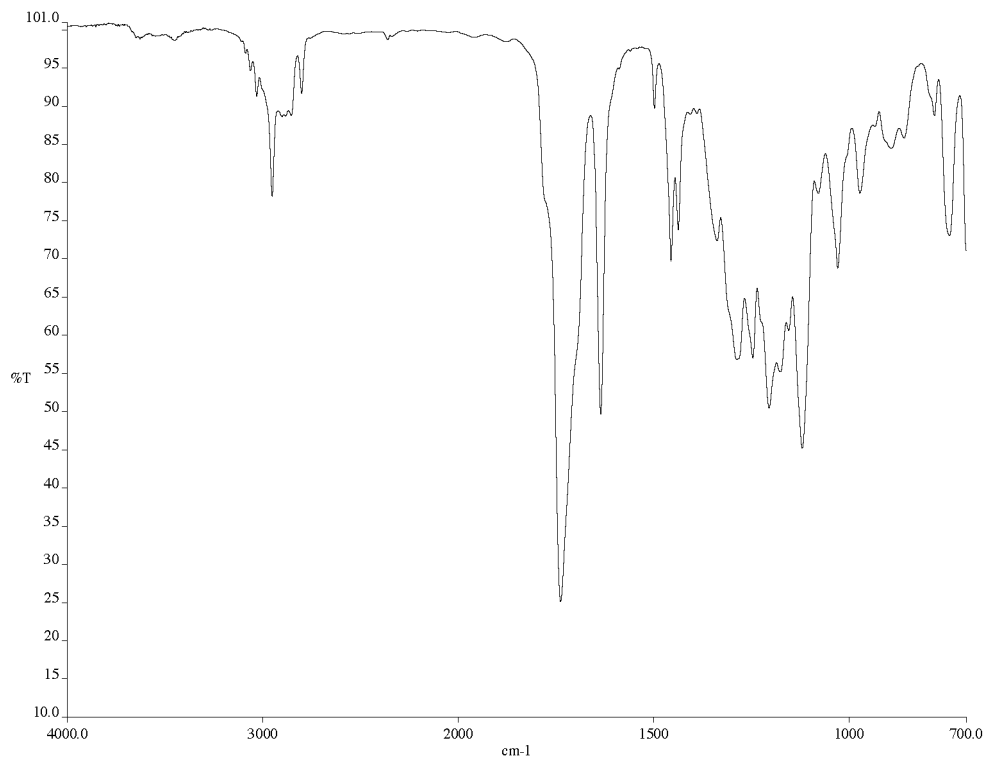


Figure A3.2.2 Infrared spectrum (thin film/NaCl) of imide **381**.

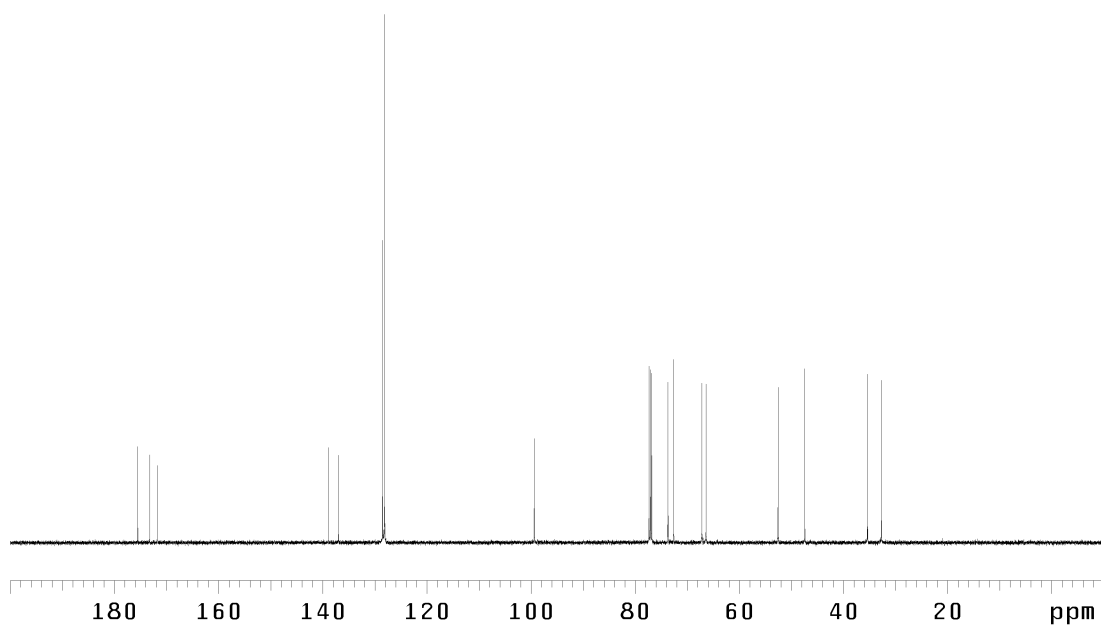


Figure A3.2.3  $^{13}\text{C}$  NMR (125 MHz,  $\text{CDCl}_3$ ) of imide **381**.

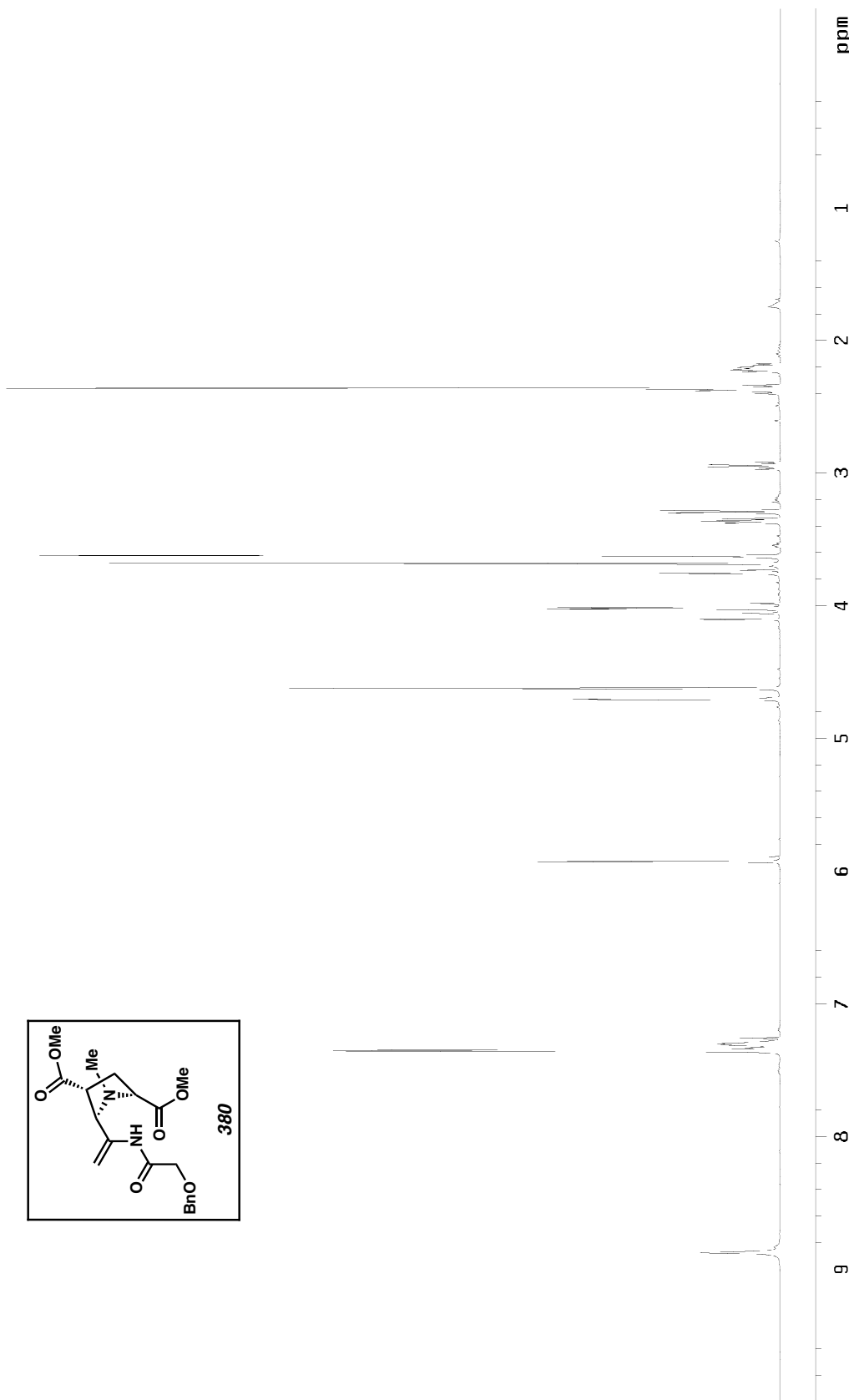


Figure A3.3.1  $^1\text{H}$  NMR (500 MHz,  $\text{CDCl}_3$ ) of *N*-acetyl enamine 380.

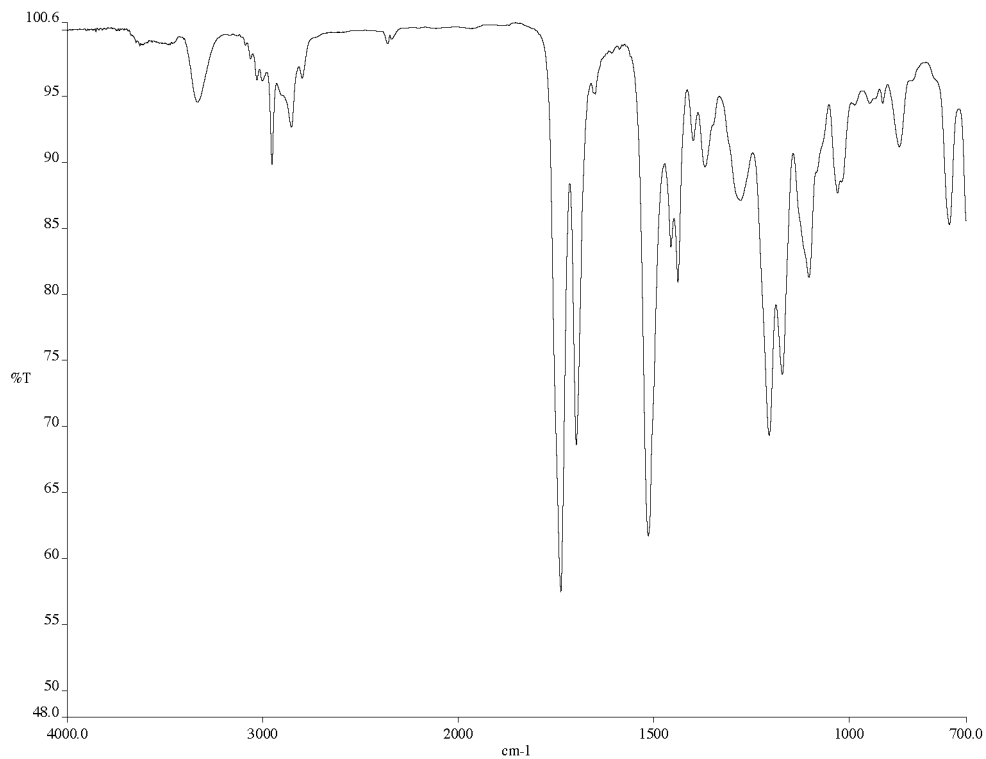


Figure A3.3.2 Infrared spectrum (thin film/NaCl) of *N*-acyl enamine **380**.

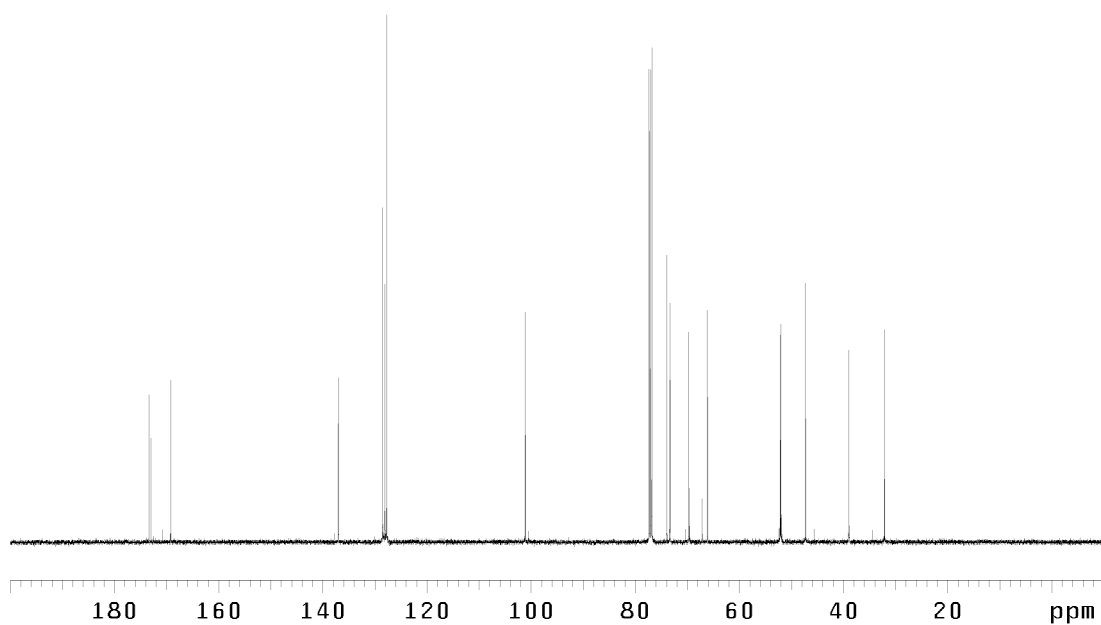


Figure A3.3.3  $^{13}\text{C}$  NMR (125 MHz,  $\text{CDCl}_3$ ) of *N*-acyl enamine **380**.

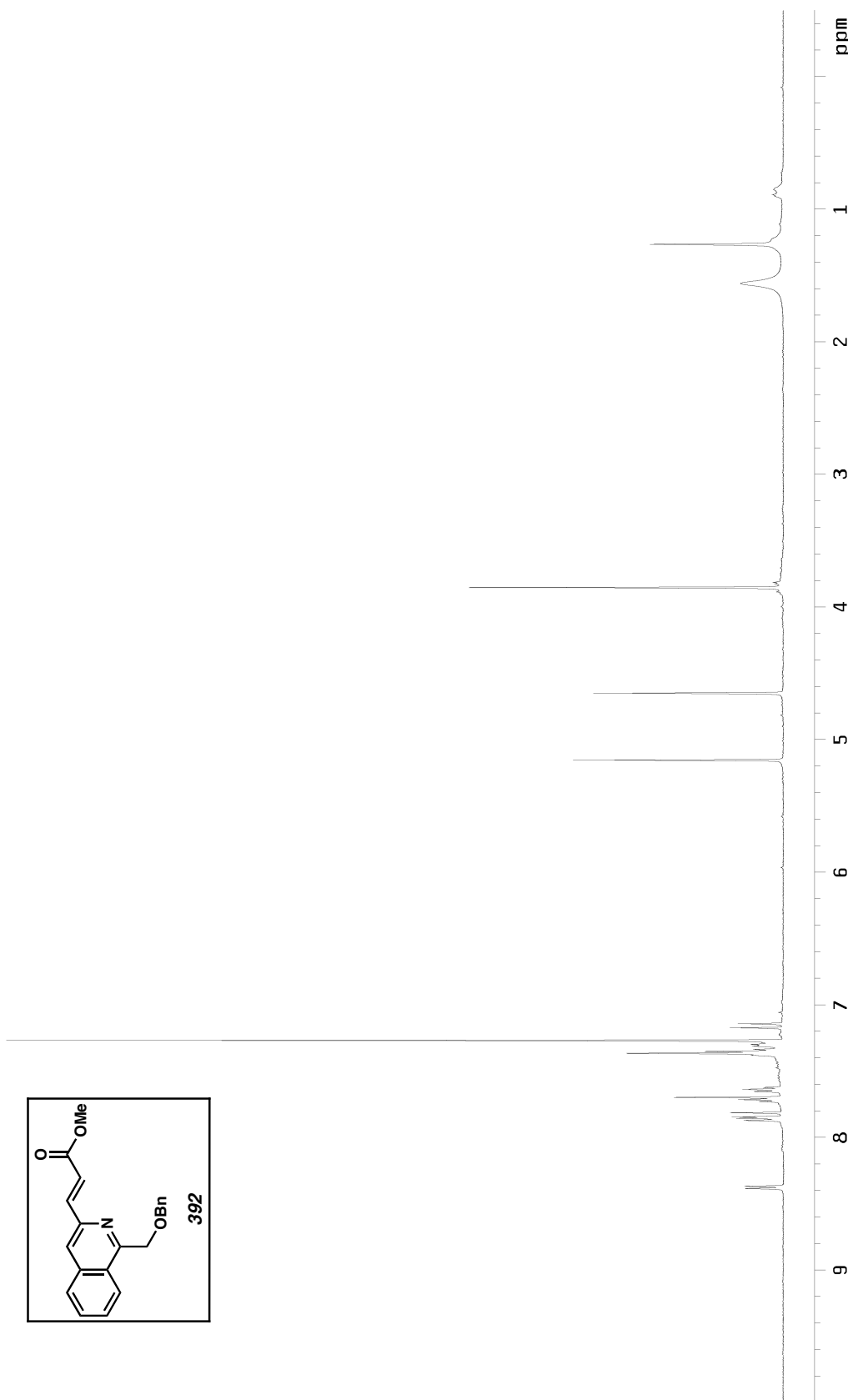


Figure A3.4.1  $^1\text{H}$  NMR (500 MHz,  $\text{CDCl}_3$ ) of isoquinoline 392.

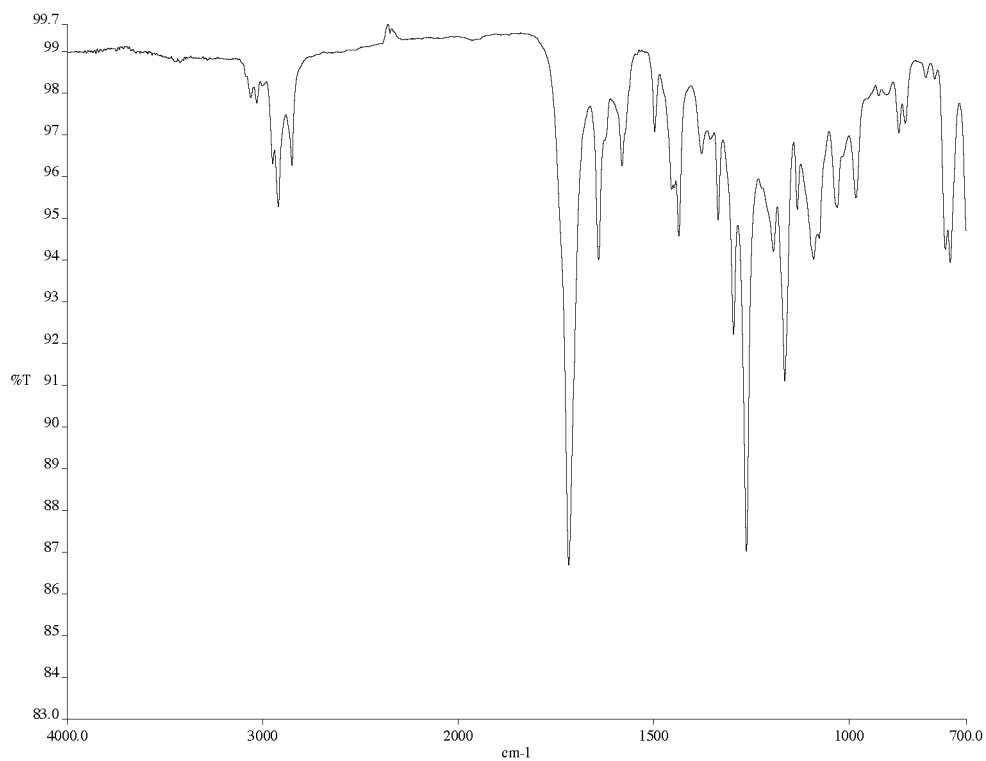


Figure A3.4.2 Infrared spectrum (thin film/NaCl) of isoquinoline **392**.

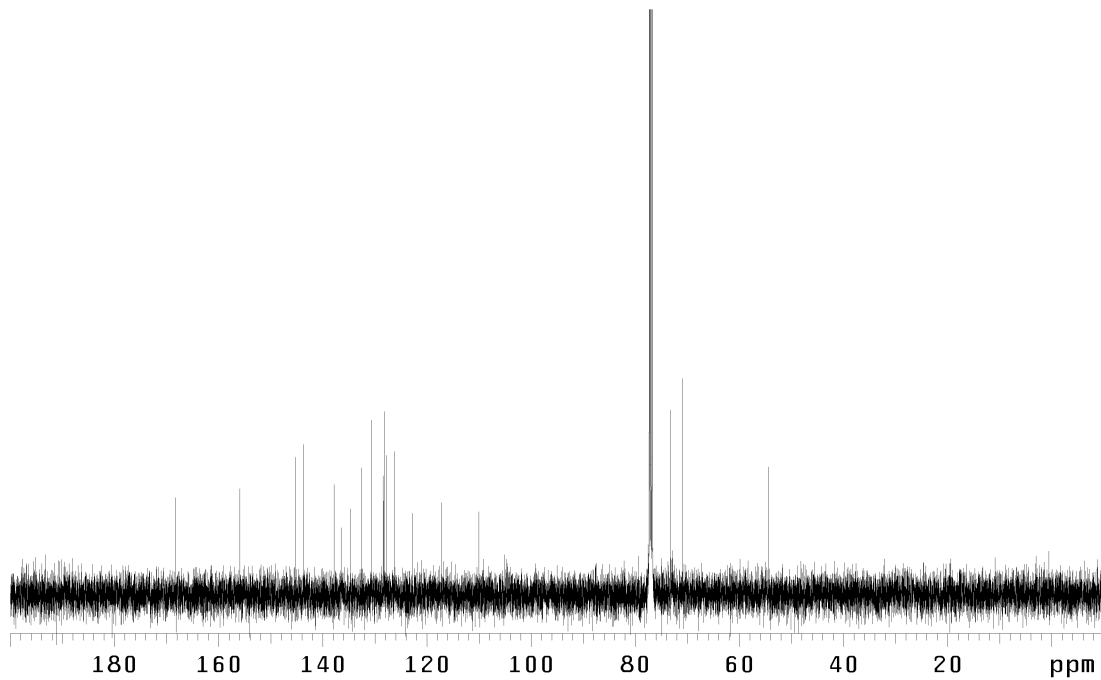


Figure A3.4.3  $^{13}\text{C}$  NMR (125 MHz,  $\text{CDCl}_3$ ) of isoquinoline **392**.

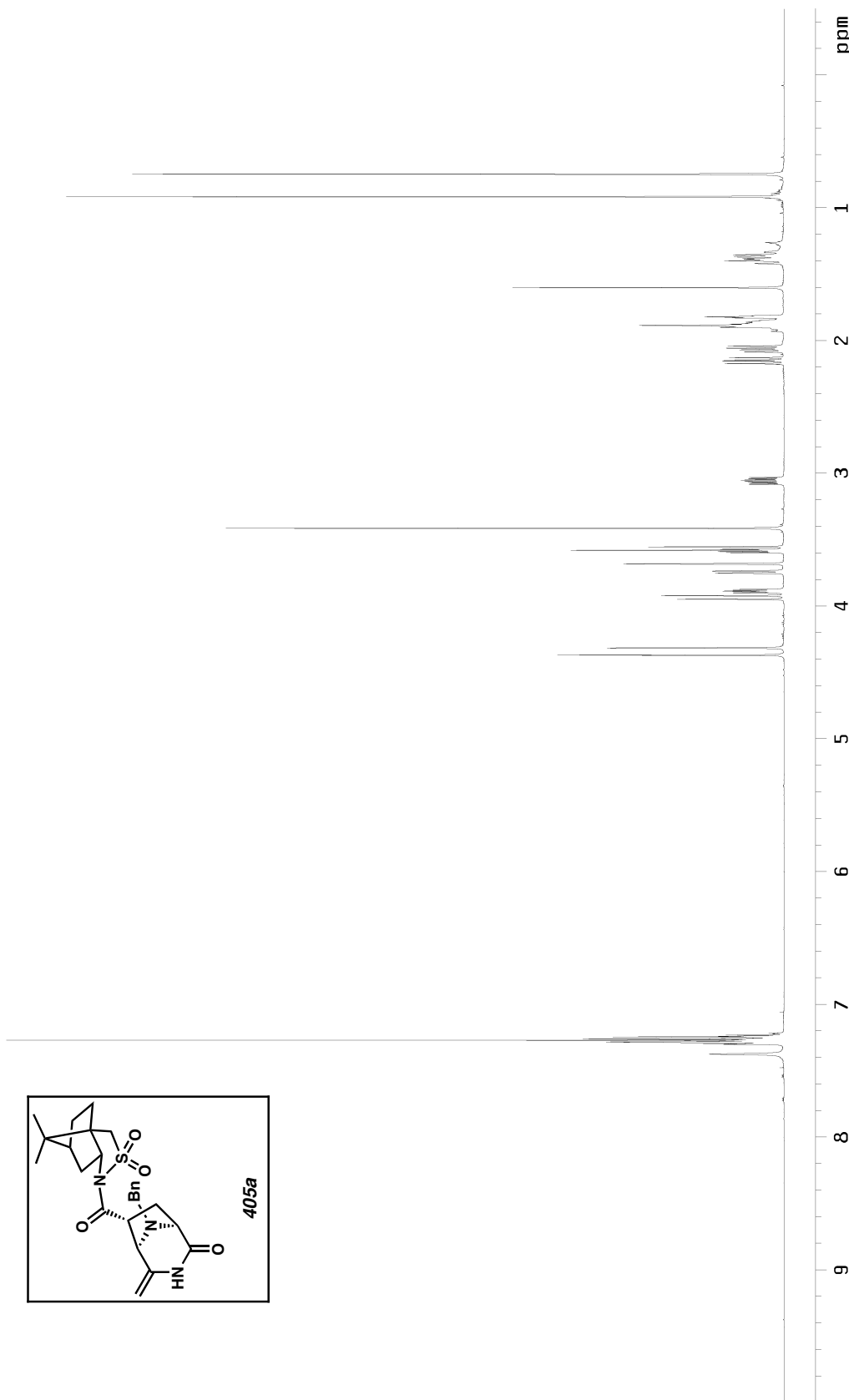


Figure A3.5.1.  $^1\text{H}$  NMR (500 MHz,  $\text{CDCl}_3$ ) of diazabicyclic **405a**.

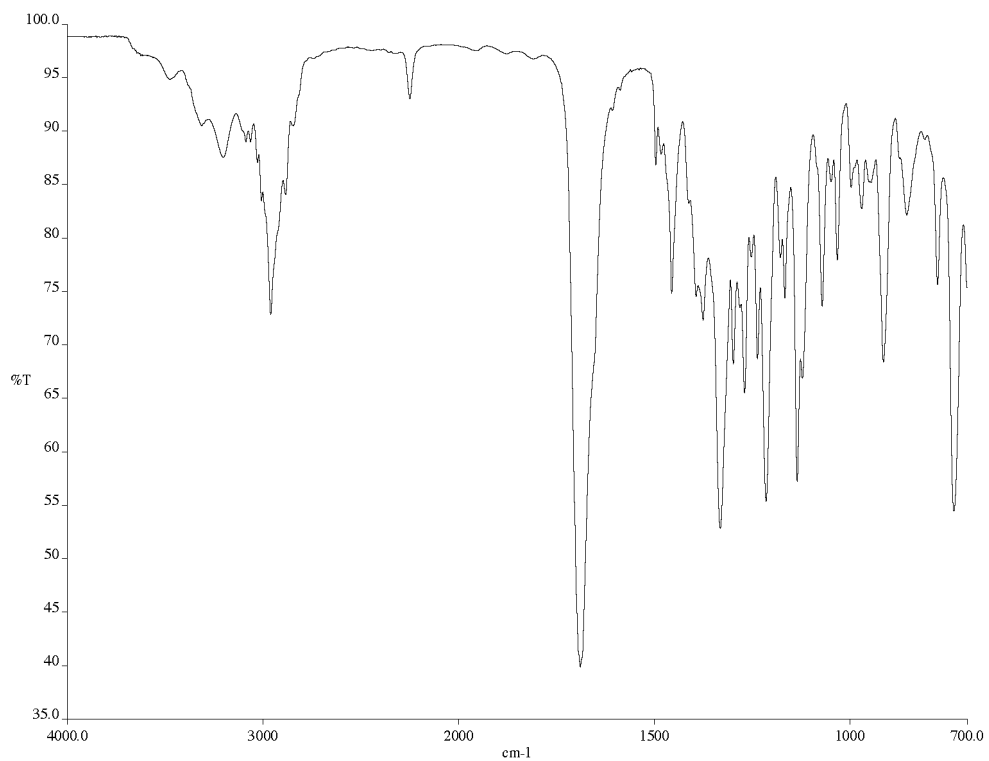


Figure A3.5.2 Infrared spectrum (thin film/NaCl) of diazabicyclic **405a**.

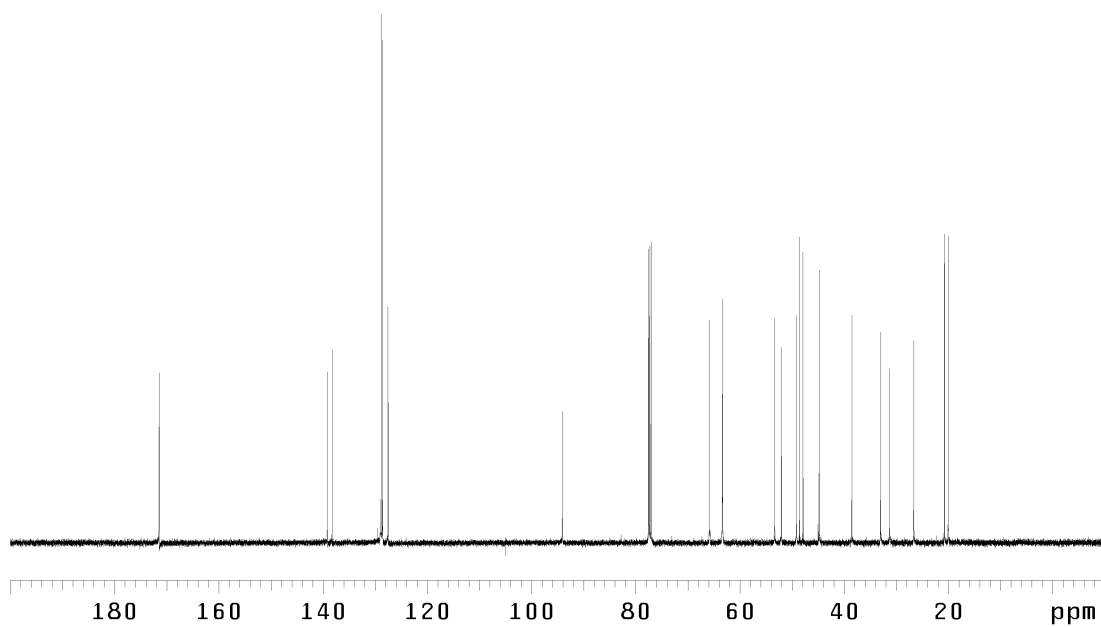


Figure A3.5.3  $^{13}\text{C}$  NMR (125 MHz,  $\text{CDCl}_3$ ) of diazabicyclic **405a**.

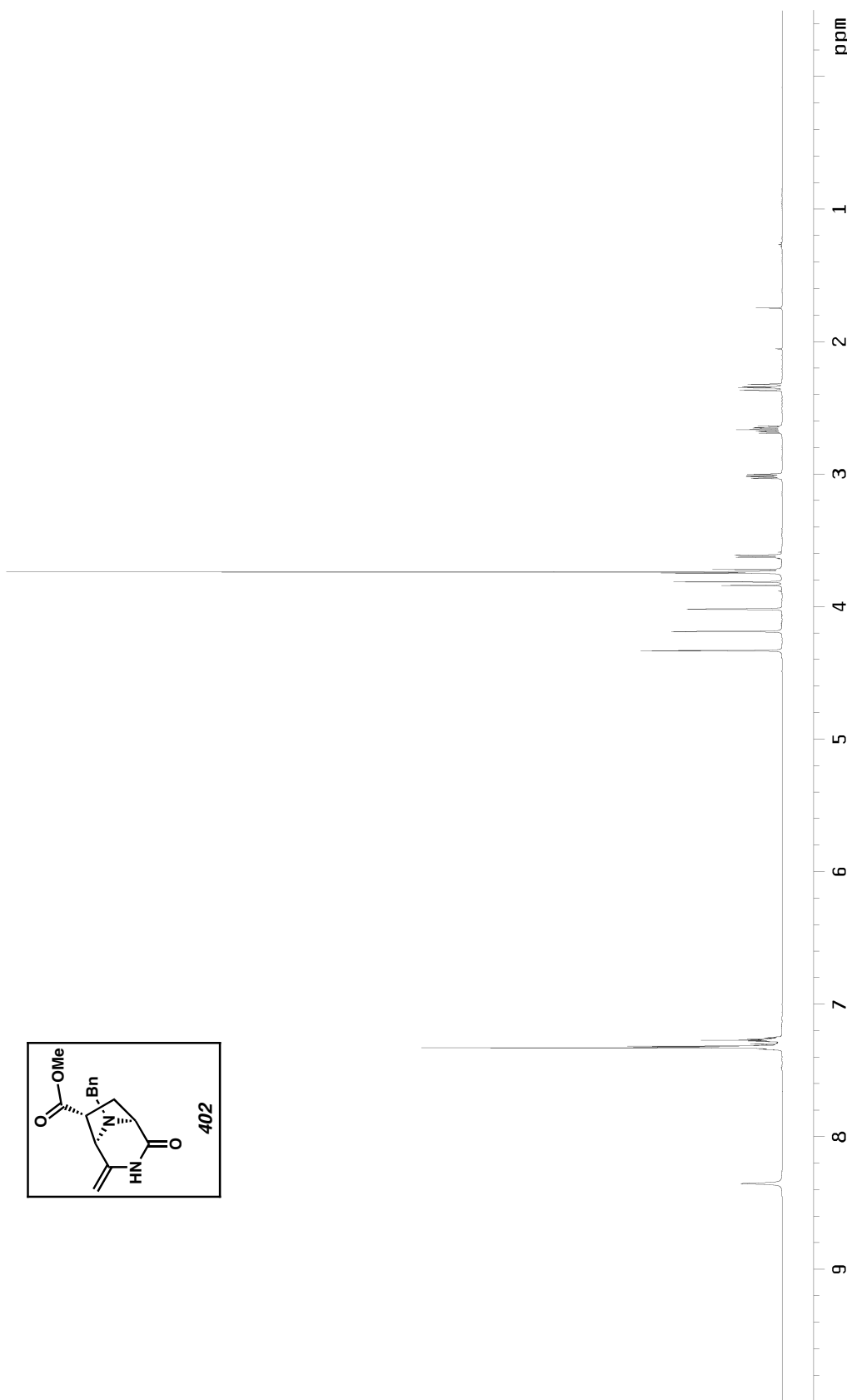


Figure A3.6.1.  $^1\text{H}$  NMR (500 MHz,  $\text{CDCl}_3$ ) of methyl ester 402.

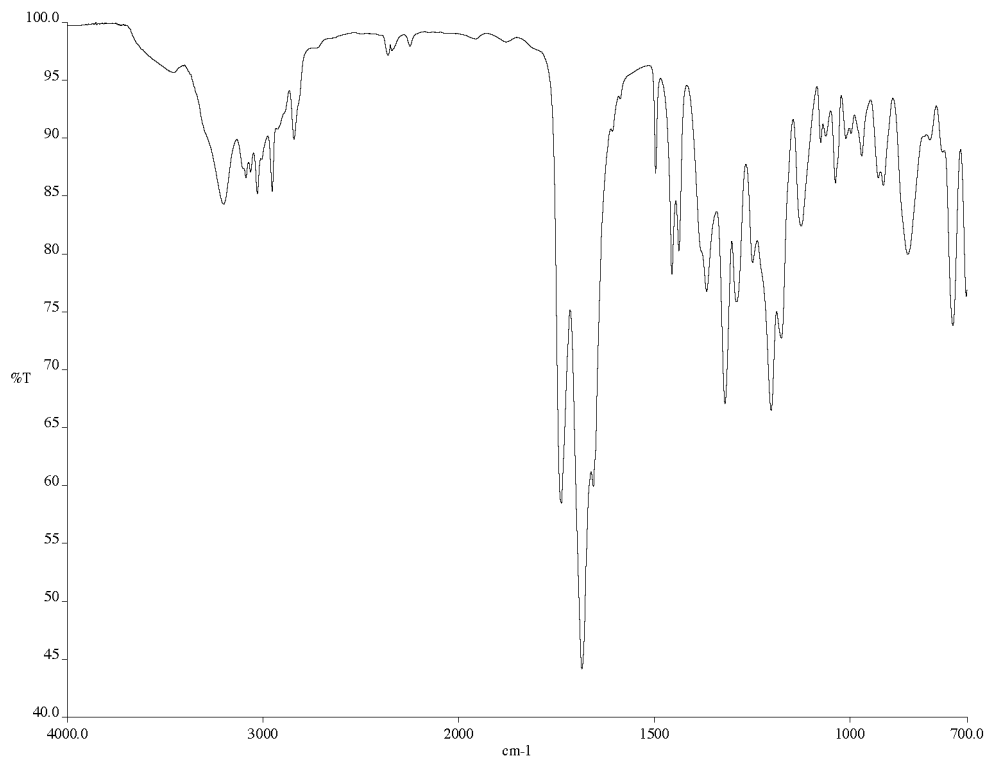


Figure A3.6.2 Infrared spectrum (thin film/NaCl) of methyl ester **402**.

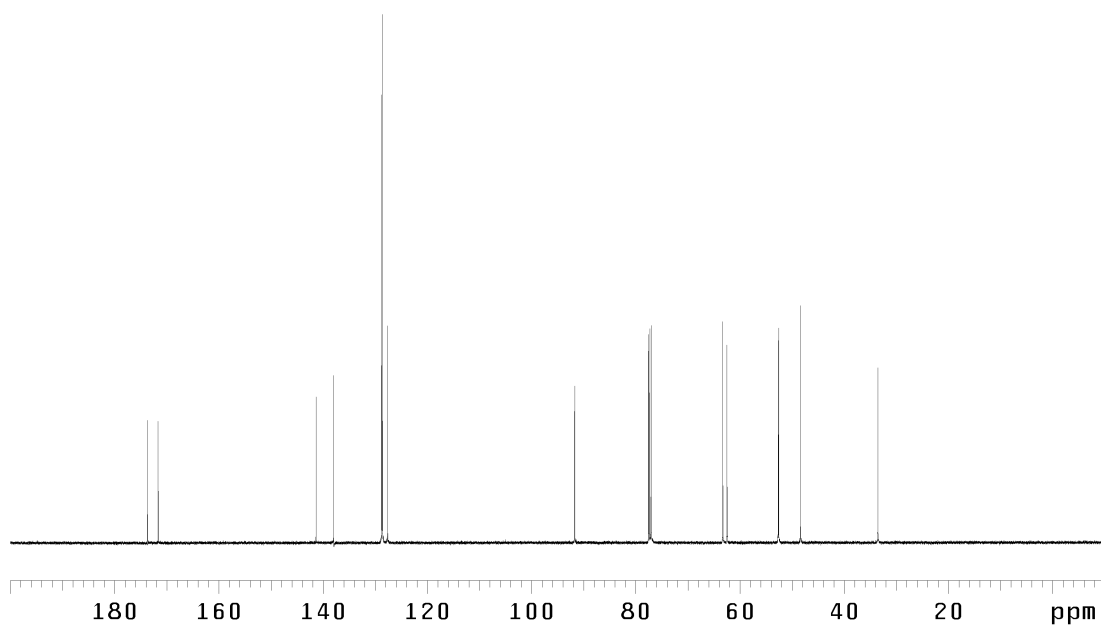
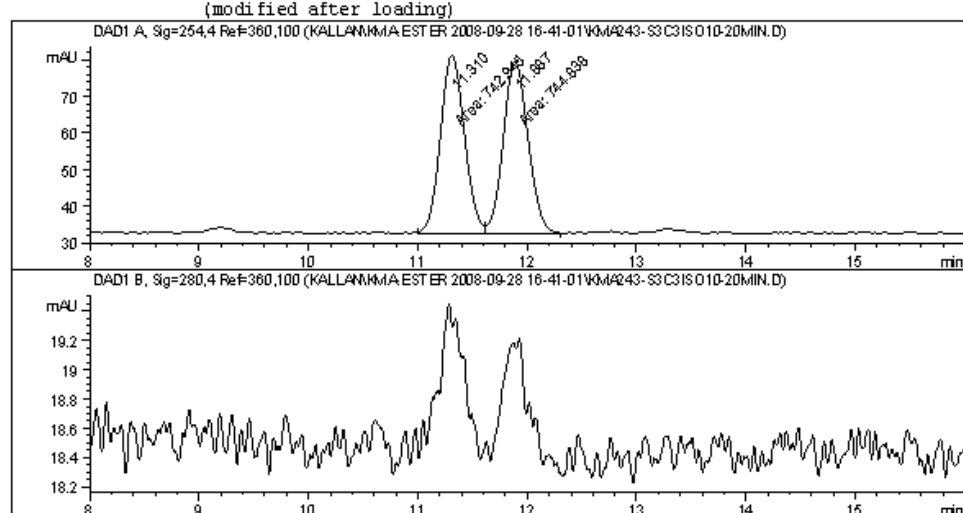


Figure A3.6.3 <sup>13</sup>C NMR (125 MHz, CDCl<sub>3</sub>) of methyl ester **402**.

Figure A3.6.4 Chiral SFC traces for racemic methyl ester **402**.

Data File C:\CHEM32\1\DATA\KALLAN\KMA-ESTER 2008-09-28 16-41-01\KMA243-S3C3IS010-20MIN.D  
Sample Name: kma-xiii-243.2

```
=====
Acq. Operator : KALLAN          Seq. Line : 2
Acq. Instrument : Instrument 1  Location : Pl-D-02
Injection Date : 9/28/2008 4:45:18 PM Inj : 1
                                                Inj Volume : 5  $\mu$ l
Acq. Method   : C:\Chem32\1\DATA\KALLAN\KMA-ESTER 2008-09-28 16-41-01\KMA-CHIRAL S3C3
                  IS010-20MIN-2.M
Last changed   : 9/28/2008 3:34:13 PM by JST
Analysis Method : C:\CHEM32\1\DATA\JST2\JST 2008-09-28 14-45-41\KMA243-2.D\DA.M (KMA-
                  CHIRAL S3C3 IS015.M)
Last changed   : 9/28/2008 5:19:28 PM by SKEDROWSKI
                  (modified after loading)
```



```
=====
Area Percent Report
=====
```

```
Sorted By      : Signal
Multiplier     : 1.0000
Dilution      : 1.0000
Use Multiplier & Dilution Factor with ISTDs
```

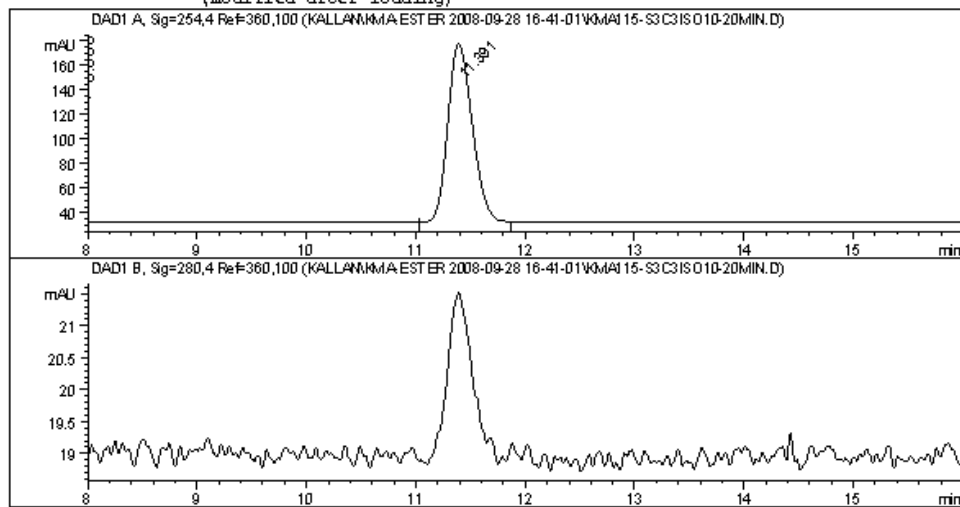
Signal 1: DAD1 A, Sig=254,4 Ref=360,100

Peak #	Ret Time [min]	Type	Width [min]	Area [mAU*s]	Height [mAU]	Area %
1	11.310	MM	0.2543	742.94531	48.68321	49.9364
2	11.887	MM	0.2632	744.83813	47.16733	50.0636
Totals :				1487.78345	95.85054	

Figure A3.6.5 Chiral SFC trace for enantioenriched methyl ester (–)-402 (&gt;99% ee).

Data File C:\CHEM32\1\DATA\KALLAN\KMA-ESTER 2008-09-28 16-41-01\KMA115-S3C3ISO10-20MIN.D  
Sample Name: kma-xiii-115.3

```
=====
Acq. Operator : KALLAN          Seq. Line : 4
Acq. Instrument : Instrument 1  Location : Pl-D-03
Injection Date : 9/28/2008 5:18:32 PM  Inj : 1
                                                Inj Volume : 5  $\mu$ l
Acq. Method : C:\Chem32\1\DATA\KALLAN\KMA-ESTER 2008-09-28 16-41-01\KMA-CHIRAL S3C3
: ISO10-20MIN-2.M
Last changed : 9/28/2008 3:34:13 PM by JST
Analysis Method : C:\CHEM32\1\DATA\JST2\JST 2008-09-28 14-45-41\KMA243-2.D\DA.M (KMA-
: CHIRAL S3C3 ISO15.M)
Last changed : 9/28/2008 5:48:22 PM by SKEDROWSKI
(modified after loading)
```



```
=====
Area Percent Report
=====
Sorted By : Signal
Multiplier : 1.0000
Dilution : 1.0000
Use Multiplier & Dilution Factor with ISTDs
```

Signal 1: DAD1 A, Sig=254,4 Ref=360,100

Peak #	RetTime [min]	Type	Width [min]	Area [mAU*s]	Height [mAU]	Area %
1	11.391	VB	0.2723	2826.86035	156.79543	100.0000

Totals : 2826.86035 156.79543

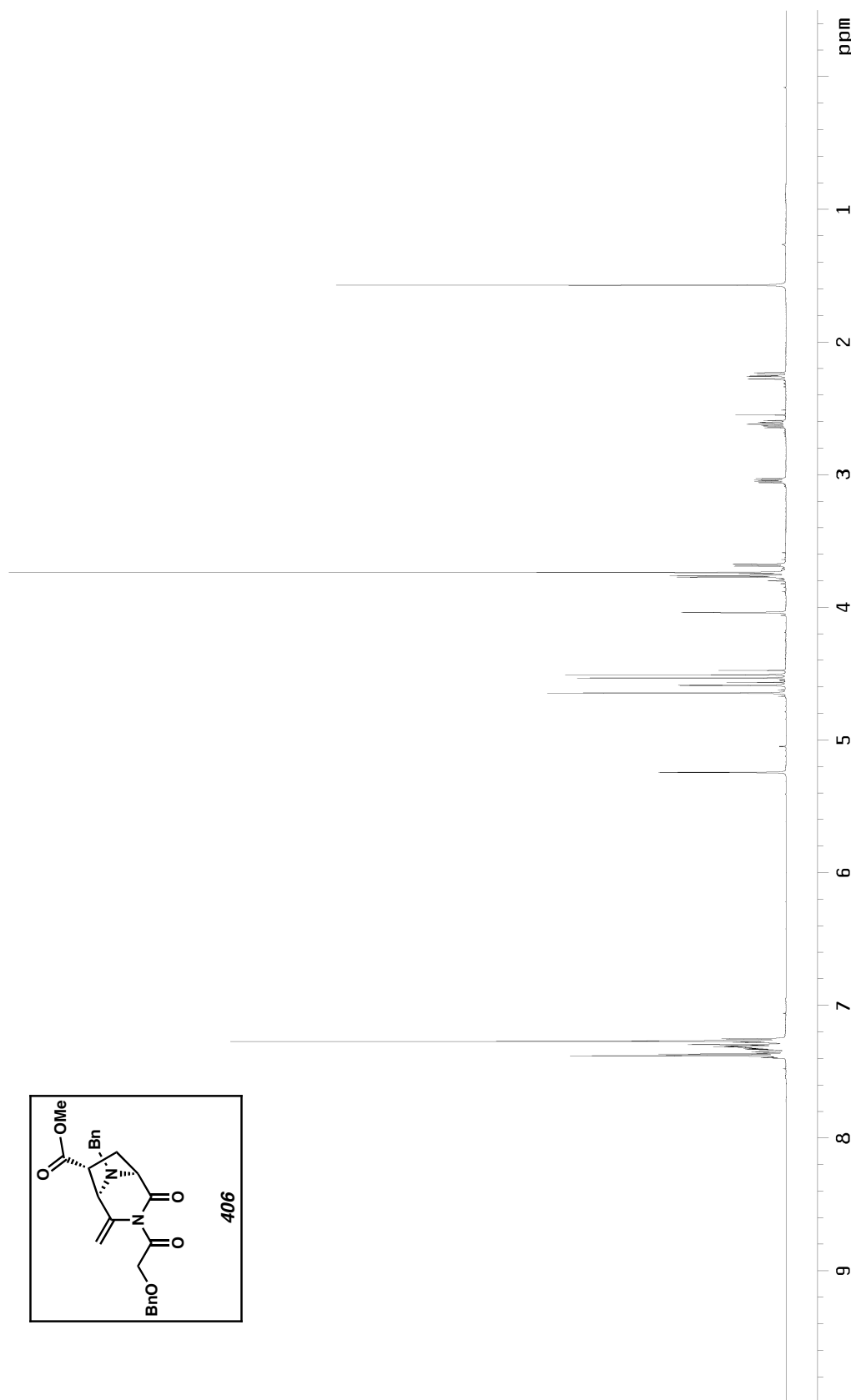


Figure A3.7.1.  $^1\text{H}$  NMR (500 MHz,  $\text{CDCl}_3$ ) of imide 406.

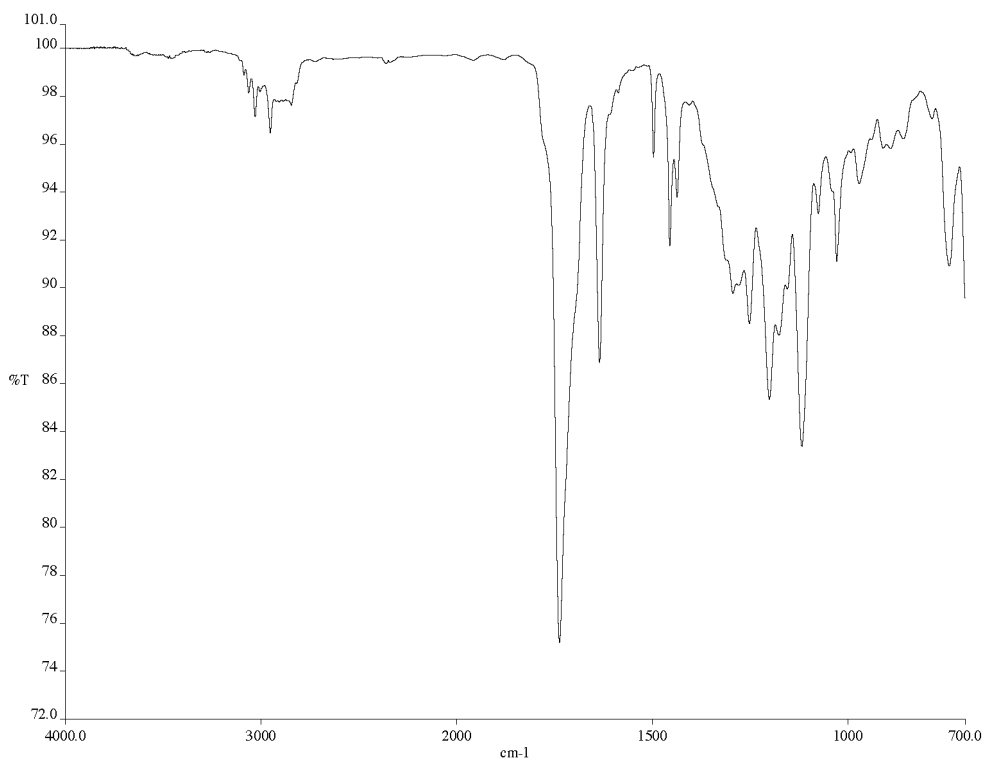


Figure A3.7.2 Infrared spectrum (thin film/NaCl) of imide **406**.

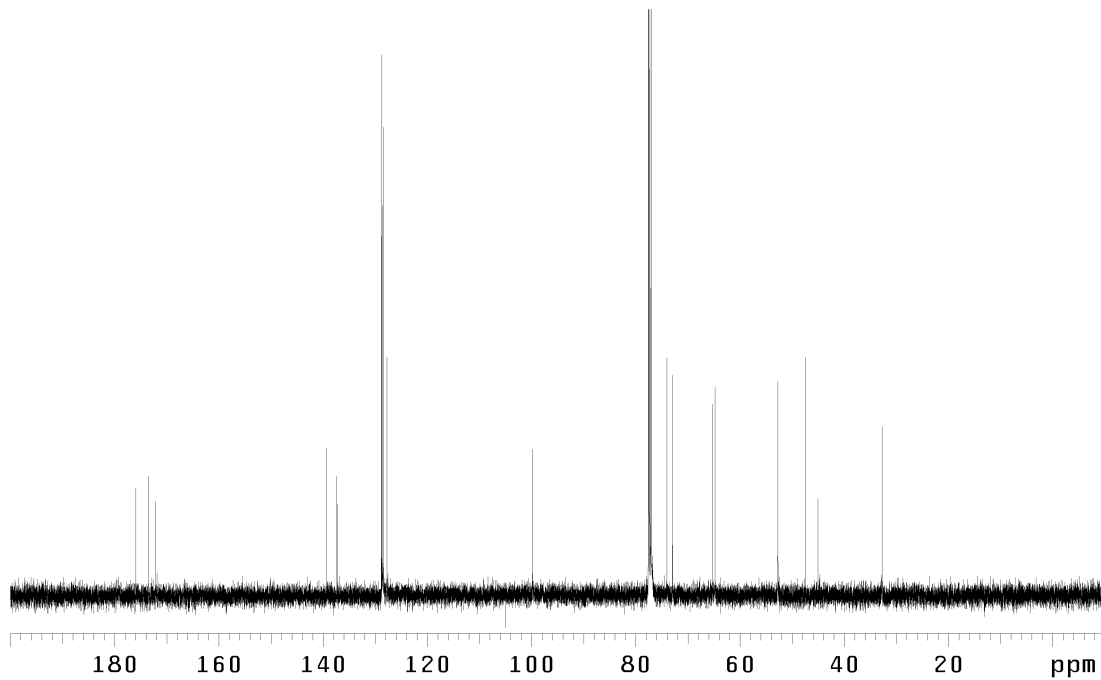


Figure A3.7.3 <sup>13</sup>C NMR (125 MHz, CDCl<sub>3</sub>) of imide **406**.

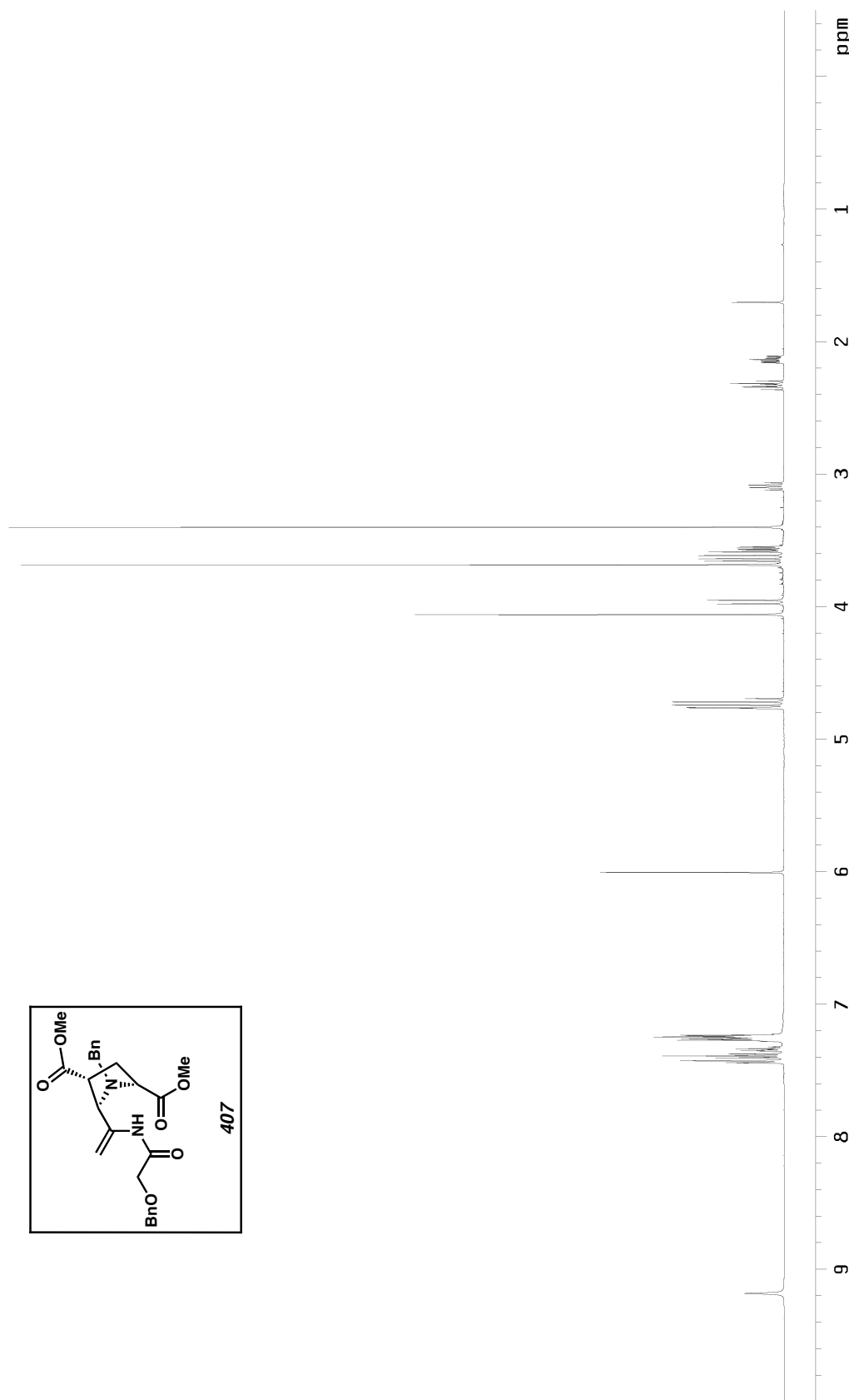


Figure A3.8.I.  $^1\text{H}$  NMR (500 MHz,  $\text{CDCl}_3$ ) of *N*-acetyl enamine 407.

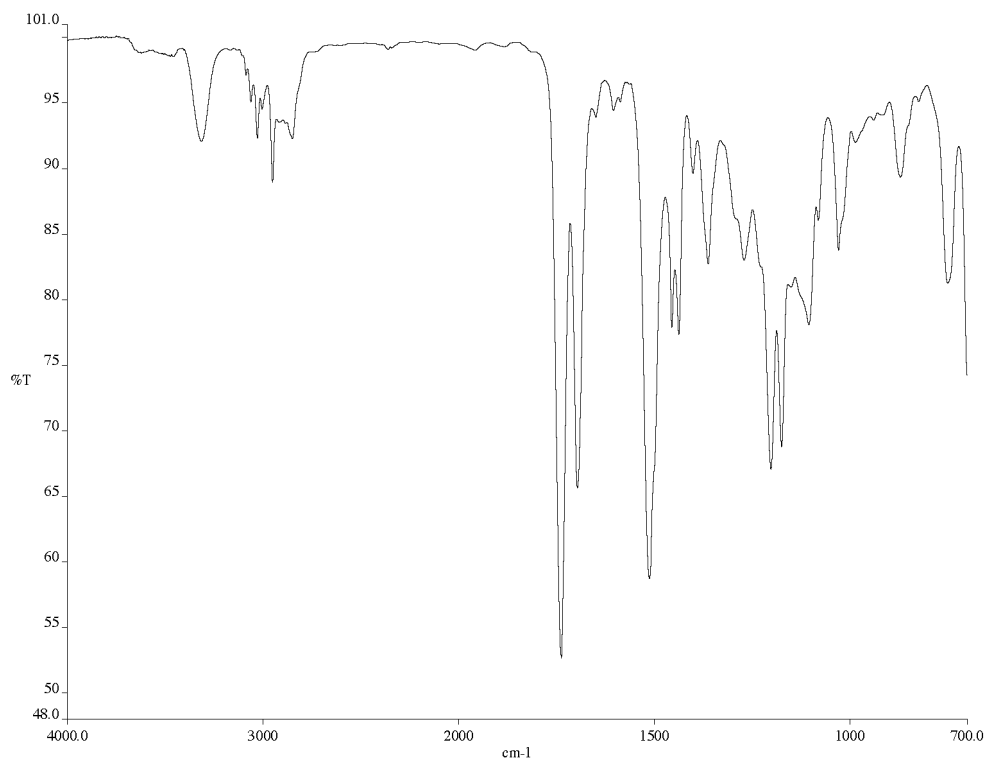


Figure A3.8.2 Infrared spectrum (thin film/NaCl) of *N*-acyl enamine **407**.

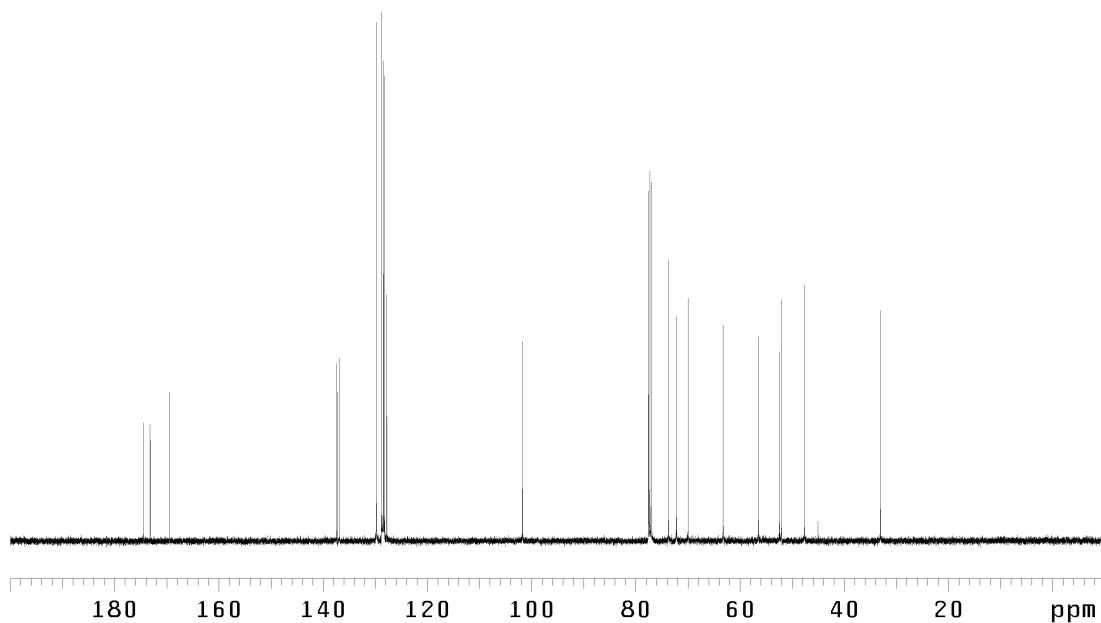


Figure A3.8.3  $^{13}\text{C}$  NMR (125 MHz,  $\text{CDCl}_3$ ) of *N*-acyl enamine **407**.

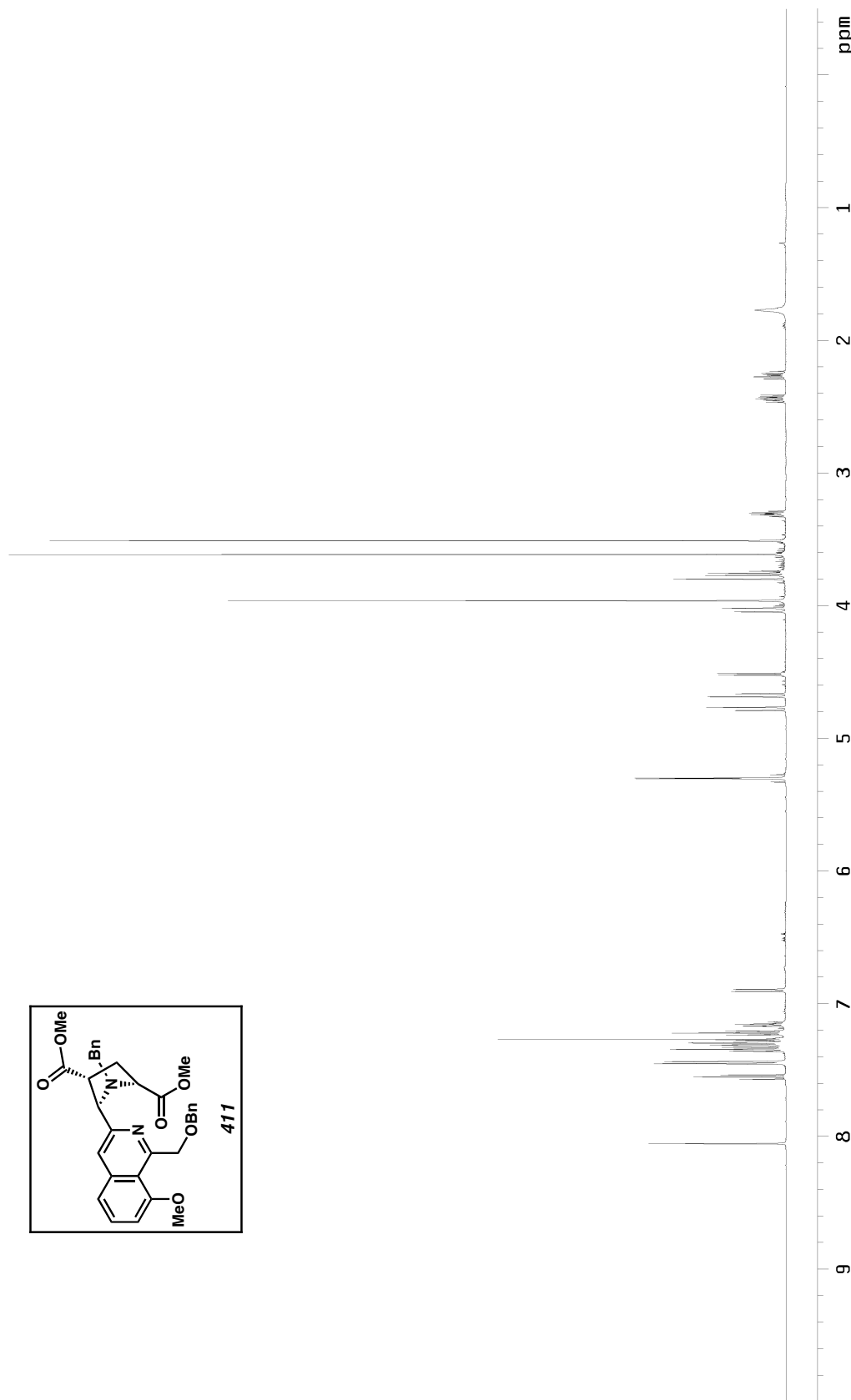


Figure A3.9.1.  $^1\text{H}$  NMR (500 MHz,  $\text{CDCl}_3$ ) of isoquinoline 411.

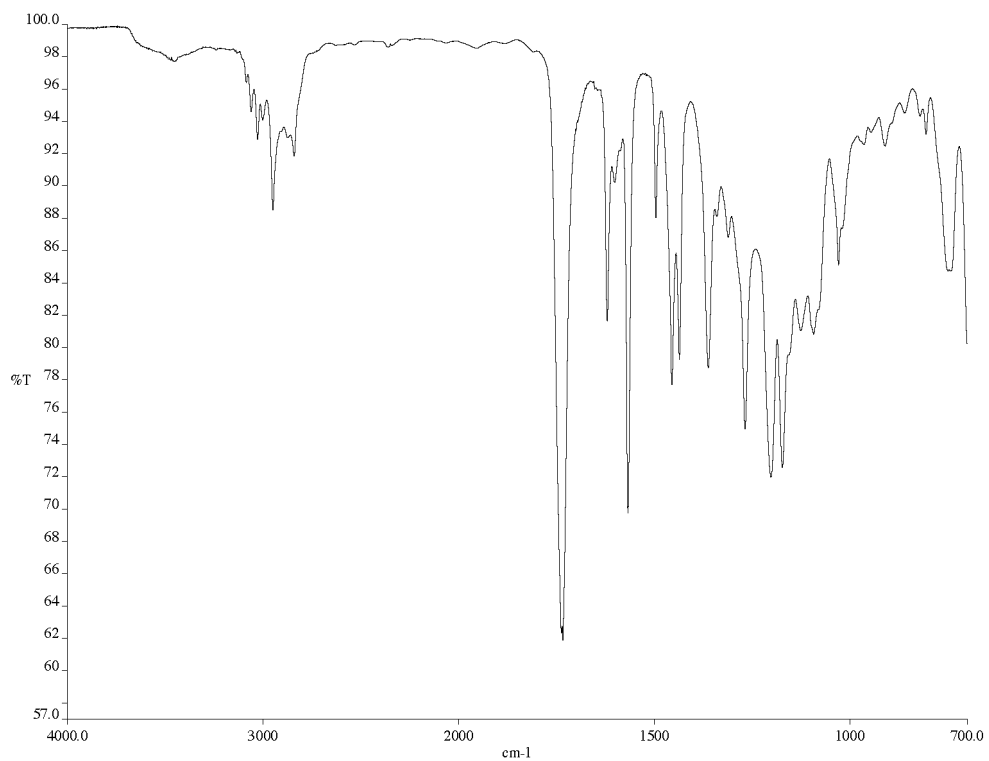


Figure A3.9.2 Infrared spectrum (thin film/NaCl) of isoquinoline **411**.

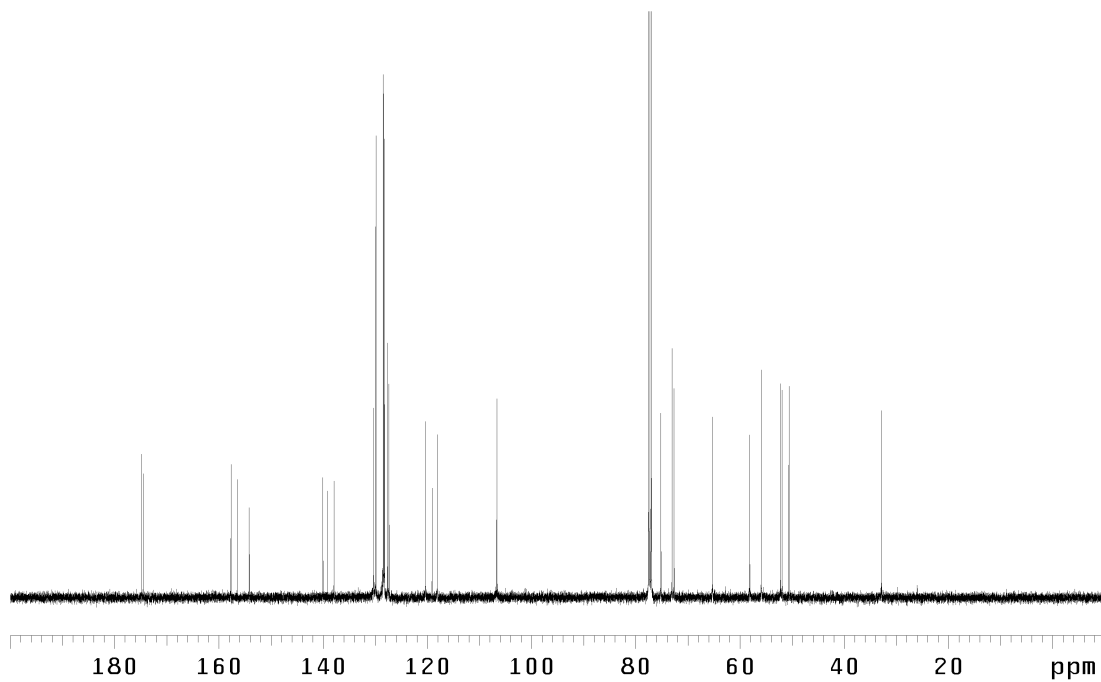


Figure A3.9.3  $^{13}\text{C}$  NMR (125 MHz,  $\text{CDCl}_3$ ) of isoquinoline **411**.

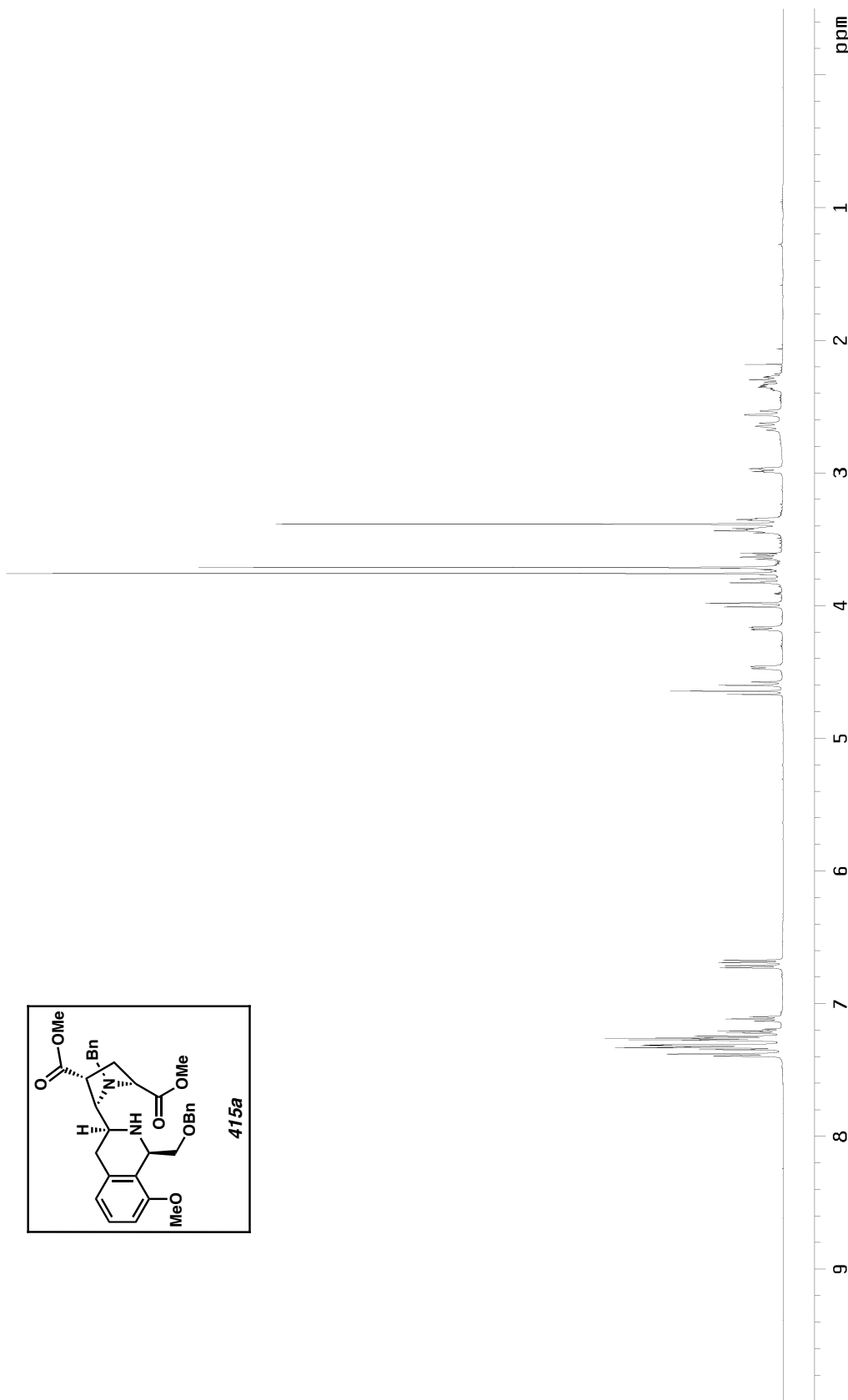


Figure A3.10.1.  $^1\text{H}$  NMR (500 MHz,  $\text{CDCl}_3$ ) of tetrahydroisoquinoline 415a.

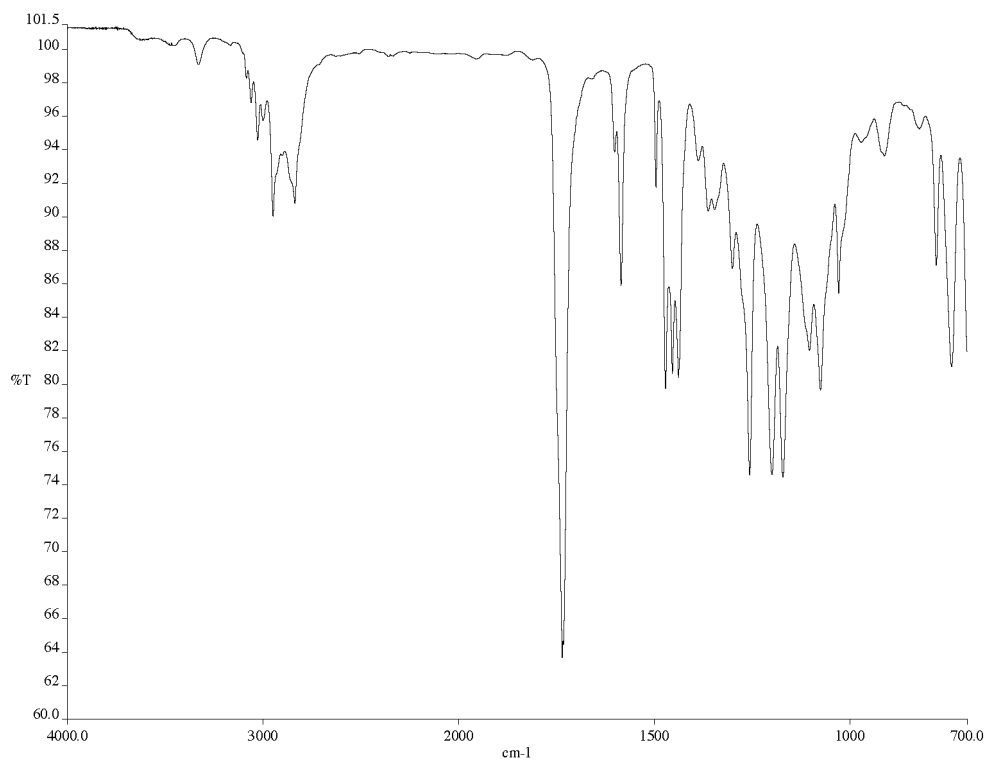


Figure A3.10.2 Infrared spectrum (thin film/NaCl) of tetrahydroisoquinoline **415a**.

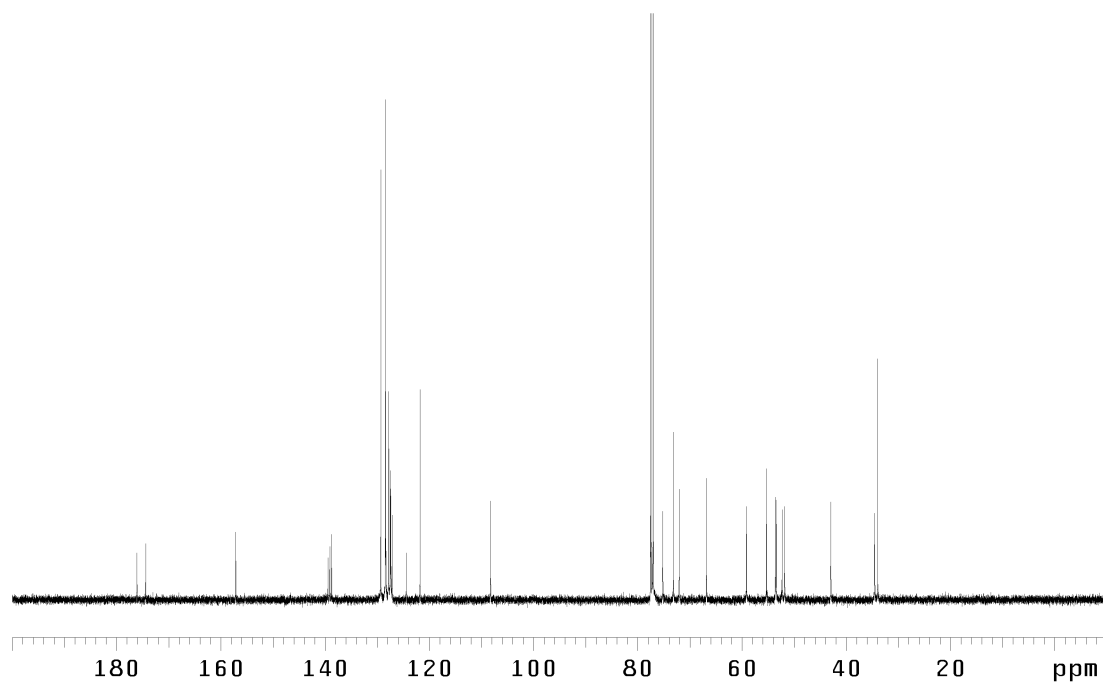


Figure A3.10.3  $^{13}\text{C}$  NMR (125 MHz,  $\text{CDCl}_3$ ) of tetrahydroisoquinoline **415a**.

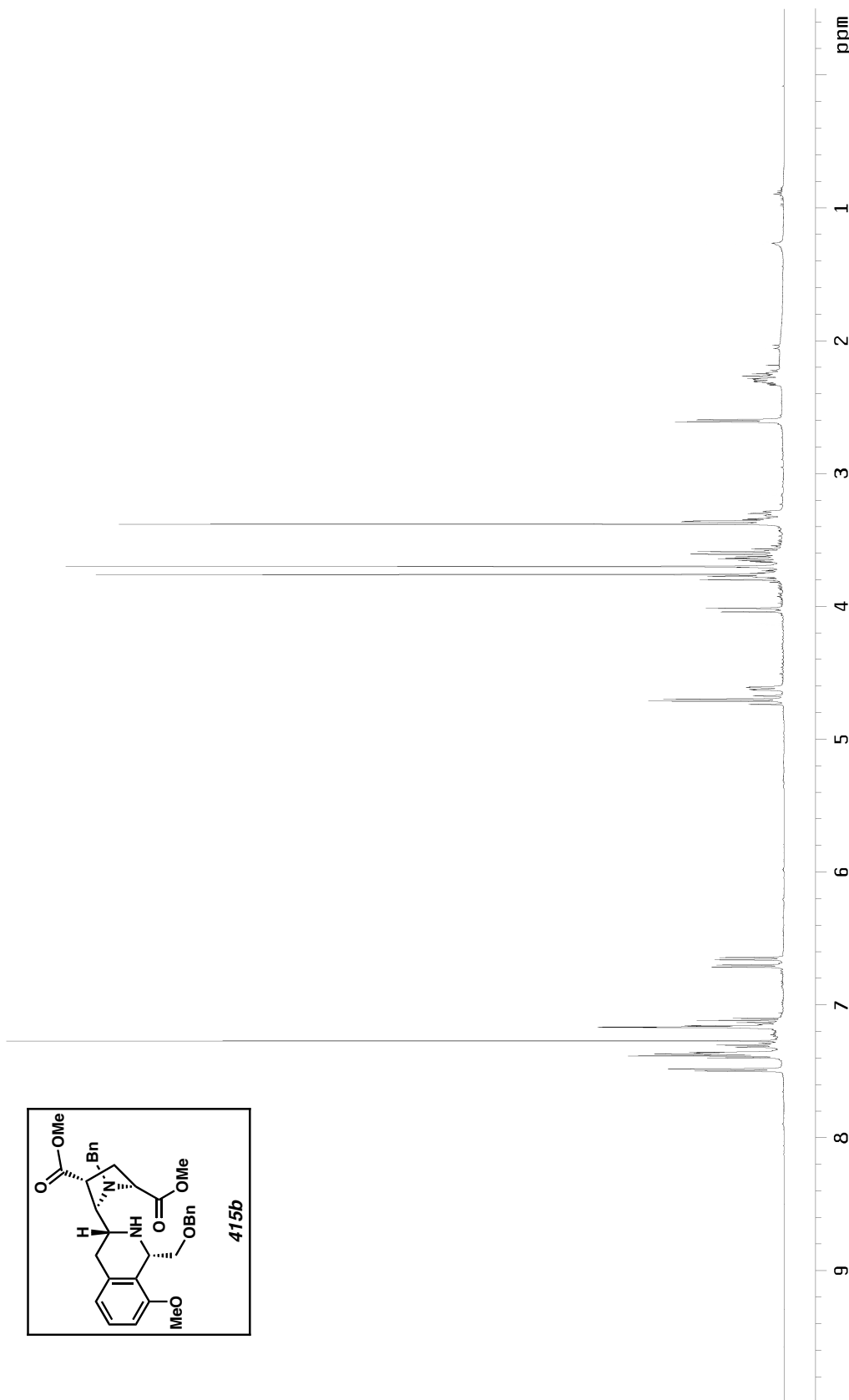


Figure A3.11.1.  $^1\text{H}$  NMR (500 MHz,  $\text{CDCl}_3$ ) of tetrahydroisoquinoline **415b**.

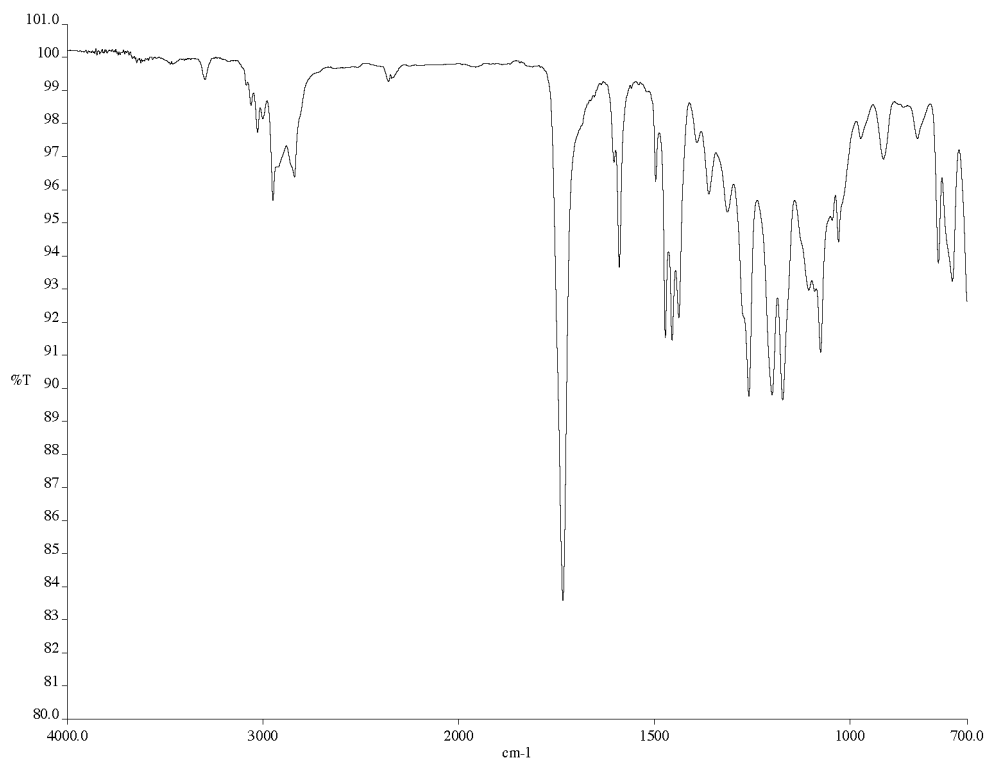


Figure A3.11.2 Infrared spectrum (thin film/NaCl) of tetrahydroisoquinoline **415b**.

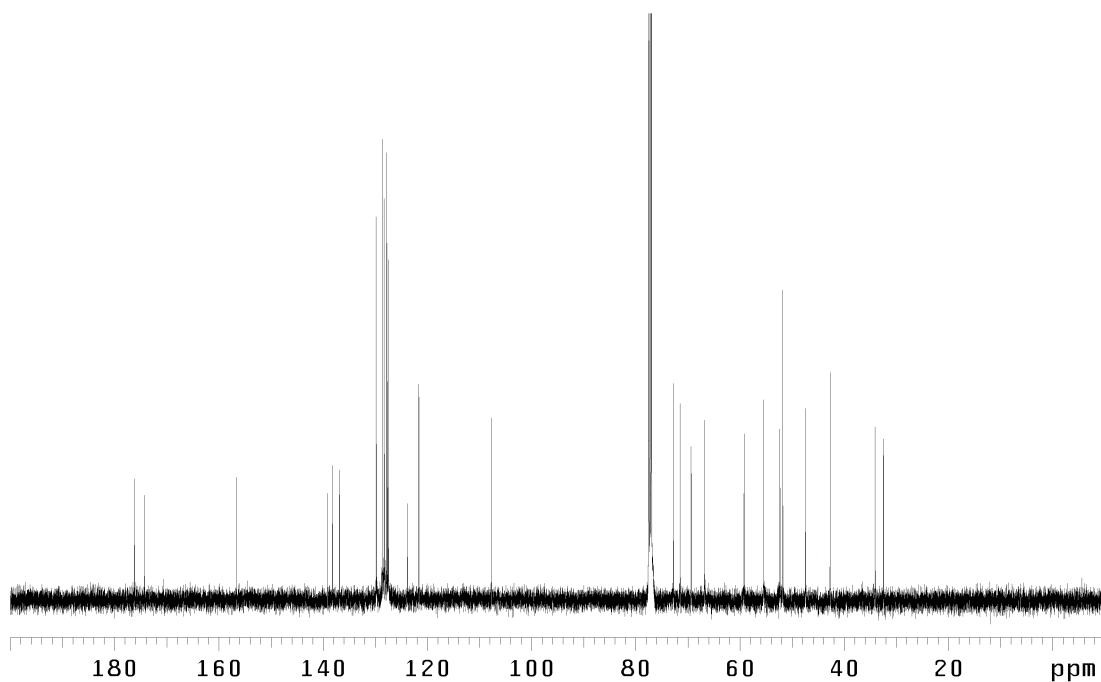


Figure A3.11.3  $^{13}\text{C}$  NMR (125 MHz,  $\text{CDCl}_3$ ) of tetrahydroisoquinoline **415b**.

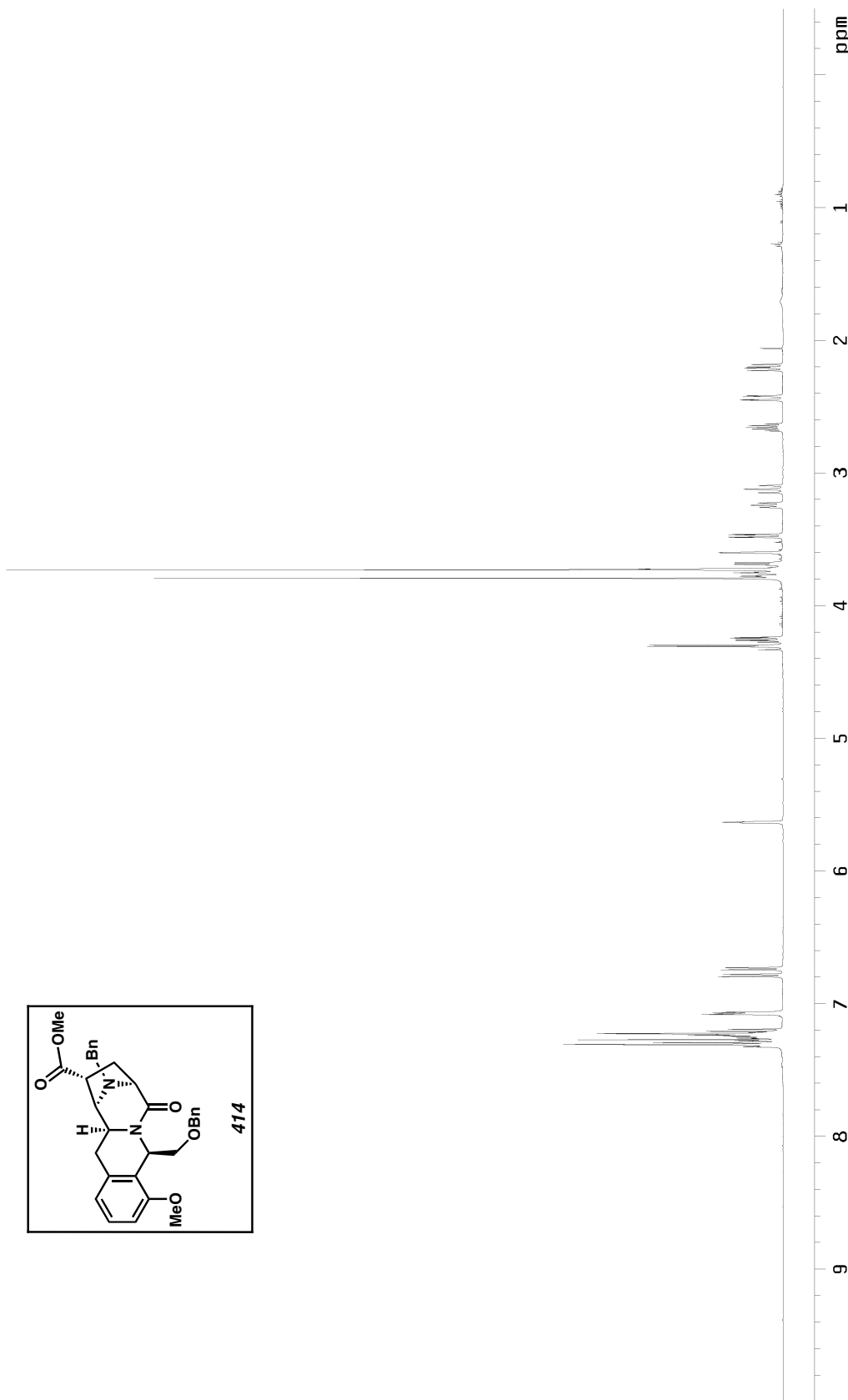


Figure A3.12.1.  $^1\text{H}$  NMR (500 MHz,  $\text{CDCl}_3$ ) of tetracycle 414.

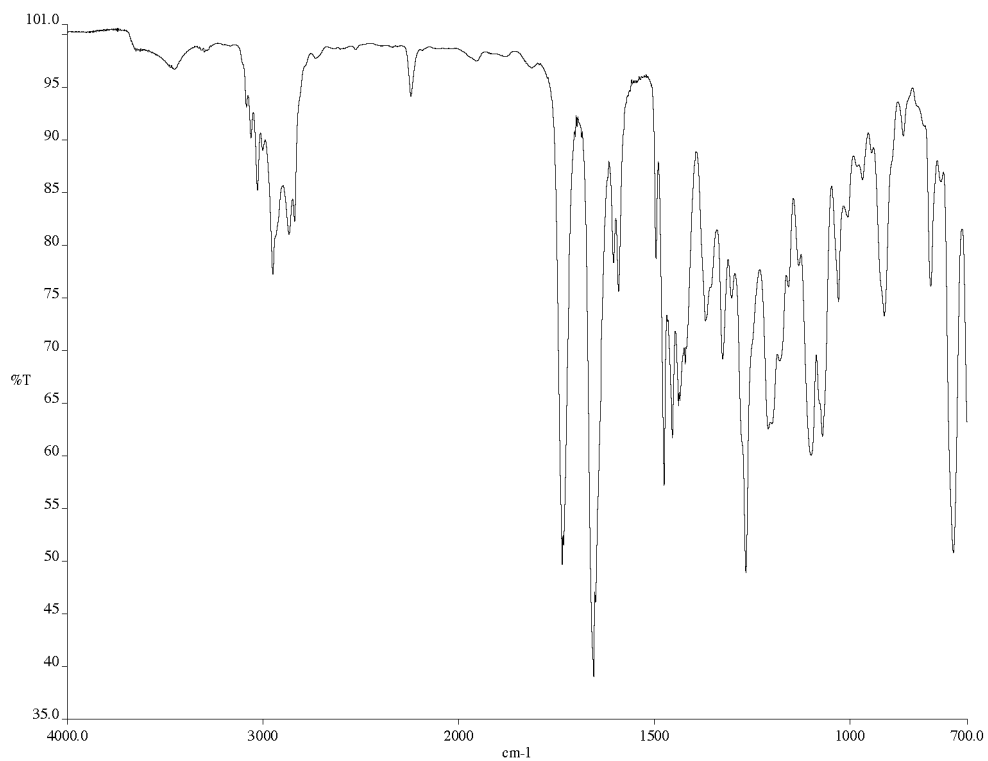


Figure A3.12.2 Infrared spectrum (thin film/NaCl) of tetracycle **414**.

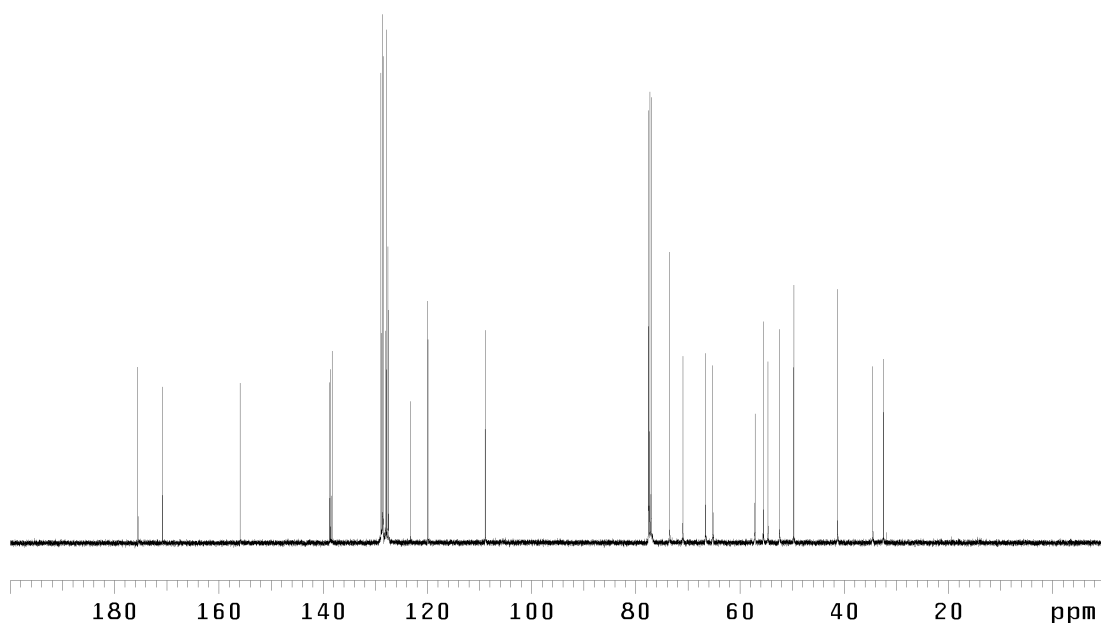


Figure A3.12.3  $^{13}\text{C}$  NMR (125 MHz,  $\text{CDCl}_3$ ) of tetracycle **414**.

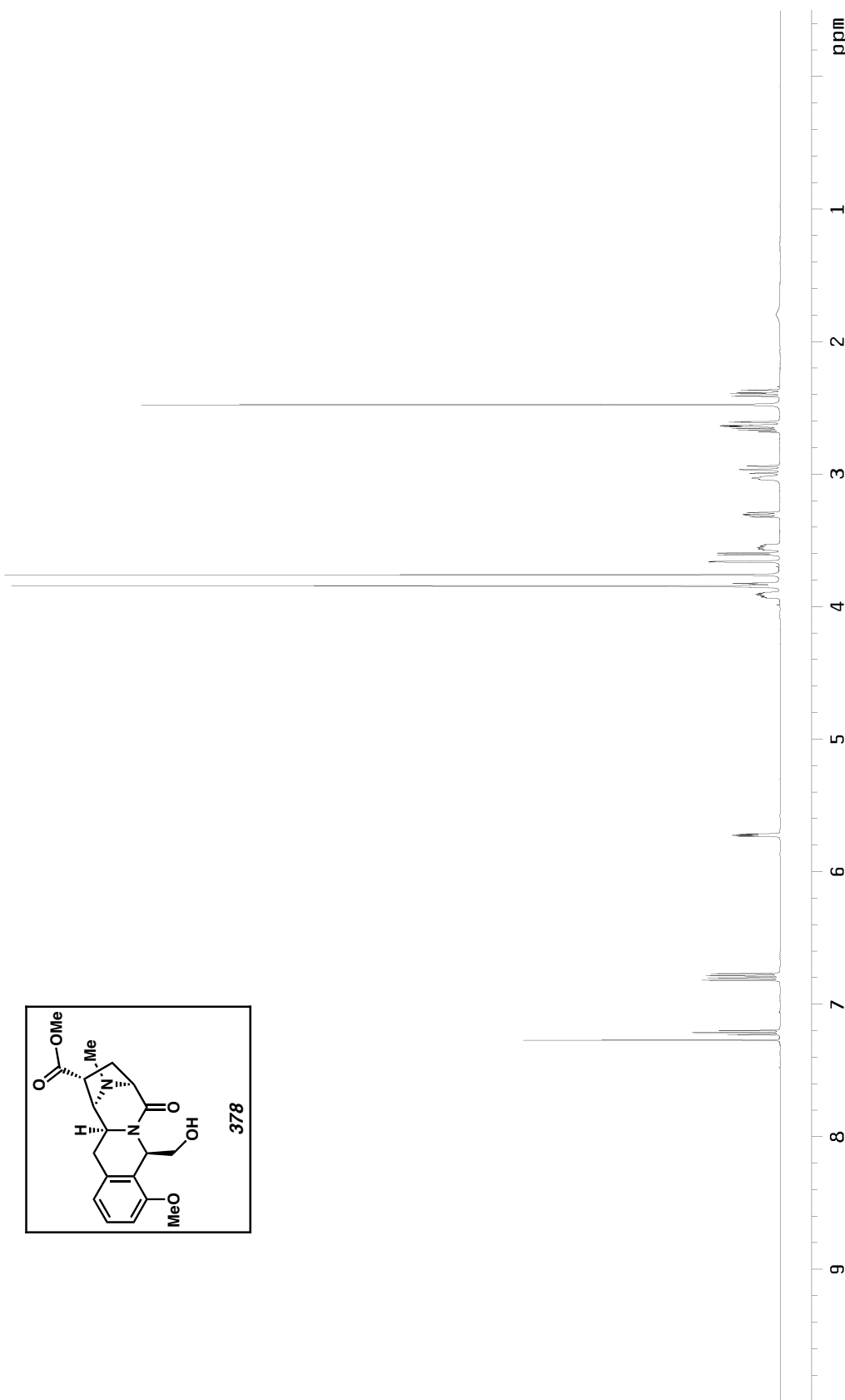


Figure A3.I3.1.  $^1\text{H}$  NMR (500 MHz,  $\text{CDCl}_3$ ) of *N*-methyl amine 378.

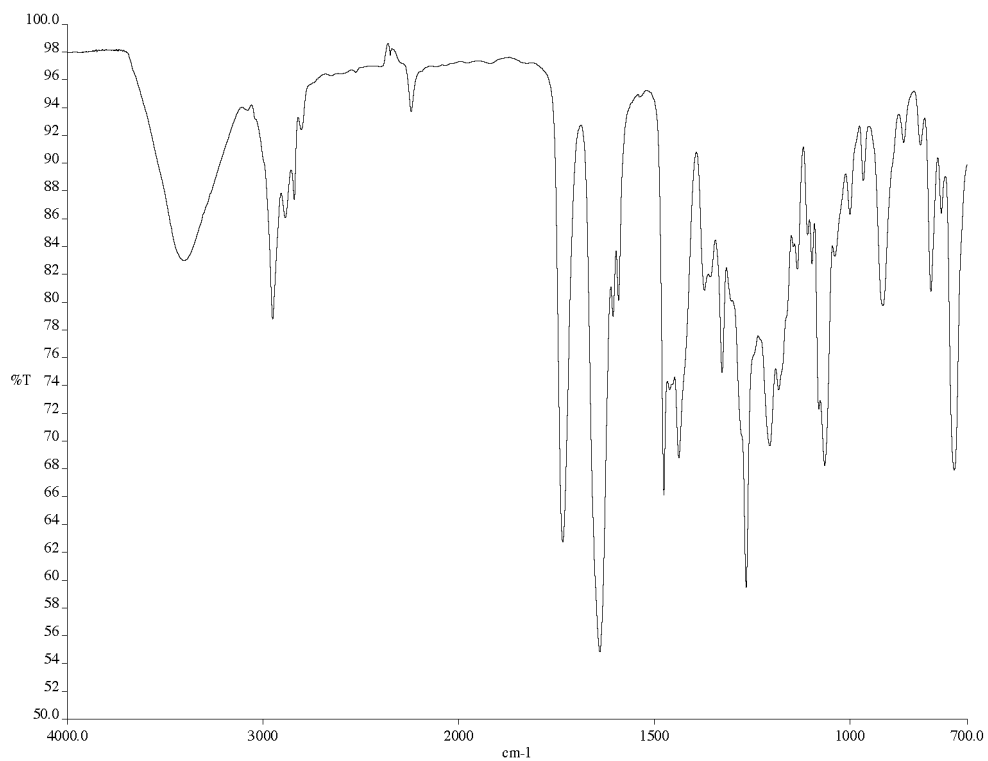


Figure A3.13.2 Infrared spectrum (thin film/NaCl) of *N*-methyl amine **378**.

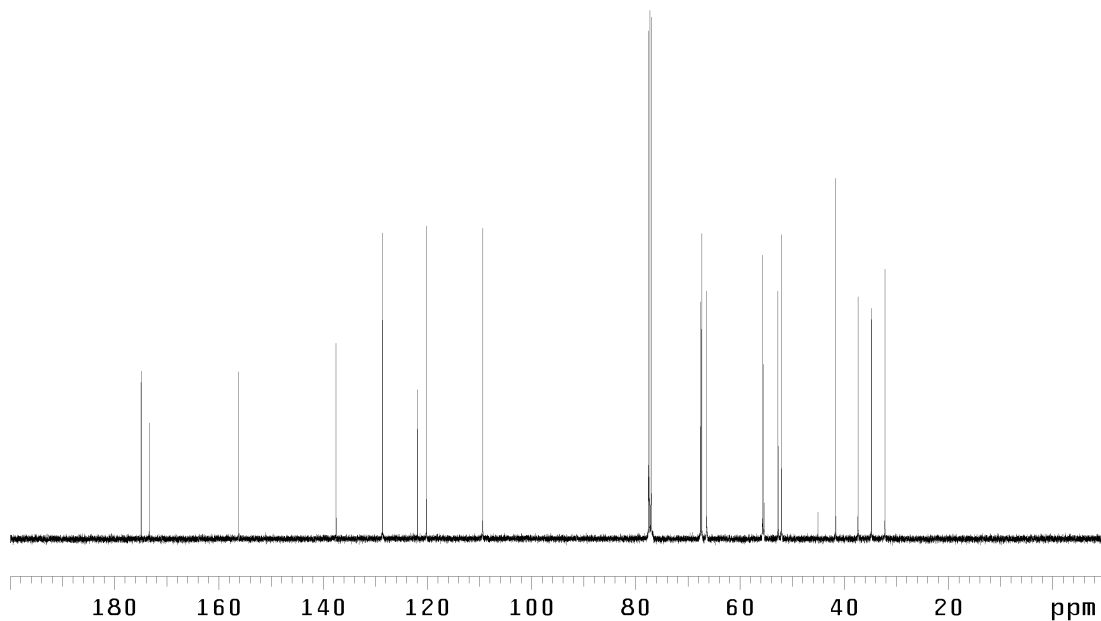


Figure A3.13.3  $^{13}\text{C}$  NMR (125 MHz,  $\text{CDCl}_3$ ) of *N*-methyl amine **378**.

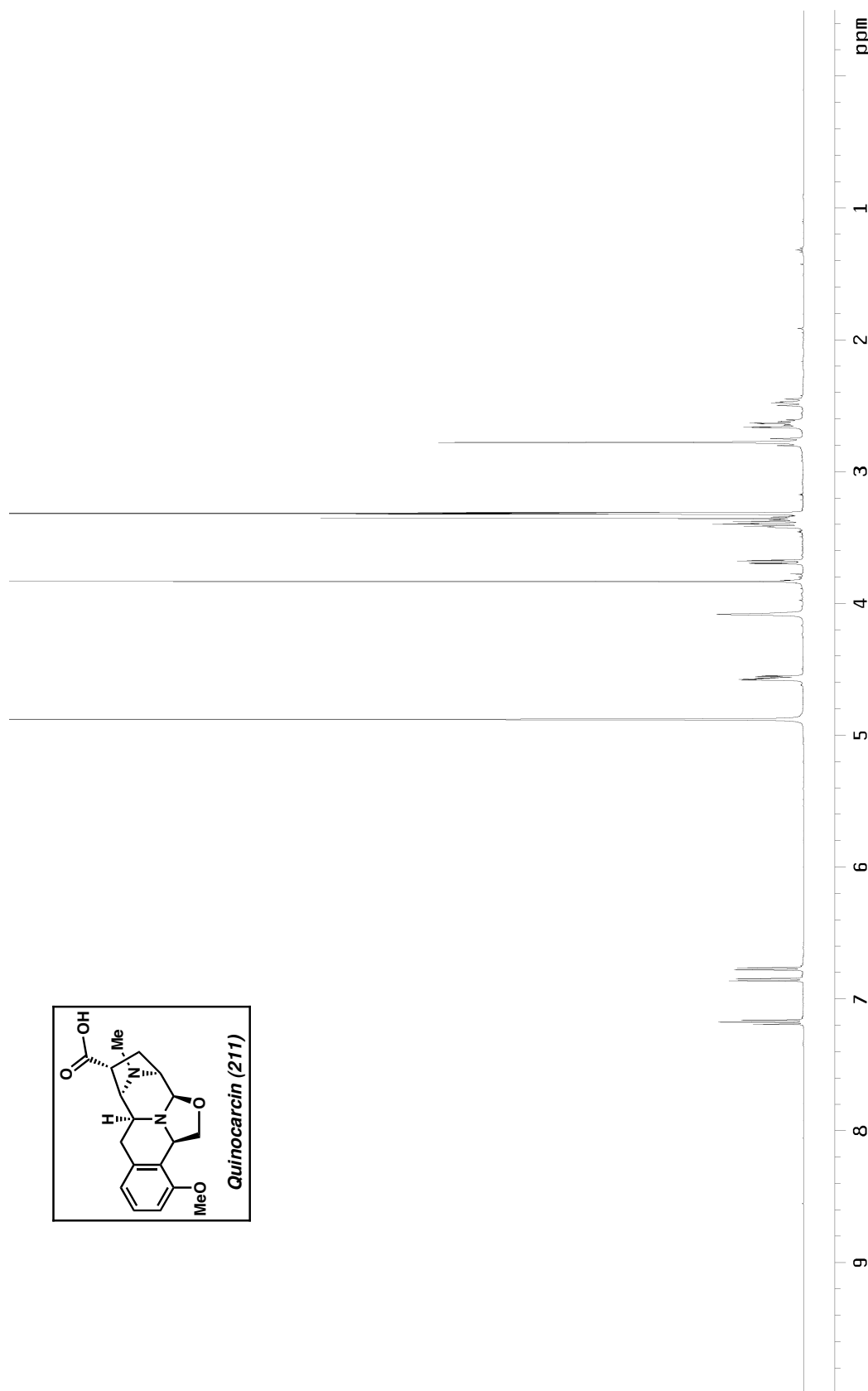


Figure A3.14.1.  $^1\text{H}$  NMR (500 MHz,  $\text{CD}_3\text{OD}$ ) of (-)-quinocarcin (211).

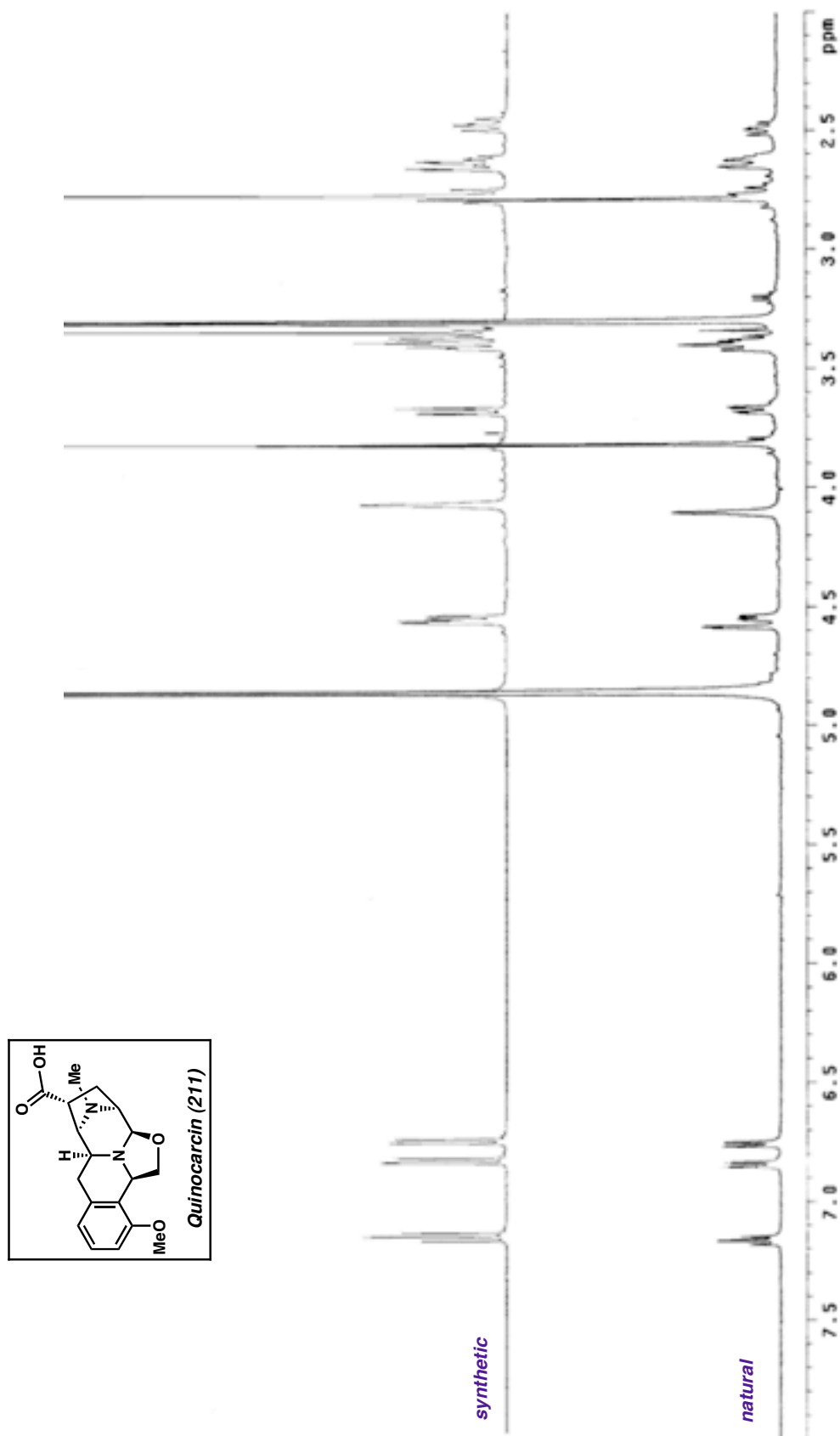


Figure A3.14.2  $^1\text{H}$  NMR comparison of synthetic (above) and natural (-)-quinocarcin (211) (500 MHz,  $\text{CD}_3\text{OD}$ ).

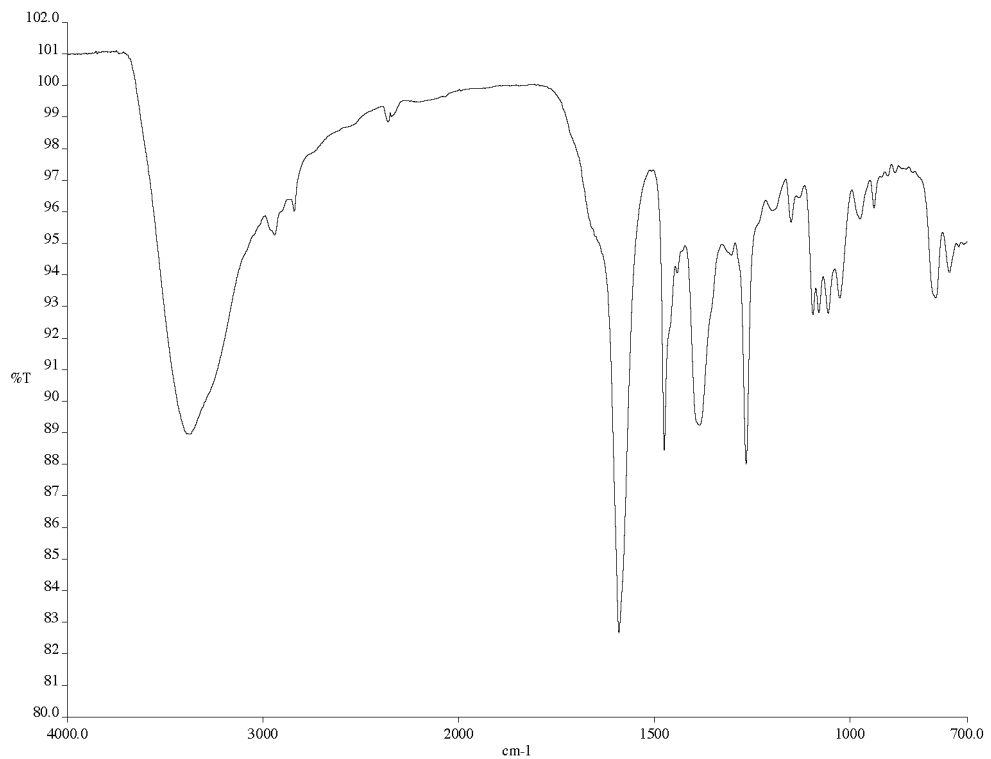


Figure A3.14.3 Infrared spectrum (thin film/NaCl) of (-)-quinocarcin (**211**).

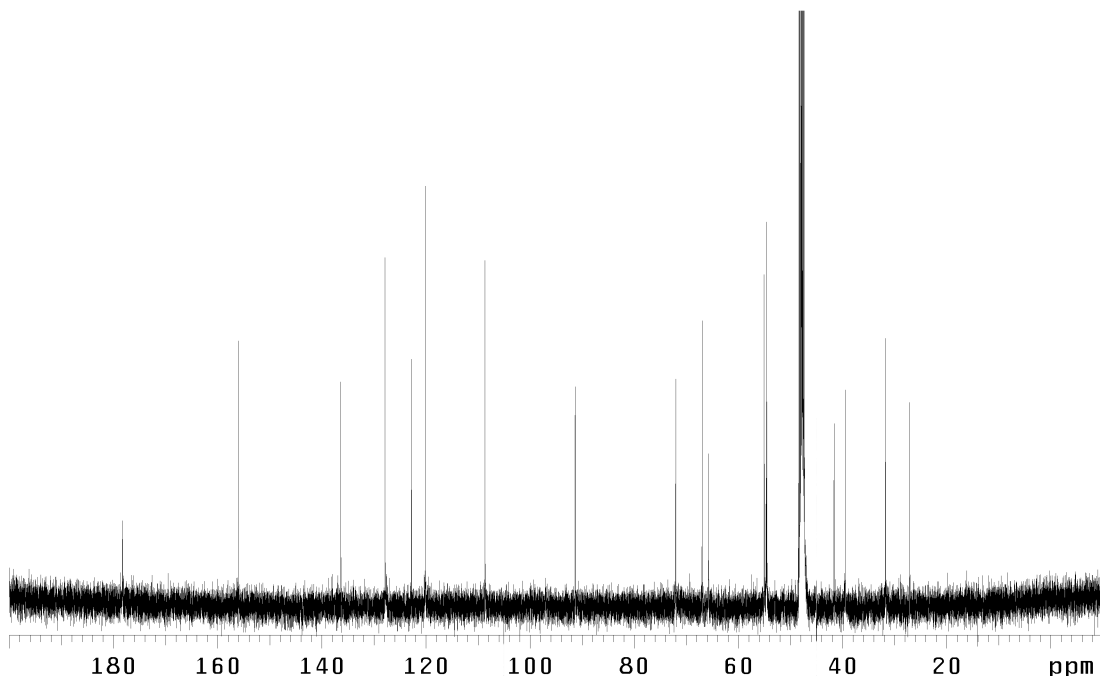


Figure A3.14.4 <sup>13</sup>C NMR (125 MHz, CD<sub>3</sub>OD) of (-)-quinocarcin (**211**).

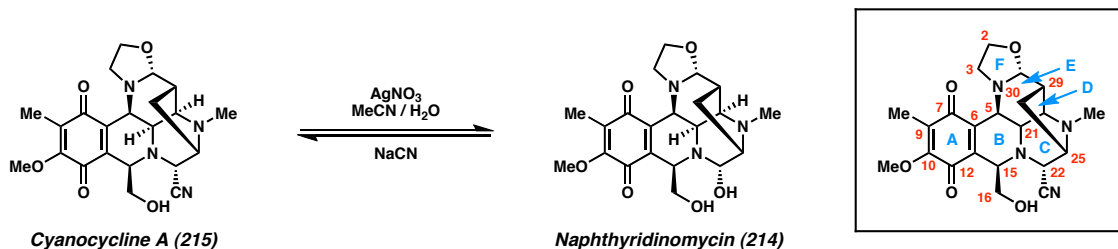
## APPENDIX 4

### *Summary of Progress Toward the Total Synthesis of (+)-Cyanocycline A*

#### A4.1 INTRODUCTION AND BACKGROUND

In 1982, researchers at Chugai Pharmaceutical Co., Ltd. isolated a new compound from a fermentation broth of *Streptomyces flavogriseus* No. 49 that showed remarkable activity as both a broad-spectrum antibiotic and antitumor agent.<sup>1</sup> The chemical was first named Antibiotic No. 49 before later being given the name cyanocycline A when it was found to contain both a nitrile and several heterocycles. Cyanocycline A (**215**) bears a striking resemblance to the previously identified natural product, naphthyridinomycin (**214**), which was first isolated from *Streptomyces lusitanus* eight years earlier by Kluepfel and coworkers (Scheme A4.1).<sup>2</sup> Interestingly, the first sample of cyanocycline A to be identified was a synthetic product isolated by Zmijewski *et al.* after treating an extraction broth of *Streptomyces lusitanus* with sodium cyanide.<sup>3</sup> Like other members of its family, cyanocycline A functions by binding to the minor groove of DNA and covalently linking to adenine and guanine nucleotides, thereby interrupting transcription.<sup>4</sup>

Scheme A4.1. Cyanocycline A and naphthyridinomycin



The tetrahydroisoquinoline alkaloids are so named because this fused bicyclic system is common to each member.<sup>5</sup> However, in a majority of cases, this ring system is featured in an oxidized form as a fused benzoquinone-piperidine, as seen in rings A and B of cyanocycline A. In addition, members of the naphthyridinomycin family are unique in that they contain an oxazolidine ring at the benzylic position of the tetrahydroisoquinoline. Cyanocycline A in particular is distinguished by the presence of an aminonitrile at C(22) in place of a carbinolamine. In total, cyanocycline A contains six rings set within a dense caged scaffold and eight stereocenters, five of which surround a single piperidine ring. Only two completed syntheses of cyanocycline A have been reported to date, both of which measure greater than 30 linear steps in length. The first synthesis was achieved by Evans in 1986,<sup>6</sup> and the second by Fukuyama one year later.<sup>7</sup> Both groups later revised their strategies to accomplish an asymmetric synthesis of the natural enantiomer of the product.<sup>8,9</sup>

## A4.2 FIRST GENERATION SYNTHETIC APPROACH<sup>†</sup>

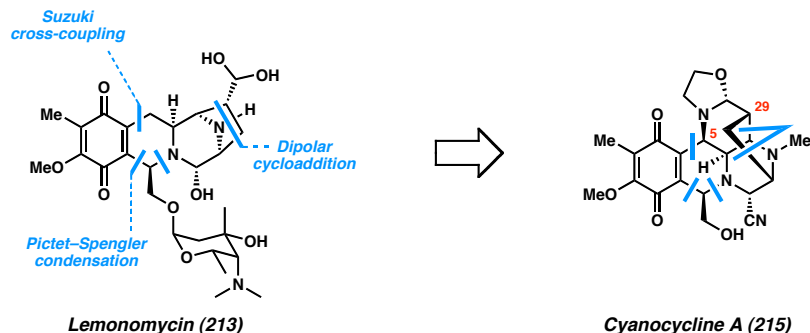
### A4.2.1 *Outline of Approach and Retrosynthetic Analysis*

Our involvement with the tetrahydroisoquinoline alkaloids began with our work toward (–)-lemonomycin (**213**), culminating in the first, and to date only total synthesis of this natural product (Figure A4.1).<sup>10,11</sup> In short, this synthesis featured a dipolar cycloaddition to construct the eastern diazabicycle, and palladium-catalyzed Suzuki cross-coupling and Pictet–Spengler reactions to form the top and bottom portions of the tetrahydroisoquinoline ring system, respectively. Given the close structural similarity between this molecule and cyanocycline A (**215**), we envisioned the use of similar procedures to form the analogous bonds in cyanocycline A. However, two notable differences separate the new target from the old: the additional presence of an oxazolidine at C(5) and the epimeric stereocenter at C(29), both of which account for the caged structure of cyanocycline A. Thus, the most significant challenges in translating our synthetic strategy from lemonomycin to cyanocycline A lay in devising a methods for introducing rings E and F.

---

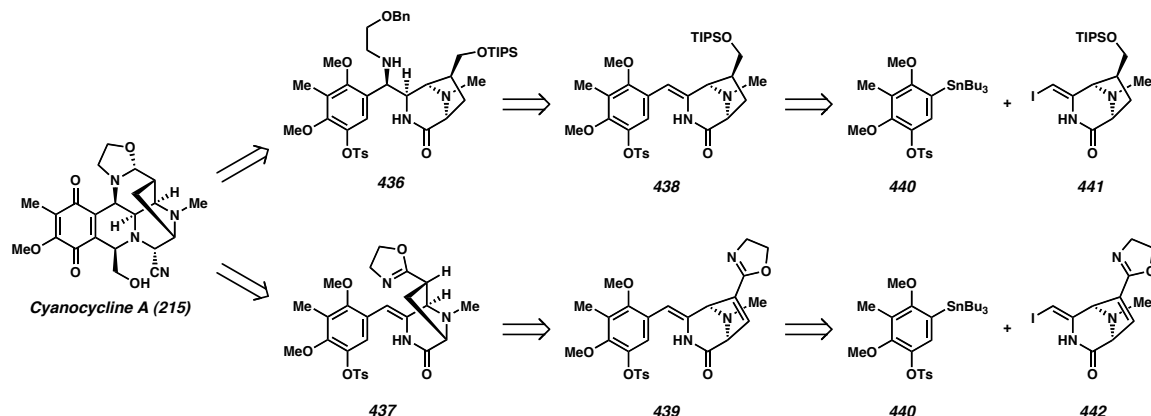
<sup>†</sup> The syntheses of silyl ether **447** and oxazoline **446** were originally designed and performed by Dr. Eric Ashley, a former graduate student in the Stoltz research group.

Figure A4.1. Translation a synthetic approach from leonomycin to cyanocycline A



Considering cyanocycline A (**215**) in a retrosynthetic sense, we envision late-stage construction of the tetrahydroisoquinoline ring system via Pictet–Spengler condensation (Scheme A4.2). Thus, removal of the lower portion of ring B leads back along two separate paths. The caged framework of the northern quadrant comprising rings E and F can be unraveled in one of two ways to reveal either amino alcohol **436** or oxazoline **437**. While these structures differ significantly from one another, they can be simplified to styrenes **438** and **439** bearing greater similarity. In the former route, doing so invokes a retrosynthetic dehydrogenation, while in the latter route, a retrosynthetic dehydroamination is required. In either case, tracing these intermediates back to styrenes **438** and **439** enables a common disconnection in each route via retrosynthetic palladium-catalyzed coupling to reveal a pair of vinyl iodides, **441** and **442**, and a common aryl stannane (**440**). The vinyl iodides displayed a close resemblance to an intermediate prepared en route to leonomycin, and so we began our efforts by targeting these compounds.

Scheme A4.2. Retrosynthetic analysis of cyanocycline A

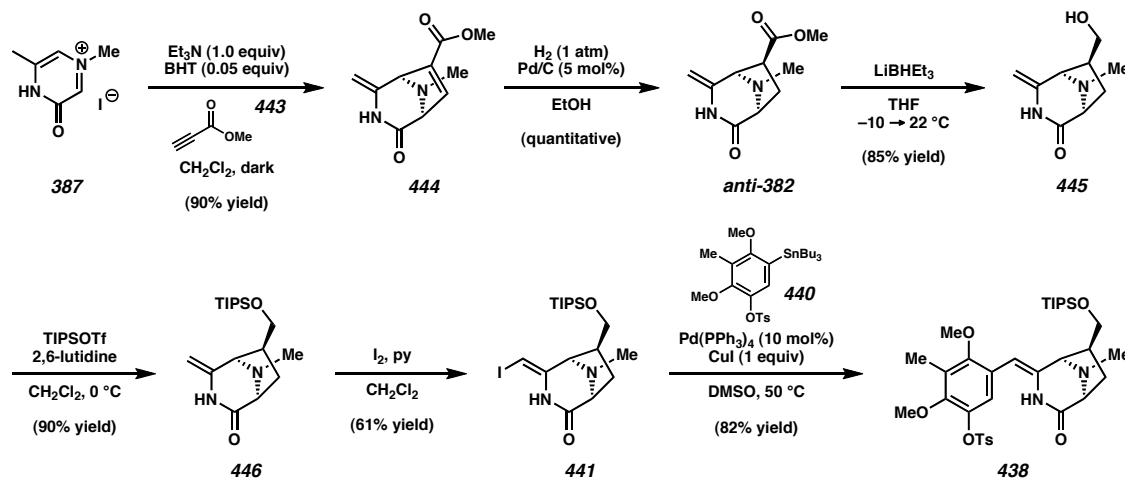


#### A4.2.2 Styrene Synthesis and Oxidative Amination

The first target of our efforts toward cyanocycline A was ester **anti-382** (Scheme A4.3). We had successfully constructed this compound using a dipolar cycloaddition between the betaine dipolar derived from oxidopyrazinium iodide **387** and methyl acrylate.<sup>12</sup> However, in this reaction, ester **anti-382** is generated as the minor diastereomer due to the unfavorable steric interactions that occur in the endo transition state leading to its formation. In order to gain access to greater quantities of **anti-382**, we therefore opted for a two-step procedure beginning with a dipolar cycloaddition between the oxidopyrazinium dipole and methyl propiolate (**443**). The resulting  $\alpha,\beta$ -unsaturated ester (**444**) was then hydrogenated from the less hindered face to produce the desired product (**anti-382**) bearing an anti relationship between the bridging amine and the methyl ester. Subsequent reduction of the ester with lithium triethylborohydride yielded a primary alcohol (**445**), which was then protected as the triisopropylsilyl ether (**446**) and selectively iodinated to produce *cis*-iodoenamine **441**. While a Suzuki cross-coupling had proven effective in the synthesis of leonomycin for introducing the western aryl

ring, attempts to apply this strategy to iodoenamine **441** were impeded by competitive reduction of the vinyl iodide. Therefore, an alternative copper-accelerated Stille cross-coupling<sup>13,14</sup> with aryl stannane **440** was selected, giving access to styrene **438** in 82% yield.

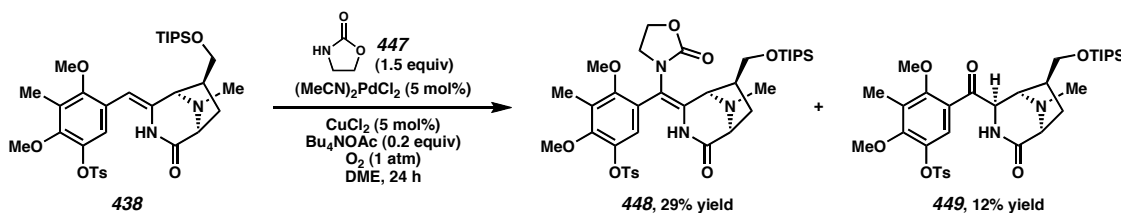
Scheme A4.3. Synthesis of silyl ether **438**



With rings A, C, and D effectively in place, we turned our attention toward the introduction of the benzylic nitrogen substituent. Seeking a method to directly incorporate the entire ethanolamine fragment comprising C(2) and C(3) of the oxazolidine backbone of the natural product, we considered an oxidative amination strategy using 2-oxazolidinone (**447**) as a masked equivalent (Scheme A4.4). Following a procedure developed by Stahl and coworkers, styrene **438** and 2-oxazolidinone (**447**) were combined in the presence of both a palladium and a copper catalyst under an oxygen atmosphere.<sup>15</sup> After 24 h, vinyl oxazolidinone **448** was produced in 29% yield accompanied by a small amount of ketone **449**, presumably formed through hydrolysis of

**448.** This result is especially noteworthy given the steric environment surrounding the olefin and the increased electron density afforded by the amide nitrogen and electron-rich arene. However, these factors may also contribute to the low yield, as evidenced by the fact that attempts to optimize the synthesis of vinyl oxazolidinone **448** met with little success.

*Scheme A4.4. Oxidative amination of styrene **438***

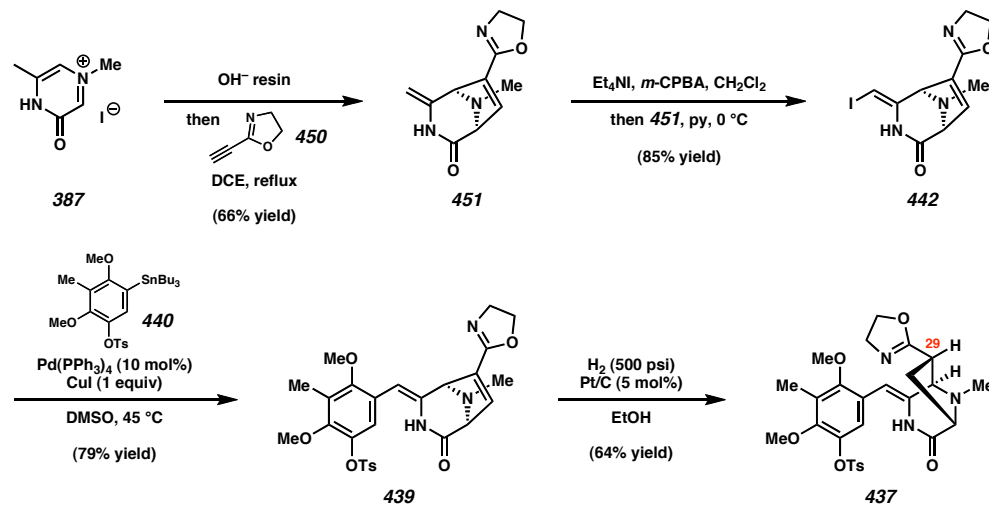


#### A4.2.3 Oxazoline Route

Having encountered difficulties installing the benzylic nitrogen substituent using an intermolecular coupling reaction, we revised our approach to attempt an intramolecular cyclization of oxazoline **437** (Scheme A4.5). Given the similarity between this structure and silyl ether **438**, we were able to apply the same general approach to its synthesis. A modified dipolar cycloaddition between the oxidopyrazinium dipole derived from **387** and propargylic oxazoline **450** furnished  $\alpha,\beta$ -unsaturated oxazoline **451**. Iodination according to the method of Sha *et al.*<sup>16</sup> provided iodoenamine **442**, which was coupled to aryl stannane **440** under copper-accelerated Stille conditions to generate styrene **439**. This product was then submitted to catalytic hydrogenation over platinum on charcoal to form the saturated oxazoline (**437**) with the desired stereochemistry at C(29). However, this compound represents the forefront of this particular synthetic route as attempts to

carry out a *6-endo*-trig cyclization to form the N–C(5) bond have resulted only in rearrangement and hydrolysis of the oxazoline.<sup>11</sup>

Scheme A4.5. Synthesis of oxazoline **437**



## A4.3 SECOND GENERATION SYNTHETIC APPROACH

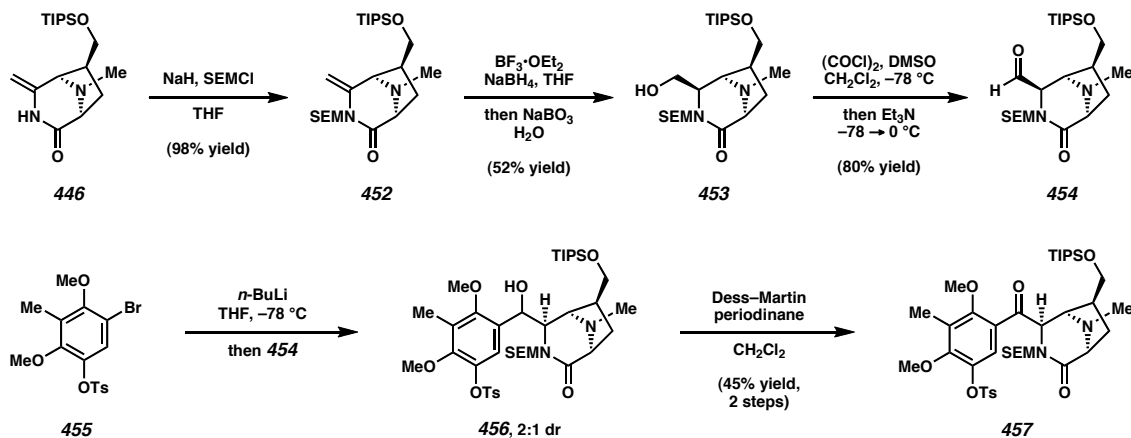
### A4.3.1 Aryllithium Addition to an Aldehyde

Our strategy thus far centered around the preparation of a styrenyl intermediate, to which the benzylic nitrogen substituent would be added in subsequent steps. However, attempts to introduce this functionality had met with difficulties associated with the crowded environment surrounding C(5) and the nucleophilicity of the target olefin. As such, we chose to investigate an alternate route in which an oxygen substituent would be installed at C(5) prior to the introduction of the aryl ring, in the hope of facilitating installation of the amine using this functional handle.

The first method we devised to accomplish this task was an addition of an aryl nucleophile to an aldehyde such as **454** (Scheme A4.6). With this goal in mind, we set

about converting enamine **446** to the desired aldehyde. This was achieved in a straightforward manner by protecting the amide nitrogen as a 2-(trimethylsilyl)ethyl aminal (**452**), hydroborating the olefin, oxidizing the resulting alkyl borane to a primary alcohol (**453**), and further oxidizing under Swern conditions. Then, in the key step, bromide **455** was treated with *n*-butyllithium. To the resulting aryllithium species was added aldehyde **454**, producing a 2:1 mixture of diastereomeric benzylic alcohols (**456**) of unassigned relative stereochemistry. Fortunately, this low selectivity proved irrelevant, as both diastereomers successfully underwent oxidation in the presence of the Dess–Martin periodinane to furnish ketone **457** as a single product.

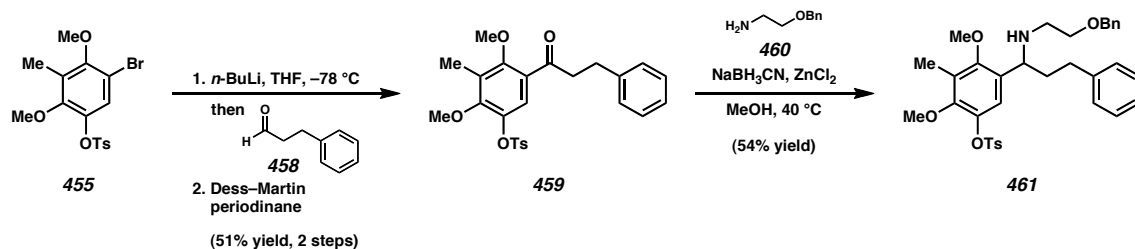
Scheme A4.6. Synthesis of benzylic ketone **457** via aldehyde **454**



While ketone **457** is the most advanced intermediate that we have prepared along this route, we have explored several potential methods for introducing the ethanolamine fragment in model systems. The most successful approach developed so far employs reductive amination. Ketone **459** was prepared in two steps from aryl bromide **455** and dihydrocinnamaldehyde (**458**) according to the previous procedure (Scheme A4.7).

Reductive amination of this model substrate with 2-(benzyloxy)ethylamine (**460**) using zinc-modified cyanoborohydride<sup>17</sup> yielded benzylic amine **461** in 54% yield. We are confident that application of these conditions to the advancement of ketone **457** will provide access to an amine such as **436**.

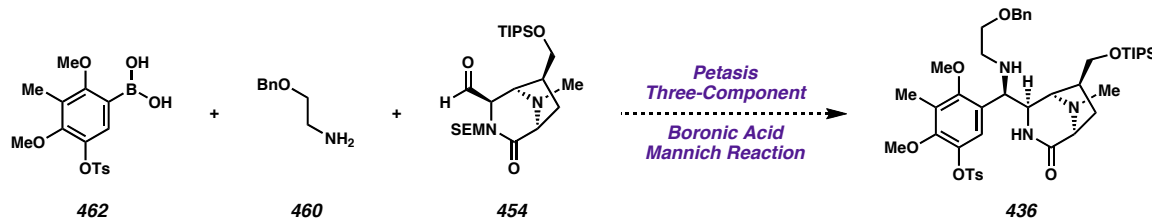
*Scheme A4.7. Reductive amination of a model benzylic ketone*



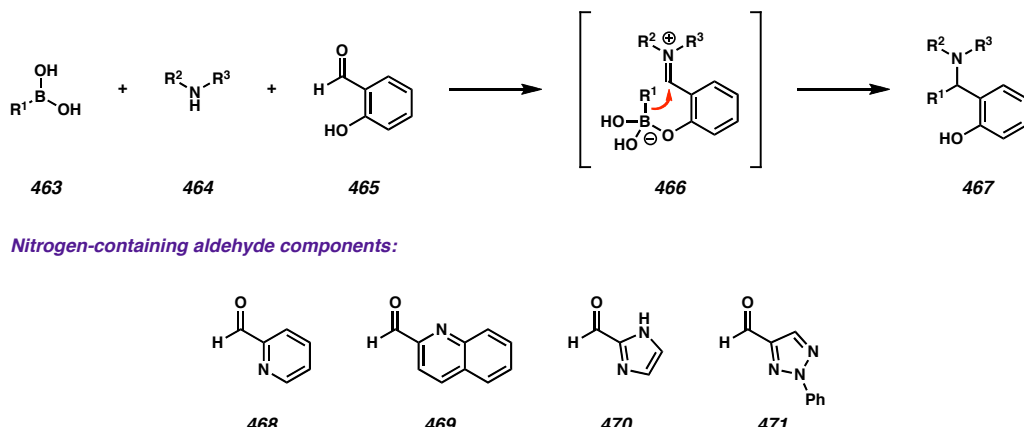
#### A4.3.2 Petasis Three-Component Boronic Acid Mannich Reaction

The stepwise synthesis of amine **461** from aryl bromide **455**, dihydrocinnamaldehyde (**458**), and amine **460** brought to mind an alternative strategy wherein assembly of benzylic amine **436** could be accomplished in a single step using a Petasis three-component Mannich-type coupling reaction between boronic acid **462**, 2-(benzyloxy)ethylamine (**460**), and aldehyde **454** (Scheme A4.8).<sup>18</sup> Since each of these components had been prepared during previous studies,<sup>19</sup> we were able to carry out the investigation of this new route quickly and with little additional effort.

Scheme A4.8. Proposed Petasis three-component coupling reaction

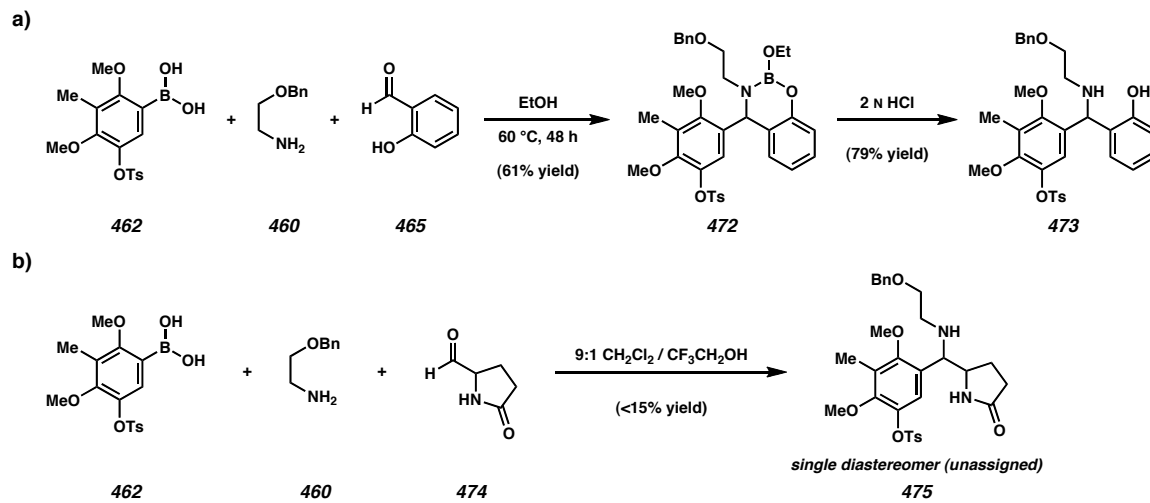


One noteworthy characteristic of the Petasis reaction is the need for a nucleophilic directing group proximal to the aldehyde. This group presumably serves to direct the intramolecular addition of the boronic acid (**463**) to the iminium (**466**) formed through condensation of the amine (**464**) and aldehyde (**465**) components, most likely through the intermediacy of a boronate anion (Scheme A4.9).<sup>20</sup> This directing group often takes the form of an alcohol or carboxylic acid situated  $\alpha$  to the aldehyde.<sup>21</sup> However, our specific approach would require a secondary amide to fulfill this role. Prior to our work, the closest analogues that had been shown to promote this reactivity in the Petasis reaction were a collection of nitrogen-containing heterocyclic aldehydes (**468–471**) reported by Bryce and Hansen.<sup>22</sup>

Scheme A4.9. Petasis three-component coupling via iminium boronate **466**

We set about examining the feasibility of our three-component strategy by first testing boronic acid **462** and amine **460** in combination with salicylaldehyde (**465**) (Scheme A4.10a). To our delight, simply heating these substrates in ethanol resulted in the formation of amino borate **472** in 61% yield, which then furnished amino alcohol **473** upon stirring in 2 N hydrochloric acid. Having demonstrated the desired reactivity with two of our three desired substrates, we then prepared amido aldehyde **474** as a model for the third component (Scheme A4.10b). Promoting the formation of amino amide **475** proved difficult in most solvents commonly used for the Petasis reaction (e.g., EtOH, *I*-PrOH, 1,4-dioxane, CH<sub>2</sub>Cl<sub>2</sub>). However, we found that by performing the reaction in a mixture of dichloromethane and 2,2,2-trifluoroethanol, we could generate small amounts of the desired product as a single diastereomer of unassigned relative stereochemistry.<sup>23</sup> Efforts to improve this yield and subsequently apply these conditions to the formation of benzylic amine **436** are currently ongoing.

Scheme A4.10. a) Evaluating the Petasis reaction with aryl boronic acid **462** and amine **460**. b) Evaluating the Petasis reaction with amido aldehyde **474**.

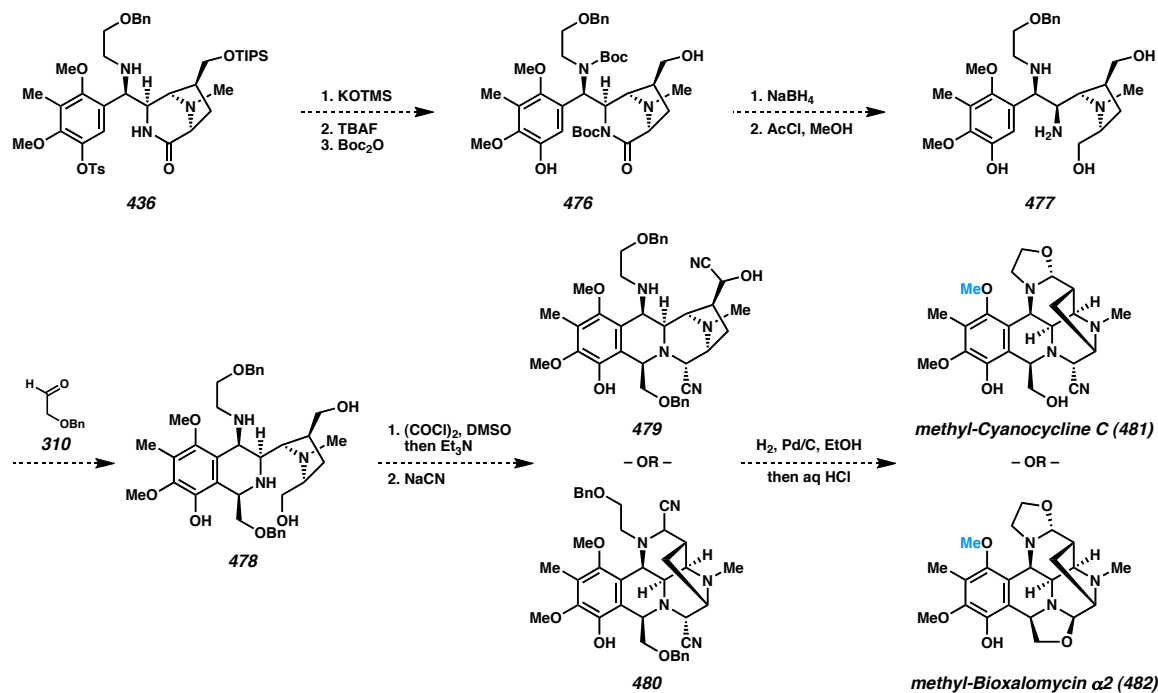


#### A4.4 FUTURE DIRECTIONS

We anticipate that either reductive amination of ketone **457** with 2-(benzyloxy)ethylamine (**460**) or three-component coupling of aryl boronic acid **462**, amine **460**, and aldehyde **454** will yield benzylic amine **436** (Scheme A4.11). This material will then be advanced toward cyanocycline A through removal of the sulfonyl and silyl protecting groups followed by *tert*-butyl carboxylation of the amide and amine to yield imide **476**. Our previous efforts toward lemonomycin indicate that the Pictet–Spengler reaction will only progress with a primary  $\beta$ -phenylethylamine.<sup>10,11</sup> As such, we plan to open the lactam ring under reductive conditions and remove the *tert*-butyl carboxyl groups to provide triamine **477**. Pictet–Spengler condensation with benzyloxyacetaldehyde (**310**) will then form tetrahydroisoquinoline **478**. From this intermediate, the synthetic route is envisioned to proceed in one of two directions. Swern oxidation of the two primary alcohols will produce an intermediate dialdehyde, which will then be treated with sodium cyanide. Each of the aldehydes is located within the vicinity of a secondary amine. Condensation of the southern amine with the proximal aldehyde is well known, and as such, the two-step procedure is expected to yield an aminonitrile at this position.<sup>24</sup> However, the fate of the northern aldehyde is less easily predicted. Lack of condensation with the nitrogen of the ethanolamine fragment is anticipated to lead to cyanohydrin **479**, while condensation will generate *bis*-aminonitrile **480**. Fortunately, these two species are expected to behave similarly, and therefore, either compound (or a mixture of the two) will be carried forward through the same series of transformations. In the next step, hydrogenolysis of the two benzyl ethers and treatment with hydrochloric acid will result in closure of the northern oxazolidine and

potential closure of the southern oxazolidine as well, furnishing either methyl-cyanocycline C (**481**) or methyl-bioxalomycin  $\alpha$ 2 (**482**).<sup>25</sup>

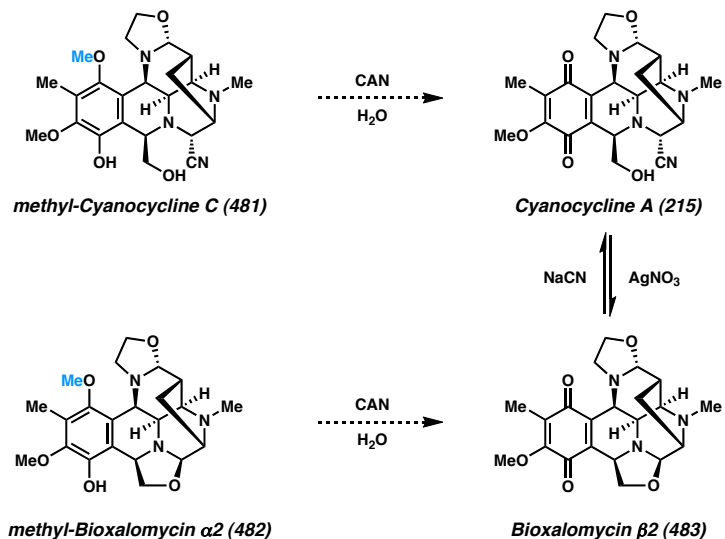
Scheme A4.11. Proposed advancement of benzylic amine **445**



In the final steps of the synthetic route, the monomethyl hydroquinone will be oxidized using ceric ammonium nitrate (CAN). Methyl-cyanocycline C (**481**) is expected to yield cyanocycline A (**215**) directly, while methyl-bioxalomycin  $\alpha$ 2 (**482**) will generate bioxalomycin  $\beta$ 2 (**483**). According to studies performed by the isolation chemists who first identified the bioxalomycins,<sup>26</sup> treatment of **483** with sodium cyanide is expected to open the oxazolidine to the amino nitrile to provide cyanocycline A (**215**). In full, our strategy is expected to furnish cyanocycline A in a total of 18–19 steps from

oxidopyrazinium iodide **387** depending on whether the route proceeds through methyl-cyanocycline C (**481**) or methyl-bioxalomycin  $\alpha$ 2 (**482**).

Scheme A4.12. Proposed completion of cyanocycline A



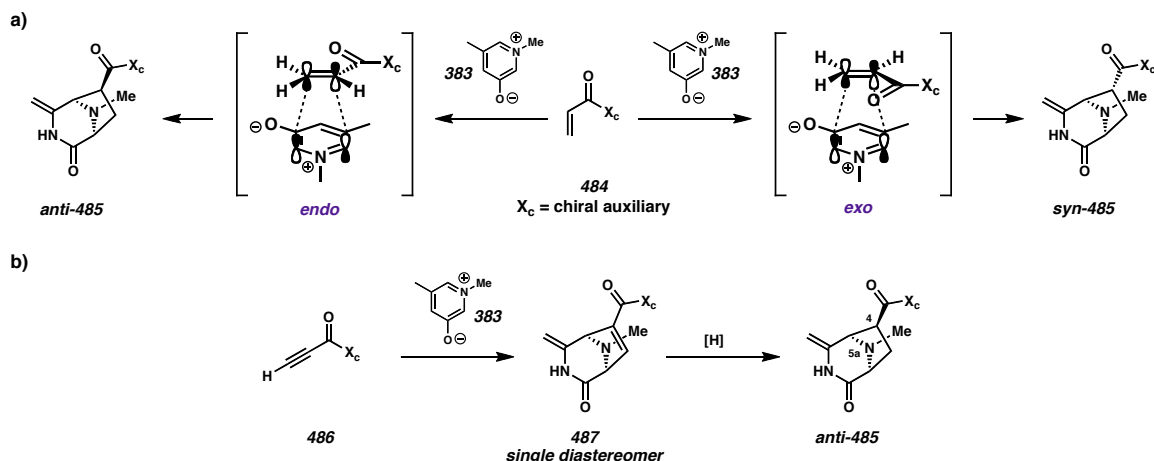
## A4.5 DESIGN OF NOVEL CHIRAL AUXILIARIES FOR A DIASTEREORESELECTIVE DIPOLAR CYCLOADDITION: APPLICATION TO THE ENANTIOSELECTIVE TOTAL SYNTHESIS OF (+)-CYANOCYCLINE A

### A4.5.1 *Introduction and Background*

Concurrent with our efforts toward a racemic total synthesis of cyanocycline A (**215**), we are exploring an enantioselective synthesis of the natural product derived from an auxiliary-controlled diastereoselective variant of the dipolar cycloaddition used to build the diazabicyclic core (e.g., **444**). While previous efforts have been made to impart asymmetry upon dipolar cycloadditions between chiral  $\alpha,\beta$ -unsaturated carbonyl compounds (**484**) and stabilized azomethine ylides (**383**),<sup>9,27,28</sup> to our knowledge, none has

succeeded in producing the anti relationship observed in cyanocycline A between N(5a) and substituents at C(29) in a single chemical step (Scheme A4.13a). This is most likely due to a preference for the less sterically congested exo transition state leading to the syn configuration (*syn*-485). To address this problem, we envisioned an asymmetric dipolar cycloaddition between betaine dipole **383** and chiral auxiliary-appended alkyne **486** to produce cycloadduct **487** as a single diastereomer. Hydrogenation of the olefin in a manner similar to the racemic route (c.f., **444** → *anti*-**382**) to produce the desired anti configuration (*anti*-**485**) in a two-step sequence (Scheme A4.13b).

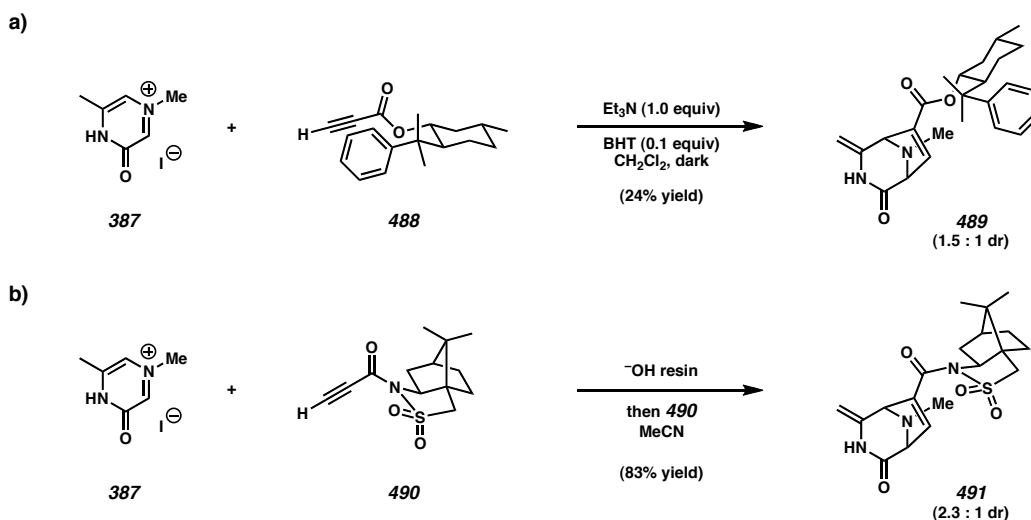
Scheme A4.13. a) 1,3-Dipolar cycloadditions between azomethine ylides and  $\alpha,\beta$ -unsaturated carbonyl compounds. b) Two-step approach to an anti cycloadduct.



With this goal in mind, the next challenge was the determination of a suitable auxiliary. Initial choices included acylated derivatives of 8-phenylmenthol<sup>29</sup> and Oppolzer's sultam<sup>30</sup> as potential candidates (Scheme A4.14). However, when the cycloaddition of oxidopyrazinium iodide **387** was carried out with the propargyl ester of 8-phenylmenthol (**488**), a nearly equivalent mixture of inseparable diastereomers (**489**)

was obtained in poor yield. Substituting ester **488** with the propargyl amide of Oppolzer's sultam (**490**) resulted in a greatly improved yield of the corresponding cycloadduct (**491**) in 2.3:1 dr. However, the diastereoselectivity remained far below the threshold for synthetic utility.

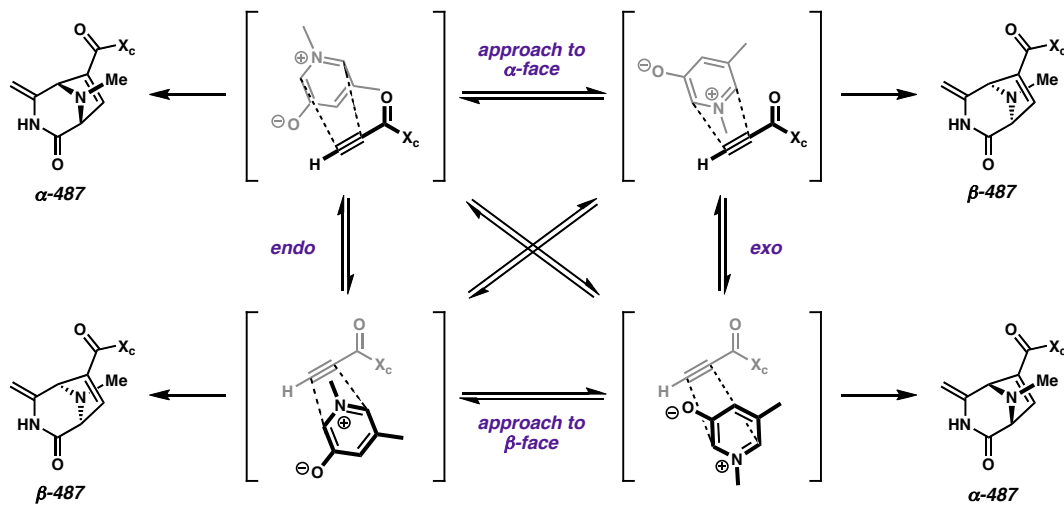
Scheme A4.14. a) Dipolar cycloaddition with propargyl ester **488**. b) Dipolar cycloaddition with propargyl amide **490**.



Our lack of success with these previously reported chiral auxiliaries led us to reevaluate the conformational requirements for effective stereochemical control. Given the rigid linear structure of the alkyne dipolarophile, it was assumed that any selectivity garnered from this reaction would originate from controlling the trajectory of the approaching dipole. Examination of the four possible relative configurations adopted by the dipole and dipolarophile during bond formation reveals that an effective auxiliary must be able to influence both the facial bias of the dipolarophile and the relative orientation of the dipole (Scheme A4.15). As was evident in the case of chiral alkynes

**488** and **490**, providing facial bias without controlling the position of the dipole results in poor diastereoselectivity.

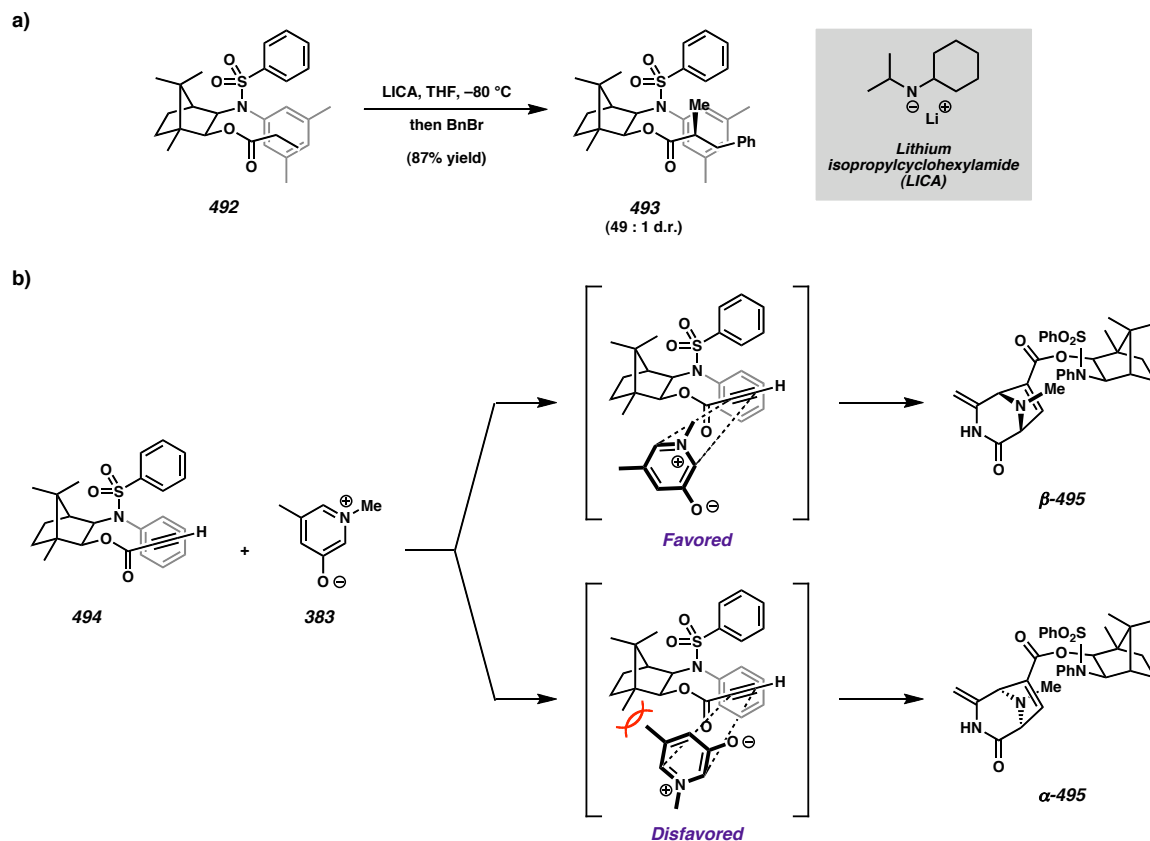
Scheme A4.15. Interplay of facial approach and dipole orientation in a dipolar cycloaddition



In 1983, Helmchen *et al.* reported the use of camphor-derived auxiliaries for the asymmetric alkylation of propionic esters (**492**) to provide  $\alpha$ -stereogenic products (**493**) in excellent diastereomeric ratios (Scheme A4.16a).<sup>31</sup> Facial control was exerted through the installation of a bulky aryl sulfonamide group on one face of the ester. We believed that these auxiliaries could be adapted to the dipolar cycloaddition when modified to bear alkyne esters (**494**) (Scheme A4.16b). In addition to providing facial bias, it was expected that interactions between the camphor bridgehead methyl group and the aryl methyl group of betaine **383** would force the dipole to adopt an exo orientation. It was noted this model would ultimately lead to cycloadduct **β-495** possessing the incorrect stereochemistry for application to cyanocycline A (**215**). However, it was our initial goal

to apply the model using the more readily available natural enantiomer of camphor before investigating this methodology in greater depth.

*Scheme A4.16. a) Asymmetric alkylation of propionic esters. b) Proposed asymmetric induction in the dipolar cycloaddition<sup>32</sup>*

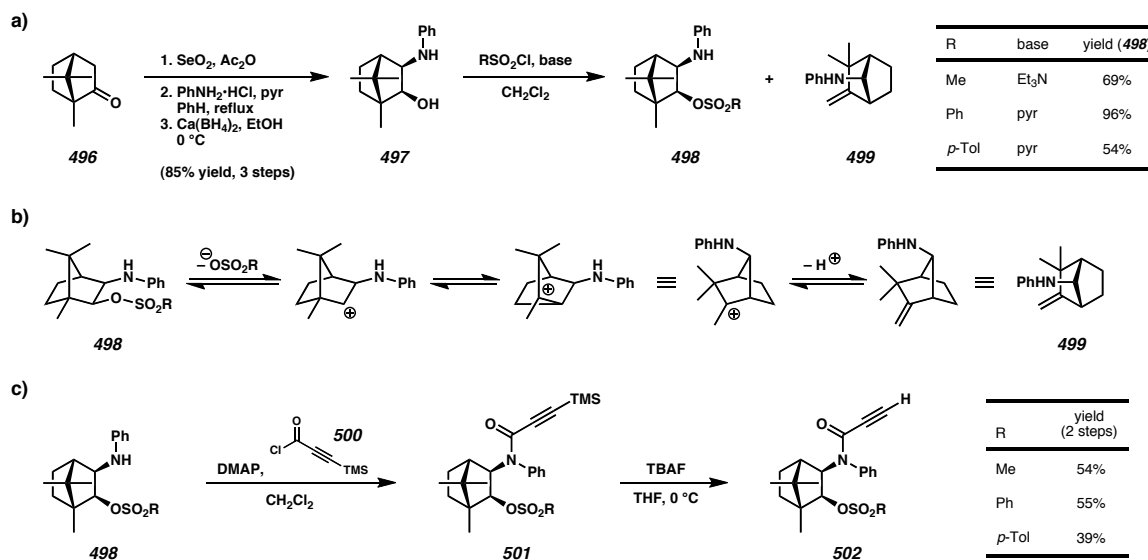


#### A4.5.2 Progress Toward an Auxiliary-Controlled Diastereoselective Dipolar Cycloaddition

Synthesis of the auxiliary began from commercially available (+)-camphor (**496**) and was advanced to amino alcohol **497** using known procedures (Scheme A4.17a).<sup>33</sup> It was expected that a small library of sulfonamides could be constructed by varying substitution

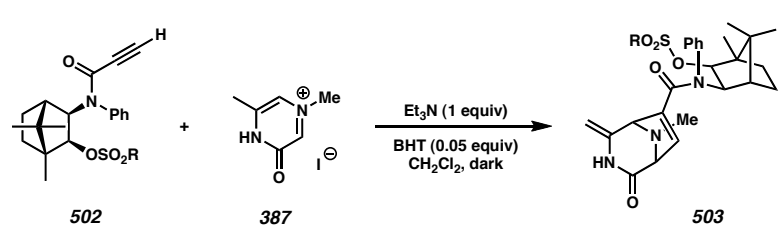
at the amine. However, treatment with a number of sulfonylating agents and acid scavengers only generated product mixtures favoring formation of the corresponding sulfonates (**498**). In addition, product yield was compromised by the formation of camphene amine **499**, believed to be the product of a non-classical cationic rearrangement following loss of the sulfonate (Scheme A4.17b). Due to the difficulty associated with determination of sulfonate versus sulfonamide formation, each product was acylated with 3-(trimethylsilyl)propioloyl chloride (**500**) and its identity was confirmed by the IR stretch of the carbonyl (Scheme A4.17c).<sup>34</sup> To our disappointment, the absorption at 1630–1640 cm<sup>−1</sup> confirmed that sulfonylation of amino alcohol **497** was indeed producing the sulfonate in favor of the sulfonamide, and subsequent acylation was therefore producing amide **501**. Though continued investigations may have produced a more reliable method for the selective functionalization of the amine, we decided instead to advance the product in hand one additional step to an alkynamide analogue of the original alkynoate target. Thus, desilylation of **501** with tetra-*n*-butylammonium fluoride produced alkynamide **502**.

Scheme A4.17. a) Synthesis of the auxiliary core. b) Non-classical cationic rearrangement. c) Completion of the propargyl amide.



Gratifyingly, when the cycloaddition was carried out with **502** according to previous conditions, it was found that cycloadduct **503** could be prepared in diastereomeric ratios as high as 10:1 (Table A4.1).<sup>35</sup> The temperature at which the reaction was performed was shown to have a significant effect upon both the yield and dr of the product. In addition, the methanesulfonate auxiliary proved effective over a range of temperatures while the phenylsulfonate reacted only at elevated temperatures. Unfortunately, the toluenesulfonate auxiliary never successfully reacted, indicating that selectivity and reactivity were likely dependent upon steric interactions between the auxiliary framework and the dipole.

Table A4.1. Dipolar cycloaddition using the sulfonate-alkynamide auxiliaries

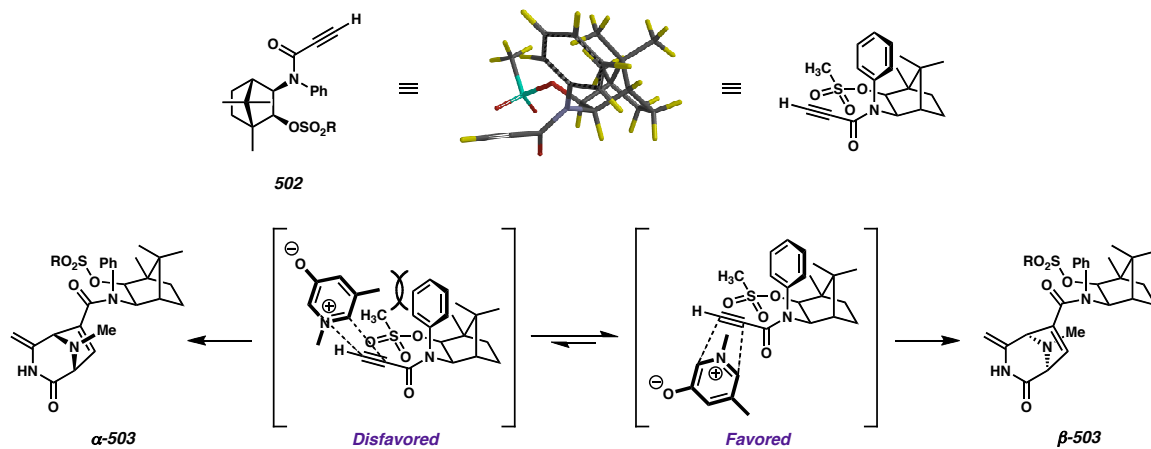


R	temp (°C)	yield	dr
Me	0	48%	10 : 1
Me	21	59%	6.4 : 1
Me	30	74%	6 : 1
Ph	30	17%	8 : 1
p-Tol	30	---	---

#### A4.5.3 A Second Generation Auxiliary

Having determined that the alkynamide auxiliary-controlled cycloaddition could indeed produce diastereomerically enriched products, it then became necessary to revise the previous selectivity model to accommodate the alkynamide analogues. In its lowest energy conformation,<sup>36</sup> the *N*-phenyl ring is expected to be rotated above the alkynamide and twisted out of conjugation with the amide  $\pi$ -system in order to avoid interactions with the bridging geminal methyl groups (Scheme A4.18). The sulfonate then blocks the back face of the alkynamide (methanesulfonate shown). Since the camphor bridgehead methyl group is no longer near the reaction center, the approach of dipole **383** is envisioned to be controlled by the *N*-phenyl ring. Positioning the dipole in an exo orientation places its aryl methyl group below the ortho substituent of the *N*-phenyl ring while the endo orientation places the methyl group in direct contact with the ring. Thus, it is believed that the cycloaddition occurs through an exo transition state to produce the diazabicycle corresponding to the stereochemistry present in cyanocycline A (**β-503**).

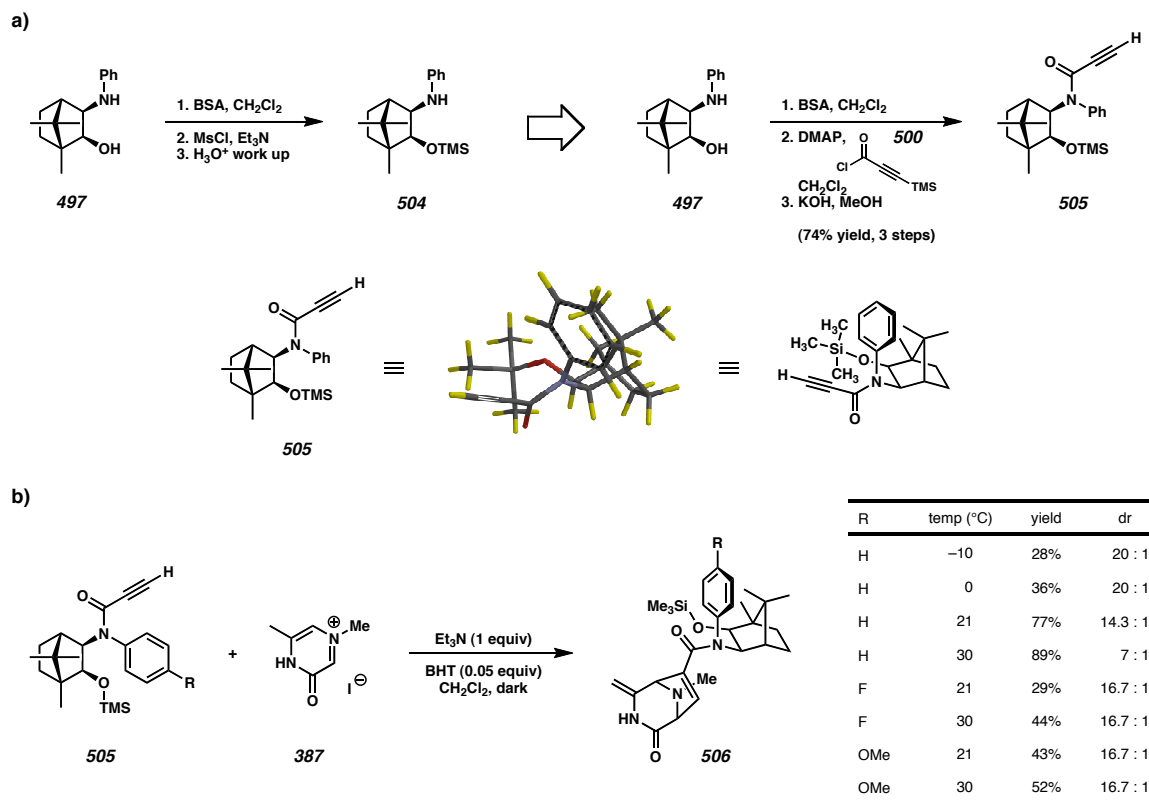
Scheme A4.18. Modified proposal for asymmetric induction in the dipolar cycloaddition



With an effective alkynamide auxiliary in hand, we turned our attention back to the sulfonamide-alkynoate auxiliaries in an effort to test our original model. In order to selectively sulfonylate the amine, a method was needed to temporarily mask the alcohol. It was expected that silylation of the alcohol followed by sulfonylation of the amine would generate an intermediate sulfonamide silyl ether that could be converted to the desired sulfonamide alcohol upon acidic work up. However, when this method was applied to amino alcohol **497** using *N,O*-bis(trimethylsilyl)acetamide followed by methanesulfonyl chloride and triethylamine, the only product isolated after acidic work up was silyl ether **504** (Scheme A4.19a). In fact, the silyl ether proved surprisingly stable toward treatment with tetra-*n*-butylammonium fluoride, producing only trace quantities of the amino alcohol (**497**). Because of this increased stability and its structural similarity to the previous auxiliary, the intermediate was advanced to alkynamide **505** and tested for competence as an auxiliary (Scheme A4.19b). To our delight, the new auxiliary proved superior to previous substrates in both yield and diastereoselectivity at all temperatures, producing cycloadduct **506** in diastereomeric ratios as high as 20:1. To

probe inductive effects in the *N*-aryl ring, substitution was introduced at the para position.<sup>37</sup> Interestingly, a general increase in diastereoselectivity was observed in the case of both electron donation and electron withdrawal, though both were accompanied by a general decrease in yield. This seems to indicate an increased steric effect with less influence directly attributable to resonance effects. However, further study is required before definitive conclusions may be drawn.

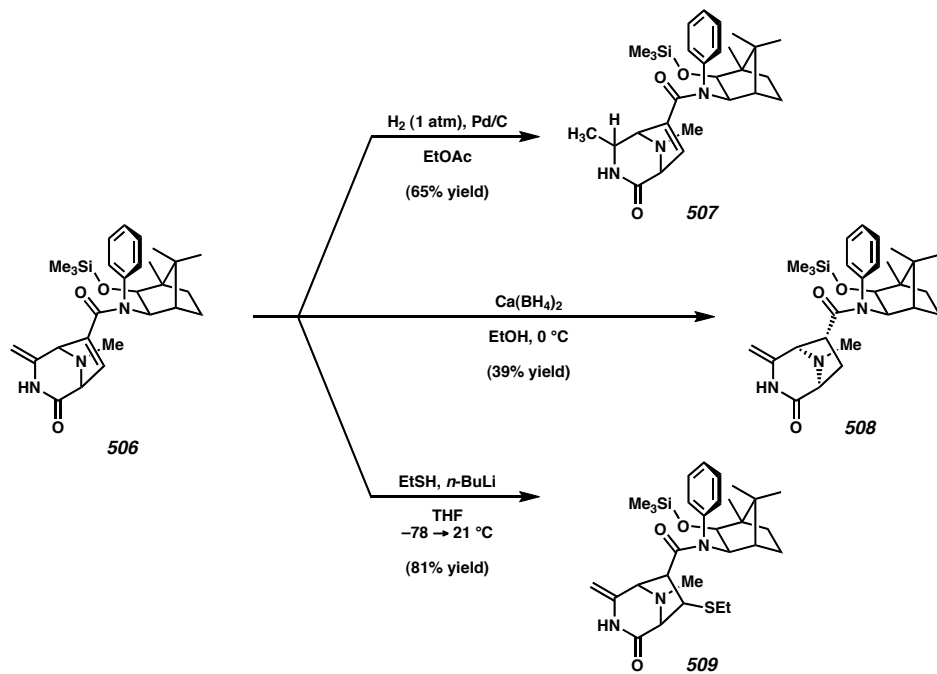
Scheme A4.19. a) Synthesis of the silyl ether auxiliary. b) Dipolar cycloaddition.



Following cycloaddition, reduction and cleavage of the auxiliary will provide an enantioenriched version of either ester **anti-382** or alcohol **445** to be integrated into the asymmetric synthesis of cyanocycline A (**215**). Attempts have been made to reduce the

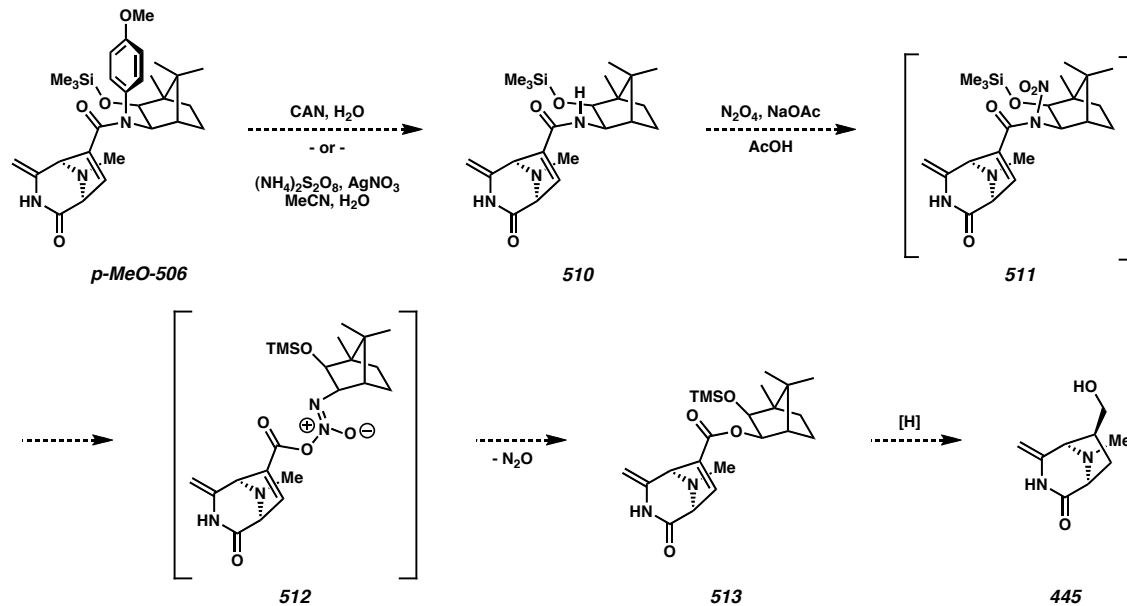
$\alpha,\beta$ -unsaturated amide prior to removal of the auxiliary (Scheme A4.20). In the case of unsubstituted auxiliary **506**, however, the majority of conditions result in either no reaction or decomposition of the starting material. Certain exceptions include catalytic hydrogenation, which results in selective reduction of the exocyclic olefin to generate **507**. Calcium borohydride displays a unique ability to reduce the  $\alpha,\beta$ -unsaturation, though it produces the undesired *syn*-diastereomer (**508**). In addition, efforts to cleave the auxiliary by hydride reduction, dissolving metal reduction, and imidate hydrolysis have failed to generate useful products. Interestingly, treatment of **506** with *n*-butyllithium and ethanethiol according to the procedure of Fukuyama<sup>38</sup> produced thioether **509** by conjugate addition of the thiolate to the  $\alpha,\beta$ -unsaturated amide.

Scheme A4.20. Attempts to advance the auxiliary-appended diazabicyclic



The difficulty encountered in auxiliary cleavage has led us to consider a two-step method beginning with removal of the *N*-aryl ring followed by reduction of the resulting secondary amide. The most likely candidate for this process is the *N*-(*p*-methoxyphenyl) ring, which is expected to be cleaved under oxidative conditions. Treatment of **p-MeO-506** with CAN or milder reagents<sup>39</sup> is expected to generate secondary amide **510**, which will be converted to ester **513** via *N*-nitro amide **511** and rearrangement to zwitterion **512** following exposure to dinitrogen tetroxide (Scheme A4.21). Reduction of the ester will then provide enantioenriched alcohol **445**, which may be advanced to cyanocycline A (**215**).

Scheme A4.21. Proposal for the removal of the amide auxiliary



#### A4.6 CONCLUSION

Our efforts toward the total synthesis of cyanocycline A have yielded a number of interesting results. A [3 + 2] cycloaddition between an oxidopyrazinium dipole and

methyl propiolate generates an unsaturated diazabicycle, which we have been able to advance to both silyl ether- and oxazolidine-containing intermediates bearing the desired stereochemistry at C(29). Carrying either of these forward to an iodoenamine, and subsequently coupling this compound with a functionalized aryl stannane furnishes one of two styrenes containing three of the six rings of the natural product. Attempts to install a benzylic oxazolidine via oxidative amination have proceeded in low yield, generating small amounts of a benzylic ketone as well. An alternative approach to the formation of the benzylic ketone employs an addition of an aryllithium species to a diazabicyclic aldehyde, followed by oxidation of the resulting benzylic alcohol. This approach has generated the ketone in reasonable yield and efforts are underway to install the ethanolamine fragment through reduction amination. Investigations toward a Petasis three-component coupling reaction to form the benzylic amine in a single step are being pursued. Completion of cyanocycline A from this key intermediate is expected to require 10–11 additional steps. Finally, examination of the alkyne dipolar cycloaddition used to form the diazabicyclic portion of the natural product has led to a model for asymmetric induction during bond formation. Application of this model to the synthesis of novel chiral auxiliaries for the control of diastereoselectivity has produced a small library of camphor-derived structures capable of achieving diastereomeric product ratios as high as 20:1. Efforts are currently underway to carry out the removal of these auxiliaries and integrate the enantioenriched diazabicyclic product into the asymmetric synthesis of (+)-cyanocycline A.

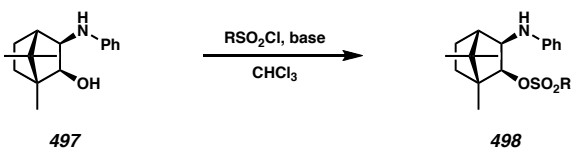
## A4.7 EXPERIMENTAL SECTION

### A4.7.1 Materials and Methods

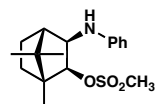
Unless otherwise stated, reactions were performed at ambient temperature (typically 20 to 23 °C) in flame-dried glassware under a nitrogen or argon atmosphere using dry, deoxygenated solvents. Solvents were dried by passage through an activated alumina column under argon. Brine solutions are saturated aqueous sodium chloride solutions. All commercially obtained reagents were used as received. Reaction temperatures were controlled by an IKAmag temperature modulator. Thin-layer chromatography (TLC) was performed using E. Merck silica gel 60 F254 pre-coated plates (0.25 mm) and visualized by UV, anisaldehyde, permanganate, or CAM staining. ICN silica gel (particle size 0.032–0.063 mm) was used for flash chromatography.  $^1\text{H}$  and  $^{13}\text{C}$  NMR spectra were recorded on a Varian Mercury 300 (at 300 MHz and 75 MHz respectively) spectrometer and are reported relative to  $\text{Me}_4\text{Si}$  ( $\delta$  0.0). Data for  $^1\text{H}$  NMR spectra are reported as follows: chemical shift ( $\delta$  ppm), multiplicity, coupling constant (Hz), and integration. Data for  $^{13}\text{C}$  NMR spectra are reported in terms of chemical shift. IR spectra were recorded on a Perkin Elmer Paragon 1000 spectrometer and are reported in frequency of absorption ( $\text{cm}^{-1}$ ). High-resolution mass spectra were obtained from the Caltech Mass Spectral Facility.

### A4.7.2 Preparative Procedures and Spectroscopic Data

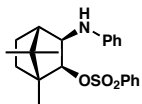
#### A4.7.2.1 General Method for the Preparation of Amino Sulfonates



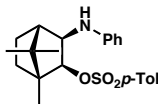
To a solution of **497** (100.0 mg, 0.408 mmol) in chloroform (2.0 mL) was added alkyl or aryl sulfonyl chloride (1.22 mmol) and triethylamine (123.4 mg, 1.22 mmol) or pyridine (96.5 mg, 1.22 mmol). After 5 h, the reaction mixture was diluted with saturated aqueous ammonium chloride (2 mL) and extracted into chloroform (25 mL x 2). The combined organics were washed with 0.1 N HCl (10 mL), brine (25 mL), dried over  $\text{Na}_2\text{SO}_4$ , concentrated, and purified via flash chromatography over silica gel (2:98  $\rightarrow$  15:85 EtOAc/hexanes) to yield **498**.



(69% yield):  $R_f$  = 0.34 (15:85 EtOAc/hexanes);  $^1\text{H}$  NMR (300 MHz,  $\text{CDCl}_3$ )  $\delta$  7.18 (t,  $J$  = 7.5 Hz, 2H), 6.70 (t,  $J$  = 7.5 Hz, 1H), 6.58 (d,  $J$  = 7.8 Hz, 2H), 4.78 (d,  $J$  = 7.8, 1H), 3.68 (d,  $J$  = 7.8, 1H), 2.78 (s, 3H), 1.91 (d,  $J$  = 4.2, 1H), 1.78–1.61 (m, 2H), 1.30–1.18 (comp m, 3H), 1.12 (s, 3H), 1.04 (s, 3H), 0.86 (s, 3H);  $^{13}\text{C}$  NMR (75 MHz,  $\text{CDCl}_3$ )  $\delta$  148.1, 129.3, 118.2, 113.6, 80.1, 63.8, 51.0, 49.3, 46.9, 33.1, 26.6, 21.8, 21.2, 11.4; IR (NaCl/thin film) 3334 br, 2953, 2865, 2854, 1590, 1426, 1118, 937, 868  $\text{cm}^{-1}$ ; HRMS (FAB+) calc'd for  $[\text{C}_{17}\text{H}_{25}\text{NO}_3\text{S}+\text{H}]^+$ :  $m/z$  324.1633, found 325.0853.



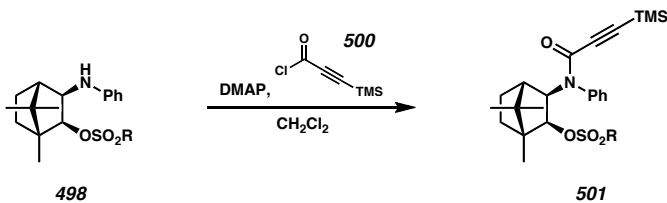
(96% yield):  $R_f = 0.21$  (10:90 EtOAc/hexanes);  $^1\text{H}$  NMR (300 MHz,  $\text{CDCl}_3$ )  $\delta$  7.92 (d,  $J = 7.2$  Hz, 2H), 7.69–7.51 (comp m, 4H), 7.44 (t,  $J = 7.2$  Hz, 2H), 6.67 (d,  $J = 7.7$  Hz, 2H), 3.99 (dd,  $J = 6.0, 3.0$  Hz, 1H), 3.74 (d,  $J = 2.7$  Hz, 1H), 3.61 (d,  $J = 6.0$  Hz, 1H), 1.69 (comp m, 3H), 1.26–1.11 (m, 2H), 0.99 (s, 3H), 0.95 (s, 3H), 0.56 (s, 3H);  $^{13}\text{C}$  NMR (75 MHz,  $\text{CDCl}_3$ )  $\delta$  139.1, 136.2, 135.4, 133.7, 133.2, 129.2, 128.8, 128.5, 128.2, 127.8, 82.5, 69.1, 67.1, 49.8, 49.0, 46.9, 33.1, 27.8, 21.7, 21.0, 14.7, 11.8; IR (NaCl/thin film) 3367 br, 2947, 2880, 1574, 1454, 1130, 940, 888  $\text{cm}^{-1}$ ; HRMS (FAB+) calc'd for  $[\text{C}_{22}\text{H}_{28}\text{NO}_3\text{S}+\text{H}]^+$ :  $m/z$  386.1790, found 386.1808.



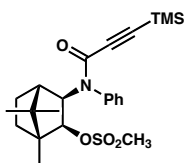
(54% yield):  $R_f = 0.42$  (15:85 EtOAc/hexanes);  $^1\text{H}$  NMR (300 MHz,  $\text{CDCl}_3$ )  $\delta$  7.79 (d,  $J = 7.2$  Hz, 2H), 7.34 (d,  $J = 7.2$  Hz, 2H), 7.22 (d,  $J = 7.5$  Hz, 2H), 6.99 (t,  $J = 7.5$  Hz, 1H), 6.82 (d,  $J = 7.6$  Hz, 2H), 3.97 (d,  $J = 6.6$  Hz, 1H), 3.79 (br s, 1H), 3.58 (d,  $J = 6.6$  Hz, 1H), 2.43 (s, 3H), 1.67–1.42 (comp m, 3H), 1.30–1.12 (comp m, 3H), 0.99 (s, 3H), 0.95 (s, 3H), 0.56 (s, 3H);  $^{13}\text{C}$  NMR (75 MHz,  $\text{CDCl}_3$ )  $\delta$  144.1, 139.2, 132.4, 129.1, 128.1, 82.5, 69.1, 49.8, 49.0, 46.9, 33.1, 27.9, 21.7, 21.0, 11.9; IR (NaCl/thin film) 3328 br, 2930, 2878, 1565, 1555, 1460, 1140, 920, 903  $\text{cm}^{-1}$ ; LRMS (APCI) calc'd for  $[\text{C}_{23}\text{H}_{29}\text{NO}_3\text{S}+\text{H}]^+$ :  $m/z$  400.2, found 400.3.

#### A4.7.2.2 General Method for the Preparation of Silyl Propargyl Amide

##### Sulfonates

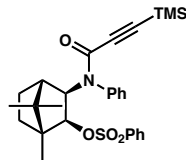


To a solution of 3-trimethylsilylpropionic acid (73.1 mg, 0.501 mmol) and dimethylformamide (2.6  $\mu$ L, 33.4  $\mu$ mol) in dichloromethane (0.84 mL) was added oxalyl chloride (45.2  $\mu$ L, 0.518 mmol) (caution: gas evolution). After 20 min, a solution of 4-dimethylaminopyridine (40.8 mg, 0.334 mmol) and **498** (0.167 mmol) in dichloromethane (0.84 mL) was added dropwise over 1 min. After an additional 30 min, the reaction mixture was diluted with dichloromethane (25 mL) and washed with saturated aqueous  $\text{NH}_4\text{Cl}$  (2 x 25 mL) followed by brine (25 mL). The organics were dried over  $\text{Na}_2\text{SO}_4$ , concentrated, and purified via flash chromatography over silica gel (5:95  $\rightarrow$  25:75 ethyl acetate:hexanes) to yield **501**.

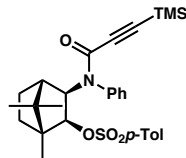


(66% yield):  $R_f$  = 0.18 (15:85 EtOAc/hexanes);  $^1\text{H}$  NMR (300 MHz,  $\text{CDCl}_3$ )  $\delta$  7.48–7.32 (comp m, 4H), 7.13 (br s, 1H), 4.93 (d,  $J$  = 7.5 Hz, 1H), 4.51 (d,  $J$  = 7.2 Hz, 1H), 3.10 (s, 3H), 2.02 (d,  $J$  = 4.2 Hz, 1H), 1.82–1.70 (m, 1H), 1.57 (app td,  $J$  = 13.5, 2.4 Hz, 1H), 1.44–1.18 (m, 2H), 1.03 (s, 3H), 0.65 (s, 3H), 0.58 (s, 3H), -0.07 (s, 9H);  $^{13}\text{C}$  NMR (75 MHz,  $\text{CDCl}_3$ )  $\delta$  182.1, 155.7, 140.2, 133.4, 130.5, 128.7, 96.7, 90.1, 65.1, 50.2, 47.9,

47.0, 39.4, 32.1, 28.6, 21.6, 21.5, 12.4, -0.8; IR (NaCl/thin film) 2960, 2873, 1632, 1586, 1495, 1347, 1174, 957, 852  $\text{cm}^{-1}$ ; HRMS (FAB+) calc'd for  $[\text{C}_{23}\text{H}_{33}\text{NO}_4\text{SSi}+\text{H}]^+$ :  $m/z$  448.1978, found 448.1954.



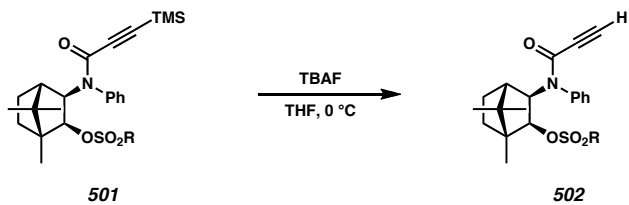
(65% yield):  $R_f$  = 0.32 (15:85 EtOAc/hexanes);  $^1\text{H}$  NMR (300 MHz,  $\text{CDCl}_3$ )  $\delta$  7.91 (d,  $J$  = 7.2 Hz, 2H), 7.68–7.48 (comp m, 4H), 7.37 (t,  $J$  = 7.2 Hz, 2H), 6.67 (d,  $J$  = 7.7 Hz, 2H), 5.24 (d,  $J$  = 7.2 Hz, 1H), 3.94 (d,  $J$  = 7.2 Hz, 1H), 2.05 (d,  $J$  = 4.2, 1H), 1.78–1.64 (comp m, 2H), 1.62–1.50 (m, 2H), 0.87 (s, 3H), 0.83 (s, 3H), 0.62 (s, 3H), 0.25 (s, 9H);  $^{13}\text{C}$  NMR (75 MHz,  $\text{CDCl}_3$ )  $\delta$  176.2, 156.6, 145.2, 144.3, 142.1, 140.0, 136.5, 135.5, 133.2, 130.5, 99.9, 93.1, 66.7, 52.2, 47.8, 45.5, 32.3, 28.5, 22.2, 22.0, 12.2, 0.2; IR (NaCl/thin film) 2986, 2964, 2873, 2848, 1638, 1567, 1500, 1212, 978  $\text{cm}^{-1}$ ; HRMS (FAB+) calc'd for  $[\text{C}_{28}\text{H}_{35}\text{NO}_4\text{SSi}+\text{H}]^+$ :  $m/z$  510.2134, found 510.2158.



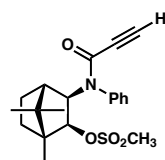
(49% yield):  $R_f$  = 0.36 (15:85 EtOAc/hexanes);  $^1\text{H}$  NMR (300 MHz,  $\text{CDCl}_3$ )  $\delta$  7.81 (d,  $J$  = 7.2 Hz, 2H), 7.30–7.18 (comp m, 4H), 7.05 (t,  $J$  = 7.5 Hz, 1H), 6.82 (d,  $J$  = 7.6 Hz, 2H), 5.18 (d,  $J$  = 6.9 Hz, 1H), 3.88 (d,  $J$  = 6.8 Hz, 1H), 2.51 (s, 3H), 2.08 (d,  $J$  = 4.2 Hz, 1H), 1.67–1.42 (comp m, 2H), 1.30–1.12 (comp m, 3H), 1.04 (s, 3H), 0.88 (s, 3H), 0.56 (s, 3H), 0.22 (s, 9H);  $^{13}\text{C}$  NMR (75 MHz,  $\text{CDCl}_3$ )  $\delta$  176.4, 156.7, 145.8, 144.8, 141.0,

139.5, 136.2, 135.5, 133.0, 130.6, 99.2, 92.8, 66.7, 52.6, 48.0, 45.1, 37.5, 32.3, 28.6, 22.1, 22.0, 12.1, 0.4; IR (NaCl/thin film) 2953, 2856, 1637, 1566, 1540, 1468, 1123, 989  $\text{cm}^{-1}$ ; HRMS (FAB+) calc'd for  $[\text{C}_{29}\text{H}_{37}\text{NO}_4\text{SSi}+\text{H}]^+$ :  $m/z$  524.2291, found 524.2267.

#### A4.7.2.3 General Method for the Preparation of Propargyl Amide Sulfonates

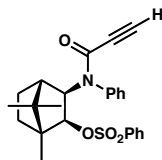


To a 0 °C solution of **501** (0.140 mmol) in tetrahydrofuran (1.4 mL) was added tetra-*n*-butylammonium fluoride (61  $\mu\text{L}$ , 0.210 mmol). After 1 h, the reaction mixture was diluted with diethyl ether (10 mL) and washed with saturated aqueous ammonium chloride (2 x 10 mL) followed by brine (10 mL). The organics were dried over sodium sulfate, concentrated, and purified via flash chromatography over silica gel (4:96  $\rightarrow$  15:85 EtOAc/hexanes) to yield **502**.

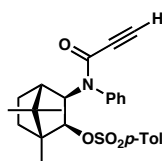


(82% yield):  $R_f$  = 0.24 (20:80 EtOAc/hexanes);  $^1\text{H}$  NMR (300 MHz,  $\text{CDCl}_3$ )  $\delta$  7.48–7.34 (comp m, 4H), 7.15 (br s, 1H), 4.97 (d,  $J$  = 7.2 Hz, 1H), 4.51 (d,  $J$  = 7.5 Hz, 1H), 3.11 (s, 3H), 2.80 (s, 1H), 2.01 (d,  $J$  = 4.2 Hz, 1H), 1.82–1.70 (m, 1H), 1.65–1.52 (m, 1H), 1.42–1.18 (m, 2H), 1.03 (s, 3H), 0.65 (s, 3H), 0.57 (s, 3H);  $^{13}\text{C}$  NMR (75 MHz,  $\text{CDCl}_3$ )  $\delta$  182.0, 155.6, 140.2, 133.4, 128.3, 128.0, 90.2, 86.4, 65.1, 50.2, 47.9, 47.0, 39.3, 32.4,

28.7, 21.6, 21.4, 12.2; IR (NaCl/thin film) 2960, 2876, 1638, 1584, 1490, 1348, 1204, 960  $\text{cm}^{-1}$ ; HRMS (FAB+) calc'd for  $[\text{C}_{20}\text{H}_{25}\text{NO}_4\text{S}+\text{H}]^+$ :  $m/z$  376.1583, found 376.1602.



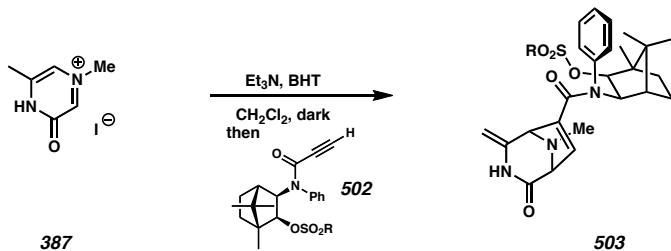
(85% yield):  $R_f = 0.20$  (20:80 EtOAc/hexanes);  $^1\text{H}$  NMR (300 MHz,  $\text{CDCl}_3$ )  $\delta$  7.91 (d,  $J = 7.2$  Hz, 2H), 7.66–7.44 (comp m, 4H), 7.37 (t,  $J = 7.2$  Hz, 2H), 6.55 (d,  $J = 7.6$  Hz, 2H), 5.24 (d,  $J = 7.2$  Hz, 1H), 3.94 (d,  $J = 7.2$  Hz, 1H), 2.27 (s, 1H), 2.03 (d,  $J = 4.3$  Hz, 1H), 1.78–1.58 (comp m, 2H), 1.18–1.14 (m, 2H), 0.88 (s, 3H), 0.83 (s, 3H), 0.62 (s, 3H);  $^{13}\text{C}$  NMR (75 MHz,  $\text{CDCl}_3$ )  $\delta$  176.0, 156.5, 145.3, 144.2, 142.6, 140.4, 136.4, 135.8, 133.3, 130.4, 91.2, 88.8, 66.5, 52.1, 47.8, 45.5, 32.2, 28.4, 22.1, 22.0, 12.3; IR (NaCl/thin film) 2990, 2970, 2868, 1639, 1568, 1523, 1210, 855  $\text{cm}^{-1}$ ; HRMS (FAB+) calc'd for  $[\text{C}_{25}\text{H}_{27}\text{NO}_4\text{S}+\text{H}]^+$ :  $m/z$  438.1739, found 438.1752.



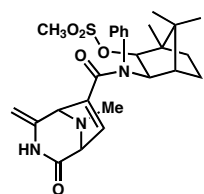
(80% yield):  $R_f = 0.30$  (20:80 EtOAc/hexanes);  $^1\text{H}$  NMR (300 MHz,  $\text{CDCl}_3$ )  $\delta$  7.73 (d,  $J = 7.2$  Hz, 2H), 7.30–7.12 (comp m, 5H), 6.78 (d,  $J = 7.5$  Hz, 2H), 5.14 (d,  $J = 7.0$  Hz, 1H), 3.70 (d,  $J = 6.8$  Hz, 1H), 2.47 (s, 3H), 2.24 (s, 1H), 2.08 (d,  $J = 4.2$  Hz, 1H), 1.71–1.44 (comp m, 3H), 1.24–1.14 (comp m, 2H), 1.02 (s, 3H), 0.88 (s, 3H), 0.56 (s, 3H);  $^{13}\text{C}$  NMR (75 MHz,  $\text{CDCl}_3$ )  $\delta$  178.0, 156.6, 145.4, 144.6, 141.4, 139.5, 136.5, 135.7, 133.6, 131.1, 92.4, 88.9, 66.7, 52.6, 48.4, 45.2, 37.6, 32.3, 28.6, 22.4, 22.3, 12.2; IR

(NaCl/thin film) 2960, 2848, 1638, 1566, 1532, 1468, 1218, 867  $\text{cm}^{-1}$ ; HRMS (FAB+) calc'd for  $[\text{C}_{26}\text{H}_{29}\text{NO}_4\text{S}+\text{H}]^+$ :  $m/z$  452.1896, found 452.1868.

#### A4.7.2.4 General Method for the Preparation of Amide Sulfonate Cycloadducts

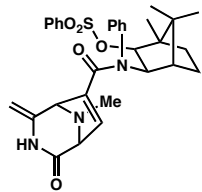


To a 0  $^{\circ}\text{C}$  suspension of oxidopyrazinium iodide **387** (40.4 mg, 0.160 mmol) and 2,6-di-*tert*-butyl-4-methylphenol (7.7 mg, 35  $\mu\text{mol}$ ) in dichloromethane (1 mL) was added triethylamine (21  $\mu\text{L}$ , 0.151 mmol). After 20 min, a solution of **502** (0.477 mmol) in dichloromethane (1 mL) was added. After an additional 24 h, the reaction mixture was diluted with dichloromethane (20 mL) and washed with saturated aqueous ammonium chloride (2 x 20 mL) followed by brine (20 mL). The organics were dried over sodium sulfate, concentrated, and purified via flash chromatography over silica gel (50:50  $\rightarrow$  100:0 EtOAc/hexanes) to yield **503**.



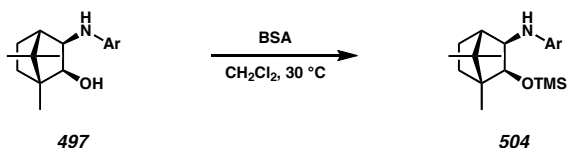
(48% yield, 10:1 dr):  $R_f = 0.11$  (75:25 EtOAc:hexanes);  $^1\text{H}$  NMR (300 MHz,  $\text{CDCl}_3$ )  $\delta$  7.42–7.33 (comp m, 4H), 7.25 (br s, 1H), 6.73 (br s, 1H), 5.48 (d,  $J = 2.4$  Hz, 1H), 4.98 (d,  $J = 7.5$  Hz, 1H), 4.51 (d,  $J = 7.2$  Hz, 1H), 4.34 (d,  $J = 1.2$  Hz, 1H), 4.22 (d,  $J = 1.2$  Hz,

1H), 4.04 (s, 1H), 3.65 (s, 1H), 2.97 (s, 3H), 2.15 (s, 3H), 1.98 (d,  $J$  = 4.2 Hz, 1H), 1.82–1.50 (comp m, 5H), 1.02 (s, 3H), 0.66 (s, 3H), 0.58 (s, 3H);  $^{13}\text{C}$  NMR (75 MHz,  $\text{CDCl}_3$ )  $\delta$  191.9, 168.6, 162.9, 140.9, 134.7, 128.8, 128.0, 124.1, 113.0, 90.4, 66.3, 53.4, 50.1, 47.7, 47.1, 39.4, 34.9, 31.9, 30.6, 28.4, 21.5, 21.3, 12.4; IR (NaCl/thin film) 3442, 2961, 1686, 1591, 1493, 1347, 1173, 954, 879  $\text{cm}^{-1}$ ; HRMS (FAB+) calc'd for  $[\text{C}_{26}\text{H}_{33}\text{N}_3\text{O}_5\text{S}+\text{H}]^+$ :  $m/z$  500.2219, found 500.2224.

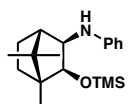


Reaction performed at 30 °C (17% yield, 8:1 dr):  $R_f$  = 0.25 (75:25 EtOAc/hexanes);  $^1\text{H}$  NMR (300 MHz,  $\text{CDCl}_3$ )  $\delta$  7.75–7.34 (comp m, 10H), 6.97 (br s, 1H), 5.63 (d,  $J$  = 2.4 Hz, 1H), 5.54 (d,  $J$  = 7.2 Hz, 1H), 4.75 (br s, 1H), 4.68 (s, 1H), 4.44 (d,  $J$  = 1.2 Hz, 1H), 4.34 (d,  $J$  = 1.2 Hz, 1H), 3.94 (d,  $J$  = 7.2 Hz, 1H), 2.17 (s, 3H), 2.04 (d,  $J$  = 4.3 Hz, 1H), 1.78–1.42 (comp m, 4H), 0.88 (s, 3H), 0.83 (s, 3H), 0.62 (s, 3H);  $^{13}\text{C}$  NMR (75 MHz,  $\text{CDCl}_3$ )  $\delta$  192.0, 169.8, 162.4, 146.3, 144.2, 140.2, 136.6, 132.5, 129.0, 127.7, 126.5, 115.1, 92.1, 66.5, 58.1, 55.8, 50.2, 46.9, 39.6, 34.7, 33.9, 33.3, 29.4, 21.7, 21.0, 14.7; IR (NaCl/thin film) 3420, 2958, 2843, 1685, 1586, 1498, 1353, 1172, 960  $\text{cm}^{-1}$ ; HRMS (FAB+) calc'd for  $[\text{C}_{31}\text{H}_{35}\text{N}_3\text{O}_5\text{S}+\text{H}]^+$ :  $m/z$  562.2376, found 562.2345.

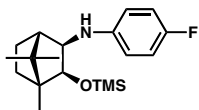
#### A4.7.2.5 General Method for the Preparation of Amino Silyl Ethers



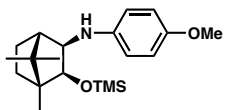
To a 30 °C solution of **497** (4.10 mmol) in dichloromethane (10.2 mL) was added *N,O*-bis(trimethylsilyl)acetamide (4.05 mL, 16.4 mmol). After 15 h, additional *N,O*-bis(trimethylsilyl)acetamide (1.01 mL, 4.09 mmol) was added. After an additional 6 h, the reaction mixture was concentrated and purified via flash chromatography over silica gel (4:96 → 10:90 EtOAc/hexanes) to yield **504**.



(91% yield):  $R_f = 0.77$  (15:85 EtOAc/hexanes);  $^1\text{H}$  NMR (300 MHz,  $\text{CDCl}_3$ )  $\delta$  7.17 (t,  $J = 7.2$  Hz, 2H), 6.64 (t,  $J = 7.2$  Hz, 1H), 6.51 (d,  $J = 7.5$  Hz, 2H), 4.57 (br s, 1H), 3.81 (d,  $J = 7.5$  Hz, 1H), 3.29 (d,  $J = 7.8$  Hz, 1H), 1.87 (d,  $J = 4.2$  Hz, 1H), 1.80–1.66 (m, 1H), 1.55 (td,  $J = 12.0, 3.3$ , 1H), 1.22–1.00 (comp m, 2H), 1.07 (s, 3H), 0.89 (s, 3H), 0.79 (s, 3H), 0.14 (s, 9H);  $^{13}\text{C}$  NMR (75 MHz,  $\text{CDCl}_3$ )  $\delta$  147.6, 126.5, 117.3, 115.1, 78.6, 58.7, 56.6, 48.9, 47.7, 32.5, 26.5, 22.0, 21.3, 11.4, 2.1; IR (NaCl/thin film) 3437 br, 3049, 2951, 2883, 1602, 1504, 1427, 1323, 1250, 1075, 910, 845  $\text{cm}^{-1}$ ; HRMS (FAB+) calc'd for  $[\text{C}_{19}\text{H}_{31}\text{NOSi}+\text{H}]^+$ :  $m/z$  318.2253, found 318.2274.

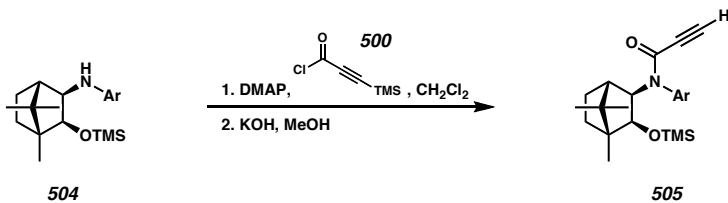


(86% yield):  $R_f = 0.68$  (15:85 EtOAc/hexanes);  $^1\text{H}$  NMR (300 MHz,  $\text{CDCl}_3$ )  $\delta$  6.88 (t,  $J = 8.7$  Hz, 2H), 6.41 (dd,  $J = 6.8, 4.5$  Hz, 2H), 4.46 (br s, 1H), 3.80 (d,  $J = 8.1$ , 1H), 3.23 (d,  $J = 7.8$  Hz, 1H), 1.83 (d,  $J = 4.2$  Hz, 1H), 1.80–1.67 (m, 1H), 1.55 (app td,  $J = 12.0, 3.0$  Hz, 1H), 1.20–1.00 (comp m, 2H), 1.06 (s, 3H), 0.89 (s, 3H), 0.79 (s, 3H), 0.14 (s, 9H);  $^{13}\text{C}$  NMR (75 MHz,  $\text{CDCl}_3$ )  $\delta$  156.3, 144.2, 118.3, 117.9, 79.0, 59.3, 56.9, 48.8, 47.5, 32.6, 26.8, 22.4, 22.2, 11.6, 3.0; IR (NaCl/thin film) 3475 br, 3061, 2967, 2884, 1589, 1500, 1350, 1252, 1105, 947  $\text{cm}^{-1}$ ; HRMS (FAB+) calc'd for  $[\text{C}_{19}\text{H}_{30}\text{FNOSi}+\text{H}]^+$ :  $m/z$  336.2159, found 336.2143.



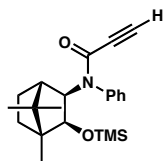
(88% yield):  $R_f = 0.55$  (15:85 EtOAc/hexanes);  $^1\text{H}$  NMR (300 MHz,  $\text{CDCl}_3$ )  $\delta$  7.26–7.24 (m, 2H), 6.85–6.78 (m, 2H), 4.24 (d,  $J = 6.3$  Hz, 1H), 3.98 (d,  $J = 6.4$  Hz, 1H), 2.75, 1.90 (d,  $J = 4.2$  Hz, 1H), 1.74–1.68 (m, 1H), 1.43–1.30 (m, 1H), 1.26–1.12 (comp m, 2H), 0.80 (s, 3H), 0.59 (s, 3H), 0.54 (s, 3H), 0.19 (s, 9H);  $^{13}\text{C}$  NMR (75 MHz,  $\text{CDCl}_3$ )  $\delta$  152.1, 140.3, 115.4, 114.9, 78.7, 58.9, 57.0, 56.5, 49.0, 48.6, 47.7, 32.0, 26.7, 22.4, 22.3, 11.5, 1.9; IR (NaCl/thin film) 3420 br, 3042, 2950, 1599, 1488, 1324, 1278, 1111  $\text{cm}^{-1}$ ; HRMS (FAB+) calc'd for  $[\text{C}_{20}\text{H}_{53}\text{NO}_2\text{Si}+\text{H}]^+$ :  $m/z$  347.2281, found 347.2235.

#### A4.7.2.6 General Method for the Preparation of Propargyl Amide Silyl Ethers

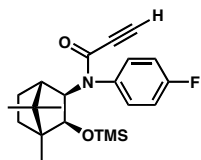


To a solution of 3-trimethylsilylpropionic acid (247.3 mg, 1.74 mmol) and dimethylformamide (16  $\mu$ L, 207  $\mu$ mol) in dichloromethane (1.6 mL) was added oxalyl chloride (0.156 mL, 1.79 mmol) (caution: gas evolution). After 20 min, a solution of 4-dimethylaminopyridine (147.4 mg, 1.21 mmol) and **504** (480 mmol) in dichloromethane (1.6 mL) was added dropwise over 1 min. After an additional 30 min, the reaction mixture was diluted with dichloromethane (25 mL) and washed with saturated aqueous ammonium chloride (2 x 25 mL) followed by brine (25 mL). The organics were dried over sodium sulfate, concentrated, and purified via flash chromatography over silica gel (4:96 EtOAc/hexanes) to provide the *C*-trimethylsilyl alkynamide.

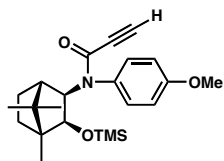
To a solution of *C*-trimethylsilyl alkynamide (2.01 g, 4.60 mmol) in methanol (60 mL) was added powdered anhydrous potassium hydroxide (660 mg, 11.8 mmol). After 5 min, the reaction mixture was diluted in ethyl acetate (100 mL) and washed with saturated sodium bicarbonate (100 mL). The organics were dried over sodium sulfate, concentrated, and purified via flash chromatography over silica gel (10:90 EtOAc/hexanes) to yield **505**.



(91% yield):  $R_f = 0.32$  (15:85 EtOAc/hexanes);  $^1\text{H}$  NMR (300 MHz,  $\text{CDCl}_3$ )  $\delta$  7.46–7.29 (comp m, 4H), 7.21–7.06 (br s, 1H), 4.30 (d,  $J = 6.9$  Hz, 1H), 4.03 (d,  $J = 6.9$  Hz, 1H), 2.72 (s, 1H), 1.94 (d,  $J = 3.9$  Hz, 1H), 1.79–1.62 (m, 1H), 1.50–1.38 (m, 1H), 1.17 (app q,  $J = 8.4$  Hz, 2H), 0.82 (s, 3H), 0.58 (s, 3H), 0.50 (s, 3H), 0.19 (s, 9H);  $^{13}\text{C}$  NMR (75 MHz,  $\text{CDCl}_3$ )  $\delta$  154.3, 140.6, 133.7, 130.6, 128.4, 128.3, 83.4, 79.5, 66.9, 49.5, 47.3, 47.0, 32.4, 29.0, 21.9, 21.7, 12.9, 0.9; IR (NaCl/thin film) 2960, 2106, 1634, 1594, 1491, 1344, 839  $\text{cm}^{-1}$ ; HRMS (FAB+) calc'd for  $[\text{C}_{22}\text{H}_{32}\text{NO}_2\text{Si}+\text{H}]^+$ :  $m/z$  370.2202, found 370.2193.

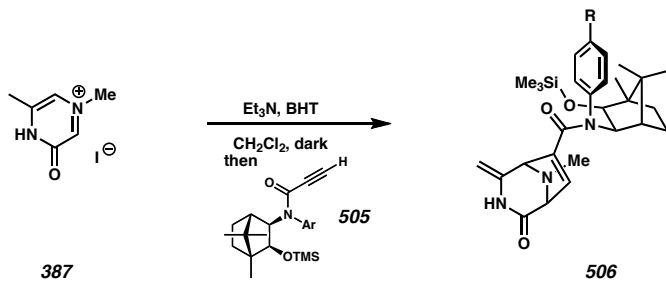


(69% yield):  $R_f = 0.47$  (15:85 EtOAc/hexanes);  $^1\text{H}$  NMR (300 MHz,  $\text{CDCl}_3$ )  $\delta$  7.41–7.32 (m, 2H), 7.18–6.94 (m, 2H), 4.28 (d,  $J = 6.9$  Hz, 1H), 4.02 (d,  $J = 6.9$  Hz, 1H), 2.76 (s, 1H), 1.88 (d,  $J = 4.2$  Hz, 1H), 1.82–1.60 (m, 1H), 1.52–1.38 (m, 1H), 1.28–1.10 (comp m, 2H), 0.82 (s, 3H), 0.60 (s, 3H), 0.52 (s, 3H), 0.19 (s, 9H);  $^{13}\text{C}$  NMR (75 MHz,  $\text{CDCl}_3$ )  $\delta$  157.4, 155.3, 140.3, 128.4, 128.3, 92.8, 90.1, 79.4, 59.5, 57.2, 49.0, 47.5, 32.7, 26.7, 22.6, 22.5, 11.6, 2.7; IR (NaCl/thin film) 3254, 1634, 1512, 1345, 1247, 1150, 835  $\text{cm}^{-1}$ ; HRMS (FAB+) calc'd for  $[\text{C}_{22}\text{H}_{30}\text{FNO}_2\text{Si}+\text{H}]^+$ :  $m/z$  388.2108, found 388.2089.



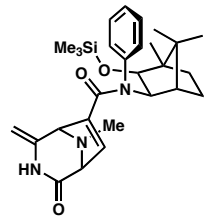
(67% yield):  $R_f = 0.40$  (15:85 EtOAc:hexanes);  $^1\text{H}$  NMR (300 MHz,  $\text{CDCl}_3$ )  $\delta$  7.30–7.28 (m, 2H), 6.90–6.81 (m, 2H), 4.27 (d,  $J = 6.3$  Hz, 1H), 4.02 (d,  $J = 6.4$  Hz, 1H), 2.75 (s, 1H), 1.91 (d,  $J = 4.2$  Hz, 1H), 1.78–1.62 (m, 1H), 1.50–1.38 (m, 1H), 1.26–1.10 (comp m, 2H), 0.82 (s, 3H), 0.59 (s, 3H), 0.54 (s, 3H), 0.19 (s, 9H);  $^{13}\text{C}$  NMR (75 MHz,  $\text{CDCl}_3$ )  $\delta$  153.0, 144.5, 140.6, 115.8, 115.2, 91.1, 90.5, 78.2, 59.3, 57.3, 56.7, 49.1, 48.8, 47.7, 32.1, 26.8, 22.7, 22.4, 11.7, 2.4; IR (NaCl/thin film) 3290, 3222, 2955, 1637, 1511, 1345, 1248, 1116, 834  $\text{cm}^{-1}$ ; HRMS (FAB+) calc'd for  $[\text{C}_{23}\text{H}_{53}\text{NO}_3\text{Si}+\text{H}]^+$ :  $m/z$  400.2308, found 400.2325.

#### A4.7.2.7 General Method for the Preparation of Silyl Ether Cycloadducts

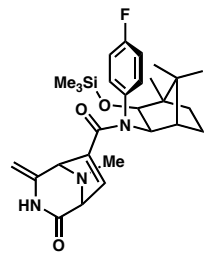


To a suspension of oxidopyrazinium iodide **387** (114.1 mg, 453 mmol) in dichloromethane (2.5 mL) were added 2,6-di-*tert*-butyl-4-methylphenol (20.0 mg, 91  $\mu\text{mol}$ ) and **505** (500.7 mg, 1.35 mmol). Triethylamine (66  $\mu\text{L}$ , 474  $\mu\text{mol}$ ) was then added in four portions at 2 h intervals. After an additional 22 h, the reaction mixture was diluted with dichloromethane (50 mL) and washed with saturated aqueous ammonium chloride (2 x 50 mL) followed by brine (50 mL). The organics were dried over sodium

sulfate, concentrated, and purified via flash chromatography over silica gel (50:50 → 75:25 EtOAc/hexanes) to yield **506**.

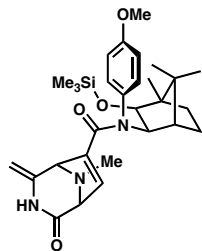


(77% yield, 14.3:1 dr):  $R_f = 0.27$  (75:25 EtOAc/hexanes);  $^1\text{H}$  NMR (300 MHz,  $\text{CDCl}_3$ )  $\delta$  7.42–7.28 (comp m, 4H), 7.14–7.02 (br s, 1H), 5.55 (d,  $J = 2.7$  Hz, 1H), 4.34 (d,  $J = 7.2$  Hz, 1H), 4.32 (s, 1H), 4.19 (d,  $J = 1.2$  Hz, 1H), 4.04 (d,  $J = 6.9$  Hz, 1H), 3.84 (s, 1H), 3.62–3.60 (br s, 1H), 2.08 (s, 3H), 1.78–1.62 (m, 1H), 1.50–1.34 (m, 1H), 1.28–1.10 (comp m, 2H), 0.80 (s, 3H), 0.58 (s, 3H), 0.47 (s, 3H), 0.10 (s, 9H);  $^{13}\text{C}$  NMR (75 MHz,  $\text{CDCl}_3$ )  $\delta$  166.2, 164.0, 141.6, 141.2, 137.9, 135.6, 128.8, 128.6, 93.2, 83.9, 71.9, 69.8, 68.2, 49.5, 47.2, 37.3, 32.5, 29.5, 22.2, 21.7, 13.0, 1.0; IR (NaCl/thin film) 3224, 2954, 1691, 1634, 1591, 1495, 1349, 903, 839  $\text{cm}^{-1}$ ; HRMS (FAB+) calc'd for  $[\text{C}_{28}\text{H}_{39}\text{N}_3\text{O}_3\text{Si}+\text{H}]^+$ :  $m/z$  494.2839, found 494.2832.



Reaction performed at 30 °C (44% yield, 16.7 dr):  $R_F 0.35$  (75:25 ethyl acetate:hexanes);  $^1\text{H}$  NMR (300 MHz,  $\text{CDCl}_3$ )  $\delta$  7.22–7.10 (m, 2H), 7.10–6.94 (m, 2H), 5.50 (d,  $J = 2.7$  Hz, 1H), 4.35 (s, 1H), 4.32 (d,  $J = 6.9$ , 1H), 4.22 (s, 1H), 4.02 (d,  $J = 6.9$ , 1H), 3.97 (s, 1H),

3.65 (s, 1H), 2.15 (s, 3H), 1.83 (d,  $J$  = 4.2 Hz, 1H), 1.78-1.62 (m, 1H), 1.50-1.33 (m, 1H), 1.24-1.08 (comp m, 2H), 0.81 (s, 3H), 0.60 (s, 3H), 0.50 (s, 3H), 0.11 (s, 9H);  $^{13}\text{C}$  (75 MHz,  $\text{CDCl}_3$ )  $\delta$  172.2, 159.5, 147.9, 139.0, 136.8, 132.1, 131.3, 114.8, 114.5, 99.3, 82.7, 82.0, 66.9, 48.6, 46.4, 46.3, 40.0, 31.5, 28.2, 25.7, 21.2, 20.9, 12.2, 0.2; IR (NaCl/film) 2954, 2874, 1686, 1635, 1509, 1350, 1249, 1222, 906, 841  $\text{cm}^{-1}$ ; HRMS (FAB+) calc'd for  $[\text{C}_{28}\text{H}_{58}\text{FN}_3\text{O}_3\text{Si}+\text{H}]^+$ :  $m/z$  512.2745, found 512.2712.



Note: T = 30 °C (52% yield):  $R_F$  0.14 (80:20 ethyl acetate:hexanes);  $^1\text{H}$  NMR (300 MHz,  $\text{CDCl}_3$ )  $\delta$  7.24-7.10 (m, 1H), 7.08-6.94 (m, 1H), 6.92-6.74 (m, 2H), 5.49 (d,  $J$  = 2.7 Hz, 1H), 4.32 (s, 1H), 4.30 (d,  $J$  = 6.7 Hz, 1H), 4.19 (s, 1H), 4.00 (d,  $J$  = 6.6 Hz, 1H), 3.91 (s, 1H), 3.80 (s, 3H), 3.62 (s, 1H), 2.12 (s, 3H), 1.86 (d,  $J$  = 4.2 Hz, 1H), 1.64-1.58 (m, 1H), 1.48-1.32 (m, 1H), 1.20-1.08 (comp m, 2H), 0.79 (s, 3H), 0.58 (s, 3H), 0.50 (s, 3H), 0.08 (s, 9H);  $^{13}\text{C}$  (75 MHz,  $\text{CDCl}_3$ )  $\delta$  158.5, 153.8, 133.8, 132.5, 130.6, 124.9, 112.6, 112.4, 82.5, 78.7, 66.0, 54.7, 48.6, 46.5, 46.1, 31.6, 29.7, 28.2, 21.1, 21.0, 12.1, 0.0; IR (NaCl/film) 3230, 2956, 1685, 1509, 1458, 1352, 1254, 1109, 905  $\text{cm}^{-1}$ ; HRMS (FAB+) calc'd for  $[\text{C}_{29}\text{H}_{41}\text{N}_3\text{O}_4\text{Si}+\text{H}]^+$ :  $m/z$  524.2945, found 524.2911.

**A4.8 NOTES AND REFERENCES**

- (1) Hayashi, T.; Noto, T.; Nawata, Y.; Okazaki, H.; Sawada, M.; Ando, K. *J. Antibiot.* **1982**, *35*, 771–777.
- (2) Kluepfel, D.; Baker, H. A.; Piattoni, G.; Sehgal, S. N.; Sidorowicz, A.; Singh, K.; Vezina, C. *J. Antibiot.* **1975**, *28*, 497–502.
- (3) Zmijewski, M. J., Jr.; Goebel, M. *J. Antibiot.* **1982**, *35*, 524–526.
- (4) Williams, R. M.; Herberich, B. *J. Am. Chem. Soc.* **1998**, *120*, 10272–10273.
- (5) For comprehensive review of the chemistry and biology of the tetrahydroisoquinoline antitumor antibiotics, see: Scott, J. D.; Williams, R. M. *Chem. Rev.* **2002**, *102*, 1669–1730.
- (6) Evans, D. A.; Illig, C. R.; Saddler, J. C. *J. Am. Chem. Soc.* **1986**, *108*, 2478–2479.
- (7) Fukuyama, T.; Li, L.; Laird, A. A.; Frank, K. *J. Am. Chem. Soc.* **1987**, *109*, 1587–1589.
- (8) Illig, C. R. Ph.D. Thesis, Harvard University, Cambridge, MA, 1987.
- (9) Fukuyama, T. *Adv. Heterocycl. Nat. Prod. Synth.* **1992**, *2*, 189–249.
- (10) Ashley, E. R.; Cruz, E. G.; Stoltz, B. M. *J. Am. Chem. Soc.* **2003**, *125*, 15000–15001.
- (11) Ashley, E. R. Ph. D. Thesis, California Institute of Technology, Pasadena, CA, 2005.
- (12) Allan, K. M.; Stoltz, B. M. *J. Am. Chem. Soc.* **2008**, *130*, 17270–17271.

(13) For examples of the copper(I)-accelerated Stille cross-coupling, see: Han, X.; Stoltz, B. M.; Corey, E. J. *J. Am. Chem. Soc.* **1999**, *121*, 7600–7605.

(14) For a review of the Stille reaction including copper(I)-accelerated conditions, see: Farina, V.; Krishnanmurthy, V.; Scott, W. J. *Org. React.* **1997**, *50*, 1–652.

(15) (a) Timokhin, V. I.; Anastasi, N. R.; Stahl, S. S. *J. Am. Chem. Soc.* **2003**, *125*, 12996–12997. (b) Brice, J. L.; Harang, J. E.; Timokhin, V. I.; Anastasi, N. R.; Stahl, S. S. *J. Am. Chem. Soc.* **2005**, *127*, 2868–2869. (c) Timokhin, V. I.; Stahl, S. S. *J. Am. Chem. Soc.* **2005**, *127*, 17888–17893. (d) Rogers, M. M.; Kotov, V.; Chatwichien, J.; Stahl, S. S. *Org. Lett.* **2007**, *9*, 4331–4334.

(16) Sha, C.-K.; Jean, T.-S.; Wang, D.-C. *Tetrahedron Lett.* **1990**, *31*, 3745–3748.

(17) Kim, S.; Oh, C. H.; Ko, J. S.; Ahn, K. H.; Kim, Y. J. *J. Org. Chem.* **1985**, *50*, 1927–1932.

(18) Petasis, N. A. *Tetrahedron Lett.* **1993**, *34*, 583–586.

(19) Boronic acid **462** was prepared during investigations related to the Suzuki cross-coupling with iodoenamine **441**.

(20) McReynolds, M. D.; Hanson, P. R. *Chemtracts* **2001**, *14*, 796–801.

(21) (a) Petasis, N. A.; Zavialov, I. A. *J. Am. Chem. Soc.* **1997**, *119*, 445–446. (b) Wang, Q.; Finn, M. G. *Org. Lett.* **2000**, *2*, 4063–4065. (c) Naskar, D.; Roy, A.; Seibel, W. L.; Portlock, D. E. *Tetrahedron Lett.* **2003**, *44*, 8865–8868. (d) Kumagai, N.; Muncipinto, G.; Schreiber, S. L. *Angew. Chem., Int. Ed.* **2006**, *45*, 3635–3638.

(22) Schlienger, N.; Bryce, M. R.; Hansen, T. K. *Tetrahedron Lett.* **2000**, *41*, 1303–1305.

(23) Nanda and Trotter demonstrated the accelerating effect of 2,2,2-trifluoroethanol and 1,1,1,3,3,3-hexafluoroisopropanol as solvent additives in the Petasis reaction. See: Nanda, K. K.; Trotter, B. W. *Tetrahedron Lett.* **2005**, *46*, 2025–2028.

(24) (a) Fukuyama, T.; Nunes, J. J. *J. Am. Chem. Soc.* **1988**, *110*, 5196–5198. (b) Chen, J.; Chen, X.; Bois-Choussy, M.; Zhu, J. *J. Am. Chem. Soc.* **2006**, *128*, 87–89. (c) Wu, Y.; Zhu, J. *Org. Lett.* **2009**, *11*, 5558–5561.

(25) The extraneous methyl groups are highlighted blue.

(26) (a) Bernan, V. S.; Montenegro, D. A.; Korshalla, J. D.; Maiese, W. M.; Steinberg, D. A.; Greenstein, M. *J. Antibiot.* **1994**, *47*, 1417–1424. (b) Zaccardi, J.; Alluri, M.; Ashcroft, J.; Bernan, V.; Korshalla, J. D.; Morton, G. O.; Siegel, M.; Tsao, R.; Williams, D. R.; Maiese, W.; Ellestad, G. A. *J. Org. Chem.* **1994**, *59*, 4045–4047.

(27) Garner *et al.* used an acrylamide derivative of Oppolzer's sultam in an asymmetric dipolar cycloaddition toward the synthesis of (–)-quinocarcin. See: (a) Garner, P.; Ho, W.-B.; Shin, H. *J. Am. Chem. Soc.* **1992**, *114*, 2767–2768. (b) Garner, P.; Ho, W.-B.; Shin, H. *J. Am. Chem. Soc.* **1993**, *115*, 10742–10753.

(28) (a) Garner, P.; Dogan, O. *J. Org. Chem.* **1994**, *59*, 4–6. (b) Dogan, O.; Garner, P. *Turk. J. Chem.* **2000**, *24*, 59–66.

(29) Fonquerna, S.; Moyano, A.; Pericàs, M. A.; Riera, A. *Tetrahedron* **1995**, *51*, 4239–4254.

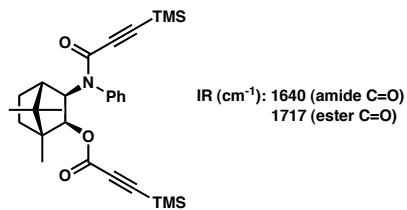
(30) Shi, M.; Wang, C.-J. *J. Chem. Res.* **2004**, *2*, 107–110.

(31) Helmchen, G.; Selim, A.; Dorsch, D.; Taufer, I. *Tetrahedron Lett.* **1983**, *24*, 3213–3216. This auxiliary was later used to control stereochemistry in [4+2] cycloadditions. See: Poll, T.; Helmchen, G.; Bauer, B. *Tetrahedron Lett.* **1984**, *25*, 2191–2194.

(32) The  $\alpha$  and  $\beta$  denotations refer to the position of the *N*-methyl tertiary amine in relation to the plane of the rest of the bicyclic. The  $\beta$  diastereomer is before the plane and the  $\alpha$  diastereomer is behind the plane.

(33) Helmchen *et al.* report the synthesis of the sulfonamide corresponding to sulfonylation of amino alcohol **497** with benzenesulfonyl chloride in the presence of pyridine. However, when we performed the same reaction, the only product isolated was benzenesulfonate **498** ( $R = Ph$ ) in up to 96% yield.

(34) The amide and ester carbonyl stretches were confirmed by synthesizing amide ester shown below via acylation of amino alcohol **497**:



(35) Diastereomeric ratios were determined by  $^1\text{H}$  NMR.

(36) The conformational energy of alkynamide **502** was minimized with semiempirical calculations carried out at the AM1 level. These calculations were performed with Spartan '02 v1.0.8 (Wavefunction, Inc.).

(37) The lowest energy conformation of each of the aryl-substituted auxiliaries was found to place the aryl ring in the same quadrant as was calculated for the unsubstituted version.

(38) Fukuyama, T.; Lin, S.-C.; Li, L. *J. Am. Chem. Soc.* **1990**, *112*, 7050–7051.

(39) Panunzio *et al.* report the mild dearylation of tertiary amides using silver(I) nitrate and aqueous ammonium persulfate, see: Bhattacharai, K.; Cainelli, G.; Panunzio, M. *Synlett* **1990**, 229–230.